Teagasc Food Research Centre, Moorepark

and

Ollscoil na hÉireann, Corcaigh

National University of Ireland, Cork

Formulation and Application of Alginate-based and Soy Protein Isolate-Stabilized Emulsion Gels

Thesis presented by

Duanquan Lin, BS, MS

for the degree of

Doctor of Philosophy

University College Cork

School of Food and Nutritional Sciences

Head of School/Department: Prof. Mairead Kiely

Supervisors: Prof. Song Miao (Teagasc) and Prof. Alan L. Kelly (UCC)

June 2021

TABLE OF CONTENTS

DECLARATION

This is to certify that the work I am submitting is my own and has not been submitted for another degree, either at University College Cork or elsewhere. All external references and sources are clearly acknowledged and identified within the contents. I have read and understood the regulations of University College Cork concerning plagiarism.

Duanquan Lin

June 2021

DEDICATION

Dedicated to my parents

Xiumei Lin

and

Yimei Zheng

ACKNOWLEDGEMENTS

First of all, I would like to thank my chief supervisor Professor Song Miao in Teagasc Food Research Centre, Moorepark, for giving me an opportunity to study in Ireland and for his consistent support and guidance throughout this PhD research programme. His assistance and encouragement helped me to accomplish this project as planned during the Covid-19 pandemic. I would also like to thank my academic supervisor Professor Alan L. Kelly from University College Cork for his hard work and valuable advice throughout this programme. I am extremely grateful for his help on academic writing.

I would like to express my sincere gratitude to the China Scholarship Council-University College Cork Joint Research Scholarship and Teagasc-The Irish Agriculture and Food Development Authority for funding this research project. I am also tankful to following people in Moorepark for their help on my experiments and guidance in the operation of instruments: Dr. Valentyn Maidannyk, Dr. Deirdre Kennedy, Dr. Sean Hogan, Ms. Helen Slattery, Ms. Martina O'Brien, Dr. Norah O'Shea, Ms. Anne Marie McAuliffe, Ms. Sarah Cooney, Dr. André Brodkorb, Dr. Laura Gómez-Mascaraque, and Mr. Bernard Corrigan.

I also would like to thank all my friends and colleagues met in Ireland, Wei Lu, Shaozong Wu, Jie Han, Xiaobin Ma, Chengdeng Chi, Runjing Li, Shaopu Wang, Yuanyuan Pu, Qingsong Zou, Xiaofeng Xia, Vinay Mishra, Sean Roche, Helen Roche, Prabin Lamichhane, Archana Bista, Ashwini Shevade, and etc, for their contributions to my wonderful life here.

Finally, I would like to give my deep thankfulness to my parents, grandparents, brothers, uncles, aunts, and cousins, for their constant love and support. I am particularly grateful to my younger brother, Duanzhe Lin, for video-chatting with me almost every day, which made my life full of enjoyment. I can not never thank you enough.

Acknowledgments

Duanquan Lin

Fermoy, Ireland

01/04/2021

ABSTRACT

Alginate gels filled with emulsion droplets (i.e., alginate-based emulsion gels) have received increased interest in recent years, and soy protein isolate (SPI), used as a emulsifier, has been widely investigated in the food industry. However, the effect of SPI on properties of alginate-based emulsion gels has rarely been reported. This study investigated three kinds of alginate-based emulsion gels containing SPI-coated droplets, according to their morphological properties (i.e., the diameter/length of gels): bulk emulsion gels (> 1 cm), emulsion macro-gel beads (1-10 mm) and emulsion micro-gel particles (0.2-1,000 μm).

For preparation of emulsion gels, the first step is to prepare emulsions containing alginate in the continuous phase, and the gelation of the continuous phase is then triggered by introducing Ca^{2+}. The addition sequence of oppositely charged dispersions may affect the structure and stability of emulsions and thus the mechanical and structural properties of bulk emulsion gels. Stable emulsions containing unflocculated alginate/SPI-coated droplets were produced by adding low levels of SPI-stabilized emulsions into alginate solutions at pH 3.0, and bulk emulsion gels prepared from the above emulsions with GDL and $CaCO_3$ had less flocculated droplets, higher L* values, and stronger mechanical properties than those prepared by adding alginate solutions into SPI-stabilized emulsions.

In terms of emulsion macro-gel beads, their Young's modulus kept increasing during the gelling process by external gelation (i.e., dropping emulsions into $CaCl_2$ solutions), before reaching a plateau accompanied by syneresis (i.e., water loss), shrinkage, and structural tightening. SPI adsorbed at the surfaces of emulsion droplets could prevent coalescence of droplets during gelation. However, the presence of SPI decreased Young's modulus of emulsion gel beads, compared to emulsion gel beads without proteins. In addition, the presence of SPI accelerated changes in Young's modulus and shrinkage during simulated gastric digestion and delayed the release of lycopene from emulsion gel beads during intestinal digestion. The pH of emulsions can also influence the gelation mechanism and

properties of emulsion gel beads. Emulsion gel beads at pH 3.0 showed lower mechanical strength, higher storage stability of encapsulated lycopene, and faster release of lycopene during *in-vitro* digestion than those at pH 7.0 or 5.0.

In terms of emulsion micro-gel particles, external/internal O/W/O emulsion-gelation methods were compared to prepare emulsion micro-gels. External gelation could produce emulsion micro-gels with small size (< 100 μm), while emulsion micro-gels prepared by internal gelation had bigger size and a more narrow size distribution. The suspensions of emulsion micro-gels prepared by external gelation had higher ϕ_{rcp}, ϕ_j, G', and G'' values than those prepared by internal gelation. Emulsion micro-gel particles prepared by external method collapsed more rapidly than those prepared by internal method during intestinal digestion. Moreover, SPI-stabilized emulsions turned into gel-like emulsions at high levels of externally-induced micro-gel particles (> 6.0%) in the presence of alginate (> 0.1%). Viscosity and creaming stability of emulsions and storage modulus (G') of gel-like emulsions increased with increasing contents of micro-gel particles in emulsions.

Findings in this study are important for structuring emulsions and emulsion gels with naturally occurring polymers to achieve improved emulsion stability and controlled release of encapsulated compounds.

SCHEMATIC OVERVIEW OF THESIS

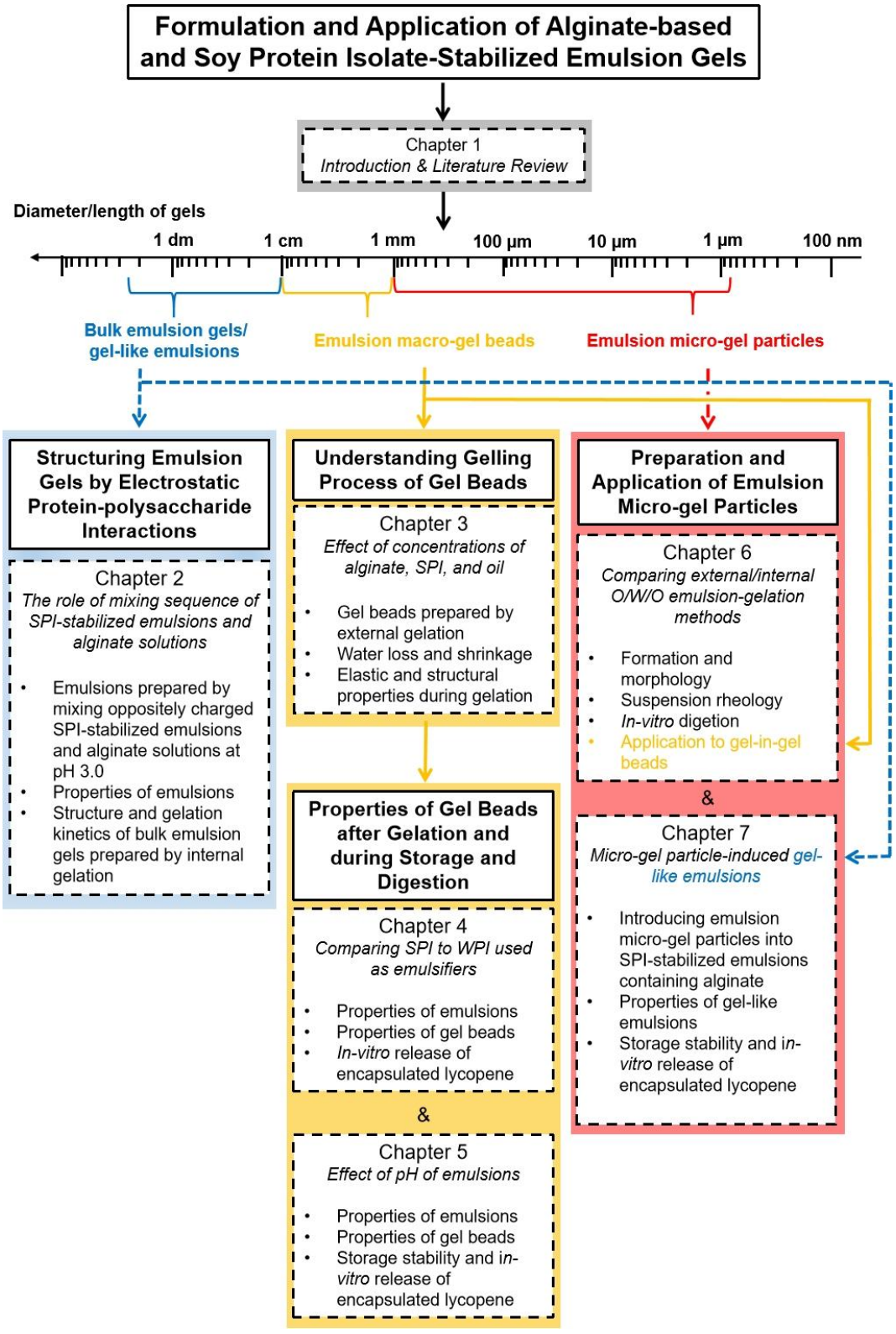

LIST OF PUBLICATIONS

Peer Reviewed Journals

1. **Lin, D.**, Kelly, A. L., & Miao*, S. (2020). Preparation, structure-property relationships and applications of different emulsion gels: Bulk emulsion gels, emulsion gel particles, and fluid emulsion gels. *Trends in Food Science & Technology, 102*, 123-137.
2. **Lin, D.**, Kelly, A. L., Maidannyk, V., & Miao*, S. (2020). Effect of concentrations of alginate, soy protein isolate and sunflower oil on water loss, shrinkage, elastic and structural properties of alginate-based emulsion gel beads during gelation. *Food Hydrocolloids, 108*, 105998.
3. **Lin, D.**, Kelly, A. L., Maidannyk, V., & Miao*, S. (2020). Effect of structuring emulsion gels by whey or soy protein isolate on the structure, mechanical properties, and *in-vitro* digestion of alginate-based emulsion gel beads. *Food Hydrocolloids, 110*, 106165.
4. **Lin, D.**, Kelly, A. L., & Miao*, S. (2021). The role of mixing sequence in structuring O/W emulsions and emulsion gels produced by electrostatic protein-polysaccharide interactions between soy protein isolate-coated droplets and alginate molecules. *Food Hydrocolloids, 113*, 106537.
5. **Lin, D.**, Kelly, A. L., & Miao*, S. (2021). Alginate-based emulsion micro-gel particles produced by an external/internal O/W/O emulsion-gelation method: Formation, suspension rheology, digestion, and application to gel-in-gel beads. *Food Hydrocolloids, 120*, 106926.
6. **Lin, D.**, Kelly, A. L., & Miao*, S. (2021). Formation and creaming stability of alginate/micro-gel particle-induced gel-like emulsions stabilized by soy protein isolate. *Food Hydrocolloids, 121*, 107040.
7. **Lin, D.**, Kelly, A. L., & Miao*, S. (2021). The impact of pH on mechanical properties, storage stability and digestion of alginate-based and soy protein isolate-stabilized emulsion gel beads with encapsulated lycopene (submitted to Food Chemistry).

LIST OF ABBREVIATIONS

AE	Mixtures by adding alginate solutions into emulsions
A_s	The section area
BHT	Butylated hydroxytoluene
CLSM	Confocal laser scanning microscopy
C_{LYC}	Lycopene concentration
cP	Centipoise
EA	Mixtures by adding emulsions into alginate solutions
G'	Storage modulus
G''	Loss modulus
GDL	Glucono-δ-lactone
$D_{3,2}$	Surface-weighted mean diameter
$D_{4,3}$	Volume-weighted mean diameter
Da	Daltons
L^*	Lightness value
LBL	Layer-by-layer
$\overline{M}$	Average molecular weight
mPa·s	Millipascal-second
O/W	Oil-in-water
O/W/O	Oil-in-water-in-oil
pI	Isoelectric point
r_{max}	The major semi-axis
R_{max}	The major axis
r_{min}	The minor semi-axis
R_{min}	The minor axis
rpm	Round per minute
$R_{release}$	Release rate

SGF	Simulated gastric fluid
SIF	Simulated intestinal fluid
SPI	Soy protein isolate
SSF	Simulated saliva fluid
v/v	Volume/volume
w/w	Weight/weight
W	Weight
WPI	Whey protein isolate
ϕ	Phase volume
ϕ_j	The jamming fraction
ϕ_m	The maximum packing fraction
ϕ_r	The relative phase volume ($\phi_r = \phi/\phi_m$)
ϕ_{rcp}	The random close packing fraction
η	Viscosity
ζ	Zeta-potential

INTRODUCTION

Emulsion gels are defined as emulsions with gel-like network structures and solid-like mechanical properties produced by gelling the continuous phase of emulsions (i.e., gels filled with emulsion droplets) or by aggregating the emulsion droplets (i.e., gel-like emulsions). The gelation of the continuous phase of emulsions can be carried out by various methods for different matrix materials such as heat treatment, enzyme treatment, acidification, and addition of ions for protein-based emulsion gels, cold-set and addition of ions for polysaccharide-based emulsion gels, and self-assembly for low molecular weight compound-based emulsion gels. Emulsion gels are classified into bulk emulsion gels, emulsion gel beads/particles, gel-like Pickering emulsions, and disrupted emulsion gels according to their morphological properties. Different properties are emphasized for different emulsion gels in previous studies, such as the importance of mechanical and release properties for bulk emulsion gels, syneresis and swelling properties for emulsion gel particles, rheological properties for micro-gel particle suspensions, and flow behavior and release property for fluid emulsion gels. Different morphological properties of emulsion gels also determine their various applications in the food industry, such as fat replacers for bulk emulsion gels, encapsulation materials and structuring agents for emulsion gel particles, and delivery systems and thickening agents for gel-like emulsions.

Alginate gels filled with emulsion droplets (i.e., alginate-based emulsions gels) have received increased interest in recent years, due to their mild gelling process, pH sensitivity and targeted release of encapsulated nutrients. In addition, alginate-based emulsion gels (including bulk emulsion gels and emulsion macro-gel beads) have been widely investigated in previous studies, in which emulsions were prepared with WPI as emulsifiers or without emulsifiers. However, alginate-based emulsion micro-gel particles and using SPI as emulsifiers in alginate-based emulsions gels have rarely been reported. Although the major

proteins in WPI and SPI are globular proteins (i.e., β-lactoglobulin in WPI and β-conglycinin (7S fraction) and glycinin (11S fraction) in SPI), WPI and SPI have different functional properties (i.e., solubility, hydrophobicity, emulsifying properties, and gelling properties). Therefore, SPI and WPI may have different impacts on properties of alginate-based emulsion gels. In addition, zeta potential of sodium alginate and SPI are pH-dependent, so different electrostatic interactions between them may occur at different pHs in the continuous phase and/or droplet surfaces of emulsions, which may affect structural and mechanical properties of emulsion gels.

In terms of applications of alginate-based emulsion gels, fat replacers in meat products and delivery systems for food nutrients are two main applications in the food industry. Previous studies mainly focused on the applications of bulk emulsion gels (as fat replacers and delivery systems) and emulsion macro-gel beads (as delivery systems). Polysaccharide-based (especially alginate-based) emulsion gels are less sensitive to gastric fluid than protein-based emulsion gels, and may protect encapsulated nutriments from harsh gastric environment, while the remaining gel structures can further collapse during intestinal digestion. However, emulsion gels normally give low effective bio-availability of encapsulated lipophilic compounds, due to insufficient digestion of the gel matrix and resulting unreleased and undigested lipid phase. Using emulsion gels with smaller size (e.g., emulsion micro/nano-gel particles) as encapsulation materials may facilitate complete digestion of the gel matrix and encapsulated lipid phase and thus improve the effective bio-availability of encapsulated food nutrients than bulk emulsion gels and emulsion macro-gel beads, which need further investigation. In addition, emulsion gels with different morphological properties (i.e, the diameter/length of gels) may also have different impacts on the properties (i.e., textural properties and sensory acceptability) of final food products, which also need further investigation.

It was therefore hypothesized that alginate-based emulsion gels with different morphological properties may have different functional properties and applications in food,

and that SPI may act emulsifiers and/or structuring agents in alginatete-based emulsion gels and thus affect properties of emulsion gels. Three kinds of emulsion gels were designed in this study, including bulk emulsion gels/gel-lile emulsions (> 1cm), emulsion macro-gel beads (1-10 mm) and emulsion micro-gel particles (0.2-1000 μm) classified according to the diameter/length of emulsion gels. The preparation methods (e.g., external and internal gelation), properties (e.g., morphology, micro-structure and mechanical properties) and applications (e.g., encapsulation materials and structuring agents) of different emulsion gels were investigated. In order to fill in the research gap in this field, this thesis addressed the following three main aspects:

(i) Structuring alginate-based bulk emulsion gels through electrostatic protein-polysaccharide interactions and the role of mixing sequence of oppositely charged SPI-stabilized emulsions and alginate solutions at pH 3.0 (i.e., Chapter 2);

(ii) Understanding gelling process of alginate-based and SPI-stabilized emulsion macro-gel beads (i.e., Chapter 3) and investigating properties of such gel beads after gelation and during storage and *in-vitro* digestion: comparing SPI to WPI as emulsifiers (i.e., Chapter 4) and the effect of pH of emulsions (i.e., Chapter 5);

(iii) Comparing external/internal O/W/O emulsion-gelation methods for preparation of alginate-based and SPI-stabilized emulsion micro-gel particles and their application to gel-in-gel beads (i.e., Chapter 6) and fabrication of emulsion micro-gel particle-induced gel-like emulsions with improved creaming stability (i.e., Chapter 7).

CHAPTER ONE

Literature Review

Part of this section was published in:

Lin, D., Kelly, A. L., & Miao*, S. (2020). Preparation, structure-property relationships and applications of different emulsion gels: Bulk emulsion gels, emulsion gel particles, and fluid emulsion gels. *Trends in Food Science & Technology, 102*, 123-137.

The work contained in this chapter was undertaken and written solely by myself with specific contributions from each co-author.

Abstract

In recent years, there has been increasing interest in emulsion gels, due to their better stability during storage and potential for prolonged intestinal drug release compared to liquid emulsions. There are three kinds of emulsion gels, classified according to their morphological properties: bulk emulsion gels, emulsion gel particles and liquid emulsion gels. Different emulsion gels result from different preparation methods, and have various structure-property relationships and applications. Many methods can be used to prepare bulk emulsion gels, involving different matrix materials, processing techniques, and purposes. This can result in different structures of gel matrices and emulsion droplets and interactions between them, which can influence the structures of bulk emulsion gels and then their mechanical and release properties. On the other hand, extrusion and impinging aerosol methods are two methods for preparing emulsion gel particles, while liquid emulsion gels can be prepared by Pickering emulsions and disrupted gel systems. Rheological, syneresis and swelling properties are critical for gel particle suspensions, while flow behavior and release properties are important to liquid emulsion gels. In addition, fat replacers and delivery systems are main applications of emulsion gels in the food industry. However, previous studies mainly focused on bulk emulsion gels, so further studies on emulsion gel particles and liquid emulsion gels are required.

Keywords: Emulsion gel; Preparation; Interaction; Structure; Property; Fat replacer; Delivery.

1.1. Introduction

Emulsion gels, also known as emulgels (Balakrishnan, et. al., 2017), are complex colloidal materials with gel-like network structures and solid-like mechanical properties formed by gelling the continuous phase of emulsions or by aggregating the emulsion droplets (de Souza Paglarini et al., 2018; Dickinson, 2012). Proteins or polysaccharides are normally used as gelling agents to trigger the gelation the continuous phase of oil-in-water (i.e., O/W) emulsions and then form emulsion gels (i.e., hydrogels filled with emulsion droplets) (Farjami & Madadlou, 2019). Low-molecular-weight organogelators (e.g., β-sitosterol and γ-oryzanol), polymeric gelators (e.g., ethylcellulose), or food-grade waxes (e.g., beeswax) can also gel the continuous phase of water-in-oil (i.e., W/O) emulsions and form emulsion gels (i.e., oleogels filled with emulsion droplets) (Bot et al., 2011). In addition, increasing the volume fraction of emulsion droplets can lead to the aggregation of emulsion droplets and thus result in emulsions with solid-like mechanical properties (i.e., gel-like emulsions) (Xu, Liu, & Tang, 2019).

During the last decade, emulsion gels have received growing interest, due to their advantages compared to emulsions, such as higher stability during storage, due to decreased oil movement and oxygen diffusion within the systems (Cofrades et al., 2017; Corstens et al., 2017; Lim et al., 2015; Ma, Wan, & Yang, 2017; Sato, Moraes, & Cunha, 2014), controlled and prolonged gastric and/or intestinal drug release because of the protection by the gel matrices (Corstens et al., 2017; Guo, Bellissimo, & Rousseau, 2017), and practical applications, including overcoming the textural problems caused by lipid particles in food products and mimicking the effect of fat on hardness and water-holding capacity of meat products (Alejandre et al., 2016; Brito-Oliveira et al., 2017).

According to the interactions between emulsion droplets and the gel matrix, emulsion droplets can be divided into active and inactive fillers (**Figure 1-1**). Active fillers are mechanically connected to the gel network through emulsifiers by non-covalent and/or

covalent bonds, especially when emulsifiers are natural molecules (e.g., proteins, egg lecithin, and soy lecithin); in contrast, inactive fillers have little chemical or physical affinity with the molecules of the gel matrix, especially when low molecular weight (LMW) emulsifiers (e.g., Tween 20, Span80, or Span 85) or no emulsifiers are used (Van Vliet, 1988). For example, it has been reported that alginate-based emulsion gels without emulsifiers were prepared by adding GDL and CaEDTA into alginate solutions containing olive oil (30%, v/v) after homogenization, in which emulsion droplets acted as inactive fillers (Sato et al., 2014).

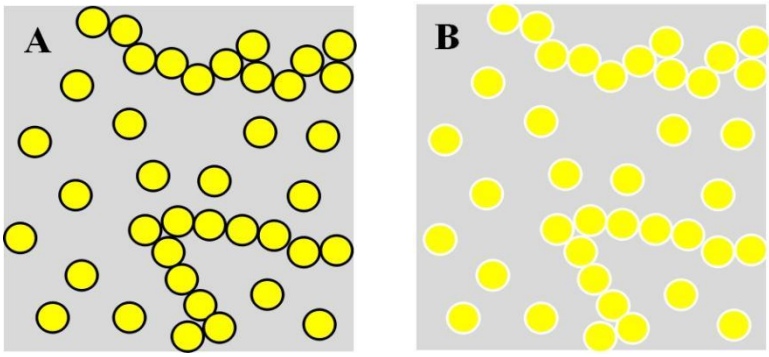

Figure 1-1. Schematic presentation of two kinds of droplet fillers in emulsion gels: (A) active fillers (e.g, emulsion droplets coated by proteins, egg lecithin, or soy lecithin), and (B) inactive fillers (e.g., emulsion droplets coated by Tween 20, Span80, or Span 85).

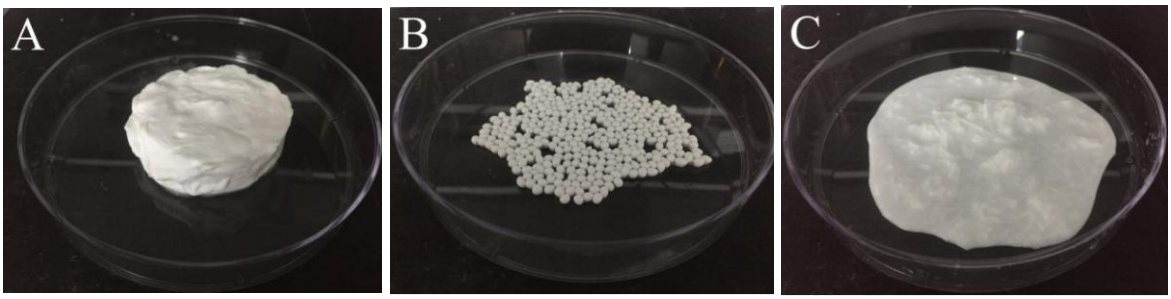

Figure 1-2. Visual appearances of alginate-based (A) bulk emulsion gels, (B) emulsion gel particles, and (C) fluid emulsion gels. Preparing alginate-based emulsion gels includes two steps: first preparing emulsions with 1 wt% sodium alginate and 0.5 wt% Tween 80 in water phase and 40 wt% sunflower oil, and then turning emulsions into emulsion gels by gelling the continuous phase of emulsions. For the preparation of bulk emulsion gels, 0.5 wt% $CaCl_2$ were added into emulsions, and the samples were allowed to gel for 6 h in stand. For the production of emulsion gel particles, emulsions were dropped into a 2.0 wt% CaCl2 solution, and the samples were allowed to gel in the $CaCl_2$ solution for 6 h with mild magnetic stirring. For producing fluid emulsion gels, 0.5 wt% $CaCl_2$ was added into emulsions, and the mixture was sheared under constant paddle stirring at 600 rpm for 6 h (original work).

Bulk emulsion gels, emulsion gel beads/particles and liquid emulsion gels are three kinds of emulsion gels (**Figure 1-2**), which exhibit their own particular properties, due to their different morphological properties. Bulk emulsion gels and emulsion gel beads/particles are solid-like emulsion gels prepared by gelling the continuous phase of emulsions, while liquid emulsion gels are gel-like emulsions prepared by aggregating the emulsion droplets or disrupted gel systems by shearing emulsion gels. The size and shape of bulk emulsion gels are determined by the emulsion volume and containers (e.g., beakers and tubes) with different shapes and sizes being used during the emulsion gel preparation, and bulk emulsion gels can also be broken into smaller pieces with different sizes and shapes. Therefore, mechanical properties (including viscoelastic and textural properties) of bulk emulsion gels are important. Emulsion gel beads/particles are normally spherical with sizes (diameters) from nano to macro (Ching, Bansal, & Bhandari, 2017). Thus, mechanical properties are also important for the macro-gel beads. However, emulsion gel beads/particles can be dispersed in aqueous media, and gel beads/particles may swell or shrink as a function of environmental conditions, resulting in changes in their size and/or physicochemical properties (Torres et al., 2017). In addition, there are two types of fluid emulsion gels: gel-like emulsions and disrupted emulsion gel systems. Fluid emulsion gels do not have solid shapes, but they have higher viscoelasticity than conventional emulsions. Gel-like emulsions are similar to bulk emulsion gels, and may also exhibit a solid state (Zou et al., 2015), while disrupted emulsion gels normally exhibit fluid characterization (Soukoulis et al., 2016). This chapter provides an overview of the current knowledge of preparation methods, structure-property relationships, and applications of different emulsion gel systems.

1.2. Preparation of different emulsion gels

1.2.1. Bulk emulsion gels

Proteins (e.g., myofibrillar protein, whey protein, soy protein, gelatin, bovine serum albumin, sodium caseinate, and casein), polysaccharides (e.g., carrageenan, gellan gum, agar,

alginate, and inulin), and LMW compounds (e.g., saponin glycyrrhizic acid and the mixture of β-sitosterol and γ-oryzanol) are normally used as matrix materials in bulk emulsion gels. According to the gelation process, preparation methods for bulk emulsion gels include heat-set, one-step cold-set, cold-set after heat treatment, enzyme treatment, acidification treatment, addition of ions, and self-assembly gelation methods. Choosing an appropriate method depends on the matrix materials (i.e., proteins, polysaccharides or LMW compounds) and applications of resultant emulsion gels such as mimicking food processing (i.e., heating process of meat), protecting encapsulated nutrients, controlled release of encapsulated nutrients, or obtaining better mechanical properties. For heat-set, one-step cold-set, cold-set after heating, and self-assembled gelation methods, the concentration of proteins, polysaccharides and LMW compounds in the water phase should be higher than the critical gelation concentration to guarantee the gelation. However, for gelation methods based on enzyme treatment, acidification treatment, or addition of ions, the concentration of matrix molecules can be below the critical gelation concentration, especially to avoid gelation during the pre-heating process (Ye & Taylor, 2009).

1.2.1.1. Protein-based bulk emulsion gels

Several methods have been studied for preparing protein-based bulk emulsion gels: heat treatment, cold-set after pre-heating, acidification, addition of ions, and enzyme treatment, depending on the gelation properties of proteins (Farjami & Madadlou, 2019).

Heat treatment can denature proteins, and denatured protein molecules can aggregate and form three-dimensional structures through chemical forces (i.e., disulfide bonds, electrostatic interactions, hydrophobic interactions, hydrogen bonds, and ionic bonds) under appropriate conditions (e.g., protein concentration, pH, and ionic strength) (Tolano-Villaverde et al., 2015). In addition, heat treatment with the assistance of microwave pretreatment is regarded as a more effective method to prepare protein-based emulsion gels compared to heat treatment without microwave treatment (Li et al., 2021). Proteins, which undergo heat-

induced gelation (e.g., myofibrillar protein (MP), whey protein isolate (WPI), and soy protein isolate (SPI)), can be used as matrix materials to prepare heat-induced bulk emulsion gels. However, recent studies mainly focused on MP- and WPI-based bulk emulsion gels (Guo et al., 2013; Wang et al., 2018a). Studying heat-induced MP-based bulk emulsion gels is important to develop high quality processed meat products such as sausages and surimi, because interactions between MPs and fat globules or oil droplets play an important role in textual properties and stability of meat products. In addition, heat treatment is the most common method for producing WPI-based bulk emulsion gels in order to investigate interactions between emulsifiers and the WPI-based gel matrices (Chen et al., 2000).

One-step cold-set or cold-set after heat treatment is normally used for preparing gelatin-based emulsion gels. The gelation mechanism of gelatin is that, when the gelatin solution is cooled below 30ºC, a self-assembly process of gelatin occurs and helices are created (Gómez-Guillén et al., 2011). Heat treatment (above 40ºC) is normally used to increase the solubility of gelatin before cold-set treatment. However, for cold-soluble gelatin, the thermal process is not necessary (Pintado et al., 2015). In addition, ethanol has recently been used to denature proteins and produce cold-set whey protein emulsion gels (Xi et al., 2019), which can also be regarded as a cold-set gelation method. The mechanism here is that ethanol can unfold proteins and then the structural cross-linking occurs between protein molecules in the continuous phase and on the surfaces of oil droplets.

The mechanism of acid-induced protein gelation is that acidification, usually carried out by adding glucono-δ-lactone (GDL), decreases the pH and neutralizes the surface charges of protein aggregates, and a gel network then forms by hydrophobic interactions and Van der Waals forces (Ringgenberg, Alexander, & Corredig, 2013). Before acidification, heat treatment is normally used to denature proteins and form protein aggregates. In such cases, two different processes can be used to produce acid-induced protein-based emulsion gels: using pre-heating-induced protein aggregates to form emulsions (Lu et al., 2020) or heating native protein-stabilized emulsion to form protein aggregates (Ye & Taylor, 2009) before

acidification. However, heating native protein-stabilized emulsions may lead to droplet flocculation, which limits the application of emulsion gels for encapsulation of heat-sensitive compounds (Mao, Roos, & Miao, 2014).

Addition of ions (normally Ca^{2+} in the form of $CaCl_2$) can promote soluble protein aggregates to form a gel network by ionic cross-linking (Wang et al., 2019). It has been reported that structures of $CaCl_2$-induced SPI emulsion gels are mainly composed of particulate clusters of protein-coated droplets, which were different from filamentous gel networks formed by microbial transglutaminase (MTGase) and GDL (Tang, Chen, & Foegeding, 2011). In addition, the concentration of Ca^{2+} can affect the structures of protein-based emulsion gels; Sok Line, Remondetto, & Subirade (2005) found that low calcium concentrations (e.g., 11.7 mM Ca^{2+}) induced emulsion gels with a fine-stranded structure, while high calcium concentrations (e.g., 40 mM or 68 mM Ca^{2+}) led to random aggregates. Therefore, $CaCl_2$ at a concentration of 8–20 mM is normally used to produce Ca^{2+}-induced emulsion gels (Liang et al., 2010; Tang, Chen, & Foegeding, 2011; Ye & Taylor, 2009).

MTGase and laccase can be used to promote cross-linking between protein molecules and improve the properties of protein-based emulsion gels (Gaspar & de Goes-Favoni, 2015; Qayum et al., 2021). Compared to other methods, enzyme treatment is a safe method to produce protein-based emulsion gels with high quality under mild process conditions (35–37ºC) and without producing any side-products (Tang et al., 2013a). It was found that the gel strength of MTGase-induced SPI-based emulsion gels was much higher than that of GDL- or $CaCl_2$-induced emulsion gels (Tang, Chen, & Foegeding, 2011). Two points should be highlighted when enzyme treatment is used to prepare protein-based emulsion gels. Firstly, the order of adding enzymes into emulsions may influence the properties of emulsion gels. Tang et al. (2013b) found that adding enzymes prior to emulsification required less enzyme, but induced emulsion gels with higher stiffness compared to adding enzymes after emulsification. Secondly, although the formation of protein aggregates is not necessary for producing enzyme-induced gels, unfolding the compact structures of globular proteins (e.g.,

SPI, WPI, and MP) can provide more target glutamine and lysine residues for the MTGase treatment. For example, pre-incubation of SPI and egg white protein (Alavi et al., 2020; Tang et al., 2013b), pre-oxidation treatment of MP (Wang, Xiong, & Sato, 2017), and breaking down disulfide bonds in bovine serum albumin (Kang et al., 2003) can improve gelation properties of proteins induced by MTGase. However, it has been found that heated SPI-stabilized emulsions after emulsification could not form gels following enzymatic treatment (Tang, Chen, & Foegeding, 2011).

1.2.1.2. Polysaccharide-based bulk emulsion gels

Several methods have been studied for preparing polysaccharide-based bulk emulsion gels, such as heat-set, cold-set after pre-heating, addition of ions, and self-assembly (crystallization), depending on the gelation properties of polysaccharides.

Curdlan is a water-soluble β-(1,3)-glucan extracted from *Alcaligenes* faecalis, and curdlan-based emulsion gels can be obtained after heating emulsions (i.e., heat-induced gelation), while cold-set after pre-heating is normally used to prepare carrageenan-, agar-, and gellan gum-based emulsion gels (Jiang et al., 2019; Zheng et al., 2020). For producing cold-set emulsion gels, polysaccharides should be dissolved at a high temperature (normally above 70°C), and/or emulsions should be prepared at a medium temperature (normally between 45°C and 70°C), after which emulsion gels are formed at a low temperature (normally less than 25°C). The gelation mechanism involves forming double helices and cross-linking helical domains to create a three-dimensional structure during cooling (Nishinari & Takahashi, 2003).

The addition of ions is normally used to produce alginate-based emulsion gels. Sodium alginate has the ability to form ‘egg-box’ shaped gels when the sodium ions are replaced by divalent cations (mostly calcium in the food industry) (Ching, Bansal, & Bhandari, 2017). Two different methods can be used to prepare alginate-based emulsion gels. Pintado et al. (2015) added $CaSO_4$ into an alginate-based emulsion to produce an alginate-based emulsion

gel directly. Sato, Moraes, & Cunha (2014) used a different method to produce emulsion gels, in which CaEDTA was added to the alginate-based emulsion first, after which an acid was then introduced to liberate calcium ions.

Inulin is an oligosaccharide which includes 2 to 60 fructose molecules connected by *β*-(2→1) glycoside bonds (Glibowski & Pikus, 2011). Inulin with a crystal structure can disperse in an aqueous environment and form a suspension, in which the most of crystals do not change their structures, except for some of smallest crystals dissolving in water. Amorphous inulin can change its structure to crystallite in water (Glibowski & Pikus, 2011). Then, small crystallites can aggregate to form larger clusters, which ultimately interact to form a gel (Bot et al., 2004). Paradiso et al. (2015) compared three different homogenization technologies (i.e., mechanical, ultrasonic and cold ultrasonic homogenization) to prepare inulin-based emulsion gels, and found that ultrasonic homogenization is a suitable method to prepare emulsion gels with better textural properties compared to the other two homogenization technologies.

A new strategy has recently been reported to prepare xanthan-based emulsion gels, in which beeswax was introduced into liquid oil to from solidified droplets and thus promote droplet-droplet interactions and strengthen gel structures (Liu et al., 2021). In addition, polysaccharide-based bulk emulsion gels can be obtained through compatibility or electrostatic attraction (i.e., self-assembly) with other polysaccharides or proteins, such as alginate/konjac glucomannan-, xanthan/konjac glucomannan-, and egg yolk protein/alginate-based emulsion gels (Yang et al., 2019; Yang et al., 2020a; Yang et al., 2020b).

1.2.1.3. Self-assembly of low molecular weight compound-based bulk emulsion gels

Many LMW organic compounds, such as glycyrrhizic acid and a combination of *β*-sitosterol and *γ*-oryzanol, can be used as oil-structuring agents, due to their self-assembly, to replace solid fats and provide required sensory and flavor properties in food products (Pernetti et al., 2007; Wan et al., 2017). These organic compounds, when in a water or oil

phase, can form soft solid-like structured gels, which are known as oleogels or organogels (Co & Marangoni, 2012), and they can be also used to produce emulsion gels.

Saponin glycyrrhizic acid (GA) is a monodesmosidic saponin which is comprised of a hydrophobic triterpenoid aglycon moiety (18 *β*-glycyrrhetinic acid) attached to a hydrophilic diglucuronic unit. GA molecules have both gelation and emulsifying properties, owing to their self-assembly ability and amphiphilic structures. GA cannot structure vegetable oil directly because of its low solubility in oil. However, GA molecules can self-assemble into long nanofibrils in water, and nanofibrils not only adsorb at the oil-water interface but also further assemble and entangle to create a supramolecular hydro-gel in water phase. Wan et al. (2017) investigated GA-based O/W emulsion gels and found that, for more polar oils, GA fibrils had a higher affinity to the oil-water interface, leading to the formation of a lot of fine multilayer emulsion droplets with smaller droplet size. Ma, Wan, & Yang (2017) used GA to produce GA-based water-in-oil-in-water ($W_1/O/W_2$) emulsion gels; a W_1/O emulsion was prepared first, before mixing with GA solutions at 80ºC, and GA-based $W_1/O/W_2$ emulsion gels were formed at room temperature by the self-assembly of GA.

The combination of *β*-sitosterol and *γ*-oryzanol can self-assemble in an oil phase to form a helical ribbon, and then these tubules can aggregate and form networks, which are known as oleogels or organogels. Thus, the combination of *β*-sitosterol and *γ*-oryzanol can be used to prepare gelled W/O emulsions by gelling the continuous phase of emulsions. However, the oil phase should be prepared at high temperature (~100ºC) to dissolve *β*-sitosterol and *γ*-oryzanol, and W/O emulsions should also be prepared at 90ºC to prevent the gelation of oil phase during emulsification. It has been reported that, when a mixture of *β*-sitosterol and *γ*-oryzanol was used to prepare W/O emulsion gels, the presence of water weakened the tubules and reduced the firmness of gelled emulsions, due to the hydration of *β*-sitosterol and the transition of crystals from anhydrous and hemihydrate into monohydrate forms (Bot et al., 2011). On the other hand, it was found that reducing the water activity and using oils

with low polarity could promote the formation of tubular micro-structure of oryzanol and sitosterol in emulsions (Sawalha et al., 2012).

1.2.2. Emulsion gel particles

Gel particles/beads can be divided into three categories according to their diameter/length: macro-gel beads (> 1 mm), micro-gel particles (0.2–1000 μm), and nanogel particles (< 0.2 μm) (Ching, Bansal, & Bhandari, 2017). In the food area, previous studies mainly focused on macro-gel beads and micro-gel particles, and alginate was the matrix material most frequently used to produce gel particles (Benavides et al., 2016; Corstens et al., 2017). Ching, Bansal, & Bhandari (2017) reviewed current technologies for producing alginate hydro-gel particles (e.g., simple dripping, jet back up extrusion, spinning disk, atomization, impinging aerosol method, emulsification technique, microfluidics, and templating method), but studies on producing emulsion gel particles have rarely been reported. Methods used to prepare emulsion gel particles include simple dripping, electrostatic extrusion, and the impinging aerosol method.

An electrostatic extrusion technique has been used to prepare alginate-based emulsion beads with diameters in the range from 960 to 1650 μm (Lević et al., 2015), in which a syringe pump and electrostatic immobilization unit (at a voltage of 6.5 kV) were used to extrude an O/W emulsion containing alginate in its continuous phase through a needle (22 gauge) into a collecting solution (0.015 g/ml of $CaCl_2$ solution). The reason for using an electrostatic immobilization unit is that electrostatic forces can disrupt the liquid filament at the tip of the needle and create a charged stream of small droplets. However, bigger beads (diameter from 2100 to 2350 μm) were formed without applying voltage, i.e., extrusion by syringe or simple dripping, which is thus a simple method to produce macro-gel beads, but this method usually leads to large particle sizes. Ching, Bansal, & Bhandari (2016) developed a spray aerosol method to prepare alginate-based emulsion micro-gel particles with the size of 36.2 to 57.8 μm. A fine aerosol mist of alginate-based emulsion and an

aerosol mist of 0.5 M calcium chloride solutions are created at the top and bottom of the chamber, respectively, using an air atomizing nozzle. Two mists combine in the chamber, and emulsion gel particles form in the chamber and are collected at the base of chamber. This is an effective and continuous method to produce emulsion gel particles with small size, but this method needs a special spray aerosol system.

1.2.3. Fluid emulsion gels

Apart from bulk emulsion gels and emulsion gel particles, fluid emulsion gels are the third type of emulsion gels. Fluid emulsion gels are different from bulk gels and gel particles with solid shapes, but fluid emulsion gels usually have a higher viscosity than conventional liquid emulsions. Fluid emulsion gels mainly include two types according to their preparation methods: gel-like emulsions and disrupted emulsion gel systems.

1.2.3.1. Gel-like emulsions

Gel-like emulsions can be obtained by aggregating emulsion droplets (Ruckenstein & Kim, 1988), and previous studies on gel-like emulsions mainly focused on gel-like Pickering emulsions (Chang et al., 2020). Pickering emulsions are a kind of emulsion which is stabilized by amphiphilic solid particles, and can be mainly divided into three categories: polysaccharide particle-, protein particle-, and polysaccharide/protein mixture-stabilized Pickering emulsions (Lv et al., 2020). In addition, some other polymer particles were also reported to be used in preparation of Pickering emulsions, such as dihydromyricetin (Geng et al., 2021). Pickering emulsions are considered as better delivery systems than conventional emulsions, owing to their enhanced storage stability against oxidation and coalescence and lower susceptibility to lipolysis. Pickering emulsions can turn into gel-like emulsions under appropriate conditions (e.g., proper solid particle type, solid particle concentration, oil phase concentration, pH, and ionic strength) (Boostani et al., 2020).

It has been reported that gel-like emulsions could be formed with 6 wt% preheated soy globulins at high glycinin contents (> 75%) with soy oil at a oil volume fraction (φ) of 0.3, and that G' and G'' values of gel-like emulsions increased as the increase of glycinin contents (from 75% to 100%), while neither unheated soy globulins nor preheated soy globulins with low glycinin contents could form gel-like emulsions (Luo, Liu, & Tang, 2013). This was probably because the formation of a gel-like network was largely attributed to hydrophobic interactions between denatured glycinin molecules adsorbed at the interface of oil droplets. However, Xu, Liu, & Tang (2019) found that, with increasing oil fractions (φ = 0.1 to 0.88), a 0.5 wt% soy β-conglycinin-stabilized Pickering emulsion could turn into a gel-like emulsion at an oil fraction of 0.7. It was also found that, with increasing wheat gluten level (emulsifier in oil-in-glycerol emulsions, 0.25–1.0 wt%), gel-like emulsions could be formed at high wheat gluten contents (>= 0.5 wt%) (Liu et al., 2016). Shao & Tang (2016) found that, with increasing oil fraction (0.2 to 0.6), pea protein-based Pickering emulsions changed from liquid to a gel-like state, while Zou et al. (2015) found that zein/tannic acid complex-stabilized Pickering emulsion gels with high oil volume fraction (φ > 0.5) could be successfully produced. Therefore, the oil phase and emulsifier contents should be high enough to assure that solid particles adsorbed at the surface of neighboring oil droplets can connect and/or react with each other (Su et al., 2020; Wouters & Delcour, 2019).

1.2.3.2. Disrupted gel systems

Fluid emulsion gels can also be prepared by breaking down bulk emulsion gels (Leon et al., 2018). Soukoulis et al. (2016) investigated so-called sheared oil-in-gel (o/g) emulsions prepared by stirring an alginate-based emulsion gel system at 1000 rpm for 6 h during the gelation process. Torres et al. (2017) developed a method to produce starch-based gel emulsions by homogenizing the bulk emulsion gels. This is a simple method to produce fluid emulsion gels with small dispersed gel particles (5–50 μm in diameter), but the gel matrix-

covered structure may be destroyed, leading to separation of the gel matrix and oil droplets during homogenization, which may influence the stability of oil droplets and/or encapsulated nutrients during storage.

1.3. Structure-property relationships of different emulsion gels

1.3.1. The structure-property relationships of bulk emulsion gels

Some properties of bulk emulsion gels are emphasized in the food industry, such as mechanical properties (e.g., rheological, and textural perception), and release properties (i.e., targeted release of encapsulated droplets and food nutrients during digestion). Many factors (e.g., structures of the gel matrices, structures of emulsion droplets, and interactions between the gel matrices and droplets) can influence the structures of bulk emulsion gels and then their mechanical and release properties.

Food emulsions normally include single emulsions (O/W and W/O emulsions) and multiple emulsions ($W_1/O/W_2$ and $O_1/W/O_2$ emulsions). After turning emulsions into bulk emulsion gels, the structures of emulsion gels therefore also include single structures (i.e., O/W and W/O) and multiple structures (i.e., $W_1/O/W_2$ and $O_1/W/O_2$). The matrix materials of O/W and $W_1/O/W_2$ emulsion gels are protein-, polysaccharide-, or organic compound-based hydro-gels, while the matrix materials of W/O and $O_1/W/O_2$ emulsion gels are organic compound-based oleogels (also known as organogels or structured oil). Moreover, properties of O/W and $W_1/O/W_2$ emulsion gels and W/O and $O_1/W/O_2$ emulsion gels differ, because the properties of emulsion gels mainly depend on the properties of matrix materials (i.e., protein-, polysaccharide-, or organic compound-based gels), although the properties of emulsion droplets and the interactions between the gel matrix and droplets also influence the properties of emulsion gels. However, O/W emulsion gels have been studied more widely than W/O, $W_1/O/W_2$ and $O_1/W/O_2$ emulsion gels, so the following discussions in this review will focus on O/W emulsion gels unless other structures are emphasized.

1.3.1.1. The structure-mechanical property relationships of bulk emulsion gels

Mechanical properties of bulk emulsion gels are closely associated with other properties (e.g., storage stability, oral perception, and controlled release) and their applications. The most common mechanical properties of bulk emulsion gels are dynamic modulus (i.e., storage and loss modulus), Young's modulus, fracture strength (i.e., strain and stress), yield strength, and hardness. There are many ways or tools to measure mechanical properties of bulk emulsion gels, such as rheometry, dynamic mechanical analysis (DMA), and textural analysis (Anseth, Bowman, & Brannon-Peppas, 1996).

1.3.1.1.1. Matrix structures

• Protein-based matrices

For protein-based bulk emulsion gels, using different proteins and preparation methods can lead to different protein matrix structures and mechanical properties, owing to different gelation mechanisms and resultant different molecular forces between protein molecules in the gel matrix. Globular proteins (e.g., SPI, WPI, and MP) and non-globular proteins (e.g., gelatin, casein, and sodium caseinate) have been widely used as matrix materials in producing bulk emulsion gels.

The heat-set gelation method has been most used to prepare globular protein-based emulsion gels, but globular protein-based emulsion gels can be also prepared through acidification treatment, addition of ions, enzyme treatment, and malondialdehyde (MDA) modification. For heat-induced emulsion gels, non-covalent cross-linking (i.e., electrostatic interactions, hydrophobic interactions, and hydrogen bonds) and inter-molecular disulfide bonds are the main forces between globular protein molecules (Wu, Xiong, & Chen, 2011). The main linking forces in GDL-induced emulsion gels are hydrophobic interactions and Van der Waals forces, while salt-bridges are the main linking forces in salt-induced emulsion gels, and MTGase-induced emulsion gels involve more covalent cross-links (i.e., ε-(γ-

glutamyl)-lysine (G-L) cross-links). Therefore, different preparation methods may lead to different mechanical properties of globular protein-based emulsion gels (Liang et al., 2020; Wang, Xiong, & Sato, 2017; Ye & Taylor, 2009); for example, it was found that $CaSO_4$-induced SPI-based emulsion gels were stiffer, with higher rigidity, than MTGase-induced gels which performed better elasticity (Wang et al., 2018b).

Gelatin can form gels under one-step cold treatment or cold treatment after pre-heating as descried in section 1.2.1.1.2. Cold-set gelatin gels, a kind of elastic polymer gel, are formed with flexible and random-coil protein chains (Sala et al., 2009). Other non-globular protein-based emulsion gels are normally prepared with enzyme treatment and acidification treatment. For example, although the main linking forces in both of acid-induced casein gels and WPC gels are non-covalent cross-links, the firmness of acid-induced sodium caseinate gels was lower than that of acid-induced WPC gels, probably due to their differences in protein structures and sensitivity to acidification treatment (Kiokias & Bot, 2005).

Overall, contributions to the connectivity of a three-dimensional protein network arise from four different kinds of molecular forces: covalent bonds, electrostatic interactions, hydrogen bonding and hydrophobic interactions. The presence of covalent bonds leads to permanent ‘chemical’ cross-linking within the network, whereas the other three types of weaker ‘physical’ forces contribute to a complex set of more temperature-dependent interactions (Chen & Dickinson, 1999b). In addition, process parameters (e.g., temperature, protein content, ionic strength, pH, the presence of other components, ultrasound pretreatment, and high-pressure homogenization) also can influence the structures and mechanical properties of protein-based bulk emulsion gels (Bi et al., 2020; Chen & Dickinson, 2000; Cheng et al., 2019).

Firstly, temperature can influence the degree of denaturation of proteins, and thus affect the stability of protein-stabilized emulsions and mechanical properties of emulsion gels. Generally, a high degree of denaturation of proteins results in low stability of protein-

stabilized emulsions but better mechanical properties of emulsion gels (Kiokias & Bot, 2005; Ye & Taylor, 2009). Chen & Dickinson (2000) also found that gelation temperature could influence the rate of gelation and the dynamic modulus of acid-induced sodium caseinate-based emulsion gels by changing the strength of physical bonding rather than the network structures.

Secondly, the influence of protein content on the mechanical properties of emulsion gels depends on the state of emulsion droplets. The mechanical properties of droplet-filled gels and inactive droplet-aggregated gels mainly depend on the gel strength of gel matrix structures, while interactions between the gel matrix (i.e., protein and polysaccharide) and lipid droplets contribute more to the active droplet-aggregated gels (Pintado et al., 2015). Therefore, increasing protein content can increase the gel strength of both kinds of emulsion gels but for different reasons (i.e., increased gel strength of protein matrix for droplet-filled gels and inactive droplet-aggregated gels, but strengthened interactions between the gel matrix and droplets and increased gel strength of protein matrix for active droplet-aggregated gels).

Thirdly, ionic strength and pH can influence inter-molecular repulsion and gel structures in emulsion gels. For example, at low ionic strength (< 50 mM NaCl) and pH values (below 4 or above 6) far away from p*I* of whey proteins, a fine-stranded network consisting of whey protein strands with a length of ~50 nm and a diameter of ~10 nm is formed; at high ionic strength (> 150 mM NaCl) and pH values near the p*I*, the strands with weak inter-molecular repulsion can accumulate and form a particulate network structure (Chen et al., 2000; Guo, Bellissimo, & Rousseau, 2017; Langton & Hermansson, 1992). However, both fine-stranded and particulate gels exhibit high gel strength (Guo, Bellissimo, & Rousseau, 2017; Tang, Chen, & Foegeding, 2011). It was found that fine-stranded whey protein gels prepared at low ionic strength (10 or 25 mM NaCl) were rubbery and soft, but that particulate whey protein gels prepared at high ionic strength (100 or 200 mM NaCl) were hard and brittle (Guo et al., 2013).

Fourthly, the presence of other components (e.g., sucrose, glucose, hydroxytyrosol, rosmarinic acid, genipin, sodium pyrophosphate, insoluble dietary fiber, and EGCG) can also influence the structures and mechanical properties of emulsion gels (Chen et al., 2019; Feng et al., 2017; Freire et al., 2017a; Montes de Oca-Ávalos et al., 2016; Wang, Jiang, & Xiong, 2019; Zhuang et al., 2019). Generally, if components can strengthen protein-protein interactions and/or reduce droplet size, they can increase gel strength of emulsion gels. However, if these components can interact with protein molecules and disturb the interactions between protein molecules, they can weaken the gel strength of emulsion gels, and these effects are normally dose-dependent. Overall, preparation methods can affect linking forces between protein molecules, and protein type and processing parameters can influence the network structures of the gel matrix, both of which can affect the mechanical properties of emulsion gels.

• Polysaccharide-based matrices

In terms of polysaccharide-based emulsion gels, polysaccharide type, preparation methods, and processing parameters can influence the structures of the polysaccharide-based gel matrix. Cold-set gellan gun-, agar-, and *κ*-carrageenan-based emulsion gels are a kind of polymer gels with strand-based structures (Kim et al., 1999; Wang et al., 2013). They normally show a predominantly elastic behavior, which resemble gelatin-based emulsion gels but differ from WPI-based emulsion gels with particulate structures (Sala et al., 2009). The network structures of alginate gels are in the shape of 'egg-box', in which sodium ions are replaced by divalent cations, and each cation can bind with four *α*-L-guluronic acid (G) residues to form a three-dimensional network structure (Ching, Bansal, & Bhandari, 2017), which can be affected by freeze-thawing treatment (Li et al., 2020). Inulin gels are formed by connection of micro-crystals, and their rheological properties resemble that of fat crystal-based networks in oil (Nourbehesht, Shekarchizadeh, & Soltanizadeh, 2018). However, there are no studies on comparing mechanical properties of emulsion gels formed by different kinds of polysaccharides.

In addition, the influence of polysaccharide content on the mechanical properties of emulsion gels depends on emulsifier type and gel structures. Most naturally occurring polysaccharides, except gum Arabic and some kinds of pectin, have weak emulsifying abilities, compared to proteins and synthetic emulsifiers (Charoen et al., 2011). Hence, the interactions between the gel matrix and emulsion droplets in polysaccharide-based emulsion gels with/without synthetic emulsifiers are normally weak, and increasing polysaccharide content can increase their gel strength, mainly due to the decreased void spaces and increased gel strength of the gel matrix (Kim et al., 1999). However, when proteins are used as emulsifiers, increasing polysaccharide content can increase the gel strength of emulsion, mainly due to increased interactions between polysaccharide molecules and droplets and/or the gel strength of polysaccharide gels. Although studies on the effects of ionic strength and pH on the mechanical properties of polysaccharide-based emulsion gels have rarely been reported, Ozturk et al. (2015) found that ionic strength and pH did not have significant influences on the stability of a gum Arabic-stabilized emulsion, which was different from a WPI-stabilized emulsion because of their different emulsification mechanisms (i.e., electrostatic repulsion for WPI and steric repulsion for gum Arabic). Therefore, it is proposed that the influence of ionic strength and pH on the structure and mechanical properties of polysaccharide-based emulsion gels differs from that for protein-based emulsion gels.

- LMW compound-based matrices

For LMW organic compound-based emulsion gels, saponin glycyrrhizic acid (GA) and the combination of β-sitosterol and γ-oryzanol have been investigated to prepare emulsion gels by self-assembly. GA can dissolve in water, and GA molecules can self-assemble to form long nanofibrils and gels in water phase, and so can be used to prepare emulsion gels with O/W or $W_1/O/W_2$ structures. The combination of β-sitosterol and γ-oryzanol can self-assemble in an oil phase to form a helical ribbon, then these tubules can aggregate and form a network, and so can be used to prepare gelled W/O emulsions. Processing parameters (e.g.,

organic compound content and solvent type) also can influence the structure and mechanical properties of organic compound-based emulsion gels. Ma, Wan, & Yang (2017) found that an emulsion stabilized by GA at a low concentration (0.5 wt%) could not form a gel, but self-standing emulsion gels could be formed and the viscoelastic modulus also significantly increased with increasing GA concentration (1–4 wt%). It was also found that no tubules were formed but only sitosterol and oryzanol crystals were present in emulsion gels at 16% total sterol concentration, while there were tubules next to the crystals at 32% total sterol concentration (Bot et al., 2011).

In addition, the polarity of solvents (i.e., oil in W/O emulsions) can influence the water activity of W/O emulsions and structures of the oil phase. It has been reported that more water molecules bind to the *β*-sitosterol molecules and formed monohydrate crystals in higher polarity oils (e.g., eugenol and castor oil), which hindered the formation of tubules and resulted in weaker emulsion gels compared to less polar oils (e.g., decane and limonene) (Sawalha et al., 2012). However, studies on comparing structures and mechanical properties of emulsion gels prepared with different kinds of organic compounds have rarely been reported. Over all, many factors (e.g., gel matrix type, preparation method, and process parameters) can affect the gel structures of bulk emulsion gels and thus their mechanical properties.

1.3.1.1.2. Properties of emulsion droplets

The properties of emulsion droplets (e.g., droplet size and surface structures) can influence the mechanical properties of bulk emulsion gels as well. Properties of emulsion droplets are normally influenced by oil phase (e.g., oil type, and oil content), and emulsifier type (e.g., LMW emulsifiers or proteins). In the food industry, emulsifiers mainly include two categories: low molecular synthetics (e.g., Span 80, Tween 80, and monoglycerides) and natural molecules (e.g., proteins, egg lecithin, and soy lecithin) (Chen et al., 2020). Emulsifiers can not only decrease the interfacial tension and thereby increase the stability of

emulsions but also affect the interactions between droplets and the gel matrix, leading to active or inactive fillers (Van Vliet, 1988). Therefore, the effect of emulsion droplets on the mechanical properties of emulsion gels depends on not only emulsion droplets (i.e., oil type, oil content, and droplet size) but also the interactions between droplets and the gel matrix (Chen et al., 2021; Farjami & Madadlou, 2019).

The effect of active fillers on the rheological properties of emulsion gels mainly depends on the stiffness of the oil droplets and the droplet volume fraction (Sala, van Vliet, Cohen Stuart, Aken, & van de Velde, 2009). The Kerner model can explain the effect of active fillers on the mechanical properties of emulsion droplet-filled gels (Kerner, 1956):

$$\frac{G^{'}_{gel}}{G^{'}_{matrix}} = \frac{15(1-v_m)(M-1)\phi_f}{(8-10v_m)M+7-5v_m-(8-10v_m)(M-1)\phi_f} + 1 \quad (1\text{-}1)$$

where $M = \frac{G^{'}_{filler}}{G^{'}_{matrix}}$, and G'_{gel}, G'_{filler}, and G'_{matrix} are the shear modulus of the overall gel, the filler droplets and the gel matrix, respectively, ϕ_{f} is the actual droplet volume fraction, and v_m is the Poisson's ratio of the gel matrix. In addition, the Kerner model modified by Lewis and Nielsen can be used to explain the effect of active fillers on the mechanical properties of emulsion droplet-aggregated gels (Lewis & Nielsen, 1970):

$$\frac{G^{'}_{gel}}{G^{'}_{matrix}} = \frac{15(1-v_m)(M-1)\psi\phi_f}{(8-10v_m)M+7-5v_m-(8-10v_m)(M-1)\psi\phi_f} + 1 \quad (1\text{-}2)$$

where $\psi\phi_{\text{f}}$ is the effective volume fraction of fillers, which takes into account the crowding effect of fillers and can be expressed as follows (Lewis & Nielsen, 1970):

$$\psi\phi_f = \left[1+\left(\frac{1-\phi_{max}}{\phi^2_{max}}\right)\phi_f\right]\phi_f \quad (1\text{-}3)$$

where ϕ_{max} is the maximum volume fraction of the fillers. According to Eq. (1-2), increasing the shear modulus and the effective volume fraction ($\psi\phi_{\text{f}}$) or actual volume fraction (ϕ_{f}) of fillers can increase the mechanical properties of emulsion gels, which has been supported by many studies (Gwartney, Larick, & Foegeding, 2004; Li et al., 2012; Oliver, Scholten, & van

Aken, 2015; Oliver, Wieck, & Scholten, 2016; Tang et al., 2013b). However, the Kerner model and the modified Kerner model are used under the assumption that M or G'_{matrix} do not change with changes in other factors (e.g., ϕ_f and G'_{filler}) (Chen & Dickinson, 1998a; Oliver et al., 2015), especially at oil volume fractions (φ) below 0.2 and protein (i.e., gel matrix) contents above 6 wt% (Guo, Bellissimo, & Rousseau, 2017). However, the shear modulus of filler droplets ($G'_{filler} = 4\gamma$ / d, where γ is surface tension and d is the average diameter of the oil droplets) is influenced by oil type, oil content, droplet size, emulsifier type, emulsifier content, and process parameters (Farjami & Madadlou, 2019; Sala et al., 2009; Van Vliet, 1988). In addition, the shear modulus of the gel matrix (G'_{matrix}) is influenced by droplet size, oil content, gel matrix type, preparation method, and process parameters (Sato, Moraes, & Cunha, 2014). Therefore, when taking those factors (e.g., droplet size, process parameters, and high oil content), which can affect the mechanical properties of both filler droplets and the gel matrix, into account, the Kerner model and the modified Kerner model cannot be applied. For instance, it has been reported that increasing the size of olive oil droplets in a gelatin-based emulsion gel led to a weaker gel strength, probably due to the increase in interfacial area, a higher amount of gelatin adsorbed to the interface, and a lower quantity of protein available in the continuous phase (Sato, Moraes, & Cunha, 2014); however, it was found that increasing the size distribution of dispersed vegetable fat in a WPI-based emulsion gel led to an increase in firmness, probably because of a larger number of contacts between droplets (Kiokias & Bot, 2006). Oliver, Wieck, & Scholten (2016) found that increasing the casein content (from 4% to 9%) could decrease the relative Young's modulus of emulsion gels at high oil volume fractions ($\phi_f > 0.15$), probably owing to the higher inhomogeneity of casein-based gel matrix and increased effective volume fraction of droplets at lower casein concentration; this indicated that the effective volume fraction ($\psi\phi_f$) plays a more important role than G'_{matrix} in affecting the mechanical properties of emulsion gels with high matrix inhomogeneity and at high oil volume fractions.

The effect of inactive fillers on the rheological properties of emulsion gels depends on the properties and concentrations of LMW emulsifiers, droplet size, and oil content, although there have been few studies on modelling the effect of inactive fillers on the rheological properties of emulsion gels. Chen & Dickinson (1999a) investigated the effect of LMW emulsifiers on the viscoelastic properties of heat-set whey protein-based emulsion gels, and found that the elastic modulus of heat-set whey protein-based emulsion gels decreased after adding a low level of diglycerol monolaurate (DGML, the surfactant/protein molar ratio (R) = 4) and diglycerol monooleate (DGMO, R = 4–32), while high levels of emulsifiers (R = 32 for DGML, and R = 64 for DGMO) could increase the storage and loss modulus of emulsion gels, probably due to depletion flocculation of the emulsion prior to heat-treatment. However, it has been reported that Tween 20 (R = 0.25–8) always decreased the mechanical properties of emulsion gels, and a high addition level (R = 8) could even break down the network structure of proteins and lead to a liquid-like emulsion (Chen & Dickinson, 1998b). It has been found that increasing oil content decreased fracture stress and stress intensity factor of agar gels and *κ*-carrageenan-locust bean gum gels (Koç et al., 2019). It has also been found that increasing solid lipid content could increase the gel strength of WPI/xanthan gum-based emulsion gels at an emulsifier content of 4 g/100 g, but decreased the gel strength at an emulsifier content of 2 g/100 g (Geremias-Andrade et al., 2017).

1.3.1.2. The structure-release property relationships of bulk emulsion gels

Bulk emulsion gels, especially O/W emulsion gels, are often used for the delivery and release of oil-soluble bioactive compounds and nutrients, such as *α*-tocopherol (Liang et al., 2010) and *β*-carotene (Soukoulis et al., 2017). Compared to emulsions, emulsion gels can provide better protection for encapsulated compounds and show slower release behavior during digestion (Cofrades et al., 2017). Many studies have focused on the matrix erosion, lipid digestion and controlled release of encapsulated compounds during digestion of emulsion gels. The digestion behaviors of protein- and polysaccharide-based emulsion gels

differ in the gastrointestinal tract because of different digestion processes of proteins and polysaccharides. For protein-based emulsion gels, Liang et al. (2010) found that gel loss (i.e., matrix erosion owing to protein degradation) and release of α-tocopherol occurred in both simulated gastric fluid (SGF) and simulated intestinal fluid (SIF), respectively, which indicated that release of α-tocopherol was controlled mainly by matrix erosion because of protein degradation. However, under simulated gastrointestinal (GI) conditions (0.5 h SGF followed by 6 h SIF), gel loss and release of α-tocopherol only occurred in the SGF step, probably due to the formation of a viscous layer on the surfaces of gel residuals. Moreover, gel rigidity of protein-based emulsions is an important factor affecting the lipid digestion in GI digestion. It has been reported that gastric digesta of a soft gel (prepared with 10 or 20 mM NaCl) mainly consisted of individual oil droplets and small gel particles (~10 mm), while gastric digesta of a hard gel (prepared with 100 or 200 mM NaCl) mainly consisted of small gel particles (~10 mm) after 240 min gastric digestion, and the remaining network structure of gel particles hindered further breakdown during intestinal digestion (Guo et al., 2016). It was also found that digestion of emulsion gels in the intestinal step was delayed by denser, more spatially heterogeneous protein matrices (Guo, Bellissimo, & Rousseau, 2017). In terms of polysaccharide-based emulsion gels, although there are fewer reports about their digestion, it was found that oil droplets could be released from agar-based emulsion gels during GI digestion in both SGF and SIF steps (2.0 h SGF followed by 4–14 h of SIF), while emulsifier type (glycerol monolaurate with different degrees of polymerization) affected the size distribution of released oil droplets (Wang et al., 2013).

Bulk emulsion gels are also used for the delivery and release of volatile flavor compounds, such as ethyl butyrate, ethyl hexanoate, ethyl octanoate, propanol, diacetyl, pentanone, hexanal, and heptanone (Hou et al., 2016; Mao, Roos, & Miao, 2014). The release of volatile compounds in the oral cavity is normally measured by a simulated nose breath device (Hou et al., 2016) or gas chromatography (GC) headspace analysis (Mao, Roos, & Miao, 2014). The release rate of volatile compounds depends on the gel matrix

structure, oil content, the nature of volatile compounds, and the interactions between flavor compounds and food ingredients (particularly oils in O/W emulsion gels) (Boland, Delahunty, & van Ruth, 2006; Guichard, 2002). It has been reported that the release rate of ethyl butyrate was significantly lower in a SPI/sugar beet pectin (SBP) complex-based emulsion gel with a compact network than SPI- or SBP-based emulsion gels, but the release rate of aroma compounds with higher hydrophobicity was not significantly influenced by the structures of emulsion gels, probably because of their high affinity for the lipid phase rather than interacting with proteins and/or polysaccharides (Hou et al., 2016). Mao, Roos, & Miao (2014) also found that emulsion gels with higher storage modulus at a high oil content (20%) had lower release rates and partition coefficients of the volatiles, and that increasing oil contents (from 5% to 20%) significantly decreased the release rate of heptanone, probably owing to its highly lipophilic characterization.

1.3.2. The structure-property relationships of emulsion gel particles

Although emulsion gel particles and bulk emulsion gels have similar structures (i.e., active fillers, inactive fillers, emulsion droplet-filled gels, and emulsion droplet-aggregated gels) and structure-property relationships, their physical properties and length scales differ (Ching, Bansal, & Bhandari, 2016).

Firstly, the rheological behavior of gel particles differs to that of bulk gels, because the micro-gel particle system is a suspension (usually gel particles in water). The rheological properties of micro-gel particle suspensions are influenced by three parameters: volume fraction (ϕ), particle modulus (modulus of particles that make up the suspension) and interaction potential (Ching, Bansal, & Bhandari, 2016). The volume fraction (ϕ) can be determined using the equation below (Ching, Bansal, & Bhandari, 2016):

$$\phi = \frac{\frac{m}{\rho}}{\frac{m}{\rho}+v} \quad (1\text{-}4)$$

where ϕ = final micro-gel suspension volume fraction, m = mass of micro-gel concentrate, ρ = density of micro-gel concentrate measured with a 50 mL calibrated pycnometer, and v = volume of water added to micro-gel concentrate. Eq. (1-4) was modified by the equations developed by Suzawa & Kaneda (2010), who calculated the volume fraction by the weight and density of emulsions but did not consider the weight loss (normally water loss) of gel particles during gelation. At low volume fraction, the flow behavior is determined by the continuous phase; at higher volume fraction, softer micro-gels will exhibit a lower storage modulus compared to hard micro-gels (Adams, Frith, & Stokes, 2004). Ching, Bansal, & Bhandari (2016) found that, at the same volume fraction, suspensions with more deformable alginate-based micro-gels exhibited a lower bulk modulus. However, it is technically difficult to investigate the rheological properties of macro-gel particles, although their mechanical properties could be investigated by a texture analyzer. It has been reported that, with increasing oil contents in alginate-based macro-gels, the elastic modulus of particles decreased, which indicates that oil droplets in alginate-based emulsion gel particles without emulsifiers were inactive fillers (Ching, Bansal, & Bhandari, 2016).

Secondly, syneresis and swelling properties are important properties of gel particles (Ching, Bansal, & Bhandari, 2017). It was found that alginate-based emulsion gel particles shrank less if they had higher oil content, and that the swelling was more pronounced for smaller particles, probably owing to the larger contact surface, but was less pronounced at increased oil contents, probably because of droplets acting as physical barriers for water transport (Lević et al., 2015).

Thirdly, encapsulation efficiency (EE), loading capacity (LC) and encapsulation yield, which are important parameters in encapsulation processes of emulsion gel particles, are affected by properties and contents of matrix material, emulsifier, and oil. It has been reported that increasing alginate contents in the water phase could increase the oil EE in lupin protein isolate (LPI)-stabilized emulsion gel particles, probably due to the formation of a stronger gel matrix and better cross-linking on the external surfaces of particles (Piornos et

al., 2017). However, when the protein content was higher than the saturation concentration, or the oil content was very low, in which excessive free protein molecules existed in the water phase, the aggregation of non-adsorbed protein molecules could lead to lower emulsion stability and lower EE (Guzey & McClements, 2006). In addition, Ruffin, Schmit, Lafitte, Dollat, & Chambin (2014) found that, compared to native WPI, using pre-heated WPI at 80ºC for 30 min as emulsifier in pectin-based emulsion gel particles slightly improved the yield and stability of encapsulated vitamin A, because of the increased viscosity of denatured WPI dispersions and the decreased particle size of emulsions.

1.3.3. The structure-property relationships of fluid emulsion gels

1.3.3.1. Gel-like emulsions

The oil content, particle content, and surface charge of particles can affect the rheological properties of gel-like Pickering emulsions and release behavior of encapsulated compounds from such emulsions (Jiang et al., 2021; Shao & Tang, 2016; Xu, Liu, & Tang, 2019). For the effect of oil content, Dai et al. (2018) found that zein/gum arabic complex-stabilized Pickering emulsion gels solidified at high oil volume fractions in emulsions (φ >= 0.5), and increasing oil volume fractions (φ = 0.5–0.7) increased the G' and G'' values of gel-like emulsions, probably due to increased interactions between emulsion droplets (Xiao et al., 2016). It was also reported that a gel-like emulsion at φ = 0.6 exhibited much lower release rate of β-carotene but higher stability during digestion than a Pickering emulsion at φ = 0.3 (Shao & Tang, 2016). In terms of the effect of particle content, Xu, Liu, & Tang (2019) found that increasing soy β-conglycinin contents from 0.2 to 1.0 wt% led to a progressive decrease in droplet size, but a progressive increase in stiffness of the gel-like emulsions at φ = 0.8. Liu et al. (2019) also found that increasing pre-heated WPI contents from 2.5 to 10 wt% led to a progressive increase in gel strength, hardness, WHC, and stability of the gel-like emulsions at 75 vol% oil; they also found that increasing protein contents could increase the bio-accessibility of β-carotene, because of reduced aggregation of the oil droplets and

retarded degradation of β-carotene during digestion, owing to a dense WPI-based gel structure around droplets. In addition, the surface charge of (nano)particles can affect their emulsification and interfacial behavior (Larson-Smith, Jackson, & Pozzo, 2012). It has been reported that electrostatic screening by adding NaCl could improve the performance of soy glycinin nanoparticles in forming gel-like emulsions and increase stiffness of the resultant gel-like emulsions, due to enhanced diffusion and adsorption of solid particles at the interface (Liu & Tang, 2016).

1.3.3.2. Disrupted gel systems

Although there are few studies on the structure-property relationships of disrupted gel systems, Torres et al. (2017) found that increasing starch contents (from 15 to 20 wt%) and oil fractions (from 0 to 20 wt%) could improve the elastic modulus of starch-based disrupted gels stabilized by octenyl succinin anhydride (OSA) modified starch, which fitted the Kerner model. It has been reported that, compared to alginate-based emulsions and bulk emulsion gels, sheared oil-in-gel (o/g) emulsions exhibited higher bio-accessibility of encapsulated β-carotene after *in-vitro* digestion, due to the lower unbound calcium content and higher colloidal stability throughout gastrointestinal passage, whereas encapsulated β-carotene in the bulk emulsion gels exhibited highest chemical stability (Soukoulis et al., 2016).

1.4. Applications of emulsion gels in the food industry

1.4.1. Use of emulsion gels as fat replacers in meat products

Emulsion gels formed by myofibrillar proteins (MPs), water and lipid not only contribute to the sensory properties (appearance and flavor) but also relate to the textural properties (water- and oil-holding, and cooking losses) of meat products (Wang et al., 2018; Zhao et al., 2017). Additives, such as extracts from herbs and spices, polyphenols, and NaCl, can influence structures of emulsion gels and the properties of meat products (Wang et al., 2018a; Zhao et al., 2017). Wang et al. (2018a) found that a low level of rosmarinic acid (RA) (12

μM/g protein) could protect thiol and ε-NH_3 groups in MP-based emulsion gels from oxidation, and thus improve the gel strength and water- and oil-holding abilities of emulsion gels; however, a high level of RA (300 μM/g protein) could induce interactions between RA and MPs, which led to aggregation of MPs and a poor emulsion gel network, while a high level of NaCl (0.6 M) could promote these interactions.

However, while health concerns around some meat products containing high fat content (over 27%) have increased in recent years, reducing fat content usually negatively influences consumer acceptance and textural properties of final products (Oliver, Scholten, & van Aken, 2015). In order to avoid undesirable textural changes and improve the nutritional value of meat products (e.g., sausages and patties), promising methods have been studied, such as replacing fat with unsaturated oil (Oliver, Scholten, & van Aken, 2015) or structured oil (e.g., olive, linseed, fish, perilla, and sunflower seed oil encapsulated in emulsion gels formed with SPI, WPI, sodium caseinate, carrageenan, gelatin, alginate, chia flour, oat bran, or inulin) (Alejandre et al., 2016; de Souza Paglarini et al., 2018; de Souza Paglarinia, Martinib, & Pollonio, 2019; Freire et al., 2018; Freire et al., 2017b; Glisic et al., 2019; Pintado et al., 2018; Pintado et al., 2021; Poyato et al., 2015; Serdaroglu, Nacak, & Karabiyikoglu, 2017). Reformulated lipid systems may show similar rheological and technological properties to saturated fats, so emulsion gels offer great potential to replace fats in meat products (de Souza Paglarini et al., 2019).

However, these methods may lead to undesirable sensory quality changes (e.g., color parameters and sensory acceptability) (dos Santos et al., 2020; Paglarini et al., 2021; Serdaroğlu & Öztürk, 2017). Oliver, Scholten, & van Aken (2015) found that physical properties of fat or oil and structural properties of the gel matrix could influence the rheological properties of fat-filled emulsion gels or oil-filled emulsion gels. Hence, the properties of fat in meat products should be considered, and the gelling agent and oil should be chosen carefully when emulsion gels are used as fat replacers (Freire et al., 2017b). It has been reported that combining emulsion gels and animal fat could be a good method to

produce healthier meat products with acceptable sensory properties (de Souza Paglarini et al., 2019). In addition, emulsion gels help to control sodium availability and perception by changing sodium mobility and binding behavior, and can thus allow reduction of the salt content in meat products (Okada & Lee, 2017). However, most studies have focused on bulk emulsion gels and their uses in solid foods, and thus more studies on emulsion gel particles and their uses in liquid foods are needed.

1.4.2. Emulsion gels used as delivery systems to encapsulate and release food nutrients

Absorption of encapsulated lipophilic food nutrients (e.g., *β*-carotene, curcumin, *n*-3 fatty acid, vitamin A, and *α*-tocopherol) in emulsion gels include several steps: release from the gel matrix as the result of mechanical, chemical and enzymatic processes throughout the oral processing and gastrointestinal passage, incorporation in the co-digested lipid droplets, interaction with endogenous lipid surface active compounds (mainly bile salts and phospholipids) promoting the formation of mixed micelles, and eventual transportation of the mixed micelles to the small intestinal epithelium (Soukoulis et al., 2016; Yonekura & Nagao, 2007). Polysaccharides (e.g., alginate, *κ*-carrageenan, and starch) and proteins (e.g., gelatin and WPI) are normally used as gelation materials in producing emulsion gels encapsulating lipophilic food nutrients, but their digestion behaviors differ. Protein-based emulsion gels are mainly disrupted in gastric digestion as the result of enzymatic hydrolysis by pepsin, and the remaining protein-based network structures can hinder further breakdown during intestinal digestion (Guo et al., 2016; Liang et al., 2010). On the other hand, polysaccharide-based (especially alginate-based) emulsion gels are less sensitive to gastric fluid than protein-based emulsion gels, and may protect the encapsulated nutriments from harsh gastric environment, and the remaining gel structures can be further disrupted during intestinal digestion (Wang et al., 2013; Xu et al., 2019).

However, emulsion gels normally give low effective bioavailability of encapsulated lipophilic compounds, due to insufficient digestion of the gel matrix and resulting unreleased

and undigested lipid phase (Liang et al., 2010; Zhang et al., 2016). Therefore, it is important to choose appropriate materials for different nutrients, which can protect encapsulated nutrients and control their release, and also do not inhibit release in the targeted gastrointestinal tract (Zhang et al., 2016). Although emulsion gels may not improve the final bio-accessibility of encapsulated food nutrients, they can improve the stability of emulsions and encapsulated nutrients during storage, exhibit slow release effects in the gastrointestinal passage compared to emulsions, and reduce the sensory perception of capsaicinoids encapsulated in emulsion gels during oral digestion (Brito-Oliveira et al., 2017; Luo et al., 2019, 2020; Ma, Wan, & Yang, 2017; Soukoulis et al., 2016; Zhang et al., 2016).

1.5. Conclusions

Various preparation methods for emulsion gels are available for different matrix materials (e.g., heat treatment, enzyme treatment, acidification, and addition of ions for protein-based emulsion gels, cold-set and addition of ions for polysaccharide-based emulsion gels, and self-assembly for LMW compound-based emulsion gels), purposes (e.g., cold-set for protecting encapsulated nutrients and better mechanical properties), and emulsion gel types (e.g., internal gelation for bulk emulsion gels, external gelation for emulsion gel particles, self-assembly for gel-like Pickering emulsions, and mechanical stir for disrupted emulsion gels). Due to differences in the morphological properties among different emulsion gels, different physical properties are emphasized, such as the importance of mechanical and release properties for bulk emulsion gels, syneresis and swelling properties for emulsion gel particles, rheological properties for micro-gel particle suspensions, and flow behavior and release property for fluid emulsion gels. In terms of bulk emulsion gels, many factors (e.g., structures of gel matrix and emulsion droplets and interactions between them) can influence their structures and thus mechanical and release properties. Structures of the gel matrix in bulk emulsion gels are affected by matrix material, preparation method, and process parameters, while structures of emulsion droplets are

affected by oil type, oil content, droplet size, and emulsifier type. In terms of emulsion gel particles, oil content and particle size can influence their syneresis and swelling properties. The rheological properties of micro-gel particle suspensions are influenced by volume fraction, particle modulus, and interaction potential. In terms of gel-like Pickering emulsions, their rheological and release properties also are influenced by many factors (e.g., oil content, particle content, and surface charge of particles). Finally, two main applications of emulsion gels in the food industry are fat replacers in meat products and delivery systems for food nutrients.

References

Adams, S., Frith, W. J., & Stokes, J. R. (2004). Influence of particle modulus on the rheological properties of agar microgel suspensions. *Journal of Rheology, 48*, 1195-1213.

Alavi, F., Emam-Djomeh, Z., Salami, M., & Mohammadian, M. (2020). Effect of microbial transglutaminase on the mechanical properties and microstructure of acid-induced gels and emulsion gels produced from thermal denatured egg white proteins. *International Journal of Biological Macromolecules, 153*, 523-532.

Alejandre, M., Poyato, C., Ansorena, D., & Astiasaran, I. (2016). Linseed oil gelled emulsion: A successful fat replacer in dry fermented sausages. *Meat Science, 121*, 107-113.

Anseth, K. S., Bowman, C. N., & Brannon-Peppas, L. (1996). Mechanical properties of hydrogels and their experimental determination. *Biomaterials, 17*, 1647-1657.

Balakrishnan, G., Nguyen, B. T., Schmitt, C., Nicolai, T., & Chassenieux, C. (2017). Heat-set emulsion gels of casein micelles in mixtures with whey protein isolate. *Food Hydrocolloids, 73*, 213-221.

Benavides, S., Cortes, P., Parada, J., & Franco, W. (2016). Development of alginate microspheres containing thyme essential oil using ionic gelation. *Food Chemistry, 204*, 77-83.

Bi, C. H., Wang, P. L., Sun, D. Y., Yan, Z. M., Liu, Y., Huang, Z. G., & Gao, F. (2020). Effect of high-pressure homogenization on gelling and rheological properties of soybean protein isolate emulsion gel. *Journal of Food Engineering, 277*, 109923.

Boland, A. B., Delahunty, C. M., & van Ruth, S. M. (2006). Influence of the texture of gelatin gels and pectin gels on strawberry flavour release and perception. *Food Chemistry, 96*, 452-460.

Boostani, S., Hosseini, S. M. H., Golmakani, M.-T., Marefati, A., Hadi, N. B. A., & Rayner, M. (2020). The influence of emulsion parameters on physical stability and rheological properties of Pickering emulsions stabilized by hordein nanoparticles. *Food Hydrocolloids, 101*, 105520.

Bot, A., den Adel, R., Regkos, C., Sawalha, H., Venema, P., & Flöter, E. (2011). Structuring in *β*-sitosterol+*γ*-oryzanol-based emulsion gels during various stages of a temperature cycle. *Food Hydrocolloids, 25*, 639-646.

Bot, A., Erle, U., Vreeker, R., & Agterof, W. G. M. (2004). Influence of crystallisation conditions on the large deformation rheology of inulin gels. *Food Hydrocolloids, 18*, 547-556.

Brito-Oliveira, T. C., Bispo, M., Moraes, I. C. F., Campanella, O. H., & Pinho, S. C. (2017). Stability of curcumin encapsulated in solid lipid microparticles incorporated in cold-set emulsion filled gels of soy protein isolate and xanthan gum. *Food Research International, 102*, 759-767.

Chang, S., Chen, X., Liu, S., & Wang, C. (2020). Novel gel-like Pickering emulsions stabilized solely by hydrophobic starch nanocrystals. *International Journal of Biological Macromolecules, 152*, 703-708.

Charoen, R., Jangchud, A., Jangchud, K., Harnsilawat, T., Naivikul, O., & McClements, D. J. (2011). Influence of biopolymer emulsifier type on formation and stability of rice bran oil-in-water emulsions: whey protein, gum arabic, and modified starch. *Journal of Food Science, 76*, E165-E172.

Chen, H., Mao, L., Hou, Z., Yuan, F., & Gao, Y. (2020). Roles of additional emulsifiers in the structures of emulsion gels and stability of vitamin E. *Food Hydrocolloids, 99*, 105372.

Chen, H. Q., Lu, Y., Yuan, F., Gao, Y. X., & Mao, L. K. (2021). Effect of interfacial compositions on the physical properties of alginate-based emulsion gels and chemical stability of co-encapsulated bioactives. *Food Hydrocolloids, 111*, 106389.

Chen, J., & Dickinson, E. (1998a). Viscoelastic properties of heat-set whey protein emulsion gels. *Journal of Texture Studies, 29*, 285-304.

Chen, J., & Dickinson, E. (1998b). Viscoelastic properties of protein-stabilized emulsions: Effect of protein-surfactant interactions. *Food Chemistry, 46*, 91-97.

Chen, J, & Dickinson, E. (1999a). Effect of monoglycerides and diglycerol-esters on viscoelasticity of heat-set whey protein emulsion gels. *International Journal of Food Science & Technology, 35*, 493-501.

Chen, J., & Dickinson, E. (1999b). Interfacial ageing effect on the rheology of a heat-set protein emulsion gel. *Food Hydrocolloids, 13*, 363-369.

Chen, J., & Dickinson, E. (2000). On the temperature reversibility of the viscoelasticity of acid-induced sodium caseinate emulsion gels. *International Dairy Journal, 10*, 541-549.

Chen, J., Dickinson, E., Langton, M., & Hermansson, A.-M. (2000). Mechanical properties and microstructure of heat-set whey protein emulsion gels: Effect of emulsifiers. *LWT - Food Science and Technology, 33*, 299-307.

Chen, J., Ren, Y., Zhang, K., Qu, J., Hu, F., & Yan, Y. (2019). Phosphorylation modification of myofibrillar proteins by sodium pyrophosphate affects emulsion gel formation and oxidative stability under different pH conditions. *Food & Function, 10*, 6568-6581.

Cheng, Y., Donkor, P. O., Ren, X., Wu, J., Agyemang, K., Ayim, I., & Ma, H. (2019). Effect of ultrasound pretreatment with mono-frequency and simultaneous dual frequency on the mechanical properties and microstructure of whey protein emulsion gels. *Food Hydrocolloids, 89*, 434-442.

Ching, S. H., Bansal, N., & Bhandari, B. (2016). Rheology of emulsion-filled alginate microgel suspensions. *Food Research International, 80*, 50-60.

Ching, S. H., Bansal, N., & Bhandari, B. (2017). Alginate gel particles–A review of production techniques and physical properties. *Critical Reviews in Food Science & Nutrition, 57*, 1133-1152.

Co, E. D., & Marangoni, A. G. (2012). Organogels: An alternative edible oil-structuring method. *Journal of the American Oil Chemists' Society, 89*, 749-780.

Cofrades, S., Bou, R., Flaiz, L., Garcimartin, A., Benedi, J., Mateos, R., Sanchez-Muniz, F. J., Olivero-David, R., & Jimenez-Colmenero, F. (2017). Bioaccessibility of hydroxytyrosol and *n*-3 fatty acids as affected by the delivery system: simple, double and gelled double emulsions. *Journal of Food Science Technology, 54*, 1785-1793.

Corstens, M. N., Berton-Carabin, C. C., Elichiry-Ortiz, P. T., Hol, K., Troost, F. J., Masclee, A. A. M., & Schroën, K. (2017). Emulsion-alginate beads designed to control *in vitro* intestinal lipolysis: Towards appetite control. *Journal of Functional Foods, 34*, 319-328.

Dai, L., Sun, C., Wei, Y., Mao, L., & Gao, Y. (2018). Characterization of Pickering emulsion gels stabilized by zein/gum arabic complex colloidal nanoparticles. *Food Hydrocolloids, 74*, 239-248.

de Souza Paglarini, C., de Figueiredo Furtado, G., Biachi, J. P., Vidal, V. A. S., Martini, S., Forte, M. B. S., et al. (2018). Functional emulsion gels with potential application in meat products. *Journal of Food Engineering, 222*, 29-37.

de Souza Paglarini, C., de Figueiredo Furtado, G., Honorio, A. R., Mokarzel, L., da Silva Vidal, V. A., Ribeiro, A. P. B., et al. (2019). Functional emulsion gels as pork back fat replacers in Bologna sausage. *Food Structure, 20*, 100105.

de Souza Paglarinia, C., Martinib, S., & Pollonio, M. A. R. (2019). Using emulsion gels made with sonicated soy protein isolate dispersions to replace fat in frankfurters. *LWT - Food Science and Technology, 99*, 453-459.

Dickinson, E. (2012). Emulsion gels: The structuring of soft solids with protein-stabilized oil droplets. *Food Hydrocolloids, 28*, 224-241.

dos Santos, M., Munekata, P. E. S., Pateiro, M., Magalhaes, G. C., Barretto, A. C. S., Lorenzo, J. M., & Pollonio, M. A. R. (2020). Pork skin-based emulsion gels as animal fat replacers in hot-dog style sausages. *LWT-Food Science and Technology, 132*, 109845.

Farjami, T., & Madadlou, A. (2019). An overview on preparation of emulsion-filled gels and emulsion particulate gels. *Trends in Food Science & Technology, 86*, 85-94.

Feng, X., Chen, L., Lei, N., Wang, S., Xu, X., Zhou, G., & Li, Z. (2017). Emulsifying properties of oxidatively stressed myofibrillar protein emulsion gels prepared with (-)-epigallocatechin-3-gallate and NaCl. *Journal of Agricultural and Food Chemistry, 65*, 2816-2826.

Freire, M., Bou, R., Cofrades, S., & Jimenez-Colmenero, F. (2017). Technological characteristics of cold-set gelled double emulsion enriched with *n*-3 fatty acids: Effect of hydroxytyrosol addition and chilling storage. *Food Research International, 100*(Pt 2), 298-305.

Freire, M., Cofrades, S., Perez-Jimenez, J., Gomez-Estaca, J., Jimenez-Colmenero, F., & Bou, R. (2018). Emulsion gels containing *n*-3 fatty acids and condensed tannins designed as functional fat replacers. *Food Research International, 113*, 465-473.

Freire, M., Cofrades, S., Serrano-Casas, V., Pintado, T., Jimenez, M. J., & Jimenez-Colmenero, F. (2017). Gelled double emulsions as delivery systems for hydroxytyrosol and *n*-3 fatty acids in healthy pork patties. *Journal of Food Science Technology, 54*, 3959-3968.

Gaspar, A. L., & de Goes-Favoni, S. P. (2015). Action of microbial transglutaminase (MTGase) in the modification of food proteins: A review. *Food Chemistry, 171*, 315-322.

Geng, S., Jiang, Z. J., Ma, H. J., Pu, P., Liu, B. G., & Liang, G. Z. (2021). Fabrication and characterization of novel edible Pickering emulsion gels stabilized by dihydromyricetin. *Food Chemistry, 343*, 128486.

Geremias-Andrade, I. M., Souki, N. P. D. B. G., Moraes, I. C. F., & Pinho, S. C. (2017). Rheological and mechanical characterization of curcumin-loaded emulsion-filled gels produced with whey protein isolate and xanthan gum. *LWT - Food Science and Technology, 86*, 166-173.

Glibowski, P., & Pikus, S. (2011). Amorphous and crystal inulin behavior in a water environment. *Carbohydrate Polymers, 83*, 635-639.

Glisic, M., Baltic, M., Glisic, M., Trbovic, D., Jokanovic, M., Parunovic, N., . . . Vasilev, D. (2019). Inulin-based emulsion-filled gel as a fat replacer in prebiotic-and PUFA-enriched dry fermented sausages. *International Journal of Food Science & Technology, 54*, 787-797.

Gómez-Guillén, M. C., Giménez, B., López-Caballero, M. E., & Montero, M. P. (2011). Functional and bioactive properties of collagen and gelatin from alternative sources: A review. *Food Hydrocolloids, 25*, 1813-1827.

Guichard, E. (2002). Interactions between flavor compounds and food ingredients and their influence on flavor perception. *Food Reviews International, 18*, 49-70.

Guo, Q., Bellissimo, N., & Rousseau, D. (2017). Role of gel structure in controlling *in vitro* intestinal lipid digestion in whey protein emulsion gels. *Food Hydrocolloids, 69*, 264-272.

Guo, Q., Ye, A., Lad, M., Dalgleish, D., & Singh, H. (2013). The breakdown properties of heat-set whey protein emulsion gels in the human mouth. *Food Hydrocolloids, 33*, 215-224.

Guo, Q., Ye, A., Lad, M., Dalgleish, D., & Singh, H. (2016). Impact of colloidal structure of gastric digesta on *in-vitro* intestinal digestion of whey protein emulsion gels. *Food Hydrocolloids, 54*, 255-265.

Guzey, D., & McClements, D. J. (2006). Formation, stability and properties of multilayer emulsions for application in the food industry. *Advances in Colloid and Interface Science, 128*, 227-248.

Gwartney, E. A., Larick, D. K., & Foegeding, E. A. (2004). Sensory texture and mechanical properties of stranded and particulate whey protein emulsion gels. *Journal of Food Science, 69*, S333-S339.

Herrero, A. M., Ruiz-Capillas, C., Pintado, T., Carmona, P., & Jiménez-Colmenero, F. (2018). Elucidation of lipid structural characteristics of chia oil emulsion gels by Raman spectroscopy and their relationship with technological properties. *Food Hydrocolloids, 77,* 212-219.

Hou, J. J., Guo, J., Wang, J. M., & Yang, X. Q. (2016). Effect of interfacial composition and crumbliness on aroma release in soy protein-sugar beet pectin mixed emulsion gels. *Journal of the Science of Food and Agriculture, 96*, 4449-4456.

Jiang, Y., Liu, L., Wang, B., Yang, X., Chen, Z., Zhong, Y., Zhang, L., Mao, Z., Xu, H., Sui, X. (2019). Polysaccharide-based edible emulsion gel stabilized by regenerated cellulose. *Food Hydrocolloids, 91*, 232-237.

Jiang, Y., Zhang, C., Yuan, J. H., Wu, Y. Y., Li, F., Waterhouse, G. I. N., et al. (2021). Exploiting the robust network structure of zein/low-acyl gellan gum nanocomplexes to create Pickering emulsion gels with favorable properties. *Food Chemistry, 349*, 129112.

Kang, Y. N., Kim, H., Shin, W. S., Woo, G., & Moon, T. W. (2003). Effect of disulfide bond reduction on bovine serum albumin-stabilized emulsion gel formed by microbial transglutaminase. *Journal of Food Science, 68*, 2215-2220.

Kerner, E. (1956). The elastic and thermo-elastic properties of composite media. *Proceedings of the Physical Society. Section B, 69*, 808.

Kim, K., Gohtani, S., Matsuno, R., & Yamano, Y. (1999). Effects of oil droplet and agar concentration on gel strength and microstructure of o-w emulsion gel. *Journal of Texture Studies, 30*, 319-335.

Kiokias, S., & Bot, A. (2005). Effect of denaturation on temperature cycling stability of heated acidified protein-stabilised o/w emulsion gels. *Food Hydrocolloids, 19*, 493-501.

Kiokias, S., & Bot, A. (2006). Temperature cycling stability of pre-heated acidified whey protein-stabilised o/w emulsion gels in relation to the internal surface area of the emulsion. *Food Hydrocolloids, 20*, 245-252.

Koç, H., Drake, M., Vinyard, C. J., Essick, G., van de Velde, F., & Foegeding, E. A. (2019). Emulsion filled polysaccharide gels: Filler particle effects on material properties, oral processing, and sensory texture. *Food Hydrocolloids, 94*, 311-325.

Langton, M., & Hermansson, A.-M. (1992). Fine-stranded and particulate gels of *β*-lactoglobulin and whey protein at varying pH. *Food Hydrocolloids, 5*, 523-539.

Larson-Smith, K., Jackson, A., & Pozzo, D. C. (2012). SANS and SAXS analysis of charged nanoparticle adsorption at oil-water interfaces. *Langmuir, 28*, 2493-2501.

Leon, A. M., Medina, W. T., Park, D. J., & Aguilera, J. M. (2018). Properties of microparticles from a whey protein isolate/alginate emulsion gel. *Food Science and Technology International, 24*, 414-423.

Lević, S., Pajić Lijaković, I., Đorđević, V., Rac, V., Rakić, V., Šolević Knudsen, T., Pavlović, V., Bugarski, B., & Nedović, V. (2015). Characterization of sodium alginate/*d*-limonene emulsions and respective calcium alginate/*d*-limonene beads produced by electrostatic extrusion. *Food Hydrocolloids, 45*, 111-123.

Lewis, T. B., & Nielsen, L. E. (1970). Dynamic mechanical properties of particulate-filled composites. *Journal of Applied Polymer Science, 14*, 1449-1471.

Li, A., Gong, T., Hou, Y., Yang, X., & Guo, Y. (2020). Alginate-stabilized thixotropic emulsion gels and their applications in fabrication of low-fat mayonnaise alternatives. *International Journal of Biological Macromolecules, 146*, 821-831.

Li, F., Kong, X., Zhang, C., & Hua, Y. (2012). Gelation behaviour and rheological properties of acid-induced soy protein-stabilized emulsion gels. *Food Hydrocolloids, 29*, 347-355.

Li, S. G., Wang, K. P., Huang, Q., & Geng, F. (2021). Microwave pretreatment enhanced the properties of ovalbumin-inulin-oil emulsion gels and improved the storage stability of pomegranate seed oil. *Food Hydrocolloids, 113*, 106548.

Liang, L., Leung Sok Line, V., Remondetto, G. E., & Subirade, M. (2010). *In vitro* release of *α*-tocopherol from emulsion-loaded *β*-lactoglobulin gels. *International Dairy Journal, 20*, 176-181.

Liang, X., Ma, C., Yan, X., Zeng, H., McClements, D. J., Liu, X., & Liu, F. (2020). Structure, rheology and functionality of whey protein emulsion gels: Effects of double cross-linking with transglutaminase and calcium ions. *Food Hydrocolloids, 102*, 105569.

Lim, S. H., Kim, H. R., Choi, S. J., & Moon, T. W. (2015). Lipid oxidation of sodium caseinate-stabilized emulsion-gels prepared using microbial transglutaminase. *Food Science and Biotechnology, 24*, 2023-2026.

Liu, C. H., Zheng, Z. J., Shi, Y. F., Zhang, Y., & Liu, Y. F. (2021). Development of low-oil emulsion gel by solidifying oil droplets: Roles of internal beeswax concentration. *Food Chemistry, 345*, 128811.

Liu, F., & Tang, C.-H. (2016). Soy glycinin as food-grade Pickering stabilizers: Part. II. Improvement of emulsification and interfacial adsorption by electrostatic screening. *Food Hydrocolloids, 60*, 620-630.

Liu, W., Gao, H. X., McClements, D. J., Zhou, L., Wu, J., & Zou, L. Q. (2019). Stability, rheology, and beta-carotene bioaccessibility of high internal phase emulsion gels. *Food Hydrocolloids, 88*, 210-217.

Liu, X., Chen, X. W., Guo, J., Yin, S. W., & Yang, X. Q. (2016). Wheat gluten based percolating emulsion gels as simple strategy for structuring liquid oil. *Food Hydrocolloids, 61*, 747-755.

Luo, N., Ye, A., Wolber, F. M., & Singh, H. (2019). Structure of whey protein emulsion gels containing capsaicinoids: Impact on in-mouth breakdown behaviour and sensory perception. *Food Hydrocolloids, 92*, 19-29.

Luo, N., Ye, A., Wolber, F. M., & Singh, H. (2020). In-mouth breakdown behaviour and sensory perception of emulsion gels containing active or inactive filler particles loaded with capsaicinoids. *Food Hydrocolloids, 108*, 106076.

Lu, Y., Mao, L., Zheng, H., Chen, H., & Gao, Y. (2020). Characterization of *β*-carotene loaded emulsion gels containing denatured and native whey protein. *Food Hydrocolloids, 102*, 105600.

Luo, L. J., Liu, F., & Tang, C. H. (2013). The role of glycinin in the formation of gel-like soy protein-stabilized emulsions. *Food Hydrocolloids, 32*, 97-105.

Lv, P. F., Wang, D., Chen, Y. L., Zhu, S. X., Zhang, J. B., Mao, L. K., et al. (2020). Pickering emulsion gels stabilized by novel complex particles of high-pressure-induced WPI gel and chitosan: Fabrication, characterization and encapsulation. *Food Hydrocolloids, 108*, 105992.

Ma, L., Wan, Z., & Yang, X. (2017). Multiple water-in-oil-in-water emulsion gels based on self-assembled saponin fibrillar network for photosensitive cargo protection. *Journal of Agricultural and Food Chemistry, 65*, 9735-9743.

Mao, L., Roos, Y. H., & Miao, S. (2014). Study on the rheological properties and volatile release of cold-set emulsion-filled protein gels. *Journal of Agricultural and Food Chemistry, 62*, 11420-11428.

Montes de Oca-Ávalos, J. M., Huck-Iriart, C., Candal, R. J., & Herrera, M. L. (2016). Sodium caseinate/sunflower oil emulsion-based gels for structuring food. *Food and Bioprocess Technology, 9*, 981-992.

Nishinari, K., & Takahashi, R. (2003). Interaction in polysaccharide solutions and gels. *Current Opinion in Colloid & Interface Science, 8*, 396-400.

Nourbehesht, N., Shekarchizadeh, H., & Soltanizadeh, N. (2018). Investigation of stability, consistency, and oil oxidation of emulsion filled gel prepared by inulin and rice bran oil using ultrasonic radiation. *Ultrason Sonochem, 42*, 585-593.

Okada, K. S., & Lee, Y. (2017). Characterization of sodium mobility and binding by ^{23}Na NMR spectroscopy in a model lipoproteic emulsion gel for sodium reduction. *Journal of Food Science, 82*, 1563-1568.

Oliver, L., Berndsen, L., van Aken, G. A., & Scholten, E. (2015). Influence of droplet clustering on the rheological properties of emulsion-filled gels. *Food Hydrocolloids, 50*, 74-83.

Oliver, L., Scholten, E., & van Aken, G. A. (2015). Effect of fat hardness on large deformation rheology of emulsion-filled gels. *Food Hydrocolloids, 43*, 299-310.

Oliver, L., Wieck, L., & Scholten, E. (2016). Influence of matrix inhomogeneity on the rheological properties of emulsion-filled gels. *Food Hydrocolloids, 52*, 116-125.

Ozturk, B., Argin, S., Ozilgen, M., & McClements, D. J. (2015). Formation and stabilization of nanoemulsion-based vitamin E delivery systems using natural biopolymers: Whey protein isolate and gum arabic. *Food Chemistry, 188*, 256-263.

Paglarini, C. D., Vidal, V. A. S., Ribeiro, W., Ribeiro, A. P. B., Bernardinelli, O. D., Herrero, A. M., et al. (2021). Using inulin-based emulsion gels as fat substitute in salt reduced Bologna sausage. *Journal of the Science of Food and Agriculture, 101*, 505-517.

Paradiso, V. M., Giarnetti, M., Summo, C., Pasqualone, A., Minervini, F., & Caponio, F. (2015). Production and characterization of emulsion filled gels based on inulin and extra virgin olive oil. *Food Hydrocolloids, 45*, 30-40.

Pernetti, M., van Malssen, K. F., Flöter, E., & Bot, A. (2007). Structuring of edible oils by alternatives to crystalline fat. *Current Opinion in Colloid & Interface Science, 12*, 221-231.

Pintado, T., Herrero, A. M., Jimenez-Colmenero, F., Pasqualin Cavalheiro, C., & Ruiz-Capillas, C. (2018). Chia and oat emulsion gels as new animal fat replacers and healthy bioactive sources in fresh sausage formulation. *Meat Science, 135*, 6-13.

Pintado, T., Munoz-Gonzalez, I., Salvador, M., Ruiz-Capillas, C., & Herrero, A. M. (2021). Phenolic compounds in emulsion gel-based delivery systems applied as animal fat replacers in frankfurters: Physico-chemical, structural and microbiological approach. *Food Chemistry, 340*, 128095.

Pintado, T., Ruiz-Capillas, C., Jimenez-Colmenero, F., Carmona, P., & Herrero, A. M. (2015). Oil-in-water emulsion gels stabilized with chia (*Salvia hispanica L.*) and cold gelling agents: Technological and infrared spectroscopic characterization. *Food Chemistry, 185*, 470-478.

Piornos, J. A., Burgos-Díaz, C., Morales, E., Rubilar, M., & Acevedo, F. (2017). Highly efficient encapsulation of linseed oil into alginate/lupin protein beads: Optimization of the emulsion formulation. *Food Hydrocolloids, 63*, 139-148.

Poyato, C., Astiasarán, I., Barriuso, B., & Ansorena, D. (2015). A new polyunsaturated gelled emulsion as replacer of pork back-fat in burger patties: Effect on lipid composition, oxidative stability and sensory acceptability. *LWT - Food Science and Technology, 62*, 1069-1075.

Qayum, A., Hussain, M., Li, M., Li, J. Q., Shi, R. J., Li, T. Q., et al. (2021). Gelling, microstructure and water-holding properties of alpha-lactalbumin emulsion gel: Impact of combined ultrasound pretreatment and laccase cross-linking. *Food Hydrocolloids, 110*, 106122.

Ringgenberg, E., Alexander, M., & Corredig, M. (2013). Effect of concentration and incubation temperature on the acid induced aggregation of soymilk. *Food Hydrocolloids, 30*, 463-469.

Ruckenstein, E., & Kim, K. J. (1988). Polymerization in gel-like emulsions. *Journal of Applied Polymer Science, 36*, 907-923.

Ruffin, E., Schmit, T., Lafitte, G., Dollat, J. M., & Chambin, O. (2014). The impact of whey protein preheating on the properties of emulsion gel bead. *Food Chemistry, 151*, 324-332.

Sala, G., van Vliet, T., Cohen Stuart, M. A., Aken, G. A. v., & van de Velde, F. (2009). Deformation and fracture of emulsion-filled gels: Effect of oil content and deformation speed. *Food Hydrocolloids, 23*, 1381-1393.

Sato, A. C. K., Moraes, K. E. F. P., & Cunha, R. L. (2014). Development of gelled emulsions with improved oxidative and pH stability. *Food Hydrocolloids, 34*, 184-192.

Sawalha, H., den Adel, R., Venema, P., Bot, A., Floter, E., & van der Linden, E. (2012). Organogel-emulsions with mixtures of beta-sitosterol and gamma-oryzanol: Influence of water activity and type of oil phase on gelling capability. *Journal of Agricultural and Food Chemistry, 60*, 3462-3470.

Serdaroglu, M., Nacak, B., & Karabiyikoglu, M. (2017). Effects of beef fat replacement with gelled emulsion prepared with olive oil on quality parameters of chicken patties. *Korean Journal of Food Science Anim Resour, 37*, 376-384.

Serdaroğlu, M., & Öztürk, B. (2017). Use of olive oil-in-water gelled emulsions in model turkey breast emulsions. *IOP Conference Series: Earth and Environmental Science, 85*, 012071.

Shao, Y., & Tang, C.-H. (2016). Gel-like pea protein Pickering emulsions at pH 3.0 as a potential intestine-targeted and sustained-release delivery system for *β*-carotene. *Food Research International, 79*, 64-72.

Sok Line, V. L., Remondetto, G. E., & Subirade, M. (2005). Cold gelation of *β*-lactoglobulin oil-in-water emulsions. *Food Hydrocolloids, 19*, 269-278.

Soukoulis, C., Cambier, S., Hoffmann, L., & Bohn, T. (2016). Chemical stability and bioaccessibility of *β*-carotene encapsulated in sodium alginate o/w emulsions: Impact of Ca^{2+} mediated gelation. *Food Hydrocolloids, 57*, 301-310.

Soukoulis, C., Tsevdou, M., Andre, C. M., Cambier, S., Yonekura, L., Taoukis, P. S., & Hoffmann, L. (2017). Modulation of chemical stability and *in vitro* bioaccessibility of beta-carotene loaded in kappa-carrageenan oil-in-gel emulsions. *Food Chemistry, 220*, 208-218.

Su, J., Guo, Q., Chen, Y., Dong, W., Mao, L., Gao, Y., & Yuan, F. (2020). Characterization and formation mechanism of lutein Pickering emulsion gels stabilized by *β*-lactoglobulin-gum arabic composite colloidal nanoparticles. *Food Hydrocolloids, 98*, 105276.

Suzawa, E., & Kaneda, I. (2010). Rheological properties of agar microgel suspensions prepared using water-in-oil emulsions. *Journal of Biorheology, 24*, 70-76.

Tang, C. H., Luo, L. J., Liu, F., & Chen, Z. (2013a). Transglutaminase-set soy globulin-stabilized emulsion gels: Influence of soy *β*-conglycinin/glycinin ratio on properties, microstructure and gelling mechanism. *Food Research International, 51*, 804-812.

Tang, C. H., Yang, M., Liu, F., & Chen, Z. (2013b). A novel process to efficiently form transglutaminase-set soy protein isolate-stabilized emulsion gels. *LWT - Food Science and Technology, 53*, 15-21.

Tang, C. H., Chen, L., & Foegeding, E. A. (2011). Mechanical and water-holding properties and microstructures of soy protein isolate emulsion gels induced by $CaCl_2$, glucono-delta-lactone (GDL), and transglutaminase: influence of thermal treatments before and/or after emulsification. *Journal of Agricultural and Food Chemistry, 59*, 4071-4077.

Tolano-Villaverde, I. J., Torres-Arreola, W., Ocaño-Higuera, V. M., & Marquez-Rios, E. (2015). Thermal gelation of myofibrillar proteins from aquatic organisms. *CyTA - Journal of Food*, 1-7.

Torres, O., Tena, N. M., Murray, B., & Sarkar, A. (2017). Novel starch based emulsion gels and emulsion microgel particles: Design, structure and rheology. *Carbohydrate Polymers, 178*, 86-94.

Van Vliet, T. (1988). Rheological properties of filled gels: Influence of filler matrix interaction. *Colloid and Polymer Science, 266*, 518-524.

Wan, Z., Sun, Y., Ma, L., Yang, X., Guo, J., & Yin, S. (2017). Responsive emulsion gels with tunable properties formed by self-assembled nanofibrils of natural saponin glycyrrhizic acid for oil structuring. *Journal of Agricultural and Food Chemistry, 65*, 2394-2405.

Wang, Q., Jiang, J., & Xiong, Y. L. (2019). Genipin-aided protein cross-linking to modify structural and rheological properties of emulsion-filled hempseed protein hydrogels. *Journal of Agricultural and Food Chemistry, 67*, 12895-12903.

Wang, S., Zhang, Y., Chen, L., Xu, X., Zhou, G., Li, Z., & Feng, X. (2018a). Dose-dependent effects of rosmarinic acid on formation of oxidatively stressed myofibrillar protein emulsion gel at different NaCl concentrations. *Food Chemistry, 243*, 50-57.

Wang, X., Luo, K., Liu, S., Adhikari, B., & Chen, J. (2019). Improvement of gelation properties of soy protein isolate emulsion induced by calcium cooperated with magnesium. *Journal of Food Engineering, 244*, 32-39.

Wang, X., Xiong, Y. L., & Sato, H. (2017). Rheological enhancement of pork myofibrillar protein-lipid emulsion composite gels via glucose oxidase oxidation/transglutaminase cross-linking pathway. *Journal of Agricultural and Food Chemistry, 65*, 8451-8458.

Wang, X. F., Luo, K. Y., Liu, S. T., Zeng, M. M., Adhikari, B., He, Z. Y., & Chen, J. (2018b). Textural and rheological properties of soy protein isolate tofu-type emulsion gels influence of soybean variety and coagulant type. *Food Biophysics, 13*, 324-332.

Wang, Z., Neves, M. A., Kobayashi, I., Uemura, K., & Nakajima, M. (2013). Preparation, characterization, and gastrointestinal digestibility of oil-in-water emulsion-agar gels. *Biosci Biotechnol Biochem, 77*, 467-474.

Wouters, A. G., & Delcour, J. A. (2019). Cereal protein based nanoparticles as agents stabilizing air-water and oil-water interfaces in food systems. *Current Opinion in Food Science, 25*, 19-27.

Wu, M., Xiong, Y. L., & Chen, J. (2011). Role of disulphide linkages between protein-coated lipid droplets and the protein matrix in the rheological properties of porcine myofibrillar protein-peanut oil emulsion composite gels. *Meat Science, 88*, 384-390.

Xi, Z., Liu, W., McClements, D. J., & Zou, L. (2019). Rheological, structural, and microstructural properties of ethanol induced cold-set whey protein emulsion gels: Effect of oil content. *Food Chemistry, 291*, 22-29.

Xiao, J., Wang, X. a., Gonzalez, A. J. P., & Huang, Q. (2016). Kafirin nanoparticles-stabilized Pickering emulsions: Microstructure and rheological behavior. *Food Hydrocolloids, 54*, 30-39.

Xu, Y. T., Liu, T. X., & Tang, C. H. (2019). Novel pickering high internal phase emulsion gels stabilized solely by soy *β*-conglycinin. *Food Hydrocolloids, 88*, 21-30.

Xu, W., Huang, L., Jin, W., Ge, P., Shah, B. R., Zhu, D., & Jing, J. (2019). Encapsulation and release behavior of curcumin based on nanoemulsions-filled alginate hydrogel beads. *International Journal of Biological Macromolecules, 134*, 210-215.

Yang, X., Gong, T., Li, D., Li, A., Sun, L., & Guo, Y. (2019). Preparation of high viscoelastic emulsion gels based on the synergistic gelation mechanism of xanthan and konjac glucomannan. *Carbohydrate Polymers, 226*, 115278.

Yang, X., Gong, T., Lu, Y. H., Li, A., Sun, L., & Guo, Y. (2020a). Compatibility of sodium alginate and konjac glucomannan and their applications in fabricating low-fat mayonnaise-like emulsion gels. *Carbohydrate Polymers, 229*, 115468.

Yang, X., Li, A., Yu, W., Li, X., Sun, L., Xue, J., & Guo, Y. (2020b). Structuring oil-in-water emulsion by forming egg yolk/alginate complexes: Their potential application in fabricating low-fat mayonnaise-like emulsion gels and redispersible solid emulsions. *International Journal of Biological Macromolecules, 147*, 595-606.

Ye, A., & Taylor, S. (2009). Characterization of cold-set gels produced from heated emulsions stabilized by whey protein. *International Dairy Journal, 19*, 721-727.

Yonekura, L., & Nagao, A. (2007). Intestinal absorption of dietary carotenoids. *Molecular Nutrition & Food Research, 51*, 107-115.

Zhao, X., Zou, Y. F., Shao, J. J., Chen, X., Han, M. Y., & Xu, X. L. (2017). Comparison of the acidic and alkaline treatment on emulsion composite gel properties of the proteins recovered from chicken breast by isoelectric solubilization/precipitation process. *Journal of Food Processing and Preservation, 41*, e12884.

Zhang, Z. P., Zhang, R. J., Zou, L. Q., Chen, L., Ahmed, Y., Bishri, W. A., Balamash, K., & McClements, D. J. (2016). Encapsulation of curcumin in polysaccharide-based hydrogel beads. *Food Hydrocolloids, 58*, 160-170.

Zheng, H., Mao, L., Cui, M., Liu, J., & Gao, Y. (2020). Development of food-grade bigels based on *κ*-carrageenan hydrogel and monoglyceride oleogels as carriers for *β*-carotene: Roles of oleogel fraction. *Food Hydrocolloids, 105,* 105855.

Zhuang, X., Jiang, X., Zhou, H., Han, M., Liu, Y., Bai, Y., Cu, X. L., Zhou, G. H. (2019). The effect of insoluble dietary fiber on myofibrillar protein emulsion gels: Oil particle size and protein network microstructure. *LWT, 101*, 534-542.

Zou, Y., Guo, J., Yin, S. W., Wang, J. M., & Yang, X. Q. (2015). Pickering emulsion gels prepared by hydrogen-bonded zein/tannic acid complex colloidal particles. *Journal of Agricultural and Food Chemistry, 63*, 7405-7414.

CHAPTER TWO

The Role of Mixing Sequence in Structuring O/W Emulsions and Emulsion Gels Produced by Electrostatic Interactions between Soy Protein Isolate-coated Droplets and Alginate

Chapter 2 was published in:

Lin, D., Kelly, A. L., & Miao*, S. (2021). The role of mixing sequence in structuring O/W emulsions and emulsion gels produced by electrostatic protein-polysaccharide interactions between soy protein isolate-coated droplets and alginate molecules. *Food Hydrocolloids, 113*, 106537.

The work contained in this chapter was undertaken and written solely by myself with specific contributions from each co-author.

Abstract

Multilayer emulsions produced by electrostatic protein-polysaccharide interactions have received increased interest recently, but the addition sequence of oppositely charged dispersions for emulsion preparation has rarely been investigated. The purpose of this study was to investigate the effect of addition sequence of oppositely charged soy protein isolate (SPI)-stabilized emulsions and alginate solutions on the stability and structure of emulsions involving electrostatic protein-polysaccharide attraction and the structural and rheological properties of emulsion gels produced by internal gelation (i.e., addition of GDL and $CaCO_3$). Stable multilayer emulsions containing unflocculated alginate/SPI-coated droplets were produced by adding low levels of SPI-stabilized emulsions into alginate solutions at pH 3.0, and emulsion gels prepared from above resultant emulsions by gelling the continuous phase containing alginate had higher L^* values and storage modulus than emulsion gels prepared by adding alginate solutions into SPI-stabilized emulsions. Unstable emulsions containing flocculated droplets were obtained on adding high levels of SPI-stabilized emulsions into alginate solutions or adding alginate solutions into SPI-stabilized emulsions (independent of concentration) at pH 3.0 with mild stirring. The findings of this study are important for preparing stable multilayer emulsions and structuring emulsion gels by changing the addition sequence of oppositely charged dispersions for emulsion preparation.

Keywords: Emulsion gel; Electrostatic interaction; Addition sequence; Structure; SPI; Alginate.

2.1. Introduction

Polysaccharide-based emulsion gels have received growing interest in the food industry recently, such as *κ*-carrageenan-, gellan gum-, agar-, inulin- and alginate-based emulsion gels (Herrero et al., 2018; Lorenzo et al., 2013; Paradiso et al., 2015; Wang et al., 2013; Zheng et al., 2020). Compared to protein-based emulsion gels, polysaccharide-based (especially alginate-based) emulsion gels are less readily digested and damaged in gastric fluid, and the remaining gel structures can be further disrupted during intestinal digestion, due to the increased repulsive forces of the uronic acid groups on alginate and ion-exchange between Na^+ ions in the digestive fluid and Ca^{2+} ions in gel beads (Bokkhim et al., 2016). These characteristics make polysaccharide-based emulsion gels ideal materials for encapsulation of compounds such as *α*-tocopherol, *β*-carotene, curcumin, and *D*-limonene (Feng et al., 2018; Lević et al., 2015; Soukoulis et al., 2017; Xu et al., 2019), which can be protected from the harsh gastric environment and released from emulsion gels during intestinal digestion.

For preparation of emulsion gels, the first step is to prepare emulsions, in which emulsifiers are normally used to decrease the droplet size and increase the stability of droplets, and these emulsions can then be turned into emulsion gels by various mechanisms for different matrix materials (e.g., heat treatment, enzyme treatment, acidification treatment, and addition of ions) (Lin, Kelly, & Miao, 2020). Use of naturally occurring proteins (e.g., whey protein isolate (WPI), soy protein isolate (SPI), lactoferrin and zein) as emulsifiers has received increased attention for replacement of synthetic chemicals (e.g., Tween 20 and Span 80) in recent years, due to increased customer demand for healthy foods (Ruffin et al., 2014; Su et al., 2016; Tang et al., 2013). In addition, electrostatic interactions between protein-coated droplets and polysaccharide molecules in the continuous phase (particularly oppositely charged proteins and polysaccharides) are critical, as these can affect the stability and structure of emulsions and thus the mechanical and structural properties of emulsion gels (Evans et al., 2013; Tavernier et al., 2017).

Previous studies have shown that pectin/WPI-, alginate/*β*-lactoglobulin-, carboxymethylcellulose/sodium caseinate-, and pectin/*β*-lactoglobulin-stabilized emulsions had better stability than protein-stabilized emulsions at pH 4–4.5 (Guzey & McClements, 2007; Harnsilawat et al., 2006; Liu et al., 2012; Salminen & Weiss, 2014), and that introducing chitosan into ovalbumin- or glycinin-stabilized emulsions could increase the stability of emulsions at pH 4.5–5.5 (Xiong et al., 2018; Yuan et al., 2013). Electrostatic interactions between oppositely charged protein-coated droplets and polysaccharide molecules led to the adsorption of polysaccharide molecules on the surfaces of protein-coated droplets, and thus the formation of polysaccharide/protein-coated bilayer droplets with increased surface charge and enhanced electrostatic repulsion (Evans et al., 2013).

Many factors can affect electrostatic interactions between oppositely charged protein-coated droplets and polysaccharide molecules, such as polymer properties (e.g., molecular weight, charge density and flexibility) and mixing conditions (e.g., the pH, ionic strength, temperature, stirring, ratio of protein to polysaccharide and addition sequence of dispersions), but the addition sequence of dispersions has rarely been discussed (Evans et al., 2013; Guzey & McClements, 2006; Ye, 2008). There are four main routes for preparing emulsions stabilized by electrostatic polysaccharide-protein complexes (Albano et al., 2019). The following discussion mainly focuses on anionic polysaccharides, because most of charged polysaccharides are anionic.

Firstly, anionic polysaccharide/anionic protein mixtures may be prepared at pH > p*I*, and then oil introduced into the system to prepare emulsions by homogenization, followed by adjusting pH below the p*I* of the protein present. Secondly, the dispersion of anionic polysaccharide/cationic protein complex may be prepared at pH < p*I*, and emulsions prepared by adding oil and homogenization. Thirdly, anionic protein-stabilized emulsions can be mixed with anionic polysaccharide solutions at pH > p*I*, and then the pH of emulsions adjusted below the p*I* of the protein present. Finally, cationic protein-stabilized emulsions

may be mixed with anionic polysaccharide solutions at pH < p*I*, which is the easiest way to prepare polysaccharide/protein-stabilized emulsions formed by electrostatic interactions.

Emulsions prepared by the first and second methods are termed mixed emulsions, in which polysaccharide-protein complexes adsorb at the droplet surfaces, while emulsions prepared by the third and fourth methods are called bilayer or layer-by-layer (LbL) emulsions (Golkar et al., 2015). Bilayer emulsions show better stability than mixed emulsions, probably because of the higher charge density of bilayer emulsions, and are normally used to prepare polysaccharide-based emulsion gels (Azarikia et al., 2017).

In addition, the addition sequence of oppositely charged protein-stabilized emulsions and polysaccharide solutions may affect the structure and stability of bilayer emulsions. It can be hypothesized that, when adding protein-stabilized emulsions into oppositely charged polysaccharide solutions, polysaccharides can attach to protein-coated droplets, leading to multilayer emulsions with or without flocculation, depending on the repulsive forces between polysaccharide/protein-coated droplets and unadsorbed polysaccharides in the continuous phase; however, when the content of protein-coated droplets exceeds a critical concentration on adding emulsions into polysaccharide solutions, polysaccharide levels may not be sufficient to interact with protein-coated droplets and bridging flocculation may occur (McClements, 2005).

On the other hand, when adding polysaccharide solutions into oppositely charged protein-stabilized emulsions, bridging flocculation may occur immediately, because insufficient polysaccharide molecules are shared by neighboring droplets; however, with continuously adding polysaccharide solutions into emulsions with strong mechanical stirring, stable emulsions without flocculation could be formed or depletion flocculation may occur (McClements, 2005). In addition, the structure of emulsion droplets can also affect the mechanical and structural properties of emulsion gels. According to the Kerner model modified by Lewis and Nielsen, emulsion gels containing flocculated droplets have

improved mechanical properties compared to emulsion droplet-filled gels (Kerner, 1956; Lewis & Nielsen, 1970).

The purpose of this study was therefore to investigate the effect of the addition sequence of SPI-stabilized emulsions and alginate solutions on the stability and structure of emulsions and the structural and rheological properties of alginate-based emulsion gels. Sodium alginate, a linear unbranched anionic polysaccharide, has been widely investigated in the field of emulsion gels. In addition, using SPI as emulsifier has received increasing interest due to its good emulsifying capacity. SPI-stabilized emulsions and alginate solutions were thus investigated at pH 3.0, under which conditions SPI is positively charged, with good solubility and emulsifying capacity, and alginate is negatively charged.

2.2. Materials and methods

2.2.1. Materials

Defatted soy flour (Bob's Red Mill, Milwaukie, Oregon, USA) and sunflower oil (Aldi Stores Ltd., Kildare, Ireland) were purchased from iHerb and Aldi, respectively. Soy protein isolate (SPI) was extracted from defatted soy flour, according to the method described by Urbonaite et al. (2015); the protein content of the SPI powder was 96.29 ± 0.03%. Sodium alginate (viscosity of 1 wt% sodium alginate solution in 0.15 M NaCl at 25°C = 210–340 cP, $\overline{M}$ = 69–117 kDa, and M/G = 71/29) was obtained from Special Ingredients (Chesterfield, UK). *D*-(+)-glucono-*δ*-lactone (GDL), calcium carbonate, sodium hydroxide, hydrochloric acid, and other analytical reagents were purchased from Sigma-Aldrich (St. Louis, MO, USA).

2.2.2. Solution/dispersion preparation

The SPI dispersion was prepared by mixing SPI powder with deionized water (0.5:94.5, w/w) and stirring at room temperature for 2 h using a magnetic stirrer, and then the pH of

dispersion was adjusted to 3.0 with 1 M HCl and NaOH. Sodium alginate (0.4%, w/w) was mixed with deionized water by shearing at 400 rpm for 30 min with a magnetic stirrer and then allowed to rest for 24 h to permit hydration. The resulting 0.4 wt% sodium alginate solutions ($A_{0.4}$) were diluted to levels of 0.025 wt% ($A_{0.025}$), 0.05 wt% ($A_{0.05}$), 0.1 wt% ($A_{0.1}$), and 0.2 wt% ($A_{0.2}$) with deionized water, and then the pH was adjusted to 3.0 with 5 M HCl and NaOH.

2.2.3. Emulsion preparation

For preparation of SPI-stabilized emulsions, sunflower oil (5.0 wt% in emulsions, w/w) was mixed with the SPI dispersions (95.0 wt% in emulsions containing 0.5 wt% SPI, w/w) at 13,000 rpm for 2 min with an Ultra-Turrax (IKA-25, Staufen, Germany). The resultant emulsions ($E_{0.5}$) were diluted into $E_{0.1}$ (i.e., containing 0.1 wt% SPI and 1.0 wt% oil), $E_{0.2}$ (i.e., containing 0.2 wt% SPI and 2.0 wt% oil), $E_{0.3}$ (i.e., containing 0.3 wt% SPI and 3.0 wt% oil), and $E_{0.4}$ (i.e., containing 0.4 wt% SPI and 4.0 wt% oil) with deionized water (pH adjusted to 3.0 using 0.1 M HCl and 0.1 M NaOH), and the pH of emulsions was then adjusted to 3.0 with 0.5 M HCl and NaOH. SPI/polysaccharide-stabilized emulsions were prepared by adding one dispersion into the other slowly (1 mL/10 seconds) with stirring at 500 rpm for 5 min using a magnetic stirrer. The resulting samples were transferred to test tubes for further investigation.

2.2.4. Properties of emulsions

2.2.4.1. Morphological properties

Samples in test tubes were allowed to rest for 2 h, and then photographs of samples were taken using a camera. The creaming or phase separation of samples may occur after being allowed to rest for 2 h. The top creaming layers were regarded as the upper portions, and the lower layers without cream were regarded as the lower portions. The turbidity and microstructure of both upper and lower portions of samples were investigated. The viscosity,

droplet size and zeta potential of the bottom portion of samples were investigated; the upper and lower portions of samples were transferred by pipettes.

2.2.4.2. Turbidity measurements

The turbidity of the upper and lower portions of mixed emulsions was analyzed with a Spectronic Genesys-5 UV spectrophotometer (Milton Roy Co., New York, USA). Samples were diluted 10 times with deionized water (pH adjusted to 3.0 by 0.1 M HCl and 0.1 M NaOH) before testing. The absorbance at 600 nm of samples was taken as the turbidity of dispersion.

2.2.4.3. Emulsion micro-structure

Optical microscopy images of the upper and lower portions of mixed emulsions were recorded using an Olympus BX51 light microscope with a built-in camera (Olympus Optical Co. Ltd., Tokyo, Japan). Samples were dropped on a microscope slide, covered with a glass coverslip, and observed using a 10× or 20× objective lens and 10× eyepiece.

2.2.4.4. Zeta potential measurements

The zeta potential of the lower portion of mixed emulsions was measured by particle electrophoresis technology using a laser particle analyzer (Nano-ZS, Malvern Instruments, Worcestershire, UK). Samples were diluted 100 times (w/w) with ultrapure water (pH adjusted to 3.0 by 0.1 M HCl and 0.1 M NaOH) before testing. The operation temperature was set at 25ºC, and the refractive index and absorption index of samples were set at 1.48 and 0.001, respectively.

2.2.4.5. Size distribution measurements

The size distributions of oil droplets in the lower portion of mixed emulsions were analyzed with a MasterSizer 3000 (Malvern Instruments Ltd., Worcestershire, UK). Samples

were added to an automated wet dispersion unit until the obscuration reached between 1 and 10%. The stirrer speed was set at 2000 rpm. The refractive index and absorption index of samples were set at 1.48 and 0.001, respectively.

2.2.4.6. Rheological measurements

The viscosity of the lower portion of mixed emulsions was tested at 25ºC using an AR 2000ex rheometer (TA Instruments, Crawley, UK) with an aluminium parallel plate (60 mm in diameter, and 0.5 mm in gap). Each sample was added in the middle of the Peltier plate and allowed to stand for 2 min before testing. The flow measurement was performed over a shear rate range of 0.1 to 100 s^{-1}, and viscosity (η) was obtained from the data analysis software. The final results of viscosity were presented at a shear rate of 100 $s^{-1.}$

2.2.5. Emulsion gel preparation

Two emulsion samples $E_{0.1}A_{0.4}$ (i.e., adding emulsions (containing 0.1 wt% SPI and 1.0 wt% oil) into 0.4 wt% alginate solutions) and $A_{0.4}E_{0.1}$ (i.e., adding 0.4 wt% alginate solutions into emulsions containing 0.1 wt% SPI and 1.0 wt% oil) were prepared at pH 3.0 according to the methods described in Section 2.2.3. The control sample was prepared by adding deionized water (pH adjusted to 3.0 by 0.1 M HCl and 0.1 M NaOH) into the same volume of alginate solutions (0.4 wt%). GDL (10 mM) was added into the above samples followed by mixing at 500 rpm for 5 min, and then $CaCO_3$ (5 mM) was added and stirred at 500 rpm for 1 min. The resultant liquid mixtures were used to prepare emulsion gels by moving 30 mL samples into a beaker and incubating at 30ºC for 3 h.

2.2.6. Properties of emulsion gels

2.2.6.1. Morphological and structural properties of emulsion gels

For recording visual appearance of emulsion gels, emulsion gels were removed from beakers into a plastic Petri dish, and then photographs of samples were taken using a digital

camera. For investigating the colour of emulsion gels, the liquid emulsion mixtures (3 mL, prepared in Section 2.2.5) containing 10 mM GDL and 5 mM $CaCO_3$ were transferred to plastic cuvettes (10 × 10 × 45 mm), and samples were incubated at 30ºC for 3 h to ensure the formation of emulsion gels. The colour parameter (L^*) of emulsion gels in cuvettes was measured using a Minolta Chroma Meter CR-400 colorimeter (Minolta Ltd., Milton Keynes, UK).

For observing the micro-structure of emulsion gels, the liquid emulsion mixtures (500 μL, prepared in Section 2.2.5) containing 10 mM GDL and 5 mM $CaCO_3$ were transferred to a glass slide, and the edge of samples between the coverslip and the glass slide was covered by a layer of silicone oil to prevent evaporation. These samples were incubated at 30ºC for 3 h to ensure the formation of emulsion gels. Optical microscopy images of emulsion gels were then recorded using an Olympus BX51 light microscope.

2.2.6.2. Dynamic rheological measurements of emulsion gels during gelation

The small deformation shear rheological properties of dispersions (time sweep) were tested at 30ºC using an AR 2000ex rheometer (TA Instruments, Crawley, UK) with an aluminium parallel plate (60 mm in diameter, and 1.0 mm in gap). Each liquid mixture sample prepared in Section 2.2.5 was added immediately in the middle of Peltier plate after preparation and allowed to stand for 2 min before testing. The edge of samples between the parallel plate and the Peltier plate was covered by a layer of silicone oil to prevent evaporation. Small-deformation shear measurement was performed at 0.01 wt% strain (within the linear viscoelastic regime) and a constant frequency of 1 Hz for 180 min. Storage modulus (G') values were obtained from the data analysis software.

2.2.7. Statistical analysis

All measurements were performed three times and were reported as mean ± standard deviation (SD). Differences between samples were analyzed using analysis of variance and a *t*-test, and $p < 0.05$ was regarded as statistically significant.

2.3. Results and discussion

2.3.1. Structuring alginate/SPI-stabilized emulsions by addition sequence

2.3.1.1. Adding SPI-stabilized emulsions into alginate solutions

Figures 2-1A and 2-1B show the visual appearance, turbidity and microscopic structures of mixtures prepared by adding various levels of SPI-stabilized emulsions (0.1–0.5 wt% SPI and 1.0–5.0 wt% oil) into 0.2 wt% alginate solutions (1:1) at pH 3.0, respectively. Adding low-concentration SPI-stabilized emulsions (0.1 wt% SPI and 1.0 wt% oil) into alginate solutions resulted in an alginate/SPI-stabilized emulsion ($E_{0.1}A_{0.2}$) without visible creaming, in which the turbidity of upper and lower portions of emulsions was not significantly different (**Figure 2-1A**), and single droplets without flocculation could be observed in both portions (**Figure 2-1B**). In contrast, adding highly concentrated SPI-stabilized emulsions (0.2–0.5 wt% SPI and 2.0–5.0 wt% oil) into alginate solutions resulted in mixtures ($E_{0.2}A_{0.2}$–$E_{0.5}A_{0.2}$) that showed creaming, in which the turbidity of upper portions was significantly higher than that of lower portions of mixtures (**Figure 2-1A**) and flocculated droplets could be observed in the upper portions of mixtures (**Figure 2-1B**).

This indicates that adding high levels of SPI-stabilized emulsions into appositely charged alginate solutions (0.2 wt%) may lead to unstable emulsions, which was probably because 0.2 wt% alginate was insufficient to fully cover high levels of oppositely charged SPI-coated droplets (0.2–0.5 wt% SPI and 2.0–5.0 wt% oil) by electrostatic interactions.

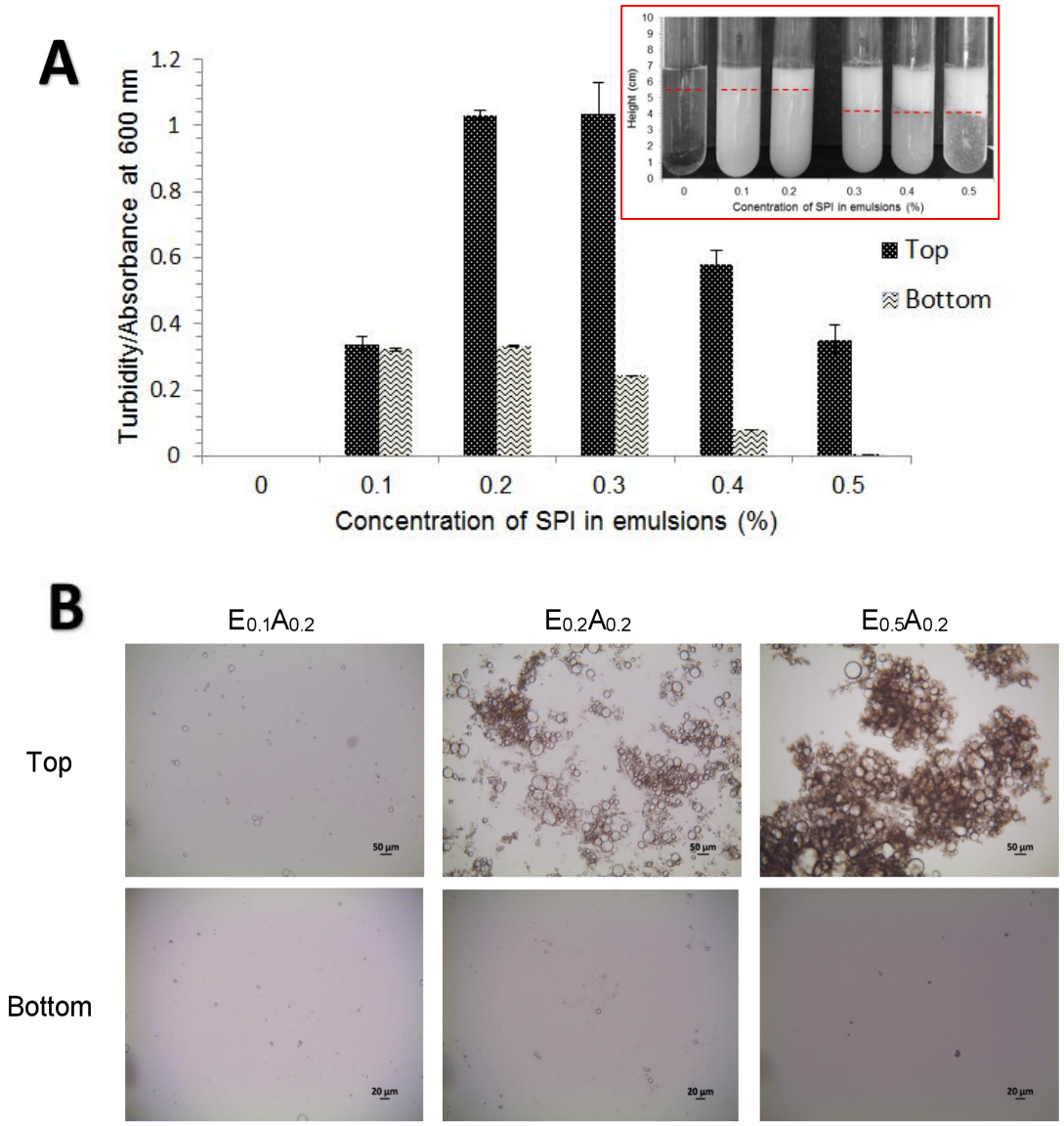

Figure 2-1. (A) Turbidity and visual appearance (top right corner) and (B) microscopic structures of alginate/SPI-stabilized emulsions prepared by adding SPI-stabilized emulsions (0.1–0.5 wt% SPI and 1.0–5.0 wt% oil) into 0.2 wt% alginate solutions (1:1) at pH 3.0. The control sample was prepared by adding deionized water (pH 3.0) into 0.2 wt% alginate solutions (1:1). All samples were measured after creaming by being allowed to stand for 2 h after preparation. Red dashed lines separate the top and bottom portions of samples.

Many factors can affect the concentration of polysaccharides which is needed to fully cover oppositely charged protein-coated droplets, such as the type and charge density of polyelectrolyte, the pH, temperature, and ionic strength of mixture system, and the concentration and size of emulsion droplets (Guzey & McClements, 2007). For example, it has been reported that emulsions containing 0.1 wt% corn oil and 0.005 wt% *β*-lactoglobulin can be fully covered by 0.003 wt% pectin solutions by electrostatic interactions at pH 4.0 (Guzey & McClements, 2007). It has also been reported that emulsions containing 5 wt% corn oil and 0.45 wt% *β*-lactoglobulin can be fully covered by 0.15 wt% pectin solutions through electrostatic interactions at pH 3.0 (Moreau et al., 2003). Therefore, the zeta-potential and viscosity of the lower liquid phases of mixtures were further studied to investigate the electrostatic interactions between SPI-coated droplets and alginate molecules (**Table 2-1**).

Table 2-1. Zeta potential, droplet/aggregate size ($D_{4,3}$) and viscosity of the lower liquid portions of alginate/SPI-stabilized emulsions prepared by adding SPI-stabilized emulsions (0.1–0.5 wt% SPI and 1.0–5.0 wt% oil) into 0.2 wt% alginate solutions (1:1) at pH 3.0.

Samples	Zeta potential (mV)	$D_{4,3}$ (*μ*m)	Viscosity (mPa·s)
$\mathbf{E_0A_{0.2}}$	-20.2 ± 1.2^{b}	/	4.51 ± 0.12^{d}
$\mathbf{E_{0.1}A_{0.2}}$	-29.3 ± 2.4^{c}	25.2 ± 4.1^{a}	4.21 ± 0.02^{d}
$\mathbf{E_{0.2}A_{0.2}}$	-31.8 ± 1.7^{c}	25.3 ± 2.0^{a}	3.01 ± 0.04^{c}
$\mathbf{E_{0.3}A_{0.2}}$	-29.8 ± 4.1^{c}	29.3 ± 2.1^{a}	2.11 ± 0.12^{b}
$\mathbf{E_{0.4}A_{0.2}}$	-26.1 ± 1.7^{c}	24.0 ± 5.9^{a}	1.74 ± 0.06^{a}
$\mathbf{E_{0.5}A_{0.2}}$	-10.3 ± 0.6^{a}	/	1.46 ± 0.09^{a}

$^{a\text{-}d}$ Values with different superscript letters in the same column are significantly different ($p < 0.01$).

SPI-coated droplets (zeta-potential of ＋29.9 ± 0.9 mV in sample $A_0E_{0.1}$) and alginate molecules (zeta-potential of －20.2 ± 1.2 mV in sample $E_0A_{0.2}$) are oppositely charged at pH 3.0, and adding low-concentrated SPI-stabilized emulsions (0.1 wt% SPI and 1.0 wt% oil) into alginate solutions decreased the zeta-potential of emulsion droplets to －29.3 ± 2.4 mV

in sample $E_{0.1}A_{0.2}$ ($p < 0.01$, **Table 2-1**). This indicates that alginate molecules were adsorbed at the surfaces of SPI-coated droplets through electrostatic interactions, and thus positively charged SPI-coated droplets turned into negatively charged alginate/SPI-coated droplets in sample $E_{0.1}A_{0.2}$. With increasing emulsion concentrations (0.2–0.4 wt% SPI and 2.0–4.0 wt% oil) in the mixtures (i.e., $E_{0.2}A_{0.2}$–$E_{0.4}A_{0.2}$), the droplets in lower portion of mixtures shown similar zeta-potential with that of $E_{0.1}A_{0.2}$ ($p > 0.01$), while creaming occurred in samples $E_{0.2}A_{0.2}$–$E_{0.4}A_{0.2}$ (**Figure 2-1A** and **Table 2-1**).

The above results indicate that alginate molecules in 0.2 wt% alginate solutions have been fully occupied in covering the surfaces of SPI-coated droplets in emulsions containing 0.1–0.2 wt% SPI and 1.0–2.0 wt% oil at pH 3.0 by electrostatic interactions between oppositely charged alginate molecules and SPI-coated droplets (Guzey & McClements, 2006). Therefore, there were no more alginate molecules available in the continuous phase to interact with further introduced SPI-stabilized droplets in samples $E_{0.2}A_{0.2}$–$E_{0.4}A_{0.2}$, and thus droplet flocculation occurred, due to electrostatic interactions between positively charged SPI-stabilized droplets and negatively charged alginate/SPI-coated droplets. Then, creaming occurred in samples $E_{0.2}A_{0.2}$–$E_{0.4}A_{0.2}$ after being allowed to stand for 2 h (**Figure 2-1A**), in which flocculated droplets moved to the upper phase and unflocculated alginate/SPI-coated droplets remained in the lower phase, which was seen from the non-significant differences in droplet size of samples $E_{0.2}A$–$E_{0.4}A$ (**Table 2-1**).

Meanwhile, the levels of remaining alginate/SPI-coated droplets in the lower phase of samples $E_{0.2}A_{0.2}$–$E_{0.5}A_{0.2}$ decreased with increased addition levels of SPI-stabilized emulsions, due to the interactions between alginate/SPI-coated droplets and further added SPI-coated droplets. This was also shown by the decreased viscosity of the lower liquid phases of samples $E_{0.1}A_{0.2}$–$E_{0.5}A_{0.2}$ (**Table 2-1**). In addition, the relatively clear lower liquid of sample $E_{0.5}A$ could not produce enough light obscuration to test its droplet size, which also indicates that there was a minimal level of alginate/SPI-coated emulsion droplets.

2.3.1.2. Adding alginate solutions into SPI-stabilized emulsions

Figures 2-2A and 2-2B show the visual appearance, turbidity and microscopic structures of mixtures prepared by adding different levels of alginate solutions (0.025–0.4 wt%) into SPI-stabilized emulsions containing 0.1 wt% SPI and 1.0 wt% oil (1:1) at pH 3.0, respectively. Adding alginate solutions into SPI-stabilized emulsions resulted in emulsions with visible creaming, in which the turbidity of upper and lower portions of emulsions were significantly different (**Figure 2-2A**) and flocculated droplets could be observed in upper portions of all samples ($A_{0.025}E_{0.1}$–$A_{0.4}E_{0.1}$) and in the lower portions of samples $A_{0.2}E_{0.1}$ and $A_{0.4}E_{0.1}$ (**Figure 2-2B**). This indicates that adding alginate solutions into SPI-stabilized emulsions with mild stirring led to unstable emulsions, independent of the concentration of alginate solutions.

In order to explain above phenomenon, the zeta-potential, droplet size and viscosity of the lower liquid phases of mixtures were further studied (**Table 2-2**). Adding 0.025 wt% alginate solutions into emulsions (containing 0.1 wt% SPI and 1.0 wt% oil) decreased the zeta-potential of the lower liquid phases of mixtures from $+29.9 \pm 0.9$ mV ($A_0E_{0.1}$) to -5.7 ± 2.1 mV ($A_{0.025}E_{0.1}$). This was probably because 0.025 wt% alginate (i.e., 0.0125 wt% in the final mixtures) was not enough to fully cover 0.1 wt% SPI molecules (i.e., 0.05 wt% SPI in the final mixtures) adsorbed at droplet surfaces, which led to bridging flocculation (i.e., insufficient alginate molecules shared by neighbouring SPI-coated droplets); then, creaming occurred on samples being allowed to stand for 2 h (**Figure 2-2A**), in which flocculated droplets moved to the upper phase, leading to few remaining emulsion droplets and alginate molecules in the lower phase. With increasing alginate concentrations (0.05–0.4 wt%), the lower liquid phase of emulsions became more negatively charged (i.e., increased absolute values of zeta-potential) and had higher viscosity (**Table 2-2**), which both indicate an increased level of alginate molecules in the lower liquid portions.

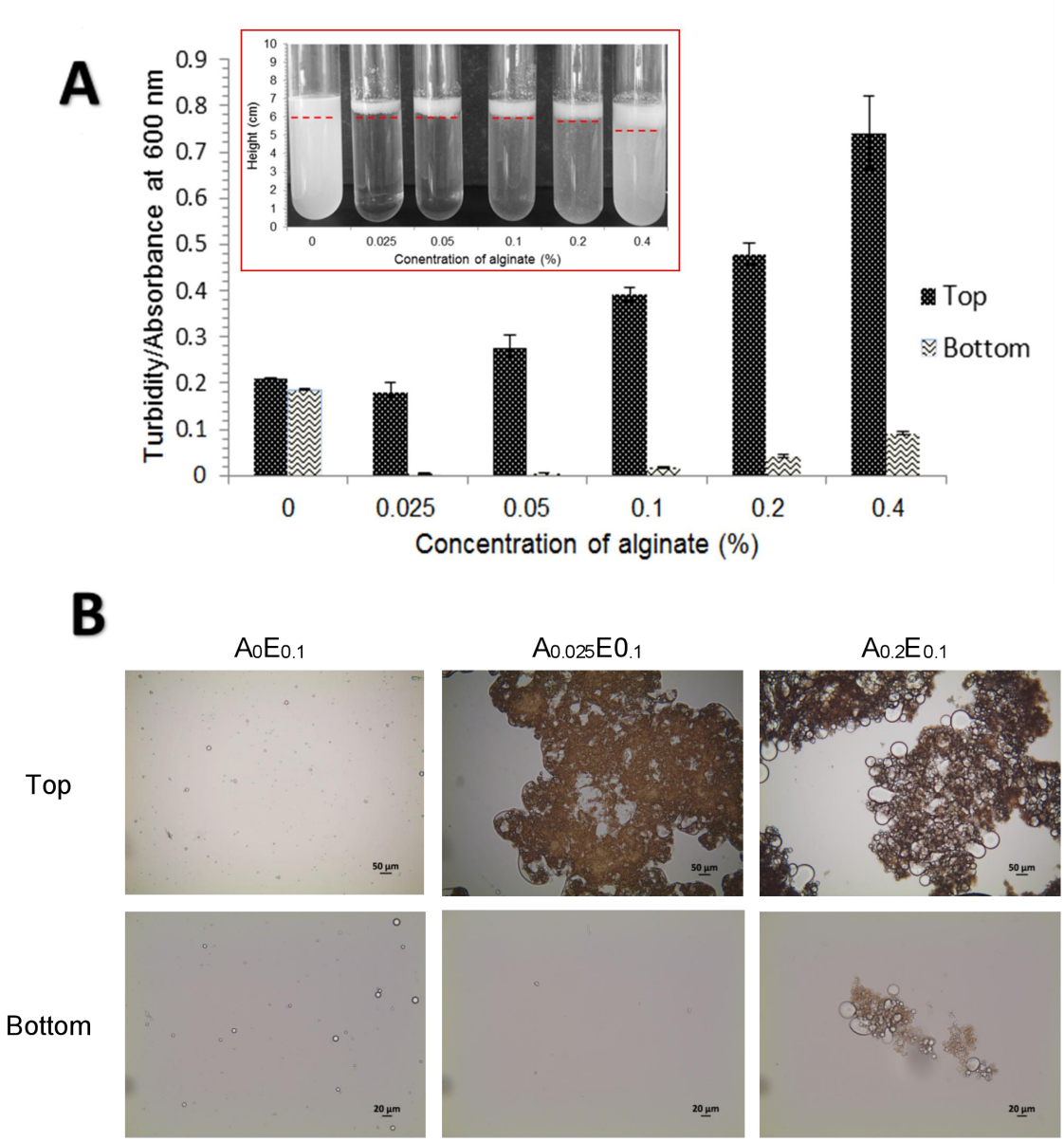

Figure 2-2. (A) Turbidity and visual appearance (top left corner) and (B) microscopic structures of alginate/SPI-stabilized emulsions prepared by adding alginate solutions (0.025–0.4 wt%) into SPI-stabilized emulsions containing 0.1 wt% SPI and 1.0 wt% oil (1:1) at pH 3.0. The control sample was prepared by adding deionized water (pH 3.0) into SPI-stabilized emulsions (1:1). All samples were measured after creaming by being allowed to stand for 2 h after preparation. Red dashed lines separate the top and bottom portions of samples.

Table 2-2. Zeta potential, droplet/aggregate size ($D_{4,3}$) and viscosity of the lower liquid portions of alginate/SPI-stabilized emulsions prepared by adding alginate solutions (0.025–0.4 wt%) into SPI-stabilized emulsions containing 0.1 wt% SPI and 1.0 wt% oil (1:1) at pH 3.0.

Samples	Zeta potential (mV)	$D_{4,3}$ (μm)	Viscosity (mPa·s)
$\mathbf{A_0E_{0.1}}$	+29.9 ± 0.9^{d}	16.9 ± 0.3^{a}	0.99 ± 0.05^{ab}
$\mathbf{A_{0.025}E_{0.1}}$	-5.7 ± 2.1^{c}	/	0.94 ± 0.02^{a}
$\mathbf{A_{0.05}E_{0.1}}$	-14.3 ± 2.2^{b}	/	1.11 ± 0.03^{b}
$\mathbf{A_{0.1}E_{0.1}}$	-20.3 ± 4.0^{ab}	/	1.72 ± 0.03^{c}
$\mathbf{A_{0.2}E_{0.1}}$	-28.9 ± 2.2^{a}	154 ± 18^{c}	3.27 ± 0.06^{d}
$\mathbf{A_{0.4}E_{0.1}}$	-27.8 ± 1.3^{a}	81.7 ± 11.0^{b}	7.39 ± 0.03^{e}

$^{a\text{-}e}$ Values with different superscript letters in the same column are significantly different ($p < 0.01$).

In addition, the particle size (**Table 2-2**) and microscopic pictures (**Figure 2-2B**) of the lower phase of mixtures show that there were some flocculated droplets in the lower phase of samples $A_{0.2}E_{0.1}$ and $A_{0.4}E_{0.1}$, but there were hardly any unflocculated alginate-SPI-coated droplets. This result was unexpected, because it has been reported that, with increasing content of polyelectrolyte (C) in oppositely charged emulsions, stable emulsions without aggregation (C = 0), bridging flocculation ($0 < C < C_{saturation}$), stable emulsions without aggregation ($C_{saturation} < C < C_{depletion}$), and depletion flocculation ($C_{depletion} < C$) may occur (McClements, 2005). However, unflocculated alginate/SPI-coated droplets were not observed in all samples in this study, although there were sufficient alginate molecules in the continuous phase (i.e., the increased viscosity of the lower liquid portions of alginate/SPI-stabilized emulsions as shown in **Table 2-2**) to dispel bridging flocculation and then form stable emulsions.

The reason for this phenomenon is probably because of the preparation method used in this study. Alginate solutions were slowly added into SPI-stabilized emulsions, and thus bridging flocculation occurred in all samples at the initial stage of the addition process, due to there being insufficient alginate molecules present; however, when large numbers of

alginate molecules were present in the continuous phase after adding higher levels of alginate solutions, the magnetic stirring force was not high enough to break bridging-flocculated droplets and promote further adsorption of alginate molecules at the surfaces of SPI-coated droplets, to form stable emulsions without droplet aggregates.

2.3.1.3. Mechanism of structuring emulsions on mixing of dispersions

In order to understand the effect of the addition sequence of dispersions on the structure, stability and rheological properties of emulsions produced by electrostatic adsorption, emulsion samples $E_{0.1}A_{0.2}$ and $A_{0.2}E_{0.1}$ were compared (**Figures 2-1 and 2-2**). $E_{0.1}A_{0.2}$ and $A_{0.2}E_{0.1}$ were prepared by the same components (i.e., 0.2 wt% alginate solutions and SPI-stabilized emulsions containing 0.1 wt% SPI and 1 wt% oil) but with different addition sequences of dispersions (i.e., adding emulsions into alginate solutions for $E_{0.1}A_{0.2}$ and adding alginate solutions into emulsions for $A_{0.2}E_{0.1}$). **Figures 2-1 and 2-2** show that $E_{0.1}A_{0.2}$ had better stability than $A_{0.2}E_{0.1}$, and that $E_{0.1}A_{0.2}$ contained unflocculated droplets while $A_{0.2}E_{0.1}$ contained flocculated droplets. This indicates that adding protein-stabilized emulsions into oppositely charged polysaccharide solutions is a better way to prepare stable multilayer emulsions induced by electrostatic adsorption than adding polysaccharide solutions into emulsions under mild stirring conditions.

The proposed mechanism is that, when adding protein-stabilized emulsions into oppositely charged polysaccharide solutions slowly, levels of polysaccharide molecules are sufficient at the beginning of the process and protein-coated droplets can be fully covered by polysaccharide molecules through electrostatic interactions, which leads to stable multilayer emulsions (**Figure 2-3A**). However, when the level of added emulsions exceeds the saturation concentration and there are not polysaccharide molecules available in the continuous phase, flocculation occurs because of electrostatic interactions between polysaccharide/protein-coated droplets and the additional protein-stabilized droplets being added. On the other hand, when adding polysaccharide solutions into oppositely charged

protein-stabilized emulsions, protein-stabilized droplets are present in excess at the beginning and they cannot be fully covered by polysaccharide molecules, which leads to bridging flocculation (**Figure 2-3B**). However, mild mixing cannot provide enough energy to break down bridging-flocculated droplets, and then stable emulsions containing unflocculated droplets do not occur, although there are sufficient polysaccharide molecules in the continuous phase after adding high levels of polysaccharide solutions.

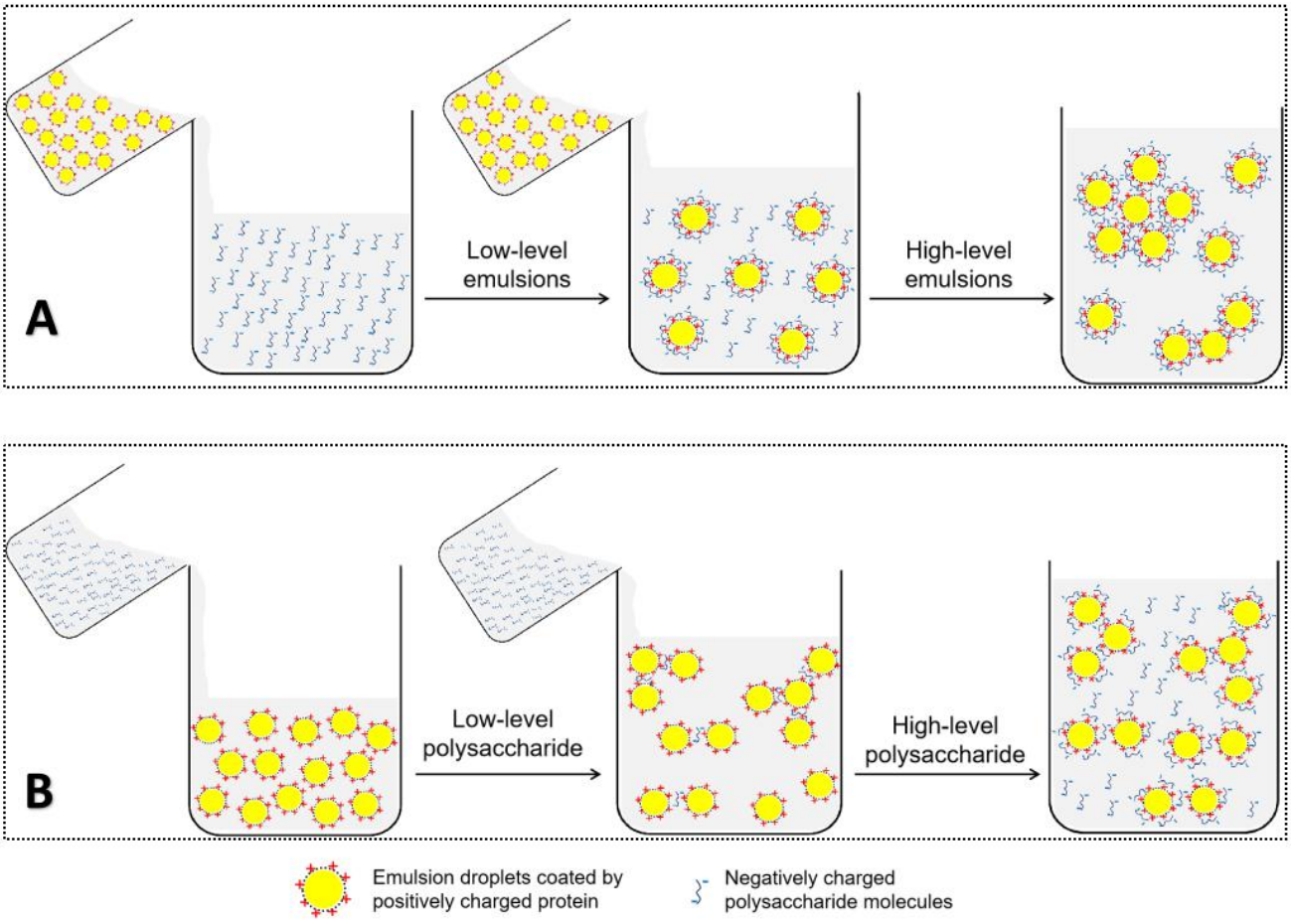

Figure 2-3. A proposed mechanism for the effect of addition sequence of oppositely charged protein-stabilized emulsions and polysaccharide solutions on the structure of emulsions: (A) adding protein-stabilized emulsions into oppositely charged polysaccharide solutions slowly or (B) adding polysaccharide solutions into oppositely charged protein-stabilized emulsions slowly.

This mechanism not only explains the effect of addition sequence of dispersions and polysaccharide/protein ratio on the structure and stability of multilayer emulsions formed by electrostatic interactions between oppositely charged protein–coated droplets and polysaccharide molecules, but also indicates that structuring polysaccharide-based and protein-stabilized emulsion gels can be controlled by changing the addition sequence of dispersions and adjusting the polysaccharide/protein ratio. It can be assumed that adding low levels of protein-stabilized emulsions into polysaccharide solutions tends to lead to formation of emulsion gels containing unflocculated emulsion droplets; however, adding polysaccharide solutions into protein-stabilized emulsions tends to give emulsion gels containing flocculated emulsion droplets. Therefore, further research was carried out to investigate the effect of addition sequence of dispersions on the structural and rheological properties of alginate-based and alginate/SPI-stabilized emulsion gels.

2.3.2. Structuring alginate/SPI-stabilized emulsion gels by addition sequence

2.3.2.1. Morphological and structural properties of emulsion gels

Figure 2-4A–F shows the visual appearance and micro-structure of gels prepared from the control sample $E_0A_{0.4}$, sample $E_{0.1}A_{0.4}$ and sample $A_{0.4}E_{0.1}$, respectively. Alginate gels (i.e., control samples) were transparent with many bubbles in matrices (**Figures 2-4A and 2-4D**). This was because the internal gelation was used in this study to trigger the formation of alginate-based gels, in which calcium ions are liberated gradually from the insoluble $CaCO_3$ particles by the interaction between GDL and $CaCO_3$, followed by the Ca^{2+}-induced association of alginate chains; CO_2 was also produced during this process and thus small CO_2 gas bubbles occurred in gel matrices.

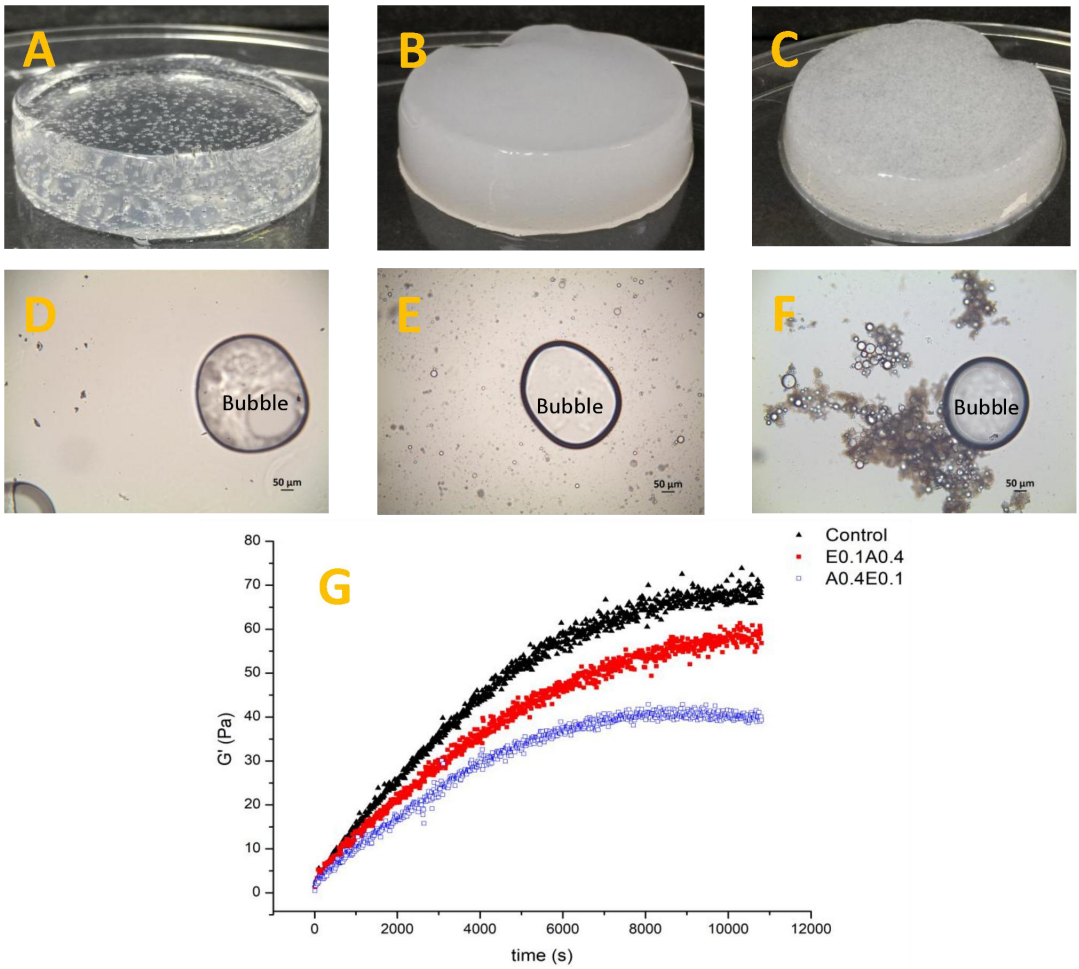

Figure 2-4. (A–C) Visual appearance and (D–F) micro-structure of emulsion gels prepared from (A and D) the control sample (i.e., adding deionized water (pH 3.0) into 0.4 wt% alginate solutions, 1:1), (B and E) sample $E_{0.1}A_{0.4}$ (i.e., adding emulsions containing 0.1 wt% SPI and 1.0 wt% oil into alginate solutions) and (C and F) sample $A_{0.4}E_{0.1}$ (i.e., adding alginate solutions into emulsions), respectively. (G) The gelation kinetics of the control sample, sample $E_{0.1}A_{0.4}$ and sample $A_{0.4}E_{0.1}$ induced by internal gelation.

Emulsion gels produced from sample $E_{0.1}A_{0.4}$ were ivory in colour with L^* values of 36.4 ± 0.2, and CO_2 bubbles also occurred in gel matrices (**Figures 2-4B and 2-4E**). This was because adding emulsions into alginate solutions (i.e., sample $E_{0.1}A_{0.4}$) led to the formation of unflocculated multilayer droplets evenly distributed in mixed emulsions with high turbidity (i.e., the absorbance of 0.470 ± 0.002 at 600 nm) and thus the formation of emulsion gels with uniform opaque appearance (Lin, Kelly, Maidannyk, et al., 2020). In contrast, emulsion gels produced from sample $A_{0.4}E_{0.1}$ were semi-transparent with L^* values

of 35.9 ± 0.3, and emulsion aggregates and CO_2 gas bubbles distributed in the matrices (**Figure 2-4C**). This was because adding alginate solutions into emulsions (i.e., sample $A_{0.4}E_{0.1}$) tended to form unstable emulsions containing flocculated droplets (**Figures 2-4F**) with low turbidity (i.e., absorbance values of 0.245 ± 0.014 at 600 nm) and thus resulted in the formation of emulsion gels with an inhomogeneous appearance.

These results indicate that the structural and morphological properties of alginate-based and alginate/SPI-stabilized emulsion gels are affected by the addition sequence of SPI-stabilized emulsions and alginate solutions for emulsion preparation. In addition, many studies have indicated that structures of emulsion gels (e.g., the matrix structure and state of droplets) affected their mechanical properties (Chen et al., 2000; Lin, Kelly, & Miao, 2020; Tang et al., 2011), so the effect of the addition sequence of SPI-stabilized emulsions and alginate solutions on the gelation kinetics of emulsion gels was further investigated.

2.3.2.2. Gelation kinetics of alginate-based emulsion gels

Figure 2-4G shows the evolution of the dynamic storage modulus (G') of the control sample, sample $E_{0.1}A_{0.4}$ and sample $A_{0.4}E_{0.1}$ during gelation. G' values of the control sample increased up to 2.5 h and then reached a plateau during gelation. The progressive introduction of calcium ions which results from the interaction between GDL and $CaCO_3$ leads to the progressive gelation of alginate molecules and gradually increased G' value of alginate gels. Many factors can influence the kinetics of alginate gel formation, such as the molecular weight of alginate, alginate concentration, calcium concentration, and applied shear rate during rheological measurements (Farrés & Norton, 2014).

The storage modulus of sample $E_{0.1}A_{0.4}$ reached a plateau at 2.5 h, which was similar to the control sample during gelation (**Figure 2-4G**). This was because emulsions produced by adding SPI-stabilized emulsions into oppositely charged alginate solutions (i.e., $E_{0.1}A_{0.4}$) tended to contain unflocculated droplets, which did not significantly affect the alginate concentration in the continuous phase, although some alginate molecules were adsorbed at

the O/W interfaces. In addition, sample $E_{0.1}A_{0.4}$ had lower G' values than the control sample during gelation, and the G' values of the control sample and sample $E_{0.1}A_{0.4}$ were 68.5 ± 1.6 Pa and 59.4 ± 1.8 Pa at plateau, respectively (**Figure 2-4G**). This was because the mechanical properties of emulsion gels are determined by the matrix (i.e., matrix material and gelation mechanism), emulsion droplets (i.e., oil type, oil content, and droplet size) and the interaction between them (i.e., active and inactive fillers) (Lin, Kelly, & Miao, 2020; Sala et al., 2009).

Positively charged SPI-coated droplets are active fillers in negatively charged alginate-based matrices in the current study, due to electrostatic attraction between them (Sala et al., 2009). According to the Kerner model (Kerner, 1956), introducing active fillers into gels can increase the mechanical properties of gels (i.e., $G'_{emulsion\ gels} > G'_{hydrogels}$ or G'_{matrix}). However, the matrix of emulsion gels plays a more important role than emulsion droplets in determining the mechanical properties of emulsion gels (i.e., $G'_{emulsion\ gels} = G'_{matrix} + 0.22\sim0.27G'_{matrix}$ according to the Kerner model) (Lin, Kelly, Maidannyk, et al., 2021). When SPI-stabilized emulsions are mixed with alginate solutions, some unadsorbed insoluble SPI particles are also introduced into the continuous phase of mixtures, which may negatively affect Ca^{2+}-induced association of alginate molecules during gelation and decrease the mechanical properties of alginate-based emulsion gels. Our previous study has indicated that alginate- and SPI/alginate-based gel beads had similar gelation kinetics (i.e., Young's modulus increased up to 6 min) induced by the external gelation, but SPI/alginate-based gel beads had lower Young's modulus than alginate-based gel beads, probably due to insoluble SPI molecules acting as solid barriers in alginate gels (Lin, Kelly, Maidannyk, et al., 2020).

Figure 2-4G also shows that sample $A_{0.4}E_{0.1}$ had a different gelation rate (i.e., reached the plateau faster, with a lower G' value of 40.3 ± 0.7 Pa at 1.9 h, compared to the control sample and sample $E_{0.1}A_{0.4}$). This was because emulsions (i.e., $A_{0.4}E_{0.1}$) produced by adding alginate solutions into oppositely charged SPI-stabilized emulsions tended to contain

flocculated droplets, which entrapped some alginate molecules in aggregates (McClements, 2015). Although the Kerner model as modified by Lewis and Nielsen indicates that aggregated droplets can increase the effective volume fraction of fillers and modulus of emulsion gels (Lewis & Nielsen, 1970), the matrix of emulsion gels plays a more important role than emulsion droplets in affecting the mechanical properties of emulsion gels. Adding alginate solutions into oppositely charged SPI-stabilized emulsions not only reduces the alginate concentration in the continuous phase, because of the formation droplet flocculation entrapping some alginate molecules, but also introduces some unadsorbed insoluble SPI particles into the continuous phase, which decreased both the G' values of emulsion gels and the time needed to reach the plateau during gelation.

2.4. Conclusions

The stability and structure of emulsions involving electrostatic protein-polysaccharide interactions can be influenced by the addition sequence of oppositely charged dispersions. Adding a low concentration of protein-stabilized emulsions into polysaccharide solutions is a better method to prepare stable emulsions than adding polysaccharide solutions into protein-stabilized emulsions with mild stirring. In addition, visual appearance, droplet structure and gel strength of emulsion gels can also be adjusted by the addition sequence of oppositely charged dispersions for emulsion preparation. Emulsions which were prepared by adding SPI-stabilized emulsions (0.1 wt% SPI and 1.0 wt% oil) into 0.4 wt% alginate solutions (i.e., $E_{0.1}A_{0.4}$) led to emulsion gels with more unflocculated droplets, higher L^* and modulus values and slower gelation kinetics than emulsion gels prepared from sample $A_{0.4}E_{0.1}$ (i.e., adding 0.4 wt% alginate solutions into SPI-stabilized emulsions containing 0.1 wt% SPI and 1.0 wt% oil). However, this study mainly focused on the effect of addition sequence on the mechanical and structural properties of emulsion gels, so further research on the application of above different emulsion gels (e.g., for encapsulation of food nutrients or as fat replacers) is needed.

References

Albano, K. M., Cavallieri, Â. L. F., & Nicoletti, V. R. (2019). Electrostatic interaction between proteins and polysaccharides: Physicochemical aspects and applications in emulsion stabilization. *Food Reviews International, 35*, 54-89.

Azarikia, F., Abbasi, S., Scanlon, M. G., & McClements, D. J. (2017). Emulsion stability enhancement against environmental stresses using whey protein–tragacanthin complex: Comparison of layer-by-layer and mixing methods. *International Journal of Food Properties, 20*, 2084-2095.

Bokkhim, H., Bansal, N., Grøndahl, L., & Bhandari, B. (2016). *In-vitro* digestion of different forms of bovine lactoferrin encapsulated in alginate micro-gel particles. *Food Hydrocolloids, 52*, 231-242.

Chen, J., Dickinson, E., Langton, M., & Hermansson, A. M. (2000). Mechanical properties and microstructure of heat-set whey protein emulsion gels: Effect of emulsifiers. *LWT - Food Science and Technology, 33*, 299-307.

Evans, M., Ratcliffe, I., & Williams, P. A. (2013). Emulsion stabilisation using polysaccharide–protein complexes. *Current Opinion in Colloid & Interface Science, 18*, 272-282.

Farrés, I. F., & Norton, I. (2014). Formation kinetics and rheology of alginate fluid gels produced by in-situ calcium release. *Food Hydrocolloids, 40*, 76-84.

Feng, W., Yue, C., Ni, Y., & Liang, L. (2018). Preparation and characterization of emulsion-filled gel beads for the encapsulation and protection of resveratrol and *α*-tocopherol. *Food Research International, 108*, 161-171.

Golkar, A., Nasirpour, A., & Keramat, J. (2015). *β*-lactoglobulin-Angum gum (Amygdalus Scoparia Spach) complexes: Preparation and emulsion stabilization. *Journal of Dispersion Science and Technology, 36*, 685-694.

Guzey, D., & McClements, D. J. (2006). Formation, stability and properties of multilayer emulsions for application in the food industry. *Advances in Colloid and Interface Science, 128*, 227-248.

Guzey, D., & McClements, D. J. (2007). Impact of electrostatic interactions on formation and stability of emulsions containing oil droplets coated by *β*-lactoglobulin−pectin complexes. *Journal of Agricultural and Food Chemistry, 55*, 475-485.

Harnsilawat, T., Pongsawatmanit, R., & McClements, D. J. (2006). Influence of pH and ionic strength on formation and stability of emulsions containing oil droplets coated by *β*-lactoglobulin−alginate interfaces. *Biomacromolecules, 7*, 2052-2058.

Herrero, A. M., Ruiz-Capillas, C., Pintado, T., Carmona, P., & Jiménez-Colmenero, F. (2018). Elucidation of lipid structural characteristics of chia oil emulsion gels by Raman spectroscopy and their relationship with technological properties. *Food Hydrocolloids, 77*, 212-219.

Kerner, E. (1956). The elastic and thermo-elastic properties of composite media. *Proceedings of the Physical Society. Section B, 69*, 808.

Lević, S., Lijaković, I. P., Đorđević, V., Rac, V., Rakić, V., Knudsen, T. Š., et al. (2015). Characterization of sodium alginate/D-limonene emulsions and respective calcium alginate/*D*-limonene beads produced by electrostatic extrusion. *Food Hydrocolloids, 45*, 111-123.

Lewis, T. B., & Nielsen, L. E. (1970). Dynamic mechanical properties of particulate-filled composites. *Journal of Applied Polymer Science, 14*, 1449-1471.

Lin, D., Kelly, A. L., Maidannyk, V., & Miao, S. (2020). Effect of concentrations of alginate, soy protein isolate and sunflower oil on water loss, shrinkage, elastic and structural properties of alginate-based emulsion gel beads during gelation. *Food Hydrocolloids, 108,* 105998.

Lin, D., Kelly, A. L., Maidannyk, V., & Miao, S. (2021). Effect of structuring emulsion gels by whey or soy protein isolate on the structure, mechanical properties, and *in-vitro* digestion of alginate-based emulsion gel beads. *Food Hydrocolloids, 110*, 106165.

Lin, D., Kelly, A. L., & Miao, S. (2020). Preparation, structure-property relationships and applications of different emulsion gels: Bulk emulsion gels, emulsion gel particles, and fluid emulsion gels. *Trends in Food Science & Technology, 102*, 123-137.

Liu, L., Zhao, Q., Liu, T., Kong, J., Long, Z., & Zhao, M. (2012). Sodium caseinate/carboxymethylcellulose interactions at oil–water interface: Relationship to emulsion stability. *Food Chemistry, 132*, 1822-1829.

Lorenzo, G., Zaritzky, N., & Califano, A. (2013). Rheological analysis of emulsion-filled gels based on high acyl gellan gum. *Food Hydrocolloids, 30*, 672-680.

McClements, D. J. (2005). Theoretical analysis of factors affecting the formation and stability of multilayered colloidal dispersions. *Langmuir, 21*, 9777-9785.

McClements, D. J. (2015). *Food emulsions: principles, practices, and techniques*. Boca Raton, FL: CRC press.

Moreau, L., Kim, H.-J., Decker, E. A., & McClements, D. J. (2003). Production and characterization of oil-in-water emulsions containing droplets stabilized by *β*-lactoglobulin−pectin membranes. *Journal of Agricultural and Food Chemistry, 51*, 6612-6617.

Paradiso, V. M., Giarnetti, M., Summo, C., Pasqualone, A., Minervini, F., & Caponio, F. (2015). Production and characterization of emulsion filled gels based on inulin and extra virgin olive oil. *Food Hydrocolloids, 45*, 30-40.

Ruffin, E., Schmit, T., Lafitte, G., Dollat, J.-M., & Chambin, O. (2014). The impact of whey protein preheating on the properties of emulsion gel bead. *Food Chemistry, 151*, 324-332.

Sala, G., Van Vliet, T., Stuart, M. A. C., Van Aken, G. A., & Van de Velde, F. (2009). Deformation and fracture of emulsion-filled gels: effect of oil content and deformation speed. *Food Hydrocolloids, 23*, 1381-1393.

Salminen, H., & Weiss, J. (2014). Electrostatic adsorption and stability of whey protein–pectin complexes on emulsion interfaces. *Food Hydrocolloids, 35*, 410-419.

Soukoulis, C., Tsevdou, M., Andre, C. M., Cambier, S., Yonekura, L., Taoukis, P. S., & Hoffmann, L. (2017). Modulation of chemical stability and *in vitro* bioaccessibility of beta-carotene loaded in kappa-carrageenan oil-in-gel emulsions. *Food Chemistry, 220*, 208-218.

Su, J., He, X., Guo, Z., Jian, J., Gao, Y., & Yuan, F. (2016). Impact on morphological characterization and emulsion stability of lactoferrin–beet pectin electrostatic complexes. *Journal of Dispersion Science and Technology, 37*, 927-940.

Tang, C. H., Chen, L., & Foegeding, E. A. (2011). Mechanical and water-holding properties and microstructures of soy protein isolate emulsion gels induced by $CaCl_2$, glucono-delta-lactone (GDL), and transglutaminase: Influence of thermal treatments before and/or after emulsification. *Journal of Agricultural and Food Chemistry, 59*, 4071-4077.

Tang, C. H., Luo, L. J., Liu, F., & Chen, Z. (2013). Transglutaminase-set soy globulin-stabilized emulsion gels: Influence of soy *β*-conglycinin/glycinin ratio on properties, microstructure and gelling mechanism. *Food Research International, 51*, 804-812.

Tavernier, I., Patel, A. R., Van der Meeren, P., & Dewettinck, K. (2017). Emulsion-templated liquid oil structuring with soy protein and soy protein : *κ*-carrageenan complexes. *Food Hydrocolloids, 65*, 107-120.

Urbonaite, V., De Jongh, H., Van Der Linden, E., & Pouvreau, L. (2015). Water holding of soy protein gels is set by coarseness, modulated by calcium binding, rather than gel stiffness. *Food Hydrocolloids, 46*, 103-111.

Wang, Z., Neves, M. A., Kobayashi, I., Uemura, K., & Nakajima, M. (2013). Preparation, characterization, and *in vitro* gastrointestinal digestibility of oil-in-water emulsion–agar gels. *Bioscience, Biotechnology, and Biochemistry*, 120659.

Xiong, W., Ren, C., Tian, M., Yang, X., Li, J., & Li, B. (2018). Emulsion stability and dilatational viscoelasticity of ovalbumin/chitosan complexes at the oil-in-water interface. *Food Chemistry, 252*, 181-188.

Xu, W., Huang, L., Jin, W., Ge, P., Shah, B. R., Zhu, D., & Jing, J. (2019). Encapsulation and release behavior of curcumin based on nanoemulsions-filled alginate hydrogel beads. *International Journal of Biological Macromolecules, 134*, 210-215.

Ye, A. (2008). Complexation between milk proteins and polysaccharides via electrostatic interaction: Principles and applications–a review. *International Journal of Food Science & Technology, 43*, 406-415.

Yuan, Y., Wan, Z.-L., Yin, S.-W., Teng, Z., Yang, X.-Q., Qi, J.-R., & Wang, X.-Y. (2013). Formation and dynamic interfacial adsorption of glycinin/chitosan soluble complex at acidic pH: Relationship to mixed emulsion stability. *Food Hydrocolloids, 31*, 85-93.

Zheng, H., Mao, L., Cui, M., Liu, J., & Gao, Y. (2020). Development of food-grade bigels based on *κ*-carrageenan hydrogel and monoglyceride oleogels as carriers for *β*-carotene: Roles of oleogel fraction. *Food Hydrocolloids*, 105855.

CHAPTER THREE

Effect of Concentrations of Alginate, Soy Protein Isolate and Sunflower Oil on Physical and Structural Properties of Emulsion Gel Beads during Gelation

Chapter 3 was published in:

Lin, D., Kelly, A. L., Maidannyk, V., & Miao*, S. (2020). Effect of concentrations of alginate, soy protein isolate and sunflower oil on water loss, shrinkage, elastic and structural properties of alginate-based emulsion gel beads during gelation. *Food Hydrocolloids, 108*, 105998.

The work contained in this chapter was undertaken and written mainly by myself with Dr. Valentyn Maidannyk's help on CLSM operation and specific contributions from supervisors.

Abstract

The aim of this chapter was to investigate the influence of concentrations of sodium alginate (0.5%–1.5% in the continuous phase of an emulsion), soy protein isolate (SPI, 0.5%–2.0% in the continuous phase) and oil phase (10%–40% in the emulsion) on the properties (including water loss, shrinkage, morphological, elastic, and structural properties) of emulsion gel beads during gelation (0–30 min). Gel beads were prepared with external gelation by dropping emulsions into $CaCl_2$ solutions using pipettes. The Young's modulus of emulsion gel beads kept increasing during gelation before reaching a plateau accompanied by syneresis (i.e., water loss), shrinkage, and structural tightening. SPI adsorbed at the surface of oil droplets could prevent coalescence of droplets during gelation. Additionally, increasing concentrations of sodium alginate and oil increased the Young's modulus of gel beads. Water loss decreased with increasing contents of alginate, SPI and oil, and shrinkage could be diminished by increasing alginate and oil contents.

Keywords: Alginate; Elastic property; Emulsion gel bead; Microstructure; Shrinkage; Soy protein isolates.

3.1. Introduction

Emulsion gels, also called emulgels, are a complex colloidal material which have some properties of both emulsions and gels (Dickinson, 2012). During the last decade, emulsion gels have received growing interest, due to their advantages compared to emulsions, such as higher storage stability by reducing oil and water phase movement and lipid oxidation (Ma, Wan, & Yang, 2017) and slower intestinal drug release, due to improved protective effects against gastric and intestinal phases (Corstens et al., 2017; Guo, Bellissimo, & Rousseau, 2017). In order to produce emulsion gels, emulsions are first prepared by mixing gelling agents, emulsifiers and oil and then turned into gels by different gelation mechanisms.

The choice of matrix materials and emulsifiers is the key factor in structuring emulsion gels. Proteins (e.g., soy protein isolate (SPI) and whey protein isolate (WPI)) and polysaccharides (e.g., agar and gellan gum) have been widely investigated as gelling agents in the formation of emulsion gels (Brito-Oliveira et al., 2017; Geremias-Andrade et al., 2017; Guo et al., 2017). Different gelling agents can form different gelation structures, and the gelation mechanism (e.g., heat, high pressure, acidification, enzymatic treatment, and addition of ions) for different gelling agents differs (Dickinson, 2012), which can affect the properties of emulsion gels and encapsulated food nutrients. Both synthetic (e.g., Tween 80 and Span 80) and natural (e.g., proteins, egg lecithin, and soy lecithin) emulsifiers can be used to prepare emulsion gels. Lipid droplets in emulsion gels can be divided into active and inactive fillers according to the interactions between gelling agents and emulsifier-coated lipid droplets (Van Vliet, 1988; Yang et al., 2020), which can also influence the properties of emulsion gels (Geremias-Andrade et al., 2017).

Alginate, a linear unbranched natural polysaccharide, is derived from brown seaweed extracts (*Phaeophyceae*) (King, 1983) and composed of two monomeric isomers: β-(1→4)-linked *D*-mannuronic acid (M) residues and α-(1→4)-linked *L*-guluronic acid (G) residues (Ching, Bansal, & Bhandari, 2017). Alginate-based emulsion gels received high attention in recent years (Lević et al., 2015; Qu et al., 2016; Zeeb et al., 2015). Alginate monomers can

form gels by ionic cross-linking with divalent cations (mostly calcium cations in the food industry) (King, 1983). External gelation and internal gelation are two methods used to prepare alginate-based emulsion gels. Pintado et al. (2015) added $CaSO_4$ into an alginate-based emulsion to directly produce an alginate-based emulsion gel (i.e., external gelation). Sato, Moraes, & Cunha (2014) added CaEDTA to an alginate-based emulsion first, after which an acid was introduced to liberate calcium ions (i.e., internal gelation). Compared these two methods, Puguan, Yu, and Kim (2014) found that gels formed by external gelation had a smoother surface and denser inner structure. In addition, alginate-based gels are not sensitive to gastric fluids, and can protect the encapsulated nutrients from harsh gastric environment, and the remaining gel structures can be further disrupted during intestinal digestion accompanied by the release of encapsulated compounds (Zhang et al., 2016).

Previous studies mainly focused on the formulation, structural properties, mechanical properties, stability, and digestion of alginate-based emulsion gels. However, there are few reports on the gelation process of alginate-based emulsion gels. It has been indicated that, during the gelation process of alginate hydro-gels prepared by external gelation, calcium cations can diffuse into alginate drops after being dropped into a calcium chloride solution (Rehm, 2009). Syneresis also occurs during this gelation process, with a consequent decrease in dimensions of gel beads (Quong et al., 1998; Rehm, 2009). However, the gelation process of alginate-based emulsion gels may differ from that of alginate gels, because the presence of lipids and emulsifiers in emulsions may affect the gelation process. Understanding the gelation process of alginate-based emulsion gels may help to produce emulsion gels with specific properties (e.g., size, water content, mechanical properties) by controlling gelation time, formulation, preparation methods and processing technologies. Therefore, further studies are needed to understand how alginate, emulsifiers and oil affect the gelation process of emulsion gel beads.

The purpose of this study was thus to investigate the gelation process of alginate-based emulsion gel beads. In order to improve the encapsulation efficiency and hygroscopicity of

alginate-based emulsion gels, proteins (e.g., lupin protein and WPI) can be used as emulsifiers (Corstens et al., 2017; Piornos et al., 2017), and polysaccharides (e.g., *Prosopis alba* exudate gum and chitosan) can be used as structural strengthening agents (Natrajan et al., 2015; Vasile, Judis, & Mazzobre, 2018). In this study, SPI was thus introduced as surfactant, due to its good emulsifying property (Lin et al., 2017; Nishinari et al., 2014). In addition, the external gelation was used, in order to obtain gel beads with denser structures, compared to internal gelation. Effect of concentrations of alginate, SPI, and sunflower oil on the shrinkage, water loss, elastic and structural properties of alginate-based emulsion gel beads during gelation were investigated.

3.2. Materials and methods

3.2.1. Materials

Defatted soy flour (Bob's Red Mill, Milwaukie, Oregon, USA) and sunflower oil (Aldi Stores Ltd., Kildare, Ireland) were purchased from iHerb and Aldi, respectively. Sodium alginate (viscosity of 1 wt% sodium alginate solution in 0.15 M NaCl at 25°C = 210–340 cP, $\overline{M}$ = 69–117 kDa, and M/G = 71/29) was obtained from Special Ingredients (Chesterfield, UK). Calcium chloride, sodium hydroxide, and hydrochloric acid were purchased from Sigma-Aldrich (St. Louis, MO, USA).

3.2.2. Preparation of soy protein isolate

SPI was prepared according to the method described by Urbonaite et al. (2015). The defatted soy flour was suspended in distilled water at a ratio of 1:10 (w/w) at 45ºC and stirred for 30 min. The pH value was then adjusted to 8.0 with 5 M NaOH, and the solution was stirred for 30 min in the water bath. The supernatant fluid was collected by centrifugation (30 min, 6000×g, 13ºC) (Sorvall LYNX 6000 Superspeed Centrifuge, Thermo Fisher Scientific, Waltham, USA). Protein isolates were obtained by isoelectric precipitation by adjusting the pH value to 4.5 with 6 M HCl. After mild stirring for 12 h at 5ºC, the

suspension was centrifuged (30 min, 6000×g, 7ºC). The sediment was re-suspended three times in deionized water at a ratio of 1:3 (w/w) and filtered by multilayer gauze to remove any remaining insoluble material. The pH value of filtrate was justified to 7.0 with 5 M NaOH. Then, the solution was freeze-dried (Free Zone 12 Freeze Dry System, Labconco Corpotation, Kansas, MO, USA). The dried SPI was kept in polyethylene bags and stored at room temperature. The protein content of SPI powder was 96.29 ± 0.03%.

3.2.3. Preparation of alginate-based and SPI-stabilized emulsions and gel beads

A dispersion of SPI (5.0 wt% in distilled water) was stirred at room temperature for 30 min using a magnetic stirrer, heated at 90ºC for 30 min, and then cooled down to room temperature. For the production of continuous phase, sodium alginate (0.5, 1.0, and 1.5 wt%) was added into the pre-heated SPI solution with adding water to reach final concentrations of SPI (0.5, 1.0, and 2.0% wt) by shearing at 400 rpm for 30 min with a magnetic stirrer and then allowed to rest for 24 h to permit hydration. For the production of O/W emulsion, sunflower oil (10, 20, and 40% wt) was added to above continuous phase and mixed at 18,000 rpm for 2 min with an Ultra-Turrax (IKA-25, Staufen, Germany). Solutions containing 1.0% alginate (1A) and dispersions containing 1.0% alginate and 1.0% SPI (1A1S) were prepared as control samples without mixing at 18,000 rpm for 2 min. **Table 3-1** shows the formulations used for preparing emulsions.

For producing gel beads, the resultant dispersions/solutions were dropped into 2 % (w/w) $CaCl_2 \cdot 2H_2O$ solutions using 5-mL measuring pipettes and a S1 pipette filler (Thermo Fisher Scientific Inc., Waltham, USA). The distance between the tip of pipette and the surface of $CaCl_2$ solutions was fixed at 10 cm. The samples were allowed to gel in $CaCl_2$ solutions for 30 min with mild magnetic stirring, and the resultant beads were rinsed with distilled water. Samples were analyzed immediately for measurement of Young's modulus, shrinkage, water loss, and morphology, and samples were kept in distilled water for observing their structures within 3 hours after being prepared.

Table 3-1. Formulations of experimental emulsions.

Samples	Water phase[a]		Oil content (% wt)
	Alginate content (% wt)	Soy protein content (% wt)	
1A (Control 1)	1.0	0	0
1A1S (Control 2)	1.0	1.0	0
1A1S20O	1.0	1.0	20
0.5A1S20O	0.5	1.0	20
1.5A1S20O	1.5	1.0	20
1A0.5S20O	1.0	0.5	20
1A2S20O	1.0	2.0	20
1A1S10O	1.0	1.0	10
1A1S40O	1.0	1.0	40

[a] The content of water phase was adjusted according to the oil content in the formulation.

3.2.4. Properties of dispersions/solutions

3.2.4.1. Structures

Confocal scanning laser microscopy (CLSM) was used to observe micro-structure of dispersions/emulsions. Dispersion/emulsion samples (500 μL) were transferred to a glass slide and stained with 50 μL of a mixture of Nile red (0.1%, w/v, in polyethylene glycol-200) and fast green (0.1%, w/v, in distilled water) at a ratio of 3:1. Confocal observation was performed using a Leica TCS SP5 microscope (Leica Microsystems GmbH, Wetzlar, Germany) at excitation and emission wavelengths of 488 nm and 633 nm, provided by an argon laser and a HeNe laser, respectively.

3.2.4.2. Viscosity

The viscosity of dispersions/solutions was tested at 25ºC using an AR 2000ex rheometer (TA Instruments, Crawley, UK) with an aluminium parallel plate (60 mm in diameter, and 0.5 mm in gap). Each sample was added in the middle of Peltier plate and allowed to stand

for 2 min before testing. The flow measurement was performed over a shear rate range of 0.1 to 100 s^{-1}, and viscosity (η) was obtained from the data analysis software.

3.2.5. Properties of emulsion gel beads

3.2.5.1. Micro-structure of gel beads

CLSM was used to observe micro-structure of gel beads. Each gel bead was cut into a thin layer (~ 1 mm), transferred to a glass slide, and stained with a mixture of Nile red (0.1%, w/v, in polyethylene glycol-200) and fast green (0.1%, w/v, in distilled water) at a ratio of 3:1. Confocal observation was performed as described in Section 3.2.4.1.

3.2.5.2. Young's modulus of gel beads

The Young's modulus of gel beads during gelation at 1, 2, 3, 4, 5, 6, 8, 10, 20, and 30 min were analyzed by a TA.XT Plus texture analyzer (Stable Micro System, Godalming, UK) according to the method described by Ching, Bansal, & Bhandari (2016) with a minor change. The surface of samples was dried with dry paper before testing. Compression tests were performed using a cylinder probe of 10-mm diameter and a 5-kg load cell. The samples were compressed to 30% strain at a crosshead speed of 0.1 mm/s, and five beads with same composition were examined one after another. Due to their ellipsoidal shapes, the cross-sectional area of samples was calculated after measuring the major axis and minor axis of samples after being placed on the platform of texture analyzer. The Young's modulus of each sample was calculated as the gradient of the stress vs. strain curve in the 5–15% strain region, where stress and strain showed good linearity.

3.2.5.3. Water loss of gel beads

The water loss of samples during gelation was determined at 1, 2, 3, 4, 5, 6, 8, 10, 20, and 30 min after dispersions/solutions were dropped into calcium chloride solutions. In this study, the water loss means the decreased water in gel beads during gelation compared to the

original dispersions/solutions. Five gel particles were obtained from calcium chloride solutions and washed with distilled water. After drying the surface, the initial weight of 5 beads was weighted (W'_i) and then they were dried in an oven at 80ºC until constant weight (W'_d). The initial weight (W_i) and the weight after drying (W_d) of dispersions/solutions (5 drops) were determined by the same method. Thus, the water loss was calculated from Eq. (3-1), if we assumed that the main content (i.e., alginate, SPI, and oil) of gel beads have no significant change during gelation, and the experiment was replicated three times:

$$\text{Water loss } (\%) = \left(\frac{W_i - W_d}{W_i} - \frac{W_d}{W_i} \times \frac{W'_i - W'_d}{W'_d}\right) \times 100\% \quad (3\text{-}1).$$

3.2.5.4. Shrinkage of gel beads

The shrinkage rate of gel beads was determined at 2, 4, 6, 8, 10, 20, and 30 min after dispersions/solutions were dropped into calcium chloride solutions. Five gel beads were obtained from the calcium chloride solutions and washed with distilled water. After drying the surface, photographs of gel beads were taken using a camera. The major semi-axis (r'_{max}) and minor semi-axis (r'_{min}) of gel beads were measured by using a digital vernier calliper, and the section area (A'_s) was calculated from Eq. (3-2). The major semi-axis (r_{max}) and minor semi-axis (r_{min}) of gel beads after gelation for 1 min were measured, and the section area (A_s) was also calculated from Eq. (3-2). The section shrinkage rate of gel beads was calculated from Eq. (3-2):

$$Section\ shrinkage\ rate\ (\%) = \frac{A_s - A'_s}{A_s} = \frac{3.14 \times r_{max} \times r_{min} - 3.14 \times r'_{max} \times r'_{min}}{3.14 \times r_{max} \times r_{min}} \times 100\% \quad (3\text{-}2).$$

It should be noted that the section shrinkage rate of samples during gelation process was compared to the section area of samples after gelation for 1 min in this study.

3.3. Results and discussion

3.3.1. Structural properties of gel beads

Structural properties are important for emulsion gels because they can influence mechanical properties of emulsion gels and release behavior of encapsulated nutrients. Many factors (e.g., structures of the gel matrix, structures of emulsion droplets, and interactions between the gel matrix and droplets) can influence the structures of overall emulsion gels. Therefore, the effect of concentrations of alginate, SPI and oil on the structures of emulsions and emulsion gels was investigated in this study.

Figure 3-1 shows the structures of emulsions/dispersions before gelation and gel beads after gelation for 30 min. In sample 1A1S, SPI formed aggregates and dispersed in alginate solutions (**Figures 3-1A and 3-1V**). This was because SPI was heated at 90ºC for 30 min in this study, and thus the solubility of SPI decreased, due to denaturation; in addition, denatured SPI exposed hydrophobic residues and thus formed aggregations in alginate solutions (Wagner & Añón, 1990). After mixing the 1A1S dispersion with oil, SPI molecules can move from the continuous phase to the O/W interfaces and are adsorbed at the surfaces of oil droplets (comparing **Figures 3-1A and 3-1B**), due to their amphipathic nature and emulsifying capacity. Hydrophobic groups of SPI adsorbed on the surface of oil droplets, and hydrophilic groups connected with the continuous phase, acting as a steric barrier against coalescence of oil droplets (Nishinari et al., 2014). However, increasing the alginate concentration to 1.5% led to more SPI aggregations in the continuous phase (comparing **Figures 3-1B and 3-1C**), because the higher viscosity of the continuous phase of emulsions hindered SPI from moving to the oil–water interfaces (Tavernier et al., 2017). Higher SPI concentrations resulted in more SPI being adsorbed at the surface of oil droplets but led to more obvious flocculation of oil droplets (comparing **Figures 3-1B and 3-1D**), probably due to the depletion flocculation of droplets coated by excessive amount of SPI (Moschakis, Murray, & Biliaderis, 2010). In addition, increasing oil content of emulsions

resulted in more compacted gel structures (comparing **Figures 3-1B and 3-1E**), due to the decreased ratio of the water phase to the oil phase.

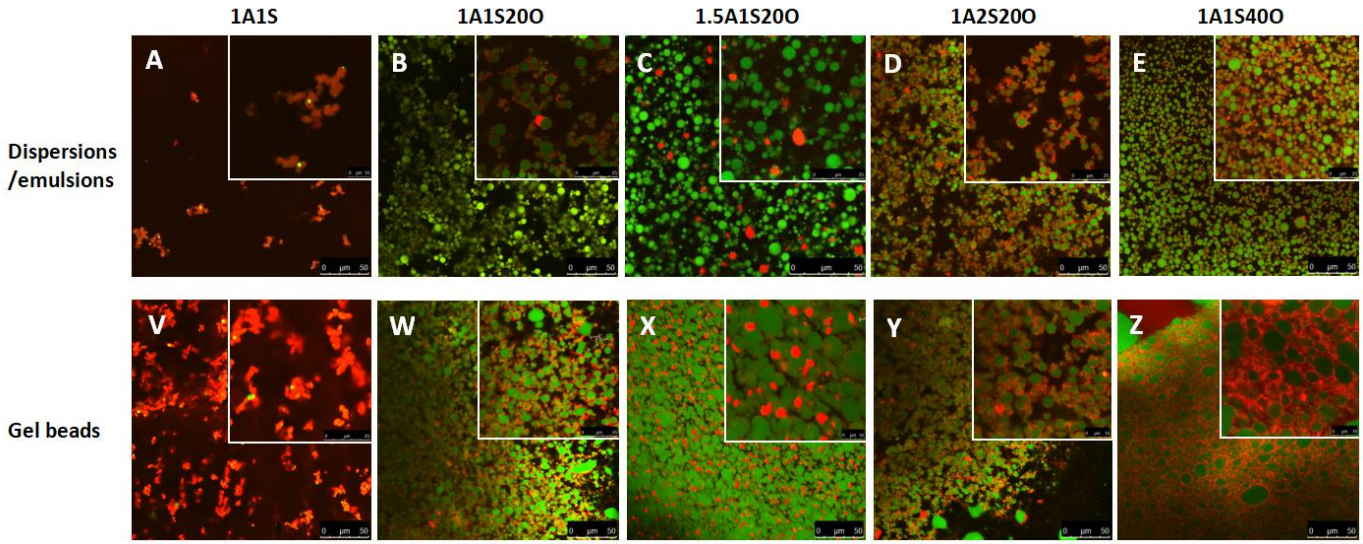

Figure 3-1. CLSM images of dispersions/emulsions (A–E) and gel beads (V–Z) after gelation for 30 min. SPI and sunflower oil were stained by red and green, respectively.

Figure 3-1 also indicates that there were more dark sections in emulsions/dispersions than gel beads in all samples, which indicates that syneresis and shrinkage of the continuous phase (i.e., the gel matrix) during gelation led to more compact filler structures. In addition, the concentrations of SPI, alginate and oil could affect the stability of droplets during gelation. As shown in **Figures 3-1B and 3-1W**, SPI-coated droplets in sample 1A1S20O could maintain their structures during gelation. This was because SPI could stabilize the O/W emulsions, and gelation, syneresis and shrinkage mainly occurred in the continuous phase during gelation, which had no significant effects on the structures of emulsion droplets. Similarly, it was found that WPI-aggregate-stabilized emulsions were stable during the gelation period (Rosa et al., 2006). Additionally, higher SPI concentration resulted in more stable droplet structures during gelation, probably because of more SPI being adsorbed at the surface of oil droplets (**Figures 3-1D and 3-1Y**). However, increasing the alginate concentration to 1.5% led to coalescence of droplets during gelation (**Figures 3-1C and 3-1X**), because increased viscosity of the continuous phase of emulsions hindered SPI from

moving to the oil–water interface and thus resulted in decreased stability of emulsion droplets during gelation. In addition, increasing the oil content to 40% also led to coalescence of droplets during gelation (**Figures 3-1E and 3-1Z**), probably because 1.0% SPI in the continuous phase was not enough to stabilize 40% oil.

3.3.2. Young's modulus of gel beads

3.3.2.1. The profiles of Young's modulus during gelation

Compression tests were carried out to study the elastic properties of gel beads during gelation. Firstly, the effect of introducing SPI and oil into alginate gels on the profiles of Young's modulus during gelation was investigated. As shown in **Figure 3-2A**, the changes of Young's modulus of gel beads containing 1% alginate (1A in short) included three steps: increasing up to 5 min, decreasing between 5 and 10 min, and then reaching a plateau. The Young's modulus of gel beads containing 1% alginate and 1% SPI (sample 1A1S) had a similar trend to that of sample 1A, but the Young's modulus of emulsion gel beads containing 1% alginate, 1% SPI, and 20% oil (sample 1A1S20O) increased first and then reached a plateau at 8 min directly (**Figure 3-2A**). It can be seen that the gelation process of alginate-based gel beads includes the maturation step (increased Young's modulus), the structural collapse step (decreased Young's modulus), and the equilibrium step (unchanged Young's modulus). Therefore, it was assumed that the gelation mechanism of alginate beads prepared by the external gelation has a direct effect on the changes in Young's modulus during gelation.

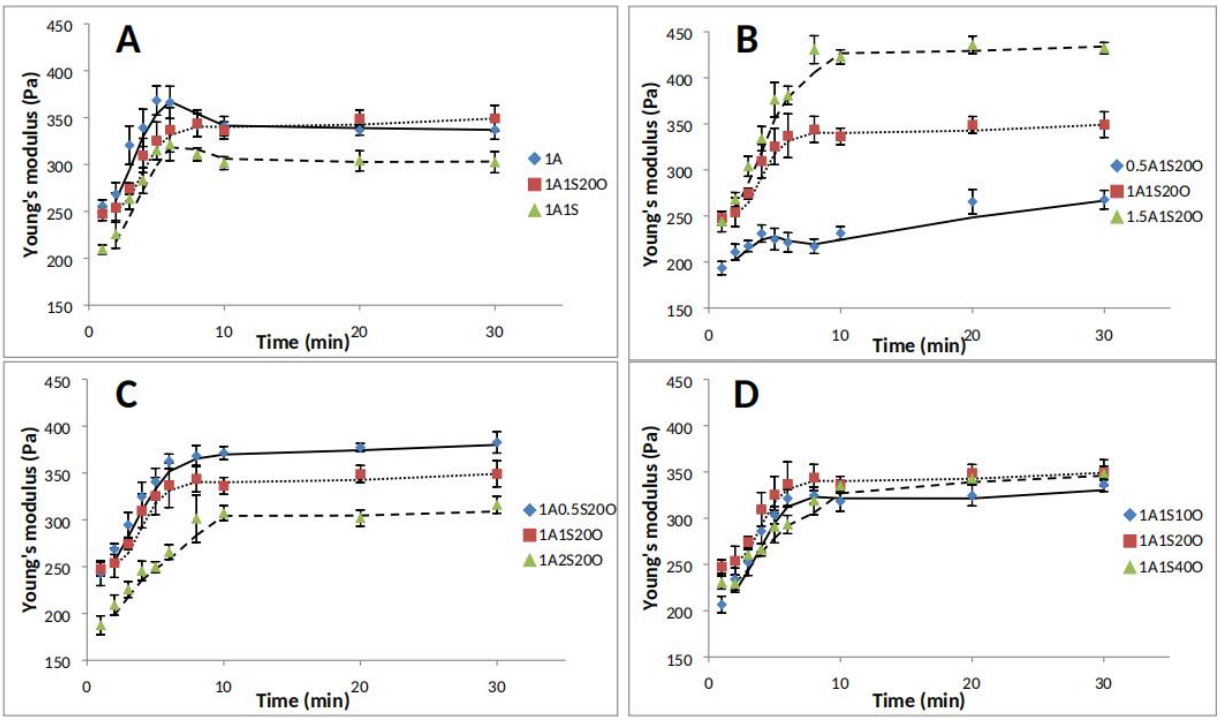

Figure 3-2. Kinetics of Young's modulus of alginate-based gel beads during gelation: (A) control groups; (B) effect of alginate concentrations (0.5–1.5% in the water phase); (C) effect of SPI concentrations (0.5–2.0% in the water phase); and (D) effect of oil contents (10–40% in the emulsion).

After being dropped into calcium chloride solutions, the surface of alginate drops can gel instantaneously, and then Ca^{2+} can diffuse from the $CaCl_2$ solutions into the interior of alginate drops, which leads to the gelation of gel beads from outside to inside and increased Young's modulus (Ching et al., 2017). This process is called the maturation step (Puguan et al., 2014). The concentration of alginate solutions and the size of gel beads are the main factors affecting the Ca^{2+} diffusion into alginate gel beads during gelation. It has been reported that higher alginate concentrations incorporated more calcium ions in alginate gel beads (Quong et al., 1998). In this study, all gel beads were prepared with 2% (w/w) $CaCl_2 \cdot 2H_2O$ solutions, and the size of samples 1A (r_{max} = 2.1 mm and r_{min} = 2.0 mm), 1A1S (r_{max} = 2.2 and r_{min} = 2.1), and 1A1S20O (r_{max} = 2.1 and r_{min} = 2.0) did not significantly differ at the end the maturation step. Therefore, it was assumed that the changes in Young's modulus of samples 1A, 1A1S, and 1A1S20O during the maturation step showed a similar

trend probably because oil and SPI had no significant effect on the Ca^{2+} diffusion from the $CaCl_2$ solutions in alginate gel beads during the maturation step.

After the maturation step, the Young's modulus of samples 1A and 1A1S decreased before reaching a constant value (**Figure 3-2A**). The concentrations of Ca^{2+} and alginate in alginate gel breads decreases from the gel surface to gel core (Quong et al., 1998), which indicates that the gel structure of the outer regions of beads is stronger than that of inside gel beads. Therefore, the fragile core structure of gel beads cannot support the whole structure, which leads to the collapse of the inner structure at the end of the maturation step and thus a decreased Young's modulus (Puguan et al., 2014). However, the Young's modulus of sample 1A1S20O reached the balance directly after the maturation step during gelation (**Figure 3-2A**). This was probably because the structures of sample 1A1S20O are totally different from that of samples 1A and 1A1S. After introducing oil into 1A1S dispersions, oil droplets disperse in the alginate solutions during homogenization, and SPI molecules move to the surface of oil droplets from the continuous phase, due to their emulsifying capacity. The resultant emulsions can turn into emulsion gels after alginate monomers are cross-linked by calcium cations, and shrinkage also occurs during this process. However, oil droplets may act as fillers and help to support the structure of gel beads from collapse after the maturation step during gelation. It has also been indicated that the oil core could support the shell of silica gels from fracture during the sol-gel process (Liang et al., 2011). Therefore, it was also assumed that oil played an important role in preventing the structural collapse of alginate gel beads during gelation.

The effect of concentrations of alginate (**Figure 3-2B**), SPI (**Figure 3-2C**) and sunflower oil (**Figure 3-2D**) on the profiles of Young's modulus of emulsion gel beads during gelation was further investigated. **Figure 3-2B** shows that the Young's modulus of sample 0.5A1S20O increased initially, decreased between 4 and 8 min, and then increased again, before reaching a plateau. In this sample, the structure of gel matrix formed by 0.5% alginate is fragile during the maturation step, which results in severe structural collapse before

compact emulsion droplets can support emulsion gel structures. However, samples 1A1S20O and 1.5A1S20O showed a similar trend, in which the Young's modulus increased up to 8 min and then reached a plateau (**Figure 3-2B**). This indicates that increasing alginate concentrations from 0.5% to 1.5% not only slowed Ca^{2+} diffusion and thus caused a slowing of the maturation step but also formed stronger alginate-based matrix structures and thus protected emulsion gel structures from collapse during gelation. **Figures 3-2C and 3-2D** show that increasing SPI concentrations from 0.5% to 2.0% and oil contents from 10% to 40% had no significant effect on the profiles of Young's modulus during gelation (i.e., reaching the plateau directly after the maturation step at around 8 min during gelation). This was probably because increasing concentrations of SPI and oil had no significant impact on calcium diffusion in emulsion gel beads, and 10% oil was high enough to prevent structural collapse of emulsion gel beads after the maturation step during gelation.

3.3.2.2. Effect of alginate, SPI and oil on the Young's modulus of gel beads after gelation

Mechanical properties are important for emulsion gels because they are closely associated with other properties (e.g., storage stability, oral perception, and controlled release of encapsulated nutrients). Many factors can affect mechanical properties of emulsion gels, such as gel strength of gel matrix structures (i.e., protein and polysaccharide), modulus of filler droplets, and interactions between oil droplets and the gel matrix. Therefore, the effect of concentrations of alginate, oil and SPI on the Young's modulus of emulsion gel beads was investigated in this study, and all samples were compared after they were allowed to gel for 30 min in $CaCl_2$ solutions (**Figures 3-2B–D**).

Figure 3-2B shows that increasing alginate concentrations from 0.5 to 1.5% significantly increased the Young's modulus of emulsion gel beads. This was expected because increasing alginate concentration could increase gel strength of alginate-based gel matrix and thus increase the Young's modulus of overall emulsion gels. Similarly, it has previously been reported that increasing agar contents (from 1.0 to 1.8%) in O/W emulsions containing 0.1

volume fraction of corn oil decreased the overall volume of void spaces and increased strand compactness of emulsion gels (Kim et al., 1999).

Figure 3-2D indicates that increasing oil contents from 10% to 40% had no significant effect on the Young's modulus of emulsion gel beads. According to the interactions between emulsifier-coated emulsion droplets and the gel matrix, oil droplets can be divided into active and inactive fillers (also known as bound and unbound fillers) in emulsion gels (Dickinson, 2012; Yang et al., 2020). Active fillers are mechanically connected to the gel network by non-covalent and/or covalent bonds through emulsifiers. For examples, it has been reported that WPI-coated oil droplets could be bound to a WPI-based gel matrix by covalent interactions (e.g., hydrophobic interactions and sulphur bridges) (Sala et al., 2008); it has been also indicated that lactoferrin-stabilized emulsion droplets could bind to a *κ*-carrageenan gel, probably because of electrostatic interactions between positively charged lactoferrin (p*I* = 8.2) and negatively charged *κ*-carrageenan at pH 7–8 (Sala et al., 2009). In addition, the Kerner model can explain the effect of active fillers on the mechanical properties of emulsion gels (Kerner, 1956). According to this model, increasing the volume fraction (ϕ_f) of active fillers can increase the mechanical properties of emulsion gels, which has been supported by many studies (Oliver et al., 2015; Sala et al., 2009). However, in this study, SPI (p*I* = 4.5) and alginate were both negatively charged at pH 6.5–7.0, so there are no electrostatic interactions between SPI-coated droplets and alginate-based gel matrices. It is also unlikely that SPI-coated droplets can connect to the alginate-based gel network by covalent interactions. Additionally, the results obtained in this study were in a disaccord with the Kerner model. Therefore, it was assumed that SPI-coated droplets were inactive fillers in alginate-based emulsion gel beads in this study.

Figure 3-2C shows that increasing SPI concentrations decreased the Young's modulus of emulsion gel beads. According to the state of emulsion droplets in gels, structures of emulsion gels can be divided into two categories: emulsion droplet-filled gels and emulsion droplet-aggregated gels (Dickinson, 2012). In emulsion droplet-filled gels, the continuous

phase (e.g., protein- and polysaccharide-based gels) forms a continuous gel matrix, and emulsion droplets are embedded in this gel matrix. In emulsion droplet-aggregated gels, emulsion droplets aggregate together and form a network structure, such that the gel matrix is disrupted by the aggregated emulsion droplets. As shown in **Figures 3-1B and 3-1D**, more aggregations of emulsion droplets occurred in sample 1A2S20O compared to sample 1A1S20O, probably because increasing SPI concentration led to more depletion flocculation of SPI-coated droplets in emulsions (Lam & Nickerson, 2013). In active droplet-aggregated gels, the crowding effect of fillers (particle interactions) increases the shear modulus of the overall gels (Oliver et al., 2015). However, SPI-coated droplets in alginate-based gel matrix may act as inactive fillers as discussed before in this study. Therefore, it was assumed that increased aggregation of SPI-coated droplets (inactive fillers) had a negative effect on the Young's modulus of alginate-based emulsion gel beads, probably because aggregated droplets (i.e., the increased phase separation between alginate-based gel matrix and SPI-coated droplets) may disturb the formation of alginate-based network structures (Dickinson, 2012; Lin et al., 2017).

3.3.3. Water loss of gel beads

During the maturation step, inter-chain interactions between stretches of alginate monomers and Ca^{2+} occurred with the diffusion of Ca^{2+} from the surface to interior of gel beads, and the formation of junctions between these stretches forced water out, which led to shrinkage and increased water loss of gel beads during gelation (Puguan et al., 2014; Rehm, 2009). **Figure 3-3** shows the effects of concentrations of alginate, SPI, and oil on the water loss from emulsion gel beads during gelation. It indicates that increasing alginate contents (from 0.5 to 1.5%) or SPI concentrations (from 0.5 to 2.0%) had no significant effect on the rates of water loss, but increasing oil contents (from 10 to 40%) could slow the water loss in terms of the profiles of water loss during gelation, probably because lower water content of the original emulsions results in slower water loss of emulsion gels during gelation.

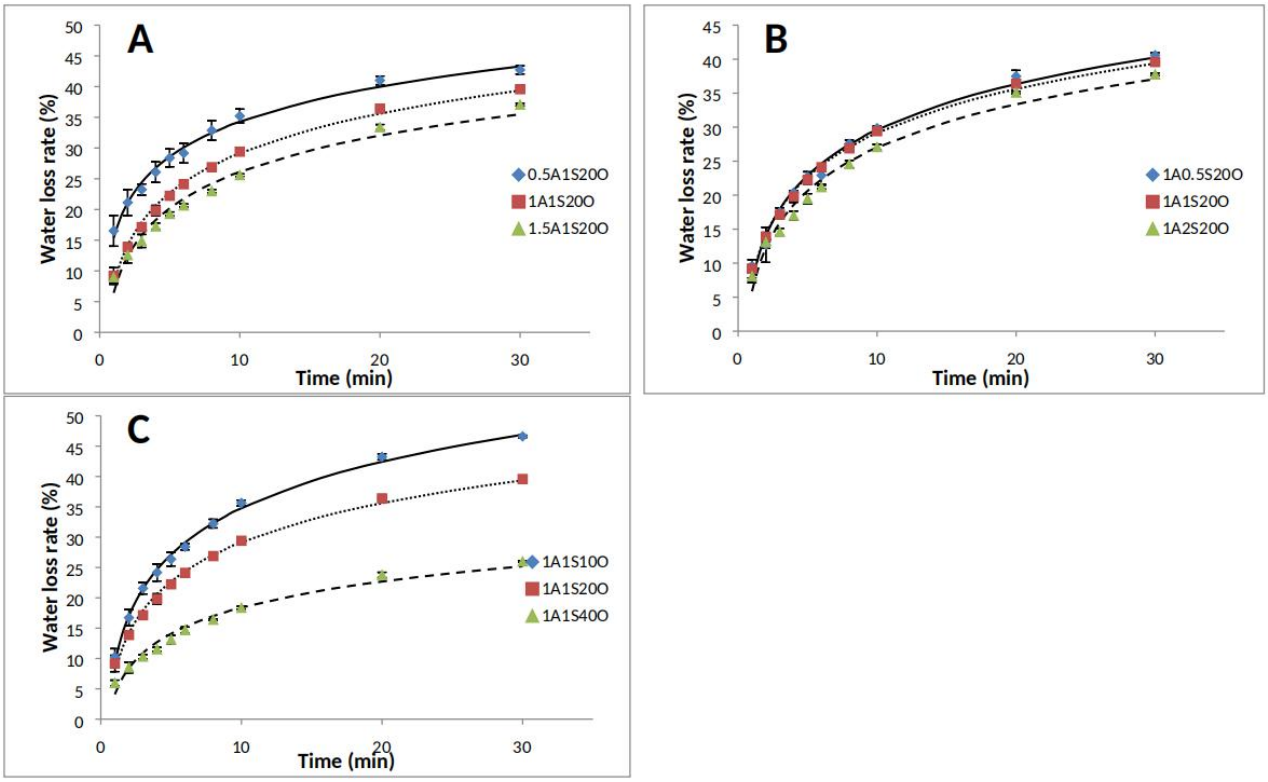

Figure 3-3. Kinetics of water loss from alginate-based gel beads during gelation: (A) effect of alginate concentrations (0.5–1.5% in the water phase); (B) effect of SPI concentrations (0.5–2.0% in the water phase); and (C) effect of oil contents (10–40% in the emulsion).

Figure 3-3 also indicates that the water loss of emulsion gel beads after gelation for 30 min decreased with increasing alginate contents (from 0.5 to 1.5%), SPI concentration (from 0.5 to 2.0%) and oil content (from 10 to 40%). Many factors can affect the water loss of emulsion gel beads during gelation, such as the concentration of $CaCl_2$ solutions, the water content of original emulsions, the strength of gel matrix, and the hydrophilicity and rigidity of fillers. It has been reported that increasing the concentration of $CaCl_2$ solution (from 0.08 M to 0.3 M) reduced the final weight of alginate gel beads due to the increased water loss (Puguan et al., 2014), but in this study all samples were dropped into the $CaCl_2$ solutions with the same concentration. Therefore, increasing alginate concentration from 0.5% to 1.5% decreased the water loss of beads from 42.3 ± 1.2% to 36.9 ± 0.3% after gelation (**Figure 3-3A**), which was probably because elastic modulus of gel beads increased with

increasing alginate concentration (**Figure 3-2B**), and gels with more rigid matrix structures had better water-holding capacity.

In addition, increasing SPI concentrations from 0.5% to 2.0% decreased the water loss of emulsion gel beads from 40.2 ± 0.6% to 37.3 ± 0.3% after gelation as well (**Figure 3-3B**), probably due to increased water-absorption capacity of SPI-coated droplets. As shown **in Figures 3-1A and 3-1B**, SPI aggregated in sample 1A1S but formed a film at the oil-water interface in sample 1A1S20O, in which hydrophobic groups of SPI connected to oil droplets and hydrophilic groups connected to water (Nishinari et al., 2014). Therefore, more SPI was adsorbed at the surface of emulsion droplets by increasing SPI concentration (**Figure 3-1D**), which resulted in increased hydrophilicity of SPI-coated droplets and increased water-retention capacity of emulsion gel beads (Wang et al., 2012). This explanation could be supported by previous conclusions by Wagner et al. (1990) that SPI with highly denatured proteins and high surface hydrophobicity exhibited the highest water-absorption capacity. Additionally, increasing oil content from 10% to 40% led to the decreased water loss of emulsion gel beads (from 46.1 ± 0.2% to 25.1 ± 0.4% after gelation) (**Figure 3-3C**), probably because the water content in original emulsions significantly decreased with increasing oil contents from 10% to 40%, and emulsion droplets could protect gel structures from collapse as well. A similar finding has been reported where increasing the oil volume fraction (13%–31.1%) in *β*-lactoglobulin-based oil-in-water emulsions improved the water-retention capacity of emulsion gels (Line, Remondetto, & Subirade, 2005).

Figure 3-4. Visual aspects of alginate-based gel beads during gelation (minimum scale mark = 1 mm).

3.3.4. Morphological properties and shrinkage of gel beads

As shown in **Figure 3-4**, alginate gel beads (1A) were transparent, but the presence of SPI decreased the transparency of alginate gel beads (1A1S) because of its yellow colour, and introducing oil led to ivory gel beads, due to the formation of emulsions. In addition, gel beads in all groups were not completely spherical, and samples 1.5A1S20O, 1A2S20O, and 1A1S40O had small tails. This was because increasing the concentrations of alginate, SPI and oil could raise the viscosity of emulsions (**Figure 3-5**), which could affect the morphological properties of emulsion gel beads. In this study, we used the simple dripping method to produce emulsion gel beads. The emulsions were pushed out from pipette and one droplet was formed at the tip before the droplet grew in size gradually and dropped into $CaCl_2$ solutions. During this process, spherical emulsion droplets were formed because of the surface tension of liquid (Ching et al., 2017). However, Lević et al. (2015) found that *D*-limonene could increase the viscosity and reduce the conductivity of the alginate liquid systems by changing structural ordering of alginate, which indicates that the high viscosity of emulsion was against the formation of spherical bead at the tip of pipette because of poor flow properties. For example, the introduction of hydroxypropylmethylcellulose (0.2%–1%) changed the rheological properties of 2% alginate solutions and produced beads with small tails (Bellich et al., 2011).

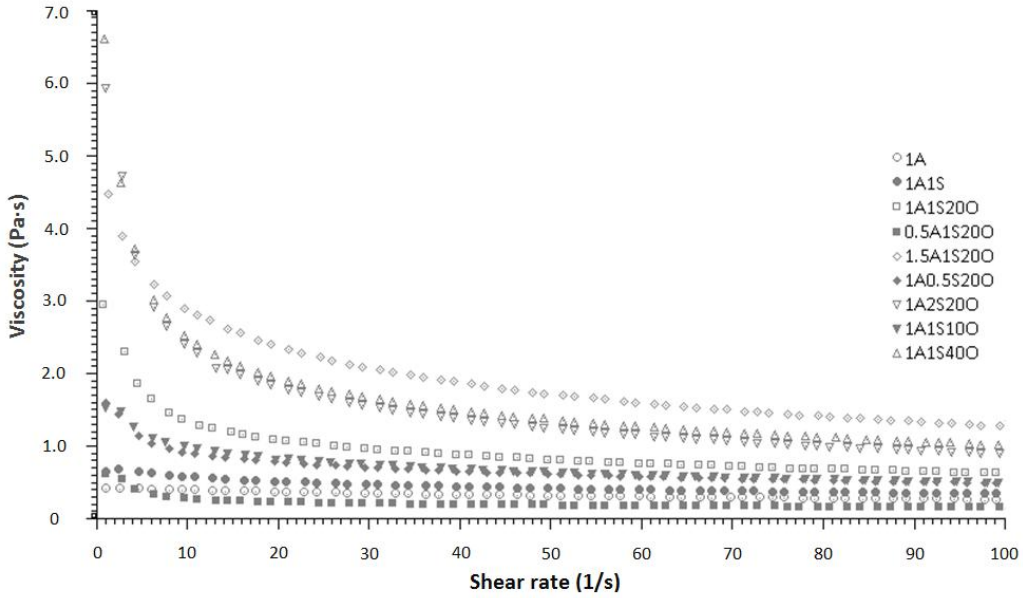

Figure 3-5. Viscosity of dispersions/emulsions with different component concentrations.

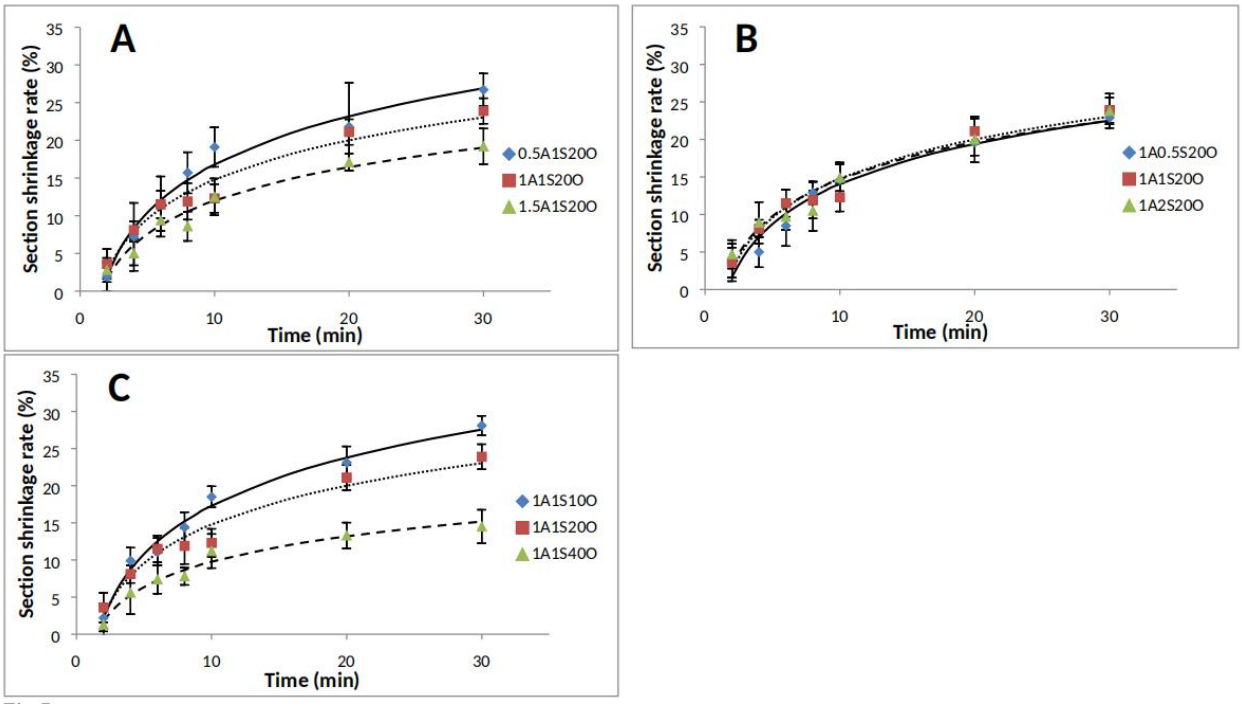

Figure 3-6. Kinetics of section shrinkage of alginate-based gel beads during gelation: (A) effect of alginate concentrations (0.5–1.5% in the water phase); (B) effect of SPI concentrations (0.5–2.0% in the water phase); and (C) effect of oil contents (10–40% in the emulsion).

Figure 3-4 also shows that the size of all samples decreased during gelation and, in order to compare their shrinkage (i.e., dimensional reduction) during gelation, the section shrinkage rates were calculated (**Figure 3-6**). The profiles of shrinkage rates show that shrinkage rates of all samples increased during gelation, probably due to syneresis (i.e., water loss) and structural collapse (Rehm, 2009). However, in terms of the profiles of shrinkage rate, increasing contents of alginate and oil could slow the shrinkage, but increasing SPI content had no significant effect on the rate of shrinkage during gelation. **Figure 3-6** also shows that the shrinkage rates decreased from 26.7 ± 2.1% to 18.2 ± 2.2% and from 27.1 ± 1.6% to 13.6 ± 2.5% after gelation with increasing concentrations of alginate (from 0.5% to 1.5%) and oil (from 10% to 40%), respectively, but increasing SPI concentration from 0.5% to 2.0% had no significant effect on the shrinkage rates of emulsion gel beads after gelation for 30 min. Many factors can affect the shrinkage of emulsion gels during gelation, such as water loss, gel stiffness, the content and properties of fillers, and interactions between fillers and the continuous phase (Smith, Scherer, & Anderson, 1995). In terms of alginate, increasing its concentration could increase the elastic modulus of emulsion gel beads (**Figure 3-2B**), which may provide resistance to shrinkage (Brinker et al., 1994). Increasing oil concentration led to more compact filler structures, which resisted further shrinkage during gelation as seen on comparing emulsion gel structures of samples 1A1S20O and 1A1S40O in **Figure 3-1**. Eichler et al. (1997) also indicated similar conclusions, in that fructose or polydextrose being introduced into polyacrylamide (PAAm) gels could act as a mechanical barrier against further volume shrinkage of PAAm gels during dehydration. However, increasing SPI concentration reduced the Young's modulus (**Figure 3-2C**) but increased water retention (i.e., decreased water loss) (**Figure 3-3B**) of emulsion gel beads, which may explain why increasing SPI concentration had no significant effects on shrinkage rates of emulsion gel beads.

3.4. Conclusions

The Young's modulus of alginate-based emulsion gel beads kept increasing before reaching a plateau during gelation process. This gelation process was accompanied by syneresis (i.e., water loss) and shrinkage, which resulted in an increased compactness of emulsion gel beads. SPI-coated droplets could maintain their structures during gelation. With increasing alginate concentration (0.5%–1.5%), the water loss decreased, the Young's modulus increased, and shrinkage rate decreased. Increasing SPI concentration (0.5%–2.0%) led to decreased Young's modulus and water loss, and undifferentiated shrinkage. Higher oil content (10%–40%) decreased water loss and section shrinkage rates, and had no significant effect on the Young's modulus. These findings underlined the effect of concentrations of components on the properties of emulsion gel beads during gelation, which are very important because the properties of emulsion gel beads may affect encapsulation, stability, and release of hydrophobic functional ingredients encapsulated in emulsion gel beads.

References

Bellich, B., Borgogna, M., Cok, M., & Cesàro, A. (2011). Release properties of hydrogels: Water evaporation from alginate gel beads. *Food Biophysics, 6*, 259-266.

Brinker, C. J., Sehgal, R., Hietala, S., Deshpande, R., Smith, D., Loy, D., & Ashley, C. (1994). Sol-gel strategies for controlled porosity inorganic materials. *Journal of Membrane Science, 94*, 85-102.

Brito-Oliveira, T. C., Bispo, M., Moraes, I. C. F., Campanella, O. H., & Pinho, S. C. (2017). Stability of curcumin encapsulated in solid lipid microparticles incorporated in cold-set emulsion filled gels of soy protein isolate and xanthan gum. *Food Research International, 102*, 759-767.

Ching, S. H., Bansal, N., & Bhandari, B. (2016). Rheology of emulsion-filled alginate microgel suspensions. *Food Research International, 80*, 50-60.

Ching, S. H., Bansal, N., & Bhandari, B. (2017). Alginate gel particles–A review of production techniques and physical properties. *Critical Reviews in Food Science & Nutrition, 57*, 1133-1152.

Corstens, M. N., Berton-Carabin, C. C., Elichiry-Ortiz, P. T., Hol, K., Troost, F. J., Masclee, A. A. M., & Schroën, K. (2017). Emulsion-alginate beads designed to control in vitro intestinal lipolysis: Towards appetite control. *Journal of Functional Foods, 34*, 319-328.

Dickinson, E. (2012). Emulsion gels: The structuring of soft solids with protein-stabilized oil droplets. *Food Hydrocolloids, 28*, 224-241.

Eichler, S., Ramon, O., Ladyzhinski, I., Cohen, Y., & Mizrahi, S. (1997). Collapse processes in shrinkage of hydrophilic gels during dehydration. *Food Research International, 30*, 719-726.

Geremias-Andrade, I. M., Souki, N. P. D. B. G., Moraes, I. C. F., & Pinho, S. C. (2017). Rheological and mechanical characterization of curcumin-loaded emulsion-filled gels produced with whey protein isolate and xanthan gum. *LWT - Food Science and Technology, 86*, 166-173.

Guo, Q., Bellissimo, N., & Rousseau, D. (2017). Role of gel structure in controlling in vitro intestinal lipid digestion in whey protein emulsion gels. *Food Hydrocolloids, 69*, 264-272.

Kerner, E. (1956). The elastic and thermo-elastic properties of composite media. *Proceedings of the Physical Society. Section B, 69*, 808.

Kim, K., Gohtani, S., Matsuno, R., & Yamano, Y. (1999). Effects of oil droplet and agar concentration on gel strength and microstructure of o-w emulsion gel. *Journal of Texture Studies, 30*, 319-335.

King, A. (1983). Brown seaweed extracts (alginates). *Food Hydrocolloids, 2*, 115-188.

Lam, R. S., & Nickerson, M. T. (2013). Food proteins: A review on their emulsifying properties using a structure-function approach. *Food Chemistry, 141*, 975-984.

Lević, S., Pajić Lijaković, I., Đorđević, V., Rac, V., Rakić, V., Šolević Knudsen, T., Pavlović, V., Bugarski, B., & Nedović, V. (2015). Characterization of sodium alginate/$_D$-limonene emulsions and respective calcium alginate/$_D$-limonene beads produced by electrostatic extrusion. *Food Hydrocolloids, 45*, 111-123.

Liang, F., Liu, J., Zhang, C., Qu, X., Li, J., & Yang, Z. (2011). Janus hollow spheres by emulsion interfacial self-assembled sol-gel process. *Chemical Communications, 47*, 1231-1233.

Lin, D., Lu, W., Kelly, A. L., Zhang, L., Zheng, B., & Miao, S. (2017). Interactions of vegetable proteins with other polymers: Structure-function relationships and applications in the food industry. *Trends in Food Science & Technology, 68*, 130-144.

Line, V. L.S., Remondetto, G. E., & Subirade, M. (2005). Cold gelation of *β*-lactoglobulin oil-in-water emulsions. *Food Hydrocolloids, 19*, 269-278.

Ma, L., Wan, Z., & Yang, X. (2017). Multiple water-in-oil-in-water emulsion gels based on self-assembled saponin fibrillar network for photosensitive cargo protection. *Journal of Agricultural and Food Chemistry, 65*, 9735-9743.

Moschakis, T., Murray, B. S., & Biliaderis, C. G. (2010). Modifications in stability and structure of whey protein-coated o/w emulsions by interacting chitosan and gum arabic mixed dispersions. *Food Hydrocolloids, 24*, 8-17.

Natrajan, D., Srinivasan, S., Sundar, K., & Ravindran, A. (2015). Formulation of essential oil-loaded chitosan-alginate nanocapsules. *Journal of Food and Drug Analysis, 23*, 560-568.

Nishinari, K., Fang, Y., Guo, S., & Phillips, G. O. (2014). Soy proteins: A review on composition, aggregation and emulsification. *Food Hydrocolloids, 39*, 301-318.

Oliver, L., Berndsen, L., van Aken, G. A., & Scholten, E. (2015). Influence of droplet clustering on the rheological properties of emulsion-filled gels. *Food Hydrocolloids, 50*, 74-83.

Pintado, T., Ruiz-Capillas, C., Jimenez-Colmenero, F., Carmona, P., & Herrero, A. M. (2015). Oil-in-water emulsion gels stabilized with chia (*Salvia hispanica L.*) and cold

gelling agents: Technological and infrared spectroscopic characterization. *Food Chemistry*, 185, 470-478.

Piornos, J. A., Burgos-Díaz, C., Morales, E., Rubilar, M., & Acevedo, F. (2017). Highly efficient encapsulation of linseed oil into alginate/lupin protein beads: Optimization of the emulsion formulation. *Food Hydrocolloids, 63*, 139-148.

Puguan, J. M., Yu, X., & Kim, H. (2014). Characterization of structure, physico-chemical properties and diffusion behavior of Ca-Alginate gel beads prepared by different gelation methods. *Journal of Colloid and Interface Science, 432*, 109-116.

Quong, D., Neufeld, R., Skjåk-Bræk, G., & Poncelet, D. (1998). External versus internal source of calcium during the gelation of alginate beads for DNA encapsulation. *Biotechnology and Bioengineering, 57*, 438-446.

Rehm, B. H. A. (Ed.). (2009). *Alginates: biology and applications*. Heidelberg: Springer.

Rosa, P., Sala, G., Van Vliet, T., & Van De Velde, F. (2006). Cold gelation of whey protein emulsions. *Journal of Texture Studies, 37*, 516-537.

Sala, G., de Wijk, R. A., van de Velde, F., & van Aken, G. A. (2008). Matrix properties affect the sensory perception of emulsion-filled gels. *Food Hydrocolloids, 22*, 353-363.

Sala, G., van Vliet, T., Cohen Stuart, M. A., Aken, G. A. v., & van de Velde, F. (2009). Deformation and fracture of emulsion-filled gels: Effect of oil content and deformation speed. *Food Hydrocolloids*, 23, 1381-1393.

Sato, A. C. K., Moraes, K. E. F. P., & Cunha, R. L. (2014). Development of gelled emulsions with improved oxidative and pH stability. *Food Hydrocolloids*, 34, 184-192.

Smith, D., Scherer, G., & Anderson, J. (1995). Shrinkage during drying of silica gel. *Journal of Non-Crystalline Solids, 188*, 191-206.

Tavernier, I., Patel, A. R., Van der Meeren, P., & Dewettinck, K. (2017). Emulsion-templated liquid oil structuring with soy protein and soy protein: *κ*-carrageenan complexes. *Food Hydrocolloids, 65*, 107-120.

Urbonaite, V., de Jongh, H. H. J., van der Linden, E., & Pouvreau, L. (2015). Water holding of soy protein gels is set by coarseness, modulated by calcium binding, rather than gel stiffness. *Food Hydrocolloids, 46*, 103-111.

Van Vliet, T. (1988). Rheological properties of filled gels: Influence of filler matrix interaction. *Colloid and Polymer Science, 266*, 518-524.

Vasile, F. E., Judis, M. A., & Mazzobre, M. F. (2018). Impact of prosopis alba exudate gum on sorption properties and physical stability of fish oil alginate beads prepared by ionic gelation. *Food Chemistry, 250*, 75-82.

Wagner, J., & Añón, M. C. (1990). Influence of denaturation, hydrophobicity and sulfhydryl content on solubility and water absorbing capacity of soy protein isolates. *Journal of Food Science, 55*, 765-770.

Wang, S., Marcone, M., Barbut, S., & Lim, L. T. (2012). The impact of anthocyanin-rich red raspberry extract (ARRE) on the properties of edible soy protein isolate (SPI) films. *Journal of Food Science, 77*, C497-505.

Wang, Z., Neves, M. A., Kobayashi, I., Uemura, K., & Nakajima, M. (2013). Preparation, characterization, and *in vitro* gastrointestinal digestibility of oil-in-water emulsion-agar gels. *Bioscience Biotechnology and Biochemistry, 77*, 467-474.

Yang, N., Feng, Y. N., Su, C. X., Wang, Q., Zhang, Y. M., Wei, Y. H., Zhao, M., Nishinari, K., Fang, Y. P. (2020). Structure and tribology of κ-carrageenan gels filled with natural oil bodies. *Food Hydrocolloids,* 105945.

Yin, L., Zhao, Z., Hu, Y., Ding, J., Cui, F., Tang, C., & Yin, C. (2008). Polymer–protein interaction, water retention, and biocompatibility of a stimuli-sensitive superporous hydrogel containing interpenetrating polymer networks. *Journal of Applied Polymer Science, 108*, 1238-1248.

Zhang, Z. P., Zhang, R. J., Zou, L. Q., Chen, L., Ahmed, Y., Bishri, W. A., Balamash, K., & McClements, D. J. (2016). Encapsulation of curcumin in polysaccharide-based hydrogel beads. *Food Hydrocolloids, 58*, 160–170.

CHAPTER FOUR

Effect of Structuring Emulsion Gels by Whey or Soy Protein Isolate on the Structure, Mechanical Properties, and *In-vitro* Digestion of Alginate-based Emulsion Gel Beads

Chapter 4 was published in:

Lin, D., Kelly, A. L., Maidannyk, V., & Miao*, S. (2020). Effect of structuring emulsion gels by whey or soy protein isolate on the structure, mechanical properties, and *in-vitro* digestion of alginate-based emulsion gel beads. *Food Hydrocolloids, 110*, 106165.

The work contained in this chapter was undertaken and written mainly by myself with Dr. Valentyn Maidannyk's help on CLSM operation and specific contributions from supervisors.

Abstract

Whey protein isolate (WPI) and soy protein isolate (SPI) were used as emulsifiers and structure-modifying agents to produce alginate-based emulsion gel beads. The purpose of this chapter was to compare the effects of WPI and SPI on the structural and mechanical properties of alginate-based emulsion gel beads and the *in-vitro* release of encapsulated lycopene from emulsion gel beads. The results of microscopy and light scattering indicated that WPI had better emulsifying properties than SPI, resulting in emulsions with smaller and more even droplet-size distribution. The rheological properties of protein/alginate mixtures and emulsions indicated strong interactions between WPI and alginate and weak interactions between SPI and alginate, resulting in increased Young's modulus of WPI-stabilized emulsion gel beads and decreased Young's modulus of SPI-stabilized emulsion gel beads, compared to gel beads without proteins. The presence of WPI and SPI increased changes of Young's modulus and shrinkage during simulated gastric digestion and delayed the release of lycopene from gel beads. Findings in this study are important for structuring emulsion gels with naturally occurring polymers to achieve controlled release of encapsulated compounds.

Keywords: Alginate; Emulsion gel bead; Lycopene; Soy protein isolate; Structure; Whey protein isolate.

4.1. Introduction

Sodium alginate is a linear unbranched natural polysaccharide, and its monomers can form gels by ionic crosslinking when sodium ions are replaced by divalent cations (mostly calcium ions in the food industry). Sodium alginate has been widely investigated in the field of emulsion gels for encapsulation of food nutrients such as thyme oil, linseed oil, resveratrol, *α*-tocopherol, *β*-carotene and *D*-limonene to improve their stability during food processing and storage (Benavides et al., 2016; Feng et al., 2018; Lević et al., 2015; Piornos et al., 2017; Soukoulis et al., 2016). There are also some advantages associated with alginate-based encapsulation techniques, such as mild gelation process with a low-cost and eco-friendly procedure and controlled release of encapsulated food nutrients because of pH sensitivity of alginate gels (i.e., shrinking at gastric environment and swelling during intestinal digestion) (Calvo, Busch, & Santagapita, 2017; George & Abraham, 2006). In alginate-based emulsion gels, proteins especially whey protein isolate (WPI) are often used as emulsifiers to improve the encapsulation efficiency during gelation and the stability of encapsulated food nutrients during storage (Feng et al., 2018; Piornos et al., 2017).

However, the presence of proteins may also change the structural and mechanical properties of alginate-based emulsion gels during gelation and digestion, which has rarely been investigated (Leon et al., 2018). Previous studies on interactions between proteins and alginate have indicated that proteins affect the gelation process and physicochemical properties of calcium-induced alginate gels through several mechanisms. Firstly, positively charged proteins can compete with calcium ions to associate with carboxylic acid sites on the negatively charged alginate molecules through electrostatic attractions (George & Abraham, 2006). Secondly, negatively charged proteins can interact with alginate through intermolecular hydrogen bonds between proteins and alginate and/or weak electrostatic attractions between carboxylic anionic groups of alginate and cationic groups of proteins, although both of them are negatively charged (Erben et al., 2019; Yang et al., 2016). Thirdly, insoluble proteins can act as solid fillers in alginate gels (Leon et al., 2018).

In addition, the presence of proteins may also affect the digestion behavior of alginate gels. It is well known that alginate gels shrink during gastric digestion, because of protonation of free carboxylate groups on alginate and thus decreased repulsive charges of alginate monomers at the acidic pH (pH 2–3) (Li et al., 2011). Alginate gels then swell during intestinal digestion, because of the increased repulsive forces at the neutral pH above the pKa of the uronic acid groups on alginate (Rayment et al., 2009) and structural disintegration of Ca^{2+}-associated networks due to ion-exchange between Na^{+} ions present in the digestive fluid and Ca^{2+} ions present in gel beads (Bajpai & Sharma, 2004; Mongar & Wassermann, 1949). This digestion behavior can protect encapsulated nutrients from the harsh gastric environment due to the shrinkage of gels during gastric digestion, and encapsulated nutrients then diffuse through the pores of alginate gel networks into the small intestine due to the swelling of gels during intestinal digestion. However, the zeta potential of proteins is also influenced by pH, which may affect the interactions between proteins and alginate and thus the physicochemical properties of alginate-based emulsions gels during digestion. Therefore, the effect of proteins on the structural and mechanical properties of alginate-based emulsion gels and the release of encapsulated nutrients during digestion need further investigation.

The properties of different proteins (e.g., solubility and amphipathy) affect their interactions with other polymers (Lin et al., 2017). WPI is the most widely used protein-based emulsifier in emulsion gels, and soy protein isolate (SPI) has received increasing interest, due to its good emulsifying and gelation properties. SPI contains more polar amino acids (492.8 mg/g) than WPI (433.7 mg/g), and WPI contains more positively charged amino acids (267.9 mg/g) than SPI (200.9 mg/g) at pH 7.0 (Peña-Ramos, Xiong, & Arteaga, 2004; Tang et al., 2006). Polar amino acids tend to form hydrogen bonds with alginate, and positively charged amino acids tend to react with alginate by electrostatic attractions. In addition, WPI has higher solubility and surface hydrophobicity than SPI (Castro et al., 2018; Voutsinas, Cheung, & Nakai, 1983). Protein solubility affects protein-water interactions, and

surface hydrophobicity influences protein-oil interactions at droplet surfaces (Pelegrine & Gasparetto, 2005).

Therefore, the objective of this study was to compare WPI to SPI in structuring alginate-based emulsion beads and delivering encapsulated nutrients to a target site (i.e., small intestine). The effect of WPI and SPI on the properties of emulsions and emulsion gel beads and the release behavior of encapsulated nutrients during *in-vitro* digestion were studied. Lycopene was encapsulated in emulsion gels to study the effect of WPI and SPI on the digestion behavior of alginate-based emulsion gels. Lycopene has a huge commercial value in the food industry, due to its high antioxidant capacity among carotenoids (Costa-Rodrigues, Pinho, & Monteiro, 2018; Liu et al., 2008). However, lycopene is highly sensitive to high temperature, oxygen and light (Bou et al., 2011; Shi et al., 2008; Ukai et al., 2014), and has limited solubility in water because of its high hydrophobicity (Shariffa et al., 2017), which limits its applications in the food industry (Srivastava & Srivastava, 2013). Therefore, encapsulating lycopene in alginate-based emulsion gels can improve its functionality and stability during food processing, storage, and digestion (Aguirre Calvo, Busch, & Santagapita, 2017; Soukoulis et al., 2016).

4.2. Materials and methods

4.2.1. Materials

Defatted soy flour (Bob's Red Mill, Milwaukie, Oregon, USA) and sunflower oil (Aldi Stores Ltd., Kildare, Ireland) were purchased from iHerb and Aldi, respectively. Sodium alginate (viscosity of 1 wt% sodium alginate solution in 0.15 M NaCl at 25°C = 210–340 mPa·s, $\overline{M}$ = 69–117 kDa, and M/G = 71/29) was obtained from Special Ingredients (Chesterfield, UK). Whey protein isolate (WPI) was purchased from Carbery Group Limited (Ballineen, Co. Cork, Ireland). Soy protein isolate (SPI) was extracted from defatted soy flour, according to the method described by Urbonaite et al. (2015), and the protein content

of SPI powder was 96.29 ± 0.03%. Tomato extract containing lycopene (0.059 mg/mg in the tomato extract), calcium chloride, sodium hydroxide, hydrochloric acid, and other analytical reagents were purchased from Sigma-Aldrich (St. Louis, MO, USA).

4.2.2. Preparation of emulsions and emulsion gel beads containing lycopene

The dispersions of WPI or SPI (4.0% in distilled water) were stirred at room temperature for 2 h using a magnetic stirrer, and then pH values of dispersions were adjusted to 7.0 with 1M HCl and NaOH. For preparing continuous phase, sodium alginate (0.4% in continuous phase) was added into the protein dispersions (4.0%) with water to reach final concentration of proteins (2.0% in continuous phase) by shearing at 400 rpm for 30 min with a magnetic stirrer and then allowed to rest for 24 h to permit hydration. The continuous phase without protein (i.e., 0.4% sodium alginate solutions) was prepared as control sample. For preparation of lycopene-capsulated emulsions, tomato extract containing lycopene (15 mg/100 g in the emulsions) was dissolved in sunflower oil (10 g oil/100 g in the emulsions) at 140°C for 30 s, and then it was cooled down to the room temperature immediately and mixed with the continuous phase (1:9, w/w) at 13,000 rpm for 2 min with an Ultra-Turrax (IKA-25, Staufen, Germany). For production of emulsion gel beads, the resultant emulsions were dropped into 2 % (w/w) $CaCl_2 \cdot 2H_2O$ solutions using 5-mL measuring pipette and a S1 pipette filler (Thermo Fisher Scientific Inc., Waltham, MA, USA), and the distance between the tip of pipette and the surface of $CaCl_2$ solutions was fixed at 10 cm. The samples were allowed to gel in $CaCl_2$ solutions for 30 min with mild magnetic stirring, and the resulted beads were rinsed with distilled water. All samples were kept in distilled water until further analyses.

4.2.3. Properties of emulsions

4.2.3.1. Viscosity

The viscosity of dispersions/solutions was tested at 25ºC using an AR 2000ex rheometer (TA Instruments, Crawley, UK) with an aluminium parallel plate (60 mm in diameter, and 0.5 mm in gap). Each sample was added in the middle of Peltier plate and allowed to stand for 2 min before testing. The flow measurement was performed over a shear rate range of 0.1 to 100 s^{-1}, and viscosity (η) was obtained from the data analysis software.

4.2.3.2. Droplet-size distributions

The droplet-size distributions of oil droplets in emulsions were analyzed with MasterSizer 3000 (Malvern Instruments Ltd., Worcestershire, UK). Samples were added to an automated wet dispersion unit until the obscuration reached between 3 and 12%. The stirrer speed was set at 2000 rpm. The refractive index and absorption index of samples were set at 1.48 and 0.001, respectively.

4.2.3.3. Structural analysis

Optical microscopy images of dispersion/emulsion samples were recorded using an Olympus BX51 light microscope with a built-in camera (Olympus Optical Co. Ltd., Tokyo, Japan). Samples were dropped on a microscope slide, covered with a glass coverslip, and observed using a 10× objective lens and a 10× eyepiece.

Confocal scanning laser microscopy (CLSM) was used to observe micro-structure of dispersions/emulsions. Dispersion/emulsion samples (500 μL) were transferred to a glass slide and stained with 50 μL of a mixture of Nile red (0.1%, w/v, in polyethylene glycol-200) and fast green (0.1%, w/v, in distilled water) at a ratio of 3:1. Confocal observation was performed using a Leica TCS SP5 microscope (Leica Microsystems GmbH, Wetzlar,

Germany) at excitation and emission wavelengths of 488 nm and 633 nm, provided by an argon laser and a HeNe laser, respectively.

4.2.4. Properties of emulsion gel beads

4.2.4.1. Water and oil contents

The gel beads before desiccation were weighted (W_i), and samples were dried in an oven at 80ºC until constant weight (W_o). The water content was calculated by Eq. (4-1):

$$\text{Water content (\%)} = \frac{W_i - W_o}{W_i} \times 100\% \quad (4\text{-}1).$$

Dry gel beads were ground and then mixed with 20 mL of hexane in a beaker. The mixture was stirred with a magnetic stirrer at room temperature for 10 min. The solvent mixture was filtered through a Whatman filter paper nº 1 into a beaker, and residues were rinsed three times with 15 mL of hexane in total. Then, the solvent was heated at 60ºC to evaporate hexane until constant weight (W_f). The oil content was calculated by Eq. (4-2):

$$\text{Oil content (\%)} = \frac{W_f}{W_i} \times 100\% \quad (4\text{-}2).$$

4.2.4.2. Lycopene content

Lycopene was extracted and quantified according to the method described by Anthon & Barrett (2006) with some modification. Samples (0.5 g of emulsion gel beads) were weighed into a screw cap tube, and 8.0 mL of hexane : acetone : ethanol (50 : 25 : 25) solutions containing 0.1% BHT was added. The control solution was prepared with 0.5 g water instead of gel beads. After mixing for 1 min by a vortex, all samples were allowed to rest for 24 h until gel beads became pale. Water (1.0 mL) was added followed by mixing for 25 s again. The mixture was left to stand for 10 min to allow phases to separate and all bubbles to disappear. All samples were protected from light throughout extraction and analysis.

Lycopene concentration (C_{LYC}) in the upper layer of mixtures was then measured by a rapid spectrometric method (Anthon & Barrett, 2006). The cuvette was rinsed with the upper layer of samples, and absorbance (A_{503}) of the upper layer was measured at 503 nm with a spectrophotometer. Lycopene concentration can be calculated by Eq. (4-3):

$$\text{Lycopene concentrate (mg/kg)} = (A_{503} \times 537 \times 8 \times 0.55)/(0.50 \times 172) = A_{503} \times 27.5 \quad (4\text{-}3)$$

where 537 g/mole is the molecular weight of lycopene, 8 mL is the volume of mixed solvent, 0.55 is the volume ratio of upper layer to the mixed solvents, 0.5 g is the weight of gel beads added, and 172 mM^{-1} is the extinction coefficient for lycopene in hexane.

4.2.4.3. Structural analysis

CLSM was used to observe the micro-structure of emulsion gel beads. Samples were cut into a thin layer (~ 1 mm) and transferred to a glass slide and stained with a mixture of Nile red (0.1%, w/v, in polyethylene glycol-200) and fast green (0.1%, w/v, in distilled water) at a ratio of 3:1. Confocal observation was performed as described in Section 4.2.3.3.

4.2.4.4. Size and Young's modulus measurement

The Young's modulus of gel beads after gelation for 30 min were analyzed by a TA.XT Plus texture analyzer (Stable Micro System, Godalming, UK). The surface of samples was dried by dry paper before testing. Compression tests were performed using a cylinder probe with 10 mm diameter and a 5-kg load cell. The samples were compressed to 30% strain at a crosshead speed of 0.1 mm/s, and five beads with same composition were examined one after another. Due to their ellipsoidal shapes, the cross-sectional area of samples was calculated after measuring the major axis (R_{max}) and minor axis (R_{min}) of gel beads using a digital vernier calliper after samples were placed on the platform of texture analyzer. The

Young's modulus of each sample was calculated as the gradient of the stress vs. strain curve in the 5–15% strain region, where stress and stain showed good linearity.

4.2.5. *In-vitro* digestion

Simulated digestion of emulsion gel beads included the oral, gastric and small intestinal phases in this study. The simulated saliva fluid (SSF), gastric fluid (SGF), and intestinal fluid (SIF) electrolyte stock solutions (i.e., 1.50× concentrates) were prepared as described by Minekus, et al. (2014) with some modification. Simulated digestion fluids are made of electrolyte stock solutions, enzymes, $CaCl_2$, and water as described below.

Oral phase: 5 g of emulsion gel beads were mixed with 2.5 mL of SSF electrolyte stock solution followed by adding 25 μL of 0.3 M $CaCl_2$ (final 0.75 mM), 475 μL of water, and 2.0 mL of 375 U/mL α-amylase solution (final 75 U/g) with pH adjustment to 7.0. The mixtures were incubated at 37°C for 2 min with continuous agitation at 300 rpm.

Gastric phase: the oral bolus (~10 g) was mixed with 5.0 mL of SGF electrolyte stock solution, 4.0 mL porcine pepsin stock solution of 10, 000 U/mL (final 2000 U/g), 5.0 μL of 0.3 M $CaCl_2$ (final 0.075 mM), 0.5 mL of 1 M HCl to reach pH 3.0 and 0.5 mL of water. The mixtures were incubated at 37°C for 2 h with continuous agitation at 300 rpm.

Intestinal phase: the gastric chyme (~20 g) was mixed with 10 mL of SIF electrolyte stock solution, 5 mL of a pancreatin solution 800 U/mL (final 100 U/g of trypsin), 4 mL bile solution of 25 g/L (Albarracin, Jose Gonzalez, & Drago, 2015), 40 μL of 0.3 M $CaCl_2$ (final 0.3 mM), 0.1 mL of 1 M NaOH to reach pH 7.0 and 0.9 mL of water. The mixtures were incubated at 37°C for 6 h with continuous agitation at 300 rpm, and 0.1 M NaOH was used to maintain the pH (7.0) during the intestinal phase.

4.2.6. Young's modulus measurement of gel beads during oral and gastric digestion

Gel beads after oral digestion and during gastric digestion at 30, 60, 90 and 120 min were collected. The surface of samples was rinsed with distilled water, and the Young's modulus of samples were analyzed according to the methods described in Section 4.2.4.4.

4.2.7. Shrinkage measurement of gel beads during gastric digestion

The section shrinkage rate of gel beads was determined after 30, 60, 90, and 120 min of gastric digestion. Five gel beads were obtained from the gastric fluid. After drying the surface, the major axis (R'_{max}) and minor axis (R'_{min}) of gel beads were measured by using a digital vernier calliper, and the cross-section area (A_t) was calculated from Eq. (4-4). The major axis (R_{max}) and minor semi-axis (R_{min}) of gel beads after oral digestion for 2 min were measured as well, and the cross-section area (A_0) was also calculated from Eq. (4-4). The section shrinkage rate of gel beads was calculated from Eq. (4-4):

$$\text{Section shrinkage rate (100\%)} = \frac{A_0 - A_t}{A_0} = \frac{3.14 \times \frac{R_{max}}{2} \times \frac{R_{min}}{2} - 3.14 \times \frac{R'_{max}}{2} \times \frac{R'_{min}}{2}}{3.14 \times \frac{R_{max}}{2} \times \frac{R_{min}}{2}} \quad (4\text{-}4)$$

where A_0 indicates the section area of samples at the beginning of gastric digestion (i.e., after oral digestion for 2 min) and A_t indicates the section area of samples after 30, 60, 90, or 120 min of gastric digestion. The section shrinkage rate of samples during gastric digestion was compared to the section area of samples after oral digestion for 2 min in this study.

4.2.8. Micro-structure of bead residuals after gastric digestion

The digesta was filtered by multilayer gauze to collect bead residuals, and CLSM was used to observe the micro-structure of emulsion gel bead, according to the method described in Section 4.2.4.3.

4.2.9. Release of lycopene during intestinal digestions

The digesta was filtered by multilayer gauze to separate bead residual and digestive juice, and the digestive juice (Wt_{juice}) was weighted. Lycopene in 1.0 g of digestive juice ($C_{LYC\text{-}J}$) was extracted and analyzed by the methods described in Section 4.2.4.2. The ratios of the amount of lycopene in digestive juice ($Wt_{LYC\text{-}J}$) to that in original beads ($Wt_{LYC\text{-}B}$) are regarded as release rates ($R_{release}$). The release rate of lycopene was estimated through Eq. (4-5):

$$\text{Release rates (\%)} = \frac{Wt_{LYC-J}}{Wt_{LYC-B}} \times 100\% = \frac{C_{LYC-J} \times Wt_{juice}}{C_{LYC-B} \times 5} \times 100\% \quad (4\text{-}5).$$

4.2.10. Statistical analysis

All measurements were performed three times and were reported as mean ± standard deviation (SD). Differences between samples were analyzed using analysis of variance and a *t*-test, and $p < 0.05$ was regarded as statistically significant.

4.3. Results and discussion

4.3.1. Properties of alginate/protein-stabilized emulsions

4.3.1.1. Structures of emulsions

As shown in **Figures 4-1A–C**, optical microscopy images of dispersions show that flocculation and coalescence occurred in dispersions without protein (i.e., the control sample), and flocculation occurred in SPI-stabilized emulsions, but WPI-stabilized emulsion droplets dispersed evenly in the continuous phase. Alginate is a naturally occurring hydrophilic polysaccharide and has poor emulsifying capacity, because it lacks hydrophobic groups (Lee & Mooney, 2012). Therefore, alginate-stabilized oil droplets have high surface tension and tend to merge into bigger oil droplets to reduce the contact area between the oil and water phases and reach the most thermodynamically stable state. In contrast, proteins

can adsorb at the O/W interfaces to prevent droplet coalescence by reducing the surface tension of droplets and decrease flocculation through droplet-droplet repulsion. However, SPI-coated droplets had more significant flocculation than WPI-coated droplets, probably due to depletion flocculation of droplets coated by excessive amount of insoluble SPI (Moschakis, Murray, & Biliaderis, 2010) and/or lower zeta-potential of SPI-coated droplets than WPI-coated droplets at pH 7.0 (Chen et al., 2020).

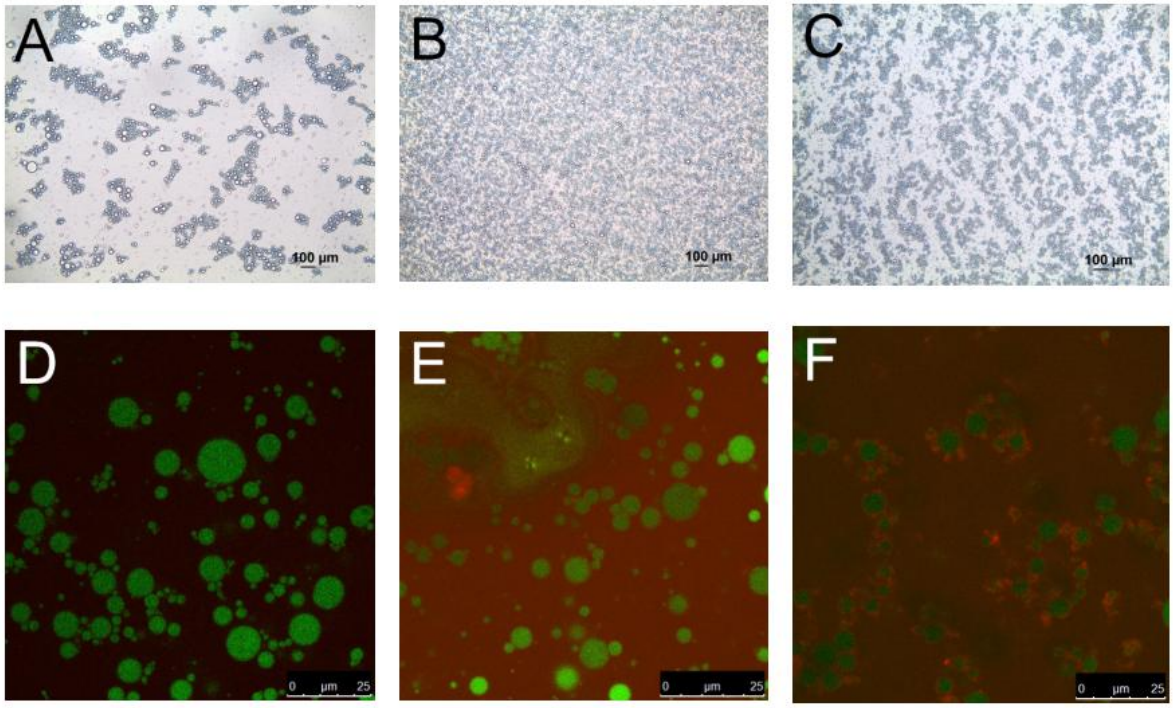

Figure 4-1. Optical microscopy and CLSM images of (A and D) dispersions without proteins, (B and E) WPI-stabilized emulsions, and (C and F) SPI-stabilized emulsions. Protein and sunflower oil were stained by red and green in CLSM figures D-F, respectively.

CLSM was further used to observe the distribution of oil and protein in dispersions. **Figures 4-1D–F** show a red background of WPI- and SPI-stabilized emulsions, which indicates that some soluble protein molecules were still found in the continuous phase. The possible reason is that protein molecules were trapped by the continuous phase, due to the interactions between protein and alginate; also, 2% protein was probably higher than the saturation level of protein to cover the 10% oil droplets. **Figures 4-1D–F** also show that more SPI molecules adsorbed at the O/W interfaces than WPI molecules, probably because

that WPI has higher solubility than SPI and thus more WPI molecules were held by alginate in the continuous phase through the interactions between them. As shown in **Figure 4-2**, optical microscopy images of alginate solutions, WPI/alginate solutions, and SPI/alginate dispersion show that more insoluble substances were observed in SPI/alginate dispersion, compared to alginate and WPI/alginate solutions. This indicates that SPI has lower solubility than WPI and tends to self-aggregate in alginate solutions.

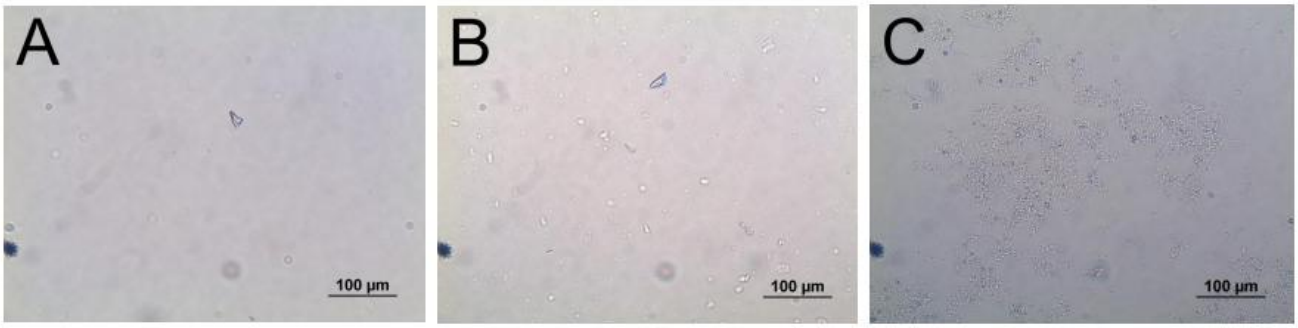

Figure 4-2. Optical microscopy images of (A) alginate solutions (0.4%, w/w), (B) WPI/alginate solutions (2.0% WPI and 0.4% alginate, w/w), and (C) SPI/alginate dispersions (2.0% SPI and 0.4% alginate, w/w).

In addition, the viscosity of alginate solutions, WPI/alginate solutions, and SPI/alginate dispersion was further investigated to demonstrate the interactions between protein and alginate. As shown in **Figure 4-3A**, WPI/alginate solutions exhibited more obvious shear-thinning behavior and higher viscosity than sodium alginate solutions and SPI/alginate dispersion, which indicates that WPI had stronger interactions with alginate than SPI. It has been reported that intermolecular associations between bovine serum albumin molecules and alginate chains occurred by electrostatic interactions between the oppositely charged amino acids and the anionic polysaccharide molecules, even though both polymers were negatively charged (Zhao et al., 2009). In addition, WPI contains many polar amino acids (Peña-Ramos, Xiong, & Arteaga, 2004), which could form hydrogen bonds between side chains of WPI amino acids and residues of alginate molecules. Therefore, the interactions between WPI and alginate were probably driven by the electrostatic interactions and hydrogen bonds

(Erben et al., 2019). On the other hand, SPI had weaker interactions with alginate, probably due to its lower solubility and fewer positively charged amino acids than WPI (i.e., 200.9 mg/g and 267.9 mg/g positively charged amino acids for SPI and WPI at pH 7.0, respectively) (Peña-Ramos, Xiong, & Arteaga, 2004; Tang et al., 2006).

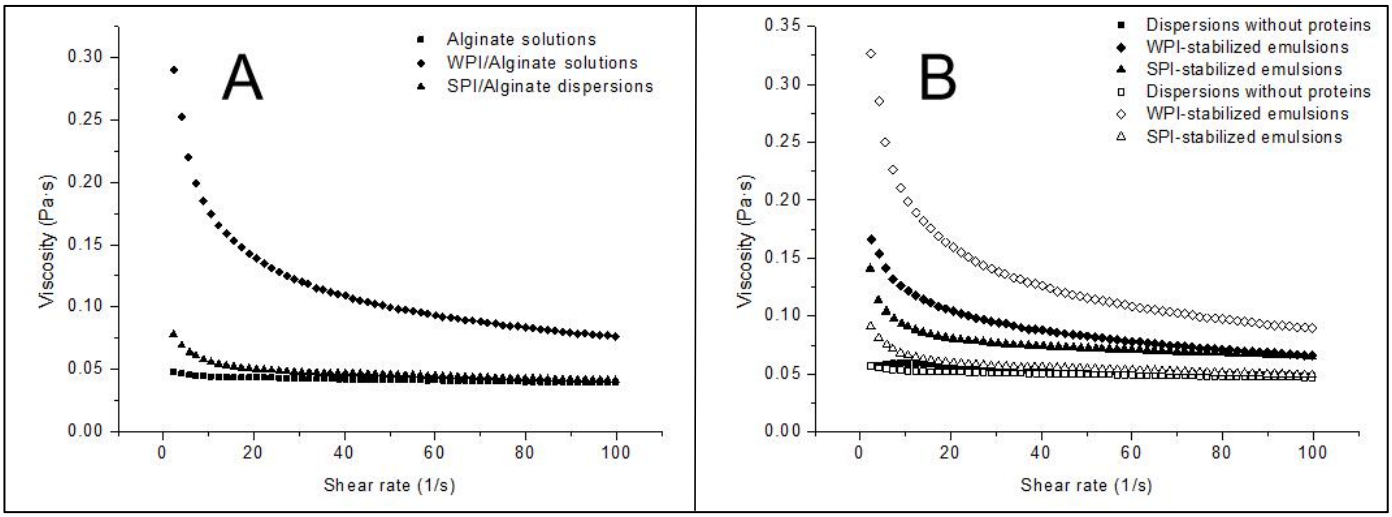

Figure 4-3. (A) Viscosity of alginate solutions (0.4%, w/w), WPI/alginate solutions (2.0% WPI and 0.4% alginate, w/w), and SPI/alginate dispersions (2.0% SPI and 0.4% alginate, w/w). (B) Viscosity of oil-in-water dispersions without proteins, WPI- and SPI-stabilized emulsions, in which solid symbols present the experimental viscosity of samples and open symbols present the calculated viscosity.

4.3.1.2. Droplet-size distributions of emulsions

Figure 4-4 shows that WPI- and SPI-stabilized emulsions had similar droplet-size distribution, while emulsions without protein (i.e., the control sample) had more large droplets than WPI- and SPI-stabilized emulsions. The droplet size in emulsions during homogenization depends on a balance between droplet disruption and droplet coalescence, so the droplet size can be affected by energy input, emulsifier type, and properties of the continuous phase. Increasing the intensity or duration of energy during homogenization can reduce the size of droplets in emulsions, but the energy input to all samples was the same in this study. The molecular properties of emulsifiers (e.g., size, conformation, flexibility, and interactions) can also affect the size of droplets in emulsions, because emulsifiers with better

hydrophobicity, higher flexibility, and/or smaller molecular size can adsorb more quickly at the surface of droplets to prevent droplet coalescence and thus produce smaller droplets during homogenization (McClements, 2015). In addition, the higher viscosity of the continuous phase can decrease droplet coalescence and thus produce smaller droplets. The poor hydrophobicity of alginate is probably the main reason leading to large droplets in the control sample, although the high viscosity of the continuous phase (i.e., alginate solutions) may also help to slow droplet coalescence.

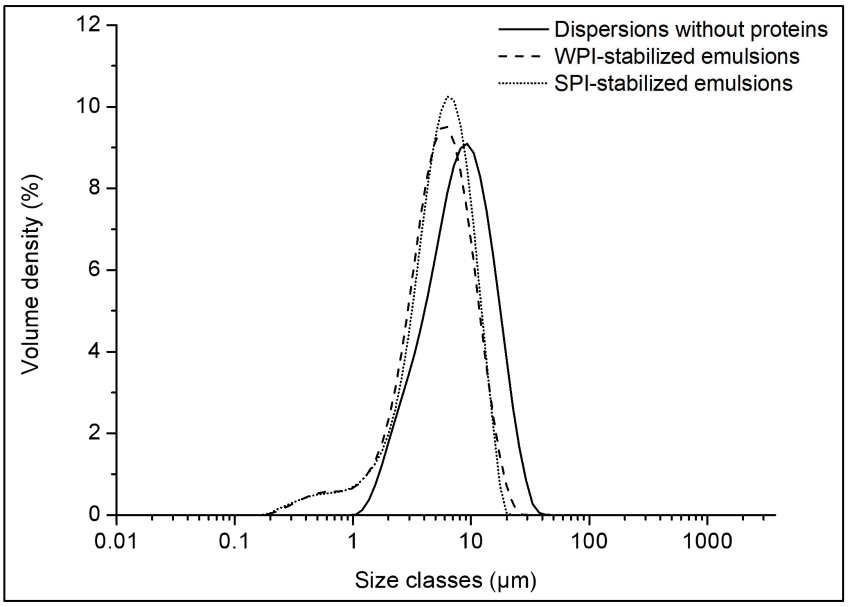

Figure 4-4. Droplet size distribution of dispersions without proteins and WPI- and SPI-stabilized emulsions.

However, many studies have indicated that WPI has higher hydrophobicity than SPI, although both of them are globular proteins with similar flexibility (Voutsinas, Cheung, & Nakai, 1983), which was at variance with the size distribution of WPI- and SPI-stabilized emulsions obtained in current study. This was probably because interactions between WPI and sodium alginate (as discussed in Section 4.3.1.1) decreased the translational diffusion coefficient of WPI (i.e., slower movement of WPI molecules from the continuous phase to the O/W interfaces). Therefore, it can be hypothesized that WPI- and SPI-stabilized emulsions had similar droplet size distribution, which was because interactions between

WPI and alginate negatively affect the adsorption kinetics of WPI, although WPI has higher hydrophobicity than SPI.

4.3.1.3. Viscosity of emulsions

Figures 4-3A and 4-3B show that adding 10% (ϕ, w/w) sunflower oil into alginate solutions or SPI/alginate dispersions increased their viscosity, while adding sunflower oil decreased the viscosity of WPI/alginate solutions. The viscosity of suspensions containing non-interacting spherical fluid particles (i.e., dispersed phase) can be calculated by the following equation (Larson, 1999; Tadros, 1994):

$$\eta = \eta_1 \left(1 + \left[\frac{\eta_1 + 2.5\eta_2}{\eta_1 + \eta_2}\right] \phi\right) \quad (4\text{-}6)$$

where η is the viscosity of dispersions, η_1 is the viscosity of the liquid surrounding the droplets, η_2 is the viscosity of the liquid in the droplets (the viscosity of sunflower oil is 0.063 ± 0.01 Pa·s), and ϕ is the dispersed phase volume fraction (i.e., 10% of the oil content in this study).

As shown in **Figure 4-3B**, the viscosity of the dispersion without protein (i.e., the control sample) could fit Eq. (4-6) well, which indicates that oil droplets in alginate solutions without protein were non-interacting spherical particles. However, the estimated viscosity of the SPI-stabilized emulsions was lower than their experimental values, and the estimated viscosity of the WPI-stabilized emulsions was higher than their experimental values. This was probably because SPI-coated emulsion droplets were flocculated. Emulsions containing flocculated droplets have higher viscosity than emulsions containing isolated droplets, because flocculated droplets trap some of the continuous phase within their

structures and therefore have a higher effective volume fraction (ϕ_{eff}) than the actual volume fraction of the dispersed phase (i.e., ϕ_{eff} > 10%) (McClements, 2015). The more obvious shear-thinning behavior of SPI-stabilized emulsions than SPI/alginate dispersions also proved that flocculation has occurred in SPI-stabilized emulsions. However, the situation is different for WPI-stabilized emulsions. As discussed in Section 4.3.1.1, WPI has strong interactions with alginate, probably driven by electrostatic interactions and hydrogen bonds. After adding oil into WPI/alginate solutions, some of WPI molecules move to the oil/water interface and then attach to the interface. The attachment of WPI molecules to the oil/water interface may lead to part of molecule structures attaching into the oil droplets, which leads to a decreased contact area between WPI and alginate and thus a decreased viscosity (η_1) of the continuous phase surrounding the droplets (as shown in **Figure 4-5**). Therefore, we hypothesized that the higher viscosity of SPI-stabilized emulsions than SPI/alginate dispersions was due to the occurrence of flocculation and the increased effective volume fraction (ϕ_{eff}), while the decreased viscosity of the continuous phase (η_1) was the main reason leading to the lower viscosity of WPI-stabilized emulsions compared to WPI/alginate solutions.

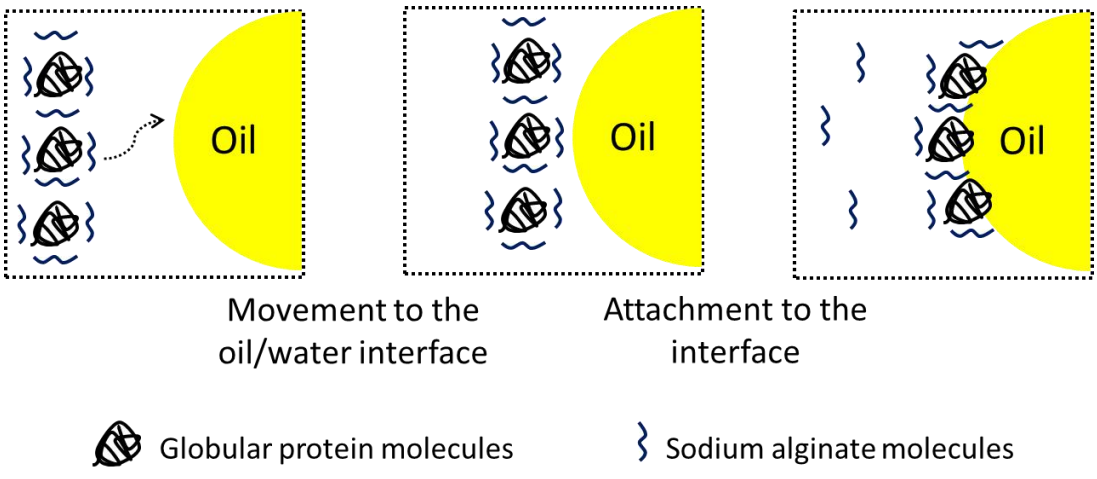

Figure 4-5. The adsorption of protein/alginate mixtures at the o/w interface (McClements, 2015).

4.3.2. Properties of alginate-based and protein-stabilized emulsion gel beads

4.3.2.1. Water and oil contents and structures of emulsion gel beads

Table 4-1 shows that SPI-stabilized emulsion gel beads had higher water content than WPI-stabilized emulsion gel beads, and emulsion gel beads without protein had lowest water content. If the oil was not lost during gelation, according to the oil content in gel beads, the water quantity in the gel beads compared to the weight of original emulsions can be calculated as 38.8 ± 3.1, 42.2 ± 2.8, and 56.4 ± 5.3 g/100g in original emulsions for emulsion gel beads without protein, WPI-stabilized emulsion gel beads, and SPI-stabilized emulsion gel beads, respectively. The results indicate that water loss in emulsion gel beads without protein, WPI-stabilized emulsion gel beads, and SPI-stabilized emulsion gel beads during gelation were 50.8 ± 3.1, 45.4 ± 2.8, and 31.4 ± 5.3 g/100g ($p < 0.05$), compared to their original emulsions, respectively. This indicates that both WPI and SPI could prevent water loss from alginate-based emulsion gel beads during gelation. This was probably associated with the solubility of proteins and interactions between protein and alginate, which affected the gelation process, structures and thus water content of alginate-based emulsion gel beads (Lin et al., 2020a).

Table 4-1. Properties of emulsion gel beads.

Samples	Water content (%)	Oil content (%)	Lycopene content (mg/kg)	Size (mm)		Young's modulus (Pa)	
				Minor axis	Major axis	Experimental value	Theoretical value predicted by the Kerner model
Gel beads without proteins	71.3 ± 1.5[a]	25.9 ± 2.1[c]	14.8 ± 1.0[c]	3.3 ± 0.1[a]	3.5 ± 0.1[a]	219 ± 8[b]	225–234
WPI-stabilized emulsion gel beads	73.1 ± 0.4[b]	23.8 ± 1.7[b]	12.4 ± 0.8[b]	3.5 ± 0.1[b]	3.6 ± 0.1[b]	233 ± 7[c]	305–318
SPI-stabilized emulsions gel beads	76.2 ± 1.3[c]	17.9 ± 1.7[a]	9.7 ± 0.7[a]	3.8 ± 0.1[c]	4.0 ± 0.2[c]	187 ± 6[a]	131–136

[a] Different lowercase letters indicate significant differences between values in a column ($p < 0.05$).

In this study, emulsion gel beads were prepared by the external gelation method, in which emulsions were dropped into $CaCl_2$ solutions. When emulsion drops contact with the $CaCl_2$ solution, the surface of drops gelatinizes immediately, and then the gelation process progresses gradually from the surface to interior of gel beads with the diffusion of Ca^{2+}. During this process, stretches of alginate monomers interact with Ca^{2+}, and the formation of junctions between them forces water out and leads to shrinkage of gel beads (Rehm, 2009). When WPI was added into this system, due to the high solubility of WPI, water molecules may serve as bridges to form hydrogen bonds between polar amino acids of WPI and residues of alginate molecules, which decreased water loss during gelation and a larger bead size. However, SPI has lower solubility and less interaction with alginate than WPI, so SPI may act as barriers to block the gelation process of alginate monomers, which led to weak gel structures, decreased water loss during gelation, and thus larger bead size as well.

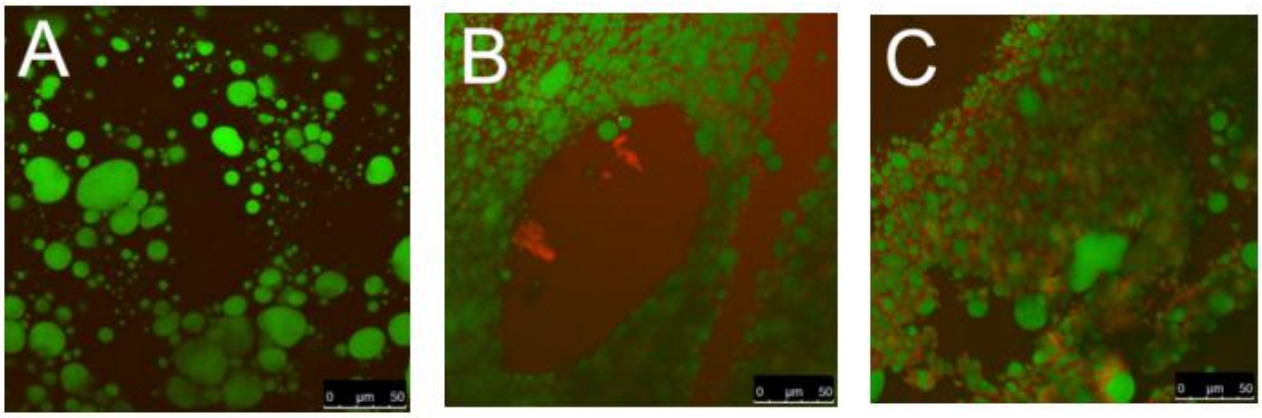

Figure 4-6. CLSM images of (A) gel beads without proteins, (B) WPI-stabilized emulsion gel beads, and (C) SPI-stabilized emulsion gel beads. Protein and sunflower oil were stained by red and green, respectively.

Figure 4-6 shows the distribution of protein and oil droplets in emulsion gel beads: more WPI was distributed in matrices (as seen by a more evenly red background) than SPI, while SPI tended to self-aggregate around oil droplets. In addition, the deformation and coalescence of emulsion droplets occurred in all gel beads during gelation, compared to their original emulsion structures before gelation (**Figure 4-1**). This was probably because, in

current study, the emulsion gel matrix structure formed by 0.4% alginate was fragile, and thus structural collapse occurred during gelation (Lin et al., 2020a).

In addition, **Table 4-1** also shows that the oil content of emulsion gel beads without protein was higher than that of WPI- and SPI-stabilized emulsion gel beads, although the oil contents in their original dispersions were the same (i.e., 10%, w/w). This was probably because, when water loss occurs during gelation, the oil content in samples increases accordingly. Emulsion gel beads without protein lost more water during gelation, so the oil content in them was higher compared to WPI- and SPI-stabilized emulsion gel beads. This was also the main reason why gel beads without protein had higher lycopene content compared to WPI- and SPI-stabilized emulsion gel beads (as shown in **Table 4-1**).

4.3.2.2. Young's modulus of emulsion gel beads

The mechanical properties of emulsion gel beads are very important, because they are closely associated with other properties (e.g., storage stability, oral perception, and controlled release) and their applications. Many factors can affect the mechanical properties of emulsion gel beads, such as matrix structure, interactions between matrix and emulsifier-stabilized droplets, oil type, oil volume fraction, and droplet size (Lin, Kelly & Miao, 2020). However, the matrix structure may be the most important factor affecting the release of nutrients encapsulated in emulsion gels during digestion. It has been reported that a denser WPI-based matrix structure delayed the digestion of lipid encapsulated in emulsion gels (Guo, Bellissimo, & Rousseau, 2017). In this study, the Young's modulus of emulsion gel beads was analyzed.

Table 4-1 shows that the Young's modulus of the control sample was higher than that of SPI-stabilized emulsion gels but lower than that of WPI-stabilized emulsion gels. The modulus of overall emulsion gels was affected by matrix and filler droplets, according to the Kerner model modified by Lewis and Nielsen (Kerner, 1956; Lewis & Nielsen, 1970):

$$\frac{G'_{gel}}{G'_{matrix}} = \frac{15(1-v_m)(M-1)\psi\phi_f}{(8-10v_m)M+7-5v_m-(8-10v_m)(M-1)\psi\phi_f} + 1 \quad (4\text{-}7)$$

where $M = \frac{G'_{filler}}{G'_{matrix}}$, G'_{gel}, G'_{filler}, and G'_{matrix} are the modulus of the overall gel, the filler droplets and the gel matrix, respectively, $\psi\phi_f$ is the effective droplet volume fraction, and v_m is the Poisson's ratio of the gel matrix.

In addition, the modulus of the filler droplets ($G'_{filler} = 4\gamma$ / d) is affected by the surface tension (γ) and the average diameter (d) of the oil droplets. It can be seen that the modulus of the overall gel (G'_{gel}) is in direct proportion to the M, $\psi\phi_f$, and G'_{matrix}. However, it should be noted that the modified Kerner model is normally used under the assumption that M or G'_{matrix} do not change with changes in other factors (e.g., ϕ_f) (Lin et al., 2020b).

According to Eq. (4-7), the theoretical values of G'_{gel}/G'_{matrix} of alginate-based emulsion gels were 1.22–1.27 with the assumption that M was 12~70 (Chen & Dickinson, 1998), $\psi\phi_f$ was 0.1, and v_m was 0.5 (Ahearne, Yang, El Haj, Then, & Liu, 2005; Langley & Green, 1989). In contrast, the experimental values of G'_{matrix} of emulsion gels without protein, and WPI- and SPI-stabilized emulsion gels (i.e., alginate, alginate/WPI, and alginate/SPI gel beads) were 184 ± 15 Pa, 250 ± 17 Pa, and 107 ± 6 Pa, respectively, which indicates that the presence of WPI led to the formation of alginate gel beads with stronger gel strength than SPI. Therefore, their experimental values of G'_{gel}/G'_{matrix} were 1.19 ± 0.04, 0.93 ± 0.03, and 1.75 ± 0.06, respectively. It can be seem that alginate-stabilized emulsion gels without protein (i.e., the control sample) fitted the modified Kerner model well; however, the experimental value of G'_{gel}/G'_{matrix} for WPI-stabilized emulsion gels was lower than the theoretical value, and the experimental value of SPI-stabilized emulsion gels was higher than the theoretical value. The possible reason was that adding oil led to the absorption of protein from the matrix to the oil/water surface, which resulted in decreased interactions between WPI and alginate molecules in the matrix, and thus a decreased G'_{matrix} of WPI-stabilized emulsion gels, but led to a less structural obstruction of SPI to the matrix and thus an

increased G'_{matrix} of SPI-stabilized emulsion gels. Therefore, we presume that the presence of oil in alginate/protein based emulsion gels affected the mechanical properties of overall emulsion gels, because oil droplets draw proteins from the matrix to the oil/water interfaces, and thus affects the mechanical properties of alginate/protein-based matrix.

4.3.3. *In-vitro* digestion behavior of emulsion gel beads containing lycopene

4.3.3.1. Young's modulus, shrinkage, and structure of emulsion gel beads during oral and gastric digestion

Alginate-based gel beads normally shrink during gastric digestion and swell during intestinal digestion, probably due to the changes in electrostatic forces in the gel matrix at different pH and/or the occurrence of ion-exchange at various ionic strength conditions (Rayment et al., 2009). The shrinkage of beads during gastric digestion can affect the structural and mechanical properties of beads and thereby their digestion behavior in the following intestinal digestion. In addition, the zeta potential of WPI and SPI also differs at different pH values, which may affect the interactions between alginate and protein molecules. Therefore, it is important to investigate the changes in mechanical properties of protein/alginate-based emulsion beads during oral and gastric digestion.

Figure 4-7A shows that the Young's modulus of gel beads without protein, WPI-stabilized emulsion beads and SPI-stabilized emulsion beads at the end of oral digestion were 1.32, 1.22, and 1.13 times higher than their original Young's modulus before digestion, respectively. A possible explanation for increased Young's modulus of alginate-based gel beads during oral digestion is that, the simulated saliva fluid (SSF) contains 13.6 mM sodium bicarbonate, which may react with calcium ions in alginate-based gel beads (i.e., $Ca^{2+} + HCO^{3-} \rightarrow CaCO_3 + H^+$) and thus lead to the dissociation of calcium ions from alginate multimers and the formation of $CaCO_3$ nanoparticles and hydrogen bonds between alginate chains (Norton, Frith, & Ablett, 2006). The $CaCO_3$ nanoparticles may also act as

physical cross-linker between carboxylic groups of alginate (Shen, Nyström, & Mezzenga, 2017). On the other hand, the presence of proteins in alginate-based emulsion beads led to a lower change rate of Young's modulus during oral digestion compared to gel beads without protein, which was probably because the presence of proteins disrupted the gelation process of alginate during the preparation, and then original gel beads contained higher levels of water, which led to lower concentrations of calcium ions in the gel matrices (Quong et al., 1998).

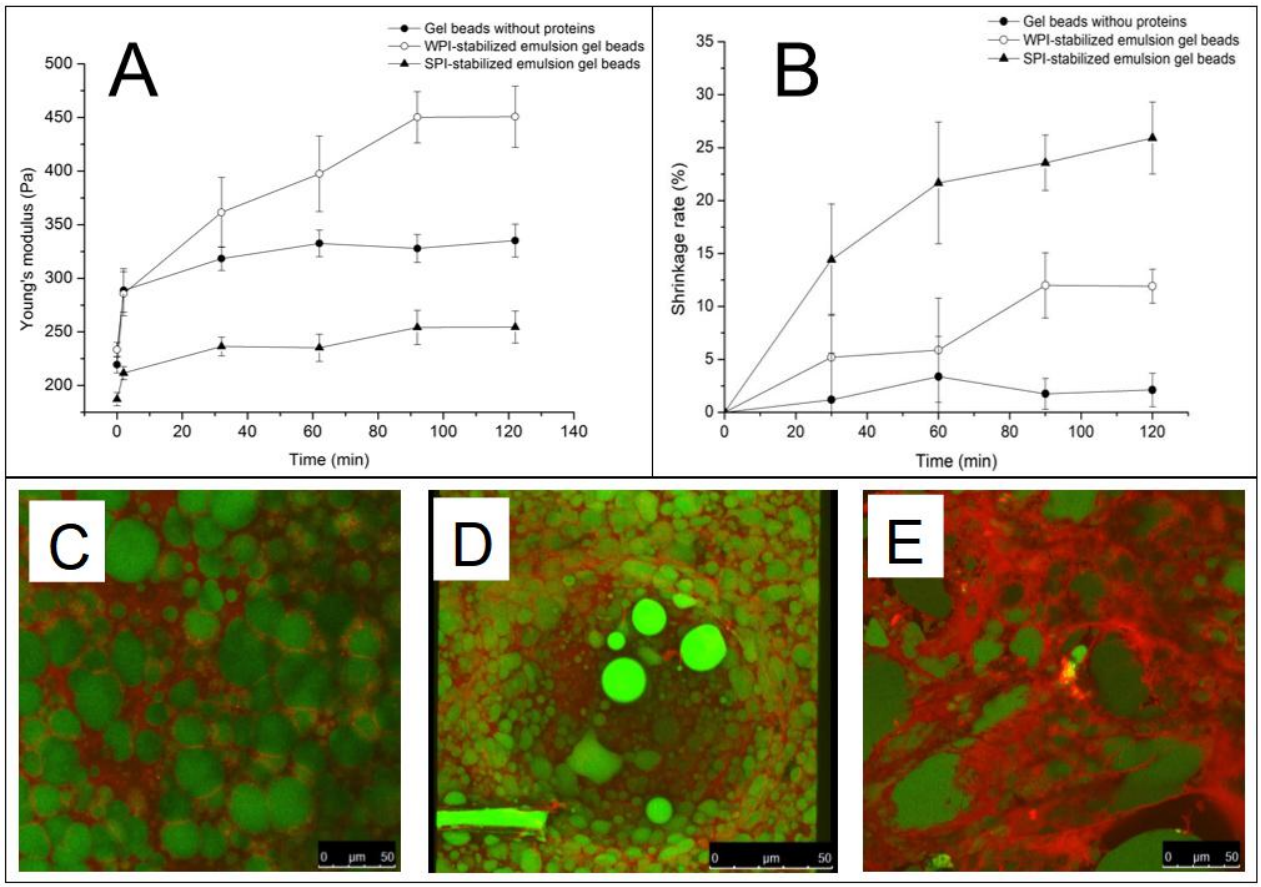

Figure 4-7. (A) Young's modulus of gel beads without proteins, WPI-stabilized emulsion gel beads, and SPI-stabilized emulsion gel beads during *in-vitro* oral and gastric digestions. (B) Shrinkage of gel beads without proteins, WPI-stabilized emulsion gel beads, and SPI-stabilized emulsion gel beads during *in-vitro* gastric digestions. CLSM images of (C) gel beads without proteins, (D) WPI-stabilized emulsion gel beads, and (E) SPI-stabilized emulsion gel beads after *in-vitro* gastric digestion for 120 min. Protein and sunflower oil were stained by red and green in CLSM figures D-F, respectively.

Figure 4-7A also shows that the Young's modulus of gel beads without protein, WPI-stabilized emulsion beads and SPI-stabilized emulsion beads at the end of gastric digestion were 1.16, 1.59, and 1.36 times higher than their Young's modulus at the end of oral digestion, respectively. The further increased Young's modulus of alginate-based gel beads during gastric digestion probably resulted from the decreased electrostatic forces between alginate monomers. The pH of digestive juice was maintained at 3.0 during gastric digestion, and pKa of alginate is at around 3.5 and thus alginate loses its negative charge at lower pH values (Li et al., 2011). Therefore, alginate monomers with lower charges had less electrostatic repulsion with each other, and a denser structure formed. On the other hand, the presence of proteins in alginate-based emulsion beads led to a higher rate of change of Young's modulus during gastric digestion compared to gel beads without protein. A possible reason is that the electrostatic attractions between alginate monomers and protein molecules increased with the decreased pH (from 7.0 to 3.0). The isoelectric point of WPI and SPI has been reported to be pH 5.0 and 4.5, respectively, and thus proteins should be positively charged at pH 3.0 during gastric digestion (Fioramonti et al., 2014).

The shrinkage of emulsion gel beads during gastric digestion may also be a critical factor. As shown in **Figure 4-7B**, emulsion gel beads without protein shrank by 2.1%, while WPI-stabilized emulsion beads and SPI-stabilized emulsion beads shrank by 11.9% and 25.9% after gastric digestion, respectively, compared to their size after oral digestion. This indicates that the presence of WPI and SPI in alginate-based emulsion gels led to more shrinkage than gel beads without protein during gastric digestion, probably also due to the electrostatic attractions between alginate and proteins at pH 3.0. In addition, the size of emulsion gel beads without protein, WPI-stabilized emulsion beads, and SPI-stabilized emulsion beads decreased from R'_{min} = 3.2 ± 0.1 mm and R'_{max} = 3.5 ± 0.2 mm to R'_{min} = 3.2 ± 0.1 mm and R'_{max} = 3.4 ± 0.1 mm, from R'_{min} = 3.3 ± 0.1 mm and R'_{max} = 3.4 ± 0.1 mm to R'_{min} = 3.0 ± 0.1 mm and R'_{max} = 3.2 ± 0.1 mm, and from R'_{min} = 3.7 ± 0.1 mm and R'_{max} = 3.8 ± 0.1 mm to R'_{min} = 3.1 ± 0.1 mm and R'_{max} = 3.3 ± 0.1 mm, respectively, during gastric digestion. This

indicates that the presence of WPI and SPI led to smaller size of alginate-based emulsion gel beads after gastric digestion and thus denser gel structures.

Figures 4-7C–E shows the distribution of protein and oil droplets in emulsion gel beads after gastric digestion. The coalescence of droplets further increased after gastric digestion, compared to their original emulsion gel structures (**Figure 4-6**). There are several likely reasons for this observation. Firstly, the decreased electrostatic forces between alginate monomers during gastric digestion may result in a denser structure of gel matrix and thus force oil droplets to merge together. Secondly, peptic hydrolysis of proteins may have reduced the stability of emulsion droplets (Liu, Gao, & Yuan, 2015). Thirdly, the decreased pH values of gel beads may decrease the zeta-potential value of WPI and SPI and lead to protein aggregation and thus a decreased emulsifying capacity (Bokkhim et al., 2016; Elizalde, Bartholomai, & Pilosof, 1996).

4.3.3.2. Lycopene release from emulsion gel beads during intestinal digestion

The visual appearance of alginate-based and protein-stabilized emulsion gels (**Figure 4-8**) and the release of encapsulated nutrient (i.e., lycopene) from gel beads during intestinal digestion (**Figure 4-9**) were studied. Alginate gels normally swell during intestinal digestion, due to the deprotonation and increased repulsive forces of the uronic acid groups on alginate at neutral pH above the pKa, and then structural degradation occurs, due to ion-exchange between Na^+ ions present in the digestive fluid and Ca^{2+} ions present in gel beads (Bajpai & Sharma, 2004; Rayment, et al., 2009). As shown in **Figure 4-8**, structural collapse of gel beads without proteins, WPI-stabilized emulsion gel beads, and SPI-stabilized emulsion gel beads occurred at 2–3 h, 4–5 h, and 3–4 h after swelling during intestinal digestion, respectively. This indicates that the presence of WPI and SPI could slow the swelling process and thus delay the structural degradation of alginate-based emulsion gel beads during intestinal digestion, probably because of the denser structures formed by electrostatic

attractions between negatively charged alginate monomers with positively charged protein molecules after gastric digestion (as discussed in Section 4.3.3.1).

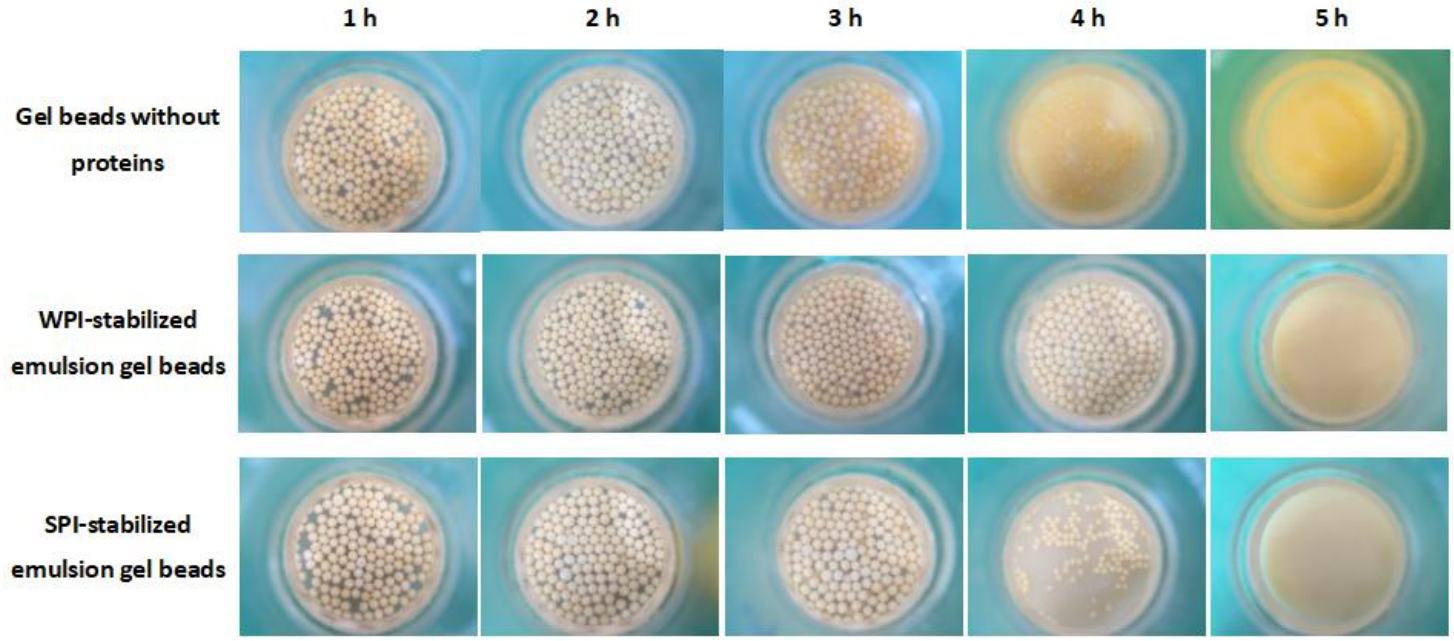

Figure 4-8. Visual appearance of gel beads without proteins, WPI-stabilized emulsion gel beads, and SPI-stabilized emulsion gel beads during *in-vitro* intestinal digestion.

Figure 4-9 shows that lycopene release from gel beads without proteins, WPI-stabilized emulsion gel beads, and SPI-stabilized emulsion gel beads commenced at 2.5–3 h, 4–4.5 h, and 3.5–4h, respectively, which corresponded with the start point of the structural collapse of gel beads (**Figure 4-8**). This indicates that lycopene was released with degradation of network structures after swelling of gel beads during intestinal digestion. It has been reported that the encapsulated nutrients can be released from gel beads by two mechanisms: diffusion through increasingly large pores and/or release following degradation of network structures during intestinal digestion, which depends on the size of pores in beads and the size of encapsulated nutrients (George & Abraham, 2006).

In this study, lycopene release was correlated with the release of oil droplets from emulsion gel beads. The size of oil droplets in gel beads (**Figures 4-7C–E**) were

significantly larger than the pores of alginate gel matrices (normally between 5 and 200 nm) (George & Abraham, 2006). Therefore, lycopene and oil droplets were released from alginate-based emulsion gel beads due to structural degradation after swelling rather than during the swelling process. **Figure 4-9** also shows that the presence of WPI and SPI in alginate-based emulsion beads delayed the release of lycopene from beads during intestinal digestion. This was because the presence of WPI and SPI slowed the swelling process, due to the denser structures formed after gastric digestion, and thus delayed the structural collapse. Therefore, it may be assumed that the digestion of gel matrix and the release of encapsulated nutrients from emulsion beads are affected by not only the gel strength but also the gel density, the matrix components of gels, and the size of droplets.

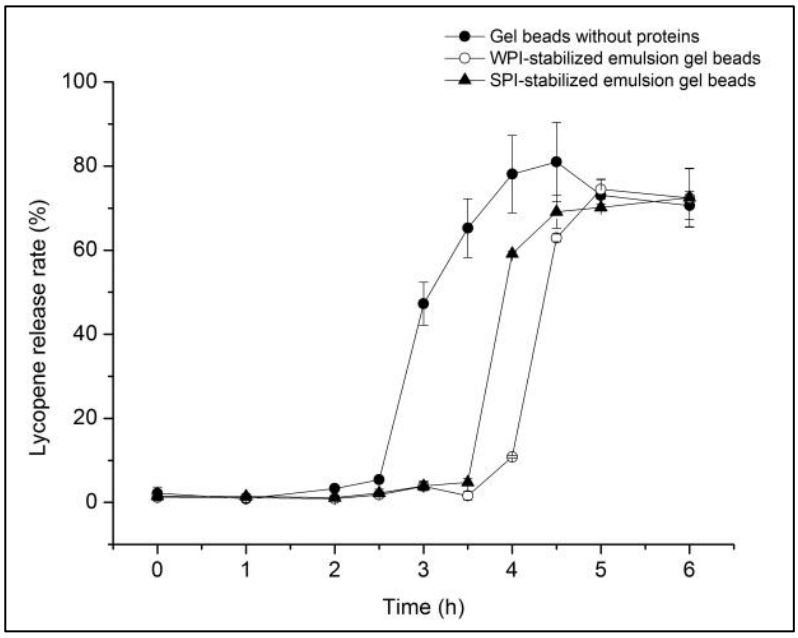

Figure 4-9. Lycopene release from gel beads without proteins, WPI-stabilized emulsion gel beads, and SPI-stabilized emulsion gel beads during *in-vitro* intestinal digestion.

4.4. Conclusions

The presence of WPI in alginate-based emulsions resulted in emulsions with higher viscosity and less flocculation of droplets than emulsions containing SPI, probably because WPI had better solubility and stronger interactions with alginate than SPI. WPI and SPI

could prevent water loss from alginate-based emulsion gel beads during gelation, resulting in lower oil and lycopene contents, compared to gel beads without proteins. The presence of WPI increased the Young's modulus of gel beads, due to increased Young's modulus of WPI/alginate complexes-based gel matrix, while the presence of SPI decreased the Young's modulus because of its low solubility, compared to alginate-based gel beads without proteins. The presence of proteins (both WPI and SPI) resulted in higher shrinkage rate and accelerated change in Young's modulus of gel beads during *in-vitro* gastric digestion, and led to delayed release of lycopene from gel beads during *in-vitro* intestinal digestion.

The findings of this study underline the role of different proteins in the properties of alginate-based emulsions and emulsion gel beads, and the delayed release of lycopene from gel beads during *in-vitro* digestion, which makes it possible to design emulsion gel beads with potential controlled released of functional hydrophobic ingredients by structuring the gel matrix and the water/oil interfaces with natural polymers (e.g., proteins) instead of synthetic chemicals (e.g., Tween 20 and Span 80). However, this study mainly focused on the effect of WPI and SPI on the mechanical and structural properties of alginate-based emulsion gel beads after gelation and during *in-vitro* digestion, so further research on the effect of WPI and SPI on the stability of encapsulated lycopene during storage and the bio-availability during intestinal digestion is needed.

References

Aguirre Calvo, T. R., Busch, V. M., & Santagapita, P. R. (2017). Stability and release of an encapsulated solvent-free lycopene extract in alginate-based beads. *LWT - Food Science and Technology, 77*, 406-412.

Ahearne, M., Yang, Y., El Haj, A. J., Then, K. Y., & Liu, K.-K. (2005). Characterizing the viscoelastic properties of thin hydrogel-based constructs for tissue engineering applications. *Journal of the Royal Society Interface, 2*, 455-463.

Albarracin, M., Jose Gonzalez, R., & Drago, S. R. (2015). Soaking and extrusion effects on physicochemical parameters, phytic acid, nutrient content and mineral bio-accessibility of whole rice grain. *International Journal of Food Science and Nutrion, 66*, 210-215.

Anthon, G., & Barrett, D. M. (2006). Standardization of a rapid spectrophotometric method for lycopene analysis. *Acta Hortic, 1*, 111-128.

Bajpai, S., & Sharma, S. (2004). Investigation of swelling/degradation behaviour of alginate beads crosslinked with Ca^{2+} and Ba^{2+} ions. *Reactive and Functional Polymers, 59*, 129-140.

Benavides, S., Cortés, P., Parada, J., & Franco, W. (2016). Development of alginate microspheres containing thyme essential oil using ionic gelation. *Food chemistry, 204*, 77-83.

Bokkhim, H., Bansal, N., Grøndahl, L., & Bhandari, B. (2016). *In-vitro* digestion of different forms of bovine lactoferrin encapsulated in alginate micro-gel particles. *Food Hydrocolloids, 52*, 231-242.

Bou, R., Boon, C., Kweku, A., Hidalgo, D., & Decker, E. A. (2011). Effect of different antioxidants on lycopene degradation in oil-in-water emulsions. *European Journal of Lipid Science and Technology, 113*, 724-729.

Calvo, T. R. A., Busch, V. M., & Santagapita, P. R. (2017). Stability and release of an encapsulated solvent-free lycopene extract in alginate-based beads. *LWT - Food Science and Technology, 77*, 406-412.

Castro, M. A. A., Alric, I., Brouillet, F., Peydecastaing, J., Fullana, S. G., & Durrieu, V. (2018). Soy protein microparticles for enhanced oral ibuprofen delivery: Preparation, characterization, and *in vitro* release evaluation. *AAPS PharmSciTech, 19*, 1124-1132.

Chen, J., & Dickinson, E. (1998). Viscoelastic properties of heat-set whey protein emulsion gels. *Journal of Texture Studies, 29*, 285-304.

Chen, L., Yokoyama, W., Liang, R., & Zhong, F. (2020). Enzymatic degradation and bioaccessibility of protein encapsulated *β*-carotene nano-emulsions during *in vitro* gastro-intestinal digestion. *Food Hydrocolloids, 100*, 105177.

Costa-Rodrigues, J., Pinho, O., & Monteiro, P. R. R. (2018). Can lycopene be considered an effective protection against cardiovascular disease? *Food Chemistry, 245*, 1148-1153.

Elizalde, B., Bartholomai, G., & Pilosof, A. (1996). The effect of pH on the relationship between hydrophilic/lipophilic characteristics and emulsification properties of soy proteins. *LWT-Food Science and Technology, 29*, 334-339.

Erben, M., Pérez, A. A., Osella, C. A., Alvarez, V. A., & Santiago, L. G. (2019). Impact of gum arabic and sodium alginate and their interactions with whey protein aggregates on bio-based films characteristics. *International Journal of Biological Macromolecules, 125*, 999-1007.

Feng, W., Yue, C., Ni, Y., & Liang, L. (2018). Preparation and characterization of emulsion-filled gel beads for the encapsulation and protection of resveratrol and *α*-tocopherol. *Food Research International, 108*, 161-171.

Fioramonti, S. A., Perez, A. A., Aríngoli, E. E., Rubiolo, A. C., & Santiago, L. G. (2014). Design and characterization of soluble biopolymer complexes produced by electrostatic self-assembly of a whey protein isolate and sodium alginate. *Food Hydrocolloids, 35*, 129-136.

George, M., & Abraham, T. E. (2006). Polyionic hydrocolloids for the intestinal delivery of protein drugs: Alginate and chitosan-A review. *Journal of Controlled Release, 114*, 1-14.

Guo, Q., Bellissimo, N., & Rousseau, D. (2017). Role of gel structure in controlling *in vitro* intestinal lipid digestion in whey protein emulsion gels. *Food Hydrocolloids, 69*, 264-272.

Kerner, E. (1956). The elastic and thermo-elastic properties of composite media. Proceedings of the physical society. *Section B, 69*, 808.

Langley, K. R., & Green, M. L. (1989). Compression and impact strength of gels, prepared from fractionated whey proteins, in relation to composition and microstructure. *Journal of Dairy Research, 56*, 275-284.

Larson, R. G. (1999). *The structure and rheology of complex fluids* (Vol. 150): Oxford university press, New York.

Lee, K. Y., & Mooney, D. J. (2012). Alginate: Properties and biomedical applications. *Progress in Polymer Science, 37*, 106-126.

Leon, A. M., Medina, W. T., Park, D. J., & Aguilera, J. M. (2018). Properties of microparticles from a whey protein isolate/alginate emulsion gel. *Food Science and Technology International, 24*, 414-423.

Lević, S., Pajić Lijaković, I., Đorđević, V., Rac, V., Rakić, V., Šolević Knudsen, T., Pavlović, V., Bugarski, B., & Nedović, V. (2015). Characterization of sodium alginate/*D*-limonene emulsions and respective calcium alginate/*D*-limonene beads produced by electrostatic extrusion. *Food Hydrocolloids, 45*, 111-123.

Lewis, T. B., & Nielsen, L. E. (1970). Dynamic mechanical properties of particulate-filled composites. *Journal of Applied Polymer Science, 14*, 1449-1471.

Li, Y., Hu, M., Du, Y., Xiao, H., & McClements, D. J. (2011). Control of lipase digestibility of emulsified lipids by encapsulation within calcium alginate beads. *Food Hydrocolloids, 25*, 122-130.

Lin, D., Kelly, A. L., Maidannyk, V., & Miao, S. (2020a). Effect of concentrations of alginate, soy protein isolate and sunflower oil on water loss, shrinkage, elastic and structural properties of alginate-based emulsion gel beads during gelation. *Food Hydrocolloids, 108*, 105998.

Lin, D., Kelly, A. L., & Miao, S. (2020b). Preparation, structure-property relationships and applications of different emulsion gels: Bulk emulsion gels, emulsion gel particles, and fluid emulsion gels. *Trends in Food Science & Technology, 102*, 123-137.

Lin, D., Lu, W., Kelly, A. L., Zhang, L., Zheng, B., & Miao, S. (2017). Interactions of vegetable proteins with other polymers: Structure-function relationships and applications in the food industry. *Trends in Food Science & Technology, 68*, 130-144.

Liu, D., Shi, J., Colina Ibarra, A., Kakuda, Y., & Jun Xue, S. (2008). The scavenging capacity and synergistic effects of lycopene, vitamin E, vitamin C, and *β*-carotene mixtures on the DPPH free radical. *LWT - Food Science and Technology, 41*, 1344-1349.

Liu, F., Gao, Y., & Yuan, F. (2015). Effects of chitosan addition on *in vitro* digestibility of protein-coated lipid droplets. *Journal of Dispersion Science and Technology, 36*, 1556-1563.

McClements, D. J. (2015). *Food emulsions: principles, practices, and techniques*. Boca Raton, FL: CRC press.

Minekus, M., Alminger, M., Alvito, P., Ballance, S., Bohn, T., Bourlieu, C., Carriere, F., Boutrou, R., Corredig, M., Dupont, D., Dufour, C., Egger, L., Golding, M., Karakaya, S., Kirkhus, B., Le Feunteun, S., Lesmes, U., Macierzanka, A., Mackie, A., Marze, S., McClements, D. J., Menard, O., Recio, I., Santos, C. N., Singh, R. P., Vegarud, G. E., Wickham, M. S., Weitschies, W., & Brodkorb, A. (2014). A standardised static *in vitro* digestion method suitable for food - an international consensus. *Food and Function, 5*, 1113-1124.

Mongar, J., & Wassermann, A. (1949). Fully swollen alginate gels as permutites: Kinetics of calcium-sodium ion exchange. *Discussions of the Faraday Society, 7*, 118-123.

Moschakis, T., Murray, B. S., & Biliaderis, C. G. (2010). Modifications in stability and structure of whey protein-coated o/w emulsions by interacting chitosan and gum arabic mixed dispersions. *Food hydrocolloids, 24*, 8-17.

Norton, I., Frith, W., & Ablett, S. (2006). Fluid gels, mixed fluid gels and satiety. *Food Hydrocolloids, 20*, 229-239.

Pelegrine, D., & Gasparetto, C. (2005). Whey proteins solubility as function of temperature and pH. *LWT-Food Science and Technology, 38*, 77-80.

Peña-Ramos, E. A., Xiong, Y. L., & Arteaga, G. E. (2004). Fractionation and characterisation for antioxidant activity of hydrolysed whey protein. *Journal of the Science of Food and Agriculture, 84*, 1908-1918.

Piornos, J. A., Burgos-Díaz, C., Morales, E., Rubilar, M., & Acevedo, F. (2017). Highly efficient encapsulation of linseed oil into alginate/lupin protein beads: Optimization of the emulsion formulation. *Food Hydrocolloids, 63*, 139-148.

Quong, D., Neufeld, R., Skjåk-Bræk, G., & Poncelet, D. (1998). External versus internal source of calcium during the gelation of alginate beads for DNA encapsulation. *Biotechnology and Bioengineering, 57*, 438-446.

Rayment, P., Wright, P., Hoad, C., Ciampi, E., Haydock, D., Gowland, P., & Butler, M. F. (2009). Investigation of alginate beads for gastro-intestinal functionality, Part 1: *In vitro* characterisation. *Food Hydrocolloids, 23*, 816-822.

Rehm, B. H. (2009). *Alginates: biology and applications* (Vol. 13): Springer.

Shariffa, Y. N., Tan, T. B., Uthumporn, U., Abas, F., Mirhosseini, H., Nehdi, I. A., Wang, Y. H., & Tan, C. P. (2017). Producing a lycopene nanodispersion: Formulation development and the effects of high pressure homogenization. *Food Research International, 101*, 165-172.

Shen, Y., Nyström, G., & Mezzenga, R. (2017). Amyloid fibrils form hybrid colloidal gels and aerogels with dispersed $CaCO_3$ nanoparticles. *Advanced Functional Materials, 27*, 1700897.

Shi, J., Dai, Y., Kakuda, Y., Mittal, G., & Xue, S. J. (2008). Effect of heating and exposure to light on the stability of lycopene in tomato purée. *Food Control, 19*, 514-520.

Soukoulis, C., Cambier, S., Hoffmann, L., & Bohn, T. (2016). Chemical stability and bioaccessibility of *β*-carotene encapsulated in sodium alginate o/w emulsions: Impact of Ca^{2+} mediated gelation. *Food hydrocolloids, 57*, 301-310.

Srivastava, S., & Srivastava, A. K. (2013). Lycopene; chemistry, biosynthesis, metabolism and degradation under various abiotic parameters. *Journal of Food Science and Technology, 52*, 41-53.

Tadros, T. F. (1994). Fundamental principles of emulsion rheology and their applications. *Colloids and Surfaces A: Physicochemical and Engineering Aspects, 91*, 39-55.

Tang, C. H., Ten, Z., Wang, X. S., & Yang, X. Q. (2006). Physicochemical and functional properties of hemp (*Cannabis sativa L.*) protein isolate. Journal of Agricultural and *Food Chemistry, 54*, 8945-8950.

Ukai, N., Lu, Y., Etoh, H., Yagi, A., Ina, K., Oshima, S., Ojima, F., Sakamoto, H., & Ishiguro, Y. (2014). Photosensitized oxygenation of lycopene. *Biosci Biotechnol Biochem, 58*, 1718-1719.

Urbonaite, V., De Jongh, H., Van Der Linden, E., & Pouvreau, L. (2015). Water holding of soy protein gels is set by coarseness, modulated by calcium binding, rather than gel stiffness. *Food Hydrocolloids, 46*, 103-111.

Voutsinas, L. P., Cheung, E., & Nakai, S. (1983). Relationships of hydrophobicity to emulsifying properties of heat denatured proteins. *Journal of Food Science, 48*, 26-32.

Yang, L. J., Guo, J., Yu, Y., An, Q. D., Wang, L. Y., Li, S. L., Huang, X. L., Mu, S. Y., & Qi, S. W. (2016). Hydrogen bonds of sodium alginate/Antarctic krill protein composite material. *Carbohydrate Polymers, 142*, 275-281.

Zhao, Y., Li, F., Carvajal, M. T., & Harris, M. T. (2009). Interactions between bovine serum albumin and alginate: An evaluation of alginate as protein carrier. *Journal of Colloid and Interface Science, 332*, 345-353.

CHAPTER FIVE

Effect of pH on Mechanical Properties, Storage Stability and *In-vitro* Digestion of Alginate-based and Soy Protein Isolate-stabilized Emulsion Gel Beads

Chapter 5 has been submitted:

Lin, D., Kelly, A. L., & Miao*, S. (2021). The impact of pH on mechanical properties, storage stability and digestion of alginate-based and soy protein isolate-stabilized emulsion gel beads with encapsulated lycopene (submitted to *Food Chemistry*).

The work contained in this chapter was undertaken and written solely by myself with specific contributions from each co-author.

Abstract

In alginate-based emulsion gels containing protein-coated droplets, pH can influence the gelation mechanism of alginate gels, and interactions between alginate molecules and protein-coated droplets, and thus properties of emulsion gels. The purpose of this chapter was to investigate the effect of pH of emulsions (i.e., pH 3–7) on the properties (e.g., droplet status, surface structures of droplets, mechanical properties, storage stability, digestion behavior) of alginate-based and soy protein isolate(SPI)-stabilized emulsion gel beads. Emulsion droplets in alginate/SPI-stabilized emulsions were coated by a single layer of SPI at pH 6–7 and a double layer of alginate/SPI at pH 3–5. Emulsion droplet flocculation only occurred in emulsions at pH 7.0. Emulsion gel beads formed at pH 3.0 had lower mechanical strength, higher storage stability, and faster release of encapsulated lycopene during *in-vitro* digestion than those formed at pH 7.0 and 5.0. The findings of this study are important for structuring emulsion gels by changing the pH of emulsions to achieve controlled release and improved storage stability of encapsulated compounds.

Keywords: Alginate; Controlled release; Emulsion gel; pH; Soy protein isolate; Surface structure.

5.1. Introduction

Emulsions gels are solidified emulsions prepared either by increasing the oil fractions in emulsions or introducing gelling agents into the continuous phase of emulsions. Emulsion gels may show higher stability and/or better protective effect on encapsulated food nutrients than fluid emulsions, due to decreased oil movement and oxygen diffusion within the systems after turning emulsions into emulsion gels (Lin et al., 2020a). Sodium alginate-based emulsion gels have received increased interest recently, and they have been used to encapsulate nutrients, such as linseed oil (Piornos et al., 2017), α-tocopherol (Feng et al., 2018), β-carotene (Soukoulis et al., 2016), lycopene (Calvo et al., 2017), and *D*-limonene (Lević et al., 2015). In addition, alginate gels normally shrink during gastric digestion, due to the protonation of free carboxylate groups and decreased repulsive forces between alginate monomers at low pH, and then swell and break during intestinal digestion, due to ion-exchange between calcium ions in gels and sodium ions in digestive juice. Therefore, alginate-based emulsion gels can protect encapsulated nutrients during gastric digestion and control and prolong intestinal release of nutrients (Pasparakis & Bouropoulos, 2006; Rayment et al., 2009).

In order to enhance the encapsulation efficiency and storage stability of encapsulated nutrients in emulsion gels, proteins such as whey protein isolate (WPI) and soy protein isolate (SPI) are often introduced as emulsifiers (Feng et al., 2018; Piornos et al., 2017). For alginate-based emulsion gels containing protein-coated droplets, pH is an important factor that affects the structural and mechanical properties of emulsion gels, stability of encapsulated nutrients, and digestion behavior of emulsion gels, which has rarely been discussed.

The pH of emulsions can affect not only the gelation mechanism of the alginate-based gel matrix but also the interactions between alginate molecules and protein-coated droplets. Sodium alginate forms weak gels by hydrogen bonds when hydrogen ions replace sodium

ions in alginate molecules under acidic condition (i.e., alginic acid gels). Sodium alginate can also form gels when calcium ions replace sodium ions (i.e., calcium-induced alginate gels) (Bennacef et al., 2021). Calcium-induced alginate gels normally have stronger mechanical properties than alginic acid gels, probably because ionic bonds have higher bond energy than hydrogen bonds (Caccavo et al., 2018). In addition, alginate is an anionic polysaccharide, while the electrical potential of protein is associated with the pH of systems (i.e., cationic protein at pH < the isoelectric point of protein (p*I*), neutral protein at p*I*, and anionic protein at pH > p*I*). Therefore, alginate molecules and protein-coated droplets show different electrostatic interactions (i.e., repulsion or attraction) at different pHs, which may affect properties of emulsion gels (i.e., structure and gel strength).

The pH of emulsion gels can also affect the stability of encapsulated food nutrients (e.g., lipids and carotenoids) in emulsion gels mainly through three mechanisms. Firstly, the pH of emulsions or emulsion gels can affect the solubility of pro-oxidant metals in the continuous phase (McClements & Decker, 2000). It has been reported that iron is more water-soluble at lower pHs, and so lipid oxidation is faster at lower pHs (Graf et al., 1984). Secondly, the pH of emulsions or emulsion gels can affect the electrical potential and/or thickness of interfacial membrane surrounding the droplets, which can affect the permeation of pro-oxidants from the continuous phase into droplets (Waraho et al., 2011). It has been reported that the lipid oxidation of WPI-stabilized emulsions at pH 3.0 was slower than that at pH 7.0, because of repulsion between positively charged WPI-coated droplets and pro-oxidant metals at pH 3.0, and attraction between negatively charged WPI-coated droplet and pro-oxidant metals at pH 7.0 (Donnelly et al., 1998). Thirdly, the pH of emulsions or emulsion gels can also affect the emulsifying capacities of emulsifiers and thus droplet size (i.e., the surface area) (McClements & Decker, 2000). It has also been reported that decreased droplet size could increase the rate of lipid oxidation in emulsions, due to the increased surface area of droplets exposed to the continuous phase (Gohtani et al., 1999). However, previous

studies mainly focused on the effect of pH on lipid oxidation in emulsions, while the effect of pH on the oxidation of encapsulated carotenoids in emulsion gels has rarely been reported.

Therefore, this study investigated the impact of pH of emulsions on properties of emulsion droplets (i.e., size, structure, and surface charge), the formation of alginate-based emulsion gel beads, and stability and release of encapsulated nutrients during storage and digestion. Lycopene was encapsulated in emulsion gels and served as an indicator to test the effect of pH on the stability and release of encapsulated nutrients in alginate-based and protein-stabilized emulsion gels during storage and digestion. SPI was used as the emulsifier in this study to investigate the effect of pH on the interactions between SPI-coated droplets and an alginate-based continuous phase. SPI is a widely used plant protein in the food industry, and use of SPI as emulsifiers to replace synthetic compounds and animal proteins has drawn increased attention in recent years (Kim et al., 2020).

5.2. Materials and methods

5.2.1. Materials

Defatted soy flour (Bob's Red Mill, Milwaukie, Oregon, USA) and sunflower oil (Aldi Stores Ltd., Kildare, Ireland) were purchased from iHerb and Aldi, respectively. Soy protein isolate (SPI) was extracted from defatted soy flour, according to the method described by Urbonaite et al. (2015); the protein content of SPI powder was 96.29 ± 0.03%. Sodium alginate (viscosity of 1.0 wt% sodium alginate solution in 0.15 M NaCl at 25°C = 210–340 cP, $\overline{M}$ = 69–117 kDa, and M/G = 71/29) was obtained from Special Ingredients (Chesterfield, UK). Tomato extract containing lycopene (0.059 mg/mg in the tomato extract), calcium chloride, sodium hydroxide, hydrochloric acid, and other analytical reagents were purchased from Sigma-Aldrich (St. Louis, MO, USA).

5.2.2. Preparation of emulsions

The SPI dispersion was prepared by mixing 0.5 g of SPI powder with 94.5 g of deionized water and stirring at room temperature for 2 h using a magnetic stirrer, and then the pH of dispersion was adjusted to 7.0 with 0.5 M HCl and NaOH. Sodium alginate solutions (1.0 wt% in deionized water) were prepared by shearing at 400 rpm for 24 h with a magnetic stirrer to permit hydration, and then the pH of solutions was adjusted to 7.0 with 1 M HCl and NaOH.

For preparation of SPI-stabilized emulsions, sunflower oil (5.0% in emulsions, w/w) was mixed with SPI dispersions at 13,000 rpm for 2 min using an Ultra-Turrax (IKA-25, Staufen, Germany). The resultant emulsions were named as primary emulsions containing 0.5% SPI and 5.0% oil. The secondary emulsions were then prepared by adding primary emulsions into 1.0% sodium alginate solutions (1:1, w/w) and stirring at 500 rpm for 5 min using a magnetic stirrer. The pH of the resulting emulsions was adjusted to 3.0, 4.0, 5.0, 6.0 and 7.0 with 0.5 M HCl and NaOH.

5.2.3. Properties of emulsions

5.2.3.1. Micro-structural analysis

Optical microscopy images of emulsions were recorded using an Olympus BX51 light microscope with a build-in camera (Olympus Optical Co. Ltd., Tokyo, Japan). Samples were dropped on a microscope slide, covered with a glass coverslip, and observed using 4× or 10× objective lens and 10× eyepiece.

5.2.3.2. Zeta potential measurement

The zeta potential of emulsions was measured by particle electrophoresis technology using a laser particle analyzer (Nano-ZS, Malvern Instruments, Worcestershire, UK), and the operation temperature was set at 25ºC. The refractive index and absorption index of samples

were set at 1.480 and 0.001, respectively. Samples were diluted to a final oil content of 0.01% (w/w) with ultrapure water (pH adjusted to 3.0–7.0 by 0.1 M HCl and 0.1 M NaOH) before testing, and the pH of diluted emulsions was adjusted to the pH value of tested emulsions with 0.5 M HCl and NaOH.

5.2.3.3. Size distribution measurement

The droplet-size distributions of emulsions were analyzed with a MasterSizer 3000 (Malvern Instruments Ltd., Worcestershire, UK). Samples were added into an automated wet dispersion unit until the obscuration reached between 1 and 10%. The stirrer speed was set at 1500 rpm, and the refractive index and absorption index of samples were set at 1.480 and 0.001, respectively.

5.2.4. Preparation of emulsion gel beads

The pH of 2% (w/w) $CaCl_2 \cdot 2H_2O$ solutions was adjusted to 3.0, 5.0, or 7.0 with 1.0 M HCl and NaOH, which was the same as the pH of secondary emulsions. The secondary emulsions were then dropped into $CaCl_2 \cdot 2H_2O$ solutions by a pipette and allowed to gel for 30 min. Samples were collected and washed with distill water after gelation and analyzed immediately for measurement of Young's modulus, size, and morphology.

5.2.5. Size and Young's modulus of emulsion gel beads

The gel strength of gel beads were measured by a texture analyzer with a 5-kg load cell (Stable Micro System, Godalming, UK), according to the method described in our precious study (Lin et al., 2021). The size (i.e., major (R_{max}) and minor (R_{min}) axis) of emulsions gel beads (5 beads in each group) were measured one after another using a vernier calliper before compression tests were performed with a 10-mm cylinder probe. The maximum strain and crosshead speed were set at 30% and 0.1 mm/s, respectively. The Young's modulus was calculated within the 5–15% strain region.

5.2.6. Encapsulation of lycopene in emulsion gel beads

For preparation of emulsion gel beads containing lycopene, tomato extract containing lycopene (15 mg/100 g in the primary emulsions) was dissolved in sunflower oil (5 g oil/100 g in the primary emulsions) at 140°C with stirring for 30 s and then it was cooled down to room temperature immediately. The primary and secondary emulsions containing lycopene were then prepared according to the methods as described in Section 5.2.2. In order to prevent the growth of microorganisms during storage, 0.02% (w/w) sodium azide was added into the primary emulsions. Emulsion gel beads containing lycopene were then prepared as described in Section 5.2.4, but only three groups of samples with pH 3.0, 5.0, or 7.0 were prepared in this section.

5.2.7. Lycopene content measurement

Gel beads with pH of 3.0, 5.0, or 7.0 (1.0 g) were mixed with organic reagents (8.0 mL) containing hexane, acetone, and ethanol (50 : 25 : 25% v/v) and 0.1% BHT in a screw-cap tube by a vortex for 1 min. Samples were then left to stand for 24 h. The absorbance of the upper layer of samples containing lycopene was then measured with a spectrophotometer at 503 nm. Lycopene concentration in gel beads was then calculated by Eq. (5-1):

$$\text{Lycopene concentration (mg/kg)} = (A_{503} \times 537 \times 8 \times 0.55) \div (1.0 \times 172) = A_{503} \times 13.74 \quad (5\text{-}1)$$

where 537 g/mole indicates the lycopene molecular weight, 8 mL is the volume of mixed organic solvents, 0.55 is the volume ratio of upper layer in mixtures after phase separation, 1.0 g is the weight of gel samples, and 172 mM^{-1} indicates the extinction coefficient of lycopene in hexane (Lin et al., 2021).

5.2.8. Storage stability of lycopene

Measurement of storage stability of emulsions gel beads were carried out as described by Song et al. (2019) and Yi et al. (2016) with some modification. Emulsion gel beads (~ 0.5 g)

containing lycopene were transferred into screw-cap tubes and stored in an incubator at 25ºC for 15 days in the dark, which were regarded as control samples. The measurement of stability of lycopene against pro-oxidant metals was carried out by adding 200 μM $FeCl_3$ in secondary emulsions during sample preparation as described in Section 5.2.6 and by incubating resulted emulsion gel beads at 25ºC for 15 days in the dark. Stability of lycopene against heat was measured by incubating emulsion gel beads at 50ºC for 5 days in the dark. Stability of lycopene against light was measured by incubating emulsion gel beads at 25ºC for 2 days under illumination with a 100 W light bulb. The light intensity on samples was 36 KLux, which was measured by a digital light meter. The remaining lycopene in emulsion gel beads during storage was extracted and measured as described in Section 5.2.7.

5.2.9. *In-vitro* digestion

Simulated oral (pH 7.0, 2 min), gastric (pH 3.0, 2 h) and small intestinal (pH 7.0, 6 h) digestions of emulsion gel beads were performed in this study (Lin et al., 2021; Minekus, et al.. 2014). Emulsion gel beads (5 g) were mixed with the simulated saliva fluid (SSF) electrolyte stock solutions (1.50× concentrates, 2.5 mL), $CaCl_2$ (final 0.75 mM), water (475 μL) and α-amylase solution (final 75 U/g) at 37°C for 2 min. The oral bolus (~10 g) was then mixed with the simulated gastric fluid (SGF) electrolyte stock solutions (1.50× concentrates, 5.0 mL), porcine pepsin stock solution (final 2000 U/g), $CaCl_2$ (final 0.075 mM), 1 M HCl (0.5 mL), and water (0.5 mL) at 37°C for 2 h. The gastric chyme (~20 g) was then mixed with the simulated intestinal fluid (SIF) electrolyte stock solutions (1.50× concentrates, 10 mL), pancreatin solution (final 100 U/g of trypsin), 25 g/L bile solution (4 mL), $CaCl_2$ (final 0.3 mM), 1 M NaOH (0.1 mL), and water (0.9 mL) at 37°C for 6 h.

5.2.10. Properties of gel beads during digestion

5.2.10.1. Young's modulus and shrinkage measurement during oral and gastric digestion

The Young's modulus of samples during digestion was analyzed as described in Section 5.2.5. In order to measure the shrinkage of gel beads during digestion, the size of five original gel beads (i.e., R_{max} and R_{min}) and the size of five gel beads during digestion (i.e., R'_{max} and R'_{min}) were measured by a vernier calliper one after another. The section shrinkage rate of gel beads during digestion was then calculated by Eq. (5-2):

$$\text{Section shrinkage rate (100\%)} = \frac{A_0 - A_t}{A_0} = \frac{3.14 \times \frac{R_{max}}{2} \times \frac{R_{min}}{2} - 3.14 \times \frac{R'_{max}}{2} \times \frac{R'_{min}}{2}}{3.14 \times \frac{R_{max}}{2} \times \frac{R_{min}}{2}} \quad (5\text{-}2)$$

where A_0 and A_t are the cross-section area of original beads before digestion and beads during digestion, respectively.

5.2.10.2. Lycopene release during intestinal digestion

The intestinal digestive juice was collected and weighted (Wt_{juice}) after filtration through gauze. The lycopene concentrations in digestive juice ($C_{LYC\text{-}J}$) and original gel beads ($C_{LYC\text{-}B}$) were measured by the method described in Section 5.2.7. The release rate of lycopene ($R_{release}$) was then calculated by Eq. (5-3):

$$\text{Release rates (\%)} = \frac{C_{LYC-J} \times Wt_{juice}}{C_{LYC-B} \times 5} \times 100\% \quad (5\text{-}3)$$

where 5 g is the weight of gel samples used for *in-vitro* digestion.

5.2.11. Statistical analysis

All measurements were performed on three times and were reported as mean ± standard deviation (SD). Differences between samples were analyzed using analysis of variance and a *t*-test, and $p < 0.05$ was regarded as statistically significant.

5.3. Results and discussion

5.3.1. Effect of pH on the properties of alginate/SPI-stabilized emulsions

5.3.1.1. Zeta-potential of emulsion droplets

In order to clarify the effect of pH on structural properties and surface charge of alginate/SPI-stabilized emulsions, SPI-stabilized emulsions (i.e., primary emulsions) were compared to alginate/SPI-stabilized emulsions (i.e., secondary emulsions) at pH 3.0–7.0. As shown in **Figure 5-1A**, the surface charge of primary emulsions changed from negative (zeta-potential of －34 ± 2 mV at pH 7.0) to positive (zeta-potential of ＋29 ± 3 mV at pH 3.0) when pH of emulsions decreased from 7.0 to 3.0, and the electrically neutral point of primary emulsions was at pH 4.0–5.0. This was associated with the zeta-potential of SPI at different pHs. The p*I* of SPI is pH 4.5, and thus SPI is positively charged at pH < p*I* and negatively charged at pH > p*I* (Malhotra & Coupland, 2004).

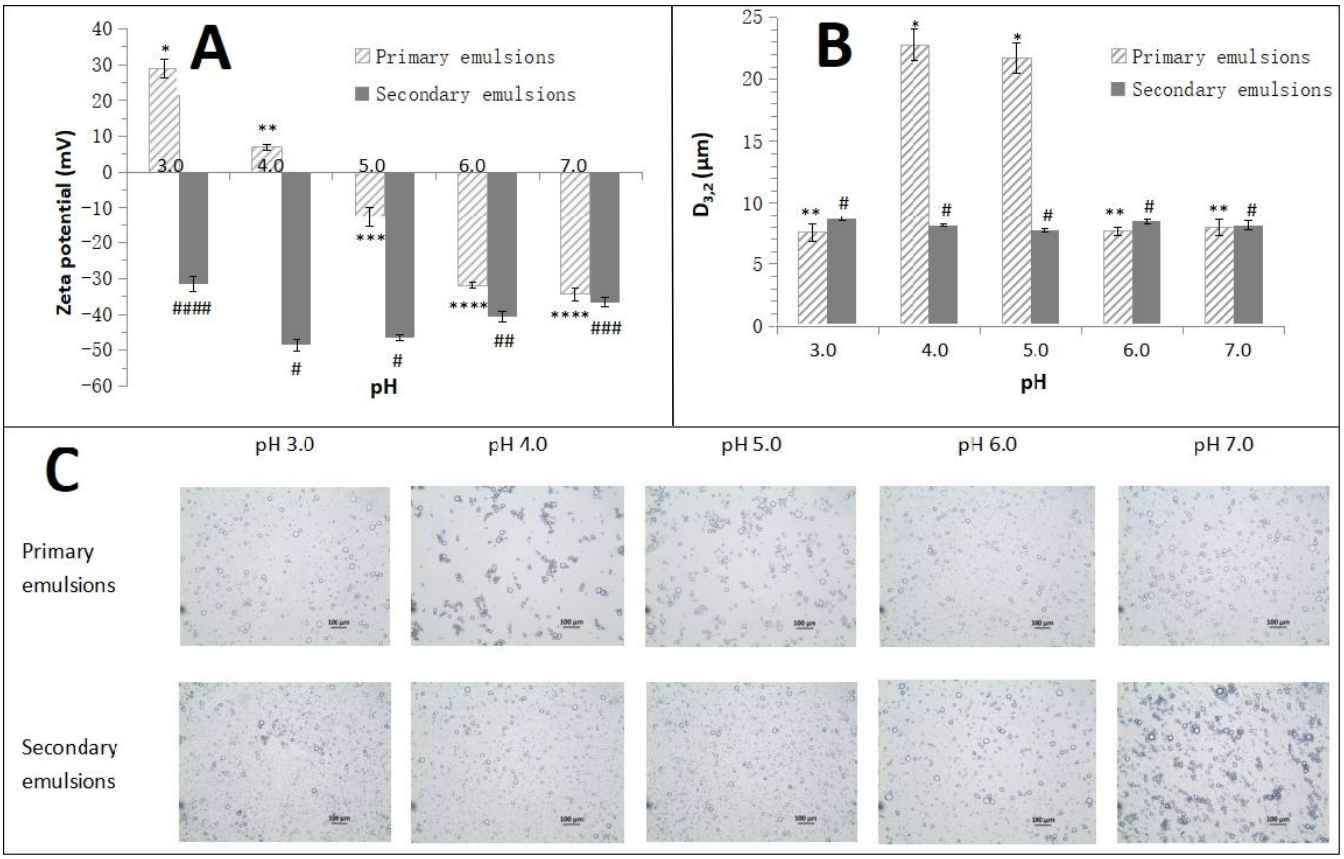

Figure 5-1. (A) Zeta potential, (B) droplet size and (C) microscopic structures of primary emulsions (i.e., SPI-stabilized emulsions) and secondary emulsions (i.e., alginate/SPI-stabilized emulsions) at pH 3.0–7.0. The symbols (* or #) indicate significant differences between primary and secondary emulsions ($p < 0.01$).

Figure 5-1A also shows that all secondary emulsions (i.e., alginate/SPI-stabilized emulsions) were negatively charged at pH 3.0–7.0. It can also be seen that primary emulsions and secondary emulsions had similar surface charge at pH 7.0, which indicates that there were not alginate molecules adsorbed at the surfaces of SPI-coated droplets in secondary emulsions at pH 7.0, because both alginate molecules and SPI-coated droplets carry strongly negative charges at pH 7.0 (Loosli et al., 2015; Zhang et al., 2015). However, secondary emulsions were more negatively charged than primary emulsions at pH 5.0–6.0 (**Figure 5-1**), which indicates that some alginate molecules were adsorbed at the surfaces of SPI-coated droplets in secondary emulsions, although both alginate molecules and SPI-coated droplets were negatively charged at pH 5.0–6.0. A possible reason for this was that the surface charge of SPI-coated droplets and alginate molecules decreased when decreasing

pH from 6.0 to 5.0 (Loosli et al., 2015), and the repulsive force between SPI-coated droplets and alginate molecules thus decreased. Therefore, alginate molecules could approach SPI-coated droplets and adsorb at the surfaces of SPI-coated droplets through inter-molecular hydrogen bonds between proteins and alginate and/or weak electrostatic attractions between carboxylic anionic groups of alginate and cationic groups of proteins, although both of them are negatively charged (Erben et al., 2019; Yang et al., 2016). In addition, positively charged primary emulsions changed into negatively charged secondary emulsions at pH 3.0–4.0, which indicates that alginate molecules were adsorbed at the surfaces of oppositely charged SPI-coated droplets through electrostatic attraction.

5.3.1.2. Droplet size and structure of emulsions

The surface charge of protein-stabilized emulsions significantly affects the emulsion stability and the state of emulsion droplets (i.e., unflocculated droplets and droplet flocculation), so the effect of pH on microscopic structures and droplet size of SPI-stabilized emulsions (i.e., primary emulsions) and alginate/SPI-stabilized emulsions (i.e., secondary emulsions) at pH 3.0–7.0 was further investigated (**Figures 5-1B and 5-1C**). As shown in **Figure 5-1C**, unflocculated emulsion droplets were evenly distributed in primary emulsions at pH 3.0, 6.0 and 7.0, because of strong electrostatic repulsion between SPI-coated droplets at pHs away from the p*I* of SPI (**Figure 5-1A**), but droplet flocculation occurred in primary emulsions at pH 4.0 and 5.0 (near the p*I* of SPI), due to the decreased surface charges and electrostatic repulsion of SPI-coated droplets (**Figure 5-1A**) (Dickinson, 2010). This was also the reason for increased droplet size in primary emulsions at pH 4.0 or 5.0, compared to that at pH 3.0, 6.0 or 7.0 (**Figure 5-1B**).

Figure 5-1B and 5-1C also show that unflocculated emulsion droplets were evenly distributed in secondary emulsions with similar droplet size at pH 3.0–6.0, due to strong electrostatic repulsion between alginate/SPI-stabilized emulsions (Zhang et al., 2015). This also indicates that the presence of alginate molecules in SPI-stabilized emulsions could

prevent droplet flocculation at pH 4.0–5.0 (near the p*I* of SPI) when comparing the microscopic structures of primary and secondary emulsions (**Figure 5-1C**), because of increased surface charge of droplets after absorption of alginate molecules at the surfaces of SPI-coated droplets (**Figure 5-1A**). Similar results have been reported, where alginate/*β*-lactoglobulin-stabilized emulsions showed better stability than *β*-lactoglobulin-stabilized emulsions at pH 5.0, due to increased electrostatic and steric repulsion between *β*-lactoglobulin-coated droplets after absorption of anionic alginate molecules at around the p*I* of *β*-lactoglobulin (Harnsilawat et al., 2006).

However, droplet flocculation occurred in secondary emulsions at pH 7.0, which differed from the state of emulsion droplets (i.e., unflocculated emulsion droplets) in primary emulsions at pH 7.0. This was probably because both alginate molecules and SPI-coated droplets were strongly negatively charged at pH 7.0, which led to depletion flocculation (Liu et al., 2012). However, **Figure 5-1C** shows that secondary emulsions at pH 7.0 had similar droplet size to that at pH 3.0–6.0. This was probably because depletion flocculation in secondary emulsions at pH 7.0 could not be detected by the measurement method used in this study. Emulsions were diluted during testing by adding emulsions into sample dispersion units containing distilled water and then electrostatic repulsion between alginate molecules and SPI-coated droplets decreased and depletion flocculation was not present during testing.

The above results indicate that the presence of alginate could change positively charged SPI-stabilized emulsions into negatively charged alginate-SPI-stabilized emulsions at pH 3.0–4.0 and prevent flocculation of SPI-stabilized emulsions at pH 4.0–5.0 (near the p*I* of SPI) but promote depletion flocculation of SPI-stabilized emulsions at pH 7.0. In addition, it has been indicated that the electrostatic interactions between polysaccharide molecules and protein-coated droplets and the state of emulsion droplets in emulsions may affect the mechanical properties of emulsion gels (Lin et al., 2020). Therefore, further research on the

effect of pH on the formation and mechanical properties of alginate-based emulsion gels containing SPI-coated droplets was carried out at pH 3.0, 5.0 and 7.0.

5.3.2. Effect of pH on mechanical properties of alginate-based emulsion gel beads

The modulus of emulsion gels is determined by the modulus of matrix and filler droplets, according to the Kerner model (Kerner, 1956):

$$\frac{G'_{gel}}{G'_{matrix}} = \frac{15(1-v_m)(M-1)\phi_f}{(8-10v_m)M+7-5v_m-(8-10v_m)(M-1)\phi_f} + 1 \quad (5\text{-}4)$$

where $M = \frac{G'_{filler}}{G'_{matrix}}$, and G'_{gel}, G'_{filler}, and G'_{matrix} are the shear modulus of the overall gel, the filler droplets and the gel matrix, respectively, ϕ_f is the actual droplet volume fraction, and v_m is the Poisson's ratio of the gel matrix. **Table 5-1** shows that alginate-based emulsion gel beads at pH 5.0 had higher Young's modulus than those at pH 7.0 and 3.0. The main reason for this was that G'_{matrix} values of alginate-based emulsion gel beads at pH 5.0 were higher than those at pH 7.0 and 3.0 (**Table 5-1**).

Table 5-1. Size and Young's modulus of emulsion gel beads (containing 0.5% alginate, 0.25% SPI and 2.5% oil) and alginate/SPI-based hydro-gel beads (containing 0.5% alginate and 0.1% SPI).

	Emulsion gel beads				**Alginate/SPI hydro-gel beads**		
	Size (mm)		**Young's modulus (Pa)**		**Size (mm)**		**Young's modulus (Pa)**
	Minor axis	**Major axis**	**Experimental value**	**Theoretical value**	**Minor axis**	**Major axis**	
pH 3.0	3.8 ± 0.2[b]	4.1 ± 0.1[b]	76 ± 7[a]	115–116	3.4 ± 0.2[a]	4.0 ± 0.3[b]	110 ± 7[a]
pH 5.0	3.2 ± 0.1[a]	3.3 ± 0.1[a]	266 ± 12[c]	235–237	3.3 ± 0.1[a]	3.5 ± 0.2[a]	224 ± 11[c]
pH 7.0	3.1 ± 0.1[a]	3.3 ± 0.1[a]	219 ± 6[b]	184–185	3.4 ± 0.1[a]	3.5 ± 0.1[a]	175 ± 6[b]

[a] Different lowercase letters indicate significant differences between values in a column ($p < 0.05$).

In this study, emulsion gel beads were prepared from secondary emulsions which were prepared by mixing 1.0% alginate solutions with primary emulsions containing 0.5% SPI and 5.0% oil (1:1), so secondary emulsions contained 0.5% alginate, 0.25% SPI and 2.5% oil. SPI was used as emulsifiers in this study, and some SPI molecules could be adsorbed at the O/W interfaces, but some unadsorbed SPI was presumably remained in the continuous phase, which could also affect G'_{matrix} of alginate-based emulsion gel beads (Lin et al., 2021). The content of unadsorbed SPI (i.e., 0.1 wt%) in the continuous phase was measured by the method described by Ye (2008). **Table 5-1** shows that alginate/SPI-based hydro-gel beads at pH 5.0 had higher modulus than that at pH 7.0, probably because, although both alginate/SPI hydro-gel beads at pH 5.0 and 7.0 were Ca^{2+}-cross-linked gels, parts of carboxylic anionic groups of alginate molecules were protonated and more hydrogen bonds formed at pH 5.0 than pH 7.0 (Zazzali et al., 2019). However, alginate gels which formed at pH 3.0 may be alginic acid gels rather than Ca^{2+}-cross-linked gels, which led to decreased modulus of alginate/gel hydro-gels at pH 3.0 compared to pH 5.0 and 7.0. It has been reported that alginic acid gels have lower modulus than Ca^{2+}-cross-linked alginate gels (Draget et al., 2006), probably because the formation of alginic acid gels was based on decreased solubility of the protonated carboxylic groups in an aqueous medium and weak hydrogen bonds between chains while, in Ca^{2+}-cross-linked gels, the divalent metallic cations cross-link the polymers, forming a compact interconnected network (Ching et al., 2017).

In addition, the theoretical values of G'_{gel}/G'_{matrix} of alginate-based emulsion gels were 1.05–1.06, under the assumption that M was 12–70, ϕ_f was 0.025, and ν_m was 0.5, according to the Kerner model (Lin et al., 2021). The theoretical values of G'_{gel}/G'_{matrix} of alginate-based emulsion gels at pH 7.0, 5.0 and 3.0 presented in **Table 5-1**. It can be seen that experimental values of G'_{gel}/G'_{matrix} of alginate-based emulsion gels at pH 7.0 and 5.0 were higher than their theoretical values. This was probably because droplet flocculation occurred in secondary emulsions at pH 7.0 (**Figure 5-1C**), which increased the actual droplet volume fraction and thus values of G'_{gel}/G'_{matrix} (Lewis & Nielsen, 1970). Meanwhile, SPI-coated

droplets could interact with the alginate-based gel matrix through intermolecular hydrogen bonds between proteins and alginate and/or weak electrostatic attractions at pH 5.0 (**Figure 5-1A**), which increased the value of M (i.e., G'_{filler}/G'_{matrix}). However, the experimental values of G'_{gel}/G'_{matrix} of alginate-based emulsion gels at pH 3.0 were lower than their theoretical values, probably because the presence of oil droplets obstructed the formation of structures of hydrogen bond-cross-linked alginic acid gels.

5.3.3. Effect of pH on storage stability and *in-vitro* release of encapsulated lycopene

5.3.3.1. Storage stability of lycopene

Figure 5-2A shows that emulsion gel beads at pH 7.0, 5.0 and 3.0 showed 63 ± 3%, 56 ± 5% and 69 ± 4% of lycopene retention, respectively, after storage for 15 days at 25ºC in the dark. According to free radical theory, the mechanism of carotenoid degradation is the interactions between carotenoid molecules and reactive peroxyl radicals (i.e., $ROO^{\cdot -}$) and/or unsaturated lipid radicals (i.e., $LOO^{\cdot -}$) (Bonne, 1999). It has been reported that lipid stability in emulsions can be affected by many factors, such as droplet characteristics (i.e., size, concentration, physical state, and chemical structures of lipids), interfacial characteristics (i.e., electrical charge, physical and chemical barriers), oxygen concentration, presence of antioxidants, and interactions between lipids and components in the aqueous phase (McClements & Decker, 2000).

In this study, the surface structure of droplets at different pHs may be the main reason leading to different lycopene stability during storage. At pH 3.0, emulsion droplets were coated by a double layer of emulsifiers as shown in **Figure 5-3** (i.e., a positively-charged SPI-based inner layer and a negatively-charged alginate-based outer layer) as discussed in Section 5.3.1.1. The negatively-charged outer layer can attract pro-oxidant metals present in the gel matrix, but the positively charged inner layer can repulse pro-oxidant metals and thus decrease metal-lipid interactions and the degradation of encapsulated lycopene. In addition,

the positively charged inner layer may also attract reactive peroxyl radicals (i.e., $ROO^{\cdot -}$) and thus decelerate the propagation step of lipid and lycopene oxidation.

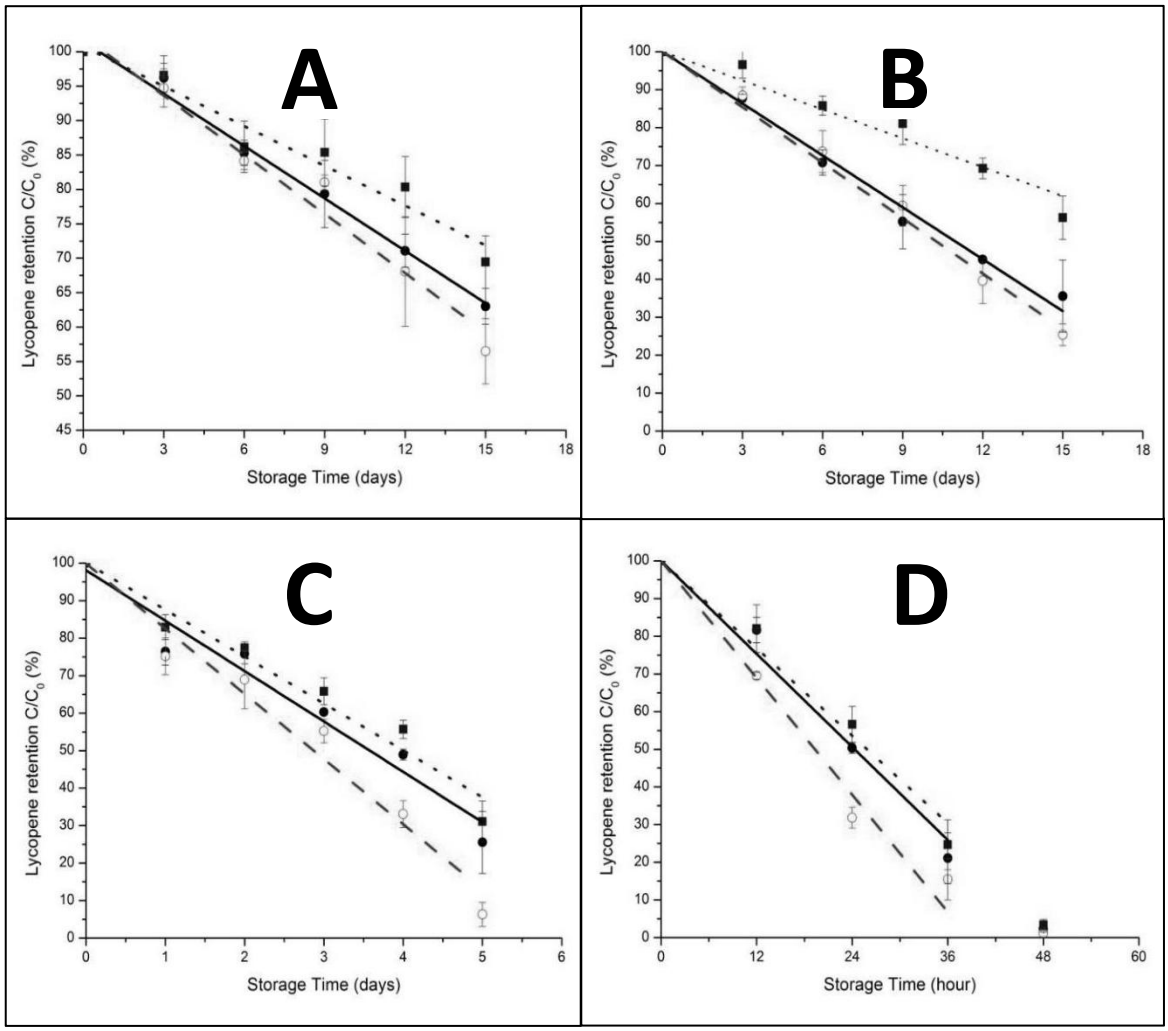

Figure 5-2. Lycopene retention in emulsion gel beads (A, C, and D) without adding $FeCl_3$ or (B) with 200 μM $FeCl_3$ at pH 7.0 (solid circles with solid lines), 5.0 (open circles with dashed lines), and 3.0 (solid squares with dotted lines) during storage. Samples were stored at (A and B) 25ºC and darkness, (C) 50ºC and darkness, or (D) 25ºC and illumination (36 KLux).

At pH 5.0, emulsion droplets were also coated by a double layer of emulsifiers, but both the SPI-based inner layer and alginate-based outer layer were negatively charged (**Figure 5-3**). Therefore, pro-oxidant metals could be attracted onto the droplet surfaces and trigger lipid and lycopene oxidation, and emulsion gel beads at 5.0 thus exhibited lower lycopene

retention than those at pH 3.0 during storage. At pH 7.0, emulsion droplets were only coated by a single layer of negatively-charged SPI molecules (**Figure 5-3**), so pro-oxidant metals could be easily attracted onto the droplet surfaces. However, emulsion gel beads at 7.0 exhibited higher lycopene retention than those at pH 5.0 during storage. This was probably because droplets at pH 5.0 were more negatively charged than those at pH 7.0 (**Figure 5-1A**), due to the absorption of alginate molecules at the droplet surfaces at pH 5.0, which led to higher attraction to pro-oxidant metals than those at pH 7.0.

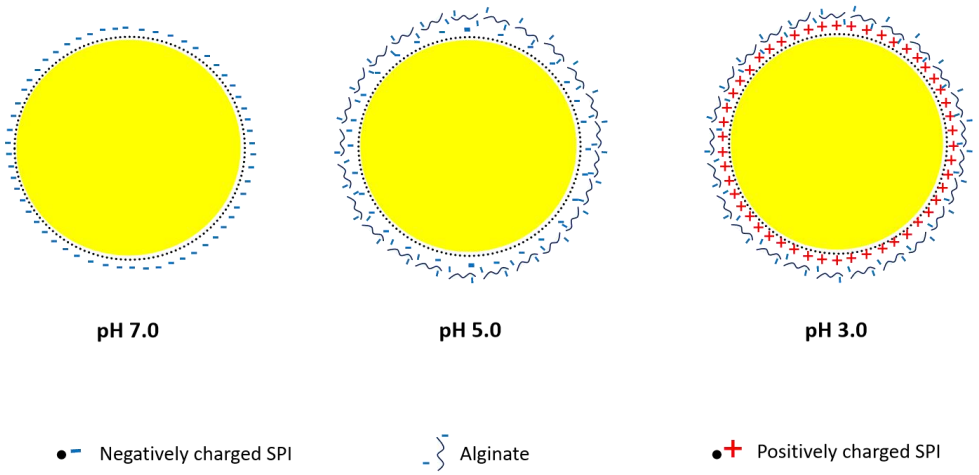

Figure 5-3. A proposed surface structures of emulsion droplets in alginate/SPI-stabilized emulsion gel beads at pH 7.0, 5.0, and 3.0.

Figure 5-2B shows that introducing 200 μM Fe^{3+} into gel beads accelerated lycopene degradation in emulsion gel beads during storage compared to the control samples (**Figure 5-2A**), but gel beads at pH 3.0 exhibited a lower acceleration rate than those at pH 7.0 and 5.0, probably because the positively charged SPI molecules on the droplet surfaces at pH 3.0 repulsed pro-oxidant metals and thus decreased the metal-lipid interactions. In addition, heating at 50ºC (**Figure 5-2C**) or exposure to light (**Figure 5-2D**) could also accelerate lycopene degradation in emulsion gel beads during storage compared to the control samples, and emulsion gel beads at pH 5.0 still showed lower lycopene retention compared to gel

beads at pH 3.0 and 7.0, probably because of the higher surface charge of droplets at pH 5.0 than those at pH 3.0 and 7.0. (**Figure 5-1A**).

5.3.3.2. In-vitro *release of lycopene*

Alginate-based emulsion gel beads can shrink during gastric digestion, which results in increased mechanical strength and denser structures, and then they can swell and break during intestinal digestion and release encapsulated nutrients by diffusion through increasingly large pores and/or following degradation of network structures (Lin et al., 2021). Therefore, the visual appearance (**Figure 5-4A**), Young's modulus (**Figure 5-4B**), and shrinkage (**Figure 5-4C**) of emulsion gel beads, and lycopene release (**Figure 5-4D**) from gel beads with different pH values during *in-vitro* digestion were further studied.

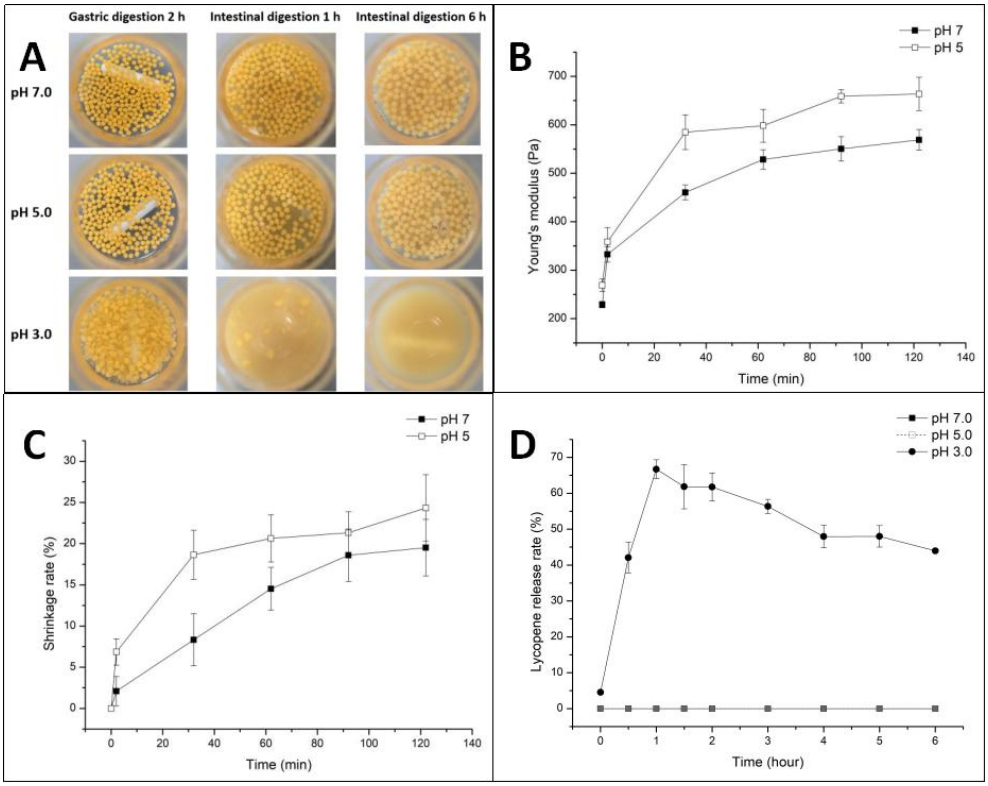

Figure 5-4. (A) Visual appearance of emulsion gel beads (containing 0.5% alginate, 0.25% SPI, and 2.5% oil) at pH 7.0, 5.0, and 3.0 during *in-vitro* digestion. (B) Young's modulus and (C) shrinkage of emulsion gel beads at pH 7.0 and 5.0 during *in-vitro* oral and gastric digestion. (D) Lycopene release from emulsion gel beads at pH 7.0, 5.0, and 3.0 during *in-vitro* intestinal digestion.

Figure 5-4A shows that emulsion gel beads at pH 3.0 were disrupted partially during oral and gastric digestion, probably due to their weak mechanical properties and the influence of stirring during *in-vitro* digestion. In contrast, emulsion gel beads at pH 5.0 and 7.0 could maintain their structures, due to their higher Young's modulus (**Table 5-1**). **Figure 5-4B** shows that the Young's modulus of emulsion gel beads at pH 5.0 and 7.0 increased during oral and gastric digestion, probably due to the interactions between calcium ions in gel beads and sodium bicarbonate which diffused from the simulated saliva fluid into gel beads during oral digestion (Lin et al., 2021; Norton et al., 2006) and the decreased electrostatic forces between alginate monomers at pH 3.0 during gastric digestion (Li et al., 2011). This could also lead to the shrinkage of gel beads during gastric digestion. **Figure 5-4C** shows that gel beads at pH 7.0 and 5.0 shrank by 20 ± 3% and 24 ± 4% after gastric digestion, respectively, compared to their original size before digestion.

Figure 5-4D shows the lycopene release from gel beads at pH 7.0, 5.0 and 3.0 during intestinal digestion (i.e., the movement of lycopene from emulsion gel beads to the digestive juice, along with the movement of emulsion droplets). It could be seen that gel beads at pH 3.0 could release lycopene from 0–1 h during intestinal digestion, due to the structural degradation of gel beads (**Figure 5-4A**), which resulted from the ion-exchange between Na^{+} ions present in the digestive fluid and Ca^{2+} ions present in gel beads (Bajpai & Sharma, 2004; Rayment et al., 2009). The lycopene content in digestive fluid decreased after 1 h during intestinal digestion, probably because the presence of enzymes and pro-oxidant metals in the digestive fluid promoted the degradation of lycopene. Similar results have been previously reported, where 20% of lycopene was lost during the gastric and duodenal digestion of lycopene-containing oleoresin (Kopec et al., 2017). In addition, lycopene did not release from gel beads at pH 5.0 and 7.0 during intestinal digestion (**Figure 5-4D**). This was probably because 0.5% alginate-based gel beads had strong gel structures at pH 5.0 and 7.0, and gel beads shrank during gastric digestion, leading to denser structures, which slowed the swelling process and thus delayed the structural degradation of alginate-based emulsion gel

beads during intestinal digestion. **Figure 5-4A** also shows from visual appearance that gel beads at pH 5.0 and 7.0 swelled but did not break during intestinal digestion.

In order to compare the effect of pH (i.e., 5.0 and 7.0) of gel beads on the release of lycopene from gel beads during *in-vitro* digestion, the alginate content of gel beads was reduced from 0.5% to 0.36% and the oil content of gel beads was increased from 2.5% to 5.0%. The visual appearance (**Figure 5-5A**), Young's modulus (**Figure 5-5B**), and lycopene release (**Figure 5-5C**) from gel beads containing 0.36% alginate and 5.0% oil at pH 5.0 and 7.0 during *in-vitro* digestion were then further studied.

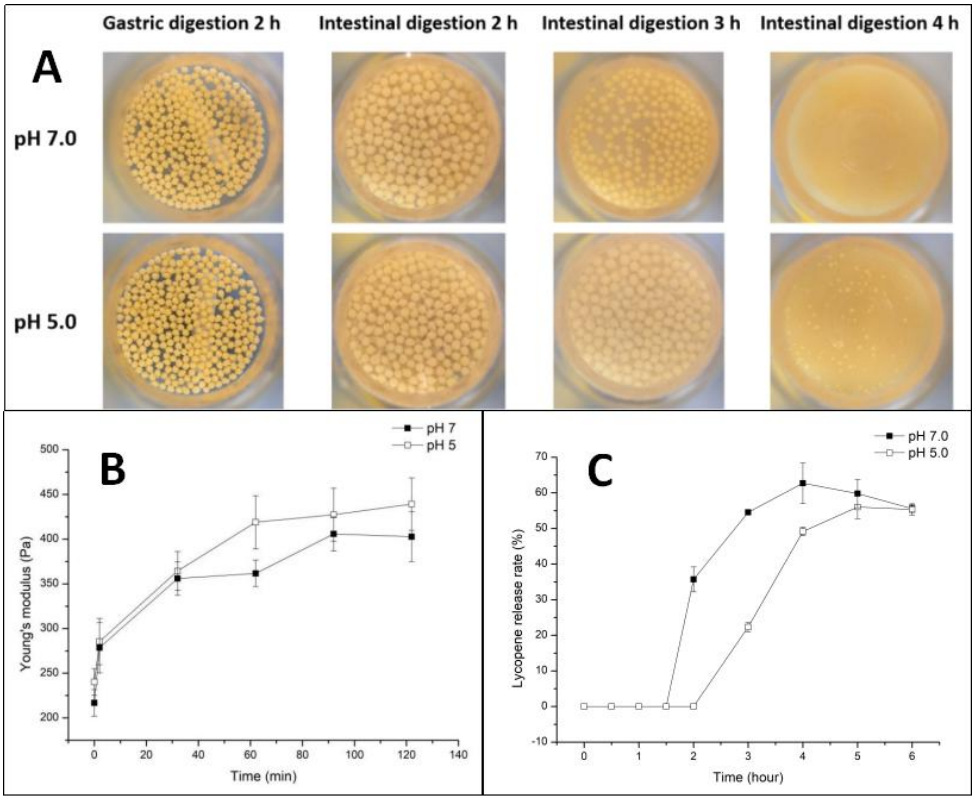

Figure 5-5. (A) Visual appearance of emulsion gel beads (containing 0.36% alginate, 0.5% SPI, and 5.0% oil) at pH 7.0 and 5.0 during *in-vitro* digestion. (B) Young's modulus of emulsion gel beads at pH 7.0 and 5.0 during *in-vitro* oral and gastric digestion. (C) Lycopene release from emulsion gel beads at pH 7.0 and 5.0 during *in-vitro* intestinal digestion.

As shown in **Figure 5-5A**, structural collapse of gel beads at pH 5.0 and 7.0 occurred 3–4 h and 2–3 h after swelling during intestinal digestion, respectively. This indicates that emulsion gel beads at pH 5.0 had slower swelling process and thus delayed structural

collapse during intestinal digestion compared to pH 7.0, probably because gel beads at pH 5.0 had stronger mechanical properties than those at pH 7.0. As shown in **Figure 5-5B**, the Young's modulus of emulsion gel beads at pH 5.0 and 7.0 increased during oral and gastric digestion, and gel beads at pH 5.0 had higher Young's modulus at the end of gastric digestion than those at pH 7.0. In addition, **Figure 5-5C** shows that the lycopene release from gel beads at pH 5.0 and 7.0 commenced at 3–3.5 h and 2.5–3 h, respectively, during intestinal digestion. This corresponded with the start point of the structural collapse of gel beads (**Figure 5-5A**). This indicates that lycopene was released with degradation of network structures after swelling of gel beads during intestinal digestion, and that stronger structures could delay the structural collapse and lycopene release during intestinal digestion.

5.4. Conclusions

The droplet states and surface structures of emulsion droplets, mechanical properties of gel beads, and storage stability and *in-vitro* release of encapsulated nutrients in alginate-based and SPI-stabilized emulsion gel beads can be influenced by the pH of emulsions. The droplets in secondary emulsions (i.e., alginate/SPI-stabilized emulsions) were coated by a single layer of SPI molecules at pH 7.0, and depletion flocculation in secondary emulsions only occurred at pH 7.0. The droplets in secondary emulsions were coated by a double layer of negatively charged SPI molecules and negatively charged alginate at pH 5.0 and a double layer of positively charged SPI molecules and negatively charged alginate at pH 3.0. Emulsion gel beads at pH 5.0 had the highest Young's modulus, and gel beads at pH 3.0 had the lowest Young's modulus among gel beads at pH 7.0, 5.0 and 3.0. Lycopene which was encapsulated in emulsion gel beads at pH 3.0 had higher storage stability and less delayed release during *in-vitro* digestion than those at pH 7.0 and 5.0. These results are important for designing alginate-based and protein-stabilized emulsion gel beads to encapsulate, store, and release lipid-soluble nutrients.

References

Bennacef, C., Desobry-Banon, S., Probst, L., & Desobry, S. (2021). Advances on alginate use for spherification to encapsulate biomolecules. *Food Hydrocolloids*, 106782.

Bonne, T. (1999). Oxidation and thermal degradation of carotenoids. *Journal of Oil Palm Research, 2*, 62-78.

Caccavo, D., Cascone, S., Lamberti, G., & Barba, A. (2018). Hydrogels: Experimental characterization and mathematical modelling of their mechanical and diffusive behaviour. *Chemical Society Reviews, 47*, 2357-2373.

Calvo, T. R. A., Busch, V. M., & Santagapita, P. R. (2017). Stability and release of an encapsulated solvent-free lycopene extract in alginate-based beads. *LWT, 77*, 406-412.

Ching, S. H., Bansal, N., & Bhandari, B. (2017). Alginate gel particles–A review of production techniques and physical properties. *Critical Reviews in Food Science and Nutrition, 57*, 1133-1152.

Dickinson, E. (2010). Flocculation of protein-stabilized oil-in-water emulsions. *Colloids and Surfaces B: Biointerfaces, 81*, 130-140.

Donnelly, J., Decker, E., & McClements, D. (1998). Iron-catalyzed oxidation of menhaden oil as affected by emulsifiers. *Journal of Food Science, 63*, 997-1000.

Draget, K. I., Skjåk-Bræk, G., & Stokke, B. T. (2006). Similarities and differences between alginic acid gels and ionically crosslinked alginate gels. *Food Hydrocolloids, 20*, 170-175.

Erben, M., Pérez, A. A., Osella, C. A., Alvarez, V. A., & Santiago, L. G. (2019). Impact of gum arabic and sodium alginate and their interactions with whey protein aggregates on bio-based films characteristics. *International Journal of Biological Macromolecules, 125*, 999-1007.

Feng, W., Yue, C., Ni, Y., & Liang, L. (2018). Preparation and characterization of emulsion-filled gel beads for the encapsulation and protection of resveratrol and α-tocopherol. *Food Research International, 108*, 161-171.

Gohtani, S., Sirendi, M., Yamamoto, N., Kajikawa, K., & Yamano, Y. (1999). Effect of droplet size on oxidation of docosahexaenoic acid in emulsion system. *Journal of Dispersion Science and Technology, 20*, 1319-1325.

Graf, E., Mahoney, J. R., Bryant, R. G., & Eaton, J. W. (1984). Iron-catalyzed hydroxyl radical formation: Stringent requirement for free iron coordination site. *Journal of Biological Chemistry, 259*, 3620-3624.

Harnsilawat, T., Pongsawatmanit, R., & McClements, D. J. (2006). Influence of pH and ionic strength on formation and stability of emulsions containing oil droplets coated by *β*-lactoglobulin− alginate interfaces. *Biomacromolecules, 7*, 2052-2058.

Kerner, E. (1956). The elastic and thermo-elastic properties of composite media. *Proceedings of the Physical Society. Section B, 69*, 808.

Kim, W., Wang, Y., & Selomulya, C. (2020). Dairy and plant proteins as natural food emulsifiers. *Trends in Food Science & Technology, 105*, 261-272.

Kopec, R. E., Gleize, B., Borel, P., Desmarchelier, C., & Caris-Veyrat, C. (2017). Are lutein, lycopene, and *β*-carotene lost through the digestive process? *Food & Function, 8*, 1494-1503.

Lević, S., Lijaković, I. P., Đorđević, V., Rac, V., Rakić, V., Knudsen, T. Š., et al. (2015). Characterization of sodium alginate/*D*-limonene emulsions and respective calcium alginate/*D*-limonene beads produced by electrostatic extrusion. *Food Hydrocolloids, 45*, 111-123.

Lewis, T. B., & Nielsen, L. E. (1970). Dynamic mechanical properties of particulate-filled composites. *Journal of Applied Polymer Science, 14*, 1449-1471.

Li, Y., Hu, M., Du, Y., Xiao, H., & McClements, D. J. (2011). Control of lipase digestibility of emulsified lipids by encapsulation within calcium alginate beads. *Food Hydrocolloids, 25*, 122-130.

Lin, D., Kelly, A. L., Maidannyk, V., & Miao, S. (2021). Effect of structuring emulsion gels by whey or soy protein isolate on the structure, mechanical properties, and in-vitro digestion of alginate-based emulsion gel beads. *Food Hydrocolloids, 110*, 106165.

Lin, D., Kelly, A. L., & Miao, S. (2020a). Preparation, structure-property relationships and applications of different emulsion gels: Bulk emulsion gels, emulsion gel particles, and fluid emulsion gels. *Trends in Food Science & Technology, 102*, 123-137.

Lin, D., Kelly, A. L., & Miao, S. (2020b). The role of mixing sequence in structuring O/W emulsions and emulsion gels produced by electrostatic protein-polysaccharide interactions between soy protein isolate-coated droplets and alginate molecules. *Food Hydrocolloids, 113*, 106537.

Liu, L., Zhao, Q., Liu, T., Kong, J., Long, Z., & Zhao, M. (2012). Sodium caseinate/carboxymethylcellulose interactions at oil–water interface: Relationship to emulsion stability. *Food Chemistry, 132*, 1822-1829.

Loosli, F., Vitorazi, L., Berret, J. F., & Stoll, S. (2015). Towards a better understanding on agglomeration mechanisms and thermodynamic properties of TiO_2 nanoparticles interacting with natural organic matter. *Water Research, 80*, 139-148.

Malhotra, A., & Coupland, J. N. (2004). The effect of surfactants on the solubility, zeta potential, and viscosity of soy protein isolates. *Food Hydrocolloids, 18*, 101-108.

McClements, D., & Decker, E. (2000). Lipid oxidation in oil-in-water emulsions: Impact of molecular environment on chemical reactions in heterogeneous food systems. *Journal of Food Science, 65*, 1270-1282.

Minekus, M., Alminger, M., Alvito, P., Ballance, S., Bohn, T., Bourlieu, C., et al. (2014). A standardised static *in vitro* digestion method suitable for food–an international consensus. *Food & Function, 5*, 1113-1124.

Norton, I., Frith, W., & Ablett, S. (2006). Fluid gels, mixed fluid gels and satiety. *Food Hydrocolloids, 20*, 229-239.

Pasparakis, G., & Bouropoulos, N. (2006). Swelling studies and in vitro release of verapamil from calcium alginate and calcium alginate–chitosan beads. *International Journal of Pharmaceutics, 323*, 34-42.

Piornos, J. A., Burgos-Díaz, C., Morales, E., Rubilar, M., & Acevedo, F. (2017). Highly efficient encapsulation of linseed oil into alginate/lupin protein beads: Optimization of the emulsion formulation. *Food Hydrocolloids, 63*, 139-148.

Rayment, P., Wright, P., Hoad, C., Ciampi, E., Haydock, D., Gowland, P., & Butler, M. F. (2009). Investigation of alginate beads for gastro-intestinal functionality, Part 1: *In vitro* characterisation. *Food Hydrocolloids, 23*, 816-822.

Song, H. Y., Moon, T. W., & Choi, S. J. (2019). Impact of antioxidant on the stability of *β*-carotene in model beverage emulsions: Role of emulsion interfacial membrane. *Food Chemistry, 279*, 194-201.

Soukoulis, C., Cambier, S., Hoffmann, L., & Bohn, T. (2016). Chemical stability and bioaccessibility of *β*-carotene encapsulated in sodium alginate o/w emulsions: Impact of Ca^{2+} mediated gelation. *Food Hydrocolloids, 57*, 301-310.

Tønnesen, H. H., & Karlsen, J. (2002). Alginate in drug delivery systems. *Drug Development and Industrial Pharmacy, 28*, 621-630.

Urbonaite, V., De Jongh, H., Van Der Linden, E., & Pouvreau, L. (2015). Water holding of soy protein gels is set by coarseness, modulated by calcium binding, rather than gel stiffness. *Food Hydrocolloids, 46*, 103-111.

Waraho, T., McClements, D. J., & Decker, E. A. (2011). Mechanisms of lipid oxidation in food dispersions. *Trends in Food Science & Technology, 22*, 3-13.

Yang, L., Guo, J., Yu, Y., An, Q., Wang, L., Li, S., et al. (2016). Hydrogen bonds of sodium alginate/Antarctic krill protein composite material. *Carbohydrate Polymers, 142*, 275-281.

Ye, A. (2008). Interfacial composition and stability of emulsions made with mixtures of commercial sodium caseinate and whey protein concentrate. *Food Chemistry, 110*, 946-952.

Yotsuyanagi, T., Yoshioka, I., Segi, N., & Ikeda, K. (1991). Acid-induced and calcium-induced gelation of alginic acid: Bead formation and pH-dependent swelling. *Chemical and Pharmaceutical Bulletin, 39*, 1072-1074.

Yi, B., Kim, M. J., & Lee, J. (2016). Effects of emulsifier charges on the oxidative stability in oil-in-water emulsions under riboflavin photosensitization. *Food Science and Biotechnology, 25*, 1003-1009.

Zazzali, I., Calvo, T. R. A., Ruíz-Henestrosa, V. M. P., Santagapita, P. R., & Perullini, M. (2019). Effects of pH, extrusion tip size and storage protocol on the structural properties of Ca (II)-alginate beads. *Carbohydrate Polymers, 206*, 749-756.

Zhang, C., Xu, W., Jin, W., Shah, B. R., Li, Y., & Li, B. (2015). Influence of anionic alginate and cationic chitosan on physicochemical stability and carotenoids bioaccessibility of soy protein isolate-stabilized emulsions. *Food Research International, 77*, 419-425.

CHAPTER SIX

Formation, Suspension Rheology, and Application of Alginate-based Emulsion Micro-gel Particles produced by an External/Internal O/W/O Emulsion-gelation Method

Chapter 6 has been accepted in:

Lin, D., Kelly, A. L., & Miao*, S. (2021). Alginate-based emulsion micro-gel particles produced by an external/internal O/W/O emulsion-gelation method: Formation, suspension rheology, digestion, and application to gel-in-gel beads, *Food Hydrocolloids*, 106926.

The work contained in this chapter was undertaken and written solely by myself with specific contributions from each co-author.

Abstract

Alginate-based emulsion gels can be used as fat replacers and encapsulation materials, but studies on emulsion micro-gel particles and nano-gel particles have rarely been reported, compared to bulk emulsion gels and emulsion macro-gel beads. This chapter investigated external/internal O/W/O emulsion-gelation methods for preparation of alginate-based emulsion micro-gel particles. The size, micro-structure, rheological properties and *in-vitro* digestion of emulsion micro-gels prepared by external/internal methods were compared. External gelation under mild stirring could produce emulsion micro-gels with small size (< 100 μm), while emulsion micro-gels prepared by internal gelation had bigger size and a more narrow size distribution. The suspensions of emulsion micro-gels prepared by external gelation had higher ϕ_{rcp}, ϕ_j, G', and G'' values than those prepared by internal gelation. Emulsion micro-gel particles swelled during intestinal digestion, but those prepared by external method were collapsed more rapidly than those prepared by internal method. Structuring emulsion gel beads by introducing emulsion micro-gel particles was also investigated. The presence of emulsion micro-gel particles prepared by external gelation increased the Young's modulus of gel beads and delayed their structural collapse and thus delayed release of encapsulated lycopene during intestinal digestion. The results of this study are critical for preparation and applications of alginate-based emulsion micro-gel particles prepared by external/internal O/W/O emulsion-gelation methods in the food industry.

Keywords: Alginate gel; Digestion; Emulsion micro-gel particle; Suspension rheology; External/internal gelation.

6.1. Introduction

Alginate-based emulsion gels have received increased interest in the food industry recently, as they can be used as fat replacers (Yang et al., 2020) and encapsulation materials for oil-soluble compounds, such as β-carotene (Soukoulis et al., 2016) and lycopene (Celli et al., 2016). Alginate-based emulsion gels offer many advantages, such as mild gelation and encapsulation process (Catarina et al., 2006), high stability of encapsulated compounds during food processing, storage and gastric digestion (Bokkhim et al., 2016), and controlled release of encapsulated compounds during intestinal digestion (Burey et al., 2008).

There are two kinds of alginate-based emulsion gels, according to their morphological properties: bulk emulsion gels and emulsion gel beads/particles (Lin et al., 2020). In addition, according to the size of alginate gel beads/particles, they can be further divided into three categories: macro-gel beads (> 1 mm), micro-gel particles (from 0.2 to 1,000 μm), and nano-gel particles (< 0.2 μm) (Ching et al., 2017). Different physical properties are emphasized for different emulsion gels (i.e., the importance of mechanical and release properties for bulk emulsion gels, mechanical properties and pH-sensitivity for emulsion macro-gel beads, and rheology and pH-sensitivity for emulsion micro-gel/nano-gel particles (Lin, et al., 2020). However, most previous studies focused on bulk emulsion gels and emulsion macro-gel beads, so further researches on emulsion micro-gel particles and emulsion nano-gel particles are needed.

Two methods have been reported to produce alginate-based emulsion micro-gel particles: the spray aerosol method and the emulsification technique (Ching et al., 2016; Ribeiro et al., 1999). A special setup is needed to prepare micro-gel particles by the spray aerosol method, in which emulsions containing alginate are sprayed from the top of the setup and $CaCl_2$ solutions are spayed from the bottom of the setup using pneumatic nozzles driven by compressed air. The mist of emulsions and $CaCl_2$ solutions contact in the chamber of the setup and then emulsion micro-gel particles form (Ching, et al., 2017). Compared to the

spray aerosol method, the emulsification technique is a simpler and more economic method, and it also has the potential to be used in industrial-scale. In this method, primary O/W emulsions containing alginate are dispersed in an oil phase by homogenization to form secondary O/W/O emulsions (i.e., the emulsification step), and then the gelling agents (divalent cations) are slowly introduced with stirring to form emulsion micro-gel particles (i.e., the gelation step) (Ribeiro, et al., 1999).

The emulsion-gelation technique includes external and internal gelation methods. Calcium chloride is often used as the gelling agent in external gelation. In contrast, in internal gelation, calcium carbonate is added into primary emulsions and then an acid is introduced as the gelling agent into secondary emulsions to liberate Ca^{2+} and trigger the progressive gelation of emulsion micro-gel particles (**Figure 6-S1**). Internal gelation has been reported to prepare emulsion micro-gel particles, in which chitosan-coated alginate micro-spheres containing soya oil were investigated (Ribeiro et al., 1999). However, external gelation has rarely been reported to prepare alginate-based emulsion micro-gel particles. It is well known that alginate-based gels produced by external or internal gelation may have different properties. It has been reported that alginate-based macro-gel beads prepared by internal gelation had faster release rate of acetaminophen than beads prepared by external gelation (Chan et al., 2006). It has also been indicated that alginate-based hydro-micro-gel particles prepared by internal gelation had looser gel structures with bigger pore sizes and a faster diffusion rate of haemoglobin into particles than those prepared by external gelation (Liu et al., 2002). Therefore, we predicted that emulsion micro-gel particles prepared by external or internal methods may also have different properties (i.e., morphology, rheology and swelling).

It is known that Ca^{2+}-cross-linked alginate gels show pH-dependent swelling, which is closely associated with the release of encapsulated drugs/compounds from alginate gels during swelling (Amiri et al., 2017; Bajpai & Sharma, 2004). Alginate gels can swell at neutral/alkaline conditions, because of the increased repulsive forces at pH values above the

pKa of the uronic acid groups of alginate molecules and/or structural disintegration of Ca^{2+}-cross-linked networks (Lin et al., 2021a; Mongar & Wassermann, 1949). The swelling properties of alginate hydro/emulsion micro-gels have been widely investigated (El-Sherbiny et al., 2011; Gómez-Mascaraque et al., 2019).

In contrast, rheology of alginate hydro/emulsion micro-gel suspensions has rarely been reported, although suspension rheology of soft micro-gel particles is critical in the determination of flow behavior and modulus of micro-gel particles. Particle suspensions may show viscous liquid-like behavior, viscoelastic liquid-like behavior or viscoelastic solid-like behavior depending on the phase volume (ϕ) of particles in suspensions. When ϕ is below the random close packing fraction (ϕ_{rcp}), particle suspensions are purely viscous with no measurable viscoelasticity (i.e., the regime I). However, when ϕ is above ϕ_{rcp} but below the jamming fraction (ϕ_j), the suspensions become shearing and viscoelastic with a measurable storage modulus (G') less than the loss modulus (G'') (i.e., the regime II). Finally, when ϕ is above ϕ_j, particle suspensions show viscoelastic solid-like behavior (e.g., the regime III) where G' becomes higher than G'' because micro-gel particles pack closely and form a weakly elastic network (Dickinson, 2015; Shewan & Stokes, 2013).

In terms of application of emulsion micro-gel particles in the food industry, previous studies mainly focused on the encapsulation of lipophilic compounds (e.g., flavors, essential oils, vitamins and fatty acids) in micro-gel particles for their targeting delivery in the digestive tract (Shewan & Stokes, 2013; Torres et al., 2016). For example, it has been reported that 85% of encapsulated dye (i.e., Sudan orange G) in alginate-based emulsion micro-gels were rapidly released within 15 min during intestinal digestion, while 35% of encapsulated dye in micro-gels coated by chitosan were slowly release within 2 h during intestinal digestion (Ribeiro et al., 1999). In addition, micro-gels can also been used as structuring agents to form gel-in-gels, which has drawn increased concerns in recent years (Husman et al., 2020; Liu et al., 2008). For instance, a microgel-in-bulk gel system was reported by Zhu et al. (2016), in which bone morphogenetic protein-2 (BMP-2) was

encapsulated in alginate-based micro-spheres, and then alginate micro-spheres were embedded into chitosan/dextran- polylactide/glycerophosphate-based bulk hydro-gels with the property of continuous release of BMP-2 from gels.

However, previous studies mainly focused on microgel-in-hydrogel systems and release of encapsulated compounds from the inner sections (i.e., micro-gels) of microgel-in-gel systems. In this study, we will further explore the effect of the presence of micro-gel particles on the properties (i.e., mechanical and digestive behavior) of emulsion macro-gels and thus the release of encapsulated lipophilic nutrients from the outer sections (i.e., macro-gels) of microgel-in-gel systems during digestion.

The purpose of this study was therefore to compare the morphology, suspension rheology and digestion behavior of alginate-based emulsion micro-gel particles produced by an external or internal O/W/O emulsion-gelation method. In addition, an example of application of micro-gel particles in the formation of gel-in-gel beads was discussed. Lycopene was encapsulated in emulsion macro-gel beads and served as an indicator to test the effect of micro-gel particles prepared by different gelation methods on the release of encapsulated nutrients in alginate-based emulsion macro-gel beads during digestion.

6.2. Materials and methods

6.2.1. Materials

Sunflower oil (Aldi Stores Ltd., Kildare, Ireland) and sodium alginate with $\overline{M}$ of 69–117 kDa (Special Ingredients, Chesterfield, UK) were purchased from local markets. Soy protein isolate (SPI) was prepared according to our previous study (Lin et al., 2019). *D*-(+)-gluconic-*δ*-lactone (GDL), calcium carbonate, calcium chloride, Tween 80, Span 80, sodium hydroxide, hydrochloric acid, and other analytical reagents were purchased from Sigma-Aldrich (St. Louis, MO, USA).

6.2.2. Preparation of emulsion micro-gel particles

Sodium alginate solutions (2.0%, w/w) were prepared with deionized water by shearing at 400 rpm for 30 min and then resting for 24 h at 4°C. For preparation of coarse emulsions, SPI powder (2.0 wt%) was mixed with deionized water (78 wt%) by stirring at room temperature for 2 h, and then sunflower oil (20 wt%) was mixed with above dispersions at 16,000 rpm for 2 min with an Ultra-Turrax (IKA-25, Staufen, Germany). The primary emulsions (i.e., O/W emulsions containing alginate) were then prepared by mixing the above coarse emulsions with 2.0% sodium alginate solutions (1:3, w/w) at 14,000 rpm for 2 min with an Ultra-Turrax. For the preparation of secondary emulsions (i.e., O/W/O emulsions), Span 80 (2.0 wt%) was mixed with sunflower oil (78 wt%) by stirring at room temperature for 5 min using a magnetic stirrer, and then primary emulsions (20 wt%) were mixed with above oil phase by stirring at 800 rpm.

External gelation was carried out by adding 1.0% $CaCl_2 \cdot 2H_2O$ solutions into secondary emulsions (1:5, w/w) and stirring at 1000 rpm for 30 min using a magnetic stirrer. For preparation of micro-gel particles by internal gelation, $CaCO_3$ was added into coarse emulsions (1:20, w/w) in advance during emulsion preparation, and then 4.0% GDL solutions were added into secondary emulsions (1:5, w/w) and stirring at 1000 rpm for 30 min using a magnetic stirrer (**Figure 6-S1**). After gelation, above resultant dispersions containing particles were added into deionized water (1:5, w/w) and mixed at 500 rpm for 2 min using a magnetic stirrer. The mixtures were left to stand for 2 h, and the oil cream on the top of mixtures was removed and the sediment of emulsion micro-gel particles were collected by filtration and washed twice by deionized water.

6.2.3. Properties of emulsion micro-gel particles

6.2.3.1. Morphological analysis

Emulsions and emulsion micro-gel particles were dropped on microscope slides without covering by glass coverslips before observing with an Olympus BX51 light micro-scope (Olympus Optical Co. Ltd., Tokyo, Japan).

6.2.3.2. Particle size distribution

The size distributions of emulsion micro-gel particles were analyzed with MasterSizer 3000 (Malvern Instruments Ltd., Worcestershire, UK). The obscuration and the stirrer speed were set at 1–10% and 2000 rpm, respectively, with the refractive index of 1.55 and the absorption index of 0.001.

6.2.3.3. Rheological analysis

Emulsion micro-gel particles were dried by filter papers twice and then particles were diluted by deionized water to the final ϕ from 1.0 to 0.1. The viscosity and modulus of particle suspensions were tested using an AR 2000ex rheometer (TA Instruments, Crawley, UK) by the method described in our previous publication (Lin et al., 2021b), but the flow and strain sweep measurements were carried out over a shear rate range of 0.1 to 1000 s^{-1} and a strain range of 1% to 50%, respectively. The final viscosity and modulus values used to calculate ϕ_{rcp} and ϕ_j were obtained at a shear rate of 100 s^{-1} (below ϕ_{rcp}) or 10 s^{-1} (above ϕ_{rcp}) and a strain of 10%.

6.2.3.4. In-vitro *digestion*

Concentrated electrolyte stock solutions (i.e., 1.5× concentrate) of simulated saliva fluid (SSF), gastric fluid (SGF), and intestinal fluid (SIF) were prepared as described by Minekus, et al. (2014) with some modification. Simulated oral digestion of emulsion micro-gel

particles was performed by mixing micro-gel particles (5 g) with SSF electrolyte stock solutions (2.5 mL), *α*-amylase (final 75 U/g), $CaCl_2$ (final 0.75 mM), and water at 37°C for 2 min. Simulated gastric digestion was performed by mixing oral bolus (~10 g) with SGF electrolyte stock solutions (4.0 mL), porcine pepsin (final 2000 U/g), $CaCl_2$ (final 0.075 mM), and water at 37°C for 2 h after adjusting pH to 3.0 with HCl. Simulated intestinal digestion was performed by mixing gastric chyme (~20 g) with SIF electrolyte stock solutions (10 mL), pancreatin (final 100 U/g of trypsin), bile (final 0.25 wt%), $CaCl_2$ (final 0.3 mM), and water at 37°C for 3 h after adjusting pH to 7.0 with NaOH.

Optical microscopy images and size distributions of emulsion micro-gel particles during *in-vitro* digestion were analyzed as described in Sections 6.2.3.1 and 6.2.3.2.

6.2.4. Preparation of emulsion gel beads containing micro-gel particles

Primary emulsions (i.e., O/W emulsions) were prepared by mixing 0.8% alginate solutions and coarse emulsions containing 5.0% oil, 0.5% SPI and 94.5% water, according to the methods described in Section 6.2.2, but the ratio of coarse emulsions to alginate solutions was 1:1. Lycopene was also encapsulated in primary emulsions by mixing 5 mg of tomato extract (containing 0.059 mg lycopene/mg) with 5.0 g of oil before preparing coarse emulsions. Micro-gel particle dispersions were then prepared by mixing filtered micro-gel particles with deionized water (3:2, w/w), and then primary emulsions were mixed with micro-gel particle dispersions (9:1, w/w). The control sample was prepared by mixing primary emulsions with deionized water (9:1, w/w). Emulsion gel beads were then prepared by dropping primary emulsions with/without micro-gel particles into 2.0% $CaCl_2 \cdot 2H_2O$ solutions using a S1 pipette filler, and gel beads were mildly stirred for 30 min and then collected and washed by deionized water.

6.2.5. Properties of emulsion gel beads containing micro-gel particles

6.2.5.1. In-vitro digestion

Simulated digestion was performed as described in Section 6.2.3.4, and properties of emulsion gel beads (i.e., shrinkage rate, Young's modulus, and visual appearance) and lycopene release from them during *in-vitro* digestion were then tested.

6.2.5.2. Measurement of Young's modulus and shrinkage during oral and gastric digestion

The sizes of gel beads including major and minor axis (R_{maj} and R_{min}) were measured by a digital vernier caliper with a sensitivity of 0.1 mm. The shrinkage rate of gel beads during digestion was calculated by comparing decreased sectional area (i.e., $A = \pi \times R_{maj} \times R_{min} \div 4$) of gel beads during digestion to that of original gel beads before digestion. The Young's modulus of gel beads was measured by a texture analyzer (Stable micro-System, Godalming, UK). The compression test was performed with the maximum strain of 30% and the crosshead speed 0.1 mm/s. The Young's modulus was calculated in the linear elastic region of gel beads (i.e., the 5–15% strain region).

6.2.5.3. Measurement of lycopene release during intestinal digestion

The supernatant (1.0 g) of digestive fluids after centrifugal separation at 4000 rpm for 15 min was mixed with 8.0 mL of hexane, acetone, and ethanol (50 : 25 : 25% v/v) containing 0.1% BHT by a vortex for 1 min, and lycopene in digestive fluid was then extracted and measured by the method described in our previous publication (Lin et al., 2021a).

6.2.6. Statistical analysis

All measurements were performed three times and were reported as mean ± standard deviation (SD). Differences between samples were analyzed using analysis of variance and a *t*-test, and $p < 0.05$ was regarded as statistically significant.

6.3. Results and discussion

6.3.1. Formation and morphology of emulsion micro-gel particles produced by external/internal emulsification methods

Figure 6-1A shows the size distributions of emulsion micro-gel particles produced by external/internal emulsion-gelation methods under mild stirring. Emulsion micro-gel particles produced by external method ($D_{4,3}$ = 39.6 ± 0.5 μm) were significantly smaller than those produced by internal method ($D_{4,3}$ = 144 ± 5 μm, $p < 0.05$) under mild stirring. In addition, a previous study indicated that particles with size over 100 μm may be detected by mouth and negatively affected sensory of food (Kim et al., 2019). Therefore, we predicted that emulsion micro-gel particles produced by the external gelation has potential to use as micro-capsules and structuring agents in food products without affecting their sensory properties.

Different gelation mechanisms of external/internal emulsion-gelation methods may be the main reason for emulsion micro-gel particles with different morphological properties. A commonly-used method to prepare micro-gel particles in previous studies was adding oil containing $CaCl_2$ particles or acetic acid into emulsions to trigger gelation, in which $CaCl_2$ or acetic acid could diffuse from oil into water phases (Liu et al., 2007; Paques et al., 2013). In this study, $CaCl_2$ or GDL solutions were added into secondary emulsions to trigger gelation under mild stirring, in which $CaCl_2$ or GDL solutions may merge with water phases in O/W/O emulsions (**Figure 6-S1**). **Figures 6-1B–E** show the micro-structure of micro-gel particles produced by external/internal methods and O/W/O emulsions which were used to prepare micro-gel particles. It could be seen that O/W droplets in O/W/O emulsions (**Figures 6-1C and 6-1E**) were smaller than micro-gel particles in both gelation methods (**Figures 6-1B and 6-1D**). This indicates that $CaCl_2$ or GDL solutions, which were introduced into O/W/O emulsions to trigger gelation, merged with O/W droplets during gelation process. A similar result was reported by Ribeiro et al. (1999), where soya oil-in-

alginate droplets, with size of around 200 μm, which were dispersed in silicone oil, were smaller than alginate emulsion micro-gel particles, with size of 250–1000 μm, produced by internal gelation. However, $CaCl_2$-induced external gelation was a faster process than GDL-induced internal gelation, so each O/W droplet merged with less $CaCl_2$ solutions in external gelation than GDL solutions in internal gelation, which resulted in smaller micro-gel particles produced by external method than those produced by internal method.

Figure 6-1A also shows that micro-gel particles produced by the internal gelation had a more narrow size distribution than those produced by external method under mild stirring. The diameter of micro-gel particles produced by internal and external methods ranged from 15 to 450 μm and from 2.5 to 110 μm, respectively. The possible reason was that random droplet coalescence occurred in O/W/O emulsions after introducing $CaCl_2$ solutions during the external gelation. It has been reported that adding $CaCl_2$ solutions into W/O emulsions to produce alginate hydro-micro-spheres by external gelation caused the disruption of the equilibrium of the system during stirring, resulting in a significant degree of congregating of micro-spheres (Chan et al., 2002).

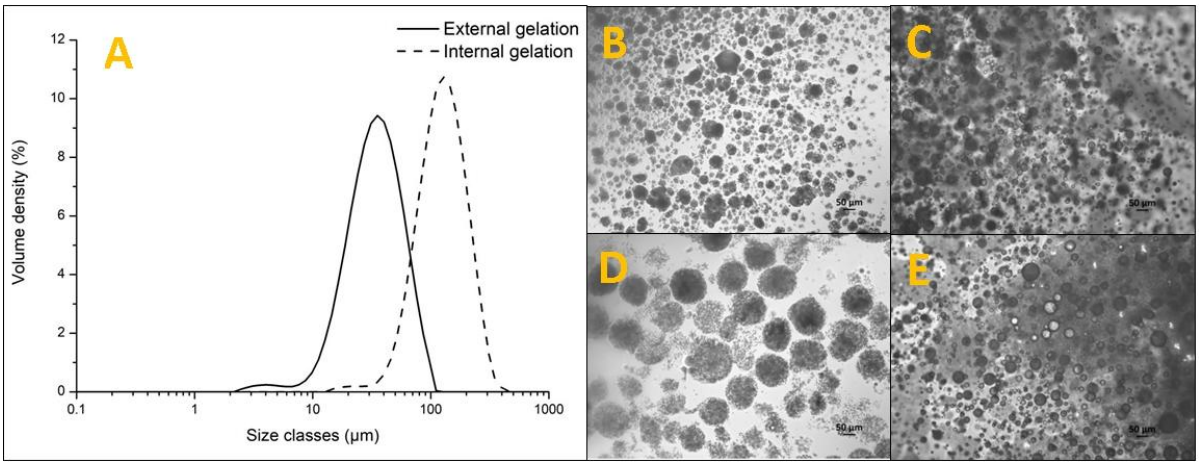

Figure 6-1. (A) The size distribution of alginate-based emulsion micro-gel particles produced by external/internal O/W/O emulsification methods, (B) the micro-structure of emulsion micro-gel particles produced by external gelation and (C) the micro-structure of O/W/O emulsions used, and (D) the micro-structure of emulsion micro-gel particles produced by internal gelation and (E) the micro-structure of O/W/O emulsions used.

6.3.2. Suspension rheology of emulsion micro-gel particles

In order to predict functions and guide production and application of micro-gel particles in the food industry, it is important to investigate the rheology of micro-gel particle suspensions. It is known that the rheology of micro-particle suspensions is affected by properties of solvents (i.e., viscosity and pH), properties of particles (i.e., size, size distribution, mechanical strength, surface properties, and interaction potential), and particle phase volume (Shewan, 2015). In regime I, the viscosity of particle suspensions (η) can be calculated by the Einstein equation (Eq. (6-1), $0 < \phi < 0.05$), Batchelor equation (Eq. (6-2), $0.05 < \phi < 0.15$), and Meron-Pierce-Quemada model (MPQ model, as shown in Eq. (6-3), $0.2 < \phi < \phi_m$):

$$\eta = \eta_s (1 + 2.5\phi) \quad (6\text{-}1)$$

$$\eta = \eta_s (1 + 2.5\phi + C_2\phi^2) \quad (6\text{-}2)$$

$$\eta = \eta_s (1 - \frac{\phi}{\phi_m})^{-2} \quad (6\text{-}3)$$

where η_s is the solvent viscosity, C_2 is a constant with a range of values from 4.2 to 6.2, and ϕ_m is the maxing packing fraction which could be assumed to be equal to ϕ_{rcp} (Shewan, 2015).

In regime III, G' of particle suspensions can be calculated by the Evans and Lips model modified by Adams (Eq. 6-4):

$$G' = aG_p^b \left[1 - \phi_r^{-1/3}\right] \quad (6\text{-}4)$$

in which a and b are constants equal to 0.4 and 1.2, respectively, G_p is the shear elastic modulus of particles, and ϕ_r is a relative phase volume (i.e., $\phi_r = \phi/\phi_m$ *or* ϕ/ϕ_{rcp}) (Shewan, 2015). Therefore, it can be assumed that alginate-based emulsion micro-gel particles with higher modulus and lower ϕ_{rcp} may lead to particle suspensions with higher modulus in

regime III. However, modelling the regime II has rarely been reported in previous studies because measuring suspension rheology around particle jamming is challenging and available experimental results are often questioned (Shewan, 2015).

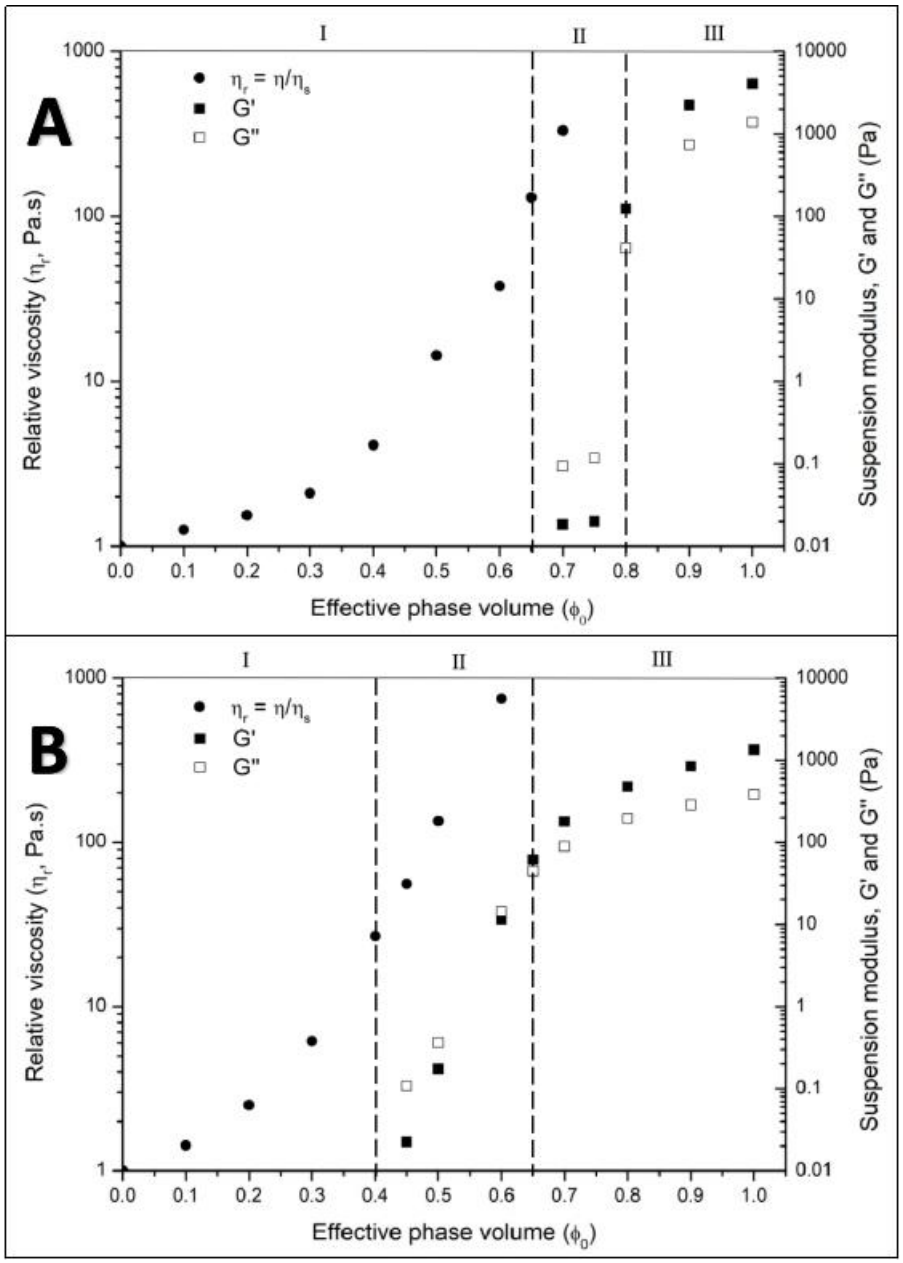

Figure 6-2. Relative viscosity (η_r), storage modulus (G') and loss modulus (G'') of suspensions of emulsion micro-gel particles produced by (A) external or (B) internal O/W/O emulsification methods as a function of phase volume (ϕ_0). Regime I ($0 < \phi < \phi_{rcp}$) indicates that particle suspensions are purely viscous; Regime II ($\phi_{rcp} < \phi < \phi_j$) indicates that particle suspensions are viscoelastic with a measurable G' less than G''; Regime III ($\phi_j < \phi < 1$) indicates that particle suspensions are solid-like with G' higher than G''.

Figure 6-2 shows the relative viscosity, G', and G'' of suspensions of alginate-based emulsion micro-gel particles produced by internal/external gelation methods compare to the phase volume (ϕ) of particles in suspensions. Suspensions of emulsion micro-gel particles produced by external gelation had higher ϕ_{rcp} and ϕ_j values than those produced by internal gelation (**Figures 6-2 and 6-S2**). The possible reason was that micro-gel particles produced by external gelation had smaller size and a wider particle size distribution than those produced by internal gelation (**Figure 6-1**). When ϕ is below the ϕ_{rcp} of particle suspensions, micro-gel particles can freely move past one another and particle suspensions are purely viscous with no measurable viscoelasticity, while, when ϕ is above the ϕ_{rcp} of particle suspensions, micro-gel particles closely contact and particle suspensions become shearing and viscoelastic. Smaller particles had higher packing density than larger particles (Ye et al., 2018), so smaller particles have a higher ϕ_{rcp}. In addition, the maximum packing fraction (ϕ_m) or ϕ_{rcp} and ϕ_j increase when the particle size distribution increases, because small particles can fit in the gaps among larger particles (Shewan, 2015).

Figure 6-2 also shows that the suspensions of micro-gel particles produced by external gelation had higher G' than those produced by internal gelation when ϕ is above the ϕ_j of particle suspensions. This indicates that micro-gel particles produced by external gelation had stronger mechanical properties than those produced by internal gelation. The possible reason was that each O/W droplet merged with less $CaCl_2$ solutions during external gelation than GDL solutions during internal gelation, and thus O/W droplets were less diluted by gelling agents during external gelation, which resulted in higher alginate concentrations in micro-gel particles produced by external gelation, compared to those produced by internal gelation.

6.3.3. Degradation of emulsion micro-gel particles during digestion

The above results indicate that different gelation methods (i.e., external or internal emulsification method) led to emulsion micro-gel particles with different morphological and

mechanical properties, which may also affect the pH-sensitivity and digestion behavior of micro-gel particles. Therefore, *in-vitro* digestion of emulsion micro-gel particles prepared by external/internal emulsification method was further investigated.

Figures 6-3 and 6-4 show the micro-structure and size distribution of emulsion micro-gel particles during simulated oral, gastric and intestinal digestion. It can be seen that emulsion micro-gel particles, which were prepared by external gelation, slightly swelled after oral and gastric digestion (**Figures 6-3 and 6-4A**). A similar finding has been reported, where alginate micro-gels ($D_{4,3}$ < 500 μm), which were prepared by dropping alginate solutions into $CaCl_2$ solutions by syringes, slightly swelled after gastric digestion at pH 3.0, probably because of ion exchange between univalent cations in stimulated gastric fluids and divalent cations in alginate micro-gels (Gómez-Mascaraque et al., 2019). On the other hand, **Figures 6-3 and 6-4B** show that emulsion micro-gel particles, which were prepared by internal gelation, shrank partially and swelled partially during gastric digestion (i.e., a wider size distribution of emulsion micro-gels after gastric digestion than those before digestion). The possible reason for such shrinkage was that remaining $CaCO_3$ in micro-gel particles further reacted with H^+ in the digestive fluid during gastric digestion. As shown in **Figure 6-S3**, remaining $CaCO_3$ particles in internally-induced micro-gel particles could be observed under a fluorescence microscopy but $CaCO_3$ particles disappeared in parallel with the shrinkage of emulsion micro-gels after incubating emulsion micro-gels in 0.1 M HCl-KCl solutions (1:1, w/w) at pH 1.2 for 2 h.

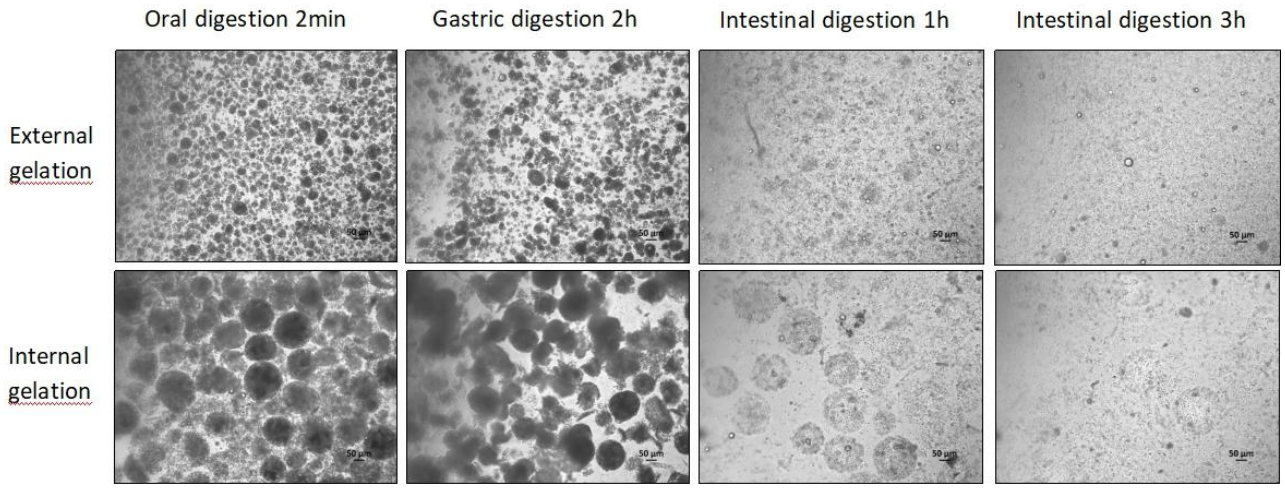

Figure 6-3. The micro-structure of emulsion micro-gel particles produced by external/internal O/W/O emulsification methods during *in-vitro* digestion.

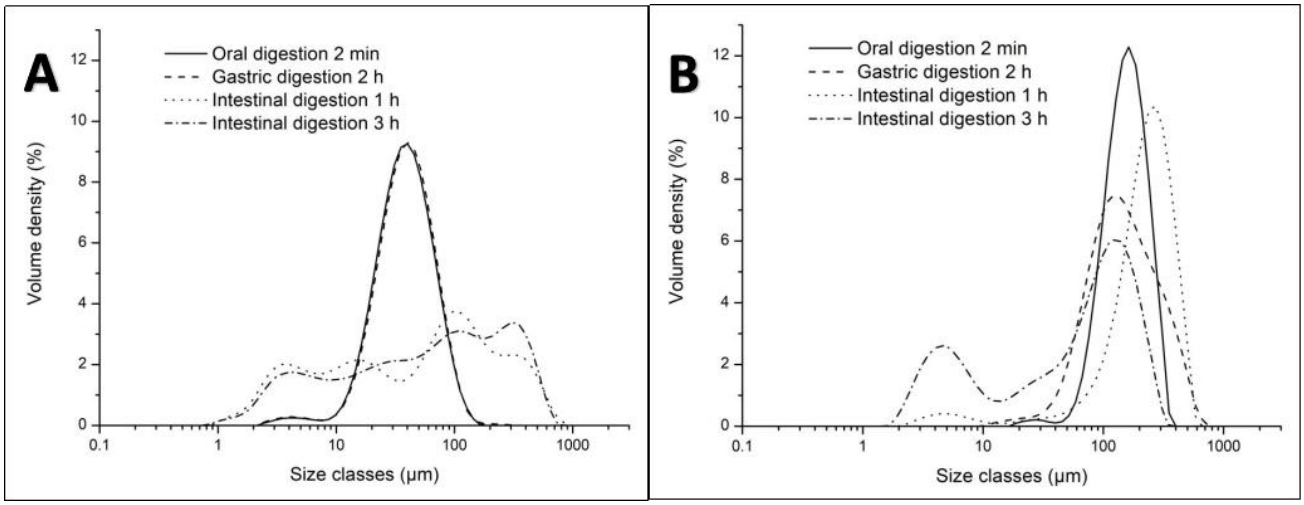

Figure 6-4. The size distribution of emulsion micro-gel particles produced by (A) external or (B) internal O/W/O emulsification methods during *in-vitro* digestion.

Figure 6-4B also shows that the size distribution of emulsion micro-gel particles prepared by internal method had two peaks (i.e., D = 4.5 μm in left peak and D = 270 μm in right peak) after intestinal digestion for 1 h, which indicates that micro-gel particles further swelled and parts of micro-particles broke, due to increased pH of digestive fluids and ion-exchange between digestive fluids and micro-particles. The area of the left-hand peak increased, but the area of the right-hand peak decreased after intestinal digestion for 3 h, which indicates further breaking of swelled particles and the presence of unbroken particles. This was also confirmed by the micro-structure of emulsion micro-gel particles prepared by internal gelation after intestinal digestion for 3 h (**Figure 6-3**), in which both swollen micro-particles and dissociative oil droplets were observed.

However, the size distribution of emulsion micro-gel particles prepared by external method had three peaks (i.e., D = 4.0 μm in left peak, D = 16.4 μm in middle peak and D = 98.1 μm in right peak) after intestinal digestion for 1 h, and the area of the right-hand peak increased and a fourth peak occurred at D = 310 μm after intestinal digestion for 3 h (**Figure 6-4A**), but unbroken micro-particles were rarely observed and large oil droplets could be observed in digestive juice (**Figure 6-3**). A possible reason for this was that coalescence between released oil droplets from emulsion micro-gel particles occurred during intestinal digestion, which led to increased droplet size. These also indicate that emulsion micro-gel particles prepared by external method were more sensitive to intestinal environment and more easily collapsed during intestinal digestion than those prepared by internal method. Many factors affect the swelling of alginate gels in solutions/buffers, such as alginate concentration, alginate type and Ca^{2+} concentration in gels, intensity of gel structures, temperature, pH and ionic strength of solutions/buffers (Pasparakis & Bouropoulos, 2006; Sriamornsak et al., 2007). It has been indicated that alginate macro-gel beads prepared using 1% $CaCl_2$ solutions had higher swelling rates in a pH 7.4 solution than gel beads prepared using 2% $CaCl_2$ solutions (Dai et al., 2008). It has been also reported that reduced swelling was observed when alginate gels exposed to low pH or lower concentrations of cations (Moe

et al., 1993). However, in this study, the main reason for different intestinal digestion behavior of emulsion micro-gel particles was probably that emulsion micro-gel particles prepared by internal method had larger size and thus may have stronger buffer capacity to pH change and ion-exchange during intestinal digestion.

6.3.4. Structuring emulsion gel beads by emulsion micro-gel particles

6.3.4.1. Effect of micro-gel particles on mechanical properties of emulsion gel beads

Figure 6-5A shows that the Young's modulus of emulsion gel beads without micro-gel particles or with 6.0 % of emulsion micro-gel particles prepared by internal/external O/W/O gelation methods were 241 ± 9 Pa, 246 ± 9 Pa, and 315 ± 19 Pa, respectively. The possible reason for similar Young's modulus of emulsion gel beads containing micro-gel particles prepared by internal gelation ($p > 0.05$) but increased Young's modulus of emulsion gel beads containing micro-gel particles prepared by external gelation ($p < 0.05$), compared to that without micro-gel particles, was that micro-gel particles prepared by external gelation had stronger Ca^{2+}-induced cross-linking with alginate molecules in the continuous phase of emulsions than micro-gel particles prepared by internal gelation.

In order to verify above explanation, rheological properties of 0.4% alginate solutions containing micro-gel particles (0–10 wt%) prepared by internal/external O/W/O gelation methods were further investigated (**Figure 6-S4**). It shows that 0.4% alginate solutions containing micro-gel particles (0–10 wt%) prepared by internal gelation showed viscoelastic properties with slightly increased viscosity and an unmeasurable G' (i.e., unstable and negative values) with increasing content of micro-gel particles, which indicated that there was little cross-linking between alginate molecules and micro-gel particles prepared by internal gelation. On the other hand, introducing high levels of micro-gel particles (6–10 wt%) prepared by external gelation into alginate solutions increased the viscosity of mixtures significantly, which showed solid-like behavior with a measurable storage modulus

(G') higher than the loss modulus (G''). This indicates that the presence of micro-gel particles prepared by external gelation could promote interactions between alginate molecules, but the mechanism needs further investigation. There are mainly two types of speculation: firstly, Ca^{2+} could be released from micro-gel particles prepared by external gelation into alginate solutions, which triggered the interactions between alginate molecules; secondly, micro-gel particles prepared by external gelation could cross-link with alginate molecules through Ca^{2+} adsorbed on the surfaces of micro-gel particles.

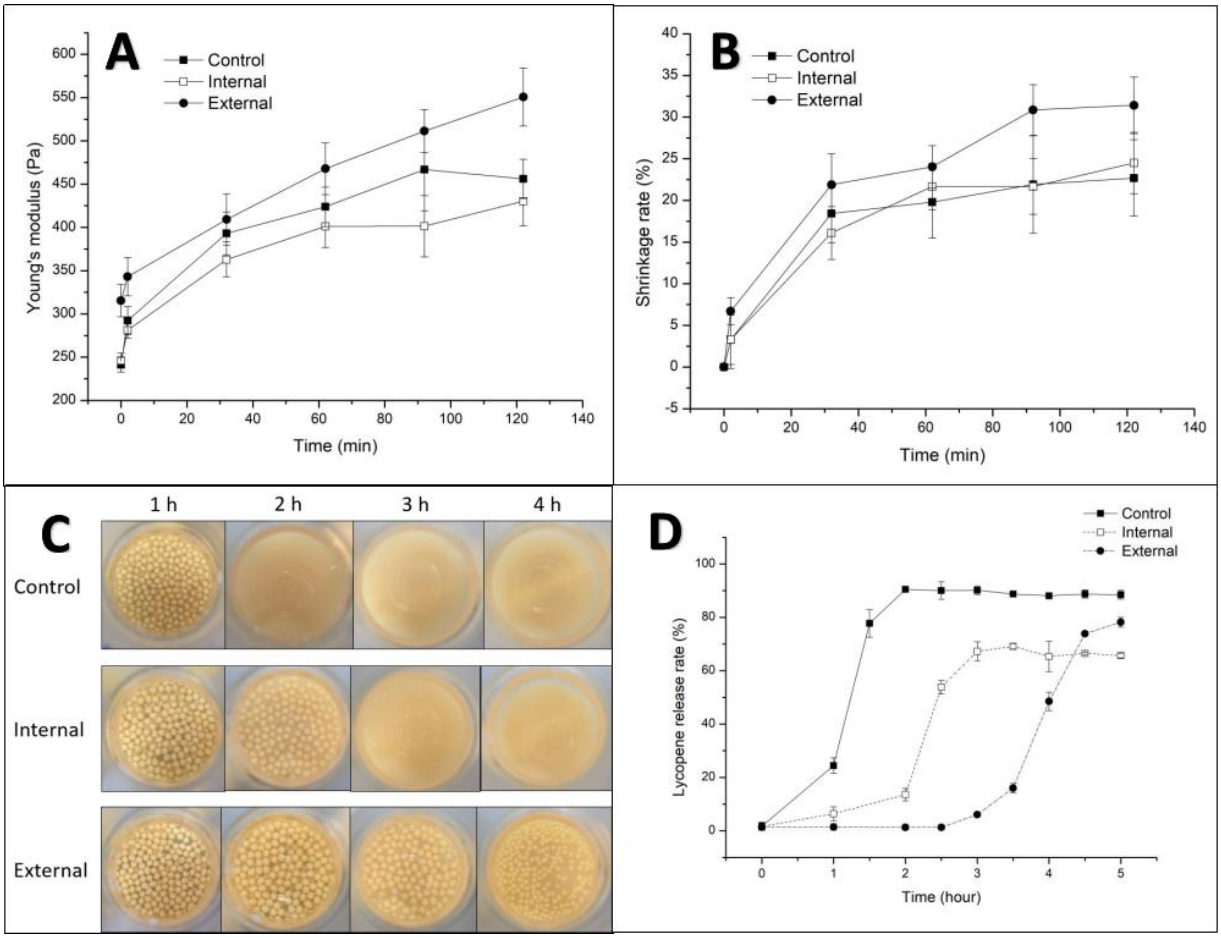

Figure 6-5. (A) Young's modulus and (B) shrinkage rate of emulsion gel beads without micro-gel particles (i.e., control samples) or with 6.0% micro-gel particles produced by external/internal O/W/O emulsification methods during oral and gastric digestion. (C) Visual appearance of emulsion gel beads and (D) lycopene release from emulsion gel beads without micro-gel particles or with 6.0% micro-gel particles produced by external/internal methods during *in-vitro* intestinal digestion.

6.3.4.2. Digestion of emulsions gels beads containing emulsion micro-gel particles

Figures 6-5A and 6-5B show that emulsion gel beads without emulsion micro-gel particles or with 6.0 % of emulsion micro-gel particles prepared by internal/external O/W/O gelation methods shrank and their Young's modulus increased during oral and gastric digestion, probably due to interactions between Ca^{2+} in gel beads and HCO_3^- in the simulated saliva fluid and decreased repulsive forces of alginate molecules under acidic conditions during gastric digestion (Lin et al., 2021a). It can also be seen that emulsion gel beads containing emulsion micro-gel particles prepared by external gelation shrank more (31 ± 3%, $p < 0.05$) and had higher Young's modulus (551 ± 33 Pa, $p < 0.05$) after gastric digestion, compared to emulsion gel beads without emulsion micro-gel particles (23 ± 5% and 456 ± 23 Pa) or with 6.0 % of emulsion micro-gel particles prepared by internal gelation (24 ± 4% and 430 ± 29 Pa).

Figures 6-5C and 6-5D show the visual images and lycopene release from gel beads during intestinal digestions. It can be seen that emulsion gel beads without emulsion micro-gel particles or with 6.0 % of emulsion micro-gel particles prepared by internal/external O/W/O gelation methods broke and released lycopene after 1–2 h, 2–3 h, and 3.5–4.5 h of intestinal digestion, respectively. The presence of micro-gel particles prepared by external gelation in emulsion gel beads could delay the structural collapse of gel beads, probably because the ion-exchange between Na^+ ions in digestive juices and Ca^{2+} ions in gel beads and the pH-dependent swelling of gel beads were delayed, due to stronger and denser structures of gel beads formed by after introducing micro-gel particles.

6.4. Conclusions

Properties (i.e., the size distribution, micro-structure, suspension rheology, and digestion behavior) of emulsion micro-gel particles produced by internal/external O/W/O gelation methods under mild stirring were compared in this study. Micro-gel particles produced by

external gelation had smaller size and a wider size distribution than those produced by internal gelation, probably due to their different gelation mechanisms. The suspensions of micro-gel particles produced by external gelation showed higher ϕ_{rcp}, ϕ_j, G', and G'' values than those prepared by internal gelation. Micro-gel particles produced by external gelation slightly swelled during gastric digestion and further swelled during intestinal digestion and then totally collapsed after intestinal digestion, while micro-gel particles produced by internal gelation partially swelled and partially shrank during gastric digestion and partially collapsed with swelling after intestinal digestion. Micro-gel particles can also be used for structuring emulsion gel beads by formation of gel-in-gel beads. Emulsion gel beads containing micro-gel particles produced by internal gelation had similar mechanical properties with the control samples without gel particles. However, introducing gel particles produced by external gelation increased mechanical strength of gel beads, which delayed structural collapse of gel beads and lycopene release from gel beads during intestinal digestion. The findings are important for the production of emulsion micro-gel particles and structuring food by emulsion micro-gel particles produced by external/internal O/W/O emulsion-gelation methods.

References

Amiri, M., Salavati-Niasari, M., Pardakhty, A., Ahmadi, M., & Akbari, A. (2017). Caffeine: A novel green precursor for synthesis of magnetic $CoFe_2O_4$ nano-particles and pH-sensitive magnetic alginate beads for drug delivery. *Materials Science and Engineering: C, 76*, 1085-1093.

Bajpai, S., & Sharma, S. (2004). Investigation of swelling/degradation behaviour of alginate beads crosslinked with Ca^{2+} and Ba^{2+} ions. *Reactive and Functional Polymers, 59*, 129-140.

Bokkhim, H., Bansal, N., Grøndahl, L., & Bhandari, B. (2016). *In-vitro* digestion of different forms of bovine lactoferrin encapsulated in alginate micro-gel particles. *Food Hydrocolloids, 52*, 231-242.

Burey, P., Bhandari, B. R., Howes, T., & Gidley, M. J. (2008). Hydrocolloid gel particles: Formation, characterization, and application. *Critical Review of Food Science & Nutrition, 48*, 361-377.

Catarina, M. S., António, J. R., Margarida, F., Domingos, F., & Francisco, V. (2006). Micro-encapsulation of hemoglobin in chitosan-coated alginate micro-spheres prepared by emulsification-internal gelation. *The AAPS Journal, 7*, E903–E913.

Celli, G. B., Teixeira, A. G., Duke, T. G., & Brooks, M. S.-L. (2016). Encapsulationof lycopene from watermelon in calcium-alginate micro-particles using an optimised inverse-gelation method by response surface methodology. *International Journal of Food Science & Technology, 51*, 1523-1529.

Chan, L. W., Lee, H. Y., & Heng, P. W. (2002). Production of alginate micro-spheres by internal gelation using an emulsification method. *International Journal of Pharmaceutics, 242*, 259-262.

Chan, L. W., Lee, H. Y., & Heng, P. W. (2006). Mechanisms of external and internal gelation and their impact on the functions of alginate as a coat and delivery system. *Carbohydrate Polymers, 63*, 176-187.

Ching, S. H., Bansal, N., & Bhandari, B. (2016). Rheology of emulsion-filled alginate micro-gel suspensions. *Food Research International, 80*, 50-60.

Ching, S. H., Bansal, N., & Bhandari, B. (2017). Alginate gel particles–A review of production techniques and physical properties. *Critical Reviews in Food Science & Nutrition, 57*, 1133-1152.

Dai, Y. N., Li, P., Zhang, J. P., Wang, A. Q., & Wei, Q. (2008). A novel pH sensitive N-succinyl chitosan/alginate hydrogel bead for nifedipine delivery. *Biopharmaceutics & Drug Disposition, 29*, 173-184.

Dickinson, E. (2015). Microgels—an alternative colloidal ingredient for stabilization of food emulsions. *Trends in Food Science & Technology, 43*, 178-188.

El-Sherbiny, I. M., Abdel-Mogib, M., Dawidar, A.-A. M., Elsayed, A., & Smyth, H. D. (2011). Biodegradable pH-responsive alginate-poly (lactic-co-glycolic acid) nano-/micro- hydrogel matrices for oral delivery of silymarin. *Carbohydrate Polymers, 83*, 1345-1354.

Gómez-Mascaraque, L. G., Martínez-Sanz, M., Hogan, S. A., López-Rubio, A., & Brodkorb, A. (2019). Nano-and micro-structural evolution of alginate beads in simulated gastrointestinal fluids. Impact of M/G ratio, molecular weight and pH. *Carbohydrate Polymers, 223*, 115121.

Husman, D., Welzel, P. B., Vogler, S., Bray, L. J., Träber, N., Friedrichs, J., et al. (2020). Multiphasic microgel-in-gel materials to recapitulate cellular mesoenvironments *in vitro*. *Biomaterials science, 8*, 101-108.

Kim, Y. N., Muttakin, S., Jung, Y. M., Heo, T. Y., & Lee, D. U. (2019). Tailoring physical and sensory properties of tofu by the addition of jet-milled, superfine, defatted soybean flour. *Foods, 8*, 617.

Lin, D., Kelly, A. L., Maidannyk, V., & Miao, S. (2021a). Effect of structuring emulsion gels by whey or soy protein isolate on the structure, mechanical properties, and *in-vitro* digestion of alginate-based emulsion gel beads. *Food Hydrocolloids, 110*, 106165.

Lin, D., Kelly, A. L., & Miao, S. (2020). Preparation, structure-property relationships and applications of different emulsion gels: Bulk emulsion gels, emulsion gel particles, and fluid emulsion gels. *Trends in Food Science & Technology, 102*, 123-137.

Lin, D., Kelly, A. L., & Miao, S. (2021b). The role of mixing sequence in structuring O/W emulsions and emulsion gels produced by electrostatic protein-polysaccharide interactions between soy protein isolate-coated droplets and alginate molecules. *Food Hydrocolloids, 113*, 106537.

Lin, D., Zhang, L., Li, R., Zheng, B., Rea, M. C., & Miao, S. (2019). Effect of plant protein mixtures on the micro-structure and rheological properties of myofibrillar protein gel derived from red sea bream (Pagrosomus major). *Food Hydrocolloids, 96*, 537-545.

Liu, W., Griffith, M., & Fengfu, L. (2008). Alginate microsphere-collagen composite hydrogel for ocular drug delivery and implantation. *Journal of Materials Science: Materials in Medicine, 19*, 3365-3371.

Liu, X. D., Yu, W. T., Lin, J. Z., & Quan, Y. (2007). Diffusion of acetic acid across oil/water interface in emulsification-internal gelation process for preparation of alginate gel beads. *Chemical Research in Chinese Universities, 23*, 579-584.

Liu, X. D, Yu, W. T, Zhang, Y., Xue, W., Yu, W., Xiong, Y., et al. (2002). Characterization of structure and diffusion behaviour of Ca-alginate beads prepared with external or internal calcium sources. *Journal of Micro-encapsulation, 19*, 775-782.

Minekus, M., Alminger, M., Alvito, P., Ballance, S., Bohn, T., Bourlieu, C., Carriere, F., Boutrou, R., Corredig, M., Dupont, D., Dufour, C., Egger, L., Golding, M., Karakaya, S., Kirkhus, B., Le Feunteun, S., Lesmes, U., Macierzanka, A., Mackie, A., Marze, S., McClements, D. J., Menard, O., Recio, I., Santos, C. N., Singh, R. P., Vegarud, G. E., Wickham, M. S., Weitschies, W., & Brodkorb, A. (2014). A standardised static *in vitro* digestion method suitable for food - an international consensus. *Food and Function, 5*, 1113-1124.

Moe, S. T., Skjaak-Braek, G., Elgsaeter, A., & Smidsroed, O. (1993). Swelling of covalently crosslinked alginate gels: Influence of ionic solutes and nonpolar solvents. *Macro-molecules, 26*, 3589-3597.

Mongar, J., & Wassermann, A. (1949). Fully swollen alginate gels as permutites: Kinetics of calcium–sodium ion exchange. *Discussions of the Faraday Society, 7*, 118-123.

Paques, J. P., van der Linden, E., van Rijn, C. J., & Sagis, L. M. (2013). Alginate submicro-n beads prepared through W/O emulsification and gelation with $CaCl_2$ nano-particles. *Food Hydrocolloids, 31*, 428-434.

Pasparakis, G., & Bouropoulos, N. (2006). Swelling studies and *in vitro* release of verapamil from calcium alginate and calcium alginate–chitosan beads. *International Journal of Pharmaceutics, 323*, 34-42.

Ribeiro, A. J., Neufeld, R. J., Arnaud, P., & Chaumeil, J. C. (1999). Micro-encapsulation of lipophilic drugs in chitosan-coated alginate micro-spheres. *International Journal of Pharmaceutics, 187*, 115-123.

Shewan, H. M. (2015). *Rheology of Soft Particle Suspensions.* (PhD thesis), School of Chemical Engineering, The University of Queensland. https://doi.org/10.14264/uql.2015.533.

Shewan, H. M., & Stokes, J. R. (2013). Review of techniques to manufacture micro-hydrogel particles for the food industry and their applications. *Journal of Food Engineering, 119*, 781-792.

Soukoulis, C., Cambier, S., Hoffmann, L., & Bohn, T. (2016). Chemical stability and bioaccessibility of *β*-carotene encapsulated in sodium alginate O/W emulsions: Impact of Ca^{2+} mediated gelation. *Food Hydrocolloids, 57*, 301-310.

Sriamornsak, P., Thirawong, N., & Korkerd, K. (2007). Swelling, erosion and release behavior of alginate-based matrix tablets. *European Journal of Pharmaceutics and Biopharmaceutics, 66*, 435-450.

Torres, O., Murray, B., & Sarkar, A. (2016). Emulsion micro-gel particles: Novel encapsulation strategy for lipophilic molecules. *Trends in Food Science & Technology, 55*, 98-108.

Yang, X., Gong, T., Lu, Y. H., Li, A., Sun, L., & Guo, Y. (2020). Compatibility of sodium alginate and konjac glucomannan and their applications in fabricating low-fat mayonnaise-like emulsion gels. *Carbohydrate Polymers, 229*, 115468.

Ye, X., Li, Y., Ai, Y., & Nie, Y. (2018). Novel powder packing theory with bimodal particle size distribution-application in superalloy. *Advanced Powder Technology, 29*, 2280-2287.

Zhu, Y., Wang, J., Wu, J., Zhang, J., Wan, Y., & Wu, H. (2016). Injectable hydrogels embedded with alginate microspheres for controlled delivery of bone morphogenetic protein-2. *Biomedical Materials, 11*, 025010.

Supplementary materials

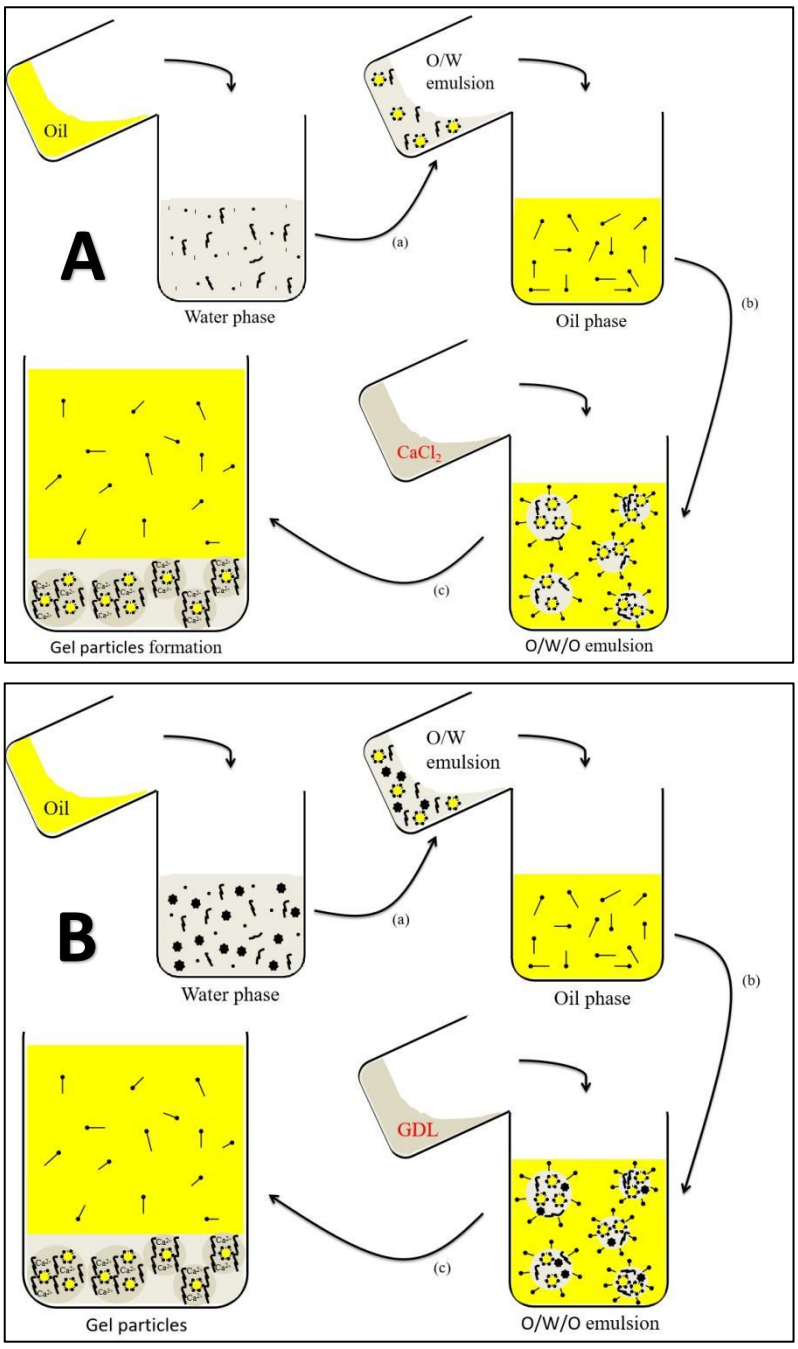

Figure 6-S1. The schematic diagram for preparation of emulsion micro-gel particles by (A) external and (B) internal emulsion gelation methods.

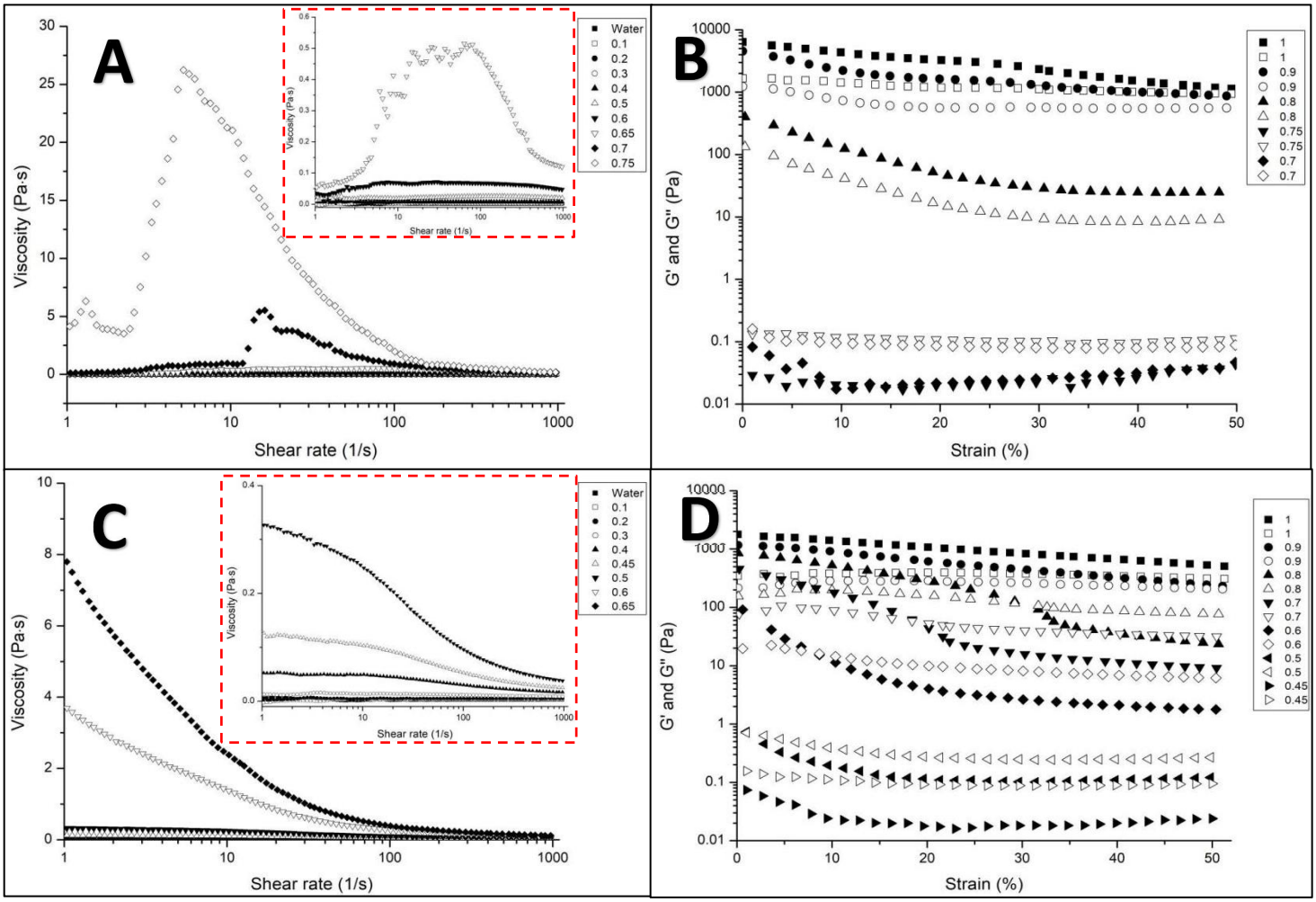

Figure 6-S2. (A) The viscosity, (B) G' (solid symbols) and G'' (open symbols) of suspensions of emulsion micro-gel particles (ϕ = 0–1) prepared by external gelation. (C) The viscosity, (D) G' (solid symbols) and G'' (open symbols) of suspensions of emulsion micro-gel particles (ϕ = 0–1) prepared by internal gelation. Dashed line-surrounded figures were zoom-in view of overlapping lines in figures A and C.

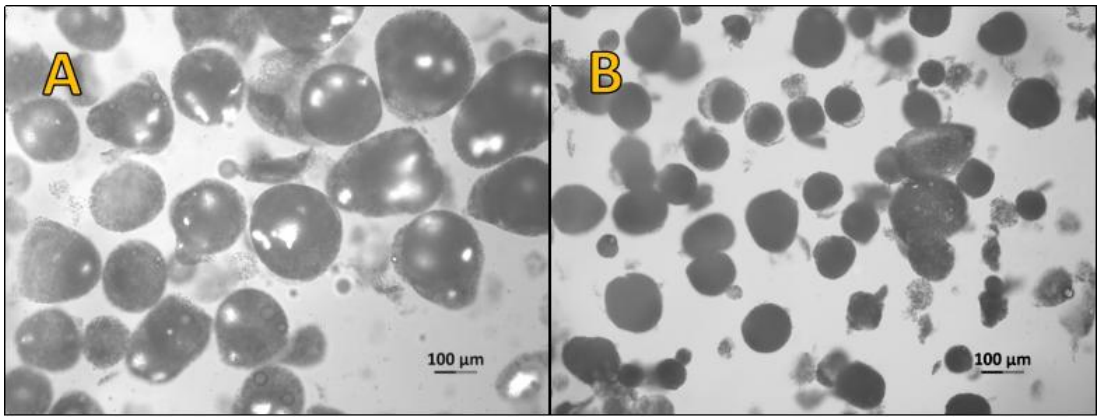

Figure 6-S3. Micro-structure of micro-gel particles prepared by internal gelation were observed under a fluorescence microscopy with a high pressure mercury burner. (A) The original particles and (B) particles incubated in 0.1 M HCl-KCl solutions (1:1, w/w) at pH 1.2 for 2 h.

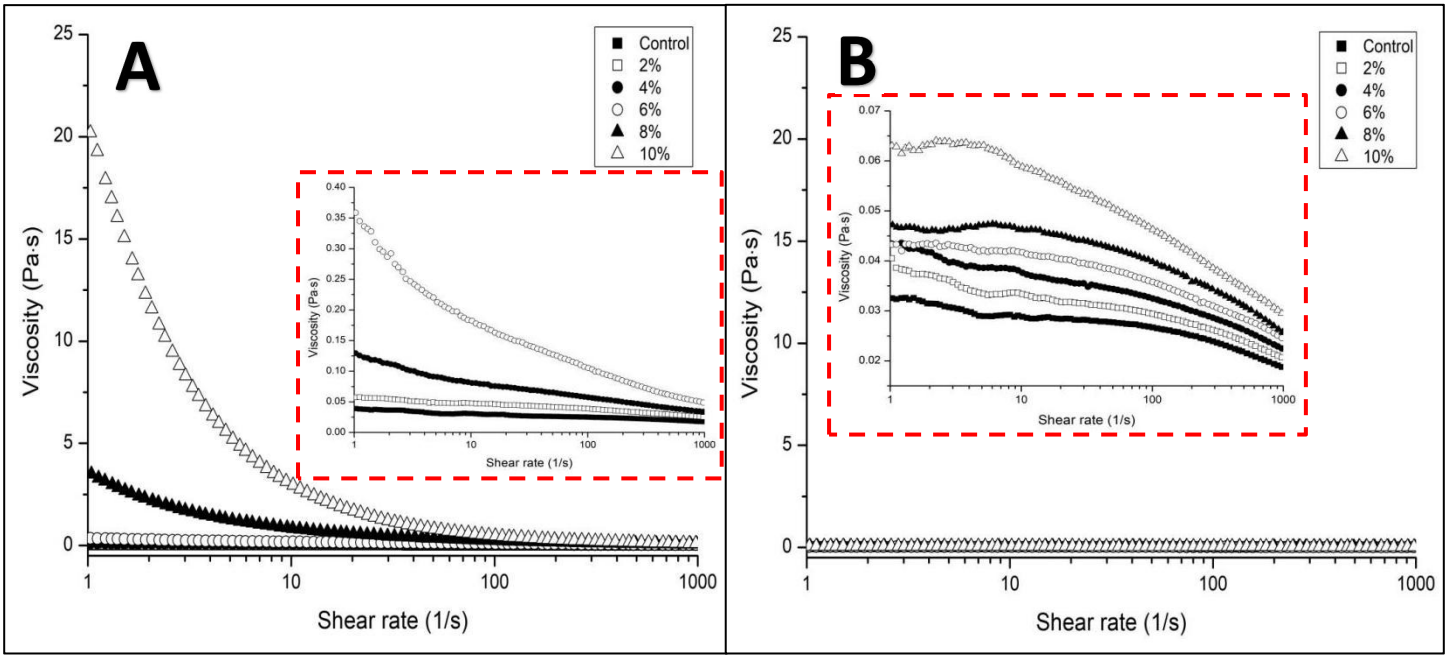

Figure 6-S4. The viscosity of 0.4% alginate solutions containing micro-gel particles (0–10 wt%) prepared by (A) external or (B) internal gelation methods. Dashed line-surrounded figures were zoom-in view of overlapping lines in figures A and B.

CHAPTER SEVEN

Improved Stability of Alginate/Soy protein isolate-stabilized Emulsions by Formation of Micro-gel Particle-induced Gel-like Emulsions

Chapter 7 has been submitted:

Lin, D., Kelly, A. L., & Miao*, S. (2021). Formation and creaming stability of alginate/micro-gel particle-induced gel-like emulsions stabilized by soy protein isolate (submitted to *Food Hydrocolloids*).

The work contained in this chapter was undertaken and written solely by myself with specific contributions from each co-author.

Abstract

Many strategies have been developed to improve stability of plant protein-stabilized emulsions, such as modifying properties of plant proteins, using plant protein-polysaccharide complexes, and forming gel-like emulsions. In this study, a novel method was investigated to enhance stability of soy protein isolate (SPI)-stabilized emulsions by introducing alginate and alginate-based micro-gel particles to form gel-like emulsions. Gel-like emulsions could be obtained at high levels of micro-gel particles (> 6.0%) in the presence of alginate (> 0.1%), while the concentration of SPI-coated droplets (0–10%) played a relatively unimportant role, probably because the gelation mechanism was interactions between alginate molecules and Ca^{2+}-induced micro-gel particles. Viscosity and creaming stability of emulsions and storage modulus (G') of gel-like emulsions increased with increasing contents of micro-gel particles in emulsions. Emulsions without micro-gel particles showed extensive creaming during storage, and emulsions containing micro-gel particles were visually stable after storage for six weeks, although all samples showed good stability to coalescence. In addition, the presence of micro-gel particles in emulsions slightly decreased the bio-accessibility of encapsulated lycopene after *in-vitro* digestion. The method presented in this study was important for improving stability of plant protein-stabilized emulsions and expanding application of plant protein-stabilized emulsions in the food industry.

Keywords: Digestion; External gelation; Gel-like emulsion; Micro-gel particle; Storage stability.

7.1. Introduction

In recent years, plant protein-stabilized emulsions, such as soy protein-, pea protein-, potato protein-, rice protein-, wheat gliadin- and zein-stabilized emulsions, have received increased interest (Lin et al., 2017), due to increased consumer demand for healthier foods (da Silva et al., 2021; Wan et al., 2015). However, compared to animal proteins (e.g., casein and whey protein) and synthetic chemicals (e.g., span 85, span 80 and Tween 20), plant proteins often result in emulsions with lower stability (especially creaming stability), probably due to low hydrophobicity and large droplet size of plant protein-stabilized droplets (Benjamin et al., 2014; Zhang et al., 2021). Many strategies therefore have been investigated to solve this problem, such as protein modification by physical, chemical and/or enzymatic treatments (Albano et al., 2019; Barać et al., 2004) and turning emulsions into emulsion gels (Lin, Kelly, & Miao, 2020).

Many methods have been reported to modify structural properties of plant proteins, in order to improve their emulsifying capacity, such as heating (Peng et al., 2016), high pressure (Chen et al., 2016; Molina et al., 2001), extrusion (Mozafarpour et al., 2019), ultrasound (O'sullivan et al., 2016), pH-shifting process (Jiang et al., 2009), enzymatic hydrolysis (Chen et al., 2011), and oxidation (Liu et al., 2015), due to improved protein solubility, reduced molecular size, and/or exposure of hidden hydrophobic residues. In addition, plant protein-polysaccharide complexes, which are formed by Maillard reaction or electrostatic interaction, can also be used to improve emulsion stability (Evans et al., 2013). It has been reported that soy protein isolate (SPI)-dextran conjugate-stabilized emulsions showed better physical and structural stability than emulsions stabilized by native SPI or SPI-dextran mixtures, probably due to higher electrostatic repulsion and steric hindrance (Zhou et al., 2020). On the other hand, the pH is crucial for stability of emulsions containing plant protein-polysaccharide complexes produced by electrostatic interaction, because electrostatic properties of proteins and polysaccharides are clearly pH-dependent (Albano et

al., 2019). Many reports have been indicated that the presence of anionic polysaccharides could increase the stability of plant protein-stabilized emulsions near the p*I* of the proteins present, due to the formation of electrostatic interaction-induced plant protein-polysaccharide complexes at the droplet interfaces and thus increased electrostatic repulsion of emulsion droplets at pH 4.0–4.5 (Lin, Kelly, & Miao, 2021b; Yildiz et al., 2018).

The final physical state of modified plant protein-stabilized emulsions is still liquid, while another widely-investigated strategy to improve stability of plant protein-stabilized emulsions is turning emulsions into emulsion gels/gel-like emulsions, due to increased viscosity and solid-like properties and thus reduced mobility of emulsion droplets. Therefore, emulsions prepared by these two methods may have different applications in the food industry. It has been reported that emulsion gels/gel-like emulsions containing plant protein-stabilized droplets may be used in meat products and solid-like delivery systems (de Souza Paglarini et al., 2019), while modified plant protein-stabilized emulsions were often used in sauce, yogurt, beverage, and liquid delivery systems (Ashaolu, 2020).

There are several methods used to prepare gel-like emulsions. Firstly, increasing the oil fraction is the simplest method to form gel-like emulsions, because of droplet flocculation/bridging (Lee et al., 2012), which has been widely reported in plant protein particle-stabilized Pickering emulsions (Liu & Tang, 2016; Zou et al., 2017). Secondly, modifying structural properties of plant proteins adsorbed at droplet surfaces may also lead to the formation of gel-like emulsions; it has been reported that SPI-stabilized emulsions turned into gel-like emulsions after microfluidization, probably due to structural deformation of proteins and increased inter-droplet interactions during microfluidization treatment (Tang & Liu, 2013). It has also been reported that soy glycinin- or potato protein-stabilized emulsion droplets could cross-link together and form gel-like emulsions by tyrosinase-induced enzymatic cross-linking (Glusac et al., 2017; Isaschar-Ovdat et al., 2015). Thirdly, introducing gelling agents into the continuous phase of emulsions can also form emulsion gels by various gelation mechanisms depending on gelling agents used, as reviewed by Lin,

Kelly, & Miao (2020). For example, alginate and $CaCO_3$ particles have been introduced into SPI-stabilized emulsions, and then emulsion gels formed after adding glucono-delta-lactone (GDL) into the system to release Ca^{2+} and trigger Ca^{2+}-induced alginate gelation (Lin, Kelly, & Miao, 2021b).

Alginate-based emulsion gels received increased interest in recent years, due to their characters (e.g., mild gelation process and slow digestion during intestinal digestion), compared to other gelling agent-based emulsion gels (Lin, Kelly, Maidannyk, et al., 2021). The alginate gelation mechanism involves sodium ions in alginate molecules being replaced by Ca^{2+} or H^{+}, which leads to Ca^{2+}-cross-linked or hydrogen bond-linked network structures. Therefore, $CaCl_2$, $CaCO_3$, and GDL are often used to trigger alginate gelation in the food industry (Draget et al., 2006). However, our previous study found that the presence of alginate-based emulsion micro-gels prepared by external gelation could increase the viscosity of alginate solutions with solid-like behavior (Lin, Kelly, & Miao, 2021a). In addition, it has also been reported that nanoparticles (e.g., TiO_2 nanorobs, carbon nanotubes, and ZnO nano-powders) could interact with proteins, lipids and polysaccharides through ionic interactions, hydrogen bonds, and/or Van der Waals interactions, and that the size, shape, and surface characters of nanoparticles (NPs) played an important role in affecting interactions between NPs and polymers (Saptarshi et al., 2013). For example, acrylamide/N-isopropylacrylamide-based nanoparticles could interact with heparin through hydrogen bonds, ionic interactions and dehydration (Zeng et al., 2012). Therefore, we predicted that Ca^{2+}-induced emulsion micro-gels could also lead to the formation of gel-like emulsions containing alginate in the continuous phase and thus improve the stability of plant protein-stabilized emulsions, which has not previously been studied.

Furthermore, there are mainly two advantages of this method. Firstly, this is a simple method to prepare gel-like emulsions by mixing micro-gel particles with emulsions, and the viscosity and gel strength of gel-like emulsions can be easily controlled by adjusting the amount of micro-gel particles for different applications in foods. In addition, a novel food

structure (i.e., microgel-in-gel emulsions) can be developed, which may be used for specific delivery systems in future. Therefore, the aim of this study was to investigate the formation and properties (i.e., rheology, morphology, droplet size, stability, digestion, and encapsulation for food nutrients) of micro-gel particle-induced gel-like emulsions containing SPI-coated droplets and alginate in the continuous phase.

7.2. Materials and methods

7.2.1. Materials

SPI containing 96.29 ± 0.03% protein was extracted from defatted soy flour (Bob's Red Mill, Milwaukie, Oregon, USA) by the method described in our previous study (Lin, Kelly, Maidannyk, et al., 2020). Sodium alginate ($\overline{M}$ = 69–117 kDa and M/G = 71/29) was obtained from Special Ingredients (Chesterfield, UK), and sunflower oil (Aldi Stores Ltd., Kildare, Ireland) was purchased from local markets. Span 80, $CaCl_2 \cdot 2H_2O$, NaOH, HCl, tomato extract, sodium azide, butylated hydroxytoluene (BHT), hexane, acetone, ethanol, and other analytical reagents were purchased from Sigma-Aldrich (St. Louis, MO, USA).

7.2.2. Preparation of emulsion micro-gel particles

The external O/W/O emulsion-gelation method was used to prepare emulsion micro-gel particles. The coarse emulsions were firstly prepared by mixing 20 wt% sunflower oil with 80wt% SPI dispersions containing 2.0 wt% SPI at 16,000 rpm for 2 min with an Ultra-Turrax (IKA-25, Staufen, Germany). The primary emulsions were then prepared by mixing coarse emulsions with 2.0 wt% sodium alginate solutions (1:3, w/w) at 14,000 rpm for 2 min. The secondary emulsions were finally prepared by mixing primary emulsions (20 wt%) with oil phase containing 78 wt% sunflower and 2.0 wt% Span 80 at 700 rpm for 5 min with a magnetic stirrer, and then $CaCl_2 \cdot 2H_2O$ solutions (1.0 wt%) were added into secondary emulsions (1:5, w/w) and stirring at 1000 rpm for 30 min. The resultant dispersions were then poured into deionized water (1:5, w/w), mixed at 500 rpm for 1 min and left to stand for

2 h. Emulsion micro-gel particles in sediments were finally collected by filtration and washed twice by deionized water after the oil cream in the top of mixtures was removed.

7.2.3. Preparation of emulsions containing micro-gel particles

The coarse emulsions were prepared as described in Section 7.2.2 and diluted with deionized water. The primary emulsions were then prepared by mixing diluted coarse emulsions (containing 0.5–2.0 % SPI and 5.0–20% SPI) with diluted sodium alginate solutions (0.2–1.0%) at a ratio of 1:1, w/w at 14,000 rpm for 2 min with an Ultra-Turrax (**Figure 7-S1**). Micro-gel particles were dried by filtration paper twice, and then micro-gel particle dispersions (10–50%, w/w) were then prepared by adding deionized water into micro-gel particles. Micro-gel particles (2.0–10 wt% in final emulsions) were then introduced into primary emulsions by mixing primary emulsions with micro-gel particle dispersions (4:1, w/w). The final emulsions containing micro-gel particles were mixed at 500 rpm for 1 min and then the properties of final emulsions were measured immediately.

7.2.4. Properties of emulsions containing micro-gel particles

7.2.4.1. Visual appearance

Emulsions (~ 10 g) were transferred into screw-cap glass bottles before resting for 2 h, and then samples were turned upside down before taking photographs of them using a camera.

7.2.4.2. Rheological measurements

The rheological properties of emulsions were measured using an AR 2000ex rheometer (TA Instruments, Crawley, UK). Emulsions were added on an aluminium parallel plate (60 mm in diameter, and 0.5 mm in gap) and allowed to stand at 20°C for 2 min before measurement. The flow measurement (the shear rate from 0.1 to 300 s^{-1}) and oscillatory measurement (the frequency from 0.1 to 10 Hz with a fixed strain of 0.1%) were then carried

out to determine the viscosity (η) and the storage (G') and loss (G'') modulus of emulsions, respectively.

7.2.4.3. Micro-structure of emulsions

An Olympus BX51 light microscope (Olympus Optical Co. Ltd., Tokyo, Japan) with a built-in camera was used to record microscopic images of emulsions.

7.2.4.4. Creaming stability measurements

The stability of emulsions to gravitational separation (i.e., creaming stability) was analyzed with a Lumisizer (LUM GmbH, Berlin, Germany). Emulsions were centrifuged at 3000 rpm and 25ºC with a scanning rate of once every 20 s for 300 profiles. The space- and time-related transmission profiles over the sample length and the fluctuation in light transmittance during centrifugation were recorded.

7.2.4.5. Size distribution measurements

A MasterSizer 3000 (Malvern Instruments Ltd., Worcestershire, UK) was used to measure the droplet-size distribution of emulsions. The obscuration rate, stirrer speed, refractive index and absorption index were set at 1% to 10%, 2000 rpm, 1.48, and 0.001, respectively.

7.2.5. Preparation and storage stability of emulsions containing lycopene

For preparation of lycopene-encapsulated emulsions, 30 mg of tomato extract (containing 0.059 mg lycopene/mg) were dissolved in 20 g of sunflower oil at 140°C with stirring for 30 s before cooling down to the room temperature, and then lycopene-encapsulated primary emulsions and final emulsions containing micro-gel particles were prepared as described in Section 7.2.3.

The final emulsions (~ 10 g) containing lycopene and micro-gel particles were transferred into screw-cap tubes and stored in a cold room at 4ºC for 6 weeks in the dark. Properties of emulsions (e.g., visual appearance, micro-structure, and droplet-size distribution) were measured every 2 weeks during storage by the methods described in Section 7.2.4, but the refractive index of 1.69 was used for the droplet-size measurement of emulsions containing lycopene. The remaining lycopene in emulsions (C_{LYC-E}) during storage was also extracted and measured as described by Lin, Kelly, Maidannyk, et al. (2021).

7.2.6. Bio-accessibility of lycopene after *in-vitro* digestion

Simulated digestion of emulsions included the oral, gastric and small intestinal phases in this study, which was performed as described in our previous study (Lin, Kelly, Maidannyk, et al., 2021). The digesta after intestinal digestion was centrifuged at 4,500 rpm and 4°C for 40 min, and the middle layer, which was regarded as the micelle fraction, was collected and weighted ($Wt_{Micelle}$). Lycopene in 0.5 g of the micelle fraction (C_{LYC-M}) was extracted and measured by the method described in our previous study (Lin, Kelly, Maidannyk, et al., 2021). The bio-accessibility of lycopene in micelle was then calculated by Eq. (7-1):

$$\text{Bio-accessibility (\%)} = \frac{C_{LYC-M} \times Wt_{Micelle}}{C_{LYM-E} \times 5} \times 100\% \quad (7\text{-}1)$$

where C_{LYC-E} is the lycopene content in original emulsions and 5 g is the weight of original emulsions used for *in-vitro* digestion.

7.3. Results and discussion

7.3.1. Effect of concentrations of alginate-based micro-gel particles, alginate, and SPI-coated droplets on the formation of gel-like emulsions

Table 7-1 shows the effect of concentrations of alginate micro-gel particles, alginate, and SPI-coated droplets on the gel point of SPI-stabilized emulsions. The establishment of gel point of emulsions in this study was based on the rheological properties of emulsions (**Figures 7-S2 and 7-S3**). At the gel point, emulsions changed from liquid-like behavior with relatively low viscosity to solid-like behavior with shear-thinning properties and G' value higher than G''.

Table 7-1. Effect of concentrations of alginate-based micro-gel particles, alginate, and SPI-coated droplets on the formation of gel-like emulsions. When the effect of alginate concentration (0–0.5 wt%) was investigated, the concentration of SPI-coated droplets was set at 5.0 wt%. When the effect of concentration of SPI-coated droplets (0–10 wt%) was investigated, the alginate concentration was set at 0.3 wt%. The results shown are based on the rheological properties of emulsions (see supplementary material).

Samples		**Alginate (wt%)**				**SPI-coated droplets (wt%)**			
		0	**0.1**	**0.3**	**0.5**	**0**	**2.5**	**5.0**	**10**
Micro-gel particles (wt%)	**0**	×[a]	×	×	×	×	×	×	×
	2	×	×	×	×	×	×	×	×
	4	×	×	×	×	×	×	×	×
	6	×	×	√	√	√	√	√	√
	8	×	×	√	√	√	√	√	√
	10	×	√[b]	√	√	√	√	√	√

[a] A cross mark indicated that emulsions were still liquid with relatively low viscosity.

[b] A check mark indicated the formation of gel-like emulsions with shear-thinning behavior and G' value higher than G''.

As shown in **Table 7-1**, gel-like emulsions could not be obtained in SPI-stabilized emulsions without alginate no matter how many micro-gel particles (0–10%) were added. When the concentration of alginate in emulsions increased to 0.1%, and 10% of micro-gel particles were added, gel-like emulsions formed, while emulsions still showed liquid-like behavior under low concentrations of micro-gel particles (0–8.0%). In addition, when the concentrations of alginate in emulsions increased to 0.3% or 0.5%, gel-like emulsions formed at high concentrations of micro-gel particles (6.0–10%). These indicate that the conditions for the formations of gel-like emulsions were the presence of alginate and addition of high levels of alginate-based micro-gel particles.

It has been reported that calcium ions were distributed at the surfaces of alginate-based macro-gel beads produced by external gelation method, as determined by electron dispersive spectroscopy (Patel et al., 2017). Therefore, it can be proposed that the mechanism of the formation of gel-like emulsions containing alginate and Ca^{2+}-induced alginate micro-gel particles is probably interactions between alginate molecules and Ca^{2+} on the surfaces of alginate micro-gel particles in the continuous phase of emulsions, which however needs further investigation. This potential mechanism for the formation of alginate-based gel-like emulsions is different from that in previous studies, in which insoluble calcium salts (e.g., $CaCO_3$, $CaSO_4$, or CaEDTA) were introduced into emulsions containing alginate before an acid (e.g., GDL or pyrophosphate) was added to release calcium ions and trigger the gelation and formation of alginate-based emulsion gels (Pintado et al., 2015; Sato et al., 2014).

Table 7-1 also shows that 0.3% of alginate solutions without SPI-coated droplets also showed solid-like behavior at high concentrations of micro-gel particles (6.0–10%), and the gel point was unchanged when the concentrations of SPI-coated droplets increased from 0% to 10%. These indicate that the concentration of SPI-coated droplets and the interactions between alginate micro-gel particles and SPI-coated droplets played a relatively unimportant role in the formation of gel-like emulsions. This was probably because the ionic bonding between alginate and Ca^{2+} is stronger than the electrostatic interactions between SPI and

Ca^{2+} (Chan et al., 2002; Lu et al., 2010), or may relate to the fact that contents of SPI in emulsions were less than 1.0% in this study, which were much lower than the concentrations of SPI (> 6.0%) needed for Ca^{2+}-induced protein gelation (Maltais et al., 2005). Therefore, it can be concluded that the gel point of emulsions was affected by the concentrations of micro-gel particles and alginate rather than the concentration of SPI-coated droplets in this study.

7.3.2. Properties of emulsions containing alginate and micro-gel particles

Figure 7-S2 shows that although emulsions containing 5.0% SPI-coated droplets, 0.1% alginate, and 10% micro-gel particles exhibited gel-like behavior (i.e., $G' > G''$), the G' of gel-like emulsions (i.e., 0.5–2.0 Pa) was low, which indicates low extents of cross-linking in the resultant gel-like emulsions. Therefore, properties of emulsions containing higher concentration of alginate (i.e., 0.3%) and various concentrations of micro-gel particles (i.e., 0–10%) were further investigated.

7.3.2.1. Rheological properties

Figure 7-1A shows that the viscosity of emulsions increased with increasing the concentrations of micro-gel particles from 0 to 10% in emulsions. This was probably because increased interactions between micro-gel particles and alginate molecules in the continuous phase decreased the fluidity of emulsions. In addition, emulsions containing higher contents of micro-gel particles (≥ 6.0%) showed more obvious shear-thinning behavior in the low range of shear rate, which also indicates that the extent of cross-linking between micro-gel particles and alginate molecules increased when increasing the concentrations of micro-gel particles. This was also confirmed by the increased values of G' and G'' of emulsions containing higher contents of micro-gel particles (≥ 6.0%) (**Figure 7-1B**). A similar result has been reported, where emulsion gels were prepared by introducing Persian gum and $CaCl_2$ into the continuous phase of whey protein isolate-stabilized

emulsions, and increasing the levels of Persian gum increased the G', G'', and η^* values of emulsion gels (Khalesi et al., 2019).

Figure 7-1B also shows that emulsions containing low levels of micro-gel particles (< 6.0%) had low G' values (< 10 Pa), while emulsions turned into gel-like emulsions ($G' > G''$) when 6.0% micro-gel particles were added, and that increasing the concentrations of micro-gel particles to 8% and 10% increased the G' of gel-like emulsions to 12–35 Pa and 64-97 Pa, respectively, in the frequency range of 0.1–10 Hz.

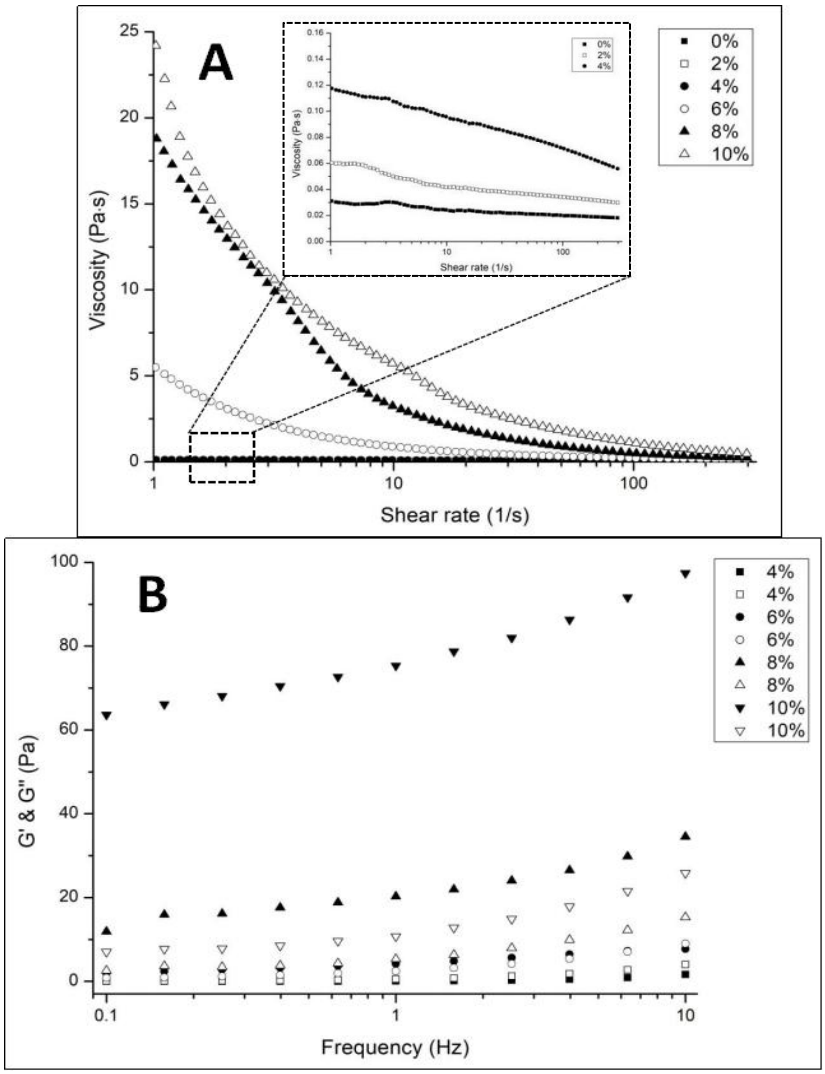

Figure 7-1. (A) Viscosity and (B) moduli (G' and G'') of emulsions containing 0–10% micro-gel particles, 0.3% alginate and 5.0% oil droplets.

In addition, the tan δ (G''/G') values also deceased from 2.43–15.9 to 0.11–0.27 when increasing the concentrations of micro-gel particles from 4.0% and 10%. This was probably because high contents of micro-gel particles in emulsions led to the formation of gel network structures, in which micro-gel particles may act as cross-linking sites between neighboring alginate molecules through interactions between alginate molecules and Ca^{2+} on the surfaces of alginate micro-gel particles and/or Ca^{2+} may release from micro-gel particles and cross-link alginate molecules in the continuous phase of emulsions. However, low concentrations of micro-gel particles (< 6.0%) were insufficient to cross-link alginate molecules and form network structures. Our results thus indicate that the viscoelasticity of gel-like emulsions can be easily adjusted by the addition amount of micro-gel particles.

7.3.2.2. Morphology, micro-structure and droplet-size

Figure 7-2A shows the visual appearance of SPI-stabilized emulsions containing 0.3% alginate and 0–10% of micro-gel particles. Emulsions without micro-gel particles moved to the bottom of bottle after inverting the glass bottle, while some emulsions containing 2.0–4.0% of micro-gel particles stuck to the inner walls of bottles, due to the slightly increased viscosity (**Figure 7-1A**). Emulsions containing 6.0% of micro-gel particles turned into gel-like emulsions and some residual gel material remained on the top and wall of bottle after inverting it, while emulsions containing 8–10% of micro-gel particles showed solid-like and self-standing behavior, and are classed as emulsion gels, probably due to high extents of cross-linking between alginate molecules and micro-gel particles in the continuous phase of emulsions. Our results indicated that SPI-stabilized emulsions, gel-like emulsions, or emulsion gels could be obtained by adjusting the content of micro-gel particles. Similar results have also been reported, where starch granule-stabilized Pickering emulsions converted from liquid-like behavior to solid-like behavior with increasing the oil volume fractions from 10% to 60% (Li et al., 2020).

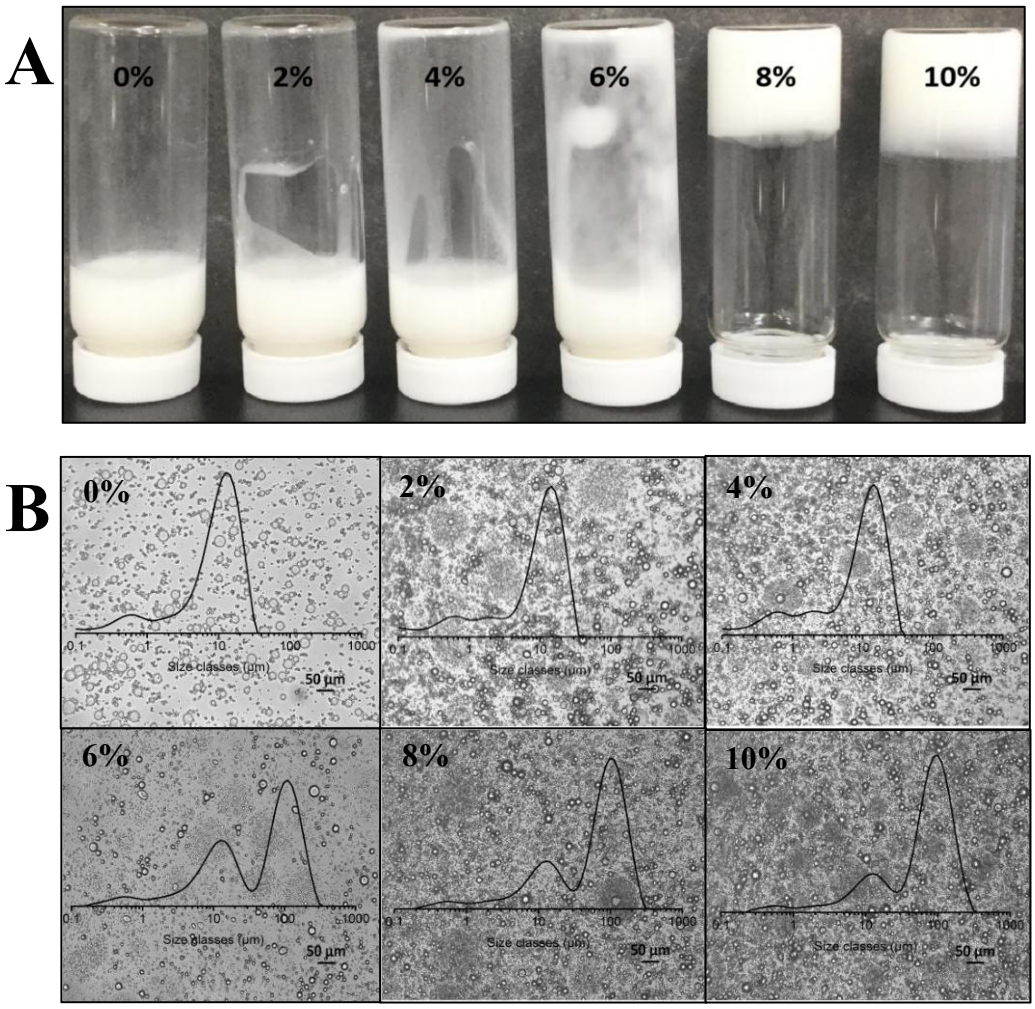

Figure 7-2. (A) Visual appearance and (B) micro-structure with droplet-size distribution of emulsions containing 0–10% micro-gel particles.

Figure 7-2B shows the micro-structure and droplet-size distribution of SPI-stabilized emulsions containing 0.3% alginate and 0–10% of micro-gel particles. Partial emulsion flocculation occurred in emulsions without micro-gel particles (i.e., the control sample), probably because the electrostatic repulsion between anionic alginate and SPI-coated droplets at pH 6–7 led to depletion flocculation (Fioramonti et al., 2015). Both micro-gel particles and emulsion droplets could be observed in samples containing 2.0–4.0% of micro-gel particles, and they had similar droplet sizes to the control sample. However, increasing the contents of micro-gel particles to 6.0–10% significantly increased the droplet size of sample (i.e., the presence of another peak at around 100 μm in the distribution), but the

micro-structure of emulsion droplets containing 6.0–10% of micro-gel particles were similar to those containing 2.0–4.0% of micro-gel particles, in which droplet coalescence did not occur. Therefore, the possible reason for increased droplet size was that the presence of micro-gel particles (D = 4.03–144 μm) (**Figure 7-S4**) were detected in samples containing higher contents of micro-gel particles (i.e., 6.0–10%), although the presence of micro-gel particles had no significant effects on the emulsion droplet-size distribution regardless of micro-gel particle concentration.

7.3.2.3. Creaming stability

Figure 7-3 shows the light transmission profiles of SPI-stabilized emulsions containing 0.3% alginate and 0–10% of micro-gel particles during centrifugation. The light transmission through the bottom of sample cells containing emulsions without micro-gel particles (i.e., the control sample in **Figure 7-3A**) increased sharply during centrifugation, which indicates the occurrence of creaming in the control sample. Creaming in emulsions is driven by the buoyancy of emulsion droplets dispersed in the continuous phase and, according to the Stokes law, the creaming rate (Cr) can be calculated through Eq. (7-2):

$$Cr = \frac{R^2(\rho_c - \rho_o)}{\eta_c} \tag{7-2}$$

where R indicates the size of droplets, ρ_c indicates the density of the continuous phase, ρ_o indicates the density of droplets, and η_c indicates the viscosity of the continuous phase (Chanamai & McClements, 2000).

However, the presence of low levels of micro-gel particles in emulsions (i.e., 2.0–4.0%) slowed the changes on the light transmission through the bottom of sample cells (**Figures 7-3B and 7-3C**), which indicates an increase in creaming stability of emulsions. This was probably because low extents of cross-linking occurred between alginate molecules and micro-gel particles in the continuous phase, which increased the viscosity of continuous phase and thus decreased the creaming rate of emulsions. Further increasing the addition

levels of micro-gel particles in emulsions to 6.0–10% led to a stable system with low light transmission in emulsions during centrifugation (**Figures 7-3D-F**), which indicated high creaming stability of emulsions, probably because of the high extents of cross-linking between alginate molecules and micro-gel particles and the formation of gel-like emulsions.

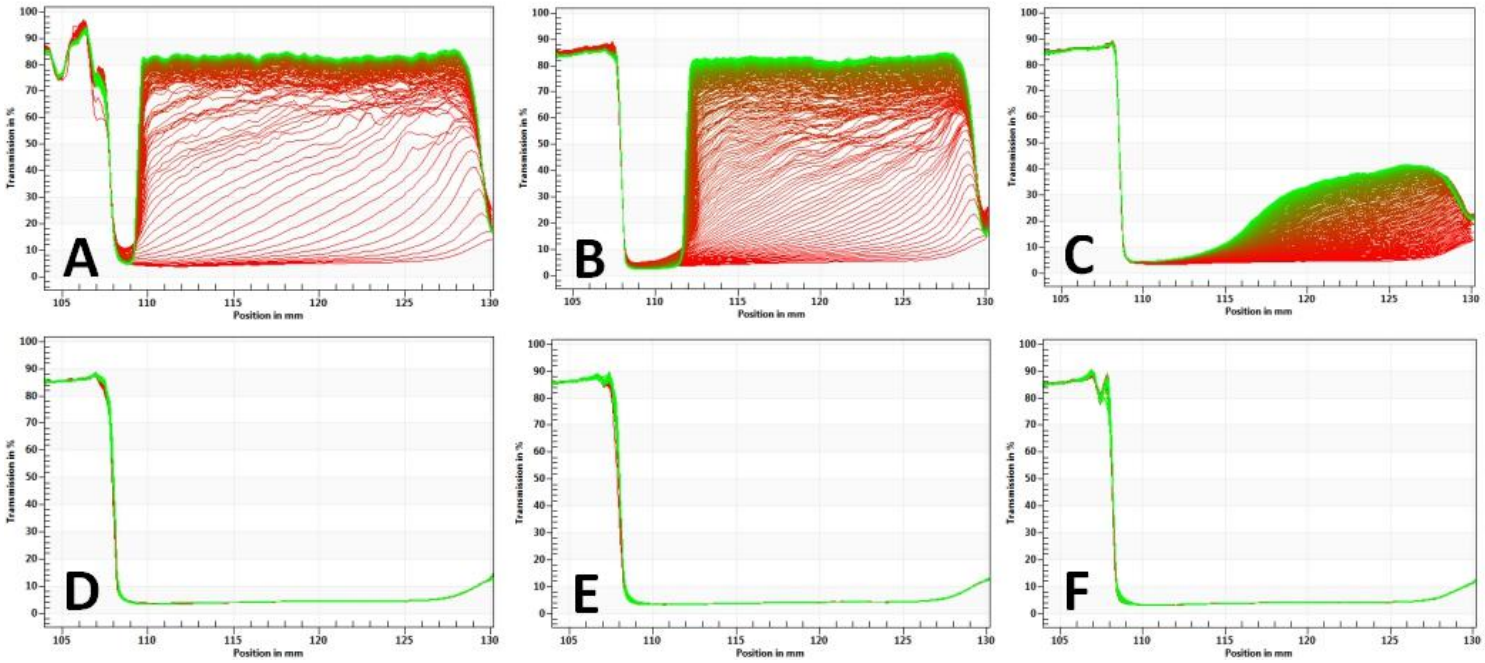

Figure 7-3. (A-F) Transmission profiles with time of emulsions containing 0%, 2.0%, 4.0%, 6.0%, 8.0%, and 10% micro-gel particles during 100 min of centrifugation at 3000 rpm.

7.3.3. Storage stability and digestion of micro-gel particle-induced gel-like emulsions with encapsulated lycopene

7.3.3.1. Storage stability of emulsions with encapsulated lycopene

The storage stability of emulsions containing 0%, 4.0%, or 8.0% of micro-gel particles and encapsulated lycopene were further investigated, by storage of samples at 4°C in the dark for six weeks. **Figure 7-4A** shows the visual appearance of emulsions during storage. It can be seen that creaming occurred in the control samples without micro-gel particles during

storage, while emulsions containing 4.0% or 8.0% of micro-gel particles showed relatively high creaming stability. This was probably because the interactions between micro-gel particles and alginate molecules increased the viscosity of the continuous phase, decreased the mobility of droplets, and thus improved the storage stability of emulsions, as discussed in Section 7.3.2.3.

The micro-structure and droplet-size distribution of emulsions during storage were also investigated (**Figure 7-4B**). The $D_{4,3}$ of droplets in emulsions containing 0% or 4.0% of micro-gel particles before storage were 9.31 ± 0.03 μm and 9.12 ± 0.02 μm with one peak in the distribution, respectively, while the $D_{4,3}$ of droplets in emulsions containing 8.0% of micro-gel particles before storage were 74.2 ± 12.7 μm with two peaks in the distribution. The droplet size of emulsions containing 0%, 4.0%, or 8.0% micro-gel particles after storage for six weeks were 9.26 ± 0.04 μm, 9.08 ± 0.04 μm, and 83.6 ± 2.2 μm, respectively. In addition, droplet coalescence was not observed from micro-structure of emulsions during storage. These indicate that all SPI-stabilized emulsions containing alginate showed good stability to coalescence regardless of the presence of micro-gel particles, probably because proteins adsorbed at the surfaces of droplets could prevent two droplets from merging to form a larger droplet (Tcholakova et al., 2006).

Figure 7-4C shows the content of lycopene encapsulated in SPI-stabilized emulsions containing 0%, 4.0%, or 8.0% of micro-gel particles during storage. It can be seen that lycopene in all samples showed high stability during storage, although their contents decreased slightly. It is well known that heating (> 100°C) and light irradiation can accelerate lycopene degradation (Ax et al., 2003; Shi et al., 2003). However, samples were stored at 4°C in the dark in this study, so lycopene were relatively stable, although the mobility of droplets in emulsions containing different levels of micro-gel particles were different.

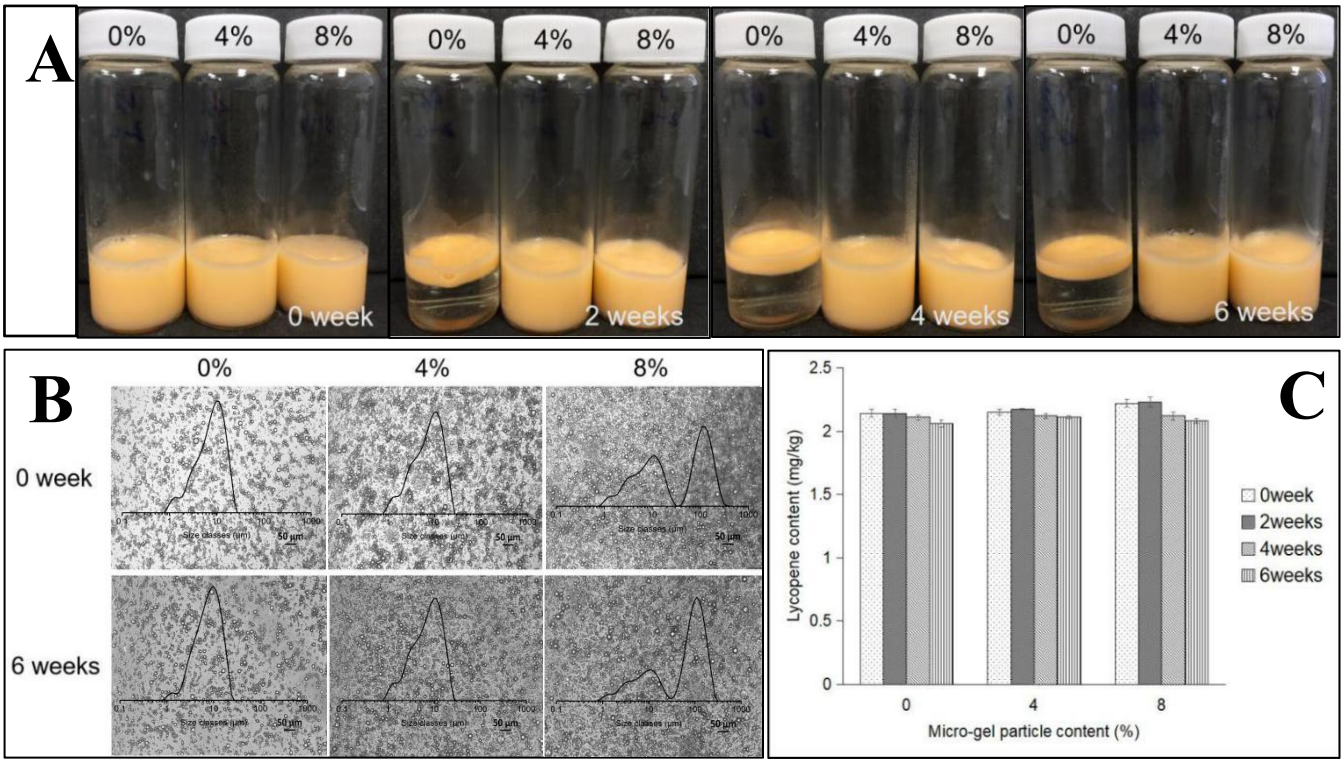

Figure 7-4. (A) Visual appearance of emulsions, (B) micro-structure with droplet-size distribution of emulsions, and (C) lycopene content in emulsions containing 0%, 4.0%, and 8.0% micro-gel particles during storage for six weeks at 4°C and darkness.

7.3.3.2. Bio-accessibility of encapsulated lycopene from emulsions during digestion

In-vitro digestion of emulsions containing 0%, 4.0%, or 8.0% of micro-gel particles and encapsulated lycopene were also studied, and **Figure 7-5** shows the micro-structure of emulsions during digestion. Emulsions after oral digestion had similar structures to those before digestion (**Figure 7-4B**). However, severe flocculation occurred during gastric digestion in all samples, probably because the pH of simulated gastric liquids was maintained at 3.0 and the surface charges of SPI-stabilized droplets and the repulsive forces between neighboring droplets decreased at such pH. It has also been reported that whey protein-stabilized emulsions underwent flocculation during simulated gastric digestion at pH 2.52–6.16 (Wang et al., 2019). **Figure 7-5** also shows that small parts of droplets could still be observed after intestinal digestion for 2 h, and some droplets were coated by membranous

cysts in emulsions containing 4.0% or 8.0% of micro-gel particles, which was probably because undigested alginate gel matrix residuals attached to the droplets.

In addition, the bio-accessibility of encapsulated lycopene after intestinal digestion was also investigated, and the lycopene bio-accessibility in emulsions containing 0%, 4.0%, or 8.0% of micro-gel particles were 56.8 ± 7.0%, 52.7 ± 7.1%, and 51.0 ± 6.7%, respectively ($p > 0.05$). It is known that carotenoids in lipids could be released and dissolved into micelles during intestinal digestion along with lipid digestion (Mutsokoti et al., 2017), while the presence of micro-gel particle-induced gel-like alginate matrices in emulsions may inhibit bio-accessibility of enzymes to lipids and thus slow lipid digestion and decrease carotenoid bio-accessibility. It has been reported that less β-carotene was released from whey protein-beet pectin-stabilized emulsions into micelles than from whey protein-

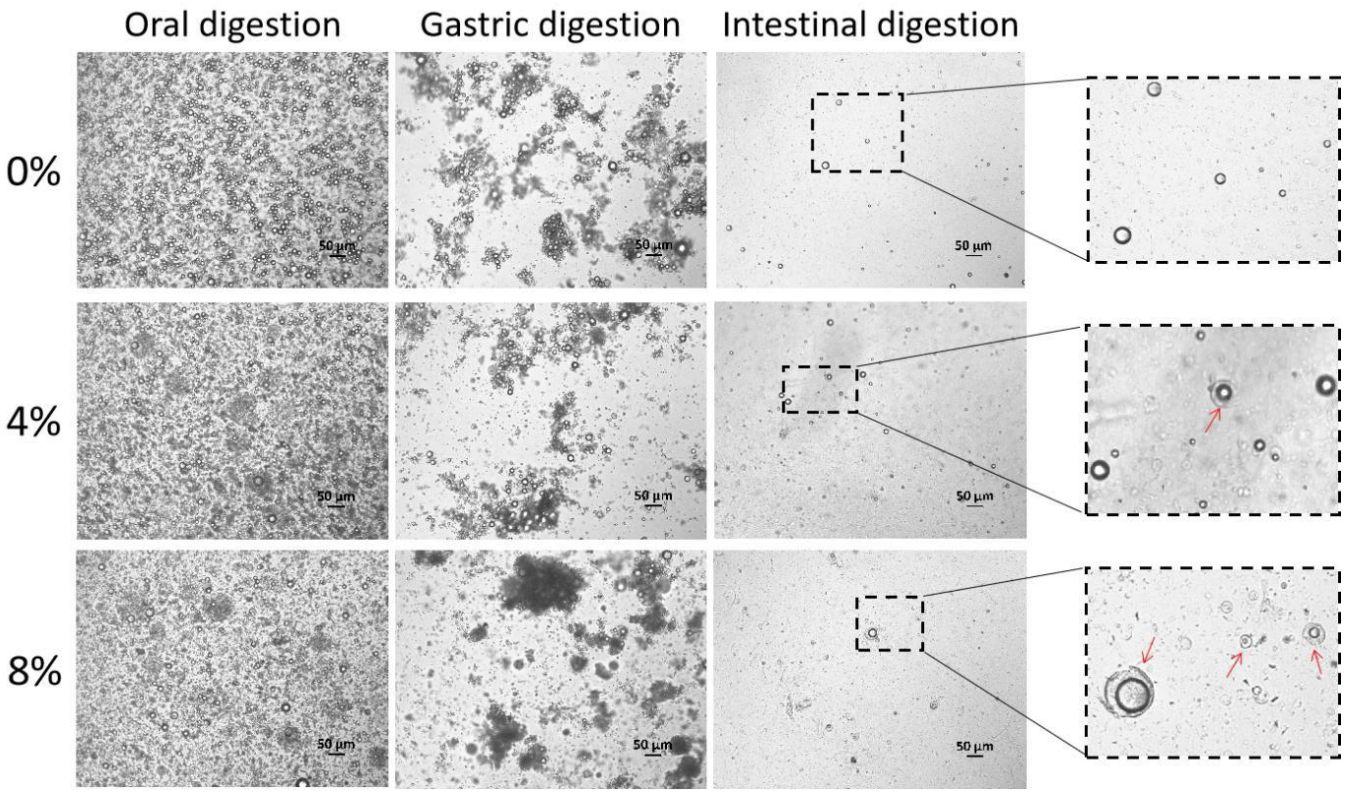

Figure 7-5. Micro-structure of emulsions containing 0%, 4.0%, and 8.0% micro-gel particles and lycopene during *in-vitro* digestion. Arrows pointed out the membranous cyst-coated droplets.

stabilized emulsions (Xu et al., 2014).

7.4. Conclusions

The formation and properties (i.e., micro-structure, rheological properties, creaming stability, storage stability, and *in-vitro* digestion) of gel-like emulsions containing alginate-based micro-gel particles and alginate molecules were investigated. The conditions for the formation of gel-like emulsions were high concentrations of micro-gel particles (≥ 6.0%) in the presence of alginate (> 0.1%), but the concentration of oil droplets (0–10%) did not affect the gel point of emulsions, which indicated that interactions between alginate molecules and micro-gel particles may be the reason for the formation of gel-like emulsions. In addition, increased viscosity and G' values of emulsions/gel-like emulsions with increasing contents of micro-gel particles in emulsions also indicated increased cross-linking between alginate molecules and micro-gel particles. The creaming stability and storage stability of emulsions were significantly improved after introducing high concentrations of micro-gel particles (≥ 6.0%) compared to the control samples without micro-gel particles, although the presence of micro-gel particles slightly decreased the *in-vitro* bio-accessibility of lycopene encapsulated in emulsions ($p > 0.05$). However, the mechanism of interactions between alginate molecules and Ca^{2+}-induced micro-gel particles (especially the surface properties of micro-gel particles), the effect of higher oil phase fraction (> 10%) on the properties of micro-gel particle-induced gel-like emulsions, and the application of these gel-like emulsions in foods, need further investigation.

References

Albano, K. M., Cavallieri, Â. L. F., & Nicoletti, V. R. (2019). Electrostatic interaction between proteins and polysaccharides: Physicochemical aspects and applications in emulsion stabilization. *Food Reviews International, 35*, 54-89.

Ashaolu, T. J. (2020). Applications of soy protein hydrolysates in the emerging functional foods: A review. *International Journal of Food Science & Technology, 55*, 421-428.

Ax, K., Mayer-Miebach, E., Link, B., Schuchmann, H., & Schubert, H. (2003). Stability of lycopene in oil-in-water emulsions. *Engineering in Life Sciences, 3*, 199-201.

Barać, M. B., Stanojević, S. P., Jovanović, S. T., & Pešić, M. B. (2004). Soy protein modification: A review. *Acta Periodica Technologica,* 35, 3-16.

Benjamin, O., Silcock, P., Beauchamp, J., Buettner, A., & Everett, D. (2014). Emulsifying properties of legume proteins compared to *β*-lactoglobulin and tween 20 and the volatile release from oil-in-water emulsions. *Journal of Food Science, 79*, E2014-E2022.

Chan, L., Jin, Y., & Heng, P. (2002). Cross-linking mechanisms of calcium and zinc in production of alginate microspheres. *International Journal of Pharmaceutics, 242*, 255-258.

Chanamai, R., & McClements, D. J. (2000). Dependence of creaming and rheology of monodisperse oil-in-water emulsions on droplet size and concentration. *Colloids and Surfaces A: Physicochemical and Engineering Aspects, 172*, 79-86.

Chen, L., Chen, J., Ren, J., & Zhao, M. (2011). Modifications of soy protein isolates using combined extrusion pre-treatment and controlled enzymatic hydrolysis for improved emulsifying properties. *Food Hydrocolloids, 25*, 887-897.

Chen, L., Chen, J., Yu, L., & Wu, K. (2016). Improved emulsifying capabilities of hydrolysates of soy protein isolate pretreated with high pressure microfluidization. *LWT-Food Science and Technology, 69*, 1-8.

da Silva, A. M. M., Almeida, F. S., & Sato, A. C. K. (2021). Functional characterization of commercial plant proteins and their application on stabilization of emulsions. *Journal of Food Engineering, 292*, 110277.

de Souza Paglarini, C., Martini, S., & Pollonio, M. A. R. (2019). Using emulsion gels made with sonicated soy protein isolate dispersions to replace fat in frankfurters. *LWT, 99*, 453-459.

Draget, K. I., Skjåk-Bræk, G., & Stokke, B. T. (2006). Similarities and differences between alginic acid gels and ionically crosslinked alginate gels. *Food Hydrocolloids, 20*, 170-175.

Evans, M., Ratcliffe, I., & Williams, P. A. (2013). Emulsion stabilisation using polysaccharide–protein complexes. *Current Opinion in Colloid & Interface Science, 18*, 272-282.

Fioramonti, S. A., Martinez, M. J., Pilosof, A. M., Rubiolo, A. C., & Santiago, L. G. (2015). Multilayer emulsions as a strategy for linseed oil microencapsulation: Effect of pH and alginate concentration. *Food Hydrocolloids, 43*, 8-17.

Glusac, J., Isaschar-Ovdat, S., Kukavica, B., & Fishman, A. (2017). Oil-in-water emulsions stabilized by tyrosinase-crosslinked potato protein. *Food Research International, 100*, 407-415.

Isaschar-Ovdat, S., Rosenberg, M., Lesmes, U., & Fishman, A. (2015). Characterization of oil-in-water emulsions stabilized by tyrosinase-crosslinked soy glycinin. *Food Hydrocolloids, 43*, 493-500.

Jiang, J., Chen, J., & Xiong, Y. L. (2009). Structural and emulsifying properties of soy protein isolate subjected to acid and alkaline pH-shifting processes. *Journal of Agricultural and Food Chemistry, 57*, 7576-7583.

Khalesi, H., Emadzadeh, B., Kadkhodaee, R., & Fang, Y. (2019). Effect of Persian gum on whey protein concentrate cold-set emulsion gel: Structure and rheology study. *International Journal of Biological Macromolecules, 125*, 17-26.

Lee, M. N., Chan, H. K., & Mohraz, A. (2012). Characteristics of Pickering emulsion gels formed by droplet bridging. *Langmuir, 28*, 3085-3091.

Li, S., Zhang, B., Li, C., Fu, X., & Huang, Q. (2020). Pickering emulsion gel stabilized by octenylsuccinate quinoa starch granule as lutein carrier: Role of the gel network. *Food Chemistry, 305*, 125476.

Lin, D., Kelly, A. L., Maidannyk, V., & Miao, S. (2020). Effect of concentrations of alginate, soy protein isolate and sunflower oil on water loss, shrinkage, elastic and structural properties of alginate-based emulsion gel beads during gelation. *Food Hydrocolloids, 108*, 105998.

Lin, D., Kelly, A. L., Maidannyk, V., & Miao, S. (2021). Effect of structuring emulsion gels by whey or soy protein isolate on the structure, mechanical properties, and in-vitro digestion of alginate-based emulsion gel beads. *Food Hydrocolloids, 110*, 106165.

Lin, D., Kelly, A. L., & Miao, S. (2020). Preparation, structure-property relationships and applications of different emulsion gels: Bulk emulsion gels, emulsion gel particles, and fluid emulsion gels. *Trends in Food Science & Technology, 102*, 123-137.

Lin, D., Kelly, A. L., & Miao, S. (2021a). Alginate-based emulsion micro-gel particles produced by an external/internal O/W/O emulsion-gelation method: Formation, suspension rheology, digestion, and application to gel-in-gel beads. *Unpublished.*

Lin, D., Kelly, A. L., & Miao, S. (2021b). The role of mixing sequence in structuring O/W emulsions and emulsion gels produced by electrostatic protein-polysaccharide interactions between soy protein isolate-coated droplets and alginate molecules. *Food Hydrocolloids, 113*, 106537.

Lin, D., Lu, W., Kelly, A. L., Zhang, L., Zheng, B., & Miao, S. (2017). Interactions of vegetable proteins with other polymers: Structure-function relationships and applications in the food industry. *Trends in Food Science & Technology, 68*, 130-144.

Liu, F., & Tang, C. H. (2016). Soy glycinin as food-grade Pickering stabilizers: Part. III. Fabrication of gel-like emulsions and their potential as sustained-release delivery systems for β-carotene. *Food Hydrocolloids, 56*, 434-444.

Liu, Q., Lu, Y., Han, J., Chen, Q., & Kong, B. (2015). Structure-modification by moderate oxidation in hydroxyl radical-generating systems promote the emulsifying properties of soy protein isolate. *Food Structure, 6*, 21-28.

Lu, X., Lu, Z., Yin, L., Cheng, Y., & Li, L. (2010). Effect of preheating temperature and calcium ions on the properties of cold-set soybean protein gel. *Food Research International, 43*, 1673-1683.

Maltais, A., Remondetto, G. E., Gonzalez, R., & Subirade, M. (2005). Formation of soy protein isolate cold-set gels: Protein and salt effects. *Journal of Food Science, 70*, C67-C73.

Molina, E., Papadopoulou, A., & Ledward, D. (2001). Emulsifying properties of high pressure treated soy protein isolate and 7S and 11S globulins. *Food Hydrocolloids, 15*, 263-269.

Mozafarpour, R., Koocheki, A., Milani, E., & Varidi, M. (2019). Extruded soy protein as a novel emulsifier: Structure, interfacial activity and emulsifying property. *Food Hydrocolloids, 93*, 361-373.

Mutsokoti, L., Panozzo, A., Pallares, A. P., Jaiswal, S., Van Loey, A., Grauwet, T., & Hendrickx, M. (2017). Carotenoid bioaccessibility and the relation to lipid digestion: A kinetic study. *Food Chemistry, 232*, 124-134.

O'sullivan, J., Park, M., & Beevers, J. (2016). The effect of ultrasound upon the physicochemical and emulsifying properties of wheat and soy protein isolates. *Journal of Cereal Science, 69*, 77-84.

Patel, M. A., AbouGhaly, M. H., Schryer-Praga, J. V., & Chadwick, K. (2017). The effect of ionotropic gelation residence time on alginate cross-linking and properties. *Carbohydrate Polymers, 155*, 362-371.

Peng, W., Kong, X., Chen, Y., Zhang, C., Yang, Y., & Hua, Y. (2016). Effects of heat treatment on the emulsifying properties of pea proteins. *Food Hydrocolloids, 52*, 301-310.

Pintado, T., Ruiz-Capillas, C., Jiménez-Colmenero, F., Carmona, P., & Herrero, A. M. (2015). Oil-in-water emulsion gels stabilized with chia (Salvia hispanica L.) and cold gelling agents: Technological and infrared spectroscopic characterization. *Food Chemistry, 185*, 470-478.

Saptarshi, S. R., Duschl, A., & Lopata, A. L. (2013). Interaction of nanoparticles with proteins: Relation to bio-reactivity of the nanoparticle. *Journal of Nanobiotechnology, 11*, 1-12.

Sato, A., Moraes, K., & Cunha, R. (2014). Development of gelled emulsions with improved oxidative and pH stability. *Food Hydrocolloids, 34*, 184-192.

Shi, J., Le Maguer, M., Bryan, M., & Kakuda, Y. (2003). Kinetics of lycopene degradation in tomato puree by heat and light irradiation. *Journal of Food Process Engineering, 25*, 485-498.

Tang, C. H., & Liu, F. (2013). Cold, gel-like soy protein emulsions by microfluidization: Emulsion characteristics, rheological and microstructural properties, and gelling mechanism. *Food Hydrocolloids, 30*, 61-72.

Tcholakova, S., Denkov, N. D., Ivanov, I. B., & Campbell, B. (2006). Coalescence stability of emulsions containing globular milk proteins. *Advances in Colloid and Interface Science, 123*, 259-293.

Wan, Z. L., Guo, J., & Yang, X. Q. (2015). Plant protein-based delivery systems for bioactive ingredients in foods. *Food & Function, 6*, 2876-2889.

Wang, X., Lin, Q., Ye, A., Han, J., & Singh, H. (2019). Flocculation of oil-in-water emulsions stabilised by milk protein ingredients under gastric conditions: Impact on *in vitro* intestinal lipid digestion. *Food Hydrocolloids, 88*, 272-282.

Xu, D., Yuan, F., Gao, Y., Panya, A., McClements, D. J., & Decker, E. A. (2014). Influence of whey protein–beet pectin conjugate on the properties and digestibility of *β*-carotene emulsion during in vitro digestion. *Food Chemistry, 156*, 374-379.

Yildiz, G., Ding, J., Andrade, J., Engeseth, N. J., & Feng, H. (2018). Effect of plant protein-polysaccharide complexes produced by mano-thermo-sonication and pH-shifting on the structure and stability of oil-in-water emulsions. *Innovative Food Science & Emerging Technologies, 47*, 317-325.

Zeng, Z., Patel, J., Lee, S. H., McCallum, M., Tyagi, A., Yan, M., & Shea, K. J. (2012). Synthetic polymer nanoparticle–polysaccharide interactions: A systematic study. *Journal of the American Chemical Society, 134*, 2681-2690.

Zhang, S. B., Yan, D. Q., Jiang, Y. S., & Ding, C. H. (2021). Competitive displacement of interfacial soy proteins by Tween 20 and its effect on the physical stability of emulsions. *Food Hydrocolloids, 113*, 106515.

Zhou, Y., Teng, F., Tian, T., Sami, R., Wu, C., Zhu, Y., et al. (2020). The impact of soy protein isolate-dextran conjugation on capsicum oleoresin (*Capsicum annuum L.*) nanoemulsions. *Food Hydrocolloids, 108*, 105818.

Zou, Y., Pan, R., Wan, Z., Guo, J., Wang, J., & Yang, X. (2017). Gel-like emulsions prepared with zein nanoparticles produced through phase separation from acetic acid solutions. *International Journal of Food Science & Technology, 52*, 2670-2676.

Supplementary materials

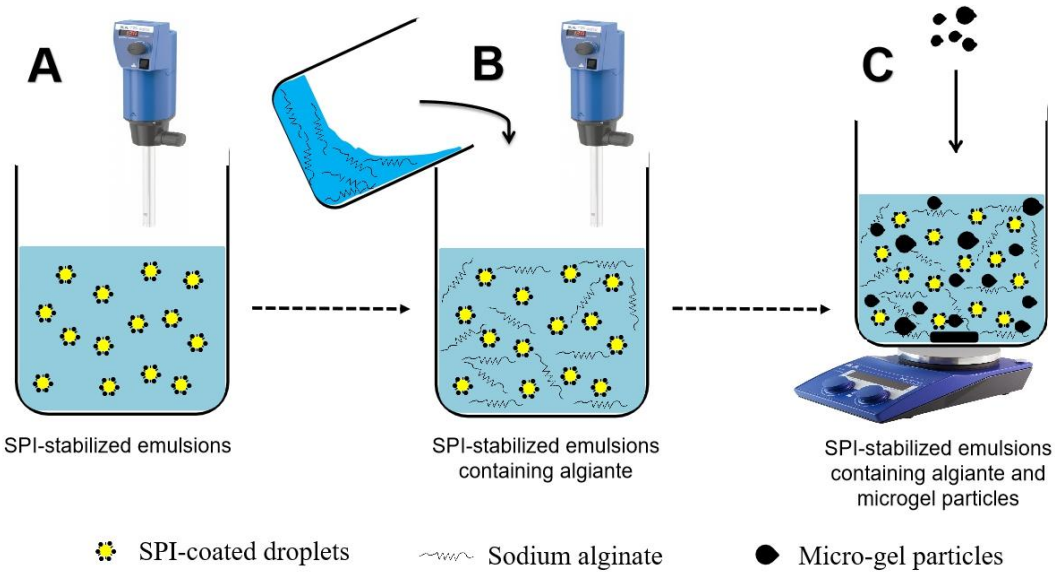

Figure 7-S1. Preparation of SPI-stabilized emulsions containing sodium alginate and micro-gel particles.

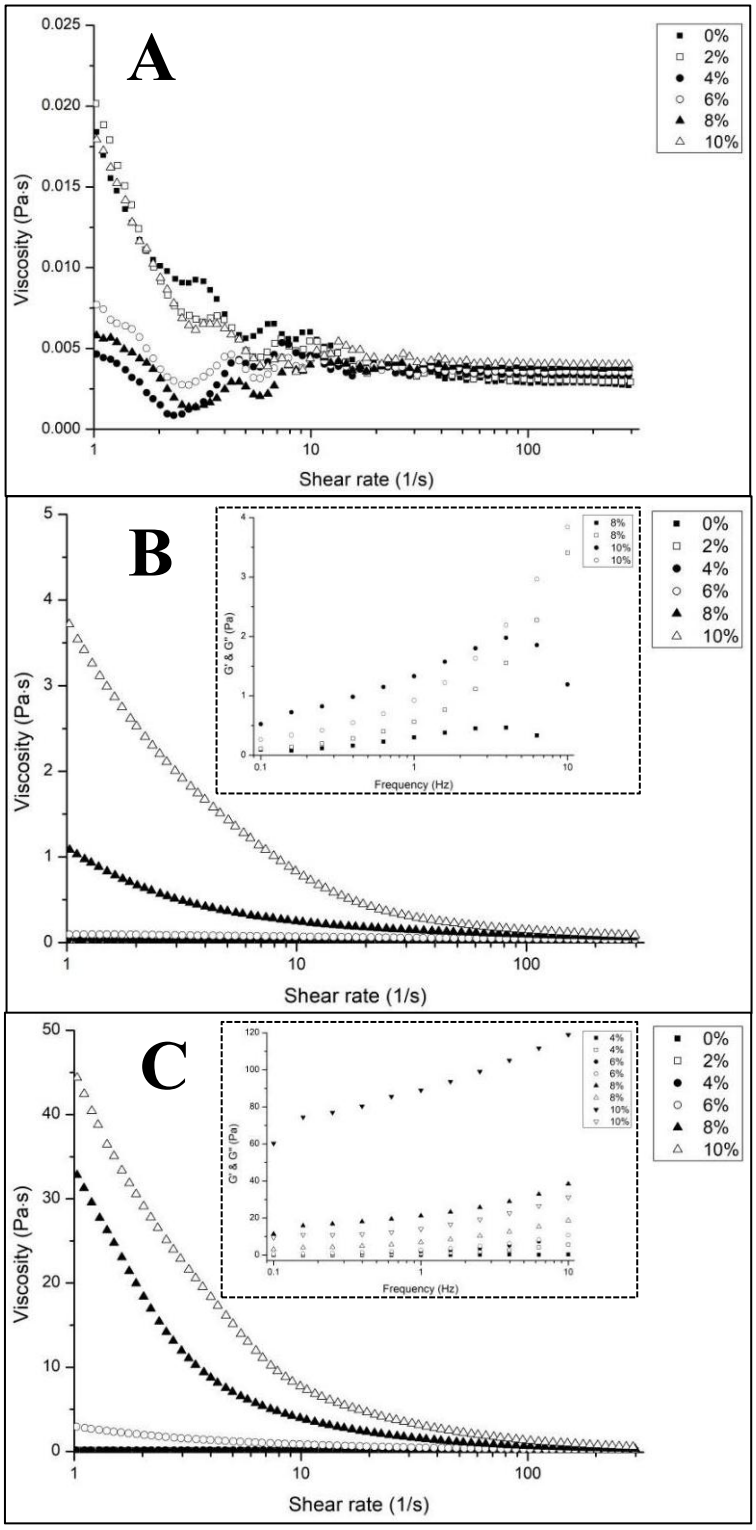

Figure 7-S2. The effect of alginate concentration (i.e., (A) 0%, (B) 0.1%, and (C) 0.5%) on viscosity and moduli (G' and G'') of emulsions containing 0–10% micro-gel particles and 5.0% oil droplets. The results of effect of 0.3% alginate were presented in **Figure 7-1**.

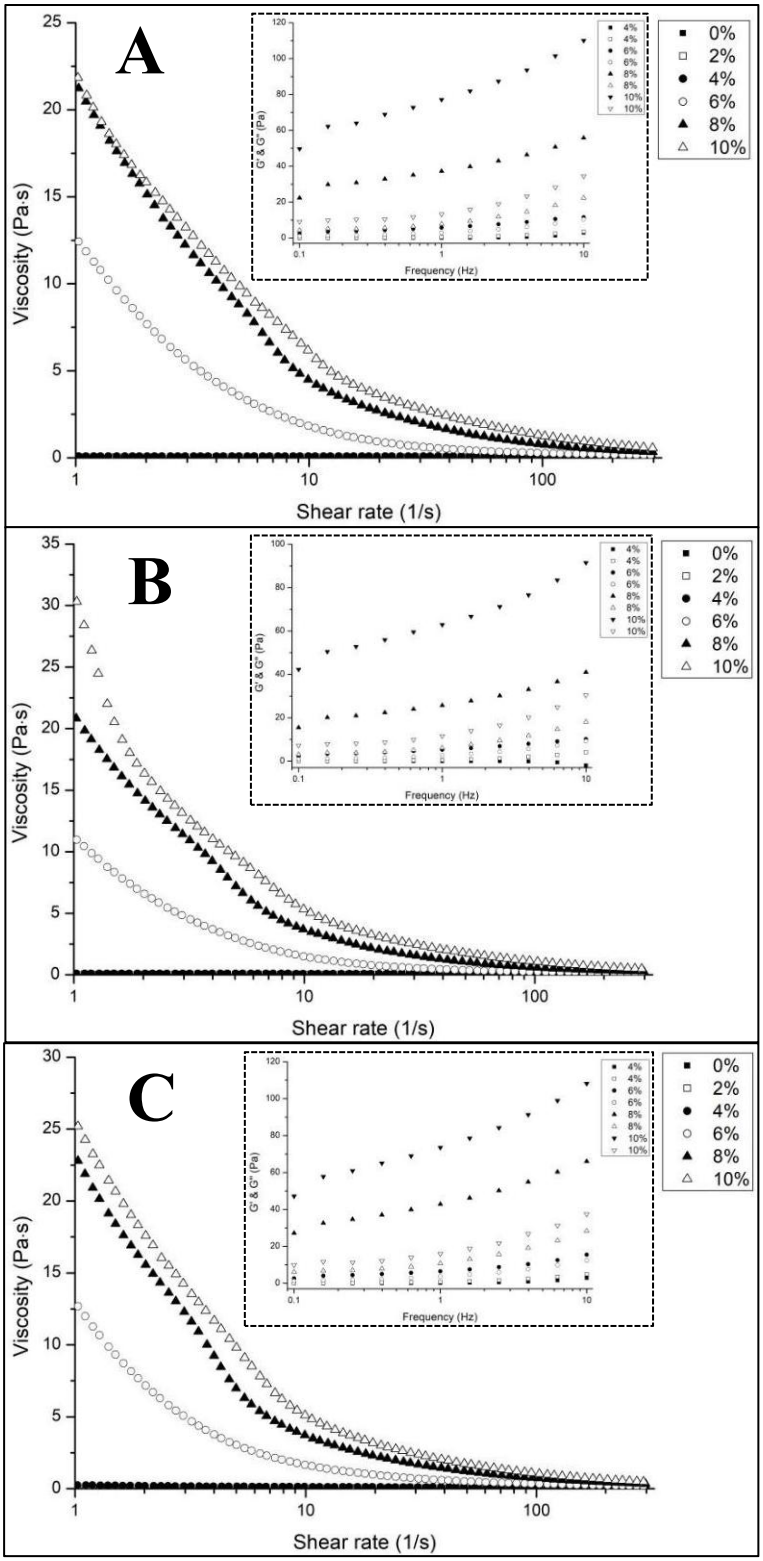

Figure 7-S3. The effect of oil phase fraction (i.e., (A) 0%, (B) 2.5%, and (C) 10%) on viscosity and moduli (G' and G'') of emulsions containing 0–10% micro-gel particles and 0.3% alginate. The results of effect of 5.0% oil were presented in **Figure 7-1**.

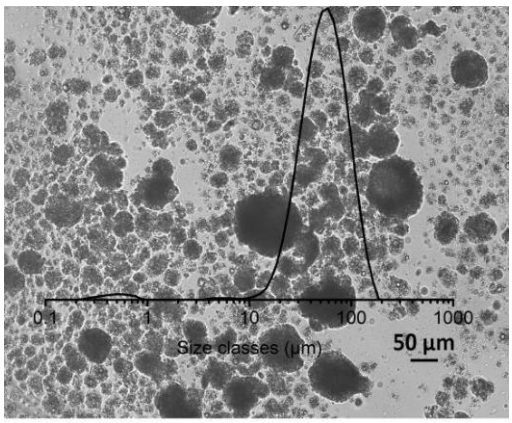

Figure 7-S4. Micro-structure and size distribution of alginate-based micro-gel particles produced by the external O/W/O emulsion-gelation method.

CHAPTER EIGHT

General Discussion and Conclusions

8.1. Overview and summary

This thesis investigated the formulation, properties and application of alginate-based and soy protein isolate (SPI)-stabilized emulsion gels. It includes three sections divided by the morphology of emulsion gels studied: (1) structuring *bulk emulsion gels* by electrostatic protein-polysaccharide interactions (**Chapter 2**) and formation of micro-gel particle-induced *gel-like emulsions* (**Chapter 7**); (2) the gelling process of *emulsion macro-gel beads* (**Chapter 3**) and the effect of emulsifiers and pH of emulsions on properties of *emulsion macro-gel beads* (**Chapters 4 and 5**); and (3) preparation and application of *emulsion micro-gel particles* (**Chapters 6 and 7**).

8.1.1. Bulk emulsion gels/gel-like emulsions

Alginate-based bulk emulsion gels/gel-like emulsions have been widely investigated (Sato et al., 2014; Soukoulis et al., 2016), in which using naturally occurring ingredients (e.g., oat bran, chia flour, and SPI) as emulsifiers has received increased interest in recent years (Herrero et al., 2018; Pintado et al., 2015). Alginate is an anionic polysaccharide, while SPI is positively charged when pH is below 4.5 (i.e., the isoelectric point (p*I*) of SPI) (Freitas et al., 2017). Therefore, electrostatic protein-polysaccharide interactions between SPI-coated droplets and alginate molecules are critical in emulsions and emulsion gels, and may influence properties of emulsions and emulsion gels (e.g., the droplet distribution and stability of emulsions and the structure and mechanical strength of emulsion gels).

Previous studies mainly focused on the improved stability of anionic polysaccharide/protein-stabilized emulsions at pH 4–4.5 (Guzey & McClements, 2007; Salminen & Weiss, 2014) and the formation and properties of polysaccharide-based and protein-stabilized emulsion gels at neutral pH or around p*I* (Feng et al., 2018; Lam & Nickerson, 2014). The studies in **Chapter 2** investigated the electrostatic protein-polysaccharide interactions between SPI-coated droplets and alginate molecules at pH 3.0

and focused on the role of mixing sequence of oppositely charged SPI-stabilized emulsions and alginate solutions in preparation of emulsions and emulsion gels. It was found that adding alginate solutions (0.025–0.4 wt%) into SPI-stabilized emulsions containing 0.1 wt% SPI and 1.0 wt% oil (1:1) and adding high concentration SPI-stabilized emulsions (0.2–0.5 wt% SPI and 2.0–5.0 wt% oil) into 0.2 wt% alginate solutions (1:1) at pH 3.0 with mild stirring resulted in unstable emulsions containing flocculated droplets. However, relatively stable emulsions containing unflocculated and negatively charged droplets could be only obtained by adding low concentration SPI-stabilized emulsions (0.1 wt% SPI and 1.0 wt% oil) into alginate solutions (0.2 wt%), and emulsion gels prepared from above resultant emulsions had less flocculated droplets and higher L^* and G' values than emulsion gels prepared by adding alginate solutions into SPI-stabilized emulsions.

SPI-stabilized emulsions normally show lower stability than animal protein- or synthetic chemical-stabilized emulsions (Benjamin et al., 2014; Zhang et al., 2021), and forming gel-like emulsions is an effective method to improve their stability. Previous studies on SPI-stabilized gel-like emulsions mainly focused on Pickering emulsions (Liu & Tang, 2016), modifying structural properties of SPI adsorbed at droplet surfaces (Tang & Liu, 2013), and introducing gelling agents (e.g., alginate and WPI) into the continuous phase of emulsions (Lin et al., 2021). A novel strategy was investigated in **Chapter 7** to enhance stability of SPI-stabilized emulsions by introducing alginate and alginate-based micro-gel particles into SPI-stabilized emulsions to form gel-like emulsions. Increasing the concentrations of micro-gel particles (from 2.0% to 10%) in alginate/SPI-stabilized emulsions gradually increased the viscosity of mixtures, and gel-like emulsions were obtained when the concentrations of micro-gel particles were higher than 6.0%. The creaming stability and storage stability of SPI-stabilized emulsions after turning into gel-like emulsions were thus significantly improved. However, the bio-accessibility of lycopene encapsulated in SPI-stabilized emulsions slightly decreased with increasing concentrations of micro-gel particles after *in-vitro* digestion.

8.1.2. Emulsion macro-gel beads

The formulation (Lević et al., 2015; Piornos et al., 2017), structural and mechanical properties (Corstens et al., 2017), digestion of alginate-based emulsion macro-gel beads, and release of encapsulated lipophilic compounds from them (Xu et al., 2019) have been widely investigated. In addition, previous studies mainly focused on alginate-based emulsion macro-gel beads stabilized by whey protein isolate (WPI) (Corstens et al., 2017), lupin protein isolate (Piornos et al., 2017), or Tween 80 and Span 80 (Xu et al., 2019). The gelling process of alginate-based emulsion macro-gel beads and using SPI as emulsifiers in alginate-based emulsion macro-gel beads have rarely been investigated.

The gelling process of alginate-based and SPI-stabilized emulsion macro-gel beads was investigated in **Chapter 3**, in which external gelation was used to produce gel beads by dropping emulsions into $CaCl_2$ solutions. It is already known that calcium cations can diffuse into alginate drops along with syneresis (i.e., water loss) and shrinkage during gelation (Quong et al., 1998; Rehm, 2009). In addition, it was found that the Young's modulus of 1% alginate-based hydro-gel beads increased up to 5 min (i.e., the maturation step), decreased between 5 and 10 min (i.e., the structural collapse step), and finally reached a plateau (i.e, the equilibrium step) during gelation for 30 min. However, there was no structural collapse step after introducing 1.0% SPI and 20% oil into gel beads (i.e., emulsion gel beads), although decreasing the alginate content in emulsions to 0.5% still led to the structural collapse of emulsion gel beads. In addition, increasing the alginate contents from 0.5 to 1.5% did not affect the speed of water loss but slowed the shrinkage of emulsion gel beads during gelation. Also, increasing the SPI concentrations from 0.5% to 2.0% did not affect the profiles of Young's modulus and the speed of water loss and shrinkage during gelation, and increasing the oil contents from 10 to 40% did not affect the profiles of Young's modulus but slowed the speed of water loss and shrinkage.

The degradation of alginate-based and SPI-stabilized emulsion macro-gel beads and the release of encapsulated lipophilic compounds (use lycopene as an example) from them during digestion were further investigated in **Chapter 4**. After simulated oral digestion, the Young's modulus of gel beads without protein (i.e., the control samples) and SPI-stabilized emulsion beads increased 1.32 and 1.13 times, respectively, than those before digestion. The Young's modulus of gel beads further increased during simulated gastric digestion (i.e., increased 1.16 and 1.36 times after 2 h of gastric digestion for control samples and SPI-stabilized emulsion beads, respectively). In addition, control samples and SPI-stabilized emulsion beads shrank by 2.11% and 25.92% after gastric digestion, respectively, compared to their size before gastric digestion, which led to SPI-stabilized emulsion gel beads with smaller size and denser structure than control samples. Therefore, structural collapse of SPI-stabilized emulsion gel beads and lycopene release from them were then delayed during intestinal digestion than control samples.

In addition, the effect of emulsion pH (i.e., pH 7.0, 5.0, and 3.0) on mechanical properties of alginate-based and SPI-stabilized emulsion macro-gel beads and the stability and release of encapsulated lycopene during storage and digestion were further investigated in **Chapter 5**. Emulsion gel beads at pH 3.0 had lower Young's modulus than those at pH 7.0 or 5.0, which was consistent with the changes on Young's modulus of SPI/alginate-based hydro-gel beads at different pHs. This indicated that the change on G'_{matrix} values was the main reason for the change on Young's modulus of emulsion macro-gel beads at different pHs. However, emulsion gel beads at pH 5.0 had a lower lycopene retention rate (i.e., 56 ± 5%) than those at pH 7.0 or 3.0 (i.e., 63 ± 3% and 69 ± 4%, respectively), probably due to different surface structures and surface charges of droplets at different pHs. In addition, gel beads at pH 3.0 show faster structural collapse and accelerated release of encapsulated lycopene than those at pH 5.0 or 7.0 during intestinal digestion, probably due to weaker mechanical properties of gel beads at pH 3.0.

The findings of this section highlighted the gelling process of alginate-based and SPI-stabilized emulsion macro-gel beads and the influence of emulsion pH on the mechanical properties and *in-vitro* digestion behavior of emulsion gel beads, which makes it possible to design emulsion gel beads with potential controlled released of encapsulated hydrophobic ingredients by structuring the gel matrix and the water/oil interfaces with naturally occurring polymers (e.g., proteins).

8.1.3. Emulsion micro-gel particles

Micro-gel particles have potential`to be used as structuring agents for adjusting rheological and textural properties of food, replacing fats, and encapsulating nutrients for their protection and targeted delivery in the food industry (Shewan & Stokes, 2013). Therefore, protein-/polysaccharide-based micro-gels have received increased interest recently. Alginate-based hydro-mirogels have also been widely investigated, in terms of their formation (Chan et al., 2002; Paques et al., 2013), properties (Leon et al., 2016), digestion behavior (Bokkhim et al., 2016), and application for encapsulation (Lupo et al., 2014; Zhang et al., 2016). In contrast, alginate-based emulsion micro-gels have rarely been studied, although it has been reported that emulsion (0.20 μm) filled alginate micro-gel particles (20–80 μm) were prepared by the impinging aerosol technique (Ching et al., 2015), and that chitosan-coated alginate-based emulsion micro-gels (500–800 μm) were prepared by the emulsion/internal gelation technique (Ribeiro et al., 1999). However, the preparation of alginate-based emulsion micro-gels by the emulsion/external gelation and their properties (i.e., suspension rheology and digestion) and applications in the food industry have rarely been investigated.

Therefore, the formation, morphology, suspension rheology, and digestive behavior of alginate-based and SPI-stabilized emulsion micro-gels prepared by the external or internal gelation were compared in **Chapter 6**, and their application to gel-in-gel beads was also investigated. The average size (i.e., $D_{4,3}$) of emulsion micro-gels prepared by the external

gelation was 39.6 ± 0.5 μm, with a size distribution from 2.5 to 110 μm, while the average size (i.e., $D_{4,3}$) of emulsion micro-gels prepared by internal gelation was 144 ± 5 μm with the size distribution from 15 to 450 μm. Externally-induced particle suspensions showed higher G', ϕ_j, and ϕ_{rcp} values than internally-induced particle suspensions. Externally- and internally-induced particles also showed different digestive behaviour. Externally-induced particles slightly swelled during simulated gastric digestion, while internally-induced particles partially shrank and partially swelled during gastric digestion. In addition, externally-induced particles showed faster structural collapse than internally-induced particles during simulated intestinal digestion. It was also found that externally-induced particles had stronger cross-linking with alginate molecules in alginate-based emulsion macro-gels, which led to increased Young's modulus and delayed structural collapse and release of encapsulated lycopene during digestion compared to internally-induced particles. Based on these findings, externally-induced particles were further investigated to trigger formation of gel-like emulsions to improve stability of alginate/SPI-stabilized emulsions in **Chapter 7**, which has been discussed in Section 8.1.1. The findings in this section set the stage for further investigation on alginate-based emulsion micro-gel particles.

8.1.4. The role of SPI in emulsion gels: Emulsifiers and structuring agents

It has been reported that 7S and 11S proteins of soy proteins showed good emulsifying capacity four decades ago (Aoki et al., 1980), and since then SPI used as emulsifiers in emulsions has been widely investigated. However, using SPI as emulsifiers in alginate-based emulsion gels has rarely been reported, although WPI was often used in alginate-based emulsion gels in previous studies (Feng et al., 2018; Ruffin et al., 2014). **Figure 3-1** shows that oil droplets can be coated by SPI in alginate/SPI-stabilized emulsions because hydrophobic groups of SPI (i.e., hydrophobic side chains of Gly, Ala, Val, Leu, Ile, Pro, Phe, Met, and Trp) can adsorb on the surfaces of oil droplets while hydrophilic groups (i.e., polar side chains of Ser, Thr, Cys, Asn, Gln, and Tyr) can connect with the water phase. SPI-

coated droplets can prevent droplet coalescence not only in emulsions during storage (**Chapter 7**) but also in emulsion gels during gelation (**Chapters 2 and 3**). **Figure 7-4B** shows that the droplet-size distribution in alginate/SPI-stabilized emulsions was stable during storage for six weeks and droplet coalescence was not observed from micro-structure of emulsions. In addition, **Figure 3-1** shows that SPI-coated droplets in alginate-based macro-gel beads maintained their structures during gelation, while droplet coalescence occurred during gelation in those samples without being coated with SPI. **Figures 2-1 and 2-4** also show that droplet coalescence did not occur in alginate-based and SPI-stabilized bulk emulsion gels during gelation.

In addition, SPI can also function as structuring agents in alginate-based emulsion gels through several mechanisms. Firstly, insoluble SPI proteins as solid fillers may obstruct the formation of alginate-based network structures. **Figure 3-2** shows that alginate/SPI-based hydro-gel beads had lower Young's modulus than alginate-based hydro-gel beads without proteins, and **Table 4-1** also shows that alginate-based and SPI-stabilized emulsion gel beads had lower Young's modulus than alginate-based emulsion gel beads without proteins. Secondly, surface properties of SPI-coated droplets differ at different pHs, and electrostatic protein-polysaccharide interactions between SPI-coated droplets and alginate molecules affect structures of emulsion gels at different pHs. **Figures 5-1 and 5-3** indicate that unflocculated droplets in alginate/SPI-stabilized emulsions at pH 3.0 and 5.0 were coated by a double layer of emulsifiers (i.e., the SPI-based inner layer and alginate-based outer layer), due to electrostatic attraction between SPI-coated droplets and alginate molecules, while droplets at pH 7.0 were coated by a single layer of negatively charged SPI and droplet flocculation occurred, due to strong electrostatic repulsion between SPI-coated droplets and alginate molecules. In addition, **Figures 2-1 and 2-2** show that adding low-level of SPI-stabilized emulsions into alginate solutions at pH 3.0 tended to form stable emulsions without flocculated droplets, while adding alginate solutions into SPI-stabilized emulsions tended to form unstable emulsions containing flocculated droplets, due to bridging

flocculation (i.e., insufficient alginate molecules shared by neighbouring SPI-coated droplets). Emulsions prepared by adding alginate solutions into SPI-stabilized emulsions led to bulk emulsion gels with flocculated droplets and lower L^* and G' values than those prepared by adding SPI-stabilized emulsions into alginate solutions (**Figure 2-4**).

8.1.5. Application of emulsion micro-gel particles: Formation of gel-in-gel systems

Embedding micro-gels into another gels to produce gel-in-gel systems and to achieve controlled release of encapsulated compounds has received growing interest in recent years (Husman et al., 2020; Liu et al., 2008). A microgel-in-bulk gel system was reported by Zhu et al. (2016), in which bone morphogenetic protein-2 (BMP-2) was encapsulated in alginate-based micro-spheres, and then alginate micro-spheres were embedded into chitosan/dextran-polylactide/glycerophosphate-based bulk hydrogels, which showed continuous release of BMP-2 from gels. A microparticle-in-macrogel system was reported by Busatto et al. (2019), in which lignin-based microparticles encapsulated with atrazine were prepared first, and then lignin microparticles were introduced into alginate-based macro-gel beads, and atrazine showed slower release from microparticle-in-macrogel beads than from lignin microparticles. A microgel-in-microgel system has also been reported (Ma et al., 2018), in which whey protein-coated oil droplets were loaded into alginate- or carrageenan-based microgels, and emulsion microgels were further embedded into carrageenan- or alginate-based microgels, and lipid digestion decreased in microgel-in-microgel systems compared to free oil droplets and those in emulsion microgels.

However, previous studies mainly focused on hydro-gel-in-hydro-gel or emulsion gel-in-hyro-gel systems. This thesis fabricated emulsion gel-in-emulsion gel systems, in which emulsion micro-gel particles were introduced into emulsion macro-gel beads in **Chapter 6**. The effect of micro-gel particles prepared by different gelation methods (i.e., external or internal gelation) on mechanical properties and digestive behavior was compared. It was found that the presence of externally-induced micro-gels led to increased Young's modulus

of alginate-based emulsion gel beads and delayed release of lycopene from them, with delayed structural collapse during *in-vitr*o intestinal digestion, compared to emulsion gel beads containing internally-induced micro-gel particles or the control samples without micro-gel particles. In addition, alginate/SPI-stabilized gel-like emulsions containing externally-induced micro-gel particles were investigated in **Chapter 7**. It was found that alginate/SPI-stabilized emulsions could turn into gel-like emulsions in the presence of high levels of micro-gel particles (> 6.0%). Micro-gel-induced gel-like emulsions showed higher creaming stability then liquid emulsions, but gel-like emulsions showed lower bio-accessibility of encapsulated lycopene after *in-vitro* digestion than liquid emulsions. The formation and properties of emulsion microgel-in-bulk emulsion gels and application of these gel-in-gel systems in food systems need further investigation.

8.2. Overall conclusions

Based on findings and discussion in this thesis, overall conclusions are shown as follows:

- Adding low-level of SPI-stabilized emulsions into oppositely charged alginate solutions at pH 3.0 led to stable emulsions, while adding high-level of SPI-stabilized emulsions into alginate solutions or adding alginate solutions into SPI-stabilized emulsions led to flocculation. In addition, emulsion flocculation accelerated gelation kinetics and decreased G' values of bulk emulsion gels, compared to stable emulsions without flocculation (**Chapter 2**);

- Young's modulus of emulsion gel beads kept increasing before reaching a plateau along with continuous water loss and shrinkage during gelation for 30 min, while the speed of shrinkage could be slowed by increasing contents of alginate (from 0.5% to 1.5%) and oil (from 10% to 40%) in emulsions (**Chapter 3**);

- Water loss and shrinkage of emulsion gel beads led to more compact filler structures during gelation, and higher SPI concentrations resulted in more stable droplet structures

during gelation, while increasing contents of alginate to 1.5% and oil to 40% led to coalescence of droplets during gelation (**Chapter 3**);

- The presence of WPI increased Young's modulus of alginate-based emulsion gel beads, while the presence of SPI decreased their Young's modulus probably because WPI had stronger interactions with alginate than SPI, although the presence of WPI or SPI delayed release of lycopene from alginate-based beads during digestion, compared to control samples without proteins (**Chapter 4**);

- Alginate-based and SPI-stabilized emulsion gel beads at pH 5.0 had higher Young's modulus than those at pH 7.0 or 3.0. Lycopene encapsulated in emulsion gel beads at pH 3.0 had higher stability than those at pH 7.0 or 5.0 during storage. In addition, lycopene showed faster release from gel beads at pH 3.0 during digestion than those at pH 7.0 or 5.0 (**Chapter 5**);

- Emulsion micro-gel particles produce by external gelation under mild stirring had smaller size, wider particle-size distribution, and faster structural collapse during *in-vitro* digestion than internally-induced micro-gels, and the suspensions of externally-induced particles exhibited higher G', ϕ_j, and ϕ_{rcp} values than those of internally-induced particles (**Chapter 6**);

- The presence of externally-induced micro-gel particles in alginate-based emulsion macro-gel beads increased their mechanical strength and thus delayed structural collapse and lycopene release during digestion, while internally-induced particles did not show such effects (**Chapter 6**);

- The presence of alginate (> 0.1%) and high levels of externally-induced emulsion micro-gel particles (> 6.0%) turned SPI-stabilized emulsions into gel-like emulsions with improved creaming stability, while the content of SPI-coated droplets (0–10%) played an relatively unimportant role in gel formation (**Chapter 7**);

- Increasing the content of micro-gel particles in alginate/SPI-stabilized emulsions increased their viscosity and G' values of gel-like emulsions but slightly decreased bio-accessibility of encapsulated lycopene after *in-vitro* digestion (**Chapter 7**).

8.3. Prospects for further study

Based on findings and discussion in this thesis, further studies on alginate-based and SPI-stabilized emulsion gels are recommended as follows:

8.3.1. Mechanism of formation of emulsion micro-gel particle-induced gel-like mixtures

Chapters 6 and 7 showed that gel-like mixtures could be obtained when adding externally-induced emulsion micro-gel particles into alginate solutions and that gel-like emulsions were formed after adding micro-gel particles into alginate/SPI-stabilized emulsions. However, the mechanism of such gelation is still unknown, although two hypotheses were given: Ca^{2+} ions may release from micro-gel particles and trigger the gelation of alginate and/or micro-gel particles may cross-link with alginate molecules through Ca^{2+} ions adsorbed on the surfaces of micro-gel particles. FTIR, SEM, Zetasizer, and calcium sensors can be used to unravel the hidden mechanism behind this phenomenon.

8.3.2. Preparation, application and safety of emulsion nano-gel particles

Nanomaterials have received growing interest in the food industry, due to their unique physicochemical properties and potential in the development of nano-sized food additives, delivery systems and innovative food packaging materials (Jain et al., 2018). Alginate-based and SPI-stabilized emulsion nano-gel particles may be produced by electrostatic atomization or the liposomal template method, which have been used to prepared nano-sized alginate hydro-gel particles (Ching et al., 2017). However, the toxicity of nanomaterials has drawn attention, due to their small size and large surface area, which allow easy dispersion and

invasion of anatomical barriers in human body (Jain et al., 2018). Therefore, it is also important to know more about the toxicological effects of emulsion nano-gel particles.

8.3.3. Surface modification to emulsion micro-/nano-gel particles

The surface properties (i.e., surface area, surface structure, surface composition, and surface charge) of micro-/nano-particles play an important role in interactions between micro-/nano-particles and other polymers (e.g., proteins, lipids and polysaccharides) through ionic interactions, hydrogen bonds, and/or Van der Waals interactions (Saptarshi et al., 2013). Therefore, the surface properties of emulsion micro-/nano-gel particles prepared by external/internal gelation, the preparation, properties, and application of complexes formed by emulsion micro-/nano-gel particles and other polymers, and modifications to surface properties of particles to modify their reactivity with other polymers, need further investigation.

8.3.4. Application of emulsion gels in food systems

Emulsion gels can be used as delivery systems for food nutrients, while the application of emulsion gels as nutrient carriers in real food systems has rarely been reported, although it has been reported that bulk emulsion gels were used as fat replacers in meat products, such as sausages (dos Santos et al., 2020) and patties (Pintado et al., 2021). Therefore, the application of emulsion gels as structuring agents and/or nutrient carriers in real food systems needs further investigation. For instance, emulsion macro-gel beads or micro-/nano-gel particles encapsulated with nutrients or flavour compounds can be introduced into solid yogurts to produce functional yogurts; also, the combination of alginate and externally induced-emulsion micro-gel particles can be introduced into semi-solid foods (e.g., salad dressing, mayonnaise, butter spread, and sauce) to structure foods with reduced fat contents or improved functional properties.

References

Aoki, H., Taneyama, O., & Inami, M. (1980). Emulsifying properties of soy protein: Characteristics of 7S and IIS proteins. *Journal of Food Science, 45*, 534-538.

Benjamin, O., Silcock, P., Beauchamp, J., Buettner, A., & Everett, D. (2014). Emulsifying properties of legume proteins compared to *β*-lactoglobulin and tween 20 and the volatile release from oil-in-water emulsions. *Journal of Food Science, 79*, E2014-E2022.

Bokkhim, H., Bansal, N., Grøndahl, L., & Bhandari, B. (2016). *In-vitro* digestion of different forms of bovine lactoferrin encapsulated in alginate micro-gel particles. *Food Hydrocolloids, 52*, 231-242.

Busatto, C. A., Taverna, M. E., Lescano, M. R., Zalazar, C., & Estenoz, D. A. (2019). Preparation and characterization of lignin microparticles-in-alginate beads for atrazine controlled release. *Journal of Polymers and the Environment, 27*, 2831-2841.

Chan, L., Lee, H., & Heng, P. (2002). Production of alginate microspheres by internal gelation using an emulsification method. *International Journal of Pharmaceutics, 242*, 259-262.

Ching, S. H., Bansal, N., & Bhandari, B. (2015). Physical stability of emulsion encapsulated in alginate microgel particles by the impinging aerosol technique. *Food Research International, 75*, 182-193.

Ching, S. H., Bansal, N., & Bhandari, B. (2017). Alginate gel particles–A review of production techniques and physical properties. *Critical Reviews in Food Science and Nutrition, 57*, 1133-1152.

Corstens, M. N., Berton-Carabin, C. C., Elichiry-Ortiz, P. T., Hol, K., Troost, F. J., Masclee, A. A., & Schroën, K. (2017). Emulsion-alginate beads designed to control *in vitro* intestinal lipolysis: Towards appetite control. *Journal of Functional Foods, 34*, 319-328.

dos Santos, M., Munekata, P. E. S., Pateiro, M., Magalhaes, G. C., Barretto, A. C. S., Lorenzo, J. M., & Pollonio, M. A. R. (2020). Pork skin-based emulsion gels as animal fat replacers in hot-dog style sausages. *LWT-Food Science and Technology, 132*, 109845.

Feng, W., Yue, C., Ni, Y., & Liang, L. (2018). Preparation and characterization of emulsion-filled gel beads for the encapsulation and protection of resveratrol and α-tocopherol. *Food Research International, 108*, 161-171.

Freitas, M. L. F., Albano, K. M., & Telis, V. R. N. (2017). Characterization of biopolymers and soy protein isolate-high-methoxyl pectin complex. *Polímeros, 27*, 62-67.

Guzey, D., & McClements, D. J. (2007). Impact of electrostatic interactions on formation and stability of emulsions containing oil droplets coated by *β*-lactoglobulin−pectin complexes. *Journal of Agricultural and Food Chemistry, 55*, 475-485.

Herrero, A. M., Ruiz-Capillas, C., Pintado, T., Carmona, P., & Jiménez-Colmenero, F. (2018). Elucidation of lipid structural characteristics of chia oil emulsion gels by Raman spectroscopy and their relationship with technological properties. *Food Hydrocolloids, 77*, 212-219.

Husman, D., Welzel, P. B., Vogler, S., Bray, L. J., Träber, N., Friedrichs, J., et al. (2020). Multiphasic microgel-in-gel materials to recapitulate cellular mesoenvironments *in vitro*. *Biomaterials Science, 8*, 101-108.

Jain, A., Ranjan, S., Dasgupta, N., & Ramalingam, C. (2018). Nanomaterials in food and agriculture: An overview on their safety concerns and regulatory issues. *Critical Reviews in Food Science and Nutrition, 58*, 297-317.

Lam, R. S., & Nickerson, M. T. (2014). The properties of whey protein–carrageenan mixtures during the formation of electrostatic coupled biopolymer and emulsion gels. *Food Research International, 66*, 140-149.

Leon, A., Medina, W., Park, D., & Aguilera, J. (2016). Mechanical properties of whey protein/Na alginate gel microparticles. *Journal of Food Engineering, 188*, 1-7.

Lević, S., Lijaković, I. P., Đorđević, V., Rac, V., Rakić, V., Knudsen, T. Š., et al. (2015). Characterization of sodium alginate/*d*-limonene emulsions and respective calcium alginate/*d*-limonene beads produced by electrostatic extrusion. *Food Hydrocolloids, 45*, 111-123.

Lin, D., Kelly, A. L., & Miao, S. (2021). The role of mixing sequence in structuring O/W emulsions and emulsion gels produced by electrostatic protein-polysaccharide interactions between soy protein isolate-coated droplets and alginate molecules. *Food Hydrocolloids, 113*, 106537.

Liu, F., & Tang, C. H. (2016). Soy glycinin as food-grade Pickering stabilizers: Part. III. Fabrication of gel-like emulsions and their potential as sustained-release delivery systems for *β*-carotene. *Food Hydrocolloids, 56*, 434-444.

Liu, W., Griffith, M., & Fengfu, L. (2008). Alginate microsphere-collagen composite hydrogel for ocular drug delivery and implantation. *Journal of Materials Science: Materials in Medicine, 19*, 3365-3371.

Lupo, B., Maestro, A., Porras, M., Gutiérrez, J. M., & González, C. (2014). Preparation of alginate microspheres by emulsification/internal gelation to encapsulate cocoa polyphenols. *Food Hydrocolloids, 38*, 56-65.

Ma, D., Tu, Z. C., Wang, H., Zhang, Z., & McClements, D. J. (2018). Microgel-in-microgel biopolymer delivery systems: Controlled digestion of encapsulated lipid droplets under simulated gastrointestinal conditions. *Journal of Agricultural and Food Chemistry, 66*, 3930-3938.

Paques, J. P., van der Linden, E., van Rijn, C. J., & Sagis, L. M. (2013). Alginate submicron beads prepared through w/o emulsification and gelation with $CaCl_2$ nanoparticles. *Food Hydrocolloids, 31*, 428-434.

Pintado, T., Munoz-Gonzalez, I., Salvador, M., Ruiz-Capillas, C., & Herrero, A. M. (2021). Phenolic compounds in emulsion gel-based delivery systems applied as animal fat replacers in frankfurters: Physico-chemical, structural and microbiological approach. *Food Chemistry, 340*,128095.

Pintado, T., Ruiz-Capillas, C., Jiménez-Colmenero, F., Carmona, P., & Herrero, A. M. (2015). Oil-in-water emulsion gels stabilized with chia (*Salvia hispanica L.*) and cold gelling agents: Technological and infrared spectroscopic characterization. *Food Chemistry, 185*, 470-478.

Piornos, J. A., Burgos-Díaz, C., Morales, E., Rubilar, M., & Acevedo, F. (2017). Highly efficient encapsulation of linseed oil into alginate/lupin protein beads: Optimization of the emulsion formulation. *Food Hydrocolloids, 63*, 139-148.

Quong, D., Neufeld, R., Skjåk-Bræk, G., & Poncelet, D. (1998). External versus internal source of calcium during the gelation of alginate beads for DNA encapsulation. *Biotechnology and Bioengineering, 57*, 438-446.

Rehm, B. H. (2009). *Alginates: biology and applications* (Vol. 13): Springer, Berlin.

Ribeiro, A. J., Neufeld, R. J., Arnaud, P., & Chaumeil, J. C. (1999). Microencapsulation of lipophilic drugs in chitosan-coated alginate microspheres. *International Journal of Pharmaceutics, 187*, 115-123.

Ruffin, E., Schmit, T., Lafitte, G., Dollat, J.-M., & Chambin, O. (2014). The impact of whey protein preheating on the properties of emulsion gel bead. *Food Chemistry, 151*, 324-332.

Salminen, H., & Weiss, J. (2014). Electrostatic adsorption and stability of whey protein–pectin complexes on emulsion interfaces. *Food Hydrocolloids, 35*, 410-419.

Saptarshi, S. R., Duschl, A., & Lopata, A. L. (2013). Interaction of nanoparticles with proteins: Relation to bio-reactivity of the nanoparticle. *Journal of Nanobiotechnology, 11*, 1-12.

Sato, A., Moraes, K., & Cunha, R. (2014). Development of gelled emulsions with improved oxidative and pH stability. *Food Hydrocolloids, 34*, 184-192.

Shewan, H. M., & Stokes, J. R. (2013). Review of techniques to manufacture micro-hydrogel particles for the food industry and their applications. *Journal of Food Engineering, 119*, 781-792.

Soukoulis, C., Cambier, S., Hoffmann, L., & Bohn, T. (2016). Chemical stability and bioaccessibility of *β*-carotene encapsulated in sodium alginate o/w emulsions: Impact of Ca^{2+} mediated gelation. *Food Hydrocolloids, 57*, 301-310.

Tang, C. H., & Liu, F. (2013). Cold, gel-like soy protein emulsions by microfluidization: Emulsion characteristics, rheological and microstructural properties, and gelling mechanism. *Food Hydrocolloids, 30*, 61-72.

Xu, W., Huang, L., Jin, W., Ge, P., Shah, B. R., Zhu, D., & Jing, J. (2019). Encapsulation and release behavior of curcumin based on nanoemulsions-filled alginate hydrogel beads. *International Journal of Biological Macromolecules, 134*, 210-215.

Zhang, S. B., Yan, D. Q., Jiang, Y. S., & Ding, C. H. (2021). Competitive displacement of interfacial soy proteins by Tween 20 and its effect on the physical stability of emulsions. *Food Hydrocolloids, 113*, 106515.

Zhang, Z., Zhang, R., Zou, L., & McClements, D. J. (2016). Protein encapsulation in alginate hydrogel beads: Effect of pH on microgel stability, protein retention and protein release. *Food Hydrocolloids, 58*, 308-315.

Zhu, Y., Wang, J., Wu, J., Zhang, J., Wan, Y., & Wu, H. (2016). Injectable hydrogels embedded with alginate microspheres for controlled delivery of bone morphogenetic protein-2. *Biomedical Materials, 11*, 025010.

APPENDIX

Publications

Trends in Food Science & Technology 102 (2020) 123–137

Contents lists available at ScienceDirect

Trends in Food Science & Technology

journal homepage: www.elsevier.com/locate/tifs

Preparation, structure-property relationships and applications of different emulsion gels: Bulk emulsion gels, emulsion gel particles, and fluid emulsion gels

Duanquan Lin[a,b], Alan L. Kelly[b], Song Miao[a,b,*]

[a] Teagasc Food Research Centre, Moorepark, Fermoy, Co. Cork, Ireland
[b] School of Food and Nutritional Sciences, University College Cork, Cork, Ireland

ARTICLE INFO

Keywords:
Emulsion gel
Preparation
Interaction
Structure
Property
Fat replacer
Delivery

ABSTRACT

Background: In recent years, there has been increasing interest in emulsion gels, due to their better stability during storage and potential for prolonged intestinal drug release compared to emulsions. There are three kinds of emulsion gels, classified according to their morphological properties: bulk emulsion gels, emulsion gel particles and liquid emulsion gels.

Scope and approach: This paper provides a comprehensive review of the mechanisms and procedures of different methods for preparing different emulsion gels and relationships between structures and properties of emulsion gels. The applications of emulsion gels in the food industry are finally discussed.

Key findings and conclusions: Different emulsion gels result from different preparation methods, and have various structure-property relationships and applications. Many methods can be used to prepare bulk emulsion gels, involving different matrix materials, processing techniques, and purposes. This can result in different structures of gel matrices and emulsion droplets, and interactions between them, which can influence the structures of bulk emulsion gels and then their mechanical and release properties. On the other hand, extrusion and impinging aerosol methods are two methods for preparing emulsion gel particles, while liquid emulsion gels can be prepared by Pickering emulsions and disrupted gel systems. Rheological, syneresis and swelling properties are critical for gel particle suspensions, while flow behavior and release properties are important to liquid emulsion gels. In addition, fat replacements and delivery systems are main applications of emulsion gels in the food industry. However, current research has mainly focused on bulk emulsion gels, so further studies on emulsion gel particles and liquid emulsion gels are required.

1. Introduction

Emulsion gels, also known as emulgels or gelled emulsions (Balakrishnan, Nguyen, Schmitt, Nicolai, & Chassenieux, 2017), are complex colloidal materials in which both emulsion droplets and gels exist (Dickinson, 2012). According to the state of emulsion droplets in gels, structures of emulsion gels can be divided into two categories: emulsion droplet-filled gels and emulsion droplet-aggregated gels (Fig. 1). In emulsion droplet-filled gels, the continuous phase (e.g., protein- and polysaccharide-based gels) forms a continuous gel matrix which can be defined as the support of emulsion gels, and emulsion droplets are embedded in this gel matrix. In emulsion droplet-aggregated gels, emulsion droplets aggregate together and form a network structure, such that the gel matrix is disrupted by the aggregated emulsion droplets. In most cases, the structural state of emulsion droplets is a combination of these two different structures (i.e., partially droplets filled in the gel matrix and partially aggregated droplets), probably owing to the inhomogeneous distribution of emulsion droplets. Moreover, according to the interactions between emulsion droplets and the gel matrix, emulsion droplets can be divided into active and inactive fillers (Fig. 2). Active fillers are mechanically connected to the gel network through emulsifiers by noncovalent and/or covalent bonds, especially when emulsifiers are natural molecules (e.g., proteins, egg lecithin, and soy lecithin); in contrast, inactive fillers have little chemical or physical affinity with the molecules of gel matrix, especially when low molecular weight (LMW) emulsifiers or no emulsifiers are used and matrix materials have weak emulsifying properties (Van Vliet, 1988).

Preparing emulsion gels normally includes two steps: first preparing emulsions and then turning emulsions into gels. During the last decade,

* Corresponding author. Teagasc Food Research Centre, Moorepark, Fermoy, Co. Cork, Ireland.
E-mail address: song.miao@teagasc.ie (S. Miao).

https://doi.org/10.1016/j.tifs.2020.05.024
Received 29 May 2019; Received in revised form 23 April 2020; Accepted 27 May 2020
Available online 03 June 2020
0924-2244/

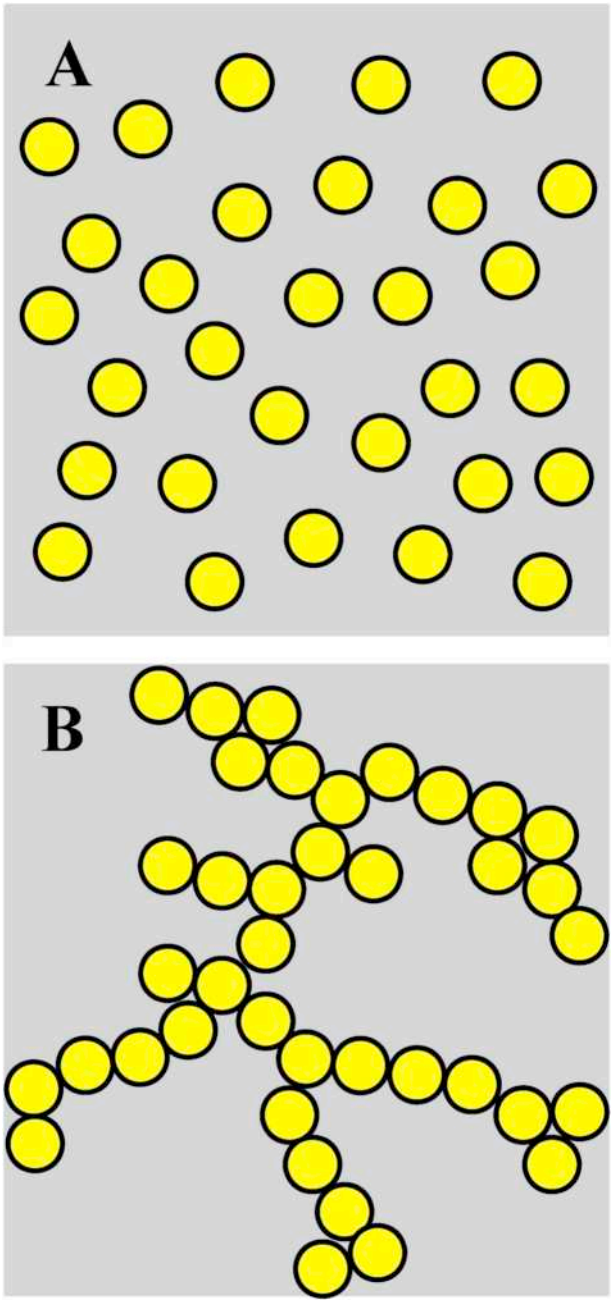

Fig. 1. Structures of two idealized models of emulsion gels: (A) emulsion droplet-filled gels, and (B) emulsion droplet-aggregated gels (Dickinson, 2012).

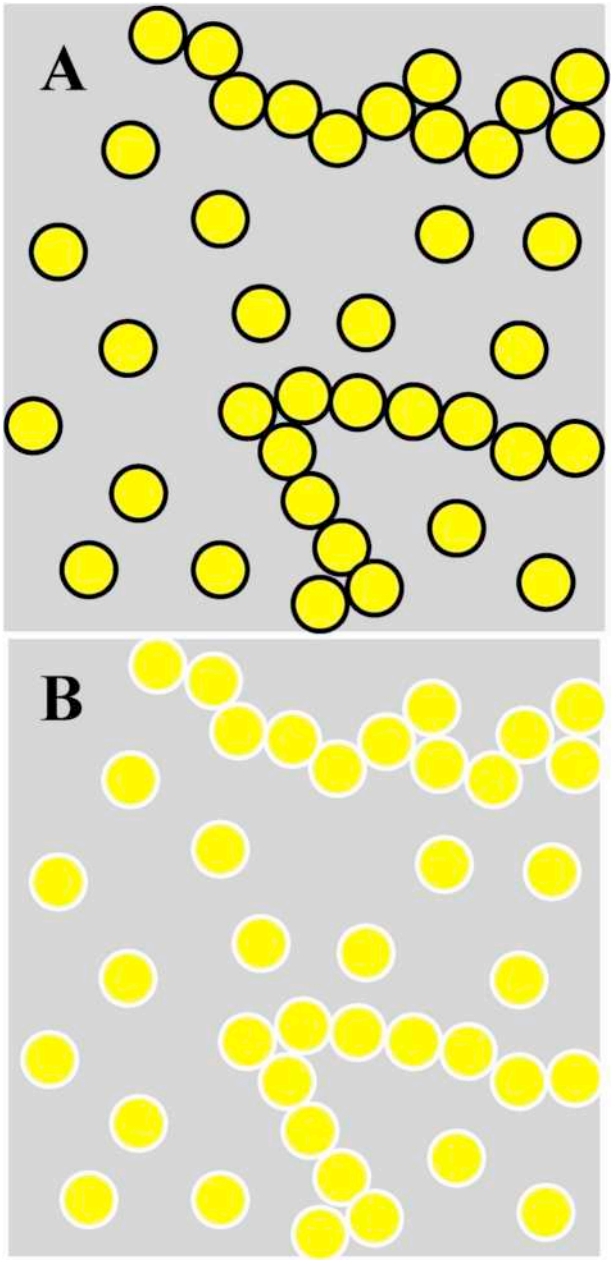

Fig. 2. Schematic presentation of two kinds of droplet fillers in emulsion gels: (A) active fillers (droplets covered by black line), and (B) inactive fillers (droplets covered by white line).

emulsion gels have received growing interest, due to their advantages compared to emulsions, such as higher stability during storage, owing to decreased oil movement and oxygen diffusion within the systems (Cofrades, Bou, Flaiz, Garcimartin, Benedi, Mateos, et al., 2017; Corstens et al., 2017; Lim, Kim, Choi, & Moon, 2015; Ma, Wan, & Yang, 2017; Sato, Moraes, & Cunha, 2014), controlled and prolonged gastric and/or intestinal drug release because of the protection by the gel matrix (Corstens et al., 2017; Guo, Bellissimo, & Rousseau, 2017), and practical applications, including overcoming the textural problems caused by lipid particles in food products and mimicking the effect of fat on hardness and water-holding capacity of meat products (Alejandre, Poyato, Ansorena, & Astiasaran, 2016; Brito-Oliveira, Bispo, Moraes, Campanella, & Pinho, 2017).

Bulk emulsion gels, emulsion gel particles and liquid emulsion gels are three kinds of emulsion gels (Fig. 3), which exhibit their own particular properties, due to their different morphological properties. The size and shape of bulk emulsion gels are determined by the emulsion volume and containers (e.g., beakers and tubes) with different shapes and sizes used during the emulsion gel preparation, and bulk emulsion gels can also be broken into smaller pieces with different sizes and shapes. Therefore, mechanical properties (including viscoelastic and textural properties) of bulk emulsion gels are important. Emulsion gel particles are normally spherical with sizes (diameters) from nano to macro (Ching, Bansal, & Bhandari, 2017). Thus, mechanical properties are also important for the macrogel particles. However, emulsion gel particles can be dispersed in aqueous media, and gel particles may swell or shrink as a function of environmental conditions, resulting in changes in their size and/or physicochemical properties (Torres, Tena, Murray, & Sarkar, 2017). There are two types of fluid emulsion gels: gel-like Pickering emulsions and disrupted emulsion gel systems. Fluid emulsion gels do not have solid shapes, but they have higher

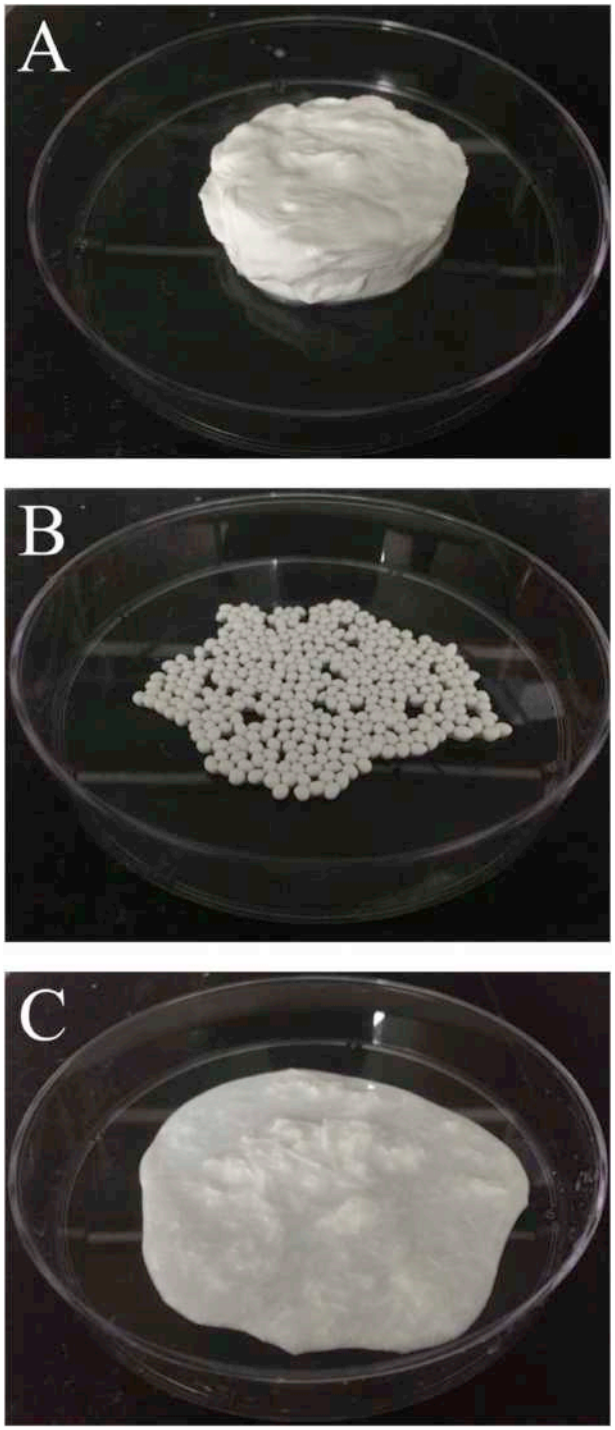

Fig. 3. Visual appearances of alginate-based (A) bulk emulsion gels, (B) emulsion gel particles, and (C) fluid emulsion gels. Preparing alginate-based emulsion gels includes two steps: first preparing emulsions with 1 wt% sodium alginate and 0.5 wt% Tween 80 in water phase and 40 wt% sunflower oil, and then turning emulsions into gels. For the preparation of bulk emulsion gel, 0.5 wt% $CaCl_2$ was added to the emulsion, and the samples were allowed to gel for 6 h in stand. For the production of emulsion gel particles, the emulsion was dropped into a 2 wt% $CaCl_2$ solution, and the samples were allowed to gel in the $CaCl_2$ solution for 6 h with mild magnetic stirring. For producing fluid emulsion gel, 0.5 wt% $CaCl_2$ was added to the emulsion, and the mixture was sheared under constant paddle stirring at 600 rpm for 6 h.

viscoelasticity than conventional emulsions. Gel-like Pickering emulsions are similar to bulk emulsion gels, exhibiting a solid state (Zou, Guo, Yin, Wang, & Yang, 2015), while disrupted emulsion gels normally exhibit fluid characterization (Soukoulis, Cambier, Hoffmann, & Bohn, 2016). This paper provides an overview of the current knowledge of preparation methods, structure-property relationships, and applications of different emulsion gel systems.

2. Preparation of different emulsion gels

2.1. Bulk emulsion gels

As shown in Table 1, proteins (e.g., myofibrillar protein, whey protein, soy protein, gelatin, bovine serum albumin, sodium caseinate, and casein), polysaccharides (e.g., carrageenan, gellan gum, agar, alginate, and inulin), and LMW compounds (e.g., sapoin glycyrrhizic acid and the mixture of β-sitosterol and γ-oryzanol) are normally used as matrix materials in bulk emulsion gels. According to the gelation process, preparation methods for bulk emulsion gels include heat-set and cold-set (including one-step cold-set, cold-set after heat treatment, enzyme treatment, acidification treatment, addition of ions, and self-assembly) gelation methods. Choosing an appropriate method depends on the matrix materials (i.e., proteins, polysaccharides or LMW compounds) and applications of prepared emulsion gels such as mimicking food processing (i.e., heating process of meat), protecting encapsulated nutrients, controlled release of encapsulated nutrients, or obtaining better mechanical properties. For heat-set, one-step cold-set, cold-set after heating, and self-assembled gelation methods, the concentration of proteins, polysaccharides and LMW compounds in the water phase should be higher than the critical gelation concentration to guarantee the gelation. However, for gelation methods based on enzyme treatment, acidification treatment, or addition of ions, the concentration of matrix molecules can be below the critical gelation concentration, especially to avoid gelation during the pre-heating process (Ye & Taylor, 2009).

2.1.1. Protein-based bulk emulsion gels

Several methods have been studied for preparing protein-based bulk emulsion gels: heat treatment, cold-set after pre-heating, acidification, addition of ions, and enzyme treatment, depending on the gelation properties of proteins (Farjami & Madadlou, 2019).

Heat treatment can denature proteins, and denatured protein molecules can aggregate and form three-dimensional structures through chemical forces (i.e., disulfide bonds, electrostatic interactions, hydrophobic interactions, hydrogen bonds, and ionic bonds) under appropriate conditions (e.g., protein concentration, pH, and ionic strength) (Tolano-Villaverde, Torres-Arreola, Ocaño-Higuera, & Marquez-Rios, 2015). Proteins (e.g., myofibrillar protein (MP), whey protein isolate (WPI), and soy protein isolate (SPI)), which undergo heat-induced gelation, can be used as matrix materials to prepare heat-induced bulk emulsion gels. However, recent studies have focused on MP- and WPI-based bulk emulsion gels (Guo, Ye, Lad, Dalgleish, & Singh, 2013; Wang, Zhang, Chen, Xu, Zhou, Li, et al., 2018). Studying heat-induced MP-based bulk emulsion gels is important to develop high quality processed meat products such as sausages and surimi, because the interactions between MPs and fat globules or oil droplets play an important role in textual properties and stability of meat products. In addition, heat treatment is the most common method for producing WPI-based bulk emulsion gels in order to investigate the interactions between emulsifiers and the WPI-based gel matrix (Chen, Dickinson, Langton, & Hermansson, 2000).

One-step cold-set or cold-set after heat treatment is normally used for preparing gelatin-based emulsion gels. The gelation mechanism of gelatin is that, when the gelatin solution is cooled below 30 °C, a self-assembly process of gelatin occurs and helices are created (Gómez-Guillén, Giménez, López-Caballero, & Montero, 2011). Heat treatment (above 40 °C) is normally used to increase the solubility of gelatin before cold-set treatment. However, for cold-soluble gelatin, the thermal process is not necessary (Pintado, Ruiz-Capillas, Jimenez-Colmenero,

Table 1
Selected examples of materials and methods used to prepare bulk emulsion gels.

Materials	Methods	Matrix	Emulsifier/oil category and content	Structure	References
Protein	Heat treatment	Myofibrillar protein (MP)	MP/soybean oil (ϕ = 0.25), peanut oil (5%) or lard and peanut oil (0–15%)	O/W	(Feng et al., 2017; Wang, Zhang, et al., 2018; Wu et al., 2011; Wu, Xiong, Chen, Tang, & Zhou, 2009)
		Myofibrillar protein	SPI/canola oil (10%)	O/W	Jiang and Xiong (2013)
		Chicken protein isolate (CPI)	CPI/pork backfat (20%)	O/W	Zhao et al. (2017)
		Whey protein isolate (WPI)	WPI, glycerol monopalmitate, Tween 20, DGML, DGMO, or lecithin/canola oil (20%), soybean oil (20%), sunflower oil (ϕ = 0.05–0.25) or triolein (ϕ = 0.3)	O/W	(Chen & Dickinson, 1998a, 1999a, 1999b; Chen et al., 2000; Guo et al., 2017; Guo et al., 2013; Gwartney et al., 2004)
	One-step cold-set	Cold-soluble gelatin	No emulsifier/olive oil (52%)	O/W	Pintado et al. (2015)
	Cold-set after heat treatment	Gelatin	No emulsifier/sunflower oil (ϕ = 0.3)	O/W	Sato et al. (2014)
		Gelatin	WPI/sunflower oil or fat (50% in emulsions) or medium-chain triglycerides (40% in emulsions)	O/W	(Oliver, Berndsen, et al., 2015; Oliver, Scholten, et al., 2015; Sala et al., 2009)
	Enzyme treatment (TGase)	Myofibrillar protein	SPI or MP/canola oil (10% or 25%)	O/W	(Jiang & Xiong, 2013; Wang et al., 2017)
		Soy protein isolate (SPI)	SPI/soy oil (ϕ = 0.2–0.6)	O/W	(Tang et al., 2011; Tang, Luo, et al., 2013; Tang, Yang, et al., 2013)
		Bovine serum albumin	Bovine serum albumin/*n*-tetradecane (ϕ = 0.45)	O/W	Kang et al. (2003)
		Sodium caseinate	Sodium caseinate/olive oil (52%) or sunflower oil (45%)	O/W	(Lim et al., 2015; Pintado et al., 2015)
		Sodium caseinate	PGPR/perilla oil (80% in W_1/O)	$W_1/O/W_2$	Freire, Bou, Cofrades, and Jimenez-Colmenero (2017)
		Gelatin	Sodium caseinate/perilla oil (80% in W_1/O)	$W_1/O/W_2$	Flaiz et al. (2016)
	Acidification treatment (GDL/citric acid)	Soy protein	Soy protein/soy oil (40% or ϕ = 0.2–0.3)	O/W	(Fang Li & Hua, 2013;Li et al., 2012; Tang et al., 2011)
		Whey protein isolate	WPI/sunflower oil (20%) or milk fat (20–30%)	O/W	(Mao et al., 2014; Ye & Taylor, 2009)
		Sodium caseinate	Sodium caseinate/sunflower oil (10%), vegetable fat (30%) or n-tetradecane (ϕ = 0.3)	O/W	(Chen & Dickinson, 2000; Dickinson & Merino, 2002; Kiokias & Bot, 2005; Montes de Oca-Ávalos et al., 2016)
		Micellar casein isolate	WPI or casein/sunflower oil or fat (50% in emulsions) or milk fat (5–25% in emulsions)	O/W	(Oliver, Scholten, et al., 2015; Oliver et al., 2016)
		Whey protein isolate	WPI, Tween 20, or lactoferrin/sunflower oil or fat (50% in emulsions) or medium-chain triglycerides (40% in emulsions)	O/W	(Oliver, Scholten, et al., 2015; Sala et al., 2009)
	Addition of ions	Soy protein	Soy protein/soy oil (ϕ = 0.2)	O/W	Tang et al. (2011)
		Whey protein isolate or β-lactoglobulin	Proteins/sunflower oil (30%) or milk fat (20–30%)	O/W	(Liang et al., 2010; Sok Line et al., 2005; Ye & Taylor, 2009)
	Malondialdehyde (MDA) modification	Myofibrillar protein	MP/soybean oil (20%)	O/W	Zhou, Sun, and Zhao (2015)
Protein/protein	Heat treatment	Micelle casein/whey protein isolate	Proteins/sunflower oil (5–15%)	O/W	Balakrishnan et al. (2017)
	Enzyme treatment (Tyrosinase)	Potato protein/zein	Potato protein and zein/olive oil (ϕ = 0.4)	O/W	Glusac, Davidesko-Vardi, Isaschar-Ovdat, Kukavica, and Fishman (2018)
Polysaccharide	Cold-set after heat treatment	κ-Carrageenan	Polysorbate 80 or no emulsifier/sunflower oil (40%) or corn oil with monoglycerides (25–75%)	O/W or bigels	(Poyato et al., 2015; Zheng, Mao, Cui, Liu, & Gao, 2020)
		Gellan gum	Tween 80/sunflower oil (10–30%)	O/W	Lorenzo, Zaritzky, and Califano (2013)
		Agar	Polyglycerol esters of fatty acids/soybean oil (20% in emulsions) or corn oil (ϕ = 0.3 in emulsions)	O/W	(Kim et al., 1999; Wang et al., 2013)
		κ-Carrageenan	WPI or Tween 20/medium-chain triglycerides (40% in emulsions)	O/W	(Sala et al., 2009)
	Addition of ions	Alginate	No emulsifier/sunflower oil (ϕ = 0.3 or 52%) or chia oil (40%)	O/W	(Herrero, Ruiz-Capillas, Pintado, Carmona, & Jiménez-Colmenero, 2018; Pintado et al., 2015; Sato et al., 2014)
	Self-assembly (crystallisation)	Inulin	Soy lecithin/olive oil (21–38%)	O/W	Paradiso et al. (2015)
Polysaccharide/polysaccharide	Self-assembly (compatibility)	Alginate/konjac glucomannan	Egg yolk or Tween 80/rapeseed oil (10–60% in emulsions)	O/W	Yang, Gong, Lu, Li, Sun, & Guo (2020)
		Xanthan/konjac glucomannan	Tween 80/rapeseed oil (20%)	O/W	Yang et al. (2019)
Protein/polysaccharide	Cold-set after heat treatment	Whey protein isolate/xanthan gum	Span 80 and Tween 60/babacu seed oil (2.8%) and tristearin (1.2%)	O/W	Geremias-Andrade et al. (2017)

(*continued on next page*)

Table 1 (*continued*)

Materials	Methods	Matrix	Emulsifier/oil category and content	Structure	References
		Soy protein isolate/xanthan gum	Span 80 and Tween 80/tristearin (4.5%)	O/W	Brito-Oliveira et al. (2017)
		Gelatin/Agar	WPI/sunflower oil (40% in emulsions)	O/W	Devezeaux de Lavergne et al. (2016)
	Enzyme treatment (TGase or laccase)	Soy protein isolate/sugar beet pectin (SBP)	Tween 20, SPI, SBP or SPI and SBP/corn oil (15%) or medium-chain triglyceride oil (10%)	O/W	(Feng et al., 2019; Hou et al., 2016)
	Acidification treatment (GDL)	Whey protein isolate/ carrageenan	WPI/canola oil (50%)	O/W	Lam and Nickerson (2014)
	Heat treatment and addition of ions	Gelatin/alginate	No emulsifier/sunflower oil (ϕ = 0.3)	O/W	Sato et al. (2014)
		Whey protein concentrate/ Persian gum	No emulsifier/milk fat (1%)	O/W	Khalesi, Emadzadeh, Kadkhodaee, and Fang (2019)
	Self-assembly (electrostatic attraction)	Egg yolk protein/alginate (pH < pKa of proteins)	Egg yolk protein/rapeseed oil (30%)	O/W	Yang et al. (2020b)
Organic compounds	Self-assembly	Sapoin glycyrrhizic acid	No emulsifier/sunflower oil, algal oil, and flaxseed oil (40%)	O/W	Wan et al. (2017)
		β-Sitosterol/*γ*-Oryzanol	No emulsifier/sunflower oil (40–90%)	W/O	(Bot et al., 2011; Sawalha et al., 2012)
		Sapoin glycyrrhizic acid	PGPR in W_1/O and no emulsifier in double emulsions/sunflower oil (70% in W_1/O)	$W_1/O/W_2$	Ma et al. (2017)

Carmona, & Herrero, 2015). In addition, ethanol has been used to denature proteins and produce cold-set whey protein emulsion gels recently (Xi, Liu, McClements, & Zou, 2019), which can also be regarded as a cold-set gelation method. The mechanism is that ethanol can unfold proteins and then the structural crosslinking forms between protein molecules in the continuous phase and on the surfaces of droplets.

The mechanism of acid-induced protein gelation is that the acidification, usually carried out by adding glucono-δ-lactone (GDL), decreases the pH and neutralize the surface charges of protein aggregates and a gel network then forms by hydrophobic interactions and Van der Waals forces (Ringgenberg, Alexander, & Corredig, 2013). Before acidification, heat treatment is normally used to denature proteins and form protein aggregates. In such cases, two different processes can be used to produce acid-induced protein-based emulsion gels: using pre-heated-induced protein aggregates to form emulsions (Lu, Mao, Zheng, Chen, & Gao, 2020) or heating native protein-stabilized emulsion to form protein aggregates (Ye & Taylor, 2009) before acidification. However, heating native protein-stabilized emulsions may lead to droplet flocculation, which limits the application of emulsion gels for encapsulation of heat-sensitive compounds (Mao, Roos, & Miao, 2014).

Addition of ions (normally Ca^{2+} in the form of $CaCl_2$) can promote soluble protein aggregates to form a gel network by ionic crosslinks (Wang, Luo, Liu, Adhikari, & Chen, 2019). It has been reported that structures of $CaCl_2$-induced SPI emulsion gels were mainly composed of particulate clusters of protein-coated droplets, which were different from filamentous gel networks formed by MTGase and GDL (Tang, Chen, & Foegeding, 2011). In addition, the concentration of Ca^{2+} can affect the structures of protein-based emulsion gels; Sok Line, Remondetto, and Subirade (2005) found that low calcium concentrations (e.g.,11.7 mM Ca^{2+}) induced emulsion gels with a fine-stranded structure, while high calcium concentrations (e.g., 40 mM or 68 mM Ca^{2+}) led to random aggregates. Therefore, $CaCl_2$ at a concentration of 8–20 mM is normally used to produce Ca^{2+}-induced emulsion gels (Liang, Leung Sok Line, Remondetto, & Subirade, 2010; Tang et al., 2011; Ye & Taylor, 2009).

Microbial transglutaminase (MTGase) can be used to promote crosslinks between protein molecules and improve the properties of protein-based emulsion gels (Gaspar & de Goes-Favoni, 2015). Compared to other methods, enzyme treatment is a safe method to produce protein-based emulsion gels with high quality under mild process conditions (35–37 °C) and without producing any side-products (Tang, Luo, Liu, & Chen, 2013). It was found that the gel strength of MTGase-induced SPI-based emulsion gels was much higher than that of GDL- or $CaCl_2$-induced emulsion gels (Tang et al., 2011). Two points should be highlighted when enzyme treatment is used to prepare protein-based emulsion gels. Firstly, the order of adding enzyme into emulsions may influence the properties of emulsion gels. Tang, Yang, Liu, and Chen (2013) found that adding enzyme prior to emulsification required less enzyme, but induced emulsion gels with higher stiffness compared to adding enzyme after emulsification. Secondly, although the formation of protein aggregates is not necessary for producing enzyme-induced gels, unfolding the compact structures of globular proteins (e.g., SPI, WPI, and MP) can provide more target glutamine and lysine residues for the MTGase treatment. For example, pre-incubation of SPI and egg white protein (Alavi, Emam-Djomeh, Salami, & Mohammadian, 2020; Tang, Yang, Liu, & Chen, 2013), pre-oxidation treatment of MP (Wang, Xiong, & Sato, 2017), and breaking down disulfide bonds in bovine serum albumin (Kang, Kim, Shin, Woo, & Moon, 2003) can improve gelation properties of proteins induced by MTGase. However, it has been found that heated SPI-stabilized emulsions after emulsification could not form gels following enzymatic treatment (Tang et al., 2011).

2.1.2. Polysaccharide-based bulk emulsion gels

Several methods have been studied for preparing polysaccharide-based bulk emulsion gels, such as heat-set, cold-set after pre-heating, addition of ions, and self-assembly (crystallisation), depending on the

gelation properties of polysaccharides.

Curdlan is a water-soluble β-(1,3)-glucan extracted from *Alcaligenes* faecalis, and curdlan-based emulsion gels can be obtained after heating emulsions (i.e., heat-set gelation), while cold-set after pre-heating is normally used to prepare carrageenan-, agar-, and gellan gum-based emulsion gels (Jiang et al., 2019). For producing cold-set emulsion gels, polysaccharides should be dissolved at a high temperature (normally more than 70 °C), and/or emulsions should be prepared at a medium temperature (normally between 45 °C and 70 °C), after which emulsion gels are formed at a low temperature (normally less than 25 °C). They are cold-set and thermo-reversible gels. The gelation mechanism involves forming double helices and cross-linking helical domains to create a three-dimensional structure during cooling (Nishinari & Takahashi, 2003).

The addition of ions is normally used to produce alginate-based emulsion gels. Sodium alginate, a linear unbranched natural polysaccharide, is derived from brown seaweed extracts (*Phaeophyceae*) (King, 1983). Sodium alginate has the ability to form 'egg-box' shaped gels when the sodium ions are replaced by divalent cations (mostly calcium in the food industry) (Ching et al., 2017). Two different methods can be used to prepare alginate-based emulsion gels. Pintado et al. (2015) added $CaSO_4$ into an alginate-based emulsion to produce an alginate-based emulsion gel directly. Sato et al. (2014) used a different method to produce emulsion gels, in which CaEDTA was added to the alginate-based emulsion first, after which an acid was then introduced to liberate calcium ions.

Inulin is an oligosaccharide which includes 2 to 60 fructose molecules connected by β-(2 → 1) glycoside bonds (Glibowski & Pikus, 2011). Inulin with a crystal structure can disperse in an aqueous environment and form a suspension in which the most of crystals do not change their structures, except some of smallest crystals dissolving in water. Amorphous inulin can change its structure to crystallite in water (Glibowski & Pikus, 2011). Then, small crystallites can aggregate to form larger clusters, which ultimately interact to form a gel (Bot, Erle, Vreeker, & Agterof, 2004). Paradiso et al. (2015) compared three different homogenization technologies (i.e., mechanical, ultrasonic and cold ultrasonic homogenization) to prepare inulin-based emulsion gels, and found that ultrasonic homogenization is a suitable method to prepare emulsion gels with better textural properties compared to the other two homogenization technologies.

2.1.3. Self-assembly of low molecular weight compound-based bulk emulsion gels

Many LMW organic compounds, such as glycyrrhizic acid and a combination of β-sitosterol and γ-oryzanol, can be used as oil-structuring agents, due to their self-assembly, to replace solid fats and provide required sensory and flavor properties in food products (Pernetti, van Malssen, Flöter, & Bot, 2007; Wan et al., 2017). These organic compounds, when in a water or oil phase, can form soft solid-like structured gels, which are known as oleogels or organogels (Co & Marangoni, 2012), and they can be also used to produce emulsion gels.

Saponin glycyrrhizic acid (GA) is a monodesmosidic saponin which is comprised of a hydrophobic triterpenoid aglycon moiety (18 β-glycyrrhetinic acid) attached to a hydrophilic diglucuronic unit. GA molecules have both gelation and emulsifying properties, owing to their self-assembly ability and amphiphilic structures. GA cannot structure vegetable oil directly because of its low solubility in oil. However, GA molecules can self-assemble into long nanofibrils in water, and nanofibrils not only absorb at the oil-water interface but also further assemble and entangle to create a supramolecular hydrogel in water phase. Wan et al. (2017) investigated GA-based O/W emulsion gels and found that, for more polar oils, GA fibrils had a higher affinity to the oil-water interface, leading to the formation of a lot of fine multilayer emulsion droplets with smaller droplet size. Ma et al. (2017) used GA to produce GA-based water-in-oil-in-water ($W_1/O/W_2$) emulsion gels; a W_1/O emulsion was prepared first, before being mixed with GA solution at 80 °C, and GA-based $W_1/O/W_2$ emulsion gels were formed at room temperature by the self-assembly of GA.

The combination of β-sitosterol and γ-oryzanol can self-assemble in an oil phase to form a helical ribbon, and then these tubules can aggregate and form networks, which are known as oleogels or organogels. Thus, the combination of β-sitosterol and γ-oryzanol can be used to prepare gelled W/O emulsions. However, the oil phase should be prepared at high temperature (~100 °C) to dissolve β-sitosterol and γ-oryzanol, and W/O emulsions should also be prepared at 90 °C to prevent the gelation of oil phase during emulsification. It has been reported that, when a mixture of β-sitosterol and γ-oryzanol was used to prepare W/O emulsion gels, the presence of water weakened the tubules and reduced the firmness of gelled emulsions, due to the hydration of β-sitosterol and the transition of crystals from anhydrous and hemihydrate into monohydrate forms (Bot et al., 2011). On the other hand, it was found that reducing the water activity and using oils with low polarity could promote the formation of tubular microstructures of oryzanol and sitosterol in emulsions (Sawalha et al., 2012).

2.2. Emulsion gel particles

Gel particles or gel beads can be divided into three categories according to their size: macrogel particles (> 1 mm), microgel particles (0.2–1000 μm), and nanogel particles (< 0.2 μm) (Ching et al., 2017). In the food area, studies have mainly focused on macrogel and microgel particles, and alginate was the matrix material most frequently used to produce gel particles. Ching et al. (2017) reviewed current technologies for producing alginate hydrogel particles (e.g., simple dripping, jet back up extrusion, spinning disk, atomization, impinging aerosol method, emulsification technique, microfluidics, and templating method), but studies on producing emulsion gel particles have rarely been reported (Lin, Kelly, Maidannyk, & Miao, 2020). As shown in Table 2, methods used to prepare emulsion gel particles include simple dripping, electrostatic extrusion, and the impinging aerosol method.

An electrostatic extrusion technique has been used to prepare alginate-based emulsion beads with diameters in the range from 960 to 1650 μm, in which a syringe pump and electrostatic immobilization unit (at a voltage of 6.5 kV) were used to extrude an alginate-based emulsion through a needle (22 gauge) into a collecting solution (0.015 g/mL of $CaCl_2$ solution) (Lević et al., 2015). The reason for using an electrostatic immobilization unit is that electrostatic forces can disrupt the liquid filament at the tip of the needle and create a charged stream of small droplets. However, bigger beads (diameter from 2100 to 2350 μm) were formed without applying voltage, i.e., extrusion by syringe or simple dripping, which is thus a simple method to produce macrogel particles, but this method usually leads to large particle sizes (Lin et al., 2020). Ching, Bansal, and Bhandari (2016) developed a spray aerosol method to prepare alginate-based emulsion microgel particles with the size of 36.2–57.8 μm. A fine aerosol mist of alginate-based emulsion and an aerosol mist of 0.5 M calcium chloride solutions are created at the top and bottom of the chamber, respectively, using an air atomizing nozzle. Two mists combine in the chamber, and emulsion gel particles form in the chamber and are collected at the base of chamber. This is an effective and continuous method to produce emulsion gel particles with small size, but this method needs a special spray aerosol system.

2.3. Fluid emulsion gels

Apart from bulk emulsion gels and emulsion gel particles, fluid emulsion gels are the third type of emulsion gels. Fluid emulsion gels are different from bulk gels and gel particles with solid shapes, but fluid emulsion gels have higher viscoelastic properties than conventional emulsions. Fluid emulsion gels mainly include two types according to their preparation methods: gel-like emulsions and disrupted emulsion gel systems (Table 3).

Table 2
Selected examples of materials and methods used to prepare emulsion gel particles.

Materials	Methods	Matrix	Emulsifier/oil category and content	Structure	References
Polysaccharide	External gelation (ionic gelation)	Alginate	No emulsifier or WPI/canola oil (1–10%), safflower oil (10%), thyme essential oil (1%), or D-limonene	O/W	(Benavides, Cortes, Parada, & Franco, 2016; Ching et al., 2016; Corstens et al., 2017; Lević et al., 2015)
		κ-Carrageenan or alginate	Tween 80/corn oil (10%) in emulsions	O/W	Zhang et al. (2016)
Protein/polysaccharide	External gelation (ionic gelation)	Pectin/WPI	WPI/oily solution of vitamin A (20%)	O/W	Ruffin et al. (2014)
		Alginate/WPI	WPI/sunflower oil (0.5–20%)	O/W	Feng, Yue, Wusigale, Ni, & Liang (2018)
		Alginate/lupin protein	Lupin protein/linseed oil (ϕ = 0.15–0.69)	O/W	Piornos et al. (2017)

Table 3
Selected examples of materials and methods used to prepare fluid emulsion gels.

Materials	Methods	Matrix	Emulsifier/oil category and content	Structure	References
Protein	Pickering emulsion/self-support	/	Soy glycinin nanoparticles/soy oil (ϕ = 0.1, 0.3, or 0.5) or unknown oil (ϕ = 0.1–0.89)	O/W	(Liu & Tang, 2016; Luo et al., 2013; Xu, Liu, et al., 2019)
		/	Pea protein isolate/soy oil (ϕ = 0.2–0.6)	O/W	Shao and Tang (2016)
		/	WPI/camellia oil (ϕ = 0.75)	O/W	Liu et al. (2019)
		/	Casein peptides/unknown oil (61% and 77%)	O/W	Wakita and Imura (2018)
		Sarcoplasmic protein	Sarcoplasmic protein/canola oil (50%)	O/W	Hemung, Benjakul, and Yongsawatdigul (2013)
		/	Wheat gluten/corn oil (60%)	Oil-in-glycerol	Liu et al. (2016)
	Electrospinning emulsion/self-support	Gelatin	Gelatin/corn oil (ϕ = 0.2–0.8)	O/W	Zhang and Zhang (2018)
Polysaccharide	Pickering emulsion/self-support	Starch granule	Octenylsuccinate quinoa starch OSQS/corn oil (30–60%)	O/W	Li, Zhang, Li, Fu, and Huang (2020)
	Disrupted gel systems (homogenization)	Starch	OSA modified starch/sunflower oil (40%)	O/W	Torres et al. (2017)
	Disrupted gel systems (mechanical shearing)	Sodium alginate	Tween 80/canola oil (5%)	O/W	Soukoulis et al. (2016)
Protein/polysaccharide	Pickering emulsion/self-support	/	Zein and gum arabic complex (ZGAPs)/medium-chain triglyceride oil (ϕ = 0.1–0.7)	O/W	Dai et al. (2018)
		/	Zein and chitosan complex (ZCCPs)/algal oil (20–70%)	O/W	Wang et al. (2016)
		/	Zein and tannic acid complex particles (ZTP)/corn oil (ϕ = 0.5)	O/W	(Zou et al., 2015; Zou, Yang, & Scholten, 2018)
		/	β-lactoglobulin and gum arabic complex/medium-chain triglyceride oil (ϕ = 0.3–0.7)	O/W	Su et al. (2020)
	Disrupted gel systems (mechanical shearing)	WPI/alginate	WPI/olive oil (5–25%)	O/W	Leon et al. (2018)

2.3.1. Gel-like emulsions

Pickering emulsions are a kind of emulsions which are stabilized by amphiphilic solid particles, and can be divided into three categories: polysaccharide particle-, protein particle- and mixture-stabilized Pickering emulsions. Pickering emulsions are considered as better delivery systems than conventional emulsions, owing to their enhanced storage stability against oxidation and coalescence and lower susceptibility to lipolysis. Pickering emulsions can turn into gel-like emulsions under appropriate conditions (e.g., proper solid particle type, solid particle concentration, oil phase concentration, pH, and ionic strength). It has been reported that gel-like emulsions could be formed with 6 wt% preheated soy globulins at high glycinin contents (> 75%) with soy oil at a oil volume fraction (ϕ) of 0.3, and that G′ and G″ values of gel-like emulsions increased as the increase of glycinin contents (from 75% to 100%), while neither unheated soy globulins nor preheated soy globulins with low glycinin contents could form gel-like emulsions (Luo, Liu, & Tang, 2013). This was probably because the formation of a gel-like network was largely attributed to hydrophobic interactions between denatured glycine molecules absorbed at the interface of oil droplets. However, Xu, Liu, and Tang (2019) found that, with increasing oil fractions (ϕ = 0.1 to 0.88), a 0.5 wt% soy *β*-conglycinin-stabilized Pickering emulsion could turn into a gel-like emulsion at an oil fraction of 0.7. It was also found that, with increasing wheat gluten level (emulsifier in oil-in-glycerol emulsions, 0.25–1.0 wt%), gel-like emulsions could be formed at high wheat gluten contents (≥ 0.5 wt%) (Liu, Chen, Guo, Yin, & Yang, 2016). Shao and Tang (2016) found that, with increasing oil fraction (0.2–0.6), pea protein-based Pickering emulsions changed from liquid to a gel-like state, while Zou et al. (2015) found that zein/tannic acid complex-stabilized Pickering emulsion gels with high oil volume fraction (ϕ > 0.5) could be successfully produced. Therefore, the oil phase and emulsifier contents should be high enough to assure that solid particles absorbed at the surface of neighboring oil droplets can connect and/or react with each other (Wouters & Delcour, 2019).

2.3.2. Disrupted gel systems

Fluid emulsion gels can also be prepared by breaking down bulk emulsion gels (Leon, Medina, Park, & Aguilera, 2018). Soukoulis et al. (2016) investigated so-called sheared oil-in-gel (o/g) emulsions prepared by stirring an alginate-based emulsion gel system at 1000 rpm for 6 h during the gelation process. Torres et al. (2017) developed a method to produce starch-based gel emulsions by homogenizing the bulk emulsion gels. This is a simple method to produce fluid emulsion gels with small dispersed gel particles (5–50 μm in diameter), but the gel matrix-covered structure may be destroyed, leading to separation of the gel matrix and oil droplets during homogenization, which may influence the stability of oil droplets and/or encapsulated nutrients during storage.

3. Structure-property relationships of different emulsion gels

3.1. Bulk emulsion gels

Some properties of bulk emulsion gels are emphasized in the food industry, such as mechanical properties (e.g., rheological, and textural perception), and release properties (including stability during storage and targeted-release in digestion). Many factors (e.g., structures of the gel matrix, structures of emulsion droplets, and interactions between the gel matrix and droplets) can influence the structures of bulk emulsion gels and then their mechanical and release properties.

Food emulsions normally include single emulsions (O/W and W/O emulsions) and multiple emulsions ($W_1/O/W_2$ and $O_1/W/O_2$ emulsions). After turning emulsions into bulk emulsion gels, their structures usually do not change. Thus, the structures of emulsion gels also include single structures (i.e., O/W and W/O) and multiple structures (i.e., $W_1/O/W_2$ and $O_1/W/O_2$). The matrix materials of O/W and $W_1/O/W_2$ emulsion gels are protein-, polysaccharide-, or organic compound-based hydrogels, while the matrix materials of W/O and $O_1/W/O_2$ emulsion gels are organic compound-based oleogels (also known as organogels or structured oil). Moreover, properties of O/W and $W_1/O/W_2$ emulsion gels and W/O and $O_1/W/O_2$ emulsion gels differ, because the properties of emulsion gels mainly depend on the properties of matrix materials (i.e., protein-, polysaccharide-, or organic compound-based gels), although the properties of emulsion droplets and the interactions between the gel matrix and droplets also influence the properties of emulsion gels. However, O/W emulsion gels have been studied more widely than W/O, $W_1/O/W_2$ and $O_1/W/O_2$ emulsion gels, so the following discussions in this review will focus on O/W emulsion gels unless other structures are emphasized.

3.1.1. The structure-mechanical property relationships of bulk emulsion gels

Mechanical properties of bulk emulsion gels are closely associated with other properties (e.g., storage stability, oral perception, and controlled release) and their applications. The most common mechanical properties of bulk emulsion gels are dynamic modulus (i.e., storage and loss modulus), Young's modulus, fracture strength (i.e., strain and stress), yield strength, and hardness. There are many ways or tools to measure mechanical properties of bulk emulsion gels, such as rheometry, dynamic mechanical analysis (DMA), and textural analysis (Anseth, Bowman, & Brannon-Peppas, 1996).

3.1.1.1. Matrix structures. For protein-based bulk emulsion gels, using different proteins and preparation methods can lead to different protein matrix structures and mechanical properties, owing to different gelation mechanisms and resultant different molecular forces between protein molecules in the gel matrix. Globular proteins (e.g., SPI, WPI, and MP) and non-globular proteins (e.g., gelatin, casein, and sodium caseinate) have been widely used as matrix materials in producing bulk emulsion gels.

The heat-set gelation method has been most used to prepare globular protein-based emulsion gels, but globular protein-based emulsion gels can be also prepared through acidification treatment, addition of ions, enzyme treatment, and MDA modification. For heat-induced emulsion gels, noncovalent cross-links (i.e., electrostatic interactions, hydrophobic interactions, and hydrogen bonds) and intermolecular disulfide bonds are the main forces between globular protein molecules (Wu, Xiong, & Chen, 2011). The main linking forces in the glucono-δ-lactone (GDL)-induced emulsion gels are hydrophobic interactions and Van der Waals forces, while salt-bridges are the main linking forces in salt-induced emulsion gels, and TGase-induced emulsion gels involve more covalent cross-links (i.e., ε-(γ-glutamyl)-lysine (G-L) cross-links). Therefore, different preparation methods may lead to different mechanical properties of globular protein-based emulsion gels (Liang et al., 2020; Wang et al., 2017; Ye & Taylor, 2009); for example, it was found that $CaSO_4$-induced SPI-based emulsion gels were stiffer and shown higher rigidity than MTGase-induced gels which performed better elasticity (Wang, Luo, Liu, Zeng, Adhikari, He, et al., 2018).

Gelatin can form gels under one-step cold treatment or cold treatment after pre-heating as descried in section 2.1.1.2. Cold-set gelatin gels, a kind of elastic polymer gel, are formed with flexible and random-coil protein chains. Therefore, gelatin-based emulsion gels are similar to gels with active-fillers (bound droplets) in which stress concentration phenomena play a larger role compared to friction phenomena (Sala, van Vliet, Cohen Stuart, Aken, & van de Velde, 2009). Other non-globular protein-based emulsion gels are normally prepared with enzyme treatment and acidification treatment. For example, although the main linking forces in acid-induced casein gels are also noncovalent cross-links, the firmness of acid-induced sodium caseinate gels was lower than that of acid-induced WPC gels, probably due to their differences in gelation mechanism (Kiokias & Bot, 2005).

Overall, contributions to the connectivity of a three-dimensional protein network arise from four different kinds of molecular forces:

covalent bonds, electrostatic interactions, hydrogen bonding and hydrophobic interactions. The presence of covalent bonds leads to permanent 'chemical' cross-links within the network, whereas the other three types of weaker 'physical' forces contribute to a complex set of more temperature-dependent interactions (Chen & Dickinson, 1999b). In addition, process parameters (e.g., temperature, protein content, ionic strength, pH, the presence of other components, ultrasound pretreatment, and high-pressure homogenization) also can influence the structures and mechanical properties of protein-based bulk emulsion gels (Bi et al., 2020; Chen & Dickinson, 2000; Cheng et al., 2019).

Firstly, temperature can influence the degree of denaturation of proteins, and thus affect the stability of protein-stabilized emulsions and mechanical properties of emulsion gels. Generally, a high degree of denaturation of proteins results in low stability of protein-stabilized emulsions but better mechanical properties of emulsion gels (Kiokias & Bot, 2005; Ye & Taylor, 2009). Chen and Dickinson (2000) also found that gelation temperature could influence the rate of gelation and the dynamic modulus of acid-induced sodium caseinate-based emulsion gels by changing the strength of physical bonds rather than the network structures.

Secondly, the influence of protein content on the mechanical properties of emulsion gels depends on the state of emulsion droplets. The mechanical properties of droplet-filled gels and inactive droplet-aggregated gels mainly depend on the gel strength of gel matrix structures, while interactions between the gel matrix (i.e., protein and polysaccharide) and lipid droplets contribute more to the active droplet-aggregated gels (Pintado et al., 2015). Therefore, increasing protein content can increase the gel strength of both kinds of emulsion gels but for different reasons (i.e., increased gel strength of protein matrix for droplet-filled gels and inactive droplet-aggregated gels, but strengthened interactions between the gel matrix and droplets and increased gel strength of protein matrix for active droplet-aggregated gels). For example, it has been reported that increasing the concentration of sodium caseinate can decrease the gelation time (T_{gel}) of sodium caseinate/sunflower oil emulsion-based gels (Montes de Oca-Ávalos, Huck-Iriart, Candal, & Herrera, 2016).

Thirdly, ionic strength and pH can influence intermolecular repulsion and gel structures in emulsion gels. For example, at low ionic strength (< 50 mM NaCl) and pH values (below 4 or above 6) far away from p*I* of whey proteins, a fine-stranded network consisting of whey protein strains with a length of ~50 nm and a diameter of ~10 nm is formed; at high ionic strength (> 150 mM NaCl) and pH values near the p*I*, the strains with weak intermolecular repulsion can accumulate and form a particulate network structure (Chen et al., 2000; Guo et al., 2017; Langton & Hermansson, 1992). However, both fine-stranded and particulate gels exhibit high gel strength (Guo et al., 2017; Tang et al., 2011). It was found that fine-stranded whey protein gels prepared at low ionic strength (10 or 25 mM NaCl) were rubbery and soft, but that particulate whey protein gels prepared at high ionic strength (100 or 200 mM NaCl) were hard and brittle (Guo et al., 2013).

Fourthly, the presence of other components (e.g., sucrose, glucose, hydroxytyrosol, rosmarinic acid, genipin, sodium pyrophosphate, insoluble dietary fiber, and EGCG) also can influence the structures and mechanical properties of emulsion gels (Chen et al., 2019; Feng et al., 2017; Freire, Bou, Cofrades, & Jimenez-Colmenero, 2017; Montes de Oca-Ávalos et al., 2016; Wang, Zhang, et al., 2018; Wang, Jiang, & Xiong, 2019; Zhuang et al., 2019). Generally, if components can strengthen protein-protein interactions and/or reduce droplet size, they can increase gel strength of emulsion gels. However, if these components can interact with protein molecules and disturb the interactions between protein molecules, they can weaken the gel strength of emulsion gels, and these effects are normally dose-dependent. Overall, preparation methods can affect linking forces between protein molecules, and protein type and processing parameters can influence the network structures of the gel matrix, both of which can affect the mechanical properties of emulsion gels.

In terms of polysaccharide-based emulsion gels, polysaccharide type, preparation methods, and processing parameters can influence the structures of the polysaccharide-based gel matrix. Cold-set gellan gun-, agar-, and κ-carrageenan-based emulsion gels are a kind of polymer gels with strand-based structures (Kim, Gohtani, Matsuno, & Yamano, 1999; Wang, Neves, Kobayashi, Uemura, & Nakajima, 2013). They normally show a predominantly elastic behavior, which resemble gelatin-based emulsion gels but differ from WPI-based emulsion gels with particulate structures (Sala et al., 2009). The network structures of alginate gels are in the shape of 'egg-box', in which sodium ion is replaced by a divalent cation, and each cation can bind with four G residues to form a three-dimensional network structure (Ching et al., 2017), which can be affected by freeze-thawing treatment (Li, Gong, Hou, Yang, & Guo, 2020). Inulin gels are formed by connection of microcrystals, and their rheological properties resemble that of fat crystal-based networks in oil (Nourbehesht, Shekarchizadeh, & Soltanizadeh, 2018). However, there are no studies on comparing mechanical properties of emulsion gels formed by different kinds of polysaccharides.

In addition, the influence of polysaccharide content on the mechanical properties of emulsion gels depends on emulsifier type and gel structures. Most naturally occurring polysaccharides, except gum Arabic and some kinds of pectin, have weak emulsifying abilities, compared to proteins and synthetic emulsifiers (Charoen et al., 2011). Hence, the interactions between the gel matrix and emulsion droplets in polysaccharide-based emulsion gels with/without synthetic emulsifiers are normally weak, and increasing polysaccharide content can increase their gel strength, mainly due to the decreased void spaces and increased gel strength of the gel matrix (Kim et al., 1999). However, when proteins are used as emulsifiers, increasing polysaccharide content can increase the gel strength of emulsion, mainly due to increased interactions between polysaccharide molecules and droplets and/or the gel strength of polysaccharide gels. Although studies on the effects of ionic strength and pH on the mechanical properties of polysaccharide-based emulsion gels have rarely been reported, Ozturk, Argin, Ozilgen, and McClements (2015) found that ionic strength and pH did not have significant influences on the stability of a gum Arabic-stabilized emulsion, which was different from a WPI-stabilized emulsion because of their different emulsification mechanisms (i.e., electrostatic repulsion for WPI and steric repulsion for gum Arabic). Therefore, it is proposed that the influence of ionic strength and pH on the structure and mechanical properties of polysaccharide-based emulsion gels differs from that on protein-based emulsion gels.

For LMW organic compound-based emulsion gels, saponin glycyrrhizic acid (GA) and the combination of β-sitosterol and γ-oryzanol have been investigated to prepare emulsion gels by self-assembly. GA, β-sitosterol and γ-oryzanol have physical properties, so they have been used to prepare different types of emulsion gels. GA can dissolve in water, and GA molecules can self-assemble to form long nanofibrils and gels in water phase, and so can be used to prepare emulsion gels with O/W or $W_1/O/W_2$ structures. The combination of β-sitosterol and γ-oryzanol can self-assemble in an oil phase to form a helical ribbon, then these tubules can aggregate and form a network, and so can be used to prepare gelled W/O emulsions. Processing parameters (e.g., organic compound content and solvent type) also can influence the structure and mechanical properties of organic compound-based emulsion gels. Ma et al. (2017) found that an emulsion stabilized by GA at a low concentration (0.5 wt%) could not form a gel, but self-standing emulsion gels could be formed and the viscoelastic modulus also significantly increased with increasing GA concentration (1–4 wt%). It was also found that no tubules were formed but only sitosterol and oryzanol crystals were present in emulsion gels at 16% total sterol concentration, while there were tubules next to the crystals at 32% total sterol concentration (Bot et al., 2011).

In addition, the polarity of solvents (i.e., oil in W/O emulsions) can influence the water activity of W/O emulsions and structures of the oil phase. It has been reported that more water molecules bind to the β-

sitosterol molecules and formed monohydrate crystals in higher polarity oils (e.g., eugenol and castor oil), which hindered the formation of tubules and resulted in weaker emulsion gels compared to less polar oils (e.g., decane and limonene) (Sawalha et al., 2012). However, studies on comparing structures and mechanical properties of emulsion gels prepared with different kinds of organic compounds have rarely been reported. Over all, many factors (e.g., gel matrix type, preparation method, and process parameters) can affect the gel structures of bulk emulsion gels and thus their mechanical properties.

3.1.1.2. Structures of emulsion droplets. The structure of emulsion droplets can influence the mechanical properties of bulk emulsion gels as well. Structures of emulsion droplets are normally influenced by oil phase (e.g., oil type, oil content, and droplet size), and emulsifier type (e.g., LMW emulsifiers or proteins). In the food industry, emulsifiers mainly include two categories: low molecular synthetics (e.g., Span 80, Tween 80, and monoglycerides) and natural molecules (e.g., proteins, egg lecithin, and soy lecithin) (Chen, Mao, Hou, Yuan, & Gao, 2020). Emulsifiers can not only decrease the interfacial tension and thereby increase the stability of emulsions but also affect the interactions between droplets and the gel matrix leading to active or inactive fillers (Van Vliet, 1988). Therefore, the effect of emulsion droplets on the mechanical properties of emulsion gels depends on not only emulsion droplets (i.e., oil type, oil content, and droplet size) but also the interactions between droplets and the gel matrix (Farjami & Madadlou, 2019).

The effect of active fillers on the rheological properties of emulsion gels mainly depends on the stiffness of the oil droplets and the droplet volume fraction (Sala et al., 2009). The Kerner model can explain the effect of active fillers on the mechanical properties of emulsion droplet-filled gels (Kerner, 1956):

$$\frac{G'_{gel}}{G'_{matrix}} = \frac{15(1-v_m)(M-1)\varphi_f}{(8-10v_m)M+7-5v_m-(8-10v_m)(M-1)\varphi_f} + 1 \quad (1)$$

where $M = \frac{G'_{filler}}{G'_{matrix}}$, and G'_{gel}, G'_{filler}, and G'_{matrix} are the shear modulus of the overall gel, the filler droplets and the gel matrix, respectively, φ_f is the actual droplet volume fraction, and v_m is the Poisson's ratio of the gel matrix. In addition, the Kerner model modified by Lewis and Nielsen can be used to explain the effect of active fillers on the mechanical properties of emulsion droplet-aggregated gels (Lewis & Nielsen, 1970):

$$\frac{G'_{gel}}{G'_{matrix}} = \frac{15(1-v_m)(M-1)\psi\varphi_f}{(8-10v_m)M+7-5v_m-(8-10v_m)(M-1)\psi\varphi_f} + 1 \quad (2)$$

where $\psi\varphi_f$ is the effective volume fraction of fillers, which takes into account the crowding effect of fillers and can be expressed as follows (Lewis & Nielsen, 1970):

$$\psi\varphi_f = \left[1+\left(\frac{1-\varphi_{max}}{\varphi_{max}^2}\right)\varphi_f\right]\varphi_f \quad (3)$$

where φ_{max} is the maximum volume fraction of the fillers. According to Eq. (2), increasing the shear modulus and the effective volume fraction ($\psi\varphi_f$) or actual volume fraction (φ_f) of fillers can increase the mechanical properties of emulsion gels, which has been supported by many studies (Gwartney, Larick, & Foegeding, 2004; Li, Kong, Zhang, & Hua, 2012; Oliver, Scholten, & van Aken, 2015; Oliver, Wieck, & Scholten, 2016; Tang, Yang, et al., 2013). However, the Kerner model and the modified Kerner model are used under the assumption that M or G'_{matrix} do not change with changes in other factors (e.g., φ_f and G'_{filler}) (Chen & Dickinson, 1998a; Oliver, Berndsen, van Aken, & Scholten, 2015), especially at oil volume fractions (ϕ) below 0.2 and protein (i.e., gel matrix) contents above 6 wt% (Guo et al., 2017). However, the shear modulus of filler droplets ($G'_{filler} = 4\gamma/d$, where γ is surface tension and d is the average diameter of the oil droplets) is influenced by oil type, oil content, droplet size, emulsifier type, emulsifier content, and process parameters (Farjami & Madadlou, 2019; Sala et al., 2009; Van Vliet, 1988). The shear modulus of the gel matrix (G'_{matrix}) is influenced by droplet size, oil content, gel matrix type, preparation method, and process parameters (Sato et al., 2014). Therefore, when taking those factors (e.g., droplet size, process parameters, and high oil content), which can affect the mechanical properties of both filler droplets and the gel matrix, into account, the Kerner model and the modified Kerner model cannot be applied. For instance, it has been reported that increasing the size of olive oil droplets in a gelatin-based emulsion gel led to a weaker gel strength, probably due to the increase in interfacial area, a higher amount of gelatin adsorbed to the interface, and a lower quantity of protein available in the continuous phase (Sato et al., 2014); however, it was found that increasing the size distribution of dispersed vegetable fat in a WPI-based emulsion gel led to an increase in firmness, probably because of a larger number of contacts between droplets (Kiokias & Bot, 2006). Oliver et al. (2016) found that increasing the casein content (from 4% to 9%) could decrease the relative Young's modulus of emulsion gels at high oil volume fractions ($\varphi_f > 0.15$), probably owing to the higher inhomogeneity of casein-based gel matrix and increased effective volume fraction of droplets at lower casein concentration; this indicated that the effective volume fraction ($\psi\varphi_f$) plays a more important role than G'_{matrix} in affecting the mechanical properties of emulsion gels with high matrix inhomogeneity and at high oil volume fractions.

The effect of inactive fillers on the rheological properties of emulsion gels depends on the properties and concentrations of LMW emulsifiers, droplet size, and oil content, although there have been few studies on modelling the effect of inactive fillers on the rheological properties of emulsion gels. Chen and Dickinson (1999a) investigated the effect of LMW emulsifiers on the viscoelastic properties of heat-set whey protein-based emulsion gels, and found that the elastic modulus of heat-set whey protein-based emulsion gels decreased after adding a low level of diglycerol monolaurate (DGML, the surfactant/protein molar ratio (R) = 4) and diglycerol monooleate (DGMO, R = 4–32), while high levels of emulsifiers (R = 32 for DGML, and R = 64 for DGMO) could recover the storage and loss modulus of emulsion gels, probably due to depletion flocculation of the emulsion prior to heat-treatment. However, it has been reported that Tween 20 (R = 0.25–8) always decreased the mechanical properties of emulsion gels, and a high addition level (R = 8) could even break down the network structure of proteins and lead to a liquid-like emulsion (Chen & Dickinson, 1998b). It has been found that increasing oil content decreased fracture stress and stress intensity factor of agar gels and κ-carrageenan-locust bean gum gels (Koç et al., 2019). It has also been found that increasing solid lipid content could increase the gel strength of emulsion gels at an emulsifier content of 4 g/100 g, but decreased the gel strength at an emulsifier content of 2 g/100 g (Geremias-Andrade, Souki, Moraes, & Pinho, 2017).

3.1.2. The structure-release property relationships of bulk emulsion gels

Bulk emulsion gels, especially O/W emulsion gels, are often used for the delivery and release of oil-soluble bioactive compounds and nutrients, such as α-tocopherol (Liang et al., 2010) and β-carotene (Soukoulis et al., 2017). Compared to emulsions, emulsion gels can provide better protection for encapsulated compounds and show slower release behavior (Cofrades et al., 2017). Many studies have focused on the matrix erosion, lipid digestion and controlled release of encapsulated compounds during digestion of emulsion gels. The digestion behaviors of protein- and polysaccharide-based emulsion gels differ in the gastrointestinal tract because of different digestion processes of proteins and polysaccharides. For protein-based emulsion gels, Liang et al. (2010) found that gel loss (i.e., matrix erosion owing to protein degradation) and release of α-tocopherol occurred in both simulated gastric fluid (SGF) and simulated intestinal fluid (SIF), respectively,

which indicated that release of α-tocopherol was controlled mainly by matrix erosion because of protein degradation. However, under simulated gastrointestinal (GI) conditions (0.5 h SGF followed by 6 h SIF), gel loss and release of α-tocopherol only occurred in the SGF step, probably due to the formation of a viscous layer at the surface of gels. Moreover, gel rigidity of protein-based emulsions is an important factor affecting the lipid digestion in GI digestion. It has been reported that gastric digesta of a soft gel (prepared with 10 or 20 mM NaCl) mainly consisted of individual oil droplets and small gel particles (~10 mm), while gastric digesta of a hard gel (prepared with 100 or 200 mM NaCl) mainly consisted of small gel particles (~10 mm) after 240 min gastric digestion, and the remaining network structure of gel particles hindered further breakdown during intestinal digestion (Guo, Ye, Lad, Dalgleish, & Singh, 2016). It was also found that digestion of emulsion gels in the intestinal step was delayed by denser, more spatially heterogeneous protein matrices (Guo et al., 2017). In terms of polysaccharide-based emulsion gels, although there are fewer reports about their digestion, it was found that oil droplets could be released from agar-based emulsion gels during GI digestion in both SGF and SIF steps (2.0 h SGF followed by 4–14 h SIF), while emulsifier type (glycerol monolaurate with different degrees of polymerization) affected the size distribution of released oil droplets (Wang et al., 2013).

Bulk emulsion gels are also used for the delivery and release of volatile flavor compounds, such as ethyl butyrate, ethyl hexanoate, ethyl octanoate, propanol, diacetyl, pentanone, hexanal, and heptanone (Hou, Guo, Wang, & Yang, 2016; Mao et al., 2014). The release of volatile compounds in the oral cavity is normally measured by a simulated nose breath device (Hou et al., 2016) or gas chromatography (GC) headspace analysis (Mao et al., 2014). The release rate of volatile compounds depends on the gel matrix structure, oil content, the nature of volatile compounds, and the interactions between flavor compounds and food ingredients (particularly oils in O/W emulsion gels) (Boland, Delahunty, & van Ruth, 2006; Guichard, 2002). It has been reported that the release rate of ethyl butyrate was significantly lower in a SPI/sugar beet pectin (SBP) complex-based emulsion gel with a compact network than SPI- or SBP-based emulsion gels, but the release rate of aroma compounds with higher hydrophobicity was not significantly influenced by the structures of emulsion gels, probably because of their high affinity for the lipid phase rather than interacting with proteins and/or polysaccharides (Hou et al., 2016). Mao et al. (2014) also found that emulsion gels with higher storage modulus at a high oil content (20%) had lower release rates and partition coefficients of the volatiles, and that increasing oil contents (from 5% to 20%) significantly decreased the release rate of heptanone, probably owing to its highly lipophilic characterization.

3.2. The structure-property relationships of emulsion gel particles

Although emulsion gel particles and bulk emulsion gels have similar structures (i.e., active fillers, inactive fillers, emulsion droplet-filled gels, and emulsion droplet-aggregated gels) and structure-property relationships, their physical properties and length scales differ (Ching et al., 2016).

Firstly, the rheological behavior of gel particles differs to that of bulk gels, because the microgel particle system is a suspension (usually gel particles in water). The rheological properties of microgel particle suspensions are influenced by three parameters: volume fraction (φ), particle modulus (modulus of particles that make up the suspension) and interaction potential (Ching et al., 2016). The volume fraction (φ) can be determined using the equation below (Ching et al., 2016):

$$\varphi = \frac{\frac{m}{\rho}}{\frac{m}{\rho} + v} \quad (4)$$

where φ = final microgel suspension volume fraction, m = mass of microgel concentrate, ρ = density of microgel concentrate measured with a 50 mL calibrated pycnometer, and v = volume of water added to microgel concentrate. Eq. (4) was modified by the equations developed by Suzawa and Kaneda (2010), who calculated the volume fraction by the weight and density of emulsions but did not consider the weight loss (normally water loss) of gel particles during gelation. At low volume fraction, the flow behavior is determined by the continuous phase; at higher volume fraction, softer microgels will exhibit a lower storage modulus compared to hard microgels (Adams, Frith, & Stokes, 2004). Ching et al. (2016) found that, at the same volume fraction, suspensions with more deformable alginate-based micorgels exhibited a lower bulk modulus. However, it is technically difficult to investigate the rheological properties of macrogel particles, although their mechanical properties could be investigated by a texture analyser (Lin et al., 2020). It has been reported that, with increasing oil contents in alginate-based macrogels, the elastic modulus of particles decreased, which indicates that oil droplets in alginate-based emulsion gel particles without emulsifiers were inactive fillers (Ching et al., 2016).

Secondly, syneresis and swelling properties are important properties of gel particles (Ching et al., 2017). It was found that alginate-based emulsion gel particles shrank less if they had higher oil content (Lin et al., 2020), and that the swelling was more pronounced for smaller particles, probably owing to the larger contact surface, but was less pronounced at increased oil contents, probably because of droplets acting as physical barriers for water transport (Lević et al., 2015).

Thirdly, encapsulation efficiency (EE), loading capacity (LC) and encapsulation yield, which are important parameters in encapsulation processes of emulsion gel particles, are affected by properties and contents of matrix material, emulsifier, and oil. It has been reported that increasing alginate contents in the water phase could increase the oil EE in lupin protein isolate (LPI)-stabilized emulsion gel particles, probably due to the formation of a stronger gel matrix and better crosslinking on the external surfaces of particles (Piornos, Burgos-Díaz, Morales, Rubilar, & Acevedo, 2017). However, when the protein content was higher than the saturation concentration, or the oil content was very low, in which excessive free protein molecules existed in the water phase, the aggregation of non-adsorbed protein molecules could lead to lower emulsion stability and lower EE (Guzey & McClements, 2006). In addition, Ruffin, Schmit, Lafitte, Dollat, and Chambin (2014) found that, compared to native WPI, using pre-heated WPI at 80 °C for 30 min as emulsifier in pectin-based emulsion gel particles slightly improved the yield and stability of encapsulated vitamin A, because of the increased viscosity of denatured WPI dispersions and the decreased particle size of emulsions.

3.3. The structure-property relationships of fluid emulsion gels

3.3.1. Gel-like emulsions

The oil content, particle content, and surface charge of particles can affect the rheological properties of gel-like Pickering emulsions and release behavior of encapsulated compounds from such emulsions (Shao & Tang, 2016; Xu, Liu, & Tang, 2019). For the effect of oil content, Dai, Sun, Wei, Mao, and Gao (2018) found that zein/gum arabic complex-stabilized Pickering emulsion gels solidified at high oil volume fractions in emulsions ($\phi \geq 0.5$), and increasing oil volume fractions ($\phi = 0.5$–0.7) increased the G′ and G″ of gel-like emulsions, probably due to increased interactions between emulsion droplets (Xiao, Wang, Gonzalez, & Huang, 2016). It was also reported that a gel-like emulsion at $\phi = 0.6$ exhibited much lower release rate of β-carotene but higher stability during digestion than a Pickering emulsion at $\phi = 0.3$ (Shao & Tang, 2016). In terms of the effect of particle content, Xu, Liu, et al. (2019) found that increasing soy β-conglycinin contents from 0.2 to 1.0 wt% led to a progressive decrease in droplet size, but a progressive increase in stiffness of the gel-like emulsions at $\phi = 0.8$. Liu et al. (2019) also found that increasing pre-heated WPI contents from 2.5 to 10 wt% led to a progressive increase in gel strength, hardness, WHC, and stability of the gel-like emulsions at 75 vol% oil; they also found

that increasing protein contents could increase the bioaccessibility of β-carotene because of the reduced aggregation of the oil droplets and retarded degradation of β-carotene during digestion, owing to a dense WPI-based gel structure around droplets. In addition, the surface charge of (nano)particles can affect their emulsification and interfacial behavior (Larson-Smith, Jackson, & Pozzo, 2012). It has been reported that electrostatic screening by adding NaCl could improve the performance of soy glycine nanoparticles in forming gel-like emulsions and increase stiffness of the resultant gel-like emulsions, due to enhanced diffusion and adsorption of solid particles at the interface (Liu & Tang, 2016).

3.3.2. Disrupted gel systems

Although there are few studies on the structure-property relationships of disrupted gel systems, Torres et al. (2017) found that increasing starch contents (from 15 to 20 wt%) and oil fractions (from 0 to 20 wt %) could improve the elastic modulus of starch-based disrupted gels stabilized by octenyl succinin anhydride (OSA) modified starch, which fitted the Kerner model. It has been reported that, compared to alginate-based emulsions and bulk emulsion gels, sheared oil-in-gel (o/g) emulsions exhibited higher bioaccessibility of encapsulated β-carotene after *in vitro* digestion, due to the lower unbound calcium content and higher colloidal stability throughout gastrointestinal passage, whereas encapsulated β-carotene in the bulk emulsion gels exhibited highest chemical stability (Soukoulis et al., 2016).

4. Applications of emulsion gels in the food industry

4.1. Use of emulsion gels as fat replacers in meat products

Emulsion gels formed by myofibrillar proteins (MPs), water and lipid not only contribute to the sensory properties (appearance and flavor) but also relate to the textural properties (water- and oil-holding, and cooking losses) of meat products (Wang, Zhang, et al., 2018; Zhao et al., 2017). Additives, such as extracts from herbs and spices, polyphenols, and NaCl, can influence structures of emulsion gels and the properties of meat products (Wang, Zhang, et al., 2018; Zhao et al., 2017). Wang, Luo, et al. (2018) and Wang, Zhang, et al. (2018) found that a low level of rosmarinic acid (RA) (12 μM/g protein) could protect thiol and ε-NH_3 groups in MP-based emulsion gels from oxidation, and thus improve the structure and water- and oil-holding abilities of emulsion gels; however, a high level of RA (300 μM/g protein) could induce interactions between RA and MPs, which led to aggregation of MPs and a poor emulsion gel network, while a high level of NaCl (0.6 M) could promote these interactions.

However, while health concerns around some meat products containing high fat content (over 27%) have increased in recent years, reducing fat content usually negatively influences consumer acceptance and textural properties of final products (Oliver, Scholten, et al., 2015). In order to avoid undesirable textural changes and improve the nutritional value of meat products (e.g., sausages and patties), promising methods have been studied, such as replacing fat with unsaturated oil (Oliver, Scholten, et al., 2015) or structured oil (e.g., olive, linseed, fish, perilla, and sunflower seed oil encapsulated in emulsion gels formed with SPI, WPI, sodium caseinate, carrageenan, gelatin, alginate, chia flour, oat bran, or inulin) (Alejandre et al., 2016; de Souza Paglarini et al., 2018; de Souza Paglarinia, Martinib, & Pollonio, 2019; Freire et al., 2018; Glisic et al., 2019; Pintado, Herrero, Jimenez-Colmenero, Pasqualin; Cavalheiro, & Ruiz-Capillas, 2018; Poyato, Astiasarán, Barriuso, & Ansorena, 2015; Serdaroglu, Nacak, & Karabiyikoglu, 2017). However, these methods may lead to undesirable sensory quality changes (e.g., color parameters and sensory acceptability) (Serdaroğlu & Öztürk, 2017). Oliver, Scholten, and van Aken (2015) found that physical properties of fat or oil and structural properties of the gel matrix could influence the rheological properties of fat-filled emulsion gels or oil-filled emulsion gels. Hence, the properties of fat in meat products should be considered, and the gelling agent and oil should be chosen carefully when emulsion gels are used as a fat replacer (Freire et al., 2017). It has been reported that combining emulsion gels and animal fat could be a good method to produce healthier meat products with acceptable sensory properties (de Souza Paglarini et al., 2019). In addition, emulsion gels help to control sodium availability and perception by changing sodium mobility and binding behavior, and can thus allow reduction of the salt content in meat products (Okada & Lee, 2017). However, most studies have focused on bulk emulsion gels and their uses in solid foods, and thus more studies on emulsion gel particles and their uses in liquid foods are needed.

4.2. Emulsion gels used as delivery systems to encapsulate and release food nutrients

Absorption of encapsulated lipophilic food nutrients (e.g., β-carotene, curcumin, *n*-3 fatty acid, vitamin A, and α-tocopherol) in emulsion gels include several steps: release from the gel matrix as the result of mechanical, chemical and enzymatic processes throughout the oral processing and gastrointestinal passage, incorporation in the co-digested lipid droplets, interaction with endogenous lipid surface active compounds (mainly bile salts and phospholipids) promoting the formation of mixed micelles, and eventual transportation of the mixed micelles to the small intestinal epithelium (Soukoulis et al., 2016; Yonekura & Nagao, 2007). Polysaccharides (e.g., alginate, κ-carrageenan, and starch) and proteins (e.g., gelatin and WPI) are normally used as gelation materials in producing emulsion gels encapsulating lipophilic food nutrients, but their digestion behaviors differ. Protein-based emulsion gels are mainly disrupted in gastric digestion as the result of enzymatic hydrolysis by pepsin, and the remaining protein-based network structures can hinder further breakdown during intestinal digestion (Guo et al., 2016; Liang et al., 2010). On the other hand, polysaccharide-based (especially alginate-based) emulsion gels are less sensitive to gastric fluid than protein-based emulsion gels, and may protect the encapsulated nutriments from harsh gastric environment, and the remaining gel structures can be further disrupted during intestinal digestion (Wang et al., 2013; Xu et al., 2019a). However, emulsion gels normally give low effective bioavailability of encapsulated lipophilic compounds, due to insufficient digestion of the gel matrix and resulting unreleased and undigested lipid phase (Liang et al., 2010; Zhang et al., 2016). Therefore, it is important to choose appropriate materials for different nutrients, which can protect encapsulated nutrients and control their release, and also do not inhibit release in the targeted gastrointestinal tract (Zhang et al., 2016). Although emulsion gels may not improve the final bioaccessibility of encapsulated food nutrients, they can improve emulsion structures and stability of nutrients during storage, and exhibit slow release effects in the gastrointestinal passage compared to emulsions (Brito-Oliveira et al., 2017; Ma et al., 2017; Soukoulis et al., 2016; Zhang et al., 2016).

5. Conclusions

Various preparation methods of emulsion gels are available for different matrix materials (e.g., heat treatment, enzyme treatment, acidification, and addition of ions for protein-based emulsion gels, cold-set and addition of ions for polysaccharide-based emulsion gels, and self-assembly for LMW compound-based emulsion gels), purposes (e.g., cold-set for protecting encapsulated nutrients and better mechanical properties), and emulsion gel types (e.g., internal gelation for bulk emulsion gels, external gelation for emulsion gel particles, self-assembly for gel-like Pickering emulsions, and mechanical stir for disrupted emulsion gels). Due to differences in the morphological properties among different emulsion gels, different physical properties are emphasized, such as the importance of mechanical and release properties for bulk emulsion gels, syneresis and swelling properties for emulsion gel particles, rheological properties for microgel particle suspensions, and flow behavior and release property for fluid emulsion

gels. In terms of bulk emulsion gels, many factors (e.g., structures of gel matrix and emulsion droplets and interactions between them) can influence their structures and thus mechanical and release properties. Structures of the gel matrix in bulk emulsion gels are affected by matrix material, preparation method, and process parameters, while structures of emulsion droplets are affected by oil type, oil content, droplet size, and emulsifier type. In terms of emulsion gel particles, oil content and particle size can influence their syneresis and swelling properties. The rheological properties of microgel particle suspensions are influenced by volume fraction, particle modulus, and interaction potential. In terms of gel-like Pickering emulsions, their rheological and release properties also are influenced by many factors (e.g., oil content, particle content, and surface charge of particles). Finally, two main applications of emulsion gels in the food industry are fat replacers in meat products and delivery systems for food nutrients.

Acknowledgement

This work was supported by China Scholarship Council (No. 201708350111) and Teagasc-The Irish Agriculture and Food Development Authority (RMIS6821).

References

Adams, S., Frith, W. J., & Stokes, J. R. (2004). Influence of particle modulus on the rheological properties of agar microgel suspensions. *Journal of Rheology, 48*, 1195–1213.

Alavi, F., Emam-Djomeh, Z., Salami, M., & Mohammadian, M. (2020). Effect of microbial transglutaminase on the mechanical properties and microstructure of acid-induced gels and emulsion gels produced from thermal denatured egg white proteins. *International Journal of Biological Macromolecules, 153*, 523–532.

Alejandre, M., Poyato, C., Ansorena, D., & Astiasaran, I. (2016). Linseed oil gelled emulsion: A successful fat replacer in dry fermented sausages. *Meat Science, 121*, 107–113.

Anseth, K. S., Bowman, C. N., & Brannon-Peppas, L. (1996). Mechanical properties of hydrogels and their experimental determination. *Biomaterials, 17*, 1647–1657.

Balakrishnan, G., Nguyen, B. T., Schmitt, C., Nicolai, T., & Chassenieux, C. (2017). Heat-set emulsion gels of casein micelles in mixtures with whey protein isolate. *Food Hydrocolloids, 73*, 213–221.

Benavides, S., Cortes, P., Parada, J., & Franco, W. (2016). Development of alginate microspheres containing thyme essential oil using ionic gelation. *Food Chemistry, 204*, 77–83.

Bi, C. H., Wang, P. L., Sun, D. Y., Yan, Z. M., Liu, Y., Huang, Z. G., et al. (2020). Effect of high-pressure homogenization on gelling and rheological properties of soybean protein isolate emulsion gel. *Journal of Food Engineering, 277*, Article 109923.

Boland, A. B., Delahunty, C. M., & van Ruth, S. M. (2006). Influence of the texture of gelatin gels and pectin gels on strawberry flavour release and perception. *Food Chemistry, 96*, 452–460.

Bot, A., den Adel, R., Regkos, C., Sawalha, H., Venema, P., & Flöter, E. (2011). Structuring in β-sitosterol + γ-oryzanol-based emulsion gels during various stages of a temperature cycle. *Food Hydrocolloids, 25*, 639–646.

Bot, A., Erle, U., Vreeker, R., & Agterof, W. G. M. (2004). Influence of crystallisation conditions on the large deformation rheology of inulin gels. *Food Hydrocolloids, 18*, 547–556.

Brito-Oliveira, T. C., Bispo, M., Moraes, I. C. F., Campanella, O. H., & Pinho, S. C. (2017). Stability of curcumin encapsulated in solid lipid microparticles incorporated in cold-set emulsion filled gels of soy protein isolate and xanthan gum. *Food Research International, 102*, 759–767.

Charoen, R., Jangchud, A., Jangchud, K., Harnsilawat, T., Naivikul, O., & McClements, D. J. (2011). Influence of biopolymer emulsifier type on formation and stability of rice bran oil-in-water emulsions: Whey protein, gum Arabic, and modified starch. *Journal of Food Science, 76*, E165–E172.

Chen, J., & Dickinson, E. (1998a). Viscoelastic properties of heat-set whey protein emulsion gels. *Journal of Texture Studies, 29*, 285–304.

Chen, J., & Dickinson, E. (1998b). Viscoelastic properties of protein-stabilized emulsions effect of protein-surfactant interactions. *Food Chemistry, 46*, 91–97.

Chen, J., & Dickinson, E. (1999a). Effect of monoglycerides and diglycerol-esters on viscoelasticity of heat-set whey protein emulsion gels. *International Journal of Food Science and Technology, 35*, 493–501.

Chen, J., & Dickinson, E. (1999b). Interfacial ageing effect on the rheology of a heat-set protein emulsion gel. *Food Hydrocolloids, 13*, 363–369.

Chen, J., & Dickinson, E. (2000). On the temperature reversibility of the viscoelasticity of acid-induced sodium caseinate emulsion gels. *International Dairy Journal, 10*, 541–549.

Chen, J., Dickinson, E., Langton, M., & Hermansson, A.-M. (2000). Mechanical properties and microstructure of heat-set whey protein emulsion gels: Effect of emulsifiers. *Lebensmittel-Wissenschaft und -Technologie- Food Science and Technology, 33*, 299–307.

Cheng, Y., Donkor, P. O., Ren, X., Wu, J., Agyemang, K., Ayim, I., et al. (2019). Effect of ultrasound pretreatment with mono-frequency and simultaneous dual frequency on the mechanical properties and microstructure of whey protein emulsion gels. *Food Hydrocolloids, 89*, 434–442.

Chen, H., Mao, L., Hou, Z., Yuan, F., & Gao, Y. (2020). Roles of additional emulsifiers in the structures of emulsion gels and stability of vitamin E. *Food Hydrocolloids, 99*, Article 105372.

Chen, J., Ren, Y., Zhang, K., Qu, J., Hu, F., & Yan, Y. (2019). Phosphorylation modification of myofibrillar proteins by sodium pyrophosphate affects emulsion gel formation and oxidative stability under different pH conditions. *Food & Function, 10*, 6568–6581.

Ching, S. H., Bansal, N., & Bhandari, B. (2016). Rheology of emulsion-filled alginate microgel suspensions. *Food Research International, 80*, 50–60.

Ching, S. H., Bansal, N., & Bhandari, B. (2017). Alginate gel particles–A review of production techniques and physical properties. *Critical Reviews in Food Science and Nutrition, 57*, 1133–1152.

Cofrades, S., Bou, R., Flaiz, L., Garcimartin, A., Benedi, J., Mateos, R., et al. (2017). Bioaccessibility of hydroxytyrosol and n-3 fatty acids as affected by the delivery system: Simple, double and gelled double emulsions. *Journal of Food Science & Technology, 54*, 1785–1793.

Co, E. D., & Marangoni, A. G. (2012). Organogels: An alternative edible oil-structuring method. *Journal of the American Oil Chemists Society, 89*, 749–780.

Corstens, M. N., Berton-Carabin, C. C., Elichiry-Ortiz, P. T., Hol, K., Troost, F. J., Masclee, A. A. M., et al. (2017). Emulsion-alginate beads designed to control *in vitro* intestinal lipolysis: Towards appetite control. *Journal of Functional Foods, 34*, 319–328.

Dai, L., Sun, C., Wei, Y., Mao, L., & Gao, Y. (2018). Characterization of Pickering emulsion gels stabilized by zein/gum Arabic complex colloidal nanoparticles. *Food Hydrocolloids, 74*, 239–248.

Devezeaux de Lavergne, M., Tournier, C., Bertrand, D., Salles, C., van de Velde, F., & Stieger, M. (2016). Dynamic texture perception, oral processing behaviour and bolus properties of emulsion-filled gels with and without contrasting mechanical properties. *Food Hydrocolloids, 52*, 648–660.

Dickinson, E. (2012). Emulsion gels: The structuring of soft solids with protein-stabilized oil droplets. *Food Hydrocolloids, 28*, 224–241.

Dickinson, E., & Merino, L. M. (2002). Effect of sugars on the rheological properties of acid caseinate-stabilized emulsion gels. *Food Hydrocolloids, 16*, 321–331.

Farjami, T., & Madadlou, A. (2019). An overview on preparation of emulsion-filled gels and emulsion particulate gels. *Trends in Food Science & Technology, 86*, 85–94.

Feng, X., Chen, L., Lei, N., Wang, S., Xu, X., Zhou, G., et al. (2017). Emulsifying properties of oxidatively stressed myofibrillar protein emulsion gels prepared with (-)-epigallocatechin-3-gallate and NaCl. *Journal of Agricultural and Food Chemistry, 65*, 2816–2826.

Feng, L., Jia, X., Zhu, Q., Liu, Y., Li, J., & Yin, L. (2019). Investigation of the mechanical, rheological and microstructural properties of sugar beet pectin/soy protein isolate-based emulsion-filled gels. *Food Hydrocolloids, 89*, 813–820.

Feng, W., Yue, C., Wusigale, Ni, Y., & Liang, L. (2018). Preparation and characterization of emulsion-filled gel beads for the encapsulation and protection of resveratrol and alpha-tocopherol. *Food Research International, 108*, 161–171.

Flaiz, L., Freire, M., Cofrades, S., Mateos, R., Weiss, J., Jimenez-Colmenero, F., et al. (2016). Comparison of simple, double and gelled double emulsions as hydroxytyrosol and n-3 fatty acid delivery systems. *Food Chemistry, 213*, 49–57.

Freire, M., Bou, R., Cofrades, S., & Jimenez-Colmenero, F. (2017). Technological characteristics of cold-set gelled double emulsion enriched with n-3 fatty acids: Effect of hydroxytyrosol addition and chilling storage. *Food Research International, 100*(Pt 2), 298–305.

Freire, M., Cofrades, S., Perez-Jimenez, J., Gomez-Estaca, J., Jimenez-Colmenero, F., & Bou, R. (2018). Emulsion gels containing n-3 fatty acids and condensed tannins designed as functional fat replacers. *Food Research International, 113*, 465–473.

Freire, M., Cofrades, S., Serrano-Casas, V., Pintado, T., Jimenez, M. J., & Jimenez-Colmenero, F. (2017). Gelled double emulsions as delivery systems for hydroxytyrosol and n-3 fatty acids in healthy pork patties. *Journal of Food Science & Technology, 54*, 3959–3968.

Gaspar, A. L., & de Goes-Favoni, S. P. (2015). Action of microbial transglutaminase (MTGase) in the modification of food proteins: A review. *Food Chemistry, 171*, 315–322.

Geremias-Andrade, I. M., Souki, N. P. D. B. G., Moraes, I. C. F., & Pinho, S. C. (2017). Rheological and mechanical characterization of curcumin-loaded emulsion-filled gels produced with whey protein isolate and xanthan gum. *Lebensmittel-Wissenschaft und -Technologie- Food Science and Technology, 86*, 166–173.

Glibowski, P., & Pikus, S. (2011). Amorphous and crystal inulin behavior in a water environment. *Carbohydrate Polymers, 83*, 635–639.

Glisic, M., Baltic, M., Glisic, M., Trbovic, D., Jokanovic, M., Parunovic, N., et al. (2019). Inulin-based emulsion-filled gel as a fat replacer in prebiotic-and PUFA-enriched dry fermented sausages. *International Journal of Food Science and Technology, 54*, 787–797.

Glusac, J., Davidesko-Vardi, I., Isaschar-Ovdat, S., Kukavica, B., & Fishman, A. (2018). Gel-like emulsions stabilized by tyrosinase-crosslinked potato and zein proteins. *Food Hydrocolloids, 82*, 53–63.

Gómez-Guillén, M. C., Giménez, B., López-Caballero, M. E., & Montero, M. P. (2011). Functional and bioactive properties of collagen and gelatin from alternative sources: A review. *Food Hydrocolloids, 25*, 1813–1827.

Guichard, E. (2002). Interactions between flavor compounds and food ingredients and their influence on flavor perception. *Food Reviews International, 18*, 49–70.

Guo, Q., Bellissimo, N., & Rousseau, D. (2017). Role of gel structure in controlling in vitro intestinal lipid digestion in whey protein emulsion gels. *Food Hydrocolloids, 69*, 264–272.

Guo, Q., Ye, A., Lad, M., Dalgleish, D., & Singh, H. (2013). The breakdown properties of

heat-set whey protein emulsion gels in the human mouth. *Food Hydrocolloids, 33*, 215–224.
Guo, Q., Ye, A., Lad, M., Dalgleish, D., & Singh, H. (2016). Impact of colloidal structure of gastric digesta on in-vitro intestinal digestion of whey protein emulsion gels. *Food Hydrocolloids, 54*, 255–265.
Guzey, D., & McClements, D. J. (2006). Formation, stability and properties of multilayer emulsions for application in the food industry. *Advances in Colloid and Interface Science, 128*, 227–248.
Gwartney, E. A., Larick, D. K., & Foegeding, E. A. (2004). Sensory texture and mechanical properties of stranded and particulate whey protein emulsion gels. *Journal of Food Science, 69*, S333–S339.
Hemung, B.-O., Benjakul, S., & Yongsawatdigul, J. (2013). pH-dependent characteristics of gel-like emulsion stabilized by threadfin bream sarcoplasmic proteins. *Food Hydrocolloids, 30*, 315–322.
Herrero, A. M., Ruiz-Capillas, C., Pintado, T., Carmona, P., & Jiménez-Colmenero, F. (2018). Elucidation of lipid structural characteristics of chia oil emulsion gels by Raman spectroscopy and their relationship with technological properties. *Food Hydrocolloids, 77*, 212–219.
Hou, J. J., Guo, J., Wang, J. M., & Yang, X. Q. (2016). Effect of interfacial composition and crumbliness on aroma release in soy protein-sugar beet pectin mixed emulsion gels. *Journal of the Science of Food and Agriculture, 96*, 4449–4456.
Jiang, Y., Liu, L., Wang, B., Yang, X., Chen, Z., Zhong, Y., et al. (2019). Polysaccharide-based edible emulsion gel stabilized by regenerated cellulose. *Food Hydrocolloids, 91*, 232–237.
Jiang, J., & Xiong, Y. L. (2013). Extreme pH treatments enhance the structure-reinforcement role of soy protein isolate and its emulsions in pork myofibrillar protein gels in the presence of microbial transglutaminase. *Meat Science, 93*, 469–476.
Kang, Y. N., Kim, H., Shin, W. S., Woo, G., & Moon, T. W. (2003). Effect of disulfide bond reduction on bovine serum albumin-stabilized emulsion gel formed by microbial transglutaminase. *Journal of Food Science, 68*, 2215–2220.
Kerner, E. (1956). The elastic and thermo-elastic properties of composite media. *Proceedings of the Physical Society. Section B, 69*, 808.
Khalesi, H., Emadzadeh, B., Kadkhodaee, R., & Fang, Y. (2019). Effect of Persian gum on whey protein concentrate cold-set emulsion gel: Structure and rheology study. *International Journal of Biological Macromolecules, 125*, 17–26.
Kim, K., Gohtani, S., Matsuno, R., & Yamano, Y. (1999). Effects of oil droplet and agar concentration on gel strength and microstructure of o-w emulsion gel. *Journal of Texture Studies, 30*, 319–335.
King, A. (1983). Brown seaweed extracts (alginates). *Food Hydrocolloids, 2*, 115–188.
Kiokias, S., & Bot, A. (2005). Effect of denaturation on temperature cycling stability of heated acidified protein-stabilised o/w emulsion gels. *Food Hydrocolloids, 19*, 493–501.
Kiokias, S., & Bot, A. (2006). Temperature cycling stability of pre-heated acidified whey protein-stabilised o/w emulsion gels in relation to the internal surface area of the emulsion. *Food Hydrocolloids, 20*, 245–252.
Koç, H., Drake, M., Vinyard, C. J., Essick, G., van de Velde, F., & Foegeding, E. A. (2019). Emulsion filled polysaccharide gels: Filler particle effects on material properties, oral processing, and sensory texture. *Food Hydrocolloids, 94*, 311–325.
Lam, R. S. H., & Nickerson, M. T. (2014). The properties of whey protein–carrageenan mixtures during the formation of electrostatic coupled biopolymer and emulsion gels. *Food Research International, 66*, 140–149.
Langton, M., & Hermansson, A.-M. (1992). Fine-stranded and particulate gels of β-lactoglobulin and whey protein at varying pH. *Food Hydrocolloids, 5*, 523–539.
Larson-Smith, K., Jackson, A., & Pozzo, D. C. (2012). SANS and SAXS analysis of charged nanoparticle adsorption at oil–water interfaces. *Langmuir, 28*, 2493–2501.
Leon, A. M., Medina, W. T., Park, D. J., & Aguilera, J. M. (2018). Properties of microparticles from a whey protein isolate/alginate emulsion gel. *Food Science and Technology International, 24*, 414–423.
Lević, S., Pajić Lijaković, I., Đorđević, V., Rac, V., Rakić, V., Šolević Knudsen, T., et al. (2015). Characterization of sodium alginate/d-limonene emulsions and respective calcium alginate/d-limonene beads produced by electrostatic extrusion. *Food Hydrocolloids, 45*, 111–123.
Lewis, T. B., & Nielsen, L. E. (1970). Dynamic mechanical properties of particulate-filled composites. *Journal of Applied Polymer Science, 14*, 1449–1471.
Liang, L., Leung Sok Line, V., Remondetto, G. E., & Subirade, M. (2010). *In vitro* release of α-tocopherol from emulsion-loaded β-lactoglobulin gels. *International Dairy Journal, 20*, 176–181.
Liang, X., Ma, C., Yan, X., Zeng, H., McClements, D. J., Liu, X., et al. (2020). Structure, rheology and functionality of whey protein emulsion gels: Effects of double cross-linking with transglutaminase and calcium ions. *Food Hydrocolloids, 102*, 105569.
Li, A., Gong, T., Hou, Y., Yang, X., & Guo, Y. (2020a). Alginate-stabilized thixotropic emulsion gels and their applications in fabrication of low-fat mayonnaise alternatives. *International Journal of Biological Macromolecules, 146*, 821–831.
Li, F., & Hua, Y. (2013). Rheological properties of acid-induced soy protein-stabilized emulsion gels in the absence and presence of N-ethylmaleimide. *Food Hydrocolloids, 30*, 641–646.
Li, F., Kong, X., Zhang, C., & Hua, Y. (2012). Gelation behaviour and rheological properties of acid-induced soy protein-stabilized emulsion gels. *Food Hydrocolloids, 29*, 347–355.
Lim, S. H., Kim, H. R., Choi, S. J., & Moon, T. W. (2015). Lipid oxidation of sodium caseinate-stabilized emulsion-gels prepared using microbial transglutaminase. *Food Science and Biotechnology, 24*, 2023–2026.
Lin, D., Kelly, A. L., Maidannyk, V., & Miao, S. (2020). Effect of concentrations of alginate, soy protein isolate and sunflower oil on water loss, shrinkage, elastic and structural properties of alginate-based emulsion gel beads during gelation. *Food Hydrocolloids, 108*, 105998.
Liu, X., Chen, X.-W., Guo, J., Yin, S.-W., & Yang, X.-Q. (2016). Wheat gluten based percolating emulsion gels as simple strategy for structuring liquid oil. *Food Hydrocolloids, 61*, 747–755.
Liu, W., Gao, H. X., McClements, D. J., Zhou, L., Wu, J., & Zou, L. Q. (2019). Stability, rheology, and beta-carotene bioaccessibility of high internal phase emulsion gels. *Food Hydrocolloids, 88*, 210–217.
Liu, F., & Tang, C.-H. (2016). Soy glycinin as food-grade Pickering stabilizers: Part. II. Improvement of emulsification and interfacial adsorption by electrostatic screening. *Food Hydrocolloids, 60*, 620–630.
Li, S., Zhang, B., Li, C., Fu, X., & Huang, Q. (2020b). Pickering emulsion gel stabilized by octenylsuccinate quinoa starch granule as lutein carrier: Role of the gel network. *Food Chemistry, 305*, Article 125476.
Lorenzo, G., Zaritzky, N., & Califano, A. (2013). Rheological analysis of emulsion-filled gels based on high acyl gellan gum. *Food Hydrocolloids, 30*, 672–680.
Lu, Y., Mao, L., Zheng, H., Chen, H., & Gao, Y. (2020). Characterization of β-carotene loaded emulsion gels containing denatured and native whey protein. *Food Hydrocolloids, 102*, Article 105600.
Luo, L.-J., Liu, F., & Tang, C.-H. (2013). The role of glycinin in the formation of gel-like soy protein-stabilized emulsions. *Food Hydrocolloids, 32*, 97–105.
Mao, L., Roos, Y. H., & Miao, S. (2014). Study on the rheological properties and volatile release of cold-set emulsion-filled protein gels. *Journal of Agricultural and Food Chemistry, 62*, 11420–11428.
Ma, L., Wan, Z., & Yang, X. (2017). Multiple water-in-oil-in-water emulsion gels based on self-assembled saponin fibrillar network for photosensitive cargo protection. *Journal of Agricultural and Food Chemistry, 65*, 9735–9743.
Montes de Oca-Ávalos, J. M., Huck-Iriart, C., Candal, R. J., & Herrera, M. L. (2016). Sodium caseinate/sunflower oil emulsion-based gels for structuring food. *Food and Bioprocess Technology, 9*, 981–992.
Nishinari, K., & Takahashi, R. (2003). Interaction in polysaccharide solutions and gels. *Current Opinion in Colloid & Interface Science, 8*, 396–400.
Nourbehesht, N., Shekarchizadeh, H., & Soltanizadeh, N. (2018). Investigation of stability, consistency, and oil oxidation of emulsion filled gel prepared by inulin and rice bran oil using ultrasonic radiation. *Ultrasonics Sonochemistry, 42*, 585–593.
Okada, K. S., & Lee, Y. (2017). Characterization of sodium mobility and binding by 23Na NMR spectroscopy in a model lipoproteic emulsion gel for sodium reduction. *Journal of Food Science, 82*, 1563–1568.
Oliver, L., Berndsen, L., van Aken, G. A., & Scholten, E. (2015). Influence of droplet clustering on the rheological properties of emulsion-filled gels. *Food Hydrocolloids, 50*, 74–83.
Oliver, L., Scholten, E., & van Aken, G. A. (2015). Effect of fat hardness on large deformation rheology of emulsion-filled gels. *Food Hydrocolloids, 43*, 299–310.
Oliver, L., Wieck, L., & Scholten, E. (2016). Influence of matrix inhomogeneity on the rheological properties of emulsion-filled gels. *Food Hydrocolloids, 52*, 116–125.
Ozturk, B., Argin, S., Ozilgen, M., & McClements, D. J. (2015). Formation and stabilization of nanoemulsion-based vitamin E delivery systems using natural biopolymers: Whey protein isolate and gum Arabic. *Food Chemistry, 188*, 256–263.
Paradiso, V. M., Giarnetti, M., Summo, C., Pasqualone, A., Minervini, F., & Caponio, F. (2015). Production and characterization of emulsion filled gels based on inulin and extra virgin olive oil. *Food Hydrocolloids, 45*, 30–40.
Pernetti, M., van Malssen, K. F., Flöter, E., & Bot, A. (2007). Structuring of edible oils by alternatives to crystalline fat. *Current Opinion in Colloid & Interface Science, 12*, 221–231.
Pintado, T., Herrero, A. M., Jimenez-Colmenero, F., Pasqualin Cavalheiro, C., & Ruiz-Capillas, C. (2018). Chia and oat emulsion gels as new animal fat replacers and healthy bioactive sources in fresh sausage formulation. *Meat Science, 135*, 6–13.
Pintado, T., Ruiz-Capillas, C., Jimenez-Colmenero, F., Carmona, P., & Herrero, A. M. (2015). Oil-in-water emulsion gels stabilized with chia (Salvia hispanica L.) and cold gelling agents: Technological and infrared spectroscopic characterization. *Food Chemistry, 185*, 470–478.
Piornos, J. A., Burgos-Díaz, C., Morales, E., Rubilar, M., & Acevedo, F. (2017). Highly efficient encapsulation of linseed oil into alginate/lupin protein beads: Optimization of the emulsion formulation. *Food Hydrocolloids, 63*, 139–148.
Poyato, C., Astiasarán, I., Barriuso, B., & Ansorena, D. (2015). A new polyunsaturated gelled emulsion as replacer of pork back-fat in burger patties: Effect on lipid composition, oxidative stability and sensory acceptability. *Lebensmittel-Wissenschaft und -Technologie- Food Science and Technology, 62*, 1069–1075.
Ringgenberg, E., Alexander, M., & Corredig, M. (2013). Effect of concentration and incubation temperature on the acid induced aggregation of soymilk. *Food Hydrocolloids, 30*, 463–469.
Ruffin, E., Schmit, T., Lafitte, G., Dollat, J. M., & Chambin, O. (2014). The impact of whey protein preheating on the properties of emulsion gel bead. *Food Chemistry, 151*, 324–332.
Sala, G., van Vliet, T., Cohen Stuart, M. A., Aken, G. A.v., & van de Velde, F. (2009). Deformation and fracture of emulsion-filled gels: Effect of oil content and deformation speed. *Food Hydrocolloids, 23*, 1381–1393.
Sato, A. C. K., Moraes, K. E. F. P., & Cunha, R. L. (2014). Development of gelled emulsions with improved oxidative and pH stability. *Food Hydrocolloids, 34*, 184–192.
Sawalha, H., den Adel, R., Venema, P., Bot, A., Floter, E., & van der Linden, E. (2012). Organogel-emulsions with mixtures of beta-sitosterol and gamma-oryzanol: Influence of water activity and type of oil phase on gelling capability. *Journal of Agricultural and Food Chemistry, 60*, 3462–3470.
Serdaroglu, M., Nacak, B., & Karabiyikoglu, M. (2017). Effects of beef fat replacement with gelled emulsion prepared with olive oil on quality parameters of chicken patties. *Korean Journal of Food Science Anim Resour, 37*, 376–384.
Serdaroğlu, M., & Öztürk, B. (2017). Use of olive oil-in-water gelled emulsions in model Turkey breast emulsions. *IOP Conference Series: Earth and Environmental Science, 85*,

Article 012071.
Shao, Y., & Tang, C.-H. (2016). Gel-like pea protein Pickering emulsions at pH3.0 as a potential intestine-targeted and sustained-release delivery system for β-carotene. *Food Research International, 79*, 64–72.
Sok Line, V. L., Remondetto, G. E., & Subirade, M. (2005). Cold gelation of β-lactoglobulin oil-in-water emulsions. *Food Hydrocolloids, 19*, 269–278.
Soukoulis, C., Cambier, S., Hoffmann, L., & Bohn, T. (2016). Chemical stability and bioaccessibility of β-carotene encapsulated in sodium alginate o/w emulsions: Impact of Ca 2+ mediated gelation. *Food Hydrocolloids, 57*, 301–310.
Soukoulis, C., Tsevdou, M., Andre, C. M., Cambier, S., Yonekura, L., Taoukis, P. S., et al. (2017). Modulation of chemical stability and *in vitro* bioaccessibility of beta-carotene loaded in kappa-carrageenan oil-in-gel emulsions. *Food Chemistry, 220*, 208–218.
de Souza Paglarinia, C., Martinib, S., & Pollonio, M. A. R. (2019). Using emulsion gels made with sonicated soy protein isolate dispersions to replace fat in frankfurters. *Lebensmittel-Wissenschaft und -Technologie- Food Science and Technology, 99*, 453–459.
de Souza Paglarini, C., de Figueiredo Furtado, G., Biachi, J. P., Vidal, V. A. S., Martini, S., Forte, M. B. S., et al. (2018). Functional emulsion gels with potential application in meat products. *Journal of Food Engineering, 222*, 29–37.
de Souza Paglarini, C., de Figueiredo Furtado, G., Honório, A. R., Mokarzel, L., da Silva Vidal, V. A., Ribeiro, A. P. B., et al. (2019). Functional emulsion gels as pork back fat replacers in Bologna sausage. *Food Structure, 20*, Article 100105.
Su, J., Guo, Q., Chen, Y., Dong, W., Mao, L., Gao, Y., et al. (2020). Characterization and formation mechanism of lutein pickering emulsion gels stabilized by β-lactoglobulin-gum Arabic composite colloidal nanoparticles. *Food Hydrocolloids, 98*, Article 105276.
Suzawa, E., & Kaneda, I. (2010). Rheological properties of agar microgel suspensions prepared using water-in-oil emulsions. *Journal of biorheology, 24*, 70–76.
Tang, C. H., Chen, L., & Foegeding, E. A. (2011). Mechanical and water-holding properties and microstructures of soy protein isolate emulsion gels induced by CaCl2, glucono-delta-lactone (GDL), and transglutaminase: Influence of thermal treatments before and/or after emulsification. *Journal of Agricultural and Food Chemistry, 59*, 4071–4077.
Tang, C.-H., Luo, L.-J., Liu, F., & Chen, Z. (2013). Transglutaminase-set soy globulin-stabilized emulsion gels: Influence of soy β-conglycinin/glycinin ratio on properties, microstructure and gelling mechanism. *Food Research International, 51*, 804–812.
Tang, C.-h., Yang, M., Liu, F., & Chen, Z. (2013). A novel process to efficiently form transglutaminase-set soy protein isolate-stabilized emulsion gels. *Lebensmittel-Wissenschaft und -Technologie- Food Science and Technology, 53*, 15–21.
Tolano-Villaverde, I. J., Torres-Arreola, W., Ocaño-Higuera, V. M., & Marquez-Rios, E. (2015). Thermal gelation of myofibrillar proteins from aquatic organisms. *CyTA - Journal of Food, 14*, 1–7.
Torres, O., Tena, N. M., Murray, B., & Sarkar, A. (2017). Novel starch based emulsion gels and emulsion microgel particles: Design, structure and rheology. *Carbohydrate Polymers, 178*, 86–94.
Van Vliet, T. (1988). Rheological properties of filled gels. Influence of filler matrix interaction. *Colloid & Polymer Science, 266*, 518–524.
Wakita, K., & Imura, T. (2018). High internal phase emulsion gels stabilized by natural casein peptides. *Journal of Oleo Science, 67*, 1579–1584.
Wang, Q., Jiang, J., & Xiong, Y. L. (2019a). Genipin-aided protein cross-linking to modify structural and rheological properties of emulsion-filled hempseed protein hydrogels. *Journal of Agricultural and Food Chemistry, 67*, 12895–12903.
Wang, X., Luo, K., Liu, S., Adhikari, B., & Chen, J. (2019b). Improvement of gelation properties of soy protein isolate emulsion induced by calcium cooperated with magnesium. *Journal of Food Engineering, 244*, 32–39.
Wang, X. F., Luo, K. Y., Liu, S. T., Zeng, M. M., Adhikari, B., He, Z. Y., et al. (2018). Textural and rheological properties of soy protein isolate tofu-type emulsion gels influence of soybean variety and coagulant type. *Food Biophysics, 13*, 324–332.
Wang, Z., Neves, M. A., Kobayashi, I., Uemura, K., & Nakajima, M. (2013). Preparation, characterization, and gastrointestinal digestibility of oil-in-water emulsion-agar gels. *Bioscience Biotechnology & Biochemistry, 77*, 467–474.
Wang, X., Xiong, Y. L., & Sato, H. (2017). Rheological enhancement of pork myofibrillar protein-lipid emulsion composite gels via glucose oxidase oxidation/transglutaminase cross-linking pathway. *Journal of Agricultural and Food Chemistry, 65*, 8451–8458.
Wang, L. J., Yin, S. W., Wu, L. Y., Qi, J. R., Guo, J., & Yang, X. Q. (2016). Fabrication and characterization of Pickering emulsions and oil gels stabilized by highly charged zein/chitosan complex particles (ZCCPs). *Food Chemistry, 213*, 462–469.
Wang, S., Zhang, Y., Chen, L., Xu, X., Zhou, G., Li, Z., et al. (2018). Dose-dependent effects of rosmarinic acid on formation of oxidatively stressed myofibrillar protein emulsion gel at different NaCl concentrations. *Food Chemistry, 243*, 50–57.
Wan, Z., Sun, Y., Ma, L., Yang, X., Guo, J., & Yin, S. (2017). Responsive emulsion gels with tunable properties formed by self-assembled nanofibrils of natural saponin glycyrrhizic acid for oil structuring. *Journal of Agricultural and Food Chemistry, 65*, 2394–2405.
Wouters, A. G., & Delcour, J. A. (2019). Cereal protein based nanoparticles as agents stabilizing air-water and oil-water interfaces in food systems. *Current Opinion in Food Science, 25*, 19–27.
Wu, M., Xiong, Y. L., & Chen, J. (2011). Role of disulphide linkages between protein-coated lipid droplets and the protein matrix in the rheological properties of porcine myofibrillar protein-peanut oil emulsion composite gels. *Meat Science, 88*, 384–390.
Wu, M., Xiong, Y. L., Chen, J., Tang, X., & Zhou, G. (2009). Rheological and microstructural properties of porcine myofibrillar protein-lipid emulsion composite gels. *Journal of Food Science, 74*, E207–E217.
Xiao, J., Wang, X.a., Gonzalez, A. J. P., & Huang, Q. (2016). Kafirin nanoparticles-stabilized Pickering emulsions: Microstructure and rheological behavior. *Food Hydrocolloids, 54*, 30–39.
Xi, Z., Liu, W., McClements, D. J., & Zou, L. (2019). Rheological, structural, and microstructural properties of ethanol induced cold-set whey protein emulsion gels: Effect of oil content. *Food Chemistry, 291*, 22–29.
Xu, W., Huang, L., Jin, W., Ge, P., Shah, B. R., Zhu, D., et al. (2019a). Encapsulation and release behavior of curcumin based on nanoemulsions-filled alginate hydrogel beads. *International Journal of Biological Macromolecules, 134*, 210–215.
Xu, Y. T., Liu, T. X., & Tang, C. H. (2019b). Novel pickering high internal phase emulsion gels stabilized solely by soy β-conglycinin. *Food Hydrocolloids, 88*, 21–30.
Yang, X., Gong, T., Li, D., Li, A., Sun, L., & Guo, Y. (2019). Preparation of high viscoelastic emulsion gels based on the synergistic gelation mechanism of xanthan and konjac glucomannan. *Carbohydrate Polymers, 226*, Article 115278.
Yang, X., Gong, T., Lu, Y.-h., Li, A., Sun, L., & Guo, Y. (2020a). Compatibility of sodium alginate and konjac glucomannan and their applications in fabricating low-fat mayonnaise-like emulsion gels. *Carbohydrate Polymers, 229*, Article 115468.
Yang, X., Li, A., Yu, W., Li, X., Sun, L., Xue, J., et al. (2020b). Structuring oil-in-water emulsion by forming egg yolk/alginate complexes: Their potential application in fabricating low-fat mayonnaise-like emulsion gels and redispersible solid emulsions. *International Journal of Biological Macromolecules, 147*, 595–606.
Ye, A., & Taylor, S. (2009). Characterization of cold-set gels produced from heated emulsions stabilized by whey protein. *International Dairy Journal, 19*, 721–727.
Yonekura, L., & Nagao, A. (2007). Intestinal absorption of dietary carotenoids. *Molecular Nutrition & Food Research, 51*, 107–115.
Zhang, C., & Zhang, H. (2018). Formation and stability of core-shell nanofibers by electrospinning of gel-like corn oil-in-water emulsions stabilized by gelatin. *Journal of Agricultural and Food Chemistry, 66*, 11681–11690.
Zhang, Z. P., Zhang, R. J., Zou, L. Q., Chen, L., Ahmed, Y., Bishri, W. A., et al. (2016). Encapsulation of curcumin in polysaccharide-based hydrogel beads. *Food Hydrocolloids, 58*, 160–170.
Zhao, X., Zou, Y.-F., Shao, J.-J., Chen, X., Han, M.-Y., & Xu, X.-L. (2017). Comparison of the acidic and alkaline treatment on emulsion composite gel properties of the proteins recovered from chicken breast by isoelectric solubilization/precipitation process. *Journal of Food Processing and Preservation, 41*, Article e12884.
Zheng, H., Mao, L., Cui, M., Liu, J., & Gao, Y. (2020). Development of food-grade bigels based on κ-carrageenan hydrogel and monoglyceride oleogels as carriers for β-carotene: Roles of oleogel fraction. *Food Hydrocolloids, 105*, Article 105855.
Zhou, F., Sun, W., & Zhao, M. (2015). Controlled formation of emulsion gels stabilized by salted myofibrillar protein under malondialdehyde (MDA)-induced oxidative stress. *Journal of Agricultural and Food Chemistry, 63*, 3766–3777.
Zhuang, X., Jiang, X., Zhou, H., Han, M., Liu, Y., Bai, Y., et al. (2019). The effect of insoluble dietary fiber on myofibrillar protein emulsion gels: Oil particle size and protein network microstructure. *Lebensmittel-Wissenschaft & Technologie, 101*, 534–542.
Zou, Y., Guo, J., Yin, S. W., Wang, J. M., & Yang, X. Q. (2015). Pickering emulsion gels prepared by hydrogen-bonded zein/tannic acid complex colloidal particles. *Journal of Agricultural and Food Chemistry, 63*, 7405–7414.
Zou, Y., Yang, X. Q., & Scholten, E. (2018). Rheological behavior of emulsion gels stabilized by zein/tannic acid complex particles. *Food Hydrocolloids, 77*, 363–371.

Food Hydrocolloids 113 (2021) 106537

Contents lists available at ScienceDirect

Food Hydrocolloids

journal homepage: http://www.elsevier.com/locate/foodhyd

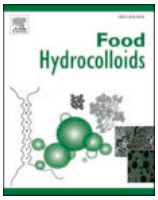

The role of mixing sequence in structuring O/W emulsions and emulsion gels produced by electrostatic protein-polysaccharide interactions between soy protein isolate-coated droplets and alginate molecules

Duanquan Lin [a,b], Alan L. Kelly [b], Song Miao [a,b,*]

[a] Teagasc Food Research Centre, Moorepark, Fermoy, Co, Cork, Ireland
[b] School of Food and Nutritional Sciences, University College Cork, Cork, Ireland

ARTICLE INFO

Keywords:
Emulsion gel
Electrostatic interaction
Addition sequence
Structure
SPI
Alginate

ABSTRACT

Multilayer emulsions produced by electrostatic protein-polysaccharide interactions have received increased interest recently, but the addition sequence of oppositely charged dispersions for emulsion preparation has rarely been investigated. The purpose of this study was to investigate the effect of addition sequence of oppositely charged soy protein isolate (SPI)-stabilized emulsions and alginate solutions on the stability and structure of emulsions involving electrostatic protein-polysaccharide attraction and the structural and rheological properties of emulsion gels produced by internal gelation. Stable multilayer emulsions containing unflocculated alginate/SPI-coated droplets were produced by adding low levels of SPI-stabilized emulsions into alginate solutions at pH 3.0, and emulsion gels prepared from the above emulsions had higher L* values and storage modulus than emulsion gels prepared by adding alginate solutions into SPI-stabilized emulsions. Unstable emulsions containing flocculated droplets were obtained on adding high levels of SPI-stabilized emulsions into alginate solutions or adding alginate solutions into SPI-stabilized emulsions (independent of concentration) at pH 3.0 with mild stirring. The findings of this study are important for preparing stable multilayer emulsions and structuring emulsion gels by changing the addition sequence of oppositely charged dispersions for emulsion preparation.

1. Introduction

Polysaccharide-based emulsion gels have received increasing interest in the food industry recently, such as κ-carrageenan-, gellan gum-, agar-, inulin- and alginate-based emulsion gels (Herrero, Ruiz-Capillas, Pintado, Carmona, & Jiménez-Colmenero, 2018; Lorenzo, Zaritzky, & Califano, 2013; Paradiso et al., 2015; Wang, Neves, Kobayashi, Uemura, & Nakajima, 2013; Zheng, Mao, Cui, Liu, & Gao, 2020). Compared to protein-based emulsion gels, polysaccharide-based (especially alginate-based) emulsion gels are less readily digested and damaged in gastric fluid, and the remaining gel structures can be further disrupted during intestinal digestion (Bokkhim, Bansal, Grøndahl, & Bhandari, 2016). These characteristics make polysaccharide-based emulsion gels ideal materials for encapsulation of compounds such as α-tocopherol, β-carotene, curcumin, and D-limonene (Feng, Yue, Ni, & Liang, 2018; Lević et al., 2015; Soukoulis et al., 2017; Xu et al., 2019), which can be protected from the harsh gastric environment and released from emulsion gels during intestinal digestion.

For preparation of emulsion gels, the first step is to prepare emulsions, in which emulsifiers are normally used to decrease the droplet size and increase the stability of droplets, and these emulsions can then be turned into emulsion gels by various mechanisms for different matrix materials (e.g., heat treatment, enzyme treatment, acidification treatment, and addition of ions) (Lin, Kelly, & Miao, 2020). Use of naturally occurring proteins (e.g., whey protein isolate (WPI), soy protein isolate (SPI), lactoferrin and zein) as emulsifiers has received increased attention for replacement of synthetic chemicals (e.g., Tween 20 and Span 80) in recent years, due to increased customer demand for healthy foods (Ruffin, Schmit, Lafitte, Dollat, & Chambin, 2014; Su et al., 2016; Tang, Luo, Liu, & Chen, 2013). In addition, electrostatic interactions between protein-coated droplets and polysaccharide molecules in the continuous phase (particularly oppositely charged proteins and polysaccharides) are critical, as these can affect the stability and structure of emulsions and thus the mechanical and structural properties of emulsion gels (Evans, Ratcliffe, & Williams, 2013; Tavernier, Patel, Van der Meeren, & Dewettinck, 2017).

* Corresponding author.
E-mail address: song.miao@teagasc.ie (S. Miao).

https://doi.org/10.1016/j.foodhyd.2020.106537
Received 25 August 2020; Received in revised form 4 December 2020; Accepted 9 December 2020
Available online 13 December 2020

Previous studies have shown that pectin/WPI-, alginate/β-lactoglobulin-, carboxymethylcellulose/sodium caseinate-, and pectin/β-lactoglobulin-stabilized emulsions had better stability than protein-stabilized emulsions at pH 4–4.5 (Guzey & McClements, 2007; Harnsilawat, Pongsawatmanit, & McClements, 2006; Liu et al., 2012; Salminen & Weiss, 2014), and that introducing chitosan into ovalbumin- or glycinin-stabilized emulsions could increase the stability of emulsions at pH 4.5–5.5 (Xiong et al., 2018; Yuan et al., 2013). Electrostatic interactions between oppositely charged protein-coated droplets and polysaccharide molecules led to the absorption of polysaccharide molecules onto the surfaces of protein-coated droplets, and thus the formation of polysaccharide/protein-coated bilayer droplets with increased surface charge and enhanced electrostatic repulsion (Evans et al., 2013).

Many factors can affect electrostatic interactions between oppositely charged protein-coated droplets and polysaccharide molecules, such as polymer properties (e.g., molecular weight, charge density and flexibility) and mixing conditions (e.g., the pH, ionic strength, temperature, stirring, ratio of protein to polysaccharide and addition sequence of dispersions), but the addition sequence of dispersions has rarely been discussed (Evans et al., 2013; Guzey & McClements, 2006; Ye, 2008). There are four main routes for preparing emulsions stabilized by electrostatic polysaccharide-protein complexes (Albano, Cavallieri, & Nicoletti, 2019). The following discussion mainly focuses on anionic polysaccharides, because most of charged polysaccharides are anionic.

Firstly, anionic polysaccharide/anionic protein mixtures may be prepared at pH > pI, and then oil introduced to the system to prepare emulsions by homogenization, followed by adjusting pH below the pI of the protein present. Secondly, the dispersion of anionic polysaccharide/cationic protein complex may be prepared at pH < pI, and emulsions prepared by adding oil and homogenization. Thirdly, anionic protein-stabilized emulsions can be mixed with anionic polysaccharide solutions at pH > pI, and then the pH of emulsions adjusted below the pI of the protein present. Finally, cationic protein-stabilized emulsions may be mixed with anionic polysaccharide solutions at pH < pI, which is the easiest way to prepare polysaccharide/protein-stabilized emulsions formed by electrostatic interactions.

Emulsions prepared by the first and second methods are termed mixed emulsions, while emulsions prepared by the third and fourth methods are called bilayer or layer-by-layer (LbL) emulsions (Golkar, Nasirpour, & Keramat, 2015). Bilayer emulsions show better stability than mixed emulsions, probably because of the higher charge density of bilayer emulsions, and are normally used to prepare polysaccharide-based emulsion gels (Azarikia, Abbasi, Scanlon, & McClements, 2017).

In addition, the addition sequence of oppositely charged protein-stabilized emulsions and polysaccharide solutions may affect the structure and stability of bilayer emulsions. It can be hypothesized that, when adding protein-stabilized emulsions into oppositely charged polysaccharide solutions, polysaccharides can attach to protein-coated droplets, leading to multilayer emulsions with or without flocculation, depending on the repulsive forces between polysaccharide/protein-coated droplets and unabsorbed polysaccharides in the continuous phase; however, when the content of protein-coated droplets exceeds a critical concentration on adding emulsions into polysaccharide solutions, polysaccharide levels may not be sufficient to interact with protein-coated droplets and bridging flocculation may occur (McClements, 2005).

On the other hand, when adding polysaccharide solutions into oppositely charged protein-stabilized emulsions, bridging flocculation may occur immediately, because insufficient polysaccharide molecules are shared by neighboring droplets; however, with continuously adding polysaccharide solutions into emulsions with strong mechanical stirring, stable emulsions without flocculation could be formed or depletion flocculation may occur (McClements, 2005). In addition, the structure of emulsion droplets can also affect the mechanical and structural properties of emulsion gels. According to the Kerner model modified by Lewis and Nielsen, emulsion gels containing flocculated droplets have improved mechanical properties compared to emulsion droplet-filled gels (Kerner, 1956; Lewis & Nielsen, 1970).

The purpose of this study was therefore to investigate the effect of the addition sequence of SPI-stabilized emulsions and alginate solutions on the stability and structure of emulsions and the structural and rheological properties of alginate-based emulsion gels. Sodium alginate, a linear unbranched anionic polysaccharide, has been widely investigated in the field of emulsion gels. In addition, using SPI as emulsifier has received increasing interest due to its good emulsifying capacity. SPI-stabilized emulsions and alginate solutions were thus investigated at pH 3.0, under which conditions SPI is positively charged, with good solubility and emulsifying capacity, and alginate is negatively charged.

2. Materials and methods

2.1. Materials

Defatted soy flour (Bob's Red Mill, Milwaukie, Oregon, USA) and sunflower oil (Aldi Stores Ltd., Kildare, Ireland) were purchased from iHerb and Aldi, respectively. Soy protein isolate (SPI) was extracted from defatted soy flour, according to the method described by Urbonaite, De Jongh, Van Der Linden, and Pouvreau (2015); the protein content of the SPI powder was 96.29 ± 0.03%. Sodium alginate (viscosity of 1 wt% sodium alginate solution in 0.15 M NaCl at 25 °C = 210–340 cP and $\overline{M}$ = 69–117 kDa) was obtained from Special Ingredients (Chesterfield, UK). *D*-(+)-Gluconic acid δ-lactone (GDL), calcium carbonate, sodium hydroxide, hydrochloric acid, and other analytical reagents were purchased from Sigma-Aldrich (St. Louis, MO, USA).

2.2. Solution/dispersion preparation

The SPI dispersion was prepared by mixing SPI powder with deionized water (0.5 : 94.5, w/w) and stirring at room temperature for 2 h using a magnetic stirrer, and then the pH of dispersion was adjusted to 3.0 with 1 M HCl and NaOH. Sodium alginate (0.4%, w/w) was mixed with deionized water by shearing at 400 rpm for 30 min with a magnetic stirrer and then allowed to rest for 24 h to permit hydration. The resulting 0.4 wt% sodium alginate solutions ($A_{0.4}$) were diluted to levels of 0.025 wt% ($A_{0.025}$), 0.05 wt% ($A_{0.05}$), 0.1 wt% ($A_{0.1}$), and 0.2 wt% ($A_{0.2}$) with deionized water, and then the pH was adjusted to 3.0 with 5 M HCl and NaOH.

2.3. Emulsion preparation

For preparation of SPI-stabilized emulsions, sunflower oil (5.0 wt% in emulsions, w/w) was mixed with the SPI dispersions (95.0 wt% in emulsions containing 0.5 wt% SPI, w/w) at 13,000 rpm for 2 min with an Ultra-Turrax (IKA-25, Staufen, Germany). The resulting emulsions ($E_{0.5}$) were diluted into $E_{0.1}$ (i.e., containing 0.1 wt% SPI and 1.0 wt% oil), $E_{0.2}$ (i.e., containing 0.2 wt% SPI and 2.0 wt% oil), $E_{0.3}$ (i.e., containing 0.3 wt% SPI and 3.0 wt% oil), and $E_{0.4}$ (i.e., containing 0.4 wt% SPI and 4.0 wt% oil) with deionized water (pH adjusted to 3.0 using 0.1 M HCl and 0.1 M NaOH), and the pH of emulsions was then adjusted to 3.0 with 0.5 M HCl and NaOH. SPI/polysaccharide-stabilized emulsions were prepared by adding one dispersion into the other slowly (1 mL/10 s) with stirring at 500 rpm for 5 min using a magnetic stirrer. The resulting samples were transferred to test tubes for further investigation.

2.4. Properties of emulsions

2.4.1. Morphological properties

Samples in test tubes were allowed to rest for 2 h, and then

photographs of samples were taken using a camera. The creaming or phase separation of samples may occur after being allowed to rest for 2 h. The top creaming layers were regarded as the upper portions, and the lower layers without cream were regarded as the lower portions. The turbidity and microstructure of both upper and lower portions of samples were investigated. The viscosity, droplet size and zeta potential of the bottom portion of samples were investigated; the upper and lower portions of samples were transferred by pipettes.

2.4.2. Turbidity measurements

The turbidity of the upper and lower portions of mixed emulsions was analysed with a Spectronic Genesys-5 UV spectrophotometer (Milton Roy Co., New York, USA). Samples were diluted 10 times with deionized water (pH adjusted to 3.0 by 0.1 M HCl and 0.1 M NaOH) before testing. The absorbance at 600 nm of samples was taken as the turbidity of dispersion.

2.4.3. Emulsion microstructure

Optical microscopy images of the upper and lower portions of mixed emulsions were recorded using an Olympus BX51 light microscope with a built-in camera (Olympus Optical Co. Ltd., Tokyo, Japan). Samples were dropped on a microscope slide, covered with a glass coverslip, and observed using a 10 × or 20 × objective lens and 10 × eyepiece.

2.4.4. Zeta potential measurements

The zeta potential of the lower portion of mixed emulsions was measured by particle electrophoresis technology using a laser particle analyser (Nano-ZS, Malvern Instruments, Worcestershire, UK). Samples were diluted 100 times (w/w) with ultrapure water (pH adjusted to 3.0 by 0.1 M HCl and 0.1 M NaOH) before testing. The operation temperature was set at 25 °C, and the refractive index and absorption index of samples were set at 1.48 and 0.001, respectively.

2.4.5. Size distribution measurements

The size distributions of oil droplets in the lower portion of mixed emulsions were analysed with a MasterSizer 3000 (Malvern Instruments Ltd., Worcestershire, UK). Samples were added to an automated wet dispersion unit until the obscuration reached between 1 and 10%. The stirrer speed was set at 2000 rpm. The refractive index and absorption index of samples were set at 1.48 and 0.001, respectively.

2.4.6. Rheological measurements

The viscosity of the lower portion of mixed emulsions was tested at 25 °C using an AR 2000ex rheometer (TA Instruments, Crawley, UK) with an aluminium parallel plate (60 mm in diameter, and 0.5 mm in gap). Each sample was added in the middle of the Peltier plate and allowed to stand for 2 min before testing. The flow measurement was performed over a shear rate range of 0.1–100 s^{-1}, and viscosity (η) was obtained from the data analysis software. The final results of viscosity were presented at a shear rate of 100 s^{-1}.

2.5. Emulsion gel preparation

Two emulsion samples $E_{0.1}A_{0.4}$ (i.e., adding emulsions (containing 0.1 wt% SPI and 1.0 wt% oil) into 0.4 wt% alginate solutions) and $A_{0.4}E_{0.1}$ (i.e., adding 0.4 wt% alginate solutions into emulsions containing 0.1 wt% SPI and 1.0 wt% oil) were prepared at pH 3.0 according to the methods described in Section 2.3. The control sample was prepared by adding deionized water (pH adjusted to 3.0 by 0.1 M HCl and 0.1 M NaOH) into the same volume of alginate solutions (0.4 wt%). GDL (10 mM) was added into the above samples followed by mixing at 500 rpm for 5 min, and then $CaCO_3$ (5 mM) was added and stirred at 500 rpm for 1 min. The resulting liquid mixtures were used to prepare emulsion gels by moving 30 mL samples into a beaker and incubating at 30 °C for 3 h.

2.6. Properties of emulsion gels

2.6.1. Morphological and microstructural properties of emulsion gels

For recording visual appearance of emulsion gels, emulsion gels were removed from beakers into a plastic Petri dish, and then photographs of samples were taken using a digital camera. For investigating the colour of emulsion gels, the liquid emulsion mixtures (3 mL, prepared in Section 2.5) containing 10 mM GDL and 5 mM $CaCO_3$ were transferred to plastic cuvettes (10 × 10 × 45 mm), and samples were incubated at 30 °C for 3 h to ensure the formation of emulsion gels. The colour parameter (L*) of emulsion gels in cuvettes was measured using a Minolta Chroma Meter CR-400 colorimeter (Minolta Ltd., Milton Keynes, UK).

For observing the microstructure of emulsion gels, the liquid emulsion mixtures (500 μl, prepared in Section 2.5) containing 10 mM GDL and 5 mM $CaCO_3$ were transferred to a glass slide, and the edge of samples between the coverslip and the glass slide was covered by a layer of silicone oil to prevent evaporation. These samples were incubated at 30 °C for 3 h to ensure the formation of emulsion gels. Optical microscopy images of emulsion gels were then recorded using an Olympus BX51 light microscope with a build-in camera (Olympus Optical Co. Ltd., Tokyo, Japan). Samples were observed using a 10 × or 20 × objective lens and 10 × eyepiece.

2.6.2. Dynamic rheological measurements of emulsion gels during gelation

The small deformation shear rheological properties of dispersions (time sweep) were tested at 30 °C using an AR 2000ex rheometer (TA Instruments, Crawley, UK) with an aluminium parallel plate (60 mm in diameter, and 1.0 mm in gap). Each liquid mixture sample prepared in Section 2.5 was added immediately in the middle of Peltier plate after preparation and allowed to stand for 2 min before testing. The edge of samples between the parallel plate and the Peltier plate was covered by a layer of silicone oil to prevent evaporation. Small-deformation shear measurement was performed at 0.01 wt% strain (within the linear viscoelastic regime) and a constant frequency of 1 Hz for 180 min. Storage modulus (G′) values were obtained from the data analysis software.

3. Results and discussion

3.1. Structuring alginate/SPI-stabilized emulsions

3.1.1. Adding SPI-stabilized emulsions into alginate solutions

Fig. 1A and B shows the visual appearance, turbidity and microscopic structures of mixtures prepared by adding various levels of SPI-stabilized emulsions (0.1–0.5 wt% SPI and 1.0–5.0 wt% oil) into 0.2 wt% alginate solutions (1:1) at pH 3.0, respectively. Adding low-concentration SPI-stabilized emulsions (0.1 wt% SPI and 1.0 wt% oil) into alginate solutions resulted in an alginate/SPI-stabilized emulsion ($E_{0.1}A_{0.2}$) without visible creaming, in which the turbidity of upper and lower portions of emulsions was not significantly different (Fig. 1A) and unflocculated droplets could be observed in both portions (Fig. 1B). In contrast, adding highly concentrated SPI-stabilized emulsions (0.2–0.5 wt% SPI and 2.0–5.0 wt% oil) into alginate solutions resulted in mixtures ($E_{0.2}A_{0.2}$–$E_{0.5}A_{0.2}$) that showed creaming, in which the turbidity of upper portions was significantly higher than that of lower portions of mixtures (Fig. 1A) and flocculated droplets could be observed in the upper portions of mixtures (Fig. 1B).

This indicates that adding high levels of SPI-stabilized emulsions into appositely charged alginate solutions (0.2 wt%) may lead to unstable emulsions, which was probably because 0.2 wt% alginate was insufficient to fully cover high levels of oppositely charged SPI-coated droplets (0.2–0.5 wt% SPI and 2.0–5.0 wt% oil) by electrostatic interactions.

Many factors can affect the concentration of polysaccharides which is needed to fully cover oppositely charged protein-coated droplets, such as the type and charge density of polyelectrolyte, the pH, temperature,

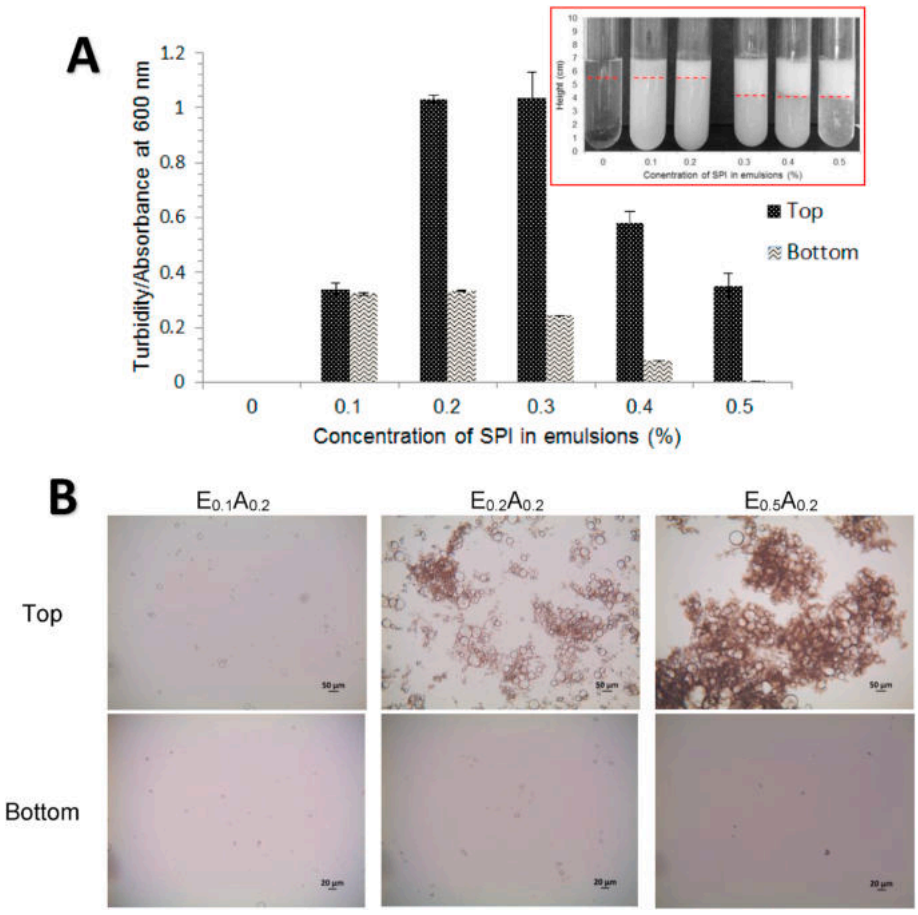

Fig. 1. (A) Turbidity and visual appearance (top right corner) and (B) microscopic structures of alginate/SPI-stabilized emulsions prepared by adding SPI-stabilized emulsions (0.1–0.5 wt% SPI and 1.0–5.0 wt% oil) into 0.2 wt% alginate solutions (1:1) at pH 3.0. The control sample was prepared by adding deionized water (pH 3.0) into 0.2 wt% alginate solutions (1:1). All samples were measured after creaming by being allowed to stand for 2 h after preparation. Red dashed lines separate the top and bottom portions of samples. (For interpretation of the references to colour in this figure legend, the reader is referred to the Web version of this article.)

and ionic strength of mixture system, and the concentration and size of emulsion droplets (Guzey & McClements, 2007). For example, it has been reported that emulsions containing 0.1 wt% corn oil and 0.005 wt % β-lactoglobulin can be fully covered by 0.003 wt% pectin solutions by electrostatic interactions at pH 4.0 (Guzey & McClements, 2007). It has also been reported that emulsions containing 5 wt% corn oil and 0.45 wt % β-lactoglobulin can be fully covered by 0.15 wt% pectin solutions through electrostatic interactions at pH 3.0 (Moreau, Kim, Decker, & McClements, 2003). Therefore, the zeta-potential and viscosity of the lower liquid phases of mixtures were further studied to investigate the electrostatic interactions between SPI-coated droplets and alginate molecules (Table 1).

SPI-coated droplets (zeta-potential of $+29.9 \pm 0.9$ mV in sample $A_0E_{0.1}$) and alginate molecules (zeta-potential of -20.2 ± 1.2 mV in sample $E_0A_{0.2}$) are oppositely charged at pH 3.0, and adding low-concentration SPI-stabilized emulsions (0.1 wt% SPI and 1.0 wt% oil) into alginate solutions decreased the zeta-potential of emulsion droplets to -29.3 ± 2.4 mV in sample $E_{0.1}A_{0.2}$ (Table 1). This indicates that alginate molecules were absorbed at the surfaces of SPI-coated droplets through electrostatic interactions, and thus positively charged SPI-coated droplets turned into negatively charged alginate/SPI-coated droplets in sample $E_{0.1}A_{0.2}$. With increasing emulsion concentrations (0.2–0.4 wt% SPI and 2.0–4.0 wt% oil) in the mixtures (i.e., $E_{0.2}A_{0.2}$–$E_{0.4}A_{0.2}$), the droplets in lower portion of mixtures shown similar zeta-potential with that of $E_{0.1}A_{0.2}$, while creaming occurred in samples $E_{0.2}A_{0.2}$–$E_{0.4}A_{0.2}$ (Fig. 1A and Table 1).

This indicates that alginate molecules in 0.2 wt% alginate solutions have been fully occupied in covering the surface of SPI-coated droplets in emulsions containing 0.1–0.2 wt% SPI and 1.0–2.0 wt% oil at pH 3.0 by electrostatic interactions between oppositely charged alginate molecules and SPI-coated droplets (Guzey & McClements, 2006). Therefore, there were no more alginate molecules available in the continuous phase to interact with further introduced SPI-stabilized droplets in samples $E_{0.2}A_{0.2}$–$E_{0.4}A_{0.2}$, and thus droplet flocculation occurred, due to the electrostatic interactions between positively charged SPI-stabilized droplets and negatively charged alginate/SPI-coated droplets. Then, creaming occurred in samples $E_{0.2}A_{0.2}$–$E_{0.4}A_{0.2}$ after being allowed to stand for 2 h (Fig. 1A), in which flocculated droplets moved to the upper phase and unflocculated alginate/SPI-coated droplets remained in the lower phase, which was seen from the non-significant differences in droplet size of samples $E_{0.2}A$–$E_{0.4}A$ (Table 1).

Meanwhile, the levels of remaining alginate/SPI-coated droplets in the lower phase of samples $E_{0.2}A_{0.2}$–$E_{0.5}A_{0.2}$ decreased with increased addition levels of SPI-stabilized emulsions, due to the interactions between alginate/SPI-coated droplets and further added SPI-coated droplets. This was also shown by the decreased viscosity of the lower liquid phases of samples $E_{0.1}A_{0.2}$–$E_{0.5}A_{0.2}$ (Table 1). In addition, the relatively

Table 1
Zeta potential, droplet/aggregate size ($d_{4,3}$) and viscosity of the lower liquid portions of alginate/SPI-stabilized emulsions prepared by adding SPI-stabilized emulsions (0.1–0.5 wt% SPI and 1.0–5.0 wt% oil) into 0.2 wt% alginate solutions (1:1) at pH 3.0.

	Zeta potential (mV)	$d_{4,3}$ (μm)	Viscosity (mPa·s)
$E_0A_{0.2}$	-20.2 ± 1.2^{b}	/	4.51 ± 0.12^{d}
$E_{0.1}A_{0.2}$	-29.3 ± 2.4^{c}	25.2 ± 4.1^{a}	4.21 ± 0.02^{d}
$E_{0.2}A_{0.2}$	-31.8 ± 1.7^{c}	25.3 ± 2.0^{a}	3.01 ± 0.04^{c}
$E_{0.3}A_{0.2}$	-29.8 ± 4.1^{c}	29.3 ± 2.1^{a}	2.11 ± 0.12^{b}
$E_{0.4}A_{0.2}$	-26.1 ± 1.7^{c}	24.0 ± 5.9^{a}	1.74 ± 0.06^{a}
$E_{0.5}A_{0.2}$	-10.3 ± 0.6^{a}	/	1.46 ± 0.09^{a}

[a-d] Values with different superscript letters in the same column are significantly different ($p < 0.01$).

clear lower liquid of sample $E_{0.5}A$ could not produce enough light obscuration to test its droplet size, which also indicates that there was a minimal level of alginate/SPI-coated emulsion droplets.

3.1.2. Adding alginate solutions into SPI-stabilized emulsions

Fig. 2A and B shows the visual appearance, turbidity and microscopic structures of mixtures prepared by adding different levels of alginate solutions (0.025–0.4 wt%) into SPI-stabilized emulsions containing 0.1 wt% SPI and 1.0 wt% oil (1:1) at pH 3.0, respectively. Adding alginate solutions into SPI-stabilized emulsions resulted in emulsions with visible creaming, in which the turbidity of upper and lower portions of emulsions were significantly different (Fig. 2A) and flocculated droplets could be observed in upper portions of all samples ($A_{0.025}E_{0.1}$–$A_{0.4}E_{0.1}$) and in the lower portions of samples $A_{0.2}E_{0.1}$ and $A_{0.4}E_{0.1}$ (Fig. 2B). This indicates that adding alginate solutions into SPI-stabilized emulsions with mild stirring led to unstable emulsions, independent of the concentration of alginate solutions.

In order to explain above phenomenon, the zeta-potential, droplet size and viscosity of the lower liquid phases of mixtures were further studied (Table 2). Adding 0.025 wt% alginate solutions into emulsions (containing 0.1 wt% SPI and 1.0 wt% oil) decreased the zeta-potential of the lower liquid phases of mixtures from $+29.9 \pm 0.9$ mV ($A_0E_{0.1}$) to -5.7 ± 2.1 mV ($A_{0.025}E_{0.1}$). This was probably because 0.025 wt% alginate (i.e., 0.0125 wt% in the final mixtures) was not enough to fully cover 0.1 wt% SPI molecules (i.e., 0.05 wt% SPI in the final mixtures) absorbed at droplet surfaces, which led to bridging flocculation (i.e., insufficient alginate molecules shared by neighboring SPI-coated droplets); then, creaming occurred on samples being allowed to stand for 2 h (Fig. 2A), in which flocculated droplets moved to the upper phase, leading to few remaining emulsion droplets and alginate molecules in the lower phase. With increasing alginate concentrations (0.05–0.4 wt %), the lower liquid phase of emulsions became more negatively charged (i.e., increased absolute values of zeta-potential) and had higher viscosity (Table 2), which both indicate an increased level of alginate molecules in the lower liquid layer.

Table 2
Zeta potential, droplet/aggregate size ($d_{4,3}$) and viscosity of the lower liquid portions of alginate/SPI-stabilized emulsions prepared by adding alginate solutions (0.025–0.4 wt%) into SPI-stabilized emulsions containing 0.1 wt% SPI and 1.0 wt% oil (1:1) at pH 3.0.

	Zeta potential (mV)	$d_{4,3}$ (μm)	Viscosity (mPa·s)
$A_0E_{0.1}$	$+29.9 \pm 0.9^{d}$	16.9 ± 0.3^{a}	0.99 ± 0.05^{ab}
$A_{0.025}E_{0.1}$	-5.7 ± 2.1^{c}	/	0.94 ± 0.02^{a}
$A_{0.05}E_{0.1}$	-14.3 ± 2.2^{b}	/	1.11 ± 0.03^{b}
$A_{0.1}E_{0.1}$	-20.3 ± 4.0^{ab}	/	1.72 ± 0.03^{c}
$A_{0.2}E_{0.1}$	-28.9 ± 2.2^{a}	154.25 ± 18.4^{c}	3.27 ± 0.06^{d}
$A_{0.4}E_{0.1}$	-27.8 ± 1.3^{a}	81.65 ± 11.0^{b}	7.39 ± 0.03^{e}

[a-e] Values with different superscript letters in the same column are significantly different ($p < 0.01$).

In addition, the particle size (Table 2) and microscopic pictures (Fig. 2B) of the lower phase of mixtures show that there were some flocculated droplets in the lower phase of samples $A_{0.2}E_{0.1}$ and $A_{0.4}E_{0.1}$, but there were hardly any unflocculated alginate-SPI-coated droplets. This result was unexpected, because it has been reported that, with increasing content of polyelectrolyte (C) in oppositely charged emulsions, stable emulsions without aggregation ($C = 0$), bridging flocculation ($0 < C < C_{saturation}$), stable emulsions without aggregation ($C_{saturation} < C < C_{depletion}$), and depletion flocculation ($C_{depletion} < C$) may occur (McClements, 2005). However, unflocculated alginate/SPI-coated droplets were not observed in all samples in this study, although there were sufficient alginate molecules in the

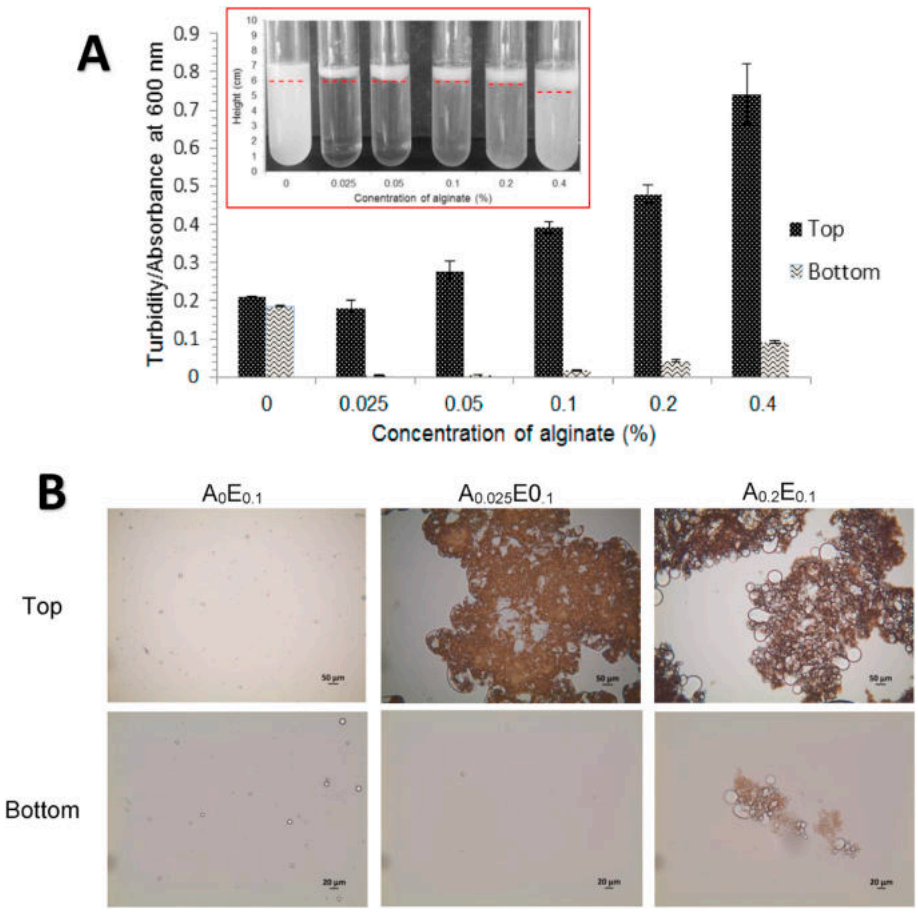

Fig. 2. (A) Turbidity and visual appearance (top left corner) and (B) microscopic structures of alginate/SPI-stabilized emulsions prepared by adding alginate solutions (0.025–0.4 wt%) into SPI-stabilized emulsions containing 0.1 wt% SPI and 1.0 wt% oil (1:1) at pH 3.0. The control sample was prepared by adding deionized water (pH 3.0) into SPI-stabilized emulsions (1:1). All samples were measured after creaming by being allowed to stand for 2 h after preparation. Red dashed lines separate the top and bottom portions of samples. (For interpretation of the references to colour in this figure legend, the reader is referred to the Web version of this article.)

continuous phase to dispel bridging flocculation and then form stable emulsions (Table 2).

The reason for this phenomenon is probably because of the preparation method used in this study. Alginate solutions were slowly added into SPI-stabilized emulsions, and thus bridging flocculation occurred in all samples at the initial stage of the addition process, due to there being insufficient alginate molecules present; however, when large numbers of alginate molecules were present in the continuous phase after adding higher levels of alginate solutions, the magnetic stirring force was not high enough to break bridging-flocculated droplets and promote further absorption of alginate molecules at the surfaces of SPI-coated droplets, to form stable emulsions without droplet aggregates.

3.1.3. Mechanism of structuring emulsions on mixing of dispersions

In order to understand the effect of the addition sequence of dispersions on the structure, stability and rheological properties of emulsions produced by electrostatic adsorption, emulsion samples $E_{0.1}A_{0.2}$ and $A_{0.2}E_{0.1}$ were compared (Figs. 1 and 2). $E_{0.1}A_{0.2}$ and $A_{0.2}E_{0.1}$ were prepared by the same components (i.e., 0.2 wt% alginate solutions and SPI-stabilized emulsions containing 0.1 wt% SPI and 1 wt% oil) but with different addition sequences of dispersions (i.e., adding emulsions into alginate solutions for $E_{0.1}A_{0.2}$ and adding alginate solutions into emulsions for $A_{0.2}E_{0.1}$). Figs. 1 and 2 show that $E_{0.1}A_{0.2}$ had better stability than $A_{0.2}E_{0.1}$, and that $E_{0.1}A_{0.2}$ contained unflocculated droplets while $A_{0.2}E_{0.1}$ contained flocculated droplets. This indicates that adding protein-stabilized emulsions into oppositely charged polysaccharide solutions is a better way to prepare stable multilayer emulsions induced by electrostatic adsorption than adding polysaccharide solutions into emulsions under mild stirring conditions.

The proposed mechanism is that, when adding protein-stabilized emulsions into oppositely charged polysaccharide solutions slowly, levels of polysaccharide molecules are sufficient at the beginning of the process and protein-coated droplets can be fully covered by polysaccharide molecules through electrostatic interactions, which leads to stable multilayer emulsions (Fig. 3A). However, when the level of added emulsions exceeds the saturation concentration and there are not polysaccharide molecules available in the continuous phase, flocculation occurs because of electrostatic interactions between polysaccharide/protein-coated droplets and the additional protein-stabilized droplets being added. On the other hand, when adding polysaccharide solutions into oppositely charged protein-stabilized emulsions, protein-stabilized droplets are present in excess at the beginning and they cannot be fully covered by polysaccharide molecules, which leads to bridging flocculation (Fig. 3B). However, mild mixing cannot provide enough energy to break down bridging-flocculated droplets, and then stable emulsions containing unflocculated droplets do not occur, although there are sufficient polysaccharide molecules in the continuous phase after adding high levels of polysaccharide solutions.

This mechanism not only explains the effect of addition sequence of dispersions and polysaccharide/protein ratio on the structure and stability of multilayer emulsions formed by electrostatic interactions between oppositely charged protein–coated droplets and polysaccharide molecules, but also indicates that structuring polysaccharide-based and protein-stabilized emulsion gels can be controlled by changing the addition sequence of dispersions and adjusting the polysaccharide/protein ratio. It can be assumed that adding low levels of protein-stabilized emulsions into polysaccharide solutions tends to lead to formation of emulsion gels containing unflocculated emulsion droplets; however, adding polysaccharide solutions into protein-stabilized emulsions tends to give emulsion gels containing flocculated emulsion droplets. Therefore, further research was carried out to investigate the effect of addition sequence of dispersions on the structural and rheological properties of alginate-based and alginate/SPI-stabilized emulsion gels.

3.2. Structuring alginate/SPI-stabilized emulsion gels by addition sequence

3.2.1. Morphological and structural properties of emulsion gels

Fig. 4A–F shows the visual appearance and microstructure of gels prepared from the control sample $E_0A_{0.4}$, sample $E_{0.1}A_{0.4}$ and sample $A_{0.4}E_{0.1}$, respectively. Alginate gels (i.e., control samples) were transparent with many bubbles in matrices (Fig. 4A and D). This was because the internal gelation was used in this study to trigger the formation of alginate-based gels, in which calcium ions are liberated gradually from the insoluble $CaCO_3$ by the interaction between GDL and $CaCO_3$,

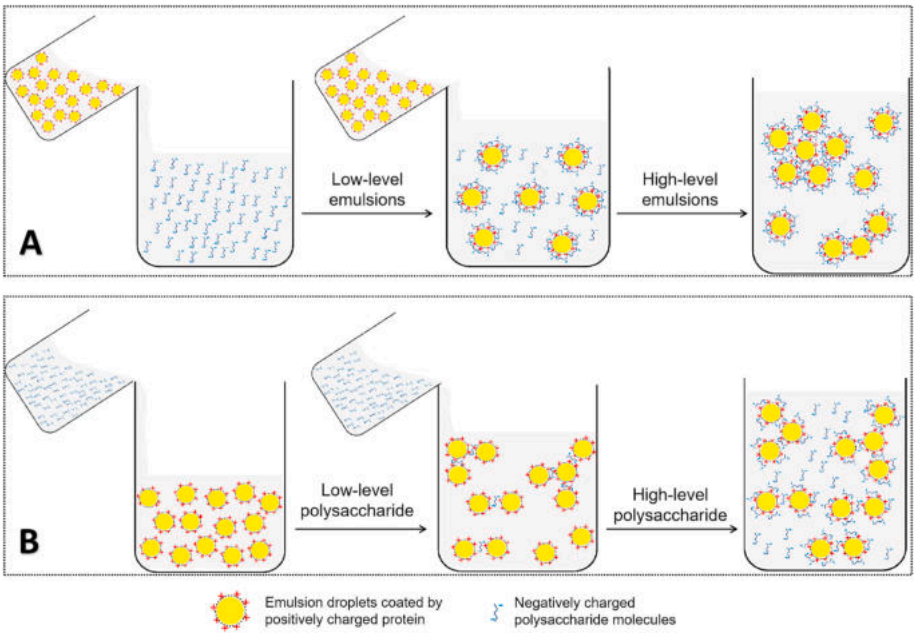

Fig. 3. A proposed mechanism for the effect of addition sequence of oppositely charged protein-stabilized emulsions and polysaccharide solutions on the structure of emulsions: (A) adding protein-stabilized emulsions into oppositely charged polysaccharide solutions slowly or (B) adding polysaccharide solutions into oppositely charged protein-stabilized emulsions slowly.

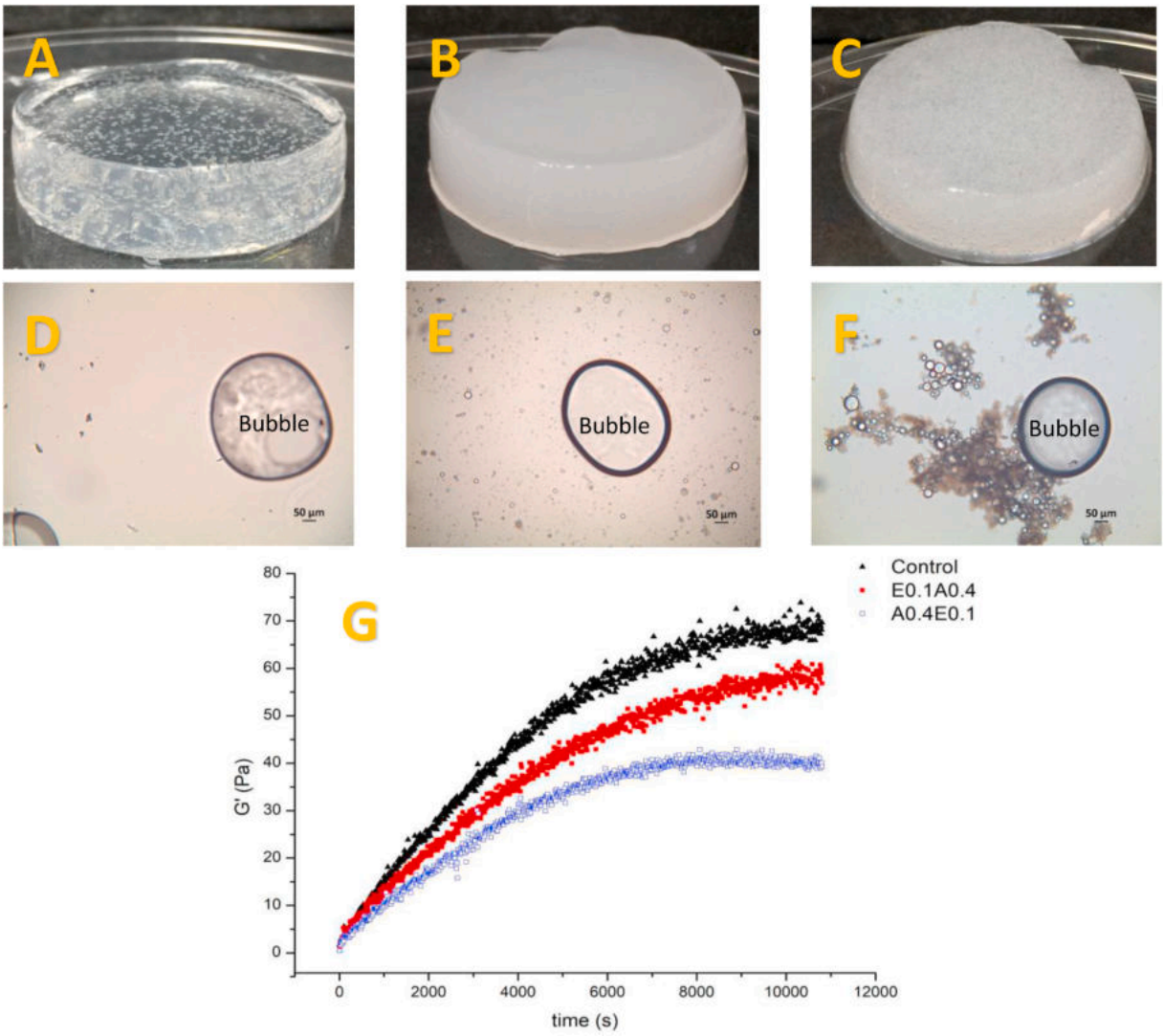

Fig. 4. (A–C) Visual appearance and (D–F) microstructure of emulsion gels prepared from (A and D) the control sample (i.e., adding deionized water (pH 3.0) into 0.4 wt% alginate solutions, 1:1) (B and E) sample $E_{0.1}A_{0.4}$ (i.e., adding emulsions containing 0.1 wt% SPI and 1.0 wt% oil into alginate solutions), and (C and F) sample $A_{0.4}E_{0.1}$ (i.e., adding alginate solutions into emulsions), respectively. (G) The gelation kinetics of the control sample, sample $E_{0.1}A_{0.4}$ and sample $A_{0.4}E_{0.1}$ induced by internal gelation.

followed by the Ca^{2+}-induced association of alginate chains; CO_2 was also produced during this process and thus small CO_2 gas bubbles occurred in gel matrices.

Emulsion gels produced from sample $E_{0.1}A_{0.4}$ were ivory in colour with L* values of 36.37 ± 0.16, and CO_2 bubbles also occurred in gel matrices (Fig. 4B and E). This was because adding emulsions into alginate solutions (i.e., sample $E_{0.1}A_{0.4}$) led to the formation of unflocculated multilayer droplets evenly distributed in mixed emulsions with high turbidity (i.e., the absorbance of 0.470 ± 0.002 at 600 nm) and thus the formation of emulsion gels with uniform opaque appearance (Lin, Kelly, Maidannyk, et al., 2020). In contrast, emulsion gels produced from sample $A_{0.4}E_{0.1}$ were semi-transparent with L* values of 35.92 ± 0.31, and emulsion aggregates and CO_2 gas bubbles distributed in the matrices (Fig. 4C). This was because adding alginate solutions into emulsions (i.e., sample $A_{0.4}E_{0.1}$) tended to form unstable emulsions containing flocculated droplets (Fig. 4F) with low turbidity (i.e., absorbance values of 0.245 ± 0.014 at 600 nm) and thus resulted in the formation of emulsion gels with an inhomogeneous appearance.

These results indicate that the structural and morphological properties of alginate-based and alginate/SPI-stabilized emulsion gels are affected by the addition sequence of SPI-stabilized emulsions and alginate solutions for emulsion preparation. In addition, many studies have indicated that structures of emulsion gels (e.g., the matrix structure and state of droplets) affected their mechanical properties (Chen, Dickinson, Langton, & Hermansson, 2000; Lin, Kelly, & Miao, 2020; Tang, Chen, & Foegeding, 2011), so the effect of the addition sequence of SPI-stabilized emulsions and alginate solutions on the gelation kinetics of emulsion gels was further investigated.

3.2.2. *Gelation kinetics of alginate-based emulsion gels*

Fig. 4G shows the evolution of the dynamic storage modulus (G') of the control sample, sample $E_{0.1}A_{0.4}$ and sample $A_{0.4}E_{0.1}$ during gelation. G' values of the control sample increased up to 2.5 h and then reached a plateau during gelation. The progressive introduction of calcium ions which results from the interaction between GDL and $CaCO_3$ leads to the progressive gelation of alginate molecules and gradually increased G' value of alginate gels. Many factors can influence the kinetics of alginate gel formation, such as the molecular weight of alginate, alginate concentration, calcium concentration, and applied shear rate during rheological measurements (Farrés & Norton, 2014).

The storage modulus of sample $E_{0.1}A_{0.4}$ reached a plateau at 2.5 h, which was similar to the control sample during gelation (Fig. 4G). This

was because emulsions produced by adding SPI-stabilized emulsions into oppositely charged alginate solutions (i.e., $E_{0.1}A_{0.4}$) tended to contain unflocculated droplets, which did not significantly affect the alginate concentration in the continuous phase, although some alginate molecules were adsorbed at the o/w interfaces. In addition, sample $E_{0.1}A_{0.4}$ had lower G' values than the control sample during gelation, and the G' values of the control sample and $E_{0.1}A_{0.4}$ were 68.5 ± 1.6 Pa and 59.4 ± 1.8 Pa at plateau, respectively (Fig. 4G). This was because the mechanical properties of emulsion gels are determined by the matrix (i.e., matrix material and gelation mechanism), emulsion droplets (i.e., oil type, oil content, and droplet size) and the interaction between them (i.e., active and inactive fillers) (Lin, Kelly, & Miao, 2020; Sala, Van Vliet, Stuart, Van Aken, & Van de Velde, 2009).

Positively charged SPI-coated droplets are active fillers in negatively charged alginate-based matrices in the current study, due to electrostatic attraction between them (Sala et al., 2009). According to the Kerner model (Kerner, 1956), introducing active fillers into gels can increase the mechanical properties of gels (i.e., $G'_{emulsion\ gels} > G'_{hydrogels}$ or G'_{matrix}). However, the matrix of emulsion gels plays a more important role than emulsion droplets in determining the mechanical properties of emulsion gels (i.e., $G'_{emulsion\ gels} = G'_{matrix} + 0.22–0.27G'_{matrix}$ according to the Kerner model) (Lin, Kelly, Maidannyk, & Miao, 2021). When SPI-stabilized emulsions are mixed with alginate solutions, some unadsorbed insoluble SPI particles are also introduced into the continuous phase of mixtures, which may negatively affect Ca^{2+}-induced association of alginate molecules during gelation and decrease the mechanical properties of alginate-based emulsion gels. Our previous study has indicated that alginate- and SPI/alginate-based gel beads had similar gelation kinetics (i.e., Young's modulus increased up to 6 min) induced by the external gelation, but SPI/alginate-based gel beads had lower Young's modulus than alginate-based gel beads, probably due to insoluble SPI molecules acting as solid barriers in alginate gels (Lin, Kelly, Maidannyk, et al., 2020).

Fig. 4G also shows that sample $A_{0.4}E_{0.1}$ had a different gelation rate (i.e., reached the plateau faster, with a lower G' value of 40.3 ± 0.7 Pa at 1.9 h, compared to the control sample and sample $E_{0.1}A_{0.4}$). This was because emulsions (i.e., $A_{0.4}E_{0.1}$) produced by adding alginate solutions into oppositely charged SPI-stabilized emulsions tended to contain flocculated droplets, which entrapped some alginate molecules in aggregates (McClements, 2015). Although the Kerner model as modified by Lewis and Nielsen indicates that aggregated droplets can increase the effective volume fraction of fillers and modulus of emulsion gels (Lewis & Nielsen, 1970), the matrix of emulsion gels plays a more important role than emulsion droplets in affecting the mechanical properties of emulsion gels. Adding alginate solutions into oppositely charged SPI-stabilized emulsions not only reduces the alginate concentration in the continuous phase, because of the formation droplet flocculation entrapping some alginate molecules, but also introduces some unabsorbed insoluble SPI particles into the continuous phase, which decreased both the G' values of emulsion gels and the time needed to reach the plateau during gelation.

4. Conclusions

The stability and structure of emulsions involving electrostatic protein-polysaccharide interactions can be influenced by the addition sequence of oppositely charged dispersions. Adding a low concentration of protein-stabilized emulsions into polysaccharide solutions is a better method to prepare stable emulsions than adding polysaccharide solutions into protein-stabilized emulsions with mild stirring. In addition, visual appearance, droplet structure and gel strength of emulsion gels can also be adjusted by the addition sequence of oppositely charged dispersions for emulsion preparation. Emulsions which were prepared by adding SPI-stabilized emulsions (0.1 wt% SPI and 1.0 wt% oil) into 0.4 wt% alginate solutions (i.e., $E_{0.1}A_{0.4}$) led to emulsion gels with more unflocculated droplets, higher L* and modulus and slower gelation kinetics than emulsion gels prepared from sample $A_{0.4}E_{0.1}$ (i.e., adding 0.4 wt% alginate solutions into SPI-stabilized emulsions containing 0.1 wt% SPI and 1.0 wt% oil). However, this study mainly focused on the effect of addition sequence on the mechanical and structural properties of emulsion gels, so further research on the application of above different emulsion gels (e.g., for encapsulation of food nutrients or as fat replacers) is needed.

CRediT authorship contribution statement

Duanquan Lin: Conceptualization, Methodology, Writing - original draft, Data curation, Investigation. **Alan L. Kelly:** Supervision, Writing - review & editing. **Song Miao:** Supervision, Conceptualization, Writing - review & editing, Funding acquisition, Project administration, Investigation.

Declaration of competing interest

The authors declare that they have no known competing financial interests or personal relationships that could have appeared to influence the work reported in this paper.

Acknowledgement

This work was supported by the China Scholarship Council (No. 201708350111) and Teagasc-The Irish Agriculture and Food Development Authority (RMIS6821).

Appendix A. Supplementary data

Supplementary data to this article can be found online at https://doi.org/10.1016/j.foodhyd.2020.106537.

References

Albano, K. M., Cavallieri, Â. L. F., & Nicoletti, V. R. (2019). Electrostatic interaction between proteins and polysaccharides: Physicochemical aspects and applications in emulsion stabilization. *Food Reviews International, 35*, 54–89.

Azarikia, F., Abbasi, S., Scanlon, M. G., & McClements, D. J. (2017). Emulsion stability enhancement against environmental stresses using whey protein–tragacanthin complex: Comparison of layer-by-layer and mixing methods. *International Journal of Food Properties, 20*, 2084–2095.

Bokkhim, H., Bansal, N., Grøndahl, L., & Bhandari, B. (2016). *In-vitro* digestion of different forms of bovine lactoferrin encapsulated in alginate micro-gel particles. *Food Hydrocolloids, 52*, 231–242.

Chen, J., Dickinson, E., Langton, M., & Hermansson, A. M. (2000). Mechanical properties and microstructure of heat-set whey protein emulsion gels: Effect of emulsifiers. *Lebensmittel-Wissenschaft und -Technologie- Food Science and Technology, 33*, 299–307.

Evans, M., Ratcliffe, I., & Williams, P. A. (2013). Emulsion stabilisation using polysaccharide–protein complexes. *Current Opinion in Colloid & Interface Science, 18*, 272–282.

Farrés, I. F., & Norton, I. (2014). Formation kinetics and rheology of alginate fluid gels produced by in-situ calcium release. *Food Hydrocolloids, 40*, 76–84.

Feng, W., Yue, C., Ni, Y., & Liang, L. (2018). Preparation and characterization of emulsion-filled gel beads for the encapsulation and protection of resveratrol and α-tocopherol. *Food Research International, 108*, 161–171.

Golkar, A., Nasirpour, A., & Keramat, J. (2015). β-lactoglobulin-Angum gum (Amygdalus Scoparia Spach) complexes: Preparation and emulsion stabilization. *Journal of Dispersion Science and Technology, 36*, 685–694.

Guzey, D., & McClements, D. J. (2006). Formation, stability and properties of multilayer emulsions for application in the food industry. *Advances in Colloid and Interface Science, 128*, 227–248.

Guzey, D., & McClements, D. J. (2007). Impact of electrostatic interactions on formation and stability of emulsions containing oil droplets coated by β-lactoglobulin−pectin complexes. *Journal of Agricultural and Food Chemistry, 55*, 475–485.

Harnsilawat, T., Pongsawatmanit, R., & McClements, D. J. (2006). Influence of pH and ionic strength on formation and stability of emulsions containing oil droplets coated by β-lactoglobulin−alginate interfaces. *Biomacromolecules, 7*, 2052–2058.

Herrero, A. M., Ruiz-Capillas, C., Pintado, T., Carmona, P., & Jiménez-Colmenero, F. (2018). Elucidation of lipid structural characteristics of chia oil emulsion gels by Raman spectroscopy and their relationship with technological properties. *Food Hydrocolloids, 77*, 212–219.

Kerner, E. (1956). The elastic and thermo-elastic properties of composite media. *Proceedings of the Physical Society Section B, 69*, 808.

Lević, S., Lijaković, I. P., Đorđević, V., Rac, V., Rakić, V., Knudsen, T.Š., et al. (2015). Characterization of sodium alginate/D-limonene emulsions and respective calcium alginate/*D*-limonene beads produced by electrostatic extrusion. *Food Hydrocolloids, 45*, 111–123.

Lewis, T. B., & Nielsen, L. E. (1970). Dynamic mechanical properties of particulate-filled composites. *Journal of Applied Polymer Science, 14*, 1449–1471.

Lin, D., Kelly, A. L., Maidannyk, V., & Miao, S. (2020a). Effect of concentrations of alginate, soy protein isolate and sunflower oil on water loss, shrinkage, elastic and structural properties of alginate-based emulsion gel beads during gelation. *Food Hydrocolloids, 108*, 105998.

Lin, D., Kelly, A. L., Maidannyk, V., & Miao, S. (2021). Effect of structuring emulsion gels by whey or soy protein isolate on the structure, mechanical properties, and *in-vitro* digestion of alginate-based emulsion gel beads. *Food Hydrocolloids, 110*, 106165.

Lin, D., Kelly, A. L., & Miao, S. (2020b). Preparation, structure-property relationships and applications of different emulsion gels: Bulk emulsion gels, emulsion gel particles, and fluid emulsion gels. *Trends in Food Science & Technology, 102*, 123–137.

Liu, L., Zhao, Q., Liu, T., Kong, J., Long, Z., & Zhao, M. (2012). Sodium caseinate/carboxymethylcellulose interactions at oil–water interface: Relationship to emulsion stability. *Food Chemistry, 132*, 1822–1829.

Lorenzo, G., Zaritzky, N., & Califano, A. (2013). Rheological analysis of emulsion-filled gels based on high acyl gellan gum. *Food Hydrocolloids, 30*, 672–680.

McClements, D. J. (2005). Theoretical analysis of factors affecting the formation and stability of multilayered colloidal dispersions. *Langmuir, 21*, 9777–9785.

McClements, D. J. (2015). *Food emulsions: Principles, practices, and techniques*. Boca Raton, FL: CRC press.

Moreau, L., Kim, H.-J., Decker, E. A., & McClements, D. J. (2003). Production and characterization of oil-in-water emulsions containing droplets stabilized by *β*-lactoglobulin−pectin membranes. *Journal of Agricultural and Food Chemistry, 51*, 6612–6617.

Paradiso, V. M., Giarnetti, M., Summo, C., Pasqualone, A., Minervini, F., & Caponio, F. (2015). Production and characterization of emulsion filled gels based on inulin and extra virgin olive oil. *Food Hydrocolloids, 45*, 30–40.

Ruffin, E., Schmit, T., Lafitte, G., Dollat, J.-M., & Chambin, O. (2014). The impact of whey protein preheating on the properties of emulsion gel bead. *Food Chemistry, 151*, 324–332.

Sala, G., Van Vliet, T., Stuart, M. A. C., Van Aken, G. A., & Van de Velde, F. (2009). Deformation and fracture of emulsion-filled gels: Effect of oil content and deformation speed. *Food Hydrocolloids, 23*, 1381–1393.

Salminen, H., & Weiss, J. (2014). Electrostatic adsorption and stability of whey protein–pectin complexes on emulsion interfaces. *Food Hydrocolloids, 35*, 410–419.

Soukoulis, C., Tsevdou, M., Andre, C. M., Cambier, S., Yonekura, L., Taoukis, P. S., et al. (2017). Modulation of chemical stability and *in vitro* bioaccessibility of beta-carotene loaded in kappa-carrageenan oil-in-gel emulsions. *Food Chemistry, 220*, 208–218.

Su, J., He, X., Guo, Z., Jian, J., Gao, Y., & Yuan, F. (2016). Impact on morphological characterization and emulsion stability of lactoferrin–beet pectin electrostatic complexes. *Journal of Dispersion Science and Technology, 37*, 927–940.

Tang, C. H., Chen, L., & Foegeding, E. A. (2011). Mechanical and water-holding properties and microstructures of soy protein isolate emulsion gels induced by $CaCl_2$, glucono-delta-lactone (GDL), and transglutaminase: Influence of thermal treatments before and/or after emulsification. *Journal of Agricultural and Food Chemistry, 59*, 4071–4077.

Tang, C. H., Luo, L. J., Liu, F., & Chen, Z. (2013). Transglutaminase-set soy globulin-stabilized emulsion gels: Influence of soy *β*-conglycinin/glycinin ratio on properties, microstructure and gelling mechanism. *Food Research International, 51*, 804–812.

Tavernier, I., Patel, A. R., Van der Meeren, P., & Dewettinck, K. (2017). Emulsion-templated liquid oil structuring with soy protein and soy protein : *κ*-Carrageenan complexes. *Food Hydrocolloids, 65*, 107–120.

Urbonaite, V., De Jongh, H., Van Der Linden, E., & Pouvreau, L. (2015). Water holding of soy protein gels is set by coarseness, modulated by calcium binding, rather than gel stiffness. *Food Hydrocolloids, 46*, 103–111.

Wang, Z., Neves, M. A., Kobayashi, I., Uemura, K., & Nakajima, M. (2013). Preparation, characterization, and *in vitro* gastrointestinal digestibility of oil-in-water emulsion–agar gels. *Bioscience Biotechnology and Biochemistry*, 120659.

Xiong, W., Ren, C., Tian, M., Yang, X., Li, J., & Li, B. (2018). Emulsion stability and dilatational viscoelasticity of ovalbumin/chitosan complexes at the oil-in-water interface. *Food Chemistry, 252*, 181–188.

Xu, W., Huang, L., Jin, W., Ge, P., Shah, B. R., Zhu, D., et al. (2019). Encapsulation and release behavior of curcumin based on nanoemulsions-filled alginate hydrogel beads. *International Journal of Biological Macromolecules, 134*, 210–215.

Ye, A. (2008). Complexation between milk proteins and polysaccharides via electrostatic interaction: Principles and applications–a review. *International Journal of Food Science and Technology, 43*, 406–415.

Yuan, Y., Wan, Z.-L., Yin, S.-W., Teng, Z., Yang, X.-Q., Qi, J.-R., et al. (2013). Formation and dynamic interfacial adsorption of glycinin/chitosan soluble complex at acidic pH: Relationship to mixed emulsion stability. *Food Hydrocolloids, 31*, 85–93.

Zheng, H., Mao, L., Cui, M., Liu, J., & Gao, Y. (2020). Development of food-grade bigels based on *κ*-carrageenan hydrogel and monoglyceride oleogels as carriers for *β*-carotene: Roles of oleogel fraction. *Food Hydrocolloids*, 105855.

Food Hydrocolloids 108 (2020) 105998

Contents lists available at ScienceDirect

Food Hydrocolloids

journal homepage: http://www.elsevier.com/locate/foodhyd

Effect of concentrations of alginate, soy protein isolate and sunflower oil on water loss, shrinkage, elastic and structural properties of alginate-based emulsion gel beads during gelation

Duanquan Lin [a,b], Alan L. Kelly [b], Valentyn Maidannyk [a], Song Miao [a,b,c,*]

[a] Teagasc Food Research Centre, Moorepark, Fermoy, Co. Cork, Ireland
[b] School of Food and Nutritional Sciences, University College Cork, Cork, Ireland
[c] China-Ireland International Cooperation Centre for Food Material Science and Structure Design, Fuzhou, China

ARTICLE INFO

Keywords:
Alginate
Elastic property
Emulsion gel bead
Microstructure
Shrinkage
Soy protein isolates

ABSTRACT

The aim of this study was to investigate the influence of concentrations of sodium alginate (0.5%–1.5% in the water phase of an emulsion), soy protein isolate (SPI, 0.5%–2.0% in the water phase) and oil phase (10%–40% in the emulsion) on the properties (including water loss, shrinkage, morphological, elastic, and structural properties) of emulsion gel beads during gelation (0–30 min). Gel beads were prepared with external gelation by dropping emulsions into $CaCl_2$ solutions using pipettes. The Young's modulus of emulsion gel beads kept increasing during gelation before reaching a plateau accompanied by syneresis (i.e., water loss), shrinkage, and structural tightening. SPI absorbed at the surface of oil droplets could prevent re-coalescence of droplets during gelation. Additionally, increasing concentrations of sodium alginate and oil increased the Young's modulus of gel beads. Water loss decreased with increasing contents of alginate, SPI and oil, and shrinkage could be diminished by increasing alginate and oil contents.

1. Introduction

Emulsion gels, also called emulgels, are a complex colloidal material which have some properties of both emulsions and gels (Dickinson, 2012). During the last decade, emulsion gels have received growing interest, due to their advantages compared to emulsions, such as higher storage stability by reducing oil and water phase movement and lipid oxidation (Ma, Wan, & Yang, 2017) and slower intestinal drug release, due to improved protective effects against gastric and intestinal phases (Corstens et al., 2017; Guo, Bellissimo, & Rousseau, 2017). In order to produce emulsion gels, emulsions are first prepared by mixing gelling agent, emulsifier and oil and then turned into gels by different gelation mechanisms.

The choice of matrix material and emulsifier is the key factor in structuring emulsion gels. Proteins (e.g., soy protein isolate (SPI) and whey protein isolate (WPI)) and polysaccharides (e.g., agar and gellan gum) have been widely investigated as gelling agents in the formation of emulsion gels (Brito-Oliveira, Bispo, Moraes, Campanella, & Pinho, 2017; Geremias-Andrade, Souki, Moraes, & Pinho, 2017; Guo et al., 2017). Different gelling agents can form different gelation structures, and the gelation mechanism (e.g., heat, high pressure, acidification, enzymatic treatment, and addition of ions) for different gelling agents differs (Dickinson, 2012), which can affect the properties of emulsion gels and encapsulated food nutrients. Both synthetic (e.g., Tween 80 and Span 80) and natural (e.g., proteins, egg lecithin, and soy lecithin) emulsifiers can be used to prepare emulsion gels. Lipid droplets in emulsion gels can be divided into active and inactive fillers according to the interactions between gelling agents and emulsifier-coated lipid droplets (Van Vliet, 1988; Yang et al., 2020), which can also influence the properties of emulsion gels (Geremias-Andrade et al., 2017).

Alginate, a linear unbranched natural polysaccharide, is derived from brown seaweed extracts (*Phaeophyceae*) (King, 1983) and composed of two monomeric isomers: β-(1 → 4)-linked D-mannuronic acid (M) residues and α-(1 → 4)-linked L-guluronic acid (G) residues (Ching, Bansal, & Bhandari, 2017). Alginate-based emulsion gels received high attention in recent years (Lević, Pajić Lijaković, Đorđević, Rac, Rakić, Šolević Knudsen et al., 2015; Qu, Zhao, Fang, Nishinari, Phillips, Wu, et al., 2016; Zeeb, Saberi, Weiss, & McClements, 2015). Alginate monomers can form gels by ionic crosslinking with divalent cations (mostly calcium cations in the food industry) (King, 1983).

* Corresponding author. Teagasc Food Research Centre, Moorepark, Fermoy, Co. Cork, Ireland.
E-mail address: song.miao@teagasc.ie (S. Miao).

https://doi.org/10.1016/j.foodhyd.2020.105998
Received 15 January 2020; Received in revised form 25 April 2020; Accepted 4 May 2020
Available online 8 May 2020

External gelation and internal gelation are two methods used to prepare alginate-based emulsion gels. Pintado, Ruiz-Capillas, Jimenez-Colmenero, Carmona, and Herrero (2015) added $CaSO_4$ into an alginate-based emulsion to directly produce an alginate-based emulsion gel. Sato, Moraes, and Cunha (2014) used internal method to produce emulsion gels, in which CaEDTA was added to an alginate-based emulsion first, after which acid was introduced to liberate calcium ions. Compared these two methods, Puguan, Yu, and Kim (2014) found that gels formed by external gelation had a smoother surface and denser inner structure. In addition, alginate-based gels are not sensitive to gastric fluids, and can protect the encapsulated nutrients from harsh gastric environment, and the remaining gel structures can be further disrupted during intestinal digestion accompanied by the release of encapsulated compounds (Zhang et al., 2016).

Previous studies mainly focused on the formulation, structural properties, mechanical properties, stability, and digestion of alginate-based emulsion gels. However, there are few reports on the gelation process of alginate-based emulsion gels. It has been indicated that, during the gelation process of alginate hydrogels prepared by external gelation, calcium cations can diffuse into alginate drops after being dropped into a calcium chloride solution (Rehm, 2009). Syneresis also occurs during this gelation process, with a consequent decrease in dimensions of gel beads (Quong, Neufeld, Skjåk-Bræk, & Poncelet, 1998; Rehm, 2009). However, the gelation process of alginate-based emulsion gels may differ from that of alginate gels, because the presence of lipids and emulsifers in emulsions may affect the gelation process. Understanding the gelation process of alginate-based emulsion gels may help to produce emulsion gels with specific properties (e.g., size, water content, mechanical properties) by controlling gelation time, formulation, preparation methods and processing technologies. Therefore, further studies are needed to understand how alginate, emulsifiers and oil affect the gelation process of emulsion gel beads.

The purpose of this study was thus to investigate the gelation process of alginate-based emulsion gel beads. In order to improve the encapsulation efficiency and hygroscopicity of alginate-based emulsion gels, proteins (e.g., lupin protein and WPI) can be used as emulsifiers (Corstens et al., 2017; Piornos, Burgos-Díaz, Morales, Rubilar, & Acevedo, 2017), and polysaccharides (e.g., *Prosopis alba* exudate gum and chitosan) can be used as structural strengthening agents (Natrajan, Srinivasan, Sundar, & Ravindran, 2015; Vasile, Judis, & Mazzobre, 2018). In this study, denatured SPI was thus introduced as surfactant, because SPI has a huge potential value in producing emulsion gels, due to its good emulsifying property, and denatured SPI has increased emulsifying capacity compared to natural SPI (Lin et al., 2017; Nishinari, Fang, Guo, & Phillips, 2014). In addition, the external gelation was used, in order to obtain gel beads with denser structures, compared to internal gelation. Therefore, effect of concentrations of alginate, SPI, and sunflower oil on the shrinkage, water loss, elastic and structural properties of alginate-based emulsion gel beads during gelation were investigated in this study.

2. Materials and methods

2.1. Materials

Defatted soy flour (Bob's Red Mill, Milwaukie, Oregon, USA) and sunflower oil (Aldi Stores Ltd., Kildare, Ireland) were purchased from iHerb and Aldi, respectively. Sodium alginate was obtained from Special Ingredients (Chesterfield, UK). Calcium chloride, sodium hydroxide, and hydrochloric acid were purchased from Sigma-Aldrich (St. Louis, MO, USA).

2.2. Preparation of soy protein isolate

SPI was prepared according to the method described by Urbonaite, de Jongh, van der Linden, and Pouvreau (2015). The defatted soy flour was suspended in distilled water at a ratio of 1:10 (w/w) at 45 °C and stirred for 30 min. The pH value was then adjusted to 8.0 with 5 M NaOH, and the solution was stirred for 30 min in the water bath. The supernatant was collected by centrifugation (30 min, 6000×g, 13 °C) (Sorvall LYNX 6000 Superspeed Centrifuge, Thermo Fisher Scientific, Waltham, USA). Protein isolates were obtained by isoelectric precipitation by adjusting the pH value to 4.5 with 6 M HCl. After mild stirring for 12 h at 5 °C, the suspension was centrifuged (30 min, 6000×g, 7 °C). The sediment was re-suspended three times in deionized water at a ratio of 1:3 (w/w) and filtered by multilayer gauze to remove any remaining insoluble material, and the filtrate was centrifuged (30 min, 6000×g, 7 °C) again. The sediment was finally suspended in deionized water at a ratio of 1:4 (w/w), and the pH value was justified to 7.0 with 5 M NaOH. Then, the solution was freeze-dried (Free Zone 12 Freeze Dry System, Labconco Corpotation, Kansas, MO, USA). The dried SPI was kept in polyethylene bags and stored at room temperature. The protein content of SPI powder was 96.29 ± 0.03%.

2.3. Preparation of alginate-based and SPI-stabilized emulsions and gel beads

A dispersion of soy protein isolate (5% wt in distilled water) was stirred at room temperature for 30 min using a magnetic stirrer, heated at 90 °C for 30 min in a waterbath, and then cooled to room temperature. For the production of continuous phase, sodium alginate (0.5, 1.0, and 1.5% wt) was added into the pre-heated soy protein isolate solution with adding water to reach final concentrations of SPI (0.5, 1.0, and 2.0% wt) by shearing at 400 rpm for 30 min with a magnetic stirrer and then allowed to rest for 24 h to permit hydration. For the production of o/w emulsions, sunflower oil (10, 20, and 40% wt) was added to above continuous phase and mixed at 18,000 rpm for 2 min with an Ultra-Turrax (IKA-25, Staufen, Germany). Solutions containing 1.0% alginate (1A) and dispersions containing 1.0% alginate and 1.0% SPI (1A1S) were prepared as control groups without mixing at 18,000 rpm for 2 min. Table 1 shows the formulations used for preparing emulsions.

For producing gel beads, the resulting dispersions/solutions were dropped into 2% (w/w) $CaCl_2{\cdot}2H_2O$ solutions using 5-ml measuring pipettes and a S1 pipette filler (Thermo Fisher Scientific Inc., Waltham, USA). The distance between the tip of pipette and the surface of $CaCl_2$ solutions was fixed at 10 cm. The samples were allowed to gel in $CaCl_2$ solutions for 30 min with mild magnetic stirring, and the resulting beads were rinsed with distilled water. Samples were analysed immediately for measurement of Young's modulus, shrinkage, water loss, and morphology, and samples were kept in distilled water for observing their structures within 3 h after being prepared.

Table 1
Formulations of experimental emulsions.

Group	Water phase[a]		Oil Con. (% wt)
	Alginate Con. (% wt)	Soy protein Con. (% wt)	
1A (Control 1)	1.0	0	0
1A1S (Control 2)	1.0	1.0	0
1A1S20O	1.0	1.0	20
0.5A1S20O	0.5	1.0	20
1.5A1S20O	1.5	1.0	20
1A0.5S20O	1.0	0.5	20
1A2S20O	1.0	2.0	20
1A1S10O	1.0	1.0	10
1A1S40O	1.0	1.0	40

[a] The content of water phase was adjusted according to the oil content in the formulation.

2.4. Properties of dispersions/solutions

2.4.1. Structures

Confocal scanning laser microscopy (CLSM) was used to observe microstructures of dispersions/emulsions. Dispersion/emulsion samples (500 μl) were transferred to a glass slide and stained with 50 μl of a mixture of Nile red (0.1%, w/v, in polyethylene glycol-200) and fast green (0.1%, w/v, in distilled water) at a ratio of 3:1. Confocal observation was performed using a Leica TCS SP5 microscope (Leica Microsystems GmbH, Wetzlar, Germany) at excitation and emission wavelengths of 488 nm and 633 nm, provided by an argon laser and a HeNe laser, respectively.

2.4.2. Viscosity

The viscosity of dispersions/solutions was tested at 25 °C using an AR 2000ex rheometer (TA Instruments, Crawley, UK) with an aluminium parallel plate (60 mm in diameter, and 0.5 mm in gap). Each sample was added in the middle of Peltier plate and allowed to stand for 2 min before testing. The flow measurement was performed over a shear rate range of 0.1–100 s^{-1}, and viscosity (η) was obtained from the data analysis software.

2.5. Microstructures of gel beads

CLSM was used to observe microstructures of gel beads. Each gel bead was cut into a thin layer (~1 mm), transferred to a glass slide, and stained with a mixture of Nile red (0.1%, w/v, in polyethylene glycol-200) and fast green (0.1%, w/v, in distilled water) at a ratio of 3:1. Confocal observation was performed by the method described in section 2.4.1.

2.6. Young's modulus of gel beads

The Young's modulus of gel beads during gelation at 1, 2, 3, 4, 5, 6, 8, 10, 20, and 30 min were analysed by a TA.XT Plus texture analyser (Stable Micro System, Godalming, UK) according the method described by Ching, Bansal, and Bhandari (2016) with a minor change. The surface of samples was dried with dry paper before testing. Compression tests were performed using a cylinder probe of 10-mm diameter and a 5-kg load cell. The samples were compressed to 30% strain at a crosshead speed of 0.1 mm/s, and five beads with same composition were examined one after another. Due to their ellipsoidal shapes, the cross-sectional area of samples was calculated after measuring the major axis and minor axis of samples after being placed on the platform of texture analyser. The Young's modulus of each sample was calculated as the gradient of the stress vs. strain curve in the 5–15% strain region, where stress and strain showed good linearity. The experiment was performed in triplicate.

2.7. Water loss of gel beads

The water loss of samples during gelation was determined at 1, 2, 3, 4, 5, 6, 8, 10, 20, and 30 min after dispersions/solutions were dropped into calcium chloride solutions. In this study, the water loss means the decreased water in gel beads during gelation compared to the original dispersions/solutions. Five gel particles were obtained from calcium chloride solutions and washed with distilled water. After drying the surface, the initial weight of 5 beads was weighted (W'_i) and then they were dried in an oven at 80 °C until constant weight (W'_d). The initial weight (W_i) and the weight after drying (W_d) of dispersions/solutions (5 drops) were determined by the same method. Thus, the water loss was calculated from Eq. (1), if we assumed that the main content (i.e., alginate, SPI, and oil) of gel beads have no significant change during gelation, and the experiment was replicated three times.

$$\text{Water loss } (\%) = \left(\frac{W_i - W_d}{W_i} - \frac{W_d}{W_i} \times \frac{W'_i - W'_d}{W'_d}\right) \times 100\% \quad (1)$$

2.8. Shrinkage of gel beads

The section shrinkage rate of gel beads was determined at 2, 4, 6, 8, 10, 20, and 30 min after dispersions/solutions were dropped into calcium chloride solutions. Five gel beads were obtained from the calcium chloride solutions and washed with distilled water. After drying the surface, photographs of gel beads were taken using a camera (iPhone 7 plus, Apple Inc., California, USA). The major semi-axis (r'_{max}) and minor semi-axis (r'_{min}) of gel beads were measured by using a digital vernier calliper, and the section area (A'_s) was calculated from Eq. (2). The major semi-axis (r_{max}) and minor semi-axis (r_{min}) of gel beads after gelation for 1 min were measured, and the section area (A_s) was also calculated from Eq. (2). The section shrinkage rate of gel beads was calculated from Eq. (2), and the experiment was replicated three times. It should be noted that the section shrinkage rate of samples during gelation process was compared to the section area of samples after gelation for 1 min in this study.

$$\text{Section shrinkage rate } (\%) = \frac{A_s - A_s^{vcross_1 6pt_p ress_1 ogo'}}{A_s} = \frac{3.14 \times r_{max} \times r_{min} - 3.14 \times r'_{max} \times r'_{min}}{3.14 \times r_{max} \times r_{min}} \times 100\% \quad (2)$$

3. Results and discussion

3.1. Structural properties of gel beads

Structural properties are important for emulsion gels because they can influence mechanical properties of emulsion gels and release behavior of encapsulated nutrients. Many factors (e.g., structures of the gel matrix, structures of emulsion droplets, and interactions between the gel matrix and droplets) can influence the structures of overall emulsion gels. Therefore, the effect of concentrations of alginate, SPI and oil on the structures of emulsions and emulsion gels was investigated in this study.

Fig. 1 shows the structures of emulsions/dispersions before gelation and gel beads after gelation for 30 min. In sample 1A1S, SPI formed aggregates and dispersed in alginate solutions (Fig. 1A and V). This was because SPI was heated at 90 °C for 30 min in this study, and thus the solubility of SPI decreased, due to denaturation; additionally, denatured SPI exposed hydrophobic residues and thus formed aggregations in alginate solutions (Wagner & Añón, 1990). After mixing the 1A1S dispersion with oil, SPI modules can move from the continuous phase to the O/W interfaces and are absorbed at the surface of oil droplets (Fig. 1A and B), due to their amphipathic nature and emulsifying capacity. Hydrophobic groups of SPI absorbed onto the surface of oil droplets, and hydrophilic groups connected with the water phase, acting as a steric barrier against coalescence of oil droplets (Nishinari et al., 2014). However, increasing the alginate concentration to 1.5% led to more SPI aggregations in the water phase (Fig. 1B and C), because the higher viscosity of the continuous phase of emulsions hindered SPI from

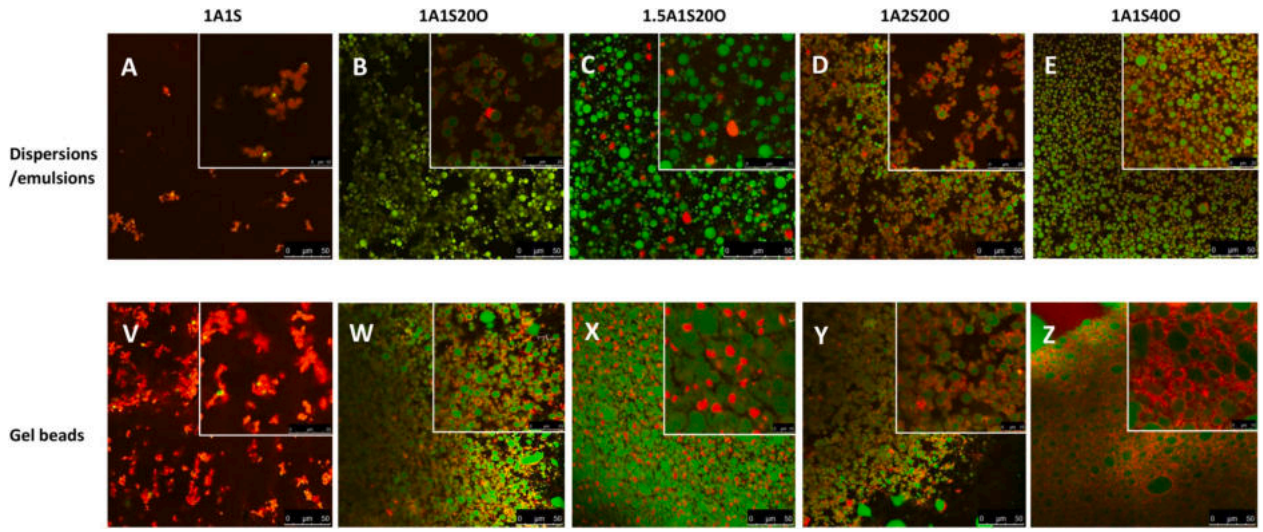

Fig. 1. CLSM images of dispersions/emulsions (A–E) and gel beads (V–Z) after gelation for 30 min. SPI and sunflower oil were stained by red and green, respectively. (For interpretation of the references to colour in this figure legend, the reader is referred to the Web version of this article.)

moving to the oil–water interface (Tavernier, Patel, Van der Meeren, & Dewettinck, 2017). Higher SPI concentrations resulted in more SPI being absorbed at the surface of oil droplets but led to more obvious flocculation of oil droplets (Fig. 1B and D), probably due to the depletion flocculation of droplets coated by excessive amount of SPI (Moschakis, Murray, & Biliaderis, 2010). In addition, increasing oil content of emulsions resulted in more compacted gel structures (Fig. 1B and E), due to the decreased ratio of the water phase to the oil phase.

Fig. 1 also indicates that there were more dark sections in emulsions/dispersions than gel beads in all samples, which indicates that syneresis and shrinkage of the water phase during gelation led to more compact filler structures. In addition, the concentrations of SPI, alginate and oil could affect the stability of droplets during gelation. As shown in Fig. 1B and W SPI-coated droplets in sample 1A1S20O could maintain their structures during gelation. This was because SPI could stabilize the o/w emulsions, and gelation, syneresis and shrinkage mainly occurred in the water phase during gelation, which had no significant effects on the structures of emulsion droplets. Similarly, it was found that WPI-aggregate-stabilized emulsions were stable during the gelation period (Rosa, Sala, Van Vliet, & Van De Velde, 2006). Additionally, higher SPI concentration resulted in more stable droplet structures during gelation, probably because of more SPI being absorbed at the surface of oil droplets (Fig. 1D and Y). However, increasing the alginate concentration to 1.5% led to re-coalescence of droplets during gelation (Fig. 1C and X), because increased viscosity of the continuous phase of emulsions hindered SPI from moving to the oil–water interface and thus resulted in decreased stability of emulsion droplets during gelation. In addition, increasing the oil content to 40% also led to re-coalescence of droplets

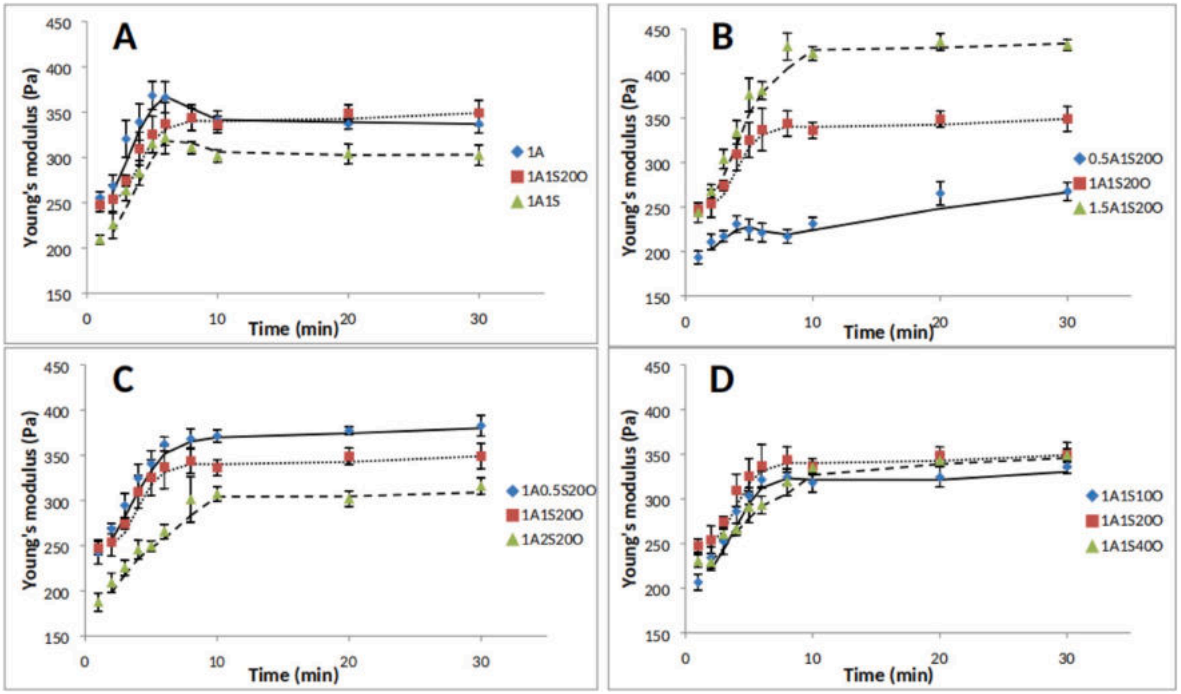

Fig. 2. Kinetics of Young's modulus of alginate-based gel beads during gelation: (A) control groups; (B) effect of alginate concentrations (0.5–1.5% in the water phase); (C) effect of SPI concentrations (0.5–2.0% in the water phase); and (D) effect of oil contents (10–40% in the emulsion).

during gelation (Fig. 1E and Z), probably because 1.0% SPI in the water phase was not enough to stabilize 40% oil.

3.2. Young's modulus of gel beads

3.2.1. The profiles of Young's modulus during gelation

Compression tests were carried out to study the elastic properties of gel beads during gelation. Firstly, the effect of introducing SPI and oil into alginate gels on the profiles of Young's modulus during gelation was investigated. As shown in Fig. 2A, the changes of Young's modulus of gel beads containing 1% alginate (1A in short) included three steps: increasing up to 5 min, decreasing between 5 and 10 min, and then reaching a plateau. The Young's modulus of gel beads containing 1% alginate and 1% SPI (sample 1A1S) had a similar trend to that of sample 1A, but the Young's modulus of emulsion gel beads containing 1% alginate, 1% SPI, and 20% oil (sample 1A1S20O) increased first and then reached a plateau at 8 min directly (Fig. 2A). It can be seen that the gelation process of alginate-based gel beads includes the maturation step (increased Young's modulus), the structural collapse step (decreased Young's modulus), and the equilibrium step (unchanged Young's modulus). Therefore, it was assumed that the gelation mechanism of alginate beads prepared by the external gelation has a direct effect on the changes in Young's modulus during gelation.

After being dropped into calcium chloride solutions, the surface of alginate drops can gel instantaneously, and then Ca^{2+} can diffuse from the $CaCl_2$ solutions into the interior of alginate drops, which leads to the gelation of gel beads from outside to inside and increased Young's modulus (Ching et al., 2017). This process is called the maturation step (Puguan et al., 2014). The concentration of alginate solutions and the size of gel beads are the main factors affecting the Ca^{2+} diffusion into alginate gel beads during gelation. It has been reported that higher alginate concentrations incorporated more calcium ions in alginate gel beads (Quong, Neufeld, Skjåk-Bræk, & Poncelet, 1998). In this study, all gel beads were prepared with 2% (w/w) $CaCl_2{\cdot}2H_2O$ solutions, and the size of samples 1A ($r_{max} = 2.1$ mm and $r_{min} = 2.0$ mm), 1A1S ($r_{max} = 2.2$ and $r_{min} = 2.1$), and 1A1S20O ($r_{max} = 2.1$ and $r_{min} = 2.0$) did not significantly differ at the end the maturation step. Therefore, it was assumed that the changes in Young's modulus of samples 1A, 1A1S, and 1A1S20O during the maturation step showed a similar trend probably because oil and SPI had no significant effect on the Ca^{2+} diffusion from the $CaCl_2$ solutions in alginate gel beads during the maturation step.

After the maturation step, the Young's modulus of samples 1A and 1A1S decreased before reaching a constant value (Fig. 2A). The concentrations of Ca^{2+} and alginate in alginate gel breads decreases from the gel surface to gel core (Quong et al., 1998), which indicates that the gel structure of the outer regions of beads is stronger than that of inside gel beads. Therefore, the fragile core structure of gel beads can not support the whole structure, which leads to the collapse of the inner structure at the end of the maturation step and thus a decreased Young's modulus (Puguan et al., 2014). However, the Young's modulus of sample 1A1S20O reached the balance directly after the maturation step during gelation (Fig. 2A). This was probably because the structures of sample 1A1S20O are totally different from that of samples 1A and 1A1S. After introducing oil into 1A1S dispersions, oil droplets disperse in the alginate solutions during homogenization, and SPI molecules move to the surface of oil droplets from the water phase, due to their emulsifying capacity. The resulting emulsions can turn into emulsion gels after alginate monomers are crosslinked by calcium cations, and shrinkage also occurs during this process. However, oil droplets may act as fillers and help to support the structure of gel beads from collapse after the maturation step during gelation. It has also been indicated that the oil core could support the shell of silica gels from fracture during the sol-gel process (Liang et al., 2011). Therefore, it was also assumed that oil played an important role on preventing the structural collapse of alginate gel beads during gelation.

The effect of concentrations of alginate (Fig. 2B), SPI (Fig. 2C) and sunflower oil (Fig. 2D) on the profiles of Young's modulus of emulsion gel beads during gelation was further investigated. Fig. 2B shows that the Young's modulus of sample 0.5A1S20O increased initially, decreased between 4 and 8 min, and then increased again, before reaching a plateau. In this sample, the structure of gel matrix formed by 0.5% alginate is fragile during the maturation step, which results in severe structural collapse before compact emulsion droplets can support emulsion gel structures. However, samples 1A1S20O and 1.5A1S20O showed a similar trend, in which the Young's modulus increased up to 8 min and then reached a plateau (Fig. 2B). This indicates that increasing alginate concentrations from 0.5% to 1.5% not only slowed Ca^{2+} diffusion and thus caused a slowing of the maturation step but also formed stronger alginate-based matrix structures and thus protected emulsion gel structures from collapse during gelation. Fig. 2C and D shows that increasing SPI concentrations from 0.5% to 2.0% and oil contents from 10% to 40% had no significant effect on the profiles of Young's modulus during gelation (i.e., reaching the plateau directly after the maturation step at around 8 min during gelation). This was probably because increasing concentrations of SPI and oil had no significant impact on calcium diffusion in emulsion gel beads, and 10% oil was high enough to prevent structural collapse of emulsion gel beads after the maturation step during gelation.

3.2.2. Effect of alginate, SPI and oil on the Young's modulus of gel beads after gelation

Mechanical properties are important for emulsion gels because they are closely associated with other properties (e.g., storage stability, oral perception, and controlled release of encapsulated nutrients). Many factors can affect mechanical properties of emulsion gels, such as gel strength of gel matrix structures (i.e., protein and polysaccharide), modulus of filler droplets, and interactions between oil droplets and the gel matrix. Therefore, the effect of concentrations of alginate, oil and SPI on the Young's modulus of emulsion gel beads was investigated in this study, and all samples were compared after they were allowed to gel for 30 min in $CaCl_2$ solutions (Fig. 2B–D).

Fig. 2B shows that increasing alginate concentrations from 0.5 to 1.5% significantly increased the Young's modulus of emulsion gel beads. This was expected because increasing alginate concentration could increase gel strength of alginate-based gel matrix and thus increase the Young's modulus of overall emulsion gels. Similarly, it has previously been reported that increasing agar content (from 1.0 to 1.8%) in o/w emulsions containing 0.1 volume fraction of corn oil decreased the overall volume of void spaces and increased strand compactness of emulsion gels (Kim, Gohtani, Matsuno, & Yamano, 1999).

Fig. 2D indicates that increasing oil contents from 10% to 40% had no significant effect on the Young's modulus of emulsion gel beads. According to the interactions between emulsifier-coated emulsion droplets and the gel matrix, oil droplets can be divided into active and inactive fillers (also known as bound and unbound fillers) in emulsion gels (Dickinson, 2012; Yang et al., 2020). Active fillers are mechanically connected to the gel network by noncovalent and/or covalent bonds through emulsifiers. For examples, it has been reported that WPI-coated oil droplets could be bound to a WPI-based gel matrix by covalent interactions (e.g., hydrophobic interactions and sulphur bridges) (Sala, de Wijk, van de Velde, & van Aken, 2008); it has been also indicated that lactoferrin-stabilized emulsion droplets could bind to a κ-carrageenan gel, probably because of electrostatic interactions between positively charged lactoferrin (pI = 8.2) and negatively charged κ-carrageenan at pH 7–8 (Sala, van Vliet, Cohen Stuart, Aken, & van de Velde, 2009). In addition, the Kerner model can explain the effect of active fillers on the mechanical properties of emulsion gels (Kerner, 1956). According to this model, increasing the volume fraction (φ_f) of active fillers can increase the mechanical properties of emulsion gels, which has been supported by many studies (Oliver, Berndsen, van Aken, & Scholten, 2015; Sala et al., 2009). However, in this study, SPI (pI = 4.5) and alginate were both negatively charged at pH 6.5–7.0, so there are no electrostatic

interactions between SPI-coated droplets and alginate-based gel matrix. It is also unlikely that SPI-coated droplets can connect to the alginate-based gel network by covalent interactions. Additionally, the results obtained in this study were in a disaccord with the Kerner model. Therefore, it was assumed that SPI-coated droplets were inactive fillers in alginate-based emulsion gel beads.

Fig. 2C shows that increasing SPI concentrations decreased the Young′s modulus of emulsion gel beads. According to the state of emulsion droplets in gels, structures of emulsion gels can be divided into two categories: emulsion droplet-filled gels and emulsion droplet-aggregated gels (Dickinson, 2012). In emulsion droplet-filled gels, the continuous phase (e.g., protein- and polysaccharide-based gels) forms a continuous gel matrix, and emulsion droplets are embedded in this gel matrix. In emulsion droplet-aggregated gels, emulsion droplets aggregate together and form a network structure, such that the gel matrix is disrupted by the aggregated emulsion droplets. As shown in Fig. 1B and D, more aggregations of emulsion droplets occurred in sample 1A2S20O compared to sample 1A1S20O, probably because increasing SPI concentration led to more depletion flocculation of SPI-coated droplets in emulsions (Lam & Nickerson, 2013). In active droplet-aggregated gels, the crowding effect of fillers (particle interactions) increases the shear modulus of the overall gels (Oliver et al., 2015). However, SPI-coated droplets in alginate-based gel matrix may act as inactive fillers as disccussed before in this study. Therefore, it was assumed that increased aggregation of SPI-coated droplets (inactive fillers) had a negative effect on the Young′s modulus of alginate-based emulsion gel beads, probably because aggregated droplets (i.e., the increased phase separation between alginate-based gel matrix and SPI-coated droplets) may disturb the formation of alginate-based network structures (Dickinson, 2012; Lin et al., 2017).

3.3. Water loss of gel beads

During the maturation step, inter-chain interactions between stretches of alginate monomers and Ca^{2+} occurred with the diffusion of Ca^{2+} from the surface to interior of gel beads, and the formation of junctions between these stretches forced water out, which led to shrinkage and increased water loss of gel beads during gelation (Puguan et al., 2014; Rehm, 2009). Fig. 3 shows the effects of concentrations of alginate, SPI, and oil on the water loss from emulsion gel beads during gelation. It indicates that increasing alginate contents (from 0.5 to 1.5%) or SPI concentration (from 0.5 to 2.0%) had no significant effect on the rares of water loss, but increasing oil content (from 10 to 40%) could slow the water loss in terms of the profiles of water loss during gelation, probably because lower water content of the original emulsions results in slower water loss of emulsion gels during gelation.

Fig. 3 also indicates that the water loss of emulsion gel beads after gelation for 30 min decreased with increasing alginate contents (from 0.5 to 1.5%), SPI concentration (from 0.5 to 2.0%) and oil content (from 10 to 40%). Many factors can affect the water loss of emulsion gel beads during gelation, such as the concentration of $CaCl_2$ solutions, the water content of original emulsions, the strength of gel matrix, and the hydrophilicity and rigidity of fillers. It has been reported that increasing the concentration of $CaCl_2$ solution (from 0.08 M to 0.3 M) reduced the final weight of alginate gel beads due to the increased water loss (Puguan et al., 2014), but in this study all samples were dropped into the $CaCl_2$ solutions with the same concentration. Therefore, increasing alginate concentration from 0.5% to 1.5% decreased the water loss of beads from 42.3 ± 1.2% to 36.9 ± 0.3% after gelation (Fig. 3A), which was probably because elastic modulus of gel beads increased with increasing alginate concentration (Fig. 2B), and gels with stronger matric structures had better water-bolding capacity.

In addition, increasing SPI concentration from 0.5% to 2.0%

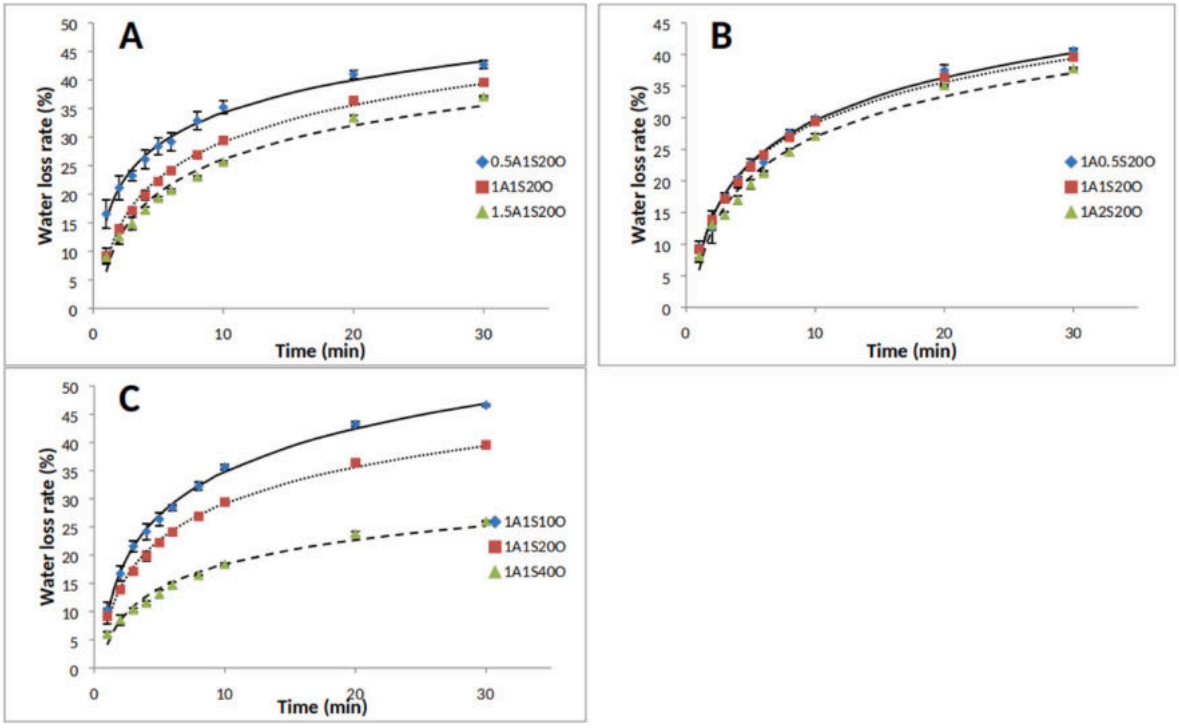

Fig. 3. Kinetics of water loss from alginate-based gel beads during gelation: (A) effect of alginate concentrations (0.5–1.5% in the water phase); (B) effect of SPI concentrations (0.5–2.0% in the water phase); and (C) effect of oil contents (10–40% in the emulsion).

decreased the water loss of emulsion gel beads from 40.2 ± 0.6% to 37.3 ± 0.3% after gelation as well (Fig. 3B), probably due to increased water-absorption capacity of SPI-coated droplets. Denatured SPI has emulsifying capacity because it has both hydrophobic and hydrophilic groups (Nishinari et al., 2014). As shown in Fig. 1A and B, SPI aggregated in sample 1A1S but formed a film at the oil-water interface in sample 1A1S20O, in which hydrophobic groups of SPI connected to oil droplets and hydrophilic groups connected to water. Therefore, more SPI was absorbed at the surface of emulsion droplets by increasing SPI concentration (Fig. 1D), which resulted in increased hydrophilicity of SPI-coated droplets and increased water-retention capacity of emulsion gel beads (Wang, Marcone, Barbut, & Lim, 2012). This explanation could be supported by previous conclusions that SPI with highly denatured proteins and high surface hydrophobicity exhibited the highest water-absorption capacity (Wagner and Añón, 1990). Additionally, increasing oil content from 10% to 40% led to the decreased water loss of emulsion gel beads (from 46.1 ± 0.2% to 25.1 ± 0.4% after gelation) (Fig. 3C), probably because the water content in original emulsions significantly decreased with increasing oil contents from 10% to 40%, and emulsion droplets could protect gel structures from collapse as well. A similar finding has been reported where increasing the oil volume fraction (13%–31.1%) in β-lactoglobulin-based oil-in-water emulsions improved the water-retention capacity of emulsion gels (Line, Remondetto, & Subirade, 2005).

3.4. Morphological properties and shrinkage of gel beads

As shown in Fig. 4, alginate gel beads (1A) were transparent, but the presence of SPI decreased the transparency of alginate gel beads (1A1S) because of its yellow colour, and introducing oil led to ivory gel beads, due to the formation of emulsions. In addition, gel beads in all groups were not completely spherical, and samples 1.5A1s20O, 1A2S20O, and 1A1S40O had small tails. This was because increasing the concentrations of alginate, SPI and oil could raise the viscosity of emulsions

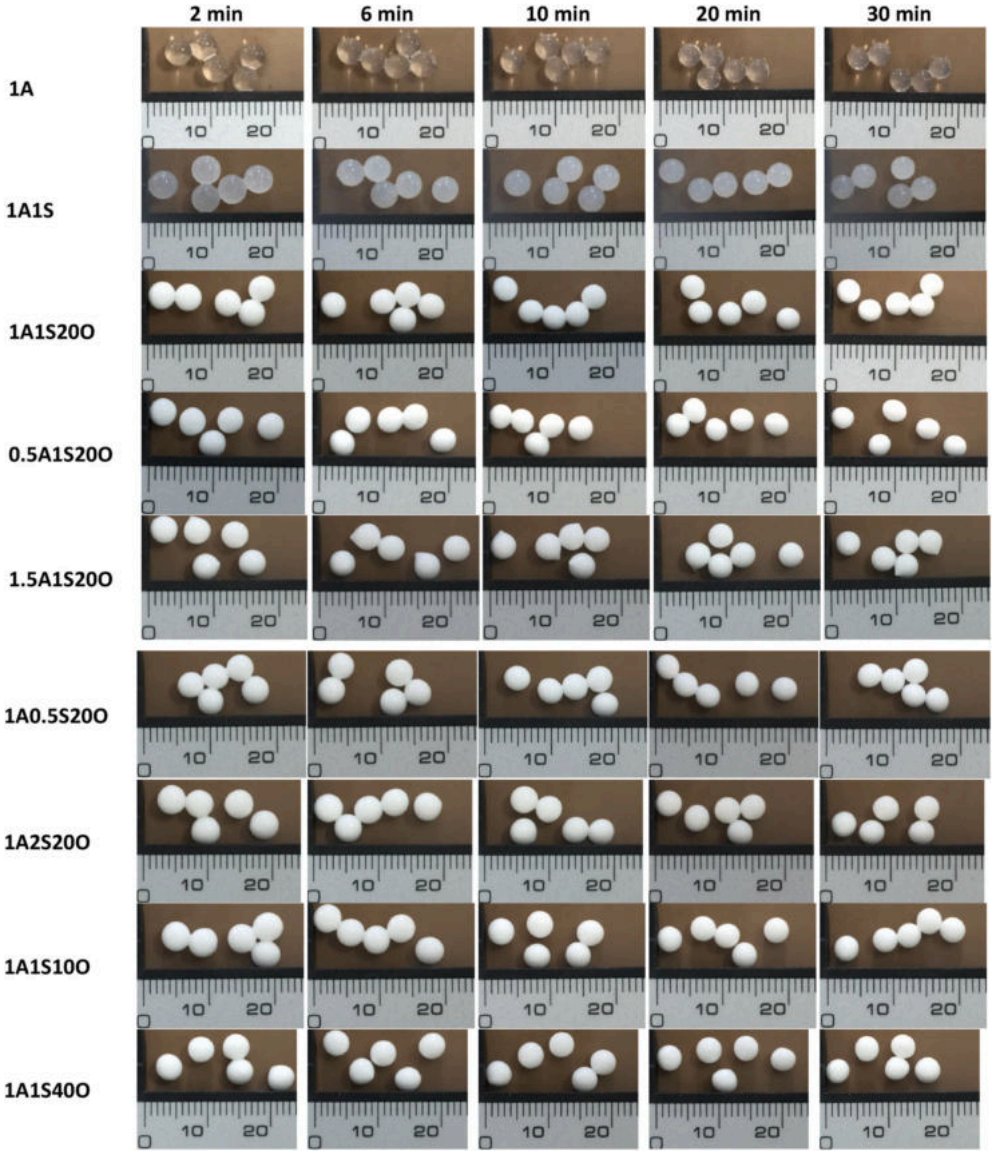

Fig. 4. Visual aspects of alginate-based gel beads during gelation (minimum scale mark = 1 mm).

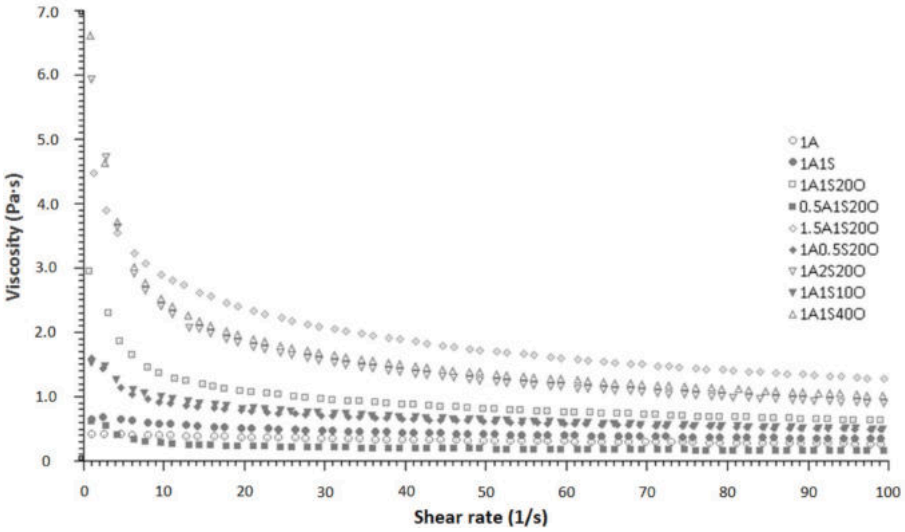

Fig. 5. Viscosity of dispersions/emulsions with different component concentrations.

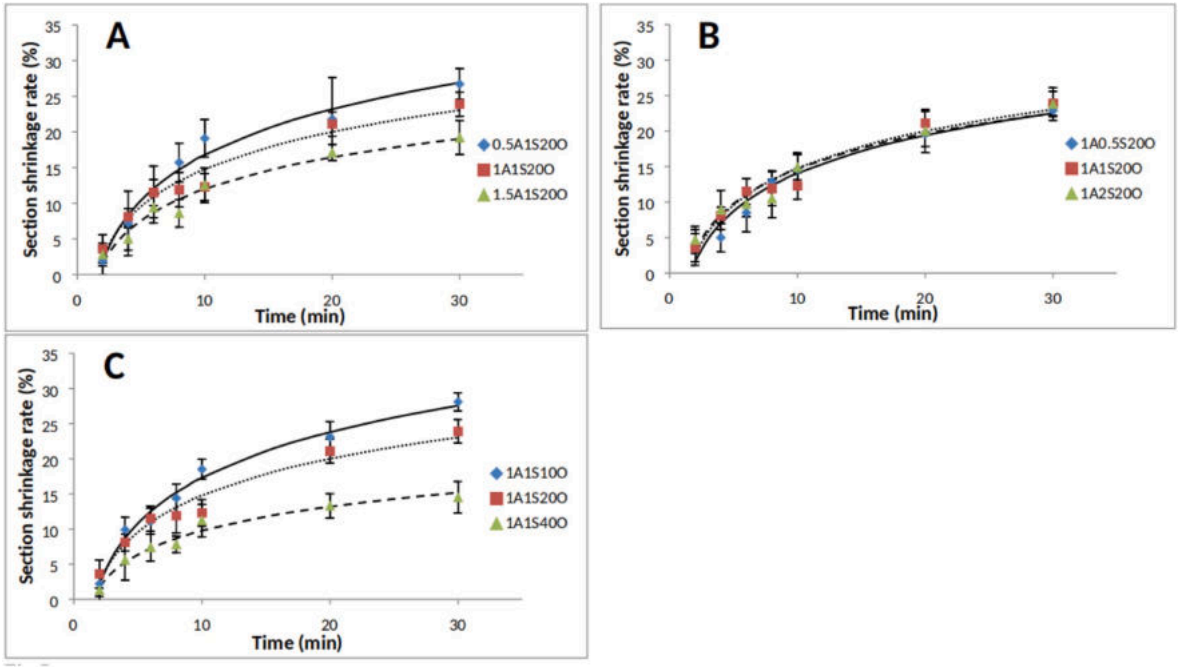

Fig. 6. Kinetics of section shrinkage of alginate-based gel beads during gelation: (A) effect of alginate concentrations (0.5–1.5% in the water phase); (B) effect of SPI concentrations (0.5–2.0% in the water phase); and (C) effect of oil contents (10–40% in the emulsion).

(Fig. 5), which could affect the morphological properties of emulsion gel beads. In this study, we used the simple dripping method to produce emulsion gel beads. The emulsions were pushed out from pipette and one droplet was formed at the tip before the droplet grew in size gradually and dropped into $CaCl_2$ solutions. During this process, spherical emulsion droplets were formed because of the surface tension of liquid (Ching et al., 2017). However, Lević et al. (2015) found that D-limonene could increase the viscosity and reduce the conductivity of the alginate liquid systems by changing structural ordering of alginate, which indicates that the high viscosity of emulsion was against the formation of spherical bead at the tip of pipet because of poor flow properties. For example, the introduction of hydroxypropylmethylcellulose (0.2%–1%) changed the rheological properties of 2% alginate solutions and produced beads with small tails (Bellich, Borgogna, Cok, & Cesàro, 2011).

Fig. 4 also shows that the size of all samples decreased during gelation and, in order to compare their shrinkage during gelation, the section shrinkage rates were calculated (Fig. 6). The profiles of shrinkage rates show that shrinkage rates of all samples increased during gelation, probably due to syneresis (i.e., water loss) and structural collapse (Rehm, 2009). However, in terms of the profiles of shrinkage rate, increasing contents of alginate and oil could slow the shrinkage, but increasing SPI content had no significant effect on the rate of shrinkage during gelation. Fig. 6 also shows that the shrinkage rates decreased from 26.7 ± 2.1% to 18.2 ± 2.2% and from 27.1 ± 1.6% to 13.6 ± 2.5%

after gelation with increasing concentrations of alginate (from 0.5% to 1.5%) and oil (from 10% to 40%), respectively, but increasing SPI concentration from 0.5% to 2.0% had no significant effect on the shrinkage rates of emulsion gel beads after gelation for 30 min. Many factors can affect the shrinkage of emulsion gels during gelation, such as water loss, gel stiffness, the content and properties of fillers, and interactions between fillers and the continuous phase (Smith, Scherer, & Anderson, 1995). In terms of alginate, increasing its concentration could increase the elastic modulus of emulsion gel beads (Fig. 2B), which may provide resistance to shrinkage (Brinker et al., 1994). Increasing oil concentration led to more compact filler structures, which resisted further shrinkage during gelation as seen on comparing emulsion gel structures of samples 1A1S20O and 1A1S40O in Fig. 1. Eichler, Ramon, Ladyzhinski, Cohen, and Mizrahi (1997) also indicated similar conclusions, in that fructose or polydextrose being introduced into polyacrylamide (PAAm) gels could act as a mechanical barrier against further volume shrinkage of PAAm gels during dehydration. However, increasing SPI concentration reduced the Young′s modulus (Fig. 2C) but increased water retention (i.e., decreased water loss) (Fig. 3B) of emulsion gel beads, which may explain why increasing SPI concentration had no significant effects on shrinkage rates of emulsion gel beads.

4. Conclusions

The Young′s modulus of alginate-based emulsion gel beads kept increasing before reaching a plateau during gelation process. This gelation process was accompanied by syneresis (i.e., water loss) and shrinkage, which resulted in an increased compactness of emulsion gel beads. SPI-coated droplets could maintain their structures during gelation. With increasing alginate concentration (0.5%–1.5%), the water loss decreased, the Young′s modulus increased, and shrinkage rate decreased. Increasing SPI concentration (0.5%–2.0%) led to decreased Young′s modulus and water loss, and undifferentiated shrinkage. Higher oil content (10%–40%) decreased water loss and section shrinkage rates, and had no significant effect on the Young′s modulus. These findings underlined the effect of concentrations of components on the properties of emulsion gel beads during gelation, which are very important because the properties of emulsion gel beads may affect encapsulation, stability, and release of hydrophobic functional ingredients encapsulated in emulsion gel beads.

Declaration of competing interest

The authors declare that they have no known competing financial interests or personal relationships that could have appeared to influence the work reported in this paper.

CRediT authorship contribution statement

Duanquan Lin: Conceptualization, Methodology, Writing - original draft, Data curation, Investigation. **Alan L. Kelly:** Supervision, Writing - review & editing. **Valentyn Maidannyk:** Investigation. **Song Miao:** Supervision, Conceptualization, Writing - review & editing, Funding acquisition, Project administration, Investigation.

Acknowledgement

This work is supported by the China Scholarship Council (No. 201708350111) and Teagasc-The Irish Agriculture and Food Development Authority (RMIS6821). The assistance of Helen Slattery with the freeze-drying system and Deirdre Kennedy with confocal scanning laser microscopy is highly appreciated.

Appendix A. Supplementary data

Supplementary data to this article can be found online at https://doi.org/10.1016/j.foodhyd.2020.105998.

References

Bellich, B., Borgogna, M., Cok, M., & Cesàro, A. (2011). Release properties of hydrogels: Water evaporation from alginate gel beads. *Food Biophysics, 6*, 259–266.
Brinker, C. J., Sehgal, R., Hietala, S., Deshpande, R., Smith, D., Loy, D., et al. (1994). Sol-gel strategies for controlled porosity inorganic materials. *Journal of Membrane Science, 94*, 85–102.
Brito-Oliveira, T. C., Bispo, M., Moraes, I. C. F., Campanella, O. H., & Pinho, S. C. (2017). Stability of curcumin encapsulated in solid lipid microparticles incorporated in cold-set emulsion filled gels of soy protein isolate and xanthan gum. *Food Research International, 102*, 759–767.
Ching, S. H., Bansal, N., & Bhandari, B. (2016). Rheology of emulsion-filled alginate microgel suspensions. *Food Research International, 80*, 50–60.
Ching, S. H., Bansal, N., & Bhandari, B. (2017). Alginate gel particles–A review of production techniques and physical properties. *Critical Reviews in Food Science and Nutrition, 57*, 1133–1152.
Corstens, M. N., Berton-Carabin, C. C., Elichiry-Ortiz, P. T., Hol, K., Troost, F. J., Masclee, A. A. M., et al. (2017). Emulsion-alginate beads designed to control in vitro intestinal lipolysis: Towards appetite control. *J. Func. Foods, 34*, 319–328.
Dickinson, E. (2012). Emulsion gels: The structuring of soft solids with protein-stabilized oil droplets. *Food Hydrocolloids, 28*, 224–241.
Eichler, S., Ramon, O., Ladyzhinski, I., Cohen, Y., & Mizrahi, S. (1997). Collapse processes in shrinkage of hydrophilic gels during dehydration. *Food Research International, 30*, 719–726.
Geremias-Andrade, I. M., Souki, N. P. D. B. G., Moraes, I. C. F., & Pinho, S. C. (2017). Rheological and mechanical characterization of curcumin-loaded emulsion-filled gels produced with whey protein isolate and xanthan gum. *Lebensmittel-Wissenschaft und -Technologie- Food Science and Technology, 86*, 166–173.
Guo, Q., Bellissimo, N., & Rousseau, D. (2017). Role of gel structure in controlling in vitro intestinal lipid digestion in whey protein emulsion gels. *Food Hydrocolloids, 69*, 264–272.
Kerner, E. (1956). The elastic and thermo-elastic properties of composite media. *Proceedings of the Physical Society Section B, 69*, 808.
Kim, K., Gohtani, S., Matsuno, R., & Yamano, Y. (1999). Effects of oil droplet and agar concentration on gel strength and microstructure of o-w emulsion gel. *Journal of Texture Studies, 30*, 319–335.
King, A. (1983). Brown seaweed extracts (alginates). *Food Hydrocolloids, 2*, 115–188.
Lam, R. S., & Nickerson, M. T. (2013). Food proteins: A review on their emulsifying properties using a structure-function approach. *Food Chemistry, 141*, 975–984.
Lević, S., Pajić Lijaković, I., Đorđević, V., Rac, V., Rakić, V., Šolević Knudsen, T., et al. (2015). Characterization of sodium alginate/$_D$-limonene emulsions and respective calcium alginate/$_D$-limonene beads produced by electrostatic extrusion. *Food Hydrocolloids, 45*, 111–123.
Liang, F., Liu, J., Zhang, C., Qu, X., Li, J., & Yang, Z. (2011). Janus hollow spheres by emulsion interfacial self-assembled sol-gel process. *Chemical Communications, 47*, 1231–1233.
Line, V. L. S., Remondetto, G. E., & Subirade, M. (2005). Cold gelation of β-lactoglobulin oil-in-water emulsions. *Food Hydrocolloids, 19*, 269–278.
Lin, D., Lu, W., Kelly, A. L., Zhang, L., Zheng, B., & Miao, S. (2017). Interactions of vegetable proteins with other polymers: Structure-function relationships and applications in the food industry. *Trends in Food Science & Technology, 68*, 130–144.
Ma, L., Wan, Z., & Yang, X. (2017). Multiple water-in-oil-in-water emulsion gels based on self-assembled saponin fibrillar network for photosensitive cargo protection. *Journal of Agricultural and Food Chemistry, 65*, 9735–9743.
Moschakis, T., Murray, B. S., & Biliaderis, C. G. (2010). Modifications in stability and structure of whey protein-coated o/w emulsions by interacting chitosan and gum Arabic mixed dispersions. *Food Hydrocolloids, 24*, 8–17.
Natrajan, D., Srinivasan, S., Sundar, K., & Ravindran, A. (2015). Formulation of essential oil-loaded chitosan-alginate nanocapsules. *Journal of Food and Drug Analysis, 23*, 560–568.
Nishinari, K., Fang, Y., Guo, S., & Phillips, G. O. (2014). Soy proteins: A review on composition, aggregation and emulsification. *Food Hydrocolloids, 39*, 301–318.
Oliver, L., Berndsen, L., van Aken, G. A., & Scholten, E. (2015). Influence of droplet clustering on the rheological properties of emulsion-filled gels. *Food Hydrocolloids, 50*, 74–83.
Pintado, T., Ruiz-Capillas, C., Jimenez-Colmenero, F., Carmona, P., & Herrero, A. M. (2015). Oil-in-water emulsion gels stabilized with chia (*Salvia hispanica L.*) and cold gelling agents: Technological and infrared spectroscopic characterization. *Food Chemistry, 185*, 470–478.
Piornos, J. A., Burgos-Díaz, C., Morales, E., Rubilar, M., & Acevedo, F. (2017). Highly efficient encapsulation of linseed oil into alginate/lupin protein beads: Optimization of the emulsion formulation. *Food Hydrocolloids, 63*, 139–148.
Puguan, J. M., Yu, X., & Kim, H. (2014). Characterization of structure, physico-chemical properties and diffusion behavior of Ca-Alginate gel beads prepared by different gelation methods. *Journal of Colloid and Interface Science, 432*, 109–116.
Quong, D., Neufeld, R., Skjåk-Bræk, G., & Poncelet, D. (1998). External versus internal source of calcium during the gelation of alginate beads for DNA encapsulation. *Biotechnology and Bioengineering, 57*, 438–446.
Rehm, B. H. A. (Ed.). (2009). *Alginates: Biology and applications*. Heidelberg: Springer.
Rosa, P., Sala, G., Van Vliet, T., & Van De Velde, F. (2006). Cold gelation of whey protein emulsions. *Journal of Texture Studies, 37*, 516–537.

Sala, G., de Wijk, R. A., van de Velde, F., & van Aken, G. A. (2008). Matrix properties affect the sensory perception of emulsion-filled gels. *Food Hydrocolloids, 22*, 353–363.

Sala, G., van Vliet, T., Cohen Stuart, M. A., Aken, G. A.v., & van de Velde, F. (2009). Deformation and fracture of emulsion-filled gels: Effect of oil content and deformation speed. *Food Hydrocolloids, 23*, 1381–1393.

Sato, A. C. K., Moraes, K. E. F. P., & Cunha, R. L. (2014). Development of gelled emulsions with improved oxidative and pH stability. *Food Hydrocolloids, 34*, 184–192.

Smith, D., Scherer, G., & Anderson, J. (1995). Shrinkage during drying of silica gel. *Journal of Non-crystalline Solids, 188*, 191–206.

Tavernier, I., Patel, A. R., Van der Meeren, P., & Dewettinck, K. (2017). Emulsion-templated liquid oil structuring with soy protein and soy protein: κ-Carrageenan complexes. *Food Hydrocolloids, 65*, 107–120.

Urbonaite, V., de Jongh, H. H. J., van der Linden, E., & Pouvreau, L. (2015). Water holding of soy protein gels is set by coarseness, modulated by calcium binding, rather than gel stiffness. *Food Hydrocolloids, 46*, 103–111.

Van Vliet, T. (1988). Rheological properties of filled gels: Influence of filler matrix interaction. *Colloid & Polymer Science, 266*, 518–524.

Vasile, F. E., Judis, M. A., & Mazzobre, M. F. (2018). Impact of Prosopis alba exudate gum on sorption properties and physical stability of fish oil alginate beads prepared by ionic gelation. *Food Chemistry, 250*, 75–82.

Wagner, J., & Añón, M. C. (1990). Influence of denaturation, hydrophobicity and sulfhydryl content on solubility and water absorbing capacity of soy protein isolates. *Journal of Food Science, 55*, 765–770.

Wang, S., Marcone, M., Barbut, S., & Lim, L. T. (2012). The impact of anthocyanin-rich red raspberry extract (ARRE) on the properties of edible soy protein isolate (SPI) films. *Journal of Food Science, 77*, C497–C505.

Yang, N., Feng, Y. N., Su, C. X., Wang, Q., Zhang, Y. M., Wei, Y. H., et al. (2020). Structure and tribology of κ-carrageenan gels filled with natural oil bodies. *Food Hydrocolloids*, 105945.

Zhang, Z. P., Zhang, R. J., Zou, L. Q., Chen, L., Ahmed, Y., Bishri, W. A., et al. (2016). Encapsulation of curcumin in polysaccharide-based hydrogel beads. *Food Hydrocolloids, 58*, 160–170.

Food Hydrocolloids 110 (2021) 106165

Contents lists available at ScienceDirect

Food Hydrocolloids

journal homepage: http://www.elsevier.com/locate/foodhyd

Effect of structuring emulsion gels by whey or soy protein isolate on the structure, mechanical properties, and *in-vitro* digestion of alginate-based emulsion gel beads

Duanquan Lin [a,b], Alan L. Kelly [b], Valentyn Maidannyk [a], Song Miao [a,b,*]

[a] Teagasc Food Research Centre, Moorepark, Fermoy, Co. Cork, Ireland
[b] School of Food and Nutritional Sciences, University College Cork, Cork, Ireland

ARTICLE INFO

Keywords:
Alginate
Emulsion gel bead
Lycopene
Soy protein isolate
Structure
Whey protein isolate

ABSTRACT

Whey protein isolate (WPI) and soy protein isolate (SPI) were used as emulsifiers and structure-modifying agents to produce alginate-based emulsion gel beads. The purpose of this study was to compare the effects of WPI and SPI on the structural and mechanical properties of alginate-based emulsion gel beads and the *in-vitro* release of encapsulated lycopene from emulsion gel beads. The results of microscopy and light scattering indicated that WPI had better emulsifying properties than SPI, resulting in emulsions with smaller and more even droplet size distribution. The rheological properties of protein/alginate mixtures and emulsions indicated strong interactions between WPI and alginate and weak interactions between SPI and alginate, resulting in increased Young's modulus of WPI-stabilized emulsion gel beads and decreased Young's modulus of SPI-stabilized emulsion gel beads, compared to gel beads without proteins. The presence of WPI and SPI increased changes of Young's modulus and shrinkage during simulated gastric digestion and delayed the release of lycopene from gel beads. Findings in this study are important for structuring emulsion gels with naturally occurring polymers to achieve controlled release of encapsulated compounds.

1. Introduction

Sodium alginate is a linear unbranched natural polysaccharide, and its monomers can form gels by ionic crosslinking when sodium ions are replaced by divalent cations (mostly calcium ions in the food industry). Sodium alginate has been widely investigated in the field of emulsion gels for encapsulation of food nutrients such as thyme oil, linseed oil, resveratrol, α-tocopherol, β-carotene and D-limonene to improve their stability during food processing and storage (Benavides, Cortés, Parada, & Franco, 2016; Feng, Yue, Ni, & Liang, 2018; Lević et al., 2015; Piornos, Burgos-Díaz, Morales, Rubilar, & Acevedo, 2017; Soukoulis, Cambier, Hoffmann, & Bohn, 2016). There are also some advantages associated with alginate-based encapsulation techniques, such as mild gelation process with a low-cost and eco-friendly procedure and controlled release of encapsulated food nutrients because of pH sensitivity of alginate gels (i.e., shrinking at gastric environment and swelling during intestinal digestion) (Calvo, Busch, & Santagapita, 2017; George & Abraham, 2006). In alginate-based emulsion gels, proteins especially whey protein isolate (WPI) are normally used as emulsifiers to improve the encapsulation efficiency during gelation and the stability of encapsulated food nutrients during storage (Feng et al., 2018; Piornos et al., 2017), However, the presence of proteins may also change the structural and mechanical properties of alginate-based emulsion gels during gelation and digestion, which has rarely been investigated (Leon, Medina, Park, & Aguilera, 2018). Previous studies on interactions between proteins and alginate have indicated that proteins affect the gelation process and physicochemical properties of calcium-induced alginate gels through several mechanisms. Firstly, positively charged proteins can compete with calcium ions to associate with carboxylic acid sites on the negatively charged alginate molecules through electrostatic attractions (George & Abraham, 2006). Secondly, negatively charged proteins can interact with alginate through intermolecular hydrogen bonds between proteins and alginate and/or weak electrostatic attractions between carboxylic anionic groups of alginate and cationic groups of proteins, although both of them are negatively charged (Erben, Pérez, Osella, Alvarez, & Santiago, 2019; Yang et al., 2016). Thirdly, insoluble proteins can act as solid fillers in alginate gels (Leon et al., 2018).

In addition, the presence of proteins may also affect the digestion

* Corresponding author. Teagasc Food Research Centre, Moorepark, Fermoy, Co. Cork, Ireland.
E-mail address: song.miao@teagasc.ie (S. Miao).

https://doi.org/10.1016/j.foodhyd.2020.106165
Received 2 March 2020; Received in revised form 6 July 2020; Accepted 8 July 2020
Available online 15 July 2020

behaviour of alginate gels. It is well known that alginate gels shrink during gastric digestion, because of the protonation of free carboxylate groups on alginate and thus decreased repulsive charges of alginate monomers at the acidic pH (pH 2–3). Alginate gels then swell during intestinal digestion, because of the increased repulsive forces at the neutral pH above the pKa of the uronic acid groups on alginate (Rayment et al., 2009) and structural disintegration of Ca^{2+}-associated networks due to ion-exchange between Na^{+} ions present in the digestive fluid and Ca^{2+} ions present in gel beads (Bajpai & Sharma, 2004; Mongar & Wassermann, 1949). This digestion behaviour can protect encapsulated nutrients from the harsh gastric environment due to the shrinkage of gels during gastric digestion, and encapsulated nutrients then diffuse through the pores of alginate gel networks into the small intestine due to the swelling of gels during intestinal digestion. However, the zeta potential of proteins is also influenced by pH, which may affect the interactions between proteins and alginate and thus the physiochemical properties of alginate-based emulsions gels during digestion. Therefore, the effect of proteins on the structural and mechanical properties of alginate-based emulsion gels and the release of encapsulated nutrients during digestion need further investigation.

The properties of different proteins (e.g., solubility and amphipathy) affect their interactions with other polymers (Lin et al., 2017). WPI is the most widely used protein-based emulsifier in emulsion gels, and soy protein isolate (SPI) has received increasing interest, due to its good emulsifying and gelation properties. SPI contains more polar amino acids (492.8 mg/g) than WPI (433.7 mg/g), and WPI contains more positively charged amino acids (267.9 mg/g) than SPI (200.9 mg/g) at pH 7.0 (Peña-Ramos, Xiong, & Arteaga, 2004; Tang, Ten, Wang, & Yang, 2006). Polar amino acids tend to form hydrogen bonds with alginate, and positively charged amino acids tend to react with alginate by electrostatic attractions. In addition, WPI has higher solubility and surface hydrophobicity than SPI (Castro et al., 2018; Voutsinas, Cheung, & Nakai, 1983). Protein solubility affects protein-water interactions, and surface hydrophobicity influences protein-oil interactions at droplet surfaces (Pelegrine & Gasparetto, 2005).

Therefore, the objective of this study was to compare WPI to SPI in structuring alginate-based emulsion beads and delivering encapsulated nutrients to a target site (i.e., small intestine). The effect of WPI and SPI on the properties of emulsions and emulsion gel beads and the release behaviour of encapsulated nutrients during *in-vitro* digestion were studied. Lycopene was encapsulated in emulsion gels to study the effect of WPI and SPI on the digestion behaviour of alginate-based emulsion gels. Lycopene has a huge commercial value in the food industry, due to its high antioxidant capacity among carotenoids (Costa-Rodrigues, Pinho, & Monteiro, 2018; Liu, Shi, Colina Ibarra, Kakuda, & Jun Xue, 2008). However, lycopene is highly sensitive to high temperature, oxygen and light (Bou, Boon, Kweku, Hidalgo, & Decker, 2011; Shi, Dai, Kakuda, Mittal, & Xue, 2008; Ukai, Lu, Etoh, Yagi, Ina, Oshima, et al., 2014), and has limited solubility in water because of its high hydrophobicity (Shariffa, Tan, Uthumporn, Abas, Mirhosseini, Nehdi, et al., 2017), which limits its applications in the food industry (Srivastava & Srivastava, 2013). Therefore, encapsulating lycopene in alginate-based emulsion gels can improve its functionality and stability during food processing, storage, and digestion (Aguirre Calvo et al., 2017; Soukoulis et al., 2016).

2. Materials and methods

2.1. Materials

Defatted soy flour (Bob's Red Mill, Milwaukie, Oregon, USA) and sunflower oil (Aldi Stores Ltd., Kildare, Ireland) were purchased from iHerb and Aldi, respectively. Sodium alginate (viscosity of 1 wt% sodium alginate solution in 0.15 M NaCl at 25 °C = 210–340 mPa s and $\overline{M}$ = 69–117 kDa) was obtained from Special Ingredients (Chesterfield, UK). Whey protein isolate (WPI) was purchased from Carbery Group Limited (Ballineen, Co. Cork, Ireland). Soy protein isolate (SPI) was extracted from defatted soy flour, according to the method described by Urbonaite, De Jongh, Van Der Linden, and Pouvreau (2015), and the protein content of SPI powder was 96.29 ± 0.03%. Tomato extract containing lycopene (0.059 mg/mg in the tomato extract), calcium chloride, sodium hydroxide, hydrochloric acid, and other analytical reagents were purchased from Sigma-Aldrich (St. Louis, MO, USA).

2.2. Preparation of emulsions and emulsion gel beads containing lycopene

The dispersions of WPI or SPI (4% in distilled water) were stirred at room temperature for 2 h using a magnetic stirrer, and then pH values of dispersions were adjusted to 7.0 with 1M HCl and NaOH. For preparing continuous phase, sodium alginate (0.4% in continuous phase) was added into the protein dispersions (4% wt) with water to reach final concentration of proteins (2.0% in continuous phase) by shearing at 400 rpm for 30 min with a magnetic stirrer and then allowed to rest for 24 h to permit hydration. The continuous phase without protein (i.e., 0.4% sodium alginate solutions) was prepared as control sample. For preparation of lycopene-capsulated emulsions, tomato extract containing lycopene (15 mg/100 g in the emulsions) was dissolved in sunflower oil (10 g oil/100 g in the emulsions) at 140 °C for 30 s, and then it was cooled down to the room temperature immediately and mixed with the continuous phase (1:9, w/w) at 13,000 rpm for 2 min with an Ultra-Turrax (IKA-25, Staufen, Germany). For production of emulsion gel beads, the resulting emulsions were dropped into 2% (w/w) $CaCl_2{\cdot}2H_2O$ solutions using 5-mL measuring pipets and a S1 pipet filler (Thermo Fisher Scientific Inc., Waltham, MA, USA), and the distance between the tip of pipet and the surface of $CaCl_2$ solutions was fixed at 10 cm. The samples were allowed to gel in $CaCl_2$ solutions for 30 min with mild magnetic stirring, and the resulting beads were rinsed with distilled water. All samples were kept in distilled water until further analyses.

2.3. Properties of emulsions

2.3.1. Viscosity

The viscosity of dispersions/solutions was tested at 25 °C using an AR 2000ex rheometer (TA Instruments, Crawley, UK) with an aluminium parallel plate (60 mm in diameter, and 0.5 mm in gap). Each sample was added in the middle of Peltier plate and allowed to stand for 2 min before testing. The flow measurement was performed over a shear rate range of 0.1–100 s^{-1}, and viscosity (η) was obtained from the data analysis software.

2.3.2. Droplet size distributions

The droplet size distributions of oil droplets in emulsions were analyzed with MasterSizer 3000 (Malvern Instruments Ltd., Worcestershire, UK). Samples were added to an automated wet dispersion unit until the obscuration reached between 3 and 12%. The stirrer speed was set at 2000 rpm. The refractive index and absorption index of samples were set at 1.48 and 0.001, respectively.

2.3.3. Structural analysis

Optical microscopy images of dispersion/emulsion samples were recorded using an Olympus BX51 light microscope with a build-in camera (Olympus Optical Co. Ltd., Tokyo, Japan). Samples were dropped on a microscope slide, covered with a glass coverslip, and observed using a 10 × objective lens and 10 × eyepiece.

Confocal scanning laser microscopy (CLSM) was used to observe microstructures of dispersions/emulsions. Dispersion/emulsion samples (500 μl) were transferred to a glass slide and stained with 50 μl of a mixture of Nile red (0.1%, w/v, in polyethylene glycol-200) and fast green (0.1%, w/v, in distilled water) at a ratio of 3:1. Confocal observation was performed using a Leica TCS SP5 microscope (Leica Microsystems GmbH, Wetzlar, Germany) at excitation and emission

wavelengths of 488 nm and 633 nm, provided by an argon laser and a HeNe laser, respectively.

2.4. Properties of emulsion gel beads

2.4.1. Water and oil contents

The gel beads before desiccation were weighted (W_i), and samples were dried in an oven at 80 °C until constant weight (W_o). The water content was calculated by Eq. (1):

$$Water\ content\ (\%) = \frac{W_i - W_o}{W_i} \times 100\% \quad (1)$$

Dry gel beads were ground and then mixed with 20 mL of hexane in a beaker. The mixture was stirred with a magnetic stirrer at room temperature for 10 min. The solvent mixture was filtered through a Whatman filter paper nº 1 into a beaker, and residues were rinsed three times with 15 mL of hexane in total. Then, the solvent was heated at 60 °C to evaporate hexane until constant weight (W_f). The oil content was calculated by Eq. (2):

$$Oil\ content\ (\%) = \frac{W_f}{W_i} \times 100\% \quad (2)$$

2.4.2. Lycopene content

Lycopene was extracted and quantified according to the method described by Anthon and Barrett (2006) with some modification. Samples (0.5 g of emulsion gel beads) were weighed into a screw cap tube, and 8.0 mL of hexane: acetone: ethanol (50 : 25: 25) solutions containing 0.1% BHT was added. The control solution was prepared with 0.5 g water instead of gel beads. After mixing for 1 min by a vortex, all samples were allowed to rest for 24 h until gel beads became pale. Water (1.0 mL) was added followed by mixing for 25 s again. The mixture was left to stand for 10 min to allow phases to separate and all bubbles to disappear. All samples were protected from light throughout extraction and analysis.

Lycopene concentrate (C_{LYC}) in the upper layer of mixtures was then measured by a rapid spectrometric method (Anthon & Barrett, 2006). The cuvette was rinsed with the upper layer of samples, and absorbance (A_{503}) of the upper layer was measured at 503 nm with a spectrophotometer. Lycopene concentration can be calculated by Eq. (3):

$$\begin{aligned} Lycopene\ concentrate\ (mg/kg) &= (A_{503} \times 537 \times 8 \times 0.55)/(0.50 \times 172) \\ &= A_{503} \times 27.5 \end{aligned} \quad (3)$$

where 537 g/mol is the molecular weight of lycopene, 8 mL is the volume of mixed solvent, 0.55 is the volume ratio of upper layer to the mixed solvents, 0.5 g is the weight of gel beads added, and 172 mM^{-1} is the extinction coefficient for lycopene in hexane.

2.4.3. Structural analysis

CLSM was used to observe the microstructure of emulsion gel beads. Samples were cut into a thin layer (~1 mm) and transferred to a glass slide and stained with a mixture of Nile red (0.1%, w/v, in polyethylene glycol-200) and fast green (0.1%, w/v, in distilled water) at a ratio of 3:1. Confocal observation was performed as described in Section 2.3.3.

2.4.4. Size and Young's modulus measurement

The Young's modulus of gel beads after gelation for 30 min were analyzed by a TA.XT Plus texture analyser (Stable Micro System, Godalming, UK). The surface of samples was dried by dry paper before testing. Compression tests were performed using a cylinder probe with 10 mm diameter and a 5-kg load cell. The samples were compressed to 30% strain at a crosshead speed of 0.1 mm/s, and five beads with same composition were examined one after another. Due to their ellipsoidal shapes, the cross-sectional area of samples was calculated after measuring the major axis (R_{max}) and minor axis (R_{min}) of gel beads using a digital vernier calliper after samples were placed on the platform of texture analyser. The Young's modulus of each sample was calculated as the gradient of the stress vs. strain curve in the 5–15% strain region, where stress and stain showed good linearity.

2.5. In-vitro digestion

Simulated digestion of emulsion gel beads included the oral, gastric and small intestinal phases in this study. The simulated saliva fluid (SSF), gastric fluid (SGF), and intestinal fluid (SIF) electrolyte stock solutions (i.e., 1.50 × concentrates) were prepared by the method of Minekus et al. (2014) with some modification. Simulated digestion fluids are made of electrolyte stock solutions, enzymes, $CaCl_2$, and water as described below.

Oral phase: 5 g of emulsion gel beads were mixed with 2.5 mL of SSF electrolyte stock solution followed by adding 25 μL of 0.3 M $CaCl_2$ (final 0.75 mM), 475 μL of water, and 2.0 mL of 375 U/mL α-amylase solution (final 75 U/g) with pH adjustment to 7.0. The mixtures were incubated at 37 °C for 2 min with continuous agitation at 300 rpm.

Gastric phase: the oral bolus (~10 g) was mixed with 5.0 mL of SGF electrolyte stock solution, 4.0 mL porcine pepsin stock solution of 10, 000 U/mL (final 2000 U/g), 5.0 μL of 0.3 M $CaCl_2$ (final 0.075 mM), 0.5 mL of 1 M HCl to reach pH 3.0 and 0.5 mL of water. The mixtures were incubated at 37 °C for 2 h with continuous agitation at 300 rpm.

Intestinal phase: the gastric chyme (~20 g) was mixed with 10 mL of SIF electrolyte stock solution, 5 mL of a pancreatin solution 800 U/mL (final 100 U/g), 4 mL bile solution of 25 g/L (Albarracin, Jose Gonzalez, & Drago, 2015), 40 μL of 0.3 M $CaCl_2$ (final 0.3 mM), 0.1 mL of 1 M NaOH to reach pH 7.0 and 0.9 mL of water. The mixtures were incubated at 37 °C for 6 h with continuous agitation at 300 rpm, and 0.1 M NaOH was used to maintain the pH (7.0) during the intestinal phase.

2.6. Young's modulus measurement of gel beads during oral and gastric digestion

Gel beads after oral digestion and during gastric digestion at 30, 60, 90 and 120 min were collected. The surface of samples was rinsed with distilled water, and the Young's modulus of samples were analyzed according to the methods described in Section 2.4.4.

2.7. Shrinkage measurement of gel beads during gastric digestion

The section shrinkage rate of gel beads was determined after 30, 60, 90, and 120 min of gastric digestion. Five gel beads were obtained from the gastric fluid and washed with distilled water. After drying the surface, the major axis (R'_{max}) and minor axis (R'_{min}) of gel beads were measured by using a digital vernier calliper, and the cross-section area (A_t) was calculated from Eq. (4). The major axis (R_{max}) and minor semi-axis (R_{min}) of gel beads after oral digestion for 2 min were measured as well, and the cross-section area (A_0) was also calculated from Eq. (4). The section shrinkage rate of gel beads was calculated from Eq. (4), and the experiment was replicated three times. The section shrinkage rate of samples during gastric digestion was compared to the section area of samples after oral digestion for 2 min in this study.

$$\text{Section shrinkage rate}\ (100\%) = \frac{A_0 - A_t}{A_0} = \frac{3.14 \times \frac{R_{max}}{2} \times \frac{R_{min}}{2} - 3.14 \times \frac{R'_{max}}{2} \times \frac{R'_{min}}{2}}{3.14 \times \frac{R_{max}}{2} \times \frac{R_{min}}{2}} \quad (4)$$

where A_0 indicates the section area of samples at the beginning of gastric digestion (i.e., after oral digestion for 2 min) and A_t indicates the section area of samples after 30, 60, 90, or 120 min of gastric digestion.

2.8. Microstructures of bead residuals after gastric digestion

The digesta was filtered by multilayer gauze to collect bead residuals, and CLSM was used to observe the microstructure of emulsion gel bead,

according to the method described in Section 2.4.3.

2.9. Release of lycopene during intestinal digestions

The digesta was filtered by multilayer gauze to separate bead residual and digestive juice, and the digestive juice (Wt_{juice}) was weighted. Lycopene in 1.0 g of digestive juice ($C_{LYC\text{-}J}$) was extracted and analyzed by the methods described in Section 2.4.2. The ratios of the amount of lycopene in digestive juice ($Wt_{LYC\text{-}J}$) to that in original beads ($Wt_{LYC\text{-}B}$) are regarded as release rates ($R_{release}$). The release rate of lycopene was estimated through Eq. (5):

$$\text{Release rates}\ (\%) = \frac{Wt_{LYC-J}}{Wt_{LYC-B}} \times 100\% = \frac{C_{LYC-J} \times Wt_{juice}}{C_{LYC-B} \times 5} \times 100\% \quad (5)$$

3. Results and discussion

3.1. Properties of alginate-based and protein-stabilized emulsions

3.1.1. Structures of emulsions

As shown in Fig. 1A–C, optical microscopy images of dispersions show that flocculation and coalescence occurred in dispersions without protein (i.e., the control sample), and flocculation occurred in SPI-stabilized emulsions, but WPI-stabilized emulsion droplets dispersed evenly in the continuous phase. Alginate is a naturally occurring hydrophilic polysaccharide and has poor emulsifying capacity, because it lacks hydrophobic groups (Lee & Mooney, 2012). Therefore, alginate-stabilized oil droplets have high surface tension and tend to merge into bigger oil droplets to reduce the contact area between the oil and water phases and reach the most thermodynamically stable state. In contrast, proteins can absorb at the o/w interface to prevent coalescence by reducing the surface tension of droplets and decrease flocculation through droplet-droplet repulsion. However, SPI-coated droplets had more significant flocculation than WPI-coated droplets, probably due to the depletion flocculation of droplets coated by excessive amount of insoluble SPI (Moschakis, Murray, & Biliaderis, 2010) and/or lower zeta-potential of SPI-coated droplets than WPI-coated droplets at pH 7.0 (Chen, Yokoyama, Liang, & Zhong, 2020).

CLSM was further used to observe the distribution of oil and protein in dispersions. Fig. 1D–F shows a red background of WPI- and SPI-stabilized emulsions, which indicates that some soluble protein molecules were still found in the continuous phase. The possible reason is that protein molecules were trapped by the continuous phase, due to the interactions between protein and alginate; also, 2% protein was probably higher than the saturation level of protein to cover the 10% oil droplets. Fig. 1D–F also show that more SPI molecules absorbed at the o/w interfaces than WPI molecules, probably because that WPI has higher solubility than SPI and thus more WPI molecules were held by alginate in the continuous phase through the interactions between them. As shown in Fig. 2, optical microscopy images of alginate solutions, WPI/alginate solutions, and SPI/alginate dispersion show that more insoluble substance was observed in SPI/alginate dispersion, compared to alginate and WPI/alginate solutions. This indicates that SPI has lower solubility than WPI and tends to self-aggregate in alginate solutions.

In addition, the viscosity of alginate solutions, WPI/alginate solutions, and SPI/alginate dispersion was further investigated to demonstrate the interactions between protein and alginate. As shown in Fig. 3A, WPI/alginate solutions exhibited more obvious shear-thinning behaviour and higher viscosity than sodium alginate solutions and SPI/alginate dispersion, which indicates that WPI had stronger interactions with alginate than SPI. It has been reported that

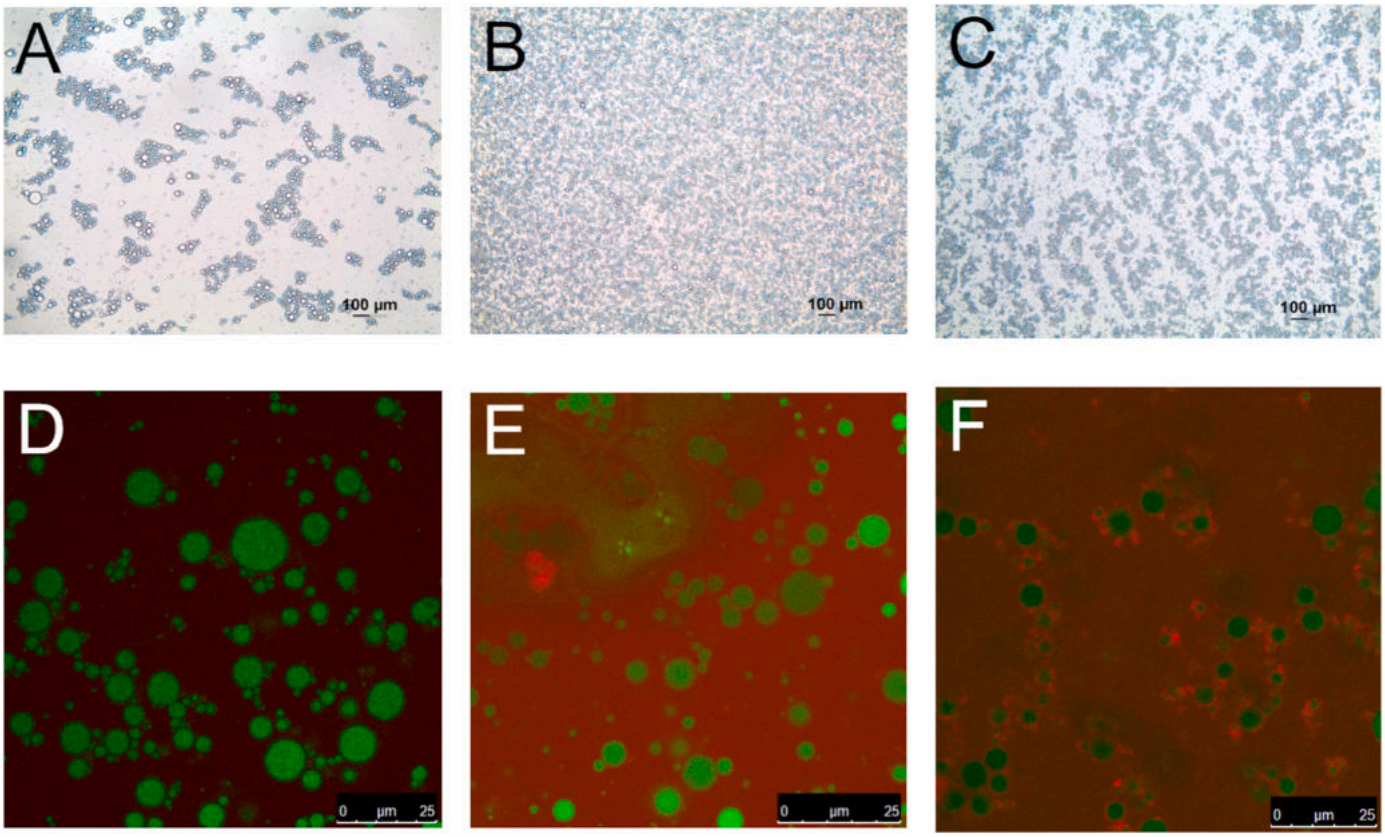

Fig. 1. Optical microscopy and CLSM images of (A and D) dispersions without proteins, (B and E) WPI-stabilized emulsions, and (C and F) SPI-stabilized emulsions. Protein and sunflower oil were stained by red and green in CLSM figures D–F, respectively. (For interpretation of the references to colour in this figure legend, the reader is referred to the Web version of this article.)

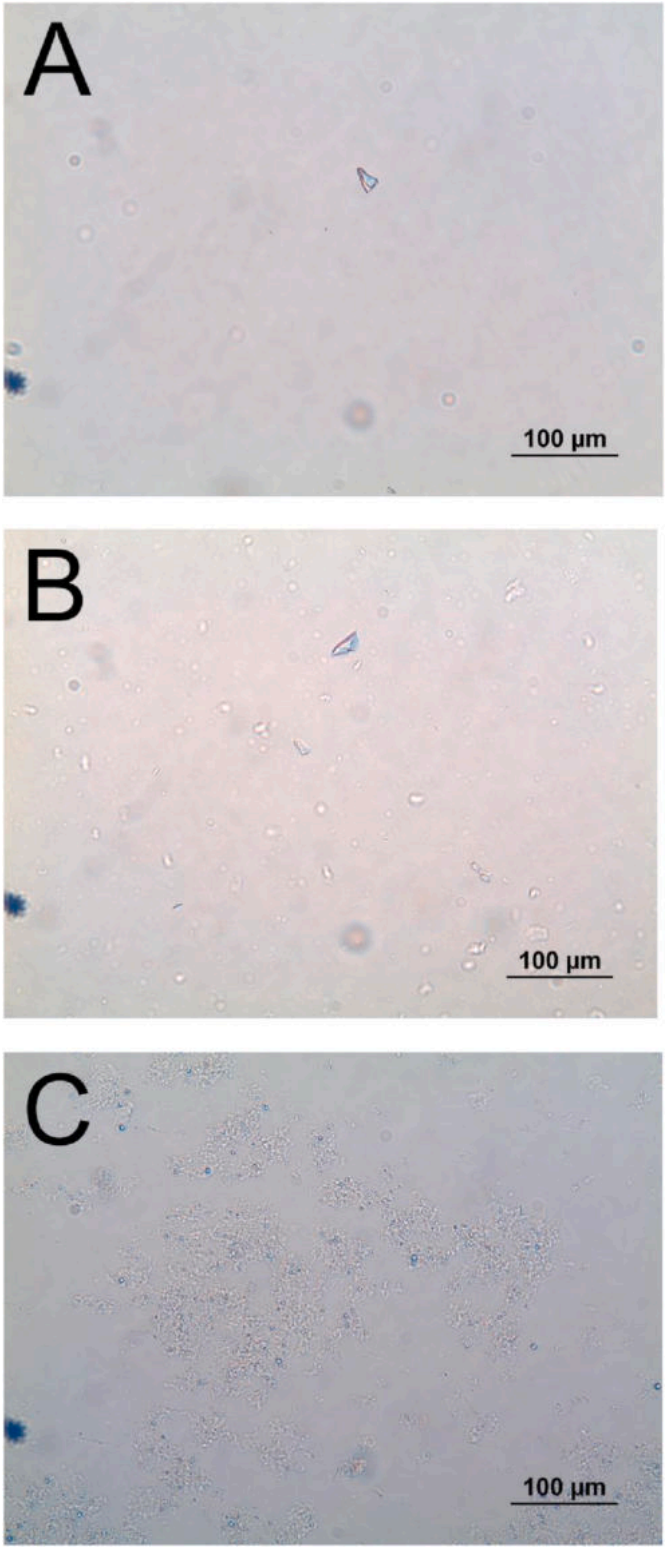

Fig. 2. Optical microscopy images of (A) alginate solutions (0.4%, w/w), (B) WPI/alginate solutions (2.0% WPI and 0.4% alginate, w/w), and (C) SPI/alginate dispersions (2.0% SPI and 0.4% alginate, w/w).

intermolecular associations between bovine serum albumin molecules and alginate chains occurred by electrostatic interactions between the oppositely charged amino acids and the anionic polysaccharide molecules, even though both polymers were negatively charged (Zhao, Li, Carvajal, & Harris, 2009). In addition, WPI contains many polar amino

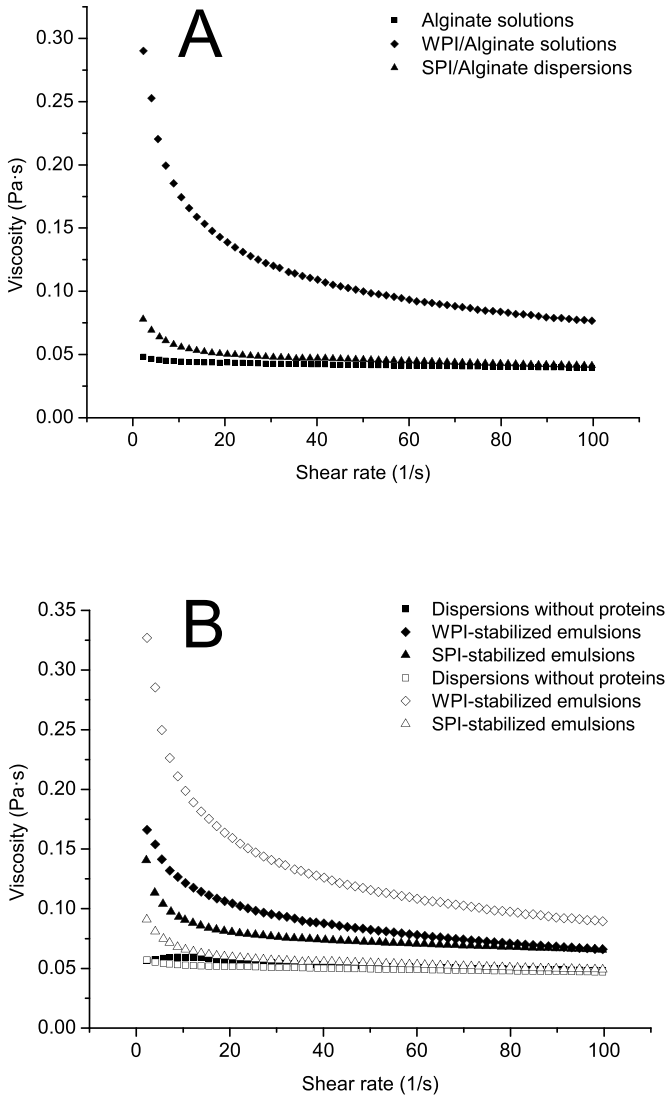

Fig. 3. (A) Viscosity of alginate solutions (0.4%, w/w), WPI/alginate solutions (2.0% WPI and 0.4% alginate, w/w), and SPI/alginate dispersions (2.0% SPI and 0.4% alginate, w/w). (B) Viscosity of dispersions without proteins, WPI- and SPI-stabilized emulsions, in which solid symbols present the experimental viscosity of samples and open symbols present the calculated viscosity.

acids (Peña-Ramos, Xiong, & Arteaga, 2004), which could form hydrogen bonds between side chains of WPI amino acids and residues of alginate molecules. Therefore, the interactions between WPI and alginate were probably driven by the electrostatic interactions and hydrogen bonds (Erben et al., 2019). On the other hand, SPI had weaker interactions with alginate, probably due to its lower solubility and fewer positively charged amino acids than WPI (i.e., 200.9 mg/g and 267.9 mg/g positively charged amino acids for SPI and WPI at pH 7.0, respectively) (Peña-Ramos, Xiong, & Arteaga, 2004; Tang et al., 2006).

3.1.2. Droplet size distributions of emulsions

Fig. 4 shows that WPI- and SPI-stabilized emulsions had similar droplet size distribution, while emulsions without protein (i.e., the control sample) had more large droplets than WPI- and SPI-stabilized emulsions. The droplet size in emulsions during homogenization depends on a balance between droplet disruption and droplet coalescence, so the droplet size can be affected by energy input, emulsifier type, and properties of the continuous phase. Increasing the intensity or duration of energy during homogenization can reduce the size of droplets in

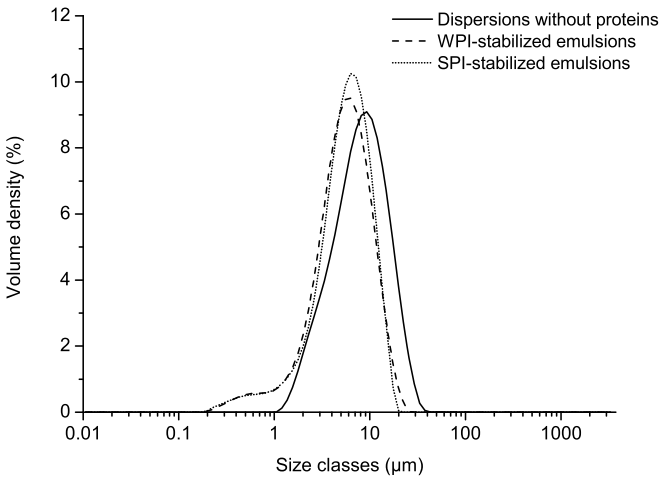

Fig. 4. Droplet size distribution of dispersions without proteins and WPI- and SPI-stabilized emulsions.

emulsions, but the energy input to all samples was the same in this study. The molecular properties of emulsifiers (e.g., size, conformation, flexibility, and interactions) can also affect the size of droplets in emulsions, because emulsifiers with better hydrophobicity, higher flexibility, and/or smaller molecular size can absorb more quickly at the surface of droplets to prevent droplet coalescence and thus produce smaller droplets during homogenization (McClements, 2015). In addition, the higher viscosity of the continuous phase can decrease droplet coalescence and thus produce smaller droplets. The poor hydrophobicity of alginate is probably the main reason leading to large droplets in the control sample, although the high viscosity of the continuous phase (i.e., alginate solutions) may also help to slow droplet coalescence.

However, many studies have indicated that WPI has higher hydrophobicity than SPI, although both of them are globular proteins with similar flexibility (Voutsinas et al., 1983), which was at variance with the size distribution of WPI- and SPI-stabilized emulsions obtained in current study. This was probably because interactions between WPI and sodium alginate (as discussed in Section 3.1.1) decreased the translational diffusion coefficient of WPI (i.e., slower movement of WPI molecules from the continuous phase to the O/W interfaces). Therefore, it can be hypothesised that WPI- and SPI-stabilized emulsions had similar droplet size distribution, which was because interactions between WPI and alginate negatively affect the adsorption kinetics of WPI, although WPI has higher hydrophobicity than SPI.

3.1.3. Viscosity of emulsions

Adding 10% (φ, w/w) sunflower oil into alginate solutions or SPI/alginate dispersions increased their viscosity, while adding sunflower oil decreased the viscosity of WPI/alginate solutions (Fig. 3A and B). The viscosity of suspensions containing non-interacting spherical fluid particles (i.e., dispersed phase) can be calculated by the following equation (Larson, 1999; Tadros, 1994):

$$\eta = \eta_1 \left(1 + \left[\frac{\eta_1 + 2.5\eta_2}{\eta_1 + \eta_2}\right]\varphi\right) \quad (6)$$

where η is the viscosity of dispersions, η_1 is the viscosity of the liquid surrounding the droplets, η_2 is the viscosity of the liquid in the droplets (the viscosity of sunflower oil is 0.063 ± 0.01 Pa s), and φ is the dispersed phase volume fraction (i.e., 10% of the oil content in this study).

As shown in Fig. 3B, the viscosity of the dispersion without protein (i.e., the control sample) could fit Eq. (6) well, which indicates that oil droplets in alginate solutions without protein were non-interacting spherical particles. However, the estimated viscosity of the SPI-stabilized emulsions was lower than their experimental values, and the estimated viscosity of the WPI-stabilized emulsions was higher than their experimental values. This indicates that SPI-coated emulsion droplets were flocculated. Emulsions containing flocculated droplets have higher viscosity than emulsions containing isolated droplets, because flocculated droplets trap some of the continuous phase within their structures and therefore have a higher effective volume fraction (φ_{eff}) than the actual volume fraction of the dispersed phase (i.e., $\varphi_{eff} >$ 10%) (McClements, 2015). The more obvious shear-thinning behaviour of SPI-stabilized emulsions than SPI/alginate dispersions also proved that flocculation has occurred in SPI-stabilized emulsions. However, the situation is different for WPI-stabilized emulsions. As discussed in Section 3.1.1, WPI has strong interactions with alginate, probably driven by electrostatic interactions and hydrogen bonds. After adding oil into WPI/alginate solutions, some of WPI molecules move to the oil/water interface and then attach to the interface. The attachment of WPI molecules to the oil/water interface may lead to part of molecule structures attaching into the oil droplets, which leads to a decreased contact area between WPI and alginate and thus a decreased viscosity (η_1) of the continuous phase surrounding the droplets (as shown in Fig. 5). Therefore, we hypothesised that the higher viscosity of SPI-stabilized emulsions than SPI/alginate dispersions was due to the occurrence of flocculation and the increased effective volume fraction (φ_{eff}), while the decreased viscosity of the continuous phase (η_1) was the main reason leading to the lower viscosity of WPI-stabilized emulsions compared to WPI/alginate solutions.

3.2. Properties of alginate-based and protein-stabilized emulsion gel beads

3.2.1. Water and oil contents and structures of emulsion gel beads

Table 1 shows that SPI-stabilized emulsion gel beads had higher water content than WPI-stabilized emulsion gel beads, and emulsion gel beads without protein had lowest water content. If the oil was not lost during gelation, according to the oil content in gel beads, the water quantity in the gel beads compared to the weight of original emulsions can be calculated as 38.78 ± 3.05, 42.22 ± 2.75, and 56.36 ± 5.29 g/100g in original emulsions for emulsion gel beads without protein, WPI-stabilized emulsion gel beads, and SPI-stabilized emulsion gel beads, respectively. The results indicate that water loss in emulsion gel beads without protein, WPI-stabilized emulsion gel beads, and SPI-stabilized emulsion gel beads during gelation were 50.82 ± 3.05, 45.38 ± 2.75, and 31.4 ± 5.29 g/100g, compared to their original emulsions, respectively. This indicates that both WPI and SPI could prevent water loss from alginate-based emulsion gel beads during gelation. This was probably associated with the solubility of proteins and interactions between protein and alginate, which affected the gelation process, structures and thus water content of alginate-based emulsion gel beads (Lin, Kelly, Maidannyk & Song, 2020).

In this study, emulsion gel beads were prepared by the external gelation method, in which emulsions were dropped into $CaCl_2$ solutions. When emulsion drops contact with the $CaCl_2$ solution, the surface of drops gelatinizes immediately, and then the gelation process progresses gradually from the surface to interior of gel beads with the diffusion of Ca^{2+}. During this process, stretches of alginate monomers interact with Ca^{2+}, and the formation of junctions between them forces water out and leads to shrinkage of gel beads (Rehm, 2009). When WPI was added into this system, due to the high solubility of WPI, water molecules may serve as bridges to form hydrogen bonds between polar amino acids of WPI and residues of alginate molecules, which decreased water loss during gelation and a larger bead size. However, SPI has lower solubility and less interaction with alginate than WPI, so SPI may act as barriers to block the gelation process of alginate monomers, which led to weak gel structures, decreased water loss during gelation, and thus larger bead size as well.

Fig. 6 shows the distribution of protein and oil droplets in emulsion gel beads: more WPI was distributed in matrices (as seen by a more

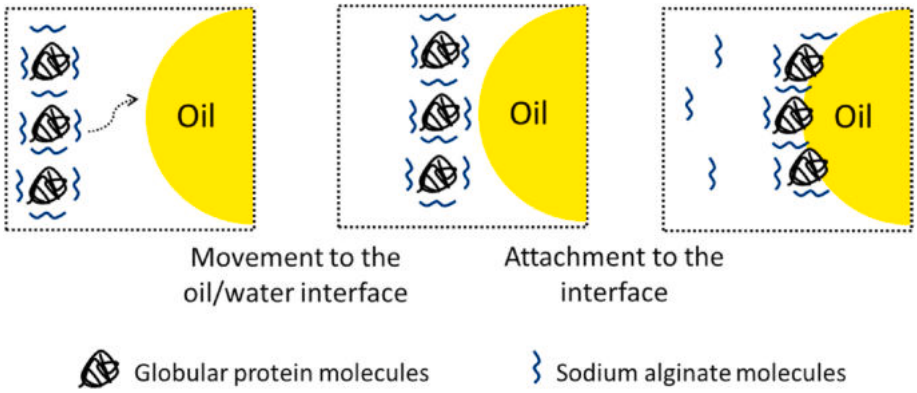

Fig. 5. The adsorption of protein/alginate mixtures at the o/w interface (McClements, 2015).

Table 1
Properties of emulsion gel beads.

Samples	Water content (%)	Oil content (%)	Lycopene content (mg/kg)	Size (mm)		Young's modulus (Pa)	
				Minor axis	Major axis	Experimental value	Theoretical value predicted by the Kerner model
Gel beads without proteins	71.32 ± 1.52	25.92 ± 2.06	14.78 ± 1.01	3.32 ± 0.08	3.46 ± 0.11	219.46 ± 7.69	224.68–233.88
WPI-stabilized emulsion gel beads	73.11 ± 0.39	23.78 ± 1.72	12.42 ± 0.81	3.52 ± 0.11	3.64 ± 0.11	233.39 ± 6.75	305.05–317.55
SPI-stabilized emulsions gel beads	76.18 ± 1.28	17.87 ± 1.68	9.66 ± 0.65	3.82 ± 0.04	4.02 ± 0.20	187.27 ± 6.11	130.52–135.86

evenly red background) than SPI, while SPI tended to self-aggregate around oil droplets. In addition, the deformation and coalescence of emulsion droplets occurred in all gel beads after gelation, compared to their original emulsion structures before gelation (Fig. 1). This was probably because, in current study, the emulsion gel matrix structure formed by 0.4% alginate was fragile, and thus structural collapse occurred during gelation (Lin, Kelly, Maidannyk, & Miao, 2020a).

In addition, Table 1 also shows that the oil content of emulsion gel beads without protein was higher than that of WPI- and SPI-stabilized emulsion gel beads, although the oil contents in their original dispersions were the same (i.e., 10%, w/w). This was probably because, when water loss occurs during gelation, the oil content in samples increases accordingly. Emulsion gel beads without protein lost the most water content during gelation, so the oil content in them was higher compared to WPI- and SPI-stabilized emulsion gel beads. This was also the main reason why gel beads without protein had higher lycopene content compared to WPI- and SPI-stabilized emulsion gel beads (as shown in Table 1).

3.2.2. *Young's modulus of emulsion gel beads*

The mechanical properties of emulsion gel beads are very important, because they are closely associated with other properties (e.g., storage stability, oral perception, and controlled release) and the applications. Many factors can affect the mechanical properties of emulsion gel beads,

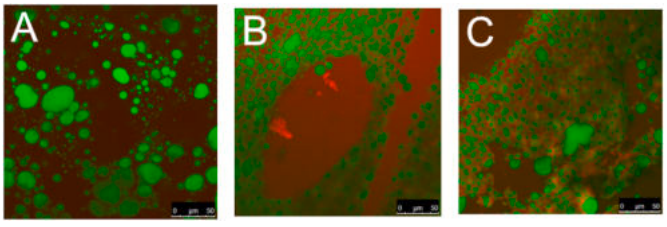

Fig. 6. CLSM images of (A) gel beads without proteins, (B) WPI-stabilized emulsion gel beads, and (C) SPI-stabilized emulsion gel beads. Protein and sunflower oil were stained by red and green, respectively. (For interpretation of the references to colour in this figure legend, the reader is referred to the Web version of this article.)

such as matrix structure, interactions between matrix and emulsifier-stabilized droplets, oil type, oil volume fraction, and droplet size (Lin, Kelly & Miao, 2020). However, the matrix structure may be the most important factor affecting the release of nutrients encapsulated in emulsion gels during digestion. It has been reported that a denser WPI-based matrix structure delayed the digestion of lipid encapsulated in emulsion gels (Guo, Bellissimo, & Rousseau, 2017). In this study, the Young's modulus of emulsion gel beads was analyzed.

Table 1 shows that the Young's modulus of the control sample was higher than that of SPI-stabilized emulsion gels but lower than that of WPI-stabilized emulsion gels. The modulus of overall emulsion gels was affected by matrix and filler droplets, according to the Kerner model modified by Lewis and Nielsen (Kerner, 1956; Lewis & Nielsen, 1970):

$$\frac{G'_{gel}}{G'_{matrix}} = \frac{15(1-\nu_m)(M-1)\psi\varphi_f}{(8-10\nu_m)M+7-5\nu_m-(8-10\nu_m)(M-1)\psi\varphi_f} + 1 \quad (7)$$

where $M = \frac{G'_{filler}}{G'_{matrix}}$, G'_{gel}, G'_{filler}, and G'_{matrix} are the modulus of the overall gel, the filler droplets and the gel matrix, respectively, $\psi\varphi_f$ is the effective droplet volume fraction, and ν_m is the Poisson's ratio of the gel matrix.

In addition, the modulus of the filler droplets ($G'_{filler} = 4\gamma/d$) is affected by the surface tension (γ) and the average diameter (d) of the oil droplets. It can be seen that the modulus of the overall gel (G'_{gel}) is in direct proportion to the M, $\psi\varphi_f$, and G'_{matrix}. However, it should be noted that the modified Kerner model is normally used under the assumption that M or G'_{matrix} do not change with changes in other factors (e.g., φ_f) (Lin, Kelly, & Miao, 2020b).

According to Eq. (7), the theoretical values of G'_{gel}/G'_{matrix} of alginate-based emulsion gels were 1.22–1.27 with the assumption that M was 12–70 (Chen & Dickinson, 1998), $\psi\varphi_f$ was 0.1, and ν_m was 0.5 (Ahearne, Yang, El Haj, Then, & Liu, 2005; Langley & Green, 1989). In contrast, the experimental values of G'_{matrix} of emulsion gels without protein, and WPI- and SPI-stabilized emulsion gels (i.e., alginate, alginate/WPI, and alginate/SPI gel beads) were 184.16 ± 14.95, 250.04 ± 16.56, and 106.98 ± 6.00 Pa, respectively. Therefore, their experimental values of G'_{gel}/G'_{matrix} were 1.19 ± 0.04, 0.93 ± 0.03, and 1.75 ± 0.06,

respectively. It can be seem that alginate-stabilized emulsion gels without protein (i.e., the control sample) fitted the modified Kerner model well; however, the experimental value of G'_{gel}/G'_{matrix} for WPI-stabilized emulsion gels was lower than the theoretical value, and the experimental value of SPI-stabilized emulsion gels was higher than the theoretical value. The possible reason was that adding oil led to the absorption of protein from the matrix to the oil/water surface, which resulted in decreased interactions between WPI and alginate molecules in the matrix, and thus a decreased G'_{matrix} of WPI-stabilized emulsion gels, but led to a less structural obstruction of SPI to the matrix and thus an increased G'_{matrix} of SPI-stabilized emulsion gels. Therefore, we presume that the presence of oil in alginate/protein based emulsion gels

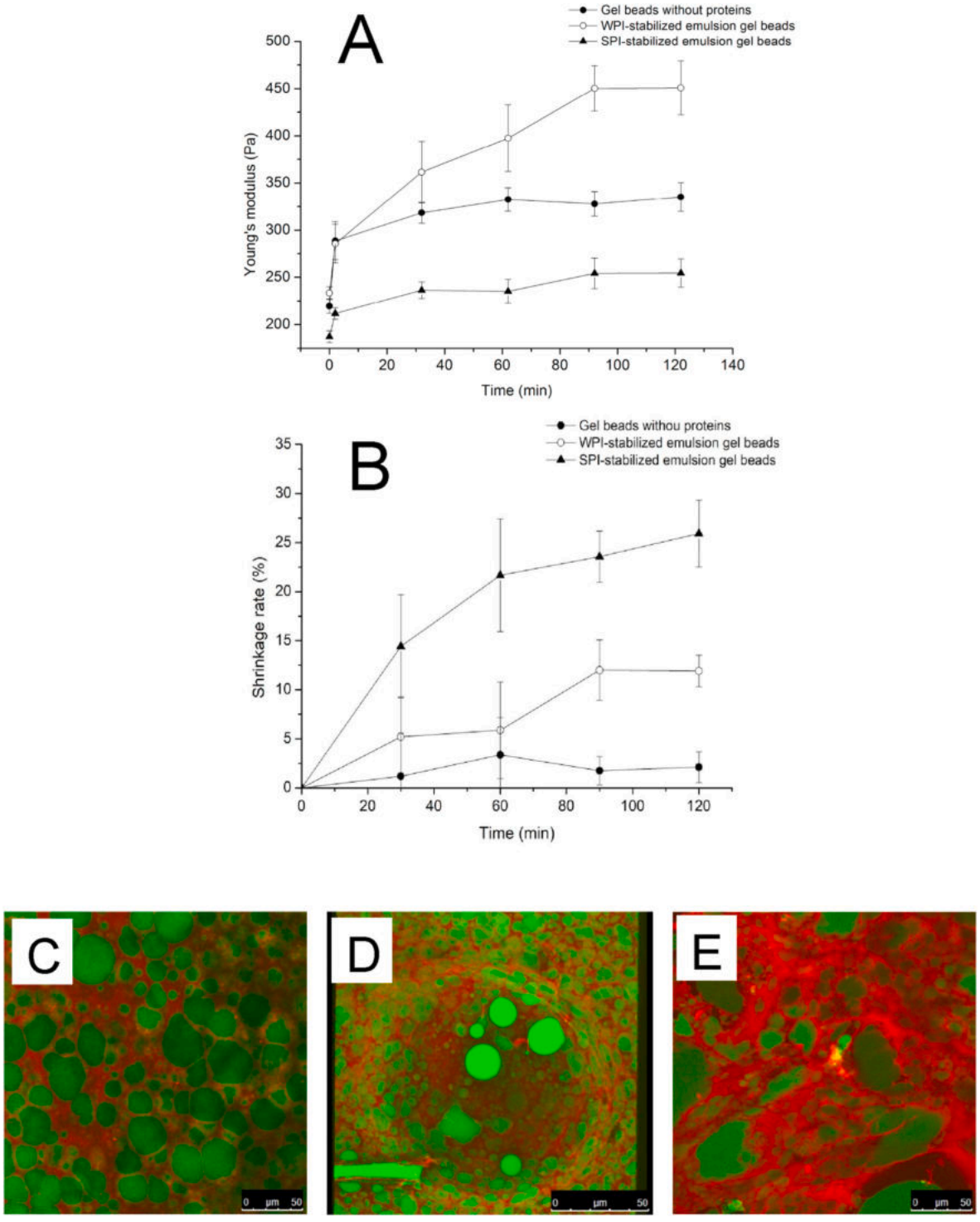

Fig. 7. (A) Young's modulus of gel beads without proteins, WPI-stabilized emulsion gel beads, and SPI-stabilized emulsion gel beads during *in-vitro* oral and gastric digestions. (B) Shrinkage of gel beads without proteins, WPI-stabilized emulsion gel beads, and SPI-stabilized emulsion gel beads during *in-vitro* gastric digestions. CLSM images of (C) gel beads without proteins, (D) WPI-stabilized emulsion gel beads, and (E) SPI-stabilized emulsion gel beads after *in-vitro* gastric digestion for 120 min. Protein and sunflower oil were stained by red and green in CLSM figures D–F, respectively. (For interpretation of the references to colour in this figure legend, the reader is referred to the Web version of this article.)

affected the mechanical properties of overall emulsion gels, because oil droplets draw proteins from the matrix to the oil/water interfaces, and thus affects the mechanical properties of alginate/protein-based matrix.

3.3. In-vitro digestion behaviour of emulsion gel beads containing lycopene

3.3.1. Young's modulus, shrinkage, and structure of emulsion gel beads during oral and gastric digestion

Alginate-based gel beads normally shrink during gastric digestion and swell during intestinal digestion, probably due to the changes in electrostatic forces in the gel matrix at different pH and the occurrence of ion-exchange at various ionic strength conditions (Rayment et al., 2009). The shrinkage of beads during gastric digestion can affect the structural and mechanical properties of beads and thereby their digestion behaviour in the following intestinal digestion. In addition, the zeta potential of WPI and SPI also differs at different pH values, which may affect the interactions between alginate and protein molecules. Therefore, it is important to investigate the changes in mechanical properties of protein/alginate-based emulsion beads during oral and gastric digestion.

Fig. 7A shows that the Young's modulus of gel beads without protein, WPI-stabilized emulsion beads and SPI-stabilized emulsion beads at the end of oral digestion were 1.32, 1.22, and 1.13 times higher than their original Young's modulus before digestion, respectively. A possible explanation for increased Young's modulus of alginate-based gel beads during oral digestion is that, the simulated saliva fluid (SSF) contains 13.6 mM sodium bicarbonate, which may react with calcium ions in alginate-based gel beads (i.e., $Ca^{2+} + HCO_3^- \rightarrow CaCO_3 + H^+$) and thus lead to the dissociation of calcium ions from alginate multimers and the formation of $CaCO_3$ nanoparticles and hydrogen bonds between alginate chains (Norton, Frith, & Ablett, 2006). The $CaCO_3$ nanoparticles can also act as physical cross-linker between carboxylic groups of alginate (Shen, Nyström, & Mezzenga, 2017). On the other hand, the presence of proteins in alginate-based emulsion beads led to a lower change rate of Young's modulus during oral digestion compared to gel beads without protein, which was probably because the presence of proteins disrupted the gelation process of alginate during the preparation, and then original gel beads contained higher levels of water, which led to lower concentrations of calcium ions in the gel matrices (Quong, Neufeld, Skjåk-Bræk, & Poncelet, 1998).

Fig. 7A also shows that the Young's modulus of gel beads without protein, WPI-stabilized emulsion beads and SPI-stabilized emulsion beads at the end of gastric digestion were 1.16, 1.59, and 1.36 times higher than their Young's modulus at the end of oral digestion, respectively. The further increased Young's modulus of alginate-based gel beads during gastric digestion probably resulted from the decreased electrostatic forces between alginate monomers. The pH of digestive juice was maintained at 3.0 during gastric digestion, and pK_a of alginate is at around 3.5 and thus alginate loses its negative charge at lower pH values (Li, Hu, Du, Xiao, & McClements, 2011). Therefore, alginate monomers with lower charges had less electrostatic repulsion with each other, and a denser structure formed. On the other hand, the presence of proteins in alginate-based emulsion beads led to a higher rate of change of Young's modulus during gastric digestion compared to gel beads without protein. A possible reason is that the electrostatic attractions occurred between negatively charged alginate monomers with positively charged protein molecules at pH 3.0. The isoelectric point of WPI and SPI had been reported to be at pH 4.5, and thus proteins are positively charged at pH 3.0 during gastric digestion (Fioramonti, Perez, Aríngoli, Rubiolo, & Santiago, 2014).

The shrinkage of emulsion gel beads during gastric digestion may also be a critical factor. As shown in Fig. 7B, emulsion gel beads without protein shrank by 2.11%, while WPI-stabilized emulsion beads and SPI-stabilized emulsion beads shrank by 11.91% and 25.92% after gastric digestion, respectively, compared to their size after oral digestion. This indicates that the presence of WPI and SPI in alginate-based emulsion gels led to more shrinkage than gel beads without protein during gastric digestion, probably also due to the electrostatic attractions between alginate and proteins at pH 3.0. In addition, the size of emulsion gel beads without protein, WPI-stabilized emulsion beads, and SPI-stabilized emulsion beads decreased from $R'_{min} = 3.24 \pm 0.13$ mm and $R'_{max} = 3.50 \pm 0.19$ mm to $R'_{min} = 3.23 \pm 0.10$ mm and $R'_{max} = 3.43 \pm 0.10$ mm, from $R'_{min} = 3.28 \pm 0.10$ mm and $R'_{max} = 3.40 \pm 0.08$ mm to $R'_{min} = 3.03 \pm 0.06$ mm and $R'_{max} = 3.23 \pm 0.06$ mm, and from $R'_{min} = 3.66 \pm 0.05$ mm and $R'_{max} = 3.82 \pm 0.11$ mm to $R'_{min} = 3.12 \pm 0.08$ mm and $R'_{max} = 3.32 \pm 0.13$ mm, respectively, during gastric digestion. This indicates that the presence of WPI and SPI led to smaller size of alginate-based emulsion gel beads after gastric digestion and thus denser gel structures.

Fig. 7C–E shows the distribution of protein and oil droplets in emulsion gel beads after gastric digestion. The coalescence of droplets further increased after gastric digestion, compared to their original emulsion gel structures (Fig. 6). There are several likely reasons for this observation. Firstly, the decreased electrostatic forces between alginate monomers during gastric digestion may result in a denser structure of gel matrix and thus force oil droplets to merge together. Secondly, peptic hydrolysis of proteins may have reduced the stability of emulsion droplets (Liu, Gao, & Yuan, 2015). Thirdly, the decreased pH values of gel beads may decrease the zeta-potential value of WPI and SPI and lead to protein aggregation and thus a decreased emulsifying capacity (Bokkhim, Bansal, Grøndahl, & Bhandari, 2016; Elizalde, Bartholomai, & Pilosof, 1996).

3.3.2. Lycopene release from emulsion gel beads during intestinal digestion

The visual appearance of alginate-based and protein-stabilized emulsion gels (Fig. 8) and the release of encapsulated nutrient (i.e., lycopene) from gel beads during intestinal digestion (Fig. 9) were studied. Alginate gels normally swell during intestinal digestion, due to the deprotonation and increased repulsive forces of the uronic acid groups on alginate at neutral pH above the pKa, and then structural degradation occurs, due to ion-exchange between Na^+ ions present in the digestive fluid and Ca^{2+} ions present in gel beads (Bajpai & Sharma, 2004; Rayment et al., 2009). As shown in Fig. 8, structural collapse of gel beads without proteins, WPI-stabilized emulsion gel beads, and SPI-stabilized emulsion gel beads occurred at 2–3 h, 4–5 h, and 3–4 h after swelling during intestinal digestion, respectively. This indicates that the presence of WPI and SPI could slow the swelling process and thus delay the structural degradation of alginate-based emulsion gel beads during intestinal digestion, probably because of the denser structures formed by electrostatic attractions between negatively charged alginate monomers with positively charged protein molecules after gastric digestion (as discussed in Section 3.3.1).

Fig. 9 shows that lycopene release from gel beads without proteins, WPI-stabilized emulsion gel beads, and SPI-stabilized emulsion gel beads commenced at 2.5–3 h, 4–4.5 h, and 3.5–4h, respectively, which corresponded with the start point of the structural collapse of gel beads (Fig. 8). This indicates that lycopene was released with degradation of network structures after swelling of gel beads during intestinal digestion. It has been reported that the encapsulated nutrients can be released from gel beads by two mechanisms: diffusion through increasingly large pores and/or release following degradation of network structures during intestinal digestion, which depends on the size of pores in beads and the size of encapsulated nutrients (George & Abraham, 2006).

In this study, lycopene release was correlated with the release of oil droplets from emulsion gel beads. The size of oil droplets in gel beads (Fig. 7C–E) were significantly larger than the pores of alginate gel matrices (normally between 5 and 200 nm) (George & Abraham, 2006). Therefore, lycopene and oil droplets were released from alginate-based emulsion gel beads due to structural degradation after swelling rather than during the swelling process. Fig. 9 also shows that the presence of WPI and SPI in alginate-based emulsion beads delayed the release of

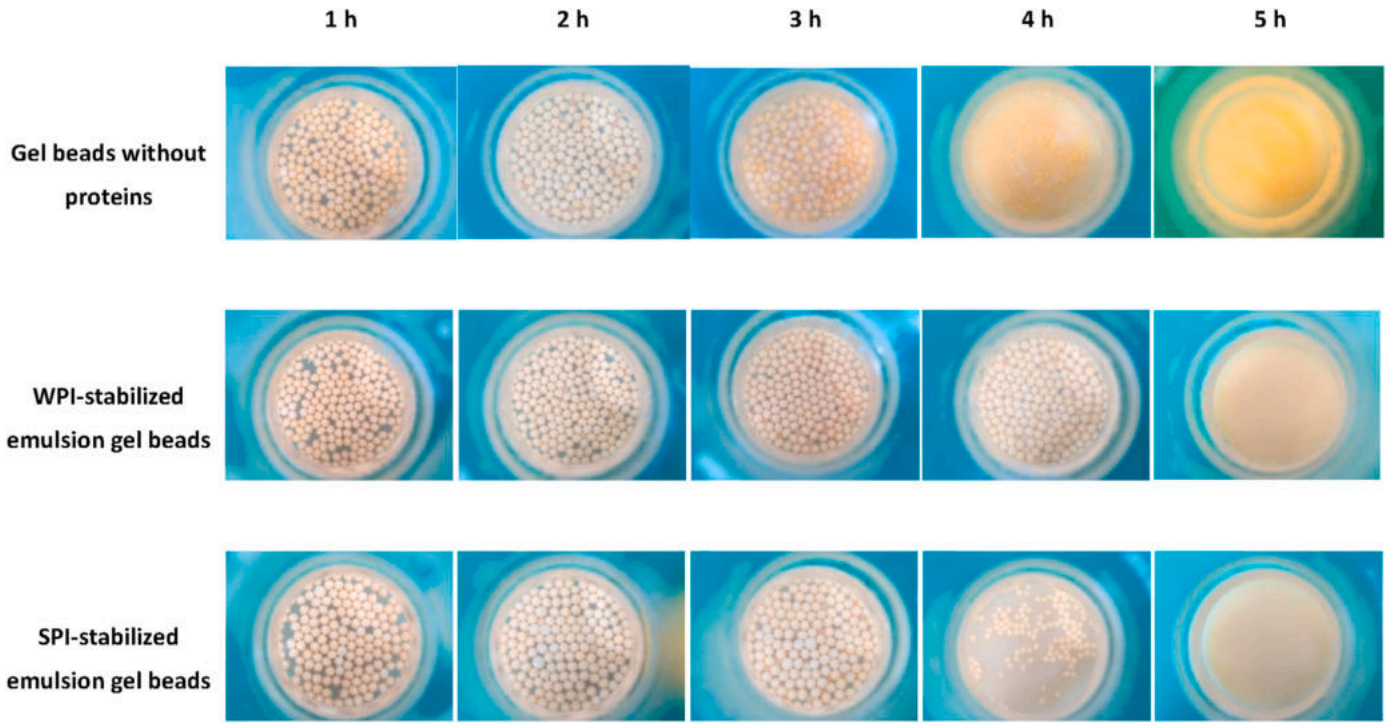

Fig. 8. Visual appearance of gel beads without proteins, WPI-stabilized emulsion gel beads, and SPI-stabilized emulsion gel beads during *in-vitro* intestinal digestion.

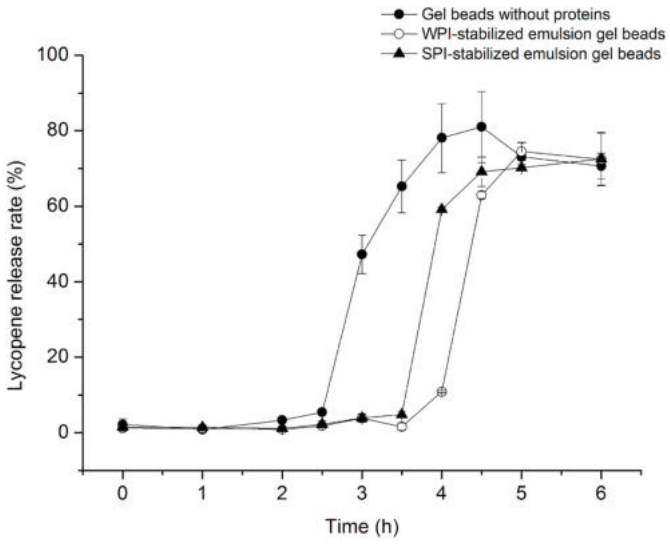

Fig. 9. Lycopene release from gel beads without proteins, WPI-stabilized emulsion gel beads, and SPI-stabilized emulsion gel beads during *in-vitro* intestinal digestion.

lycopene from beads during intestinal digestion. This was because the presence of WPI and SPI slowed the swelling process, due to the denser structures formed after gastric digestion, and thus delayed the structural collapse. Therefore, it may be assumed that the digestion of gel matrix and the release of encapsulated nutrients from emulsion beads are affected by not only the gel strength but also the gel density, the matrix components of gels, and the size of droplets.

4. Conclusions

The presence of WPI in alginate-based emulsions resulted in emulsions with higher viscosity, smaller droplet size distribution, and less flocculation of droplets than emulsions containing SPI, probably because WPI had better solubility and stronger interactions with alginate than SPI. WPI and SPI could prevent water loss from alginate-based emulsion gel beads during gelation, resulting in lower oil and lycopene contents, compared to gel beads without proteins. The presence of WPI increased the Young's modulus of gel beads, due to increased Young's modulus of WPI/alginate complexes-based gel matrix, while the presence of SPI decreased the Young's modulus because of its low solubility, compared to alginate-based gel beads without proteins. The presence of proteins (both WPI and SPI) resulted in higher shrinkage rate and higher ratio of change in Young's modulus of gel beads during *in-vitro* gastric digestion, and led to delayed release of lycopene from gel beads during *in-vitro* intestinal digestion.

The findings of this study underline the role of different proteins in the properties of alginate-based emulsions and emulsion gel beads, and the delayed release of lycopene from gel beads during *in-vitro* digestion, which makes it possible to design emulsion gel beads with potential controlled released of functional hydrophobic ingredients by structuring the gel matrix and the water/oil interfaces with natural polymers (e.g., proteins) instead of synthetic chemicals (e.g., Tween 20 and Span 80). However, this study mainly focused on the effect of WPI and SPI on the mechanical and structural properties of alginate-based emulsion gel beads after gelation and during *in-vitro* digestion, so further research on the effect of WPI and SPI on the stability of encapsulated lycopene during storage and the bio-availability during intestinal digestion is needed.

Declaration of competing interest

The authors declare that they have no known competing financial interests or personal relationships that could have appeared to influence the work reported in this paper.

CRediT authorship contribution statement

Duanquan Lin: Conceptualization, Methodology, Writing - original draft, Data curation, Investigation. **Alan L. Kelly:** Supervision, Writing - review & editing. **Valentyn Maidannyk:** Investigation. **Song Miao:** Supervision, Conceptualization, Writing - review & editing, Funding acquisition, Project administration, Investigation.

Acknowledgement

This work is supported by the China Scholarship Council (No. 201708350111) and Teagasc-The Irish Agriculture and Food Development Authority (RMIS6821).

Appendix A. Supplementary data

Supplementary data to this article can be found online at https://doi.org/10.1016/j.foodhyd.2020.106165.

References

Aguirre Calvo, T. R., Busch, V. M., & Santagapita, P. R. (2017). Stability and release of an encapsulated solvent-free lycopene extract in alginate-based beads. *Lebensmittel-Wissenschaft und -Technologie- Food Science and Technology, 77*, 406–412.

Ahearne, M., Yang, Y., El Haj, A. J., Then, K. Y., & Liu, K.-K. (2005). Characterizing the viscoelastic properties of thin hydrogel-based constructs for tissue engineering applications. *Journal of The Royal Society Interface, 2*, 455–463.

Albarracin, M., Jose Gonzalez, R., & Drago, S. R. (2015). Soaking and extrusion effects on physicochemical parameters, phytic acid, nutrient content and mineral bio-accessibility of whole rice grain. *International Journal of Food Sciences & Nutrition, 66*, 210–215.

Anthon, G., & Barrett, D. M. (2006). Standardization of a rapid spectrophotometric method for lycopene analysis. *Acta Horticulturae, 1*, 111–128.

Bajpai, S., & Sharma, S. (2004). Investigation of swelling/degradation behaviour of alginate beads crosslinked with Ca^{2+} and Ba^{2+} ions. *Reactive and Functional Polymers, 59*, 129–140.

Benavides, S., Cortés, P., Parada, J., & Franco, W. (2016). Development of alginate microspheres containing thyme essential oil using ionic gelation. *Food Chemistry, 204*, 77–83.

Bokkhim, H., Bansal, N., Grøndahl, L., & Bhandari, B. (2016). *In-vitro* digestion of different forms of bovine lactoferrin encapsulated in alginate micro-gel particles. *Food Hydrocolloids, 52*, 231–242.

Bou, R., Boon, C., Kweku, A., Hidalgo, D., & Decker, E. A. (2011). Effect of different antioxidants on lycopene degradation in oil-in-water emulsions. *European Journal of Lipid Science and Technology, 113*, 724–729.

Calvo, T. R. A., Busch, V. M., & Santagapita, P. R. (2017). Stability and release of an encapsulated solvent-free lycopene extract in alginate-based beads. *Lebensmittel-Wissenschaft und -Technologie- Food Science and Technology, 77*, 406–412.

Castro, M. A. A., Alric, I., Brouillet, F., Peydecastaing, J., Fullana, S. G., & Durrieu, V. (2018). Soy protein microparticles for enhanced oral ibuprofen delivery: Preparation, characterization, and in vitro release evaluation. *AAPS PharmSciTech, 19*, 1124–1132.

Chen, J., & Dickinson, E. (1998). Viscoelastic properties of heat-set whey protein emulsion gels. *Journal of Texture Studies, 29*, 285–304.

Chen, L., Yokoyama, W., Liang, R., & Zhong, F. (2020). Enzymatic degradation and bioaccessibility of protein encapsulated β-carotene nano-emulsions during *in vitro* gastro-intestinal digestion. *Food Hydrocolloids, 100*, Article 105177.

Costa-Rodrigues, J., Pinho, O., & Monteiro, P. R. R. (2018). Can lycopene be considered an effective protection against cardiovascular disease? *Food Chemistry, 245*, 1148–1153.

Elizalde, B., Bartholomai, G., & Pilosof, A. (1996). The effect of pH on the relationship between hydrophilic/lipophilic characteristics and emulsification properties of soy proteins. *LWT-Food Science and Technology, 29*, 334–339.

Erben, M., Pérez, A. A., Osella, C. A., Alvarez, V. A., & Santiago, L. G. (2019). Impact of gum Arabic and sodium alginate and their interactions with whey protein aggregates on bio-based films characteristics. *International Journal of Biological Macromolecules, 125*, 999–1007.

Feng, W., Yue, C., Ni, Y., & Liang, L. (2018). Preparation and characterization of emulsion-filled gel beads for the encapsulation and protection of resveratrol and α-tocopherol. *Food Research International, 108*, 161–171.

Fioramonti, S. A., Perez, A. A., Aríngoli, E. E., Rubiolo, A. C., & Santiago, L. G. (2014). Design and characterization of soluble biopolymer complexes produced by electrostatic self-assembly of a whey protein isolate and sodium alginate. *Food Hydrocolloids, 35*, 129–136.

George, M., & Abraham, T. E. (2006). Polyionic hydrocolloids for the intestinal delivery of protein drugs: Alginate and chitosan—a review. *Journal of Controlled Release, 114*, 1–14.

Guo, Q., Bellissimo, N., & Rousseau, D. (2017). Role of gel structure in controlling in vitro intestinal lipid digestion in whey protein emulsion gels. *Food Hydrocolloids, 69*, 264–272.

Kerner, E. (1956). The elastic and thermo-elastic properties of composite media. *Proceedings of the Physical Society. Section B, 69*, 808.

Langley, K. R., & Green, M. L. (1989). Compression and impact strength of gels, prepared from fractionated whey proteins, in relation to composition and microstructure. *Journal of Dairy Research, 56*, 275–284.

Larson, R. G. (1999). *The structure and rheology of complex fluids* (Vol. 150). New York: Oxford university press.

Lee, K. Y., & Mooney, D. J. (2012). Alginate: Properties and biomedical applications. *Progress in Polymer Science, 37*, 106–126.

Leon, A. M., Medina, W. T., Park, D. J., & Aguilera, J. M. (2018). Properties of microparticles from a whey protein isolate/alginate emulsion gel. *Food Science and Technology International, 24*, 414–423.

Lević, S., Pajić Lijaković, I., Đorđević, V., Rac, V., Rakić, V., Šolević Knudsen, T., et al. (2015). Characterization of sodium alginate/D-limonene emulsions and respective calcium alginate/D-limonene beads produced by electrostatic extrusion. *Food Hydrocolloids, 45*, 111–123.

Lewis, T. B., & Nielsen, L. E. (1970). Dynamic mechanical properties of particulate-filled composites. *Journal of Applied Polymer Science, 14*, 1449–1471.

Li, Y., Hu, M., Du, Y., Xiao, H., & McClements, D. J. (2011). Control of lipase digestibility of emulsified lipids by encapsulation within calcium alginate beads. *Food Hydrocolloids, 25*, 122–130.

Lin, D., Kelly, A. L., Maidannyk, V., & Miao, S. (2020a). *Effect of concentrations of alginate, soy protein isolate and sunflower oil on water loss, shrinkage, elastic and structural properties of alginate-based emulsion gel beads during gelation*. Food Hydrocolloids, 105998.

Lin, D., Kelly, A. L., & Miao, S. (2020b). Preparation, structure-property relationships and applications of different emulsion gels: Bulk emulsion gels, emulsion gel particles, and fluid emulsion gels. *Trends in Food Science & Technology* (in press).

Lin, D., Lu, W., Kelly, A. L., Zhang, L., Zheng, B., & Miao, S. (2017). Interactions of vegetable proteins with other polymers: Structure-function relationships and applications in the food industry. *Trends in Food Science & Technology, 68*, 130–144.

Liu, F., Gao, Y., & Yuan, F. (2015). Effects of chitosan addition on in vitro digestibility of protein-coated lipid droplets. *Journal of Dispersion Science and Technology, 36*, 1556–1563.

Liu, D., Shi, J., Colina Ibarra, A., Kakuda, Y., & Jun Xue, S. (2008). The scavenging capacity and synergistic effects of lycopene, vitamin E, vitamin C, and β-carotene mixtures on the DPPH free radical. *Lebensmittel-Wissenschaft und -Technologie- Food Science and Technology, 41*, 1344–1349.

McClements, D. J. (2015). *Food emulsions: Principles, practices, and techniques*. Boca Raton, FL: CRC press.

Minekus, M., Alminger, M., Alvito, P., Ballance, S., Bohn, T., Bourlieu, C., et al. (2014). A standardised static in vitro digestion method suitable for food - an international consensus. *Food and Function, 5*, 1113–1124.

Mongar, J., & Wassermann, A. (1949). Fully swollen alginate gels as permutites: Kinetics of calcium–sodium ion exchange. *Discussions of the Faraday Society, 7*, 118–123.

Moschakis, T., Murray, B. S., & Biliaderis, C. G. (2010). Modifications in stability and structure of whey protein-coated o/w emulsions by interacting chitosan and gum Arabic mixed dispersions. *Food Hydrocolloids, 24*, 8–17.

Norton, I., Frith, W., & Ablett, S. (2006). Fluid gels, mixed fluid gels and satiety. *Food Hydrocolloids, 20*, 229–239.

Pelegrine, D., & Gasparetto, C. (2005). Whey proteins solubility as function of temperature and pH. *LWT-Food Science and Technology, 38*, 77–80.

Peña Ramos, E. A., Xiong, Y. L., & Arteaga, G. E. (2004). Fractionation and characterisation for antioxidant activity of hydrolysed whey protein. *Journal of the Science of Food and Agriculture, 84*, 1908–1918.

Piornos, J. A., Burgos-Díaz, C., Morales, E., Rubilar, M., & Acevedo, F. (2017). Highly efficient encapsulation of linseed oil into alginate/lupin protein beads: Optimization of the emulsion formulation. *Food Hydrocolloids, 63*, 139–148.

Quong, D., Neufeld, R., Skjåk-Bræk, G., & Poncelet, D. (1998). External versus internal source of calcium during the gelation of alginate beads for DNA encapsulation. *Biotechnology and Bioengineering, 57*(4), 438–446.

Rayment, P., Wright, P., Hoad, C., Ciampi, E., Haydock, D., Gowland, P., et al. (2009). Investigation of alginate beads for gastro-intestinal functionality, Part 1: *In vitro* characterisation. *Food Hydrocolloids, 23*, 816–822.

Rehm, B. H. (2009). *Alginates: Biology and applications* (Vol. 13). Springer.

Shariffa, Y. N., Tan, T. B., Uthumporn, U., Abas, F., Mirhosseini, H., Nehdi, I. A., et al. (2017). Producing a lycopene nanodispersion: Formulation development and the effects of high pressure homogenization. *Food Research International, 101*, 165–172.

Shen, Y., Nyström, G., & Mezzenga, R. (2017). Amyloid fibrils form hybrid colloidal gels and aerogels with dispersed $CaCO_3$ nanoparticles. *Advanced Functional Materials, 27*, Article 1700897.

Shi, J., Dai, Y., Kakuda, Y., Mittal, G., & Xue, S. J. (2008). Effect of heating and exposure to light on the stability of lycopene in tomato purée. *Food Control, 19*, 514–520.

Soukoulis, C., Cambier, S., Hoffmann, L., & Bohn, T. (2016). Chemical stability and bioaccessibility of β-carotene encapsulated in sodium alginate o/w emulsions: Impact of Ca^{2+} mediated gelation. *Food Hydrocolloids, 57*, 301–310.

Srivastava, S., & Srivastava, A. K. (2013). Lycopene; chemistry, biosynthesis, metabolism and degradation under various abiotic parameters. *Journal of Food Science & Technology, 52*, 41–53.

Tadros, T. F. (1994). Fundamental principles of emulsion rheology and their applications. *Colloids and Surfaces A: Physicochemical and Engineering Aspects, 91*, 39–55.

Tang, C.-H., Ten, Z., Wang, X.-S., & Yang, X.-Q. (2006). Physicochemical and functional properties of hemp (Cannabis sativa L.) protein isolate. *Journal of Agricultural and Food Chemistry, 54*, 8945–8950.

Ukai, N., Lu, Y., Etoh, H., Yagi, A., Ina, K., Oshima, S., et al. (2014). Photosensitized oxygenation of lycopene. *Bioscience Biotechnology & Biochemistry, 58*, 1718–1719.
Urbonaite, V., De Jongh, H., Van Der Linden, E., & Pouvreau, L. (2015). Water holding of soy protein gels is set by coarseness, modulated by calcium binding, rather than gel stiffness. *Food Hydrocolloids, 46*, 103–111.
Voutsinas, L. P., Cheung, E., & Nakai, S. (1983). Relationships of hydrophobicity to emulsifying properties of heat denatured proteins. *Journal of Food Science, 48*, 26–32.
Yang, L. J., Guo, J., Yu, Y., An, Q. D., Wang, L. Y., Li, S. L., et al. (2016). Hydrogen bonds of sodium alginate/Antarctic krill protein composite material. *Carbohydrate Polymers, 142*, 275–281.
Zhao, Y., Li, F., Carvajal, M. T., & Harris, M. T. (2009). Interactions between bovine serum albumin and alginate: An evaluation of alginate as protein carrier. *Journal of Colloid and Interface Science, 332*, 345–353.

Food Hydrocolloids 120 (2021) 106926

Contents lists available at ScienceDirect

Food Hydrocolloids

journal homepage: www.elsevier.com/locate/foodhyd

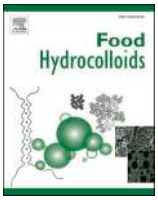

Alginate-based emulsion micro-gel particles produced by an external/internal O/W/O emulsion-gelation method: Formation, suspension rheology, digestion, and application to gel-in-gel beads

Duanquan Lin [a,b], Alan L. Kelly [b], Song Miao [a,*]

[a] Teagasc Food Research Centre, Moorepark, Fermoy, Co. Cork, Ireland
[b] School of Food and Nutritional Sciences, University College Cork, Cork, Ireland

ARTICLE INFO

Keywords:
Alginate gel
Digestion
Emulsion micro-gel particle
Suspension rheology
External/internal gelation

ABSTRACT

Alginate-based emulsion gels can be used as fat replacers and encapsulation materials, but studies on emulsion micro-gel particles and nano-gel particles have rarely been reported, compared to bulk emulsion gels and emulsion macro-gel beads. This study investigated external/internal O/W/O emulsion-gelation methods for preparation of alginate-based emulsion micro-gel particles. The size, micro-structure, rheological properties, and *in-vitro* digestion of emulsion micro-gels prepared by external/internal methods were compared. The external gelation could produce emulsion micro-gels with small size (<100 μm), while emulsion micro-gels prepared by the internal gelation had bigger size and a more narrow size distribution. The suspensions of emulsion micro-gels prepared by the external gelation had higher φ_{rcp}, φ_j, G', and G'' values than those prepared by the internal gelation. Emulsion micro-gel particles swelled during intestinal digestion, but those prepared by the external method were collapsed faster than those prepared by the internal method. Structuring emulsion gel beads by introducing emulsion micro-gel particles was also investigated. The presence of emulsion micro-gel particles prepared by the external gelation improved the Young's modulus of gel beads, delayed their structural collapse and thus delayed release of encapsulated lycopene during intestinal digestion. The results of this study are critical for preparation and applications of alginate-based emulsion micro-gel particles prepared by external/internal O/W/O emulsion-gelation methods in the food industry.

1. Introduction

Alginate-based emulsion gels have received increased interest in the food industry recently, as they can be used as fat replacers (Yang et al., 2020) and encapsulation materials for oil-soluble compounds, such as *β*-carotene (Soukoulis et al., 2016) and lycopene (Celli et al., 2016). Alginate-based emulsion gels offer many advantages, such as mild gelation and encapsulation process (Catarina et al., 2006), high stability of encapsulated compounds during food processing, storage and gastric digestion (Bokkhim et al., 2016), and controlled release of encapsulated compounds during intestinal digestion (Burey et al., 2008).

There are two kinds of alginate-based emulsion gels, according to their morphological properties: bulk emulsion gels and emulsion gel beads/particles (Lin et al., 2020). In addition, according to the size of alginate gel beads/particles, they can be further divided into three categories: macro-gel beads (>1 mm), micro-gel particles (from 0.2 to 1000 μm), and nano-gel particles (<0.2 μm) (Ching et al., 2017). Different physical properties are emphasized for different emulsion gels (i.e., the importance of mechanical and release properties for bulk emulsion gels, mechanical properties and pH-sensitivity for emulsion macro-gel beads, and rheology and pH-sensitivity for emulsion micro-gel/nano-gel particles) (Lin et al., 2020). However, most of previous studies focused on bulk emulsion gels and emulsion macro-gel beads, so further research on emulsion micro-gel particles and emulsion nano-gel particles is needed.

Two methods have been reported to produce alginate-based emulsion micro-gel particles: the spray aerosol method and the emulsification technique (Ching et al., 2016; Ribeiro et al., 1999). A special setup is needed to prepare micro-gel particles by the spray aerosol method, in which emulsions containing alginate are sprayed from the top of the setup and $CaCl_2$ solutions are spayed from the bottom of the setup using pneumatic nozzles driven by compressed air. The mist of emulsions and $CaCl_2$ solutions contact in the chamber of the setup and then emulsion micro-gel

* Corresponding author.
E-mail address: song.miao@teagasc.ie (S. Miao).

https://doi.org/10.1016/j.foodhyd.2021.106926
Received 11 April 2021; Received in revised form 23 May 2021; Accepted 29 May 2021
Available online 9 June 2021

particles form (Ching et al., 2017). Compared to the spray aerosol method, the emulsification technique is a simpler and more economic method, and it also has the potential to be used in industrial-scale. In this method, primary O/W emulsions containing alginate are dispersed in an oil phase by homogenization to form secondary O/W/O emulsions (i.e., the emulsification step), and then the gelling agents (divalent cations) are slowly introduced with stirring to form emulsion micro-gel particles (i.e., the gelation step) (Ribeiro et al., 1999).

The emulsion-gelation technique includes external and internal gelation methods. Calcium chloride is normally used as the gelling agent in the external gelation. In contrast, in the internal gelation, calcium carbonate is added into primary emulsions and then an acid is introduced as the gelling agent into secondary emulsions to liberate Ca^{2+} and trigger the progressive gelation of emulsion micro-gel particles. The internal gelation has been reported to prepare emulsion micro-gel particles, in which chitosan-coated alginate micro-spheres containing soya oil were investigated (Ribeiro et al., 1999). However, the external gelation has rarely been reported to prepare alginate-based emulsion micro-gel particles. It is well known that alginate-based gels produced by the external or internal gelation may have different properties. It has been reported that alginate-based macro-gel beads prepared by the internal gelation had faster release rate of acetaminophen than beads prepared by the external gelation (Chan et al., 2006). It has also been indicated that alginate-based hydro-micro-gel particles prepared by the internal gelation had looser gel structures with bigger pore sizes and a faster diffusion rate of haemoglobin into particles than those prepared by the external gelation (Liu et al., 2002). Therefore, we predicted that emulsion micro-gel particles prepared by external or internal methods may also have different properties (i.e., morphology, rheology and swelling).

It is known that Ca^{2+}-cross-linked alginate gels show pH-dependent swelling, which is closely associated with the release of encapsulated drug/compound from alginate gels during swelling (Amiri et al., 2017; Bajpai & Sharma, 2004). Alginate gels can swell at neutral/alkaline conditions, because of the increased repulsive forces at pH values above the pKa of the uronic acid groups of alginate molecules and/or structural disintegration of Ca^{2+}-cross-linked networks (Lin, Kelly, Maidannyk, & Miao, 2021; Mongar & Wassermann, 1949). The swelling properties of alginate hydro/emulsion micro-gels have been widely investigated (El-Sherbiny et al., 2011; Gómez-Mascaraque et al., 2019).

In contrast, rheology of alginate hydro/emulsion micro-gel suspensions has rarely been reported, although suspension rheology of soft micro-gel particles is critical in the determination of flow behavior and modulus of micro-gel particles. Particle suspensions may show viscous liquid-like behavior, viscoelastic liquid-like behavior or viscoelastic solid-like behavior depending on the phase volume (φ) of particles in suspensions. When φ is below the random close packing fraction (φ_{rcp}), particle suspensions are purely viscous with no measurable viscoelasticity (i.e., the regime I). However, when φ is above φ_{rcp} but below the jamming fraction (φ_j), the suspensions become shearing and viscoelastic with a measurable storage modulus (G') less than the loss modulus (G'') (i.e., the regime II). Finally, when φ is above φ_j, particle suspensions show viscoelastic solid-like behavior (e.g., the regime III) where G' becomes higher than G'' because micro-gel particles pack closely and form a weakly elastic network (Dickinson, 2015; Shewan & Stokes, 2013).

In terms of application of emulsion micro-gel particles in the food industry, previous studies mainly focused on the encapsulation of lipophilic compounds (e.g., flavors, essential oils, vitamins and fatty acids) in micro-gel particles for their targeted delivery in the digestive tract (Shewan & Stokes, 2013; Torres et al., 2016). For example, it has been reported that 85% of encapsulated dye (i.e., Sudan orange G) in alginate-based emulsion micro-gels were rapidly released within 15 min during intestinal digestion, while 35% of encapsulated dye in micro-gels coated by chitosan were slowly release within 2 h during intestinal digestion (Ribeiro et al., 1999). In addition, micro-gels can also been used as structuring agents to form gel-in-gels, which has drawn increased interest in recent years (Husman et al., 2020; Liu et al., 2008). For instance, a microgel-in-bulk gel system was reported by Zhu et al. (2016), in which bone morphogenetic protein-2 (BMP-2) was encapsulated in alginate-based micro-spheres, and then alginate micro-spheres were embedded into chitosan/dextran-polylactide/glycerophosphate -based bulk hydro-gels, which showed continuous release of BMP-2 from gels.

However, previous studies mainly focused on microgel-in-hydrogel systems and release of encapsulated compounds from the inner sections (i.e., micro-gels) of microgel-in-gel systems. In this study, we will further explore the effect of the presence of micro-gel particles on the properties (i.e., mechanical and digestive behavior) of emulsion macro-gels and thus the release of encapsulated lipophilic nutrients from the outer sections (i.e., macro-gels) of microgel-in-gel systems during digestion.

The purpose of this study was therefore to compare the morphology, suspension rheology and digestion behavior of alginate-based emulsion micro-gel particles produced by an external or internal O/W/O emulsion-gelation method. In addition, an example of application of micro-gel particles in the formation of microgel-in-emulsion-macrogels was discussed. Lycopene was encapsulated in emulsion macro-gel beads and served as an indicator to test the effect of micro-gel particles by different gelation methods on the release of encapsulated nutrients from alginate-based emulsion macro-gel beads during digestion.

2. Materials and methods

2.1. Materials

Sunflower oil (Aldi Stores Ltd., Kildare, Ireland) and sodium alginate with $\overline{M}$ of 69–117 kDa (Special Ingredients, Chesterfield, UK) were purchased from local markets. Soy protein isolate (SPI) was prepared according to our previous study (Lin et al., 2019). *D*-(+)-Gluconic acid δ-lactone (GDL), calcium carbonate, calcium chloride, Tween 80, Span 80, sodium hydroxide, hydrochloric acid, and other analytical reagents were purchased from Sigma-Aldrich (St. Louis, MO, USA).

2.2. Preparation of emulsion micro-gel particles

Sodium alginate solutions (2.0%, w/w) were prepared with deionized water by shearing at 400 rpm for 30 min and then resting for 24 h at 4°C. For preparation of coarse emulsions, SPI powder (2.0 wt%) was mixed with deionized water (78 wt%) by stirring at room temperature for 2 h, and then sunflower oil (20 wt%) was mixed with above dispersions at 16,000 rpm for 2 min with an Ultra-Turrax (IKA-25, Staufen, Germany). The primary emulsions (i.e., O/W emulsions containing alginate) were then prepared by mixing the above coarse emulsions with 2.0% sodium alginate solutions (1: 3, w/w) at 14,000 rpm for 2 min with an Ultra-Turrax. For the preparation of secondary emulsions (i.e., O/W/O emulsions), Span 80 (2.0 wt%) was mixed with sunflower oil (78 wt%) by stirring at room temperature for 5 min using a magnetic stirrer, and then primary emulsions (20 wt%) were mixed with above oil phase by stirring at 800 rpm.

The external gelation was carried out by adding 1.0% $CaCl_2{\cdot}2H_2O$ solutions into secondary emulsions (1:5, w/w) and stirring at 1000 rpm for 30 min using a magnetic stirrer. For preparation of micro-gel particles by the internal gelation, $CaCO_3$ was added into coarse emulsions (1:20, w/w) in advance during emulsion preparation, and then 4.0% GDL solutions were added into secondary emulsions (1:5, w/w) and stirring at 1000 rpm for 30 min using a magnetic stirrer. After gelation, above resulted dispersions containing particles were added into deionized water (1: 5, w/w) and mixed at 500 rpm for 2 min using a magnetic stirrer. The mixtures were left to stand for 2 h, and the oil cream on the top of mixtures was removed and the sediment of emulsion micro-gel particles were collected by filtration and washed twice by deionized water.

2.3. Properties of emulsion micro-gel particles

2.3.1. Morphological analysis

Emulsions and emulsion micro-gel particles were dropped on microscope slides without covering by glass coverslips before observing with an Olympus BX51 light micro-scope (Olympus Optical Co. Ltd., Tokyo, Japan).

2.3.2. Particle size distribution

The size distributions of emulsion micro-gel particles were analyzed with MasterSizer 3000 (Malvern Instruments Ltd., Worcestershire, UK). The obscuration and the stirrer speed were set at 1–10% and 2000 rpm, respectively, with the refractive index of 1.55 and the absorption index of 0.001.

2.3.3. Rheological analysis

Emulsion micro-gel particles were dried by filter papers twice and then particles were diluted by deionized water to the final φ from 1.0 to 0.1. The viscosity and modulus of particle suspensions were tested using an AR 2000ex rheometer (TA Instruments, Crawley, UK) by the method described in our previous publication (Lin, Kelly, & Miao, 2021), but the flow and strain sweep measurements were carried out over a shear rate range of 0.1–1000 s^{-1} and a strain range of 1%–50%, respectively. The final viscosity and modulus values used to calculate φ_{rcp} and φ_j were obtained at a shear rate of 100 s^{-1} (below φ_{rcp}) or 10 s^{-1} (above φ_{rcp}) and a strain of 10%.

2.3.4. In-vitro digestion

Concentrated electrolyte stock solutions (i.e., 1.5 × concentrate) of simulated saliva fluid (SSF), gastric fluid (SGF), and intestinal fluid (SIF) were prepared as described by Minekus et al. (2014) with some modification. Simulated oral digestion of emulsion micro-gel particles was performed by mixing micro-gel particles (5 g) with SSF electrolyte stock solutions (2.5 mL), α-amylase (final 75 U/g), $CaCl_2$ (final 0.75 mM), and water at 37°C for 2 min. Simulated gastric digestion was performed by mixing oral bolus (~10 g) with SGF electrolyte stock solutions (5.0 mL), porcine pepsin (final 2000 U/g), $CaCl_2$ (final 0.075 mM), and water at 37°C for 2 h after adjusting pH to 3.0 with HCl. Simulated intestinal digestion was performed by mixing gastric chyme (~20 g) with SIF electrolyte stock solutions (10 mL), pancreatin (final 100 U/g), bile (final 0.25 wt%), $CaCl_2$ (final 0.3 mM), and water at 37°C for 3 h after adjusting pH to 7.0 with NaOH.

Optical microscopy images and size distributions of emulsion micro-gel particles during *in-vitro* digestion were analyzed as described in Sections 2.3.1 and 2.3.2.

2.4. Preparation of emulsion gel beads containing micro-gel particles

Primary emulsions (i.e., O/W emulsions) were prepared by mixing 0.8% alginate solutions and coarse emulsions containing 5.0% oil, 0.5% SPI and 94.5% water, according to the methods described in Section 2.2, but the ratio of coarse emulsions to alginate solutions was 1:1. Lycopene was also encapsulated in primary emulsions by mixing 5 mg of tomato extract (containing 0.059 mg lycopene/mg) with 5.0 g of oil before preparing coarse emulsions. Micro-gel particle dispersions were then prepared by mixing filtered micro-gel particles with deionized water (3:2, w/w), and then primary emulsions were mixed with micro-gel particle dispersions (9:1, w/w). The control sample was prepared by mixing primary emulsions with deionized water (9:1, w/w). Emulsion gel beads were then prepared by dropping primary emulsions with/without micro-gel particles into 2.0% $CaCl_2{\cdot}2H_2O$ solutions using a S1 pipette filler, and gel beads were mildly stirred for 30 min and then collected and washed by deionized water.

2.5. Properties of emulsion gel beads containing micro-gel particles

2.5.1. In-vitro digestion

Simulated digestion was performed as described in Section 2.3.4, and properties of emulsion gel beads (i.e., shrinkage rate, Young's modulus, and visual appearance) and lycopene release from them during *in-vitro* digestion were then tested.

2.5.2. Measurement of Young's modulus and shrinkage during oral and gastric digestion

The size of gel beads including major and minor axis (R_{maj} and R_{min}) was measured by a digital vernier caliper with a sensitivity of 0.1 mm. The shrinkage rate of gel beads during digestion was calculated by comparing decreased sectional area (i.e., $A = \pi \times R_{maj} \times R_{min} \div 4$) of gel beads during digestion to that of original gel beads before digestion. The Young's modulus of gel beads was measured by a texture analyzer (Stable micro-System, Godalming, UK). The compression test was performed with the maximum strain of 30% and the crosshead speed 0.1 mm/s. The Young's modulus was calculated in the linear elastic region of gel beads (i.e., the 5–15% strain region).

2.5.3. Measurement of lycopene release during intestinal digestion

The supernatant (1.0 g) of digestive fluids after centrifugal separation at 4000 rpm for 15 min was mixed with 8.0 mL of hexane, acetone, and ethanol (50 : 25: 25% v/v) containing 0.1% BHT by a vortex for 1 min, and lycopene in digestive fluids was then extracted and measured by the method described in our previous publication (Lin, Kelly, Maidannyk, & Miao, 2021).

2.6. Statistical analysis

All measurements were performed three times and results are reported as mean ± standard deviation (SD). Differences between samples were analyzed using analysis of variance and a *t*-test, and a p value < 0.05 was regarded as statistically significant.

3. Results and discussion

3.1. Formation and morphology of emulsion micro-gel particles produced by external/internal emulsification methods

Fig. 1A shows the size distributions of emulsion micro-gel particles produced by external/internal emulsion-gelation methods. Micro-gel particles produced by the external method ($D_{4,3}$ = 39.6 ± 0.5 μm) were significantly smaller than those produced by the internal method ($D_{4,3}$ = 144 ± 5 μm, $p < 0.05$). In addition, a previous study indicated that particles with size over 100 μm may be detected by mouth and negatively affected sensory of food (Kim et al., 2019). Therefore, we predict that emulsion micro-gel particles produced by the external gelation has potential to be used as micro-capsules and structuring agents in food without affecting sensory properties of final products.

Different gelation mechanisms of external/internal emulsion-gelation methods may be the main reason for emulsion micro-gel particles with different morphological properties. A commonly-used method to prepare micro-gel particles in previous studies was adding oil containing $CaCl_2$ particles or acetic acid into emulsions to trigger gelation, in which $CaCl_2$ or acetic acid could diffuse from oil into water phases (Liu et al., 2007; Paques et al., 2013). In this study, $CaCl_2$ or GDL solutions were added into secondary emulsions to trigger gelation, in which $CaCl_2$ or GDL solutions may merge with water phases in O/W/O emulsions. Fig. 1B–E shows the micro-structure of micro-gel particles produced by external/internal methods and O/W/O emulsions which were used to prepare micro-gel particles. It could be seen that O/W droplets in O/W/O emulsions (Fig. 1C and E) were smaller than micro-gel particles in both gelation methods (Fig. 1B and D). This indicates that $CaCl_2$ or GDL solutions, which were introduced into O/W/O

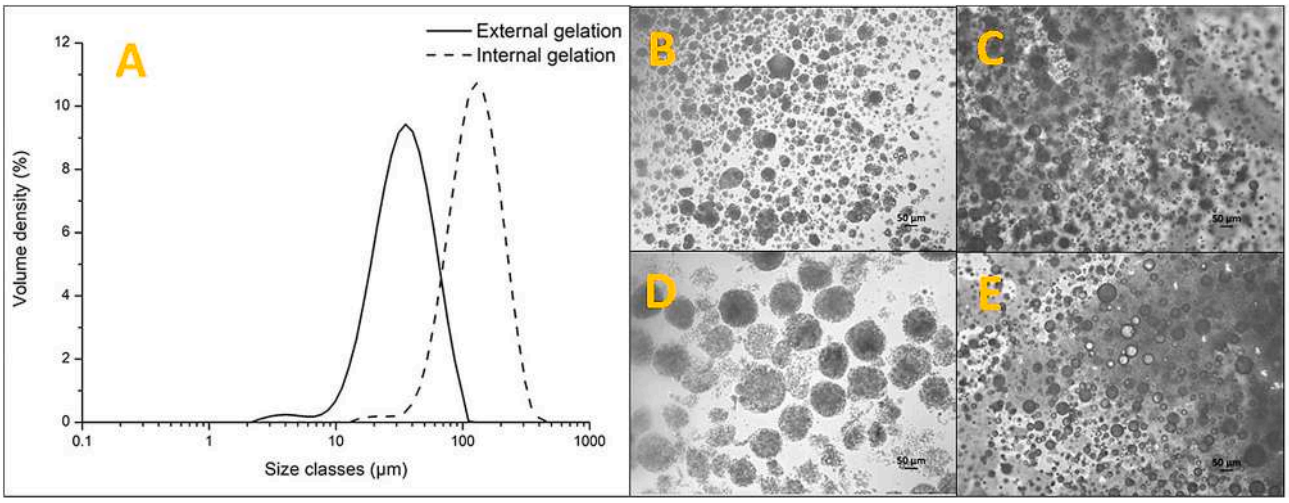

Fig. 1. (A) The size distribution of alginate-based emulsion micro-gel particles produced by external/internal O/W/O emulsification methods, (B) the micro-structure of emulsion micro-gel particles produced by the external gelation and (C) the micro-structure of O/W/O emulsions used, and (D) the micro-structure of emulsion micro-gel particles produced by the internal gelation and (E) the micro-structure of O/W/O emulsions used.

emulsions to trigger gelation, merged with O/W droplets during gelation process. A similar result was reported by Ribeiro et al. (1999), where soya oil-in-alginate droplets, with size of around 200 μm, which were dispersed in silicone oil, were smaller than alginate emulsion micro-gel particles, with size of 250–1000 μm, produced by the internal gelation. However, $CaCl_2$-induced external gelation was a faster process than GDL-induced internal gelation, so each O/W droplet merged with less $CaCl_2$ solutions in the external gelation than GDL solutions in the internal gelation, which resulted in smaller micro-gel particles produced by the external method than those produced by the internal method.

Fig. 1A also shows that micro-gel particles produced by the internal gelation had a more narrow size distribution than those produced by the external method. The diameter of micro-gel particles produced by internal and external methods ranged from 15 to 450 μm and from 2.5 to 110 μm, respectively. The possible reason was that random droplet coagulation occurred in O/W/O emulsions after introducing $CaCl_2$ solutions during the external gelation. It has been reported that adding $CaCl_2$ solutions into W/O emulsions to produce alginate hydro-micro-spheres by the external gelation caused the disruption of the equilibrium of the system during stirring, resulting in a significant degree of clumping of micro-spheres (Chan et al., 2002).

3.2. Suspension rheology of emulsion micro-gel particles

In order to predict functions and guide production and application of micro-gel particles in the food industry, it is important to investigate the rheology of micro-gel particle suspensions. It is known that the rheology of micro-particle suspensions is affected by properties of solvents (i.e., viscosity and pH), properties of particles (i.e., size, size distribution, mechanical strength, surface properties, and interaction potential), and particle phase volume (Shewan, 2015). In regime I, the viscosity of particle suspensions (η) can be calculated by the Einstein equation (Eq. (1), $0 < \varphi < 0.05$), Batchelor equation (Eq. (2), $0.05 < \varphi < 0.15$), and Meron-Pierce-Quemada model (i.e., MPQ model, as shown in (Eq. (3), $0.2 < \varphi < \varphi_m$):

$$\eta = \eta_s(1 + 2.5\varphi) \tag{1}$$

$$\eta = \eta_s\left(1 + 2.5\varphi + C_2\varphi^2\right) \tag{2}$$

$$\eta = \eta_s\left(1 - \frac{\varphi}{\varphi_m}\right)^{-2} \tag{3}$$

in which η_s is the solvent viscosity, C_2 is a constant with a range of values from 4.2 to 6.2, and φ_m is the maxing packing fraction, which could be assumed to be equal to φ_{rcp} (Shewan, 2015).

In regime III, G' of particle suspensions can be calculated by the Evans and Lips model modified by Adams (Eq. (4)):

$$G' = aG_p^b\left[1 - \varphi_r^{-1/3}\right] \tag{4}$$

in which a and b are constants equal to 0.4 and 1.2, respectively, G_p is the shear elastic modulus of particles, and φ_r is a relative phase volume (i.e., $\varphi_r = \varphi/\varphi_m$ *or* φ/φ_{rcp}) (Shewan, 2015). Therefore, it can be assumed that alginate-based emulsion micro-gel particles with higher modulus and lower φ_{rcp} may lead to particle suspensions with higher modulus in regime III. However, modelling of regime II has rarely been reported in previous studies because measuring suspension rheology around particle jamming is challenging and available experimental results are often questioned (Shewan, 2015).

Fig. 2 shows the relative viscosity, G', and G'' of suspensions of alginate-based emulsion micro-gel particles produced by internal/external gelation methods compare to the phase volume (φ) of particles in suspensions. Suspensions of emulsion micro-gel particles produced by the external gelation had higher φ_{rcp} and φ_j values than those produced by the internal gelation (Figs. 2 and S1). The possible reason was that micro-gel particles produced by the external gelation had smaller size and a wider particle size distribution than those produced by the internal gelation (Fig. 1). When φ is below the φ_{rcp} of particle suspensions, micro-gel particles can freely move past one another and particle suspensions are purely viscous with no measurable viscoelasticity, while, when φ is above the φ_{rcp} of particle suspensions, micro-gel particles closely contact and particle suspensions become shearing and viscoelastic. Smaller particles had higher packing density than larger particles (Ye et al., 2018), so smaller particles have a higher φ_{rcp}. In addition, the maximum packing fraction (φ_m) or φ_{rcp} increases when the particle size distribution increases, because small particles can fit in the gaps among larger particles (Shewan, 2015).

Fig. 2 also shows that the suspensions of micro-gel particles produced by the external gelation had higher G' than those produced by the internal gelation when φ is above the φ_{rcp} of particle suspensions. This indicates that micro-gel particles produced by the external gelation had stronger mechanical properties than those produced by the internal gelation. The possible reason was that each O/W droplet merged with less $CaCl_2$ solutions during the external gelation than GDL solutions during the internal gelation, which resulted in higher alginate concentrations in micro-gel

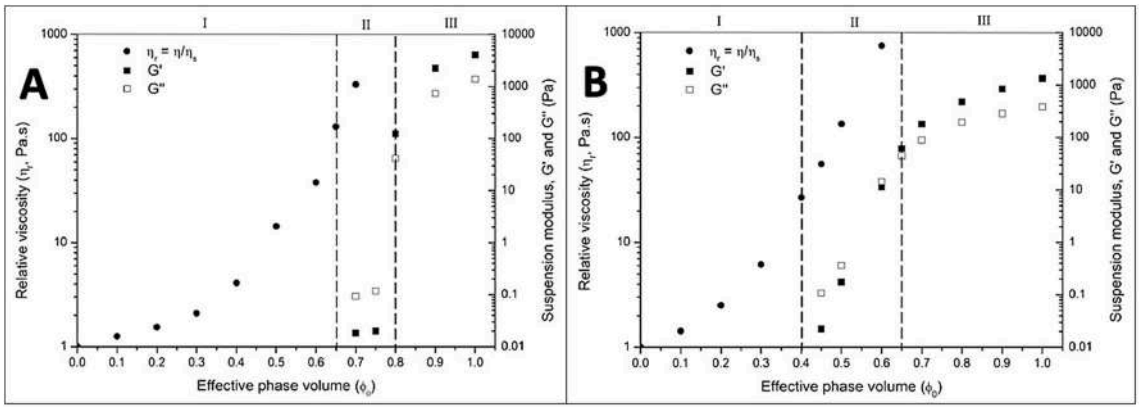

Fig. 2. Relative viscosity (η_r), storage modulus (G') and loss modulus (G'') of suspensions of emulsion micro-gel particles produced by (A) external or (B) internal O/W/O emulsification methods as a function of phase volume (φ_0). Regime I ($0 < \varphi < \varphi_{rcp}$) indicates that particle suspensions are purely viscous; Regime II ($\varphi_{rcp} < \varphi < \varphi_j$) indicates that particle suspensions are viscoelastic with a measurable G' less than G''; Regime III ($\varphi_j < \varphi < 1$) indicates that particle suspensions are solid-like with G' higher than G''.

particles produced by the external gelation, compared to those produced by the internal gelation.

3.3. Digestion of emulsion micro-gel particles

The above results indicate that different gelation methods (i.e., external or internal emulsification method) led to emulsion micro-gel particles with different morphological and mechanical properties, which may also affect the pH-sensitivity and digestion behavior of micro-gel particles. Therefore, *in-vitro* digestion of emulsion micro-gel particles prepared by external/internal emulsification methods was further investigated.

Figs. 3 and 4 show the micro-structure and size distribution of emulsion micro-gel particles during simulated oral, gastric and intestinal digestion. It can be seen that emulsion micro-gel particles, which were prepared by the external gelation, slightly swelled after oral and gastric digestion (Figs. 3 and 4A). A similar finding has been reported, where alginate micro-gels ($D_{4,3} < 500$ μm), which were prepared by dropping alginate solutions into $CaCl_2$ solutions by syringes, slightly swelled after gastric digestion at pH 3.0, probably because of ion-exchange between monovalent cations in stimulated gastric fluids and divalent cations in alginate micro-gels (Gómez-Mascaraque et al., 2019). On the other hand, Figs. 3 and 4B show that emulsion micro-gel particles which were prepared by the internal gelation shrank partially and swelled partially during gastric digestion. The possible reason for such shrinkage was that remaining $CaCO_3$ in micro-gel particles further reacted with H^+ in the digestive fluids during gastric digestion. As shown in Fig. S2, $CaCO_3$ particles in micro-gel particles, which were prepared by the internal gelation, could be observed under a fluorescence microscopy but disappeared after incubating in 0.1 M HCl–KCl solutions (1:1, w/w) at pH 1.2 for 2 h.

Fig. 4B also shows that the size distribution of emulsion micro-gel particles prepared by the internal method had two peaks (i.e., D = 4.5 μm in left peak and D = 270 μm in right peak) after intestinal digestion for 1 h, which indicates that micro-gel particles further swelled and parts of micro-particles broke, due to increased pH of digestive fluids and ion-exchange between digestive fluids and micro-particles. The area of the left-hand peak increased, but the area of the right-hand peak decreased after intestinal digestion for 3 h, which indicates further breaking of swelled particles and the presence of unbroken particles. This was also confirmed by the micro-structure of emulsion micro-gel particles prepared by the internal gelation after gastric digestion (Fig. 3), in which both swollen micro-particles and dissociative oil droplets were observed.

However, the size distribution of emulsion micro-gel particles prepared by the external method had three peaks (i.e., D = 4.0 μm in left peak, D = 16 μm in middle peak and D = 98 μm in right peak) after intestinal digestion for 1 h, and the area of the right-hand peak increased and a fourth peak occurred at D = 310 μm after intestinal digestion for 3 h (Fig. 4A), but unbroken micro-particles were rarely observed and large

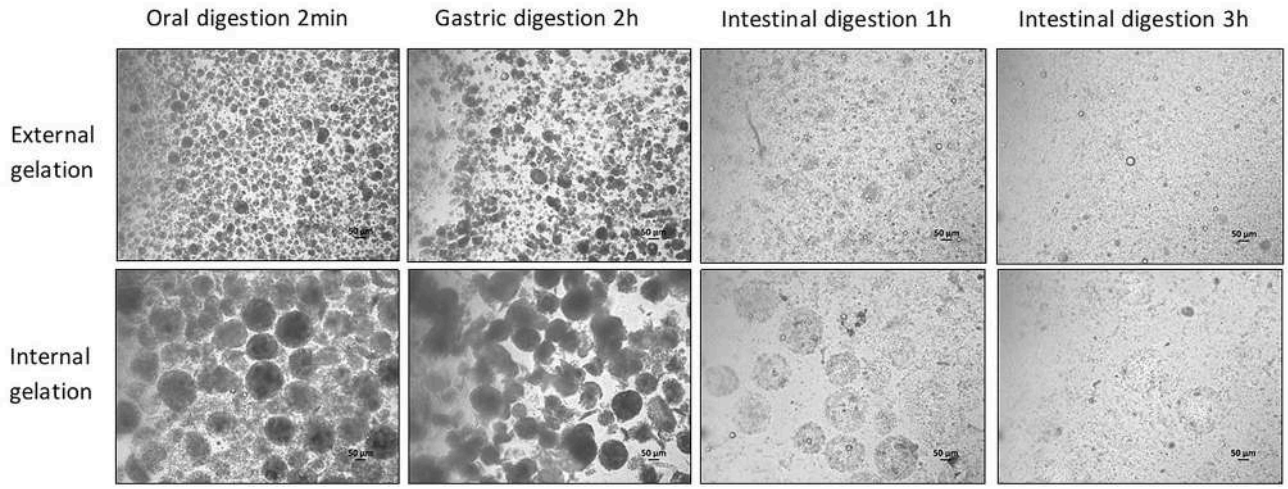

Fig. 3. The micro-structure of emulsion micro-gel particles produced by external/internal O/W/O emulsification methods during *in-vitro* digestion.

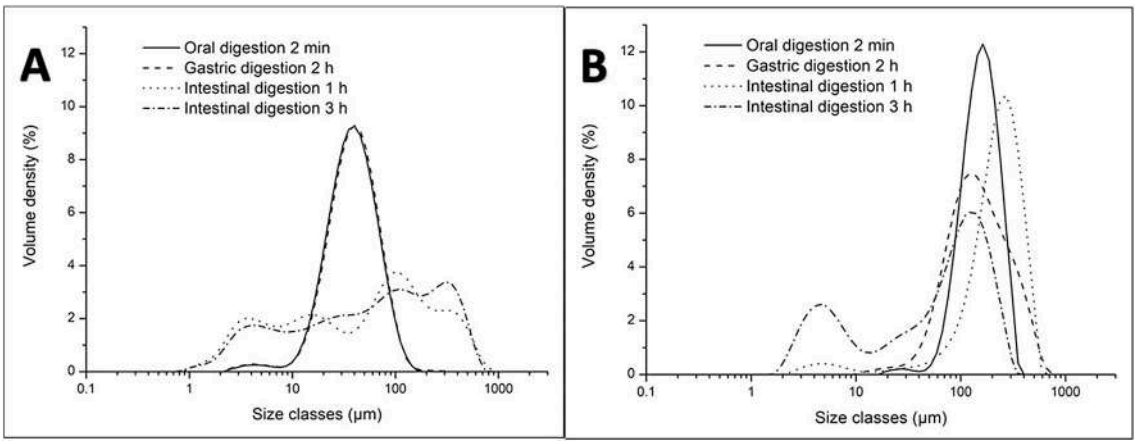

Fig. 4. The size distribution of emulsion micro-gel particles produced by (A) external or (B) internal O/W/O emulsification methods during *in-vitro* digestion.

oil droplets could be observed in digestive juice (Fig. 3). The possible reason was that released oil droplets from emulsion micro-gel particles could emerge into bigger droplets during intestinal digestion, which led to increased droplet size. These also indicate that emulsion micro-gel particles prepared by the external method were more sensitive to intestinal environment and more easily collapsed during intestinal digestion than those prepared by the internal method. Many factors affect the swelling of alginate gels in solutions/buffers, such as alginate concentration, alginate type and Ca^{2+} concentration in gels, intensity of gel structures, temperature, pH and ionic strength of solutions/buffers (Pasparakis & Bouropoulos, 2006; Sriamornsak et al., 2007). It has been indicated that alginate macro-gel beads prepared using 1% $CaCl_2$ solutions had higher swelling rates in a pH 7.4 solution than gel beads prepared using 2% $CaCl_2$ solutions (Dai et al., 2008). It has been also reported that reduced swelling was observed when alginate gels exposed to low pH or lower concentrations of cations (Moe et al., 1993). However, in this study, the main reason for different intestinal digestion behavior of emulsion micro-gel particles was probably that emulsion micro-gel particles prepared by the internal method had larger size and thus may have stronger buffer capacity to pH change and ion-exchange during intestinal digestion.

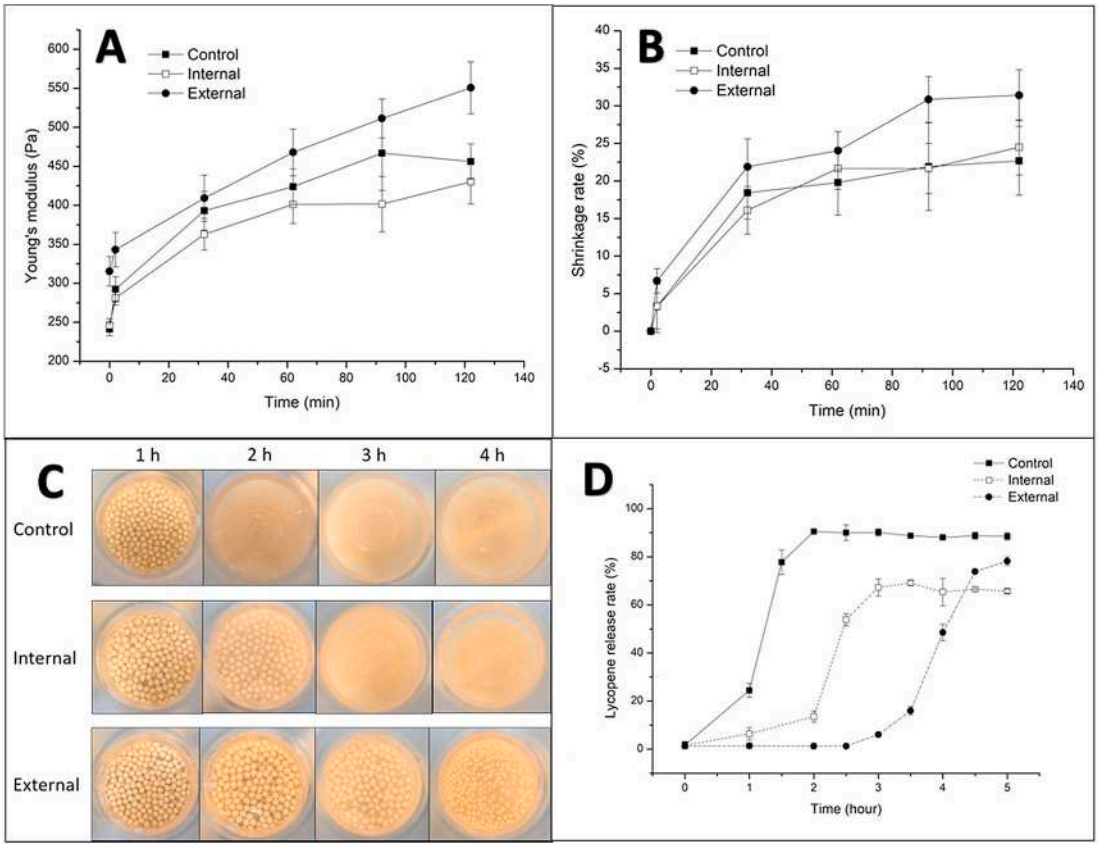

Fig. 5. (A) Young's modulus and (B) shrinkage rate of emulsion gel beads without micro-gel particles (i.e., control samples) or with 6.0% micro-gel particles produced by external/internal O/W/O emulsification methods during oral and gastric digestion. (C) Visual appearance of emulsion gel beads and (D) lycopene release from emulsion gel beads without micro-gel particles or with 6.0% micro-gel particles produced by external/internal methods during *in-vitro* intestinal digestion.

3.4. Structuring emulsions gels beads by emulsion micro-gel particles

3.4.1. Effect of micro-gel particles on mechanical properties of emulsion gel beads

Fig. 5A shows that the Young's modulus of emulsion gel beads without micro-gel particles or with 6.0% of emulsion micro-gel particles prepared by internal/external O/W/O gelation methods were 241 ± 9 Pa, 246 ± 9 Pa, and 315 ± 19 Pa, respectively. The possible reason for similar Young's modulus of emulsion gel beads containing micro-gel particles prepared by the internal gelation ($p > 0.05$) but increased Young's modulus of emulsion gel beads containing micro-gel particles prepared by the external gelation ($p < 0.05$), compared to that without micro-gel particles, was that micro-gel particles prepared by the external gelation had stronger Ca^{2+}-induced cross-linking with alginate molecules in the continuous phase of emulsions than micro-gel particles prepared by the internal gelation.

In order to verify above explanation, rheological properties of 0.4% alginate solutions containing micro-gel particles (0–10 wt%) prepared by internal/external O/W/O gelation methods were further investigated (Fig. S3). It shows that 0.4% alginate solutions containing micro-gel particles (0–10 wt%) prepared by the internal gelation showed viscoelastic properties with slightly increased viscosity and an unmeasurable G' (i.e., negative values) with increasing content of micro-gel particles, which indicated that there was little cross-linking between alginate molecules and micro-gel particles prepared by the internal gelation. On the other hand, introducing high levels of micro-gel particles (6–10 wt %) prepared by the external gelation into alginate solutions increased the viscosity of mixtures significantly, which showed solid-like behavior with a measurable G' higher than G''. This indicates that the presence of micro-gel particles prepared by the external gelation could promote interactions between alginate molecules, but the mechanism needs further investigation. There are mainly two types of speculation: firstly, Ca^{2+} could be released from micro-gel particles prepared by the external gelation into alginate solutions, which triggered the interactions between alginate molecules; secondly, micro-gel particles prepared by the external gelation could cross-link with alginate molecules through Ca^{2+} absorbed on the surfaces of micro-gel particles.

3.4.2. Digestion of emulsions gels beads containing emulsion micro-gel particles

Fig. 5A and B shows that emulsion gel beads without emulsion micro-gel particles or with 6.0% of emulsion micro-gel particles prepared by internal/external O/W/O gelation methods shrank and their Young's modulus increased during oral and gastric digestion, probably due to the interactions between Ca^{2+} in gel beads and HCO_3^- in the simulated saliva fluid and decreased repulsive forces of alginate molecules under acidic conditions during gastric digestion (Lin, Kelly, Maidannyk, & Miao, 2021). It can also be seen that emulsion gel beads containing emulsion micro-gel particles prepared by the external gelation shrank more (31 ± 3%) and had higher Young's modulus (551 ± 33 Pa) after gastric digestion, compared to emulsion gel beads without emulsion micro-gel particles (23 ± 5% and 456 ± 23 Pa, $p < 0.05$) or with 6.0% of emulsion micro-gel particles prepared by the internal gelation (24 ± 4% and 430 ± 29 Pa, $p < 0.05$).

Fig. 5C and D shows the visual images and lycopene release from gel beads during intestinal digestions. Emulsion gel beads without emulsion micro-gel particles or with 6.0% of emulsion micro-gel particles prepared by internal/external O/W/O gelation methods broke and released lycopene after 1–2 h, 2–3 h, and 3.5–4.5 h of intestinal digestion, respectively. The presence of micro-gel particles prepared by the external gelation in emulsion gel beads could delay the structural collapse of gel beads, probably because the ion-exchange between Na^+ ions in digestive juice and Ca^{2+} ions in gel beads and the pH-dependent swelling of gel beads were delayed, due to stronger and denser structures of gel beads after introducing micro-gel particles (Fig. 5A and B).

4. Conclusions

Properties (i.e., the size distribution, micro-structure, suspension rheology, and digestion behavior) of emulsion micro-gel particles produced by internal/external O/W/O gelation methods were compared in this study. Micro-gel particles produced by the external gelation had smaller size and a wider size distribution than those produced by the internal gelation, probably due to their different gelation mechanisms. The suspensions of micro-gel particles produced by the external gelation showed higher φ_{rcp}, φ_j, G', and G'' values than those prepared by the internal gelation. Micro-gel particles produced by the external gelation slightly swelled during gastric digestion and further swelled during intestinal digestion and then totally collapsed after intestinal digestion, while micro-gel particles produced by the internal gelation partially swelled and partially shrank during gastric digestion and partially collapsed with swelling after intestinal digestion. Micro-gel particles can also be used for structuring emulsion gel beads by formation of gel-in-gel beads. Emulsion gel beads containing micro-gel particles produced by the internal gelation had similar mechanical properties with the control samples without gel particles. However, introducing gel particles produced by the external gelation increased mechanical strength of gel beads, which delayed structural collapses of gel beads and lycopene release from gel beads during intestinal digestion. The findings are important for the production of emulsion micro-gel particles and structuring food by emulsion micro-gel particles produced by external/internal O/W/O emulsion-gelation methods.

CRediT authorship contribution statement

Duanquan Lin: Conceptualization, Methodology, Writing - original draft, Data curation, Investigation. **Alan L. Kelly:** Supervision, Writing - review & editing. **Song Miao:** Supervision, Conceptualization, Writing - review & editing, Funding acquisition, Project administration, Investigation.

Declaration of competing interest

The authors declare that they have no known competing financial interests or personal relationships that could have appeared to influence the work reported in this paper.

Acknowledgement

This work was supported by the China Scholarship Council (No. 201708350111) and Teagasc-The Irish Agriculture and Food Development Authority (RMIS6821).

Appendix A. Supplementary data

Supplementary data to this article can be found online at https://doi.org/10.1016/j.foodhyd.2021.106926.

References

Amiri, M., Salavati-Niasari, M., Pardakhty, A., Ahmadi, M., & Akbari, A. (2017). Caffeine: A novel green precursor for synthesis of magnetic $CoFe_2O_4$ nano-particles and pH-sensitive magnetic alginate beads for drug delivery. *Materials Science and Engineering: C, 76*, 1085–1093.

Bajpai, S., & Sharma, S. (2004). Investigation of swelling/degradation behaviour of alginate beads crosslinked with Ca^{2+} and Ba^{2+} ions. *Reactive and Functional Polymers, 59*, 129–140.

Bokkhim, H., Bansal, N., Grøndahl, L., & Bhandari, B. (2016). *In-vitro* digestion of different forms of bovine lactoferrin encapsulated in alginate micro-gel particles. *Food Hydrocolloids, 52*, 231–242.

Burey, P., Bhandari, B. R., Howes, T., & Gidley, M. J. (2008). Hydrocolloid gel particles: Formation, characterization, and application. *Critical Reviews in Food Science and Nutrition, 48*, 361–377.

Catarina, M. S., António, J. R., Margarida, F., Domingos, F., & Francisco, V. (2006). Micro-encapsulation of hemoglobin in chitosan-coated alginate micro-spheres prepared by emulsification-internal gelation. *The AAPS Journal, 7*, E903–E913.

Celli, G. B., Teixeira, A. G., Duke, T. G., & Brooks, M. S.-L. (2016). Encapsulationof lycopene from watermelon in calcium-alginate micro-particles using an optimised inverse-gelation method by response surface methodology. *International Journal of Food Science and Technology, 51*, 1523–1529.

Chan, L. W., Lee, H. Y., & Heng, P. W. (2002). Production of alginate micro-spheres by internal gelation using an emulsification method. *International Journal of Pharmaceutics, 242*, 259–262.

Chan, L. W., Lee, H. Y., & Heng, P. W. (2006). Mechanisms of external and internal gelation and their impact on the functions of alginate as a coat and delivery system. *Carbohydrate Polymers, 63*, 176–187.

Ching, S. H., Bansal, N., & Bhandari, B. (2016). Rheology of emulsion-filled alginate micro-gel suspensions. *Food Research International, 80*, 50–60.

Ching, S. H., Bansal, N., & Bhandari, B. (2017). Alginate gel particles–A review of production techniques and physical properties. *Critical Reviews in Food Science and Nutrition, 57*, 1133–1152.

Dai, Y. N., Li, P., Zhang, J. P., Wang, A. Q., & Wei, Q. (2008). A novel pH sensitive N-succinyl chitosan/alginate hydrogel bead for nifedipine delivery. *Biopharmaceutics & Drug Disposition, 29*, 173–184.

Dickinson, E. (2015). Microgels—an alternative colloidal ingredient for stabilization of food emulsions. *Trends in Food Science & Technology, 43*, 178–188.

El-Sherbiny, I. M., Abdel-Mogib, M., Dawidar, A.-A. M., Elsayed, A., & Smyth, H. D. (2011). Biodegradable pH-responsive alginate-poly (lactic-co-glycolic acid) nano-/micro- hydrogel matrices for oral delivery of silymarin. *Carbohydrate Polymers, 83*, 1345–1354.

Gómez-Mascaraque, L. G., Martínez-Sanz, M., Hogan, S. A., López-Rubio, A., & Brodkorb, A. (2019). Nano-and micro-structural evolution of alginate beads in simulated gastrointestinal fluids. Impact of M/G ratio, molecular weight and pH. *Carbohydrate Polymers, 223*, 115121.

Husman, D., Welzel, P. B., Vogler, S., Bray, L. J., Träber, N., Friedrichs, J., et al. (2020). Multiphasic microgel-in-gel materials to recapitulate cellular mesoenvironments in vitro. *Biomaterials science, 8*, 101–108.

Kim, Y. N., Muttakin, S., Jung, Y. M., Heo, T. Y., & Lee, D. U. (2019). Tailoring physical and sensory properties of tofu by the addition of jet-milled, superfine, defatted soybean flour. *Foods, 8*, 617.

Lin, D., Kelly, A. L., Maidannyk, V., & Miao, S. (2021a). Effect of structuring emulsion gels by whey or soy protein isolate on the structure, mechanical properties, and *in-vitro* digestion of alginate-based emulsion gel beads. *Food Hydrocolloids, 110*, 106165.

Lin, D., Kelly, A. L., & Miao, S. (2020). Preparation, structure-property relationships and applications of different emulsion gels: Bulk emulsion gels, emulsion gel particles, and fluid emulsion gels. *Trends in Food Science & Technology, 102*, 123–137.

Lin, D., Kelly, A. L., & Miao, S. (2021b). The role of mixing sequence in structuring O/W emulsions and emulsion gels produced by electrostatic protein-polysaccharide interactions between soy protein isolate-coated droplets and alginate molecules. *Food Hydrocolloids, 113*, 106537.

Lin, D., Zhang, L., Li, R., Zheng, B., Rea, M. C., & Miao, S. (2019). Effect of plant protein mixtures on the micro-structure and rheological properties of myofibrillar protein gel derived from red sea bream (Pagrosomus major). *Food Hydrocolloids, 96*, 537–545.

Liu, W., Griffith, M., & Fengfu, L. (2008). Alginate microsphere-collagen composite hydrogel for ocular drug delivery and implantation. *Journal of Materials Science: Materials in Medicine, 19*, 3365–3371.

Liu, X. D., Yu, W. T., Lin, J. Z., & Quan, Y. (2007). Diffusion of acetic acid across oil/water interface in emulsification-internal gelation process for preparation of alginate gel beads. *Chemical Research in Chinese Universities, 23*, 579–584.

Liu, X. D., Yu, W. T., Zhang, Y., Xue, W., Yu, W., Xiong, Y., et al. (2002). Characterization of structure and diffusion behaviour of Ca-alginate beads prepared with external or internal calcium sources. *Journal of Microencapsulation, 19*, 775–782.

Minekus, M., Alminger, M., Alvito, P., Ballance, S., Bohn, T., Bourlieu, C., Carriere, F., Boutrou, R., Corredig, M., Dupont, D., Dufour, C., Egger, L., Golding, M., Karakaya, S., Kirkhus, B., Le Feunteun, S., Lesmes, U., Macierzanka, A., Mackie, A., … Brodkorb, A. (2014). A standardised static *in vitro* digestion method suitable for food - an international consensus. *Food and Function, 5*, 1113–1124.

Moe, S. T., Skjaak-Braek, G., Elgsaeter, A., & Smidsroed, O. (1993). Swelling of covalently crosslinked alginate gels: Influence of ionic solutes and nonpolar solvents. *Macromolecules, 26*, 3589–3597.

Mongar, J., & Wassermann, A. (1949). Fully swollen alginate gels as permutites: Kinetics of calcium–sodium ion exchange. *Discussions of the Faraday Society, 7*, 118–123.

Paques, J. P., van der Linden, E., van Rijn, C. J., & Sagis, L. M. (2013). Alginate submicron beads prepared through W/O emulsification and gelation with $CaCl_2$ nanoparticles. *Food Hydrocolloids, 31*, 428–434.

Pasparakis, G., & Bouropoulos, N. (2006). Swelling studies and *in vitro* release of verapamil from calcium alginate and calcium alginate–chitosan beads. *International Journal of Pharmaceutics, 323*, 34–42.

Ribeiro, A. J., Neufeld, R. J., Arnaud, P., & Chaumeil, J. C. (1999). Micro-encapsulation of lipophilic drugs in chitosan-coated alginate micro-spheres. *International Journal of Pharmaceutics, 187*, 115–123.

Shewan, H. M. (2015). *Rheology of soft particle suspensions. (PhD thesis)*. School of Chemical Engineering. https://doi.org/10.14264/uql.2015.533. The University of Queensland.

Shewan, H. M., & Stokes, J. R. (2013). Review of techniques to manufacture micro-hydrogel particles for the food industry and their applications. *Journal of Food Engineering, 119*, 781–792.

Soukoulis, C., Cambier, S., Hoffmann, L., & Bohn, T. (2016). Chemical stability and bioaccessibility of β-carotene encapsulated in sodium alginate O/W emulsions: Impact of Ca^{2+} mediated gelation. *Food Hydrocolloids, 57*, 301–310.

Sriamornsak, P., Thirawong, N., & Korkerd, K. (2007). Swelling, erosion and release behavior of alginate-based matrix tablets. *European Journal of Pharmaceutics and Biopharmaceutics, 66*, 435–450.

Torres, O., Murray, B., & Sarkar, A. (2016). Emulsion micro-gel particles: Novel encapsulation strategy for lipophilic molecules. *Trends in Food Science & Technology, 55*, 98–108.

Yang, X., Gong, T., Lu, Y. H., Li, A., Sun, L., & Guo, Y. (2020). Compatibility of sodium alginate and konjac glucomannan and their applications in fabricating low-fat mayonnaise-like emulsion gels. *Carbohydrate Polymers, 229*, 115468.

Ye, X., Li, Y., Ai, Y., & Nie, Y. (2018). Novel powder packing theory with bimodal particle size distribution-application in superalloy. *Advanced Powder Technology, 29*, 2280–2287.

Zhu, Y., Wang, J., Wu, J., Zhang, J., Wan, Y., & Wu, H. (2016). Injectable hydrogels embedded with alginate microspheres for controlled delivery of bone morphogenetic protein-2. *Biomedical Materials, 11*, Article 025010.

Food Hydrocolloids 121 (2021) 107040

Contents lists available at ScienceDirect

Food Hydrocolloids

journal homepage: www.elsevier.com/locate/foodhyd

Formation and creaming stability of alginate/micro-gel particle-induced gel-like emulsions stabilized by soy protein isolate

Duanquan Lin [a,b], Alan L. Kelly [b], Song Miao [a,*]

[a] Teagasc Food Research Centre, Moorepark, Fermoy, Co. Cork, Ireland
[b] School of Food and Nutritional Sciences, University College Cork, Cork, Ireland

ARTICLE INFO

Keywords:
Digestion
External gelation
Gel-like emulsion
Micro-gel particle
Storage stability

ABSTRACT

Many strategies have been developed to improve stability of plant protein-stabilized emulsions, such as modifying properties of plant proteins, using plant protein-polysaccharide complexes, and forming gel-like emulsions. In this study, a novel method was investigated to enhance creaming stability of soy protein isolate (SPI)-stabilized emulsions by introducing alginate and alginate-based micro-gel particles to form gel-like emulsions. Gel-like emulsions could be obtained at high levels of micro-gel particles (>6.0%) in the presence of alginate (>0.1%), while the concentration of SPI-coated droplets (0–10%) played a relatively unimportant role, probably because the gelation mechanism was interactions between alginate molecules and Ca^{2+}-induced micro-gel particles. Viscosity and creaming stability of emulsions and storage modulus (G') of gel-like emulsions increased with increasing contents of micro-gel particles in emulsions. Emulsions without micro-gel particles showed extensive creaming during storage, and emulsions containing micro-gel particles were visually stable after storage for six weeks, although all samples showed good stability to coalescence. In addition, the presence of micro-gel particles in emulsions slightly decreased the bioaccessibility of encapsulated lycopene after *in-vitro* digestion. The method presented in this study was important for improving creaming stability of plant protein-stabilized emulsions and expanding application of plant protein-stabilized emulsions in food industry.

1. Introduction

In recent years, plant protein-stabilized emulsions, such as soy protein-, pea protein-, potato protein-, rice protein-, wheat gliadin- and zein-stabilized emulsions, have received increased interest (Lin et al., 2017), due to increased consumer demand for healthier foods (da Silva, Almeida, & Sato, 2021; Wan, Guo, & Yang, 2015). However, compared to animal proteins (e.g., casein and whey protein) and synthetic chemicals (e.g., span 85, span 80 and Tween 20), plant proteins often result in emulsions with lower stability (especially creaming stability), probably due to low hydrophobicity and inter-facial tension of plant protein-stabilized droplets (Benjamin, Silcock, Beauchamp, Buettner, & Everett, 2014; Zhang, Yan, Jiang, & Ding, 2021). Many strategies therefore have been investigated to solve this problem, such as protein modification by physical, chemical and/or enzymatic treatments (Albano, Cavallieri, & Nicoletti, 2019; Barać, Stanojević, Jovanović, & Pešić, 2004) and turning emulsions into emulsion gels (Lin, Kelly, & Miao, 2020).

Many methods have been reported to modify structural properties of plant proteins, in order to improve their emulsifying capacity, such as heating (Peng et al., 2016), high pressure (Chen, Chen, Yu, & Wu, 2016; Molina, Papadopoulou, & Ledward, 2001), extrusion (Mozafarpour, Koocheki, Milani, & Varidi, 2019), ultrasound (O'sullivan, Park, & Beevers, 2016), pH-shifting process (Jiang, Chen, & Xiong, 2009), enzymatic hydrolysis (Chen, Chen, Ren, & Zhao, 2011), and oxidation (Liu, Lu, Han, Chen, & Kong, 2015), due to improved protein solubility, reduced molecular size, and/or exposure of hidden hydrophobic residues. In addition, plant protein-polysaccharide complexes, which are formed by Maillard reaction or electrostatic interaction, can also be used to improve emulsion stability (Evans, Ratcliffe, & Williams, 2013). It has been reported that soy protein isolate (SPI)-dextran conjugate-stabilized emulsions showed better physical and structural stability than emulsions stabilized by native SPI or SPI-dextran mixtures, probably due to higher electrostatic repulsion and steric hindrance (Zhou et al., 2020). On the other hand, the pH is crucial for stability of emulsions containing plant protein-polysaccharide complexes produced by electrostatic interaction, because electrostatic properties of proteins and polysaccharides are clearly pH-dependent (Albano et al., 2019). Many

* Corresponding author.
E-mail address: song.miao@teagasc.ie (S. Miao).

https://doi.org/10.1016/j.foodhyd.2021.107040
Received 20 April 2021; Received in revised form 6 June 2021; Accepted 12 July 2021
Available online 14 July 2021
0268-005X/

reports have been indicated that the presence of anionic polysaccharides could increase the stability of plant protein-stabilized emulsions near the p*I* of the proteins present, due to the formation of electrostatic interaction-induced plant protein-polysaccharide complexes at the droplet interfaces and thus increased electrostatic repulsion of emulsion droplets at pH 4.0–4.5 (Lin, Kelly, & Miao, 2021b; Yildiz, Ding, Andrade, Engeseth, & Feng, 2018).

The final physical state of modified plant protein-stabilized emulsions is still liquid, while another widely-investigated strategy to improve stability of plant protein-stabilized emulsions is turning emulsions into emulsion gels/gel-like emulsions, due to increased viscosity and solid-like properties and thus reduced mobility of emulsion droplets. Therefore, emulsions prepared by these two methods may have different applications in the food industry. It has been reported that emulsion gels/gel-like emulsions containing plant protein-stabilized droplets may be used in meat products and solid-like delivery systems (de Souza Paglarini et al., 2018), while modified plant protein-stabilized emulsions were often used in sauce, yogurt, beverage, and liquid delivery systems (Ashaolu, 2020).

There are several methods used to prepare gel-like emulsions. Firstly, increasing the oil fraction is the simplest method to obtain gel-like emulsions, because of droplet flocculation/bridging (Lee, Chan, & Mohraz, 2012), which has been widely reported in plant protein particle-stabilized Pickering emulsions (Liu & Tang, 2016; Zou et al., 2017). Secondly, modifying structural properties of plant proteins absorbed at droplet surfaces may also lead to the formation of gel-like emulsions; it has been reported that SPI-stabilized emulsions turned into gel-like emulsions after microfluidization, probably due to structural deformation of proteins and increased inter-droplet interactions during microfluidization treatment (Tang & Liu, 2013). It has also been reported that soy glycinin- or potato protein-stabilized emulsion droplets could cross-link together and form gel-like emulsions by tyrosinase-induced enzymatic cross-linking (Glusac, Isaschar-Ovdat, Kukavica, & Fishman, 2017; Isaschar-Ovdat, Rosenberg, Lesmes, & Fishman, 2015). Thirdly, introducing gelling agents into the continuous phase of emulsions can also form emulsion gels by various gelation mechanisms depending on gelling agents used, as reviewed by Lin, Kelly, and Miao (2020). For example, alginate and $CaCO_3$ particles have been introduced into SPI-stabilized emulsions, and then emulsion gels formed after adding glucono-delta-lactone (GDL) into the system to release Ca^{2+} and trigger Ca^{2+}-induced alginate gelation (Lin et al., 2021b).

Alginate-based emulsion gels received increased interest in recent years, due to their characters (e.g., mild gelation process and slow digestion during intestinal digestion), compared to other gelling agent-based emulsion gels (Lin, Kelly, Maidannyk, & Miao, 2021). The alginate gelation mechanism involves sodium ions in alginate molecules being replaced by Ca^{2+} or H^{+}, which leads to Ca^{2+}-cross-linked or hydrogen bond-linked network structures. Therefore, $CaCl_2$, $CaCO_3$, and GDL are often used to trigger alginate gelation in the food industry (Draget, Skjåk-Bræk, & Stokke, 2006). However, our previous study found that the presence of alginate-based emulsion micro-gels prepared by external gelation could increase the viscosity of alginate solutions with solid-like behavior (Lin, Kelly, & Miao, 2021a). In addition, it has also been reported that nanoparticles (NPs) could interact with proteins, lipids and polysaccharides through ionic interactions, hydrogen bonds, and/or Van der Waals interactions, and that the size, shape, and surface characters of NPs played an important role in affecting interactions between NPs and polymers (Saptarshi, Duschl, & Lopata, 2013). For example, acrylamide/N-isopropylacrylamide-based NPs could interact with heparin through hydrogen bonds, ionic interactions and dehydration (Zeng et al., 2012). Therefore, we predicted that Ca^{2+}-induced emulsion micro-gels could also lead to the formation of gel-like emulsions containing alginate in the continuous phase and thus improve the creaming stability of plant protein-stabilized emulsions, which has not previously been studied.

Furthermore, there are mainly two advantages of this method. Firstly, this is a simple method to prepare gel-like emulsions by mixing micro-gel particles with emulsions, and the viscosity and gel strength of gel-like emulsions can be easily controlled by adjusting the amount of micro-gel particles for different applications in foods. In addition, a novel food structure (i.e., microgel-in-gel-like emulsions) can be developed, which may be used for specific delivery systems in future. Therefore, the aim of this study was to investigate the formation and properties (i.e., rheology, morphology, droplet size, creaming stability, digestion, and encapsulation for food nutrients) of alginate/microgel-induced gel-like emulsions and to improve creaming stability of SPI-stabilized emulsions by formation of such gel-like emulsions.

2. Materials and methods

2.1. Materials

SPI containing 96.29 ± 0.03% protein was extracted from defatted soy flour (Bob's Red Mill, Milwaukie, Oregon, USA) by the method described in our previous study (Lin, Kelly, Maidannyk, & Miao, 2020). Sodium alginate ($\overline{M}$ = 69–117 kDa) was obtained from Special Ingredients (Chesterfield, UK), and sunflower oil (Aldi Stores Ltd., Kildare, Ireland) was purchased from local markets. Span 80, $CaCl_2{\cdot}2H_2O$, NaOH, HCl, tomato extract, sodium azide, butylated hydroxytoluene (BHT), hexane, acetone, ethanol, and other analytical reagents were purchased from Sigma-Aldrich (St. Louis, MO, USA).

2.2. Preparation of emulsion micro-gel particles

The external O/W/O emulsion-gelation method was used to prepare emulsion micro-gel particles. The coarse emulsions were firstly prepared by mixing 20 wt% sunflower oil with 80 wt% SPI dispersions containing 2.0 wt% SPI at 16,000 rpm for 2 min with an Ultra-Turrax (IKA-25, Staufen, Germany). The primary emulsions were then prepared by mixing coarse emulsions with 2.0 wt% sodium alginate solutions (1: 3, w/w) at 14,000 rpm for 2 min. The secondary emulsions were finally prepared by mixing primary emulsions (20 wt%) with oil phase containing 78 wt% sunflower and 2.0 wt% Span 80 at 700 rpm for 5 min with a magnetic stirrer, and then $CaCl_2{\cdot}2H_2O$ solutions (1.0 wt%) were added into secondary emulsions (1:5, w/w) and stirring at 1000 rpm for 30 min. The resultant dispersions were then poured into deionized water (1: 5, w/w), mixed at 500 rpm for 1 min and left to stand for 2 h. Emulsion micro-gel particles in sediments were finally collected by filtration and washed twice by deionized water after the oil cream in the top of mixtures was removed.

2.3. Preparation of emulsions containing micro-gel particles

SPI dispersions were firstly prepared by stirring SPI powders (2 g) with deionized water (78 g) for 2 h. Sodium alginate solutions (2.0 wt% in deionized water) were also prepared by stirring for 24 h to permit hydration. Coarse emulsions (i.e., SPI-stabilized emulsions) were then prepared by mixing 20 wt% sunflower oil with 80 wt% SPI dispersions at 16,000 rpm for 2 min with an Ultra-Turrax (IKA-25, Staufen, Germany). The primary emulsions (i.e., alginate/SPI-stabilized emulsions) were then prepared by mixing coarse emulsions (containing 0.5–2.0% SPI and 5.0–20% SPI) with sodium alginate solutions (0.2–1.0%) at a ratio of 1: 1, w/w and homogenizing at 14,000 rpm for 2 min with an Ultra-Turrax. The coarse emulsions and sodium alginate solutions were diluted with deionized water before mixing.

For preparation of alginate/SPI-stabilized emulsions containing micro-gel particles, gel particles, which were prepared as described in Section 2.2, were firstly dried using filter paper to absorb free water from gaps in particle clusters. In order to increase the dispersibility of micro-gel particles in emulsions, gel particle dispersions (10–50% in

deionized water, w/w) were then prepared by adding deionized water into micro-gel particles and stirring mildly for 1 min using a magnetic stirrer. Emulsions containing micro-gel particles (2.0–10 wt% in final emulsions) were finally prepared by mixing primary emulsions with micro-gel particle dispersions (4:1, w/w) at 500 rpm for 1 min using a magnetic stirrer and the properties of final emulsions were then measured immediately. The control samples were prepared by mixing primary emulsions with deionized water (4:1, w/w) using a magnetic stirrer.

2.4. Properties of emulsions containing micro-gel particles

2.4.1. Visual appearance

Emulsions (~10 g) were transferred into screw-cap glass bottles before resting for 2 h, and then samples were turned upside down before taking photographs of them using a smart phone camera (iPhone 7, Apple, Cupertino, CA, USA). A black cardboard was placed under samples and another was placed in the background before taking photos.

2.4.2. Rheological measurements

The rheological properties of emulsions were measured using an AR 2000ex rheometer (TA Instruments, Crawley, UK). Emulsions were added on an aluminium parallel plate (60 mm in diameter, and 0.5 mm in gap) and allowed to stand at 20 °C for 2 min before measurement. The flow measurement (the shear rate from 0.1 to 300 s^{-1}) and oscillatory measurement (the frequency from 0.1 to 10 Hz with a fixed strain of 0.1%) were then carried out to determine the viscosity (η) and the storage (G') and loss (G'') modulus of emulsions, respectively.

2.4.3. Micro-structure of emulsions

An Olympus BX51 light microscope (Olympus Optical Co. Ltd., Tokyo, Japan) with a built-in camera was used to record microscopic images of emulsions. Samples were dropped on a microscope slide using pipettes without covering with glass coverslips and observed using 4 × or 10 × objective lens and 10 × eyepiece. Images were then taken using the camera control software ProgRes CapturePro 2.10 (Jenoptik, Jena, Germany).

2.4.4. Creaming stability measurements

The stability of emulsions to gravitational separation (i.e., creaming stability) was analyzed with a Lumisizer (LUM GmbH, Berlin, Germany). Emulsions were centrifuged at 3000 rpm and 25 °C with a scanning rate of once every 20 s for 300 profiles. The space- and time-related transmission profiles over the sample length and the fluctuation in light transmittance during centrifugation were recorded.

2.4.5. Size distribution measurements

A MasterSizer 3000 (Malvern Instruments Ltd., Worcestershire, UK) was used to measure the droplet-size distribution of emulsions. The obscuration rate, stirrer speed, refractive index and absorption index were set at 1%–10%, 2000 rpm, 1.48, and 0.001, respectively.

2.5. Preparation and storage stability of emulsions containing lycopene

For preparation of lycopene-encapsulated emulsions, 30 mg of tomato extract (containing 0.059 mg lycopene/mg) were dissolved in 20 g of sunflower oil at 140 °C with stirring for 30 s before cooling down to the room temperature, and then lycopene-encapsulated primary emulsions containing micro-gel particles were prepared as described in Section 2.3.

Emulsions (~10 g) containing lycopene and micro-gel particles were transferred into screw-cap tubes and stored in a cold room at 4 °C for 6 weeks in the dark. Properties of emulsions (e.g., visual appearance, micro-structure, and droplet-size distribution) were measured every 2 weeks during storage as described in Section 2.4, but the refractive index of 1.69 was used for the droplet-size measurement of emulsions containing lycopene. The remaining lycopene in emulsions ($C_{LYC\text{-}E}$) during storage was also extracted and measured as described by Lin et al. (2021).

2.6. Bioaccessibility of lycopene after in-vitro digestion

Simulated digestion of emulsions included the oral, gastric and small intestinal phases in this study, which was performed as described in our previous study (Lin et al., 2021). The digesta after intestinal digestion was centrifuged at 4500 rpm (~1900×*g*) and 4 °C for 40 min (Mikro 200R, Hettich, Tuttlingen, Germany), and the middle layer, which was regarded as the micelle fraction, was collected and weighted ($Wt_{Micelle}$). Lycopene in 0.5 g of the micelle fraction ($C_{LYC\text{-}M}$) was extracted and measured by the method described in our previous study (Lin et al., 2021). The bioaccessibility of lycopene in the micelle was then calculated by Eq. (1):

$$\text{Bioaccessibility}\ (\%) = \frac{Wt_{LYC-M}}{Wt_{LYC-E}} = \frac{C_{LYC-M} \times Wt_{Micelle}}{C_{LYC-E} \times 5} \times 100\% \quad (1)$$

where $Wt_{LYC\text{-}M}$ and $Wt_{LYC\text{-}E}$ are the amount of lycopene in the micellar phase and that in the original emulsions before digestion, respectively, $C_{LYC\text{-}E}$ is the lycopene content in original emulsions, and 5 g is the weight of original emulsions used for *in-vitro* digestion.

3. Results and discussion

3.1. Effect of concentrations of alginate-based micro-gel particles, alginate, and SPI-coated droplets on the formation of gel-like emulsions

Table 1 shows the effect of concentrations of alginate-based micro-gel particles, alginate, and SPI-coated droplets on the gel point of SPI-stabilized emulsions. The establishment of gel point of emulsions in this study was based on the rheological properties of emulsions (Figs. S1 and S2). At the gel point, emulsions changed from liquid-like behavior, with relatively low viscosity, to solid-like behavior, with shear-thinning properties and G' value higher than G''.

As shown in Table 1, gel-like emulsions could not be obtained in SPI-stabilized emulsions without alginate no matter how many micro-gel particles (0–10%) were added. When the concentration of alginate in emulsions increased to 0.1%, and 10% of micro-gel particles were added, gel-like emulsions formed, while emulsions still showed liquid-like behavior under low concentrations of micro-gel particles (0–8.0%). In addition, when the concentrations of alginate in emulsions

Table 1
Effect of concentrations of alginate-based micro-gel particles, alginate, and SPI-coated droplets on the formation of gel-like emulsions. When the effect of alginate concentration (0–0.5 wt%) was investigated, the concentration of SPI-coated droplets was set at 5.0 wt%. When the effect of concentration of SPI-coated droplets (0–10 wt%) was investigated, the alginate concentration was set at 0.3 wt%. The results shown are based on the rheological properties of emulsions (see supplementary material).

Samples		Alginate (wt%)				SPI-coated droplets (wt%)			
		0	0.1	0.3	0.5	0	2.5	5.0	10
Micro-gel particles (wt %)	0	× [a]	×	×	×	×	×	×	×
	2	×	×	×	×	×	×	×	×
	4	×	×	×	×	×	×	×	×
	6	×	×	✓	✓	✓	✓	✓	✓
	8	×	×	✓	✓	✓	✓	✓	✓
	10	×	√ [b]	✓	✓	✓	✓	✓	✓

[a] A cross mark indicated that emulsions were still liquid with relatively low viscosity.

[b] A check mark indicated the formation of gel-like emulsions with shear-thinning behavior and G' value higher than G''.

increased to 0.3% or 0.5%, gel-like emulsions formed at high concentrations of micro-gel particles (6.0–10%). These indicate that the conditions for the formations of gel-like emulsions were the presence of alginate and addition of high levels of micro-gel particles.

It has been reported that calcium ions were distributed at the surfaces of alginate-based macro-gel beads produced by external gelation, as determined by electron dispersive spectroscopy (Patel, AbouGhaly, Schryer-Praga, & Chadwick, 2017). Therefore, it can be proposed that the mechanism of the formation of gel-like emulsions containing alginate and Ca^{2+}-induced alginate micro-gel particles is probably interactions between alginate molecules and Ca^{2+} on the surfaces of alginate micro-gel particles in the continuous phase of emulsions, which however needs further investigation. This potential mechanism for the formation of alginate-based gel-like emulsions is different from that in previous studies, in which insoluble calcium salts (e.g., $CaCO_3$, $CaSO_4$, or CaEDTA) were introduced into emulsions containing alginate before an acid (e.g., GDL or pyrophosphate) was added to release calcium ions and trigger the gelation and formation of alginate-based emulsion gels (Pintado, Ruiz-Capillas, Jiménez-Colmenero, Carmona, & Herrero, 2015; Sato, Moraes, & Cunha, 2014).

Table 1 also shows that 0.3% of alginate solutions without SPI-coated droplets also showed solid-like behavior at high concentrations of micro-gel particles (6.0–10%), and the gel point was unchanged when the concentrations of SPI-coated droplets increased from 0% to 10%. These indicate that the concentration of SPI-coated droplets and interactions between alginate micro-gel particles and SPI-coated droplets played a relatively unimportant role in the formation of gel-like emulsions. This was probably because the ionic bonding between alginate and Ca^{2+} is stronger than electrostatic interactions between SPI and Ca^{2+} (Chan, Jin, & Heng, 2002; Lu, Lu, Yin, Cheng, & Li, 2010), or may relate to the fact that contents of SPI in emulsions were less than 1.0% in this study, which were much lower than the concentrations of SPI (>6.0%) needed for Ca^{2+}-induced protein gelation (Maltais, Remondetto, Gonzalez, & Subirade, 2005). Therefore, it can be concluded that the gel point of emulsions was affected by the concentrations of micro-gel particles and alginate rather than the concentration of SPI-coated droplets in this study.

3.2. Properties of emulsions containing alginate and micro-gel particles

Fig. S1 shows that although emulsions containing 5.0% SPI-coated droplets, 0.1% alginate, and 10% micro-gel particles exhibited gel-like behavior (i.e., $G' > G''$), the G' values of gel-like emulsions (i.e., 0.5–2.0 Pa) were low, which indicates low extents of cross-linking in the resultant gel-like emulsions. Therefore, properties of emulsions containing 5.0% SPI-coated droplets, higher concentration of alginate (i.e., 0.3%) and various concentrations of micro-gel particles (i.e., 0–10%) were further examined.

3.2.1. Rheological properties

Fig. 1A shows that the viscosity of emulsions increased with increasing the concentrations of micro-gel particles from 0 to 10% in emulsions. This was probably because increased interactions between micro-gel particles and alginate molecules in the continuous phase decreased the fluidity of emulsions. In addition, emulsions containing higher contents of micro-gel particles (≥6.0%) showed more obvious shear-thinning behavior in the low range of shear rate, which also indicates that the extent of cross-linking between micro-gel particles and alginate molecules increased when increasing the concentrations of micro-gel particles. This was also confirmed by the increased values of G' and G'' of emulsions containing higher contents of micro-gel particles (≥6.0%) (Fig. 1B). A similar result has been reported, where emulsion gels were prepared by introducing Persian gum and $CaCl_2$ into the continuous phase of whey protein isolate-stabilized emulsions, and increasing the levels of Persian gum increased the G', G'', and η^* values of emulsion gels (Khalesi, Emadzadeh, Kadkhodaee, & Fang, 2019).

Fig. 1B also shows that emulsions containing low levels of micro-gel particles (<6.0%) had low G' values (<10 Pa), while emulsions turned into gel-like emulsions ($G' > G''$) when 6.0% micro-gel particles were added, and that increasing the concentrations of micro-gel particles to 8% and 10% increased the G' of gel-like emulsions to 12–35 Pa and 64–97 Pa, respectively, in the frequency range of 0.1–10 Hz.

In addition, the tan δ (G''/G') values also deceased from 2.43 to 15.9 to 0.11–0.27 when increasing the concentrations of micro-gel particles from 4.0% to 10%. This was probably because high contents of micro-gel particles in emulsions led to the formation of network structures, in which micro-gel particles may act as cross-linking sites between neighboring alginate molecules through interactions between alginate molecules and Ca^{2+} on the surfaces of alginate micro-gel particles. However, low concentrations of micro-gel particles (<6.0%) were insufficient to cross-link alginate molecules and form network structures.

Our results thus indicate that the viscoelasticity of gel-like emulsions can be easily adjusted by the addition amount of micro-gel particles. In addition, the G' values of gel-like emulsions gradually increased with increasing oscillatory frequency (Fig. 1B), which also indicates the formation of non-covalent bond-cross-linked network structures in gel-like emulsions. The similar phenomenon has also been reported in SPI-stabilized gel-like emulsions produced by microfluidization (Tang & Liu, 2013).

3.2.2. Morphology, micro-structure and droplet-size distribution

Fig. 2A shows the visual appearance of SPI-stabilized emulsions containing 0.3% alginate and 0–10% of micro-gel particles. Emulsions without micro-gel particles moved to the bottom of bottle after inverting the glass bottle, while some emulsions containing 2.0–4.0% of micro-gel particles stuck to the inner walls of bottles, due to the slightly increased viscosity (Fig. 1A). Emulsions containing 6.0% of micro-gel particles

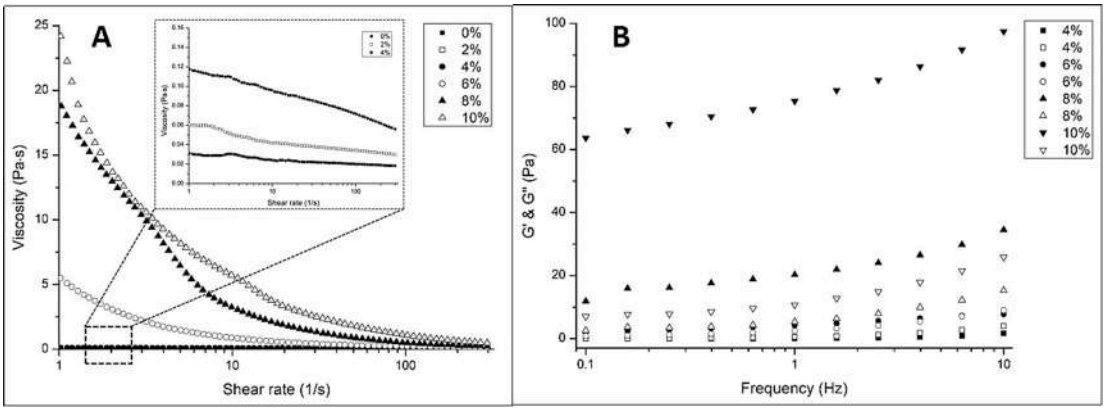

Fig. 1. (A) Viscosity and (B) moduli (G' and G'') of emulsions containing 0–10% micro-gel particles, 0.3% alginate and 5.0% oil droplets.

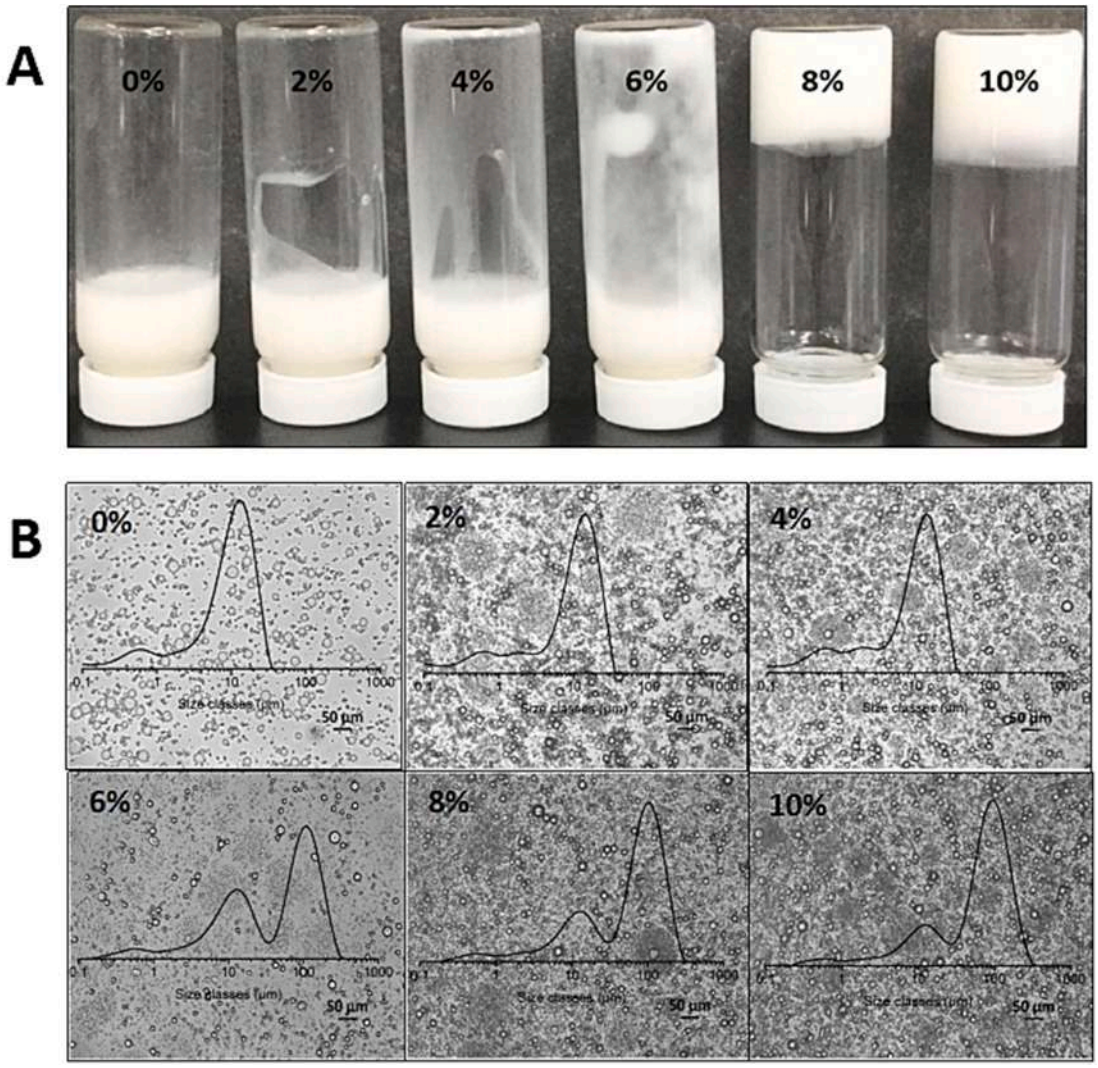

Fig. 2. (A) Visual appearance and (B) micro-structure with droplet-size distribution of emulsions containing 5.0% oil droplets, 0.3% alginate and 0–10% micro-gel particles.

turned into gel-like emulsions and some residual gel material remained on the top and wall of bottle after inverting it, while emulsions containing 8–10% of micro-gel particles showed solid-like and self-standing behavior, and are classed as emulsion gels, probably due to high extents of cross-linking between alginate molecules and micro-gel particles in the continuous phase of emulsions. Our results indicated that SPI-stabilized liquid emulsions, gel-like emulsions, or emulsion gels could be obtained by adjusting the content of micro-gel particles. Similar results have also been reported, where starch granule-stabilized Pickering emulsions converted from liquid-like behavior to solid-like behavior with increasing the oil volume fractions from 10% to 60% (Li, Zhang, Li, Fu, & Huang, 2020).

Fig. 2B shows the micro-structure and droplet-size distribution of SPI-stabilized emulsions containing 0.3% alginate and 0–10% of micro-gel particles. Partial emulsion flocculation occurred in emulsions without micro-gel particles (i.e., the control sample), probably because the electrostatic repulsion between anionic alginate and SPI-coated droplets at pH 6–7 led to depletion flocculation (Fioramonti, Martinez, Pilosof, Rubiolo, & Santiago, 2015). Both micro-gel particles and emulsion droplets could be observed in samples containing 2.0–4.0% of micro-gel particles, and they had similar droplet sizes to the control sample. However, increasing the contents of micro-gel particles to 6.0–10% significantly increased the droplet size of sample (i.e., the presence of another peak at around 100 μm in the distribution), but the micro-structure of emulsion droplets containing 6.0–10% of micro-gel particles were similar to those containing 2.0–4.0% of micro-gel particles, in which droplet coalescence did not occur. Therefore, the possible reason for increased droplet size was that the presence of micro-gel particles with $D_{4,3}$ of 63.3 ± 7.4 μm (Fig. S3) were detected in samples containing higher contents of micro-gel particles (i.e., 6.0–10%), although the presence of micro-gel particles had no significant effects on the emulsion droplet-size distribution, regardless of micro-gel particle concentration.

3.2.3. Creaming stability

Fig. 3 shows the light transmission profiles of SPI-stabilized emulsions containing 0.3% alginate and 0–10% of micro-gel particles during centrifugation. The light transmission through the bottom of sample cells containing emulsions without micro-gel particles (i.e., the control sample in Fig. 3A) increased sharply during centrifugation, which indicates the occurrence of creaming in the control sample. Creaming in emulsions is driven by the buoyancy of emulsion droplets dispersed in the continuous phase and, according to the Stokes law, the creaming rate (Cr) can be calculated through Eq. (2):

$$Cr = \frac{R^2(\rho_c - \rho_o)}{\eta_c} \quad (2)$$

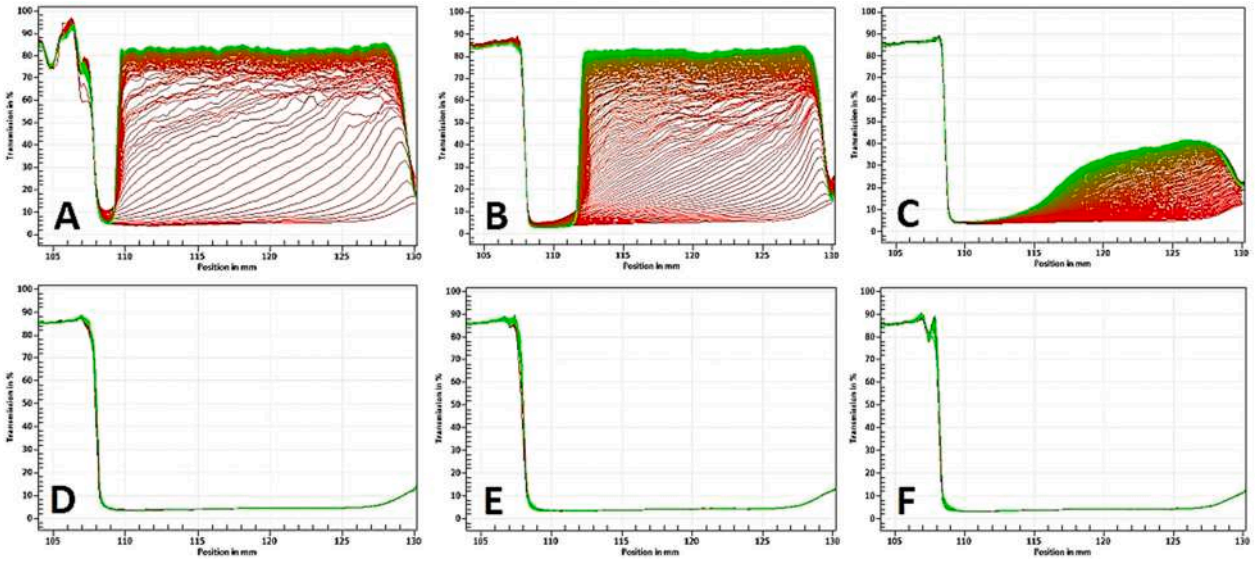

Fig. 3. (A–F) Transmission profiles with time of emulsions containing 5.0% oil droplets, 0.3% alginate and 0%, 2.0%, 4.0%, 6.0%, 8.0%, or 10% micro-gel particles during 100 min of centrifugation at 3000 rpm.

where R indicates the size of droplets, ρ_c indicates the density of the continuous phase, ρ_o indicates the density of droplets, and η_c indicates the viscosity of the continuous phase (Chanamai & McClements, 2000).

However, the presence of low levels of micro-gel particles in emulsions (i.e., 2.0–4.0%) slowed the changes on the light transmission through the bottom of sample cells (Fig. 3B and C), which indicates an increase in creaming stability of emulsions. This was probably because low extents of cross-linking occurred between alginate molecules and micro-gel particles in the continuous phase, which increased the viscosity of the continuous phase and thus decreased the creaming rate of emulsions. Further increasing the addition levels of micro-gel particles in emulsions to 6.0–10% led to a stable system with low light transmission in emulsions during centrifugation (Fig. 3D–F), which indicated high creaming stability of emulsions, probably because of the high extents of cross-linking between alginate molecules and micro-gel particles and the formation of gel-like emulsions.

3.3. Storage stability and digestion of alginate/microgel-induced gel-like emulsions with encapsulated lycopene

3.3.1. Storage stability of emulsions with encapsulated lycopene

The storage stability of emulsions containing 0%, 4.0%, or 8.0% of micro-gel particles and encapsulated lycopene were further investigated, by storage of samples at 4 °C in the dark for six weeks. Fig. 4A shows the visual appearance of emulsions during storage. It can be seen

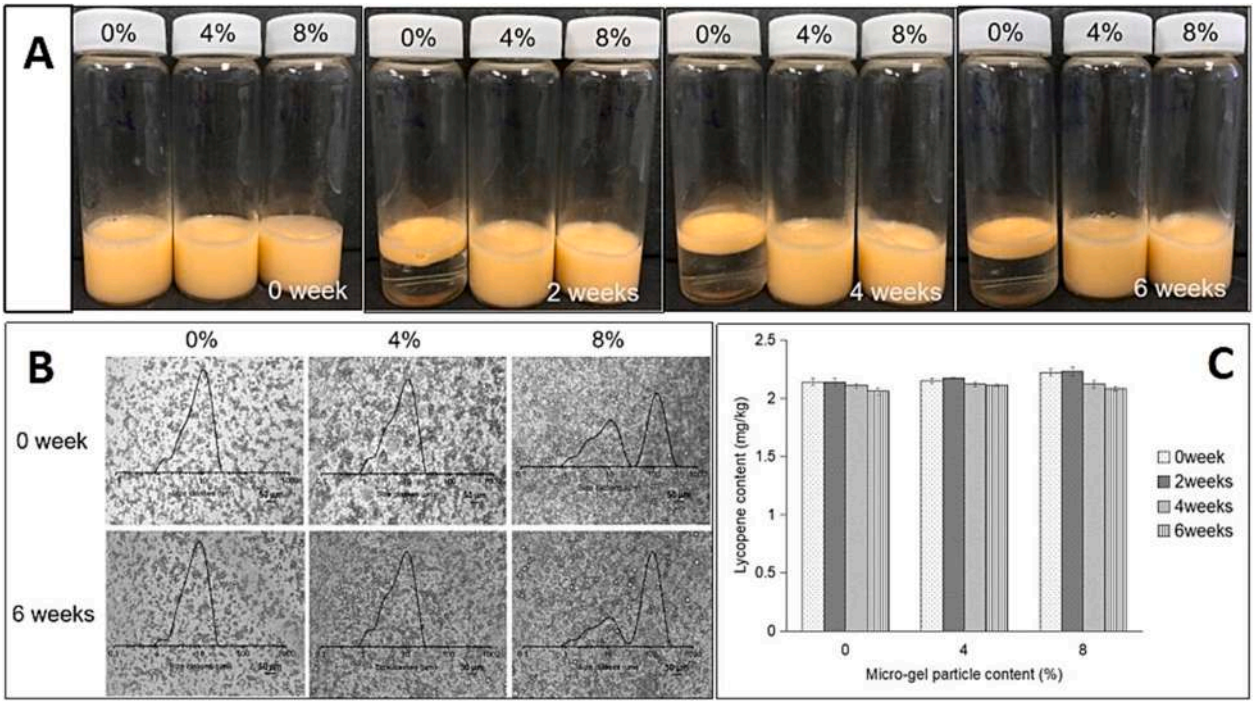

Fig. 4. (A) Visual appearance of emulsions, (B) micro-structure with droplet-size distribution of emulsions, and (C) lycopene content in emulsions containing 5.0% oil droplets, 0.3% alginate and 0%, 4.0%, or 8.0% micro-gel particles during storage for six weeks at 4 °C and darkness.

that creaming occurred in the control samples without micro-gel particles during storage, while emulsions containing 4.0% or 8.0% of micro-gel particles showed relatively high creaming stability. This was probably because the interactions between micro-gel particles and alginate molecules increased the viscosity of the continuous phase, decreased the mobility of droplets, and thus improved the storage stability of emulsions, as discussed in Section 3.2.3.

The micro-structure and droplet-size distribution of emulsions during storage were also investigated (Fig. 4B). The $D_{4,3}$ of droplets in emulsions containing 0% or 4.0% of micro-gel particles before storage were 9.31 ± 0.03 μm and 9.12 ± 0.02 μm with one peak in the distribution, respectively, while the $D_{4,3}$ of droplets in emulsions containing 8.0% of micro-gel particles before storage were 74.2 ± 12.7 μm, with two peaks in the distribution. The droplet size of emulsions containing 0%, 4.0%, or 8.0% micro-gel particles after storage for six weeks were 9.26 ± 0.04 μm, 9.08 ± 0.04 μm, and 83.6 ± 2.2 μm, respectively. In addition, droplet coalescence was not observed from micro-structure of emulsions during storage. These indicate that all SPI-stabilized emulsions containing alginate showed good stability to coalescence regardless of the presence of micro-gel particles, probably because proteins absorbed at the surfaces of droplets could prevent two droplets from merging to form a larger droplet (Tcholakova, Denkov, Ivanov, & Campbell, 2006).

Fig. 4C shows the content of lycopene encapsulated in SPI-stabilized emulsions containing 0%, 4.0%, or 8.0% of micro-gel particles during storage. Lycopene in all samples showed high stability during storage, although their contents decreased slightly. It is well known that heating (>100 °C) and light irradiation can accelerate lycopene degradation (Ax, Mayer-Miebach, Link, Schuchmann, & Schubert, 2003; Shi, Le Maguer, Bryan, & Kakuda, 2003). However, samples were stored at 4 °C in the dark in this study, so lycopene were relatively stable, although the mobility of droplets in emulsions containing different levels of micro-gel particles were different.

3.3.2. *Bioaccessibility of encapsulated lycopene from emulsions after digestion*

In-vitro digestion of emulsions containing 0%, 4.0%, or 8.0% of micro-gel particles and encapsulated lycopene were also studied, and Fig. 5 shows the micro-structure of emulsions during digestion. Emulsions after oral digestion had similar structures to those before digestion (Fig. 4B). However, severe flocculation occurred during gastric digestion in all samples, probably because the pH of simulated gastric liquids was maintained at 3.0 and the surface charges of SPI-stabilized droplets and the repulsive forces between neighboring droplets decreased at such pH. It has also been reported that whey protein-stabilized emulsions underwent flocculation during simulated gastric digestion at pH 2.52–6.16 (Wang, Lin, Ye, Han, & Singh, 2019). Fig. 5 also shows that small parts of droplets could still been observed after intestinal digestion for 2 h, and some droplets were coated by membranous cysts in emulsions containing 4.0% or 8.0% of micro-gel particles, which was probably because undigested gel-like alginate films attached to the droplets.

In addition, the bioaccessibility of encapsulated lycopene after intestinal digestion was also investigated, and the lycopene bioaccessibility in emulsions containing 0%, 4.0%, or 8.0% of micro-gel particles were 56.78 ± 6.98%, 52.65 ± 7.13%, and 50.95 ± 6.65%, respectively. It is known that carotenoids in lipids could be released and dissolved into micelles during intestinal digestion along with lipid digestion (Mutsokoti et al., 2017), while the presence of microgel-induced gel-like alginate matrices in emulsions may inhibit availability of enzymes to lipids and thus slow lipid digestion and decrease carotenoid bioaccessibility. It has been reported that less β-carotene was released from whey protein-beet pectin-stabilized emulsions into micelles than from whey protein-stabilized emulsions (Xu et al., 2014).

4. Conclusions

The formation and properties (i.e., micro-structure, rheological properties, creaming stability, storage stability, and *in-vitro* digestion) of

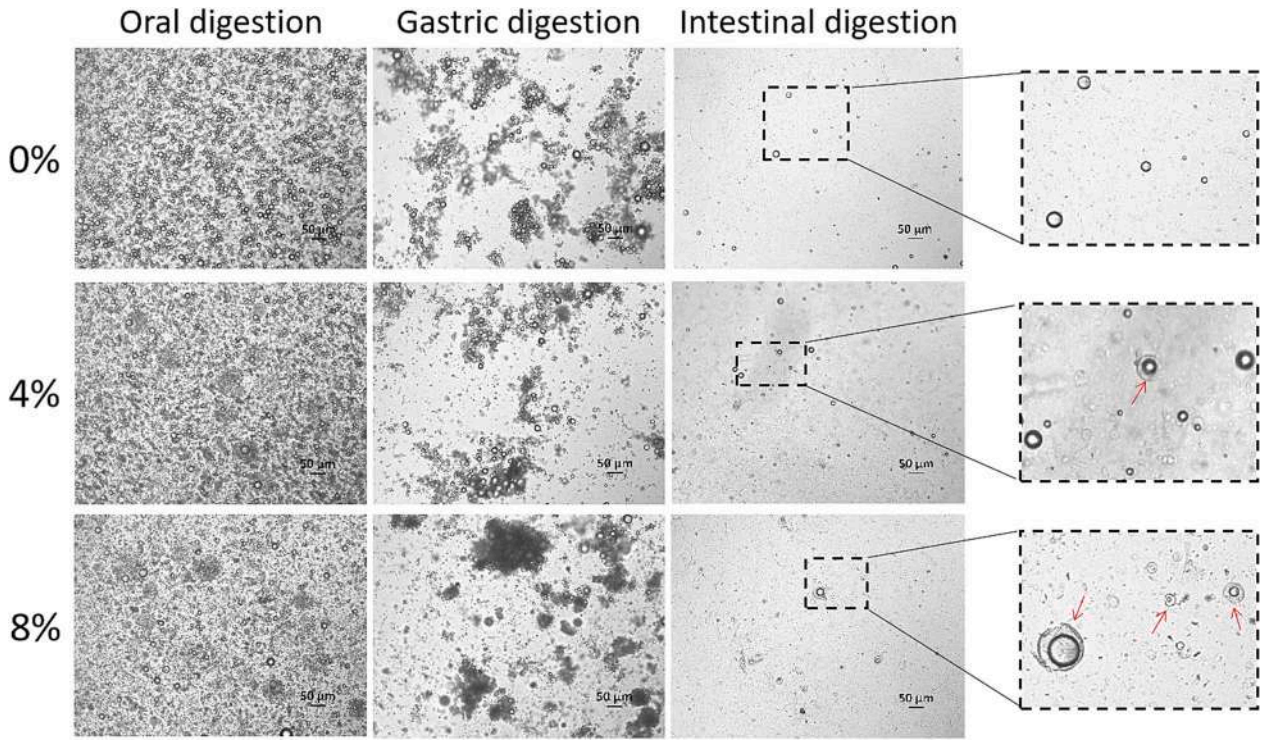

Fig. 5. Micro-structure of emulsions containing 5.0% oil droplets, 0.3% alginate and 0%, 4.0%, or 8.0% micro-gel particles during *in-vitro* digestion. Arrows pointed out the membranous cyst-coated droplets.

gel-like emulsions containing alginate-based micro-gel particles and alginate molecules were investigated. The conditions for the formation of gel-like emulsions were high concentrations of micro-gel particles (≥6.0%) in the presence of alginate (>0.1%), but the concentration of oil droplets (0–10%) did not affect the gel point of emulsions, which indicated that interactions between alginate molecules and micro-gel particles may be the reason for the formation of gel-like emulsions. In addition, increased viscosity and G' values of emulsions/gel-like emulsions with increasing contents of micro-gel particles in emulsions also indicated increased cross-linking between alginate molecules and micro-gel particles. The creaming stability and storage stability of emulsions were significantly improved after introducing high concentrations of micro-gel particles (≥6.0%) compared to the control samples without micro-gel particles, although the presence of micro-gel particles slightly decreased the *in-vitro* bioaccessibility of lycopene encapsulated in emulsions. However, the mechanism of interactions between alginate molecules and Ca^{2+}-induced micro-gel particles (especially the surface properties of micro-gel particles), the effect of higher oil phase fraction (>10%) on the properties of alginate/microgel-induced gel-like emulsions, and the application of these gel-like emulsions in foods, need further investigation.

CRediT author contribution statement

Duanquan Lin: Methodology, Writing - original draft, Data curation, Investigation. Alan L. Kelly: Supervision, Writing - review & editing. Song Miao: Supervision, Conceptualization, Writing - review & editing, Funding acquisition, Project administration, Investigation.

Declaration of competing interest

The authors declare that they have no known competing financial interests or personal relationships that could have appeared to influence the work reported in this paper.

Acknowledgement

This work was supported by the China Scholarship Council (No. 201708350111) and Teagasc-The Irish Agriculture and Food Development Authority (RMIS6821 and MDDT1392).

Appendix A. Supplementary data

Supplementary data to this article can be found online at https://doi.org/10.1016/j.foodhyd.2021.107040.

References

Albano, K. M., Cavallieri, Â. L. F., & Nicoletti, V. R. (2019). Electrostatic interaction between proteins and polysaccharides: Physicochemical aspects and applications in emulsion stabilization. *Food Reviews International, 35*, 54–89.

Ashaolu, T. J. (2020). Applications of soy protein hydrolysates in the emerging functional foods: A review. *International Journal of Food Science and Technology, 55*, 421–428.

Ax, K., Mayer-Miebach, E., Link, B., Schuchmann, H., & Schubert, H. (2003). Stability of lycopene in oil-in-water emulsions. *Engineering in Life Science, 3*, 199–201.

Barać, M. B., Stanojević, S. P., Jovanović, S. T., & Pešić, M. B. (2004). Soy protein modification: A review. *Acta Periodica Technologica, 35*, 3–16.

Benjamin, O., Silcock, P., Beauchamp, J., Buettner, A., & Everett, D. (2014). Emulsifying properties of legume proteins compared to *β*-lactoglobulin and tween 20 and the volatile release from oil-in-water emulsions. *Journal of Food Science, 79*, E2014–E2022.

Chanamai, R., & McClements, D. J. (2000). Dependence of creaming and rheology of monodisperse oil-in-water emulsions on droplet size and concentration. *Colloids and Surfaces A: Physicochemical and Engineering Aspects, 172*, 79–86.

Chan, L., Jin, Y., & Heng, P. (2002). Cross-linking mechanisms of calcium and zinc in production of alginate microspheres. *International Journal of Pharmaceutics, 242*, 255–258.

Chen, L., Chen, J., Ren, J., & Zhao, M. (2011). Modifications of soy protein isolates using combined extrusion pre-treatment and controlled enzymatic hydrolysis for improved emulsifying properties. *Food Hydrocolloids, 25*, 887–897.

Chen, L., Chen, J., Yu, L., & Wu, K. (2016). Improved emulsifying capabilities of hydrolysates of soy protein isolate pretreated with high pressure microfluidization. *LWT-Food Science and Technology, 69*, 1–8.

Draget, K. I., Skjåk-Bræk, G., & Stokke, B. T. (2006). Similarities and differences between alginic acid gels and ionically crosslinked alginate gels. *Food Hydrocolloids, 20*, 170–175.

Evans, M., Ratcliffe, I., & Williams, P. A. (2013). Emulsion stabilisation using polysaccharide–protein complexes. *Current Opinion in Colloid & Interface Science, 18*, 272–282.

Fioramonti, S. A., Martinez, M. J., Pilosof, A. M., Rubiolo, A. C., & Santiago, L. G. (2015). Multilayer emulsions as a strategy for linseed oil microencapsulation: Effect of pH and alginate concentration. *Food Hydrocolloids, 43*, 8–17.

Glusac, J., Isaschar-Ovdat, S., Kukavica, B., & Fishman, A. (2017). Oil-in-water emulsions stabilized by tyrosinase-crosslinked potato protein. *Food Research International, 100*, 407–415.

Isaschar-Ovdat, S., Rosenberg, M., Lesmes, U., & Fishman, A. (2015). Characterization of oil-in-water emulsions stabilized by tyrosinase-crosslinked soy glycinin. *Food Hydrocolloids, 43*, 493–500.

Jiang, J., Chen, J., & Xiong, Y. L. (2009). Structural and emulsifying properties of soy protein isolate subjected to acid and alkaline pH-shifting processes. *Journal of Agricultural and Food Chemistry, 57*, 7576–7583.

Khalesi, H., Emadzadeh, B., Kadkhodaee, R., & Fang, Y. (2019). Effect of Persian gum on whey protein concentrate cold-set emulsion gel: Structure and rheology study. *International Journal of Biological Macromolecules, 125*, 17–26.

Lee, M. N., Chan, H. K., & Mohraz, A. (2012). Characteristics of Pickering emulsion gels formed by droplet bridging. *Langmuir, 28*, 3085–3091.

Lin, D., Kelly, A. L., Maidannyk, V., & Miao, S. (2020). Effect of concentrations of alginate, soy protein isolate and sunflower oil on water loss, shrinkage, elastic and structural properties of alginate-based emulsion gel beads during gelation. *Food Hydrocolloids, 108*, 105998.

Lin, D., Kelly, A. L., Maidannyk, V., & Miao, S. (2021). Effect of structuring emulsion gels by whey or soy protein isolate on the structure, mechanical properties, and in-vitro digestion of alginate-based emulsion gel beads. *Food Hydrocolloids, 110*, 106165.

Lin, D., Kelly, A. L., & Miao, S. (2020). Preparation, structure-property relationships and applications of different emulsion gels: Bulk emulsion gels, emulsion gel particles, and fluid emulsion gels. *Trends in Food Science & Technology, 102*, 123–137.

Lin, D., Kelly, A. L., & Miao, S. (2021a). *Alginate-based emulsion micro-gel particles produced by an external/internal O/W/O emulsion-gelation method: Formation, suspension rheology, digestion, and application to gel-in-gel beads, 120* p. 106926). Food Hydrocolloids.

Lin, D., Kelly, A. L., & Miao, S. (2021b). The role of mixing sequence in structuring O/W emulsions and emulsion gels produced by electrostatic protein-polysaccharide interactions between soy protein isolate-coated droplets and alginate molecules. *Food Hydrocolloids, 113*, 106537.

Lin, D., Lu, W., Kelly, A. L., Zhang, L., Zheng, B., & Miao, S. (2017). Interactions of vegetable proteins with other polymers: Structure-function relationships and applications in the food industry. *Trends in Food Science & Technology, 68*, 130–144.

Liu, Q., Lu, Y., Han, J., Chen, Q., & Kong, B. (2015). Structure-modification by moderate oxidation in hydroxyl radical-generating systems promote the emulsifying properties of soy protein isolate. *Food Structure, 6*, 21–28.

Liu, F., & Tang, C. H. (2016). Soy glycinin as food-grade Pickering stabilizers: Part. III. Fabrication of gel-like emulsions and their potential as sustained-release delivery systems for β-carotene. *Food Hydrocolloids, 56*, 434–444.

Li, S., Zhang, B., Li, C., Fu, X., & Huang, Q. (2020). Pickering emulsion gel stabilized by octenylsuccinate quinoa starch granule as lutein carrier: Role of the gel network. *Food Chemistry, 305*, 125476.

Lu, X., Lu, Z., Yin, L., Cheng, Y., & Li, L. (2010). Effect of preheating temperature and calcium ions on the properties of cold-set soybean protein gel. *Food Research International, 43*, 1673–1683.

Maltais, A., Remondetto, G. E., Gonzalez, R., & Subirade, M. (2005). Formation of soy protein isolate cold-set gels: Protein and salt effects. *Journal of Food Science, 70*, C67–C73.

Molina, E., Papadopoulou, A., & Ledward, D. (2001). Emulsifying properties of high pressure treated soy protein isolate and 7S and 11S globulins. *Food Hydrocolloids, 15*, 263–269.

Mozafarpour, R., Koocheki, A., Milani, E., & Varidi, M. (2019). Extruded soy protein as a novel emulsifier: Structure, interfacial activity and emulsifying property. *Food Hydrocolloids, 93*, 361–373.

Mutsokoti, L., Panozzo, A., Pallares, A. P., Jaiswal, S., Van Loey, A., Grauwet, T., et al. (2017). Carotenoid bioaccessibility and the relation to lipid digestion: A kinetic study. *Food Chemistry, 232*, 124–134.

O'sullivan, J., Park, M., & Beevers, J. (2016). The effect of ultrasound upon the physicochemical and emulsifying properties of wheat and soy protein isolates. *Journal of Cereal Science, 69*, 77–84.

Patel, M. A., AbouGhaly, M. H., Schryer-Praga, J. V., & Chadwick, K. (2017). The effect of ionotropic gelation residence time on alginate cross-linking and properties. *Carbohydrate Polymers, 155*, 362–371.

Peng, W., Kong, X., Chen, Y., Zhang, C., Yang, Y., & Hua, Y. (2016). Effects of heat treatment on the emulsifying properties of pea proteins. *Food Hydrocolloids, 52*, 301–310.

Pintado, T., Ruiz-Capillas, C., Jiménez-Colmenero, F., Carmona, P., & Herrero, A. M. (2015). Oil-in-water emulsion gels stabilized with chia (Salvia hispanica L.) and cold gelling agents: Technological and infrared spectroscopic characterization. *Food Chemistry, 185*, 470–478.

Saptarshi, S. R., Duschl, A., & Lopata, A. L. (2013). Interaction of nanoparticles with proteins: Relation to bio-reactivity of the nanoparticle. *Journal of Nanobiotechnology, 11*, 1–12.

Sato, A., Moraes, K., & Cunha, R. (2014). Development of gelled emulsions with improved oxidative and pH stability. *Food Hydrocolloids, 34*, 184–192.

Shi, J., Le Maguer, M., Bryan, M., & Kakuda, Y. (2003). Kinetics of lycopene degradation in tomato puree by heat and light irradiation. *Journal of Food Process Engineering, 25*, 485–498.

da Silva, A. M. M., Almeida, F. S., & Sato, A. C. K. (2021). Functional characterization of commercial plant proteins and their application on stabilization of emulsions. *Journal of Food Engineering, 292*, 110277.

de Souza Paglarini, C., de Figueiredo Furtado, G., Biachi, J. P., Vidal, V. A. S., Martini, S., Forte, M. B. S., et al. (2018). Functional emulsion gels with potential application in meat products. *Journal of Food Engineering, 222*, 29–37.

Tang, C. H., & Liu, F. (2013). Cold, gel-like soy protein emulsions by microfluidization: Emulsion characteristics, rheological and microstructural properties, and gelling mechanism. *Food Hydrocolloids, 30*, 61–72.

Tcholakova, S., Denkov, N. D., Ivanov, I. B., & Campbell, B. (2006). Coalescence stability of emulsions containing globular milk proteins. *Advances in Colloid and Interface Science, 123*, 259–293.

Wang, X., Lin, Q., Ye, A., Han, J., & Singh, H. (2019). Flocculation of oil-in-water emulsions stabilised by milk protein ingredients under gastric conditions: Impact on *in vitro* intestinal lipid digestion. *Food Hydrocolloids, 88*, 272–282.

Wan, Z. L., Guo, J., & Yang, X. Q. (2015). Plant protein-based delivery systems for bioactive ingredients in foods. *Food & Function, 6*, 2876–2889.

Xu, D., Yuan, F., Gao, Y., Panya, A., McClements, D. J., & Decker, E. A. (2014). Influence of whey protein–beet pectin conjugate on the properties and digestibility of β-carotene emulsion during in vitro digestion. *Food Chemistry, 156*, 374–379.

Yildiz, G., Ding, J., Andrade, J., Engeseth, N. J., & Feng, H. (2018). Effect of plant protein-polysaccharide complexes produced by mano-thermo-sonication and pH-shifting on the structure and stability of oil-in-water emulsions. *Innovative Food Science & Emerging Technologies, 47*, 317–325.

Zeng, Z., Patel, J., Lee, S. H., McCallum, M., Tyagi, A., Yan, M., et al. (2012). Synthetic polymer nanoparticle–polysaccharide interactions: A systematic study. *Journal of the American Chemical Society, 134*, 2681–2690.

Zhang, S. B., Yan, D. Q., Jiang, Y. S., & Ding, C. H. (2021). Competitive displacement of interfacial soy proteins by Tween 20 and its effect on the physical stability of emulsions. *Food Hydrocolloids, 113*, 106515.

Zhou, Y., Teng, F., Tian, T., Sami, R., Wu, C., Zhu, Y., et al. (2020). The impact of soy protein isolate-dextran conjugation on capsicum oleoresin (*Capsicum annuum L.*) nanoemulsions. *Food Hydrocolloids, 108*, 105818.

Zou, Y., Pan, R., Wan, Z., Guo, J., Wang, J., & Yang, X. (2017). Gel-like emulsions prepared with zein nanoparticles produced through phase separation from acetic acid solutions. *International Journal of Food Science and Technology, 52*, 2670–2676.